

https://dspace.org/

Assessing the Magmatic Ni-Cu-(Co-PGE) Sulphide Potential of the Kunene AMCG Complex

Manuel, Agex Cordeiro Ferreira

2024-08

University of the Witwatersrand, Johannesburg

https://hdl.handle.net/10539/46605

Manuel, Agex Cordeiro Ferreira. (2024). Assessing the Magmatic Ni-Cu-(Co-PGE) Sulphide Potential of the Kunene AMCG Complex. [Master's dissertation, University of the Witwatersrand, Johannesburg]. WIReDSpace. https://hdl.handle.net/10539/46605

Downloaded from a DSpace repository. https://dspace.org/



Assessing the Magmatic Ni-Cu-(Co-PGE) Sulphide Potential of the Kunene AMCG Complex

by

Agex Cordeiro Ferreira Manuel

(2562515)

A Dissertation

Submitted in requirements for the degree of

Master of Sciences

in

Geosciences

in the Faculty of Science, University of the Witwatersrand, Johannesburg, South Africa

Supervisor: Dr. Ben Hayes

Co-supervisor: Prof. Grant Bybee

August 2024

DECLARATION

I declare that this dissertation is my own, unaided work. It is being submitted for the Degree of Master of Sciences at the University of the Witwatersrand, Johannesburg. It has not been submitted before for any degree or examination at any other University.



ACF Manuel

2nd of August 2024 at Johannesburg

List of Abbreviations

AMCG	Anorthosite-Mangerite-Charnockite-Granite
CAB	Continental Arc Basalts
CFB	Continental Flood Basalts
CHUR	Chondritic Uniform Reservoir
Cpx	Clinopyroxene
EMC	Epupa Metamorphic Complex
Fo	Forsterite
HCl	Hydrochloric acid
HF	Hydrofluoric acid
HLIS	Harp Lake Intrusive Suite
HNO_3	Nitric acid
H_3PO_4	Phosphoric acid
ICP-MS	Inductively Coupled Plasma-Mass Spectrometry
ICP-O/AES	Inductively Coupled Plasma-Optical/Atomic Emission Spectroscopy
KC	Kunene Complex
L/HREE	Light/Heavy Rare Earth Element
$LiBO_2/LiB_4O_7$	Lithium metaborate/Lithium tetraborate
MCR-K	Keweenaw basalts from Mid-Continental Basalt
MPD	Mean Percentage Difference
MUM	Mafic-Ultramafic
NPS	Nain Plutonic Suite
Ol	Olivine
Opx	Orthopyroxene
PCIGR	Pacific Centre of Isotope and Geochemical Research
PM	Primitive Mantle
RGS	Red Granite Suite
SQAMC	Schist-Quartzite-Amphibolite-Marble Complex
TIMS	Thermal Ionization Mass Spectometry
UJ	University of Johannesburg
UP	University of Pretoria
VBI	Voisey's Bay Intrusion
VCDT	Vienna-Canyon Diablo Troilite
WIGL	Wits Isotope Geochemistry Laboratory
Wits	University of the Witwatersrand

Acknowledgements

The successful conclusion of this thesis was only possible because of the support received in various ways and capacities. To my supervisors, Ben Hayes and Grant Bybee, I am grateful for your huge valuable experiences and advice, mentorship as well as persistence to maintain the focus on each task and within the objectives. To the Kunene Team, it was awesome to tap into this well of experience and get continuous feedback and encouragement throughout the project. I also thank the University of the Witwatersrand, in particular the School of Geosciences and its various research facilities as well as its collaborations for the commitment to allow to achieve the objectives of this research. To the crew of Room 203D in 2021-2023, it was special to be around you and get social and incentive supports as well as critical discussions pertaining to the various project topics in that room and with them, I earned a degree but also life lessons and different perspectives of life. My gratitude also goes to Busisiwe Khoza whom dedicated her precious time while abdicating her time slot for me to collect my isotopic analytical data. I thank Anglo American, CIMERA and NRF for the sponsorship that made this personal achievement and much-long goal possible (a reality) with their funding support. To my family, and soulmate, a special thanks for being there for me in that amazing run always willing to support and for the unconditional sacrifice! To all, I would like to thank for making this research project a great learning experience and making me ready for the next chapter in my professional career and its challenges.

Table of Contents

Chapter 1: Introduction 1

Chapter 2: Geological Background 6

2.1 Kunene AMCG Complex 6

2.2 MUM Intrusions of the Kunene Complex 13

2.2.1 Oncócua Intrusion 13

2.2.2 Ohamaremba Intrusion 17

2.2.3 Otjijanjasemo Intrusion 19

2.2.4 Ombuku North & South Intrusions 20

2.2.5 Other Peripheral MUM Intrusions of the KC 23

2.3 Nain Plutonic Suite and Voisey's Bay/Other Intrusions 24

2.3.1 Nain Plutonic Suite and Voisey's Bay 26

2.3.2 Ore-forming Processes in the Voisey's Bay Intrusion (VBI) 32

2.3.3 Other Mafic-Ultramafic Intrusions 36

Chapter 3: Methods 42

3.1 Sampling and Fieldwork 42

3.2 Petrography 44

3.3 Bulk Rock Major and Trace Element Database 44

3.4 Electron Probe Microanalysis 45

3.5 Radiogenic (Sr-Nd) Isotope Analyses 46

3.6 Sulphur Isotope Analyses 48

Chapter 4: Results 49

4.1 Fieldwork 49

4.2 Petrography and *in situ* Mineral Compositions of the Mafic-Ultramafic Intrusions 51

4.2.1 Oncócua Intrusion 58

4.2.2 Ohamaremba Intrusion 62

4.2.3 Otjijanjasemo Intrusion 66

4.2.4 Ombuku North Intrusion 68

4.2.5 Sulphides of the MUM Intrusions 72

4.3 Major Oxide and Trace Element Geochemistry 74

4.4 Sulphur Isotopes 91

4.5 Radiogenic Sr-Nd Isotopes 92
Chapter 5: Discussion 99
5.1 The Genetic Relationship of the Mafic-Ultramafic Intrusions to the KC Anorthosite Suite 104
5.2 Evidence of Ore-forming Processes in the Mafic-Ultramafic Intrusions to the KC 111
5.2.1 Cumulate Rocks in the MUM Intrusions and Fo-Ni Relationship in Olivine .. 111
5.2.2 Crustal Contamination 117
5.2.3 Subsequent Magma Influxes and Upgrading of Sulphide 122
5.3 Limitations and Suggestions 127
Chapter 6: Conclusion 129
Chapter 7: References 132
Chapter 8: Appendices 140

List of Figures

Figure 1: Spatial distribution of Proterozoic massif-type anorthosites (red dots). 2
Figure 2: Geological map of the Kunene Anorthosite-Mangerite-Charnockite-Granite (AMCG) Complex showing the locations of the peripheral mafic-ultramafic intrusions (red boxes) in this study. 5
Figure 3: Geological map of the Kunene Complex highlighting the six domains (demarcated by black-dashed lines) based on remote sensing data and high-precision geochronological data. 9
Figure 4: A geological map of the Oncócua Intrusion showing the main lithologies and sample locations. 15
Figure 5: A geological map of the Ohamaremba intrusion showing the major lithologies and sample locations. 18
Figure 6: Google Earth satellite image of the Otjijanjasemo intrusion showing the outcrop samples collected by the Kunene Team and past Otjijanjasemo drillholes. 20
Figure 7: Geological maps of the Ombuku intrusions. 22
Figure 8: Regional structural map highlighting the Nain Plutonic Suite location associated with trans-lithospheric structural controls. 26
Figure 9: Geological map of the Nain Plutonic Suite (NPS) showing Voisey's Bay and the Mushuau intrusions as well as the surrounding basement rocks. 28
Figure 10: Genetic model of the Voisey's Bay deposit looking-west section and showing the mineralised zones and loci for magma interaction with basement rocks. 30
Figure 11: Geological map of the Harp Lake Intrusive Suite showing the several intrusions and associated sulphide mineral occurrences. 39
Figure 12: Photographs of outcrops (A-H & L-M) and drillcores (I-K) taken during fieldwork in the Mafic-Ultramafic intrusions (mainly Oncócua intrusion) of the Kunene Complex that show a range of mafic to ultramafic lithologies and textures. 50
Figure 13: Lithological variation and classification of the MUM intrusions. 51
Figure 14: The modal abundances of the MUM intrusions plotted on mineral ternary plots (A, Ol-Plag-Cpx; B, Ol-Plag-Silica). 54
Figure 15: Molar Fo-Ni (ppm) compositions of olivine for Ohamaremba, Otjijanjasemo, Ombuku North, and Oncócua. 56
Figure 16: Boxplots showing the range of the Fo composition of olivine (A, Molar Fo; B, Ni in ppm) with outliers (black dots). 57
Figure 17: Ternary composition diagram for pyroxene with the mineral compositions of pyroxene plotted for Oncócua, Otjijanjasemo, Ombuku North, and Ohamaremba. . 58
Figure 18: Transmitted light photomicrographs (all XPL; 4x magnification) of three samples from Oncócua. 60
Figure 19: Transmitted-Light Photomicrographs (all XPL; 4x magnification) of two samples from Ohamaremba. 64
Figure 20: Transmitted light photomicrographs (all XPL; 4x magnification) of two samples from Otjijanjasemo. 67

Figure 21: Transmitted-Light Photomicrographs (all XPL; 4x magnification) of three samples from Ombuku North and South. 70
Figure 22: Reflected-Light Photomicrographs (all PPL; 4x magnification) of three drillcore samples from Ohamaremba (KSAT-157), Oncocua (ONC1-59) and Ombuku North (4-778) 73
Figure 23: A FeO-MgO (wt%) diagram that includes the parent magma compositions of world-class magmatic Nickel sulphide mineralised intrusions globally.* 75
Figure 24: Mg# vs Al_2O_3 plot to discriminate the compositions of cumulate and non-cumulate rocks. 76
Figure 25: Whole rock data of the MUM intrusions used to determine the normative mineralogy of the samples by CIPW(Cross, Iddings, Pirsson and Washington) Norm and plotted in the ternary plots of crystallisation sequences of basaltic liquids. 78
Figure 26: Whole rock data of the MUM intrusions plotted in a Ternary Si-Al-Mg+Fe diagram. 79
Figure 27: Major oxides and trace element ratio diagrams to assess the magmatic affinity of the MUM intrusions. 80
Figure 28: Trace element ratios and major oxides of the MUM intrusions to assess magma sources and magma evolution in the crust. 81
Figure 29: Primitive mantle normalised multi-element diagrams of the MUM intrusions (average values for particular rock types from each intrusion are shown in each diagram) and the KC anorthosite suite. 84
Figure 30: Trace element ratio diagrams to assess magma sources and magma-crust interaction for the MUM intrusions. 88
Figure 31: Diagrams of primitive mantle normalised PGE (Platinum Group Elements) and some base metals. 90
Figure 32: Plot of Ni vs Cu to assess metal enrichment in the MUM intrusions showing which intrusions are likely to be Ni enriched over Cu. 91
Figure 33: $\delta^{34}S$ values from the MUM intrusions and their associated basement rocks from north to south across the entire western and southern margin of the Kunene Complex. 92
Figure 34: Initial Sr-Nd isotopic compositions of Oncócua and basement rocks. 94
Figure 35: Covariant plots of $\varepsilon_{Nd(t)}$ for Oncócua and its basement rocks (corrected at 1.4 Ga and 1.8 Ga) versus $\delta^{34}S$ and selected trace element ratios. 98
Figure 36: A Timeline showing the published geochronological data for the MUM intrusions, KC and basement rocks. 105
Figure 37: Molar Fo-Ni (ppm) compositions of olivine for Ohamaremba, Otjijanjasemo, Ombuku North, and Oncócua showing the model fractionation curves for Voisey's Bay. 113
Figure 38: Chromium profiles in pyroxene grains of the MUM intrusions for chromium zoning. 124

List of Tables

Table 1: Lithostratigraphic units surrounding the Kunene AMCG Complex (the data are from compilations of authors cited in the Comments). *11*
Table 2: List of samples used in this study along with summary of the data collected for each sample in this MSc. *43*
Table 3: Average primitive mantle normalised trace element ratios of the MUM intrusions and the KC anorthosite suite. *85*
Table 4: Radiogenic Sr-Nd Isotopic Data for Oncócua and its basement rocks including a BHVO2 standard measurement. *95*
Table 5: Summary result of the data of the MUM intrusions. *100*

Chapter 1: Introduction

Proterozoic massif-type anorthosites have attained economic interest among prospectors and geologists since the discovery of the mafic-ultramafic Voisey's Bay magmatic Ni-Cu-(Co-PGE) sulphide deposit in the Mesoproterozoic Nain Plutonic Suite (NPS: Myers et al., 2008; Saumur & Cruden, 2016) in Labrador (Canada) (Fig. 1). The Voisey's Bay Intrusion (VBI) hosts a world-class Ni-sulphide deposit with 124.4 Mt (reserves + resources) grading 1.66% Ni, 0.88% Cu and 0.05% Co at the time of the discovery (Li et al., 2000). The VBI has a well-developed ore-forming model that involves crustal assimilation and the formation of immiscible sulphide liquids in its parent magmas (e.g., Naldrett, 1999; Li et al., 2000; Barnes et al., 2016). This model has been applied to other mafic-ultramafic (MUM) intrusions in the NPS to assess their economic potential, such as the Mushuau troctolitic-melatroctolitic intrusion and Pants Lake gabbroic-troctolitic intrusion, as well as MUM intrusions in the Harp Lake Intrusive Suite (Amelin et al., 2000; Smith, 2006; Kerr & Smith, 2000). An understanding of the VBI ore-forming model is therefore critical to assessing the nickel sulphide potential of other Proterozoic anorthosites globally.

Critical processes have been identified in the development of any kind of Ni-sulphide deposit and are summarised in Naldrett (2010). Field observations, textures, mineralogy, whole rock geochemistry (major and trace elements), as well as radiogenic and stable isotope signatures, show that certain ore-forming processes were, in general, critical for the formation of a magmatic Ni-Cu-(Co-PGE) sulphide ore deposit in the VBI and other magmatic Ni-sulphide deposits elsewhere. The stages in the generation of a magmatic nickel sulphide deposit summarised by Naldrett (2010) are as follows: (1) Partial melting of the mantle to produce high-temperature MgO-rich magmas that are capable of carrying significant quantities of dissolved sulphur, nickel and platinum-group elements; (2) the transportation of magma from the mantle and its emplacement into the crust; (3) magma-crust interaction; (4) assimilation of sulphur-bearing country-

rock resulting in sulphur saturation and the segregation of immiscible sulphide liquids in the magma; (5) additional ascent of both magma and immiscible sulphide liquids into shallower chambers/conduits in the crust where the sulphides accumulate in a trap; (6) magma replenishment through the same magma conduits led to metal tenor upgrading of the pre-existing sulphides; (7) finally, the host magma and the sulphides were then left to cool and crystallise to form a nickel sulphide ore deposit.

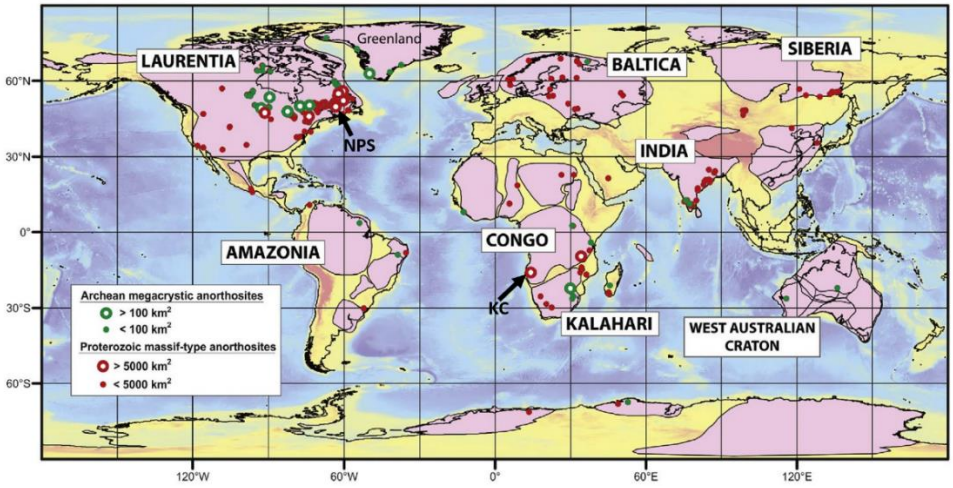


Figure 1: Spatial distribution of Proterozoic massif-type anorthosites (red dots). Locations of the Kunene Complex (KC) and Nain Plutonic Suite (NPS) are shown (black arrow). This map has been modified from Ashwal and Bybee (2017).

The Mesoproterozoic Kunene Anorthosite-Mangerite-Charnockite-Granite (AMCG) Complex (KC: Simpson & Otto, 1960; Silva, 1990; Ashwal & Twist, 1994; Slejko et al., 2002; Maier et al., 2013; Bybee et al., 2019; Lehmann et al., 2023) contains the largest (>18,000 km^2) known suite of Proterozoic massif-type anorthosites on Earth and is exposed in southern Angola and northern Namibia (Fig. 1). Its overall extent may be up to 35,000 km^2, according to subsurface satellite gravity data, as much of its eastern portion is covered by Kalahari sediments (Rey-Moral et al., 2022). The KC has also been one of the least studied AMCG complexes on Earth partly because of access difficulties due to its remote location (Ashwal, 1993; Ashwal & Twist, 1994; Bybee et al., 2019). The KC and NPS share many general similarities such as their (i) age of emplacement, (ii) long duration of magmatism, (iii) emplacement into

Palaeoproterozoic basement rocks, and (iv) lithologies, including volumetrically minor MUM intrusions located at the margins of the anorthosites. Following the discovery of the VBI ore deposit in 1993 there was some exploration in the KC, particularly in the MUM intrusions that are present at its western margin, in both Angola and Namibia. However, no significant magmatic sulphide deposit has yet been discovered in this region. In the development of any mineral system model for nickel sulphide exploration in the KC region, it is important to have a thorough understanding of the geological setting of the NPS, as well as the ore-forming processes involved in the formation of the magmatic VBI sulphide deposit (e.g., Barnes et al., 2016).

Due to several exploration challenges, including the relatively small sizes of intrusions hosting magmatic sulphides and the general lack of alteration haloes that characterise large-scale hydrothermal ore deposits, magmatic Ni-Cu-Co-PGE sulphide deposits are difficult to find. The mineral system approach allows the application of a wide range of tools to predict and detect common features of potential exploration targets for magmatic Ni-sulphide deposits that are otherwise hidden and difficult to identify in the field by exploration geologists (Barnes et al., 2016; Barnes, 2023). Naldrett (2010) and Barnes et al. (2016) report extensively on the applications of the mineral system approach. The mineral system approach looks at magmatic sulphide deposits from the perspective of a series of critical lithospheric-scale processes involved in the ore formation, including magma sources, transportation of magma, enrichment of magma, and the trapping of upgraded ores. It is important to note that these prediction and detection tools are mappable in the field and include the following: the source and composition of ore-forming silicate and sulphide magma (usually magmatism with high-Mg and low-Ti contents) and the relationship to pre-existing cratonic architecture (e.g., Fig. 1); magmatic and structural control that contributed to the formation of an open protracted-flow magma conduit system; incorporation of crustal S-bearing rocks as magma ascends to the crust to trigger segregation and the formation of immiscible sulphide liquid; favourable intrusion geometry and emplacement style to allow deposition; reworking and upgrading by fresh undepleted-chalcophile magma using the

same open conduit system; and cooling and crystallisation of magma and related sulphides; and favourable structural and erosional history after emplacement to allow preservation and detectability. These components are critical for ore formation, and evidence of the presence of these ore-forming processes can be found using petrological and geochemical techniques.

This research project focuses on assessing the magmatic Ni-Cu-(Co-PGE) sulphide potential of the MUM intrusions in the KC by identifying the evidence of ore-forming processes and to produce a mineral system approach to future mineral exploration in the KC (Fig. 2). The broad geological similarities of the KC and NPS highlighted above suggest that the geological environment of the MUM intrusions in the KC may have been conducive to the formation of a Ni-sulphide ore deposit like that at Voisey's Bay.

The aim of this MSc research project is to assess the magmatic Ni-Cu-(Co-PGE) sulphide potential of the MUM intrusions in the KC. To assess the potential mineralisation, the scope and objectives of this study will involve a literature review of the NPS and the VBI, so that a clear mineral system approach can be developed and applied to the KC and a petrological and geochemical study of the MUM intrusions in the KC to look for evidence of ore-forming processes. Important research questions include (i) establishing whether the MUM intrusions are coeval with the KC, (ii) assessing the composition of the basement rocks to the MUM intrusions to establish potential external sources of sulphur, (iii) looking for evidence of magma replenishment and (iv) determining if immiscible sulphide liquids were segregated from the basaltic magmas related to the KC. This approach will allow a thorough insight into the ore-forming processes of the MUM intrusions while assessing the economic potential of the KC using the mineral system approach developed for magmatic Ni sulphide deposits.

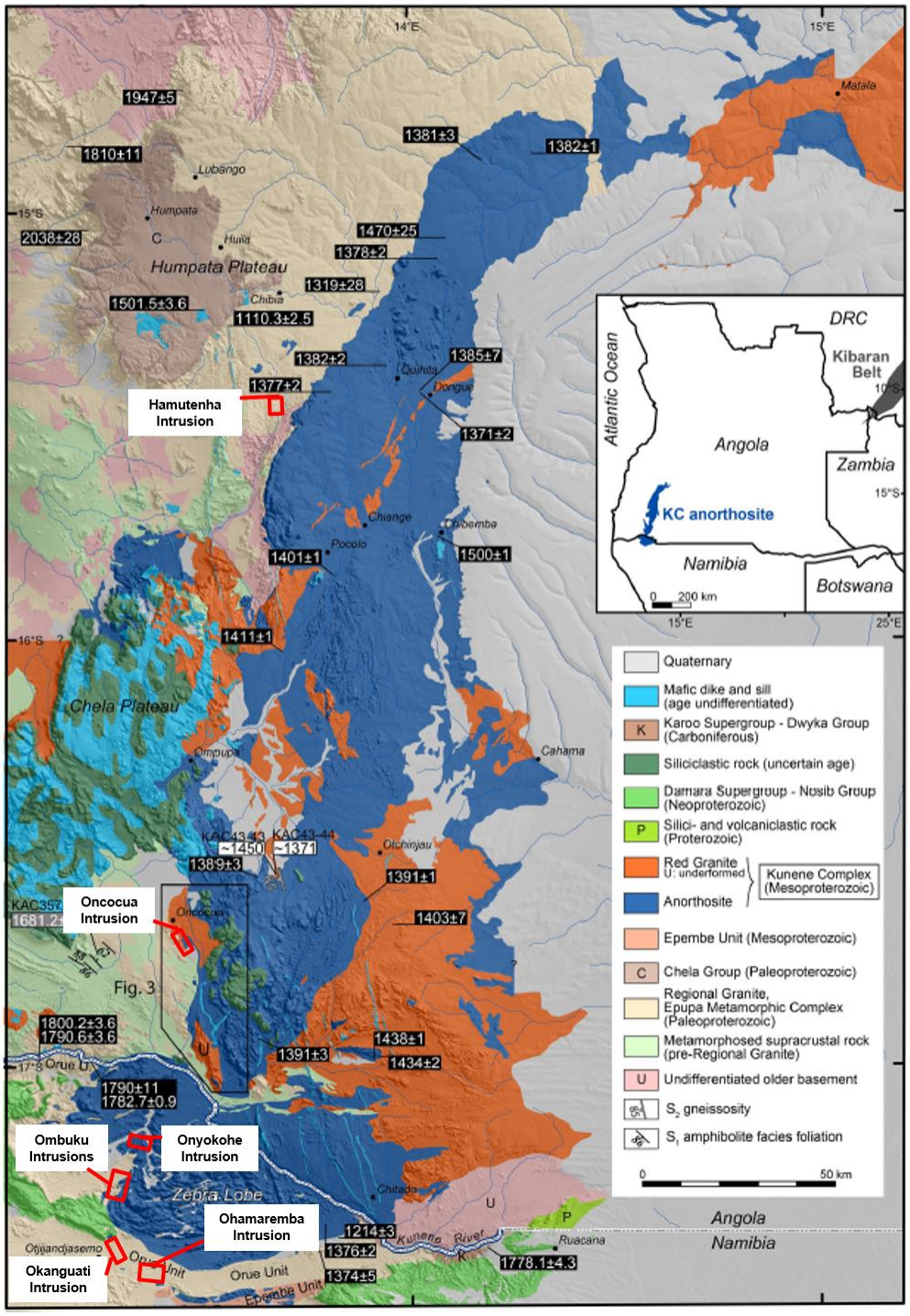


Figure 2: Geological map of the Kunene Anorthosite-Mangerite-Charnockite-Granite (AMCG) Complex showing the locations of the peripheral mafic-ultramafic intrusions (red boxes) in this study. Various $^{40}Ar/^{39}Ar$ ages (grey boxes) and U-Pb ages (white boxes) and age data from past publications (black boxes) are also shown. This map has been modified after Lehmann et al. (2020).

Chapter 2: Geological Background

2.1 Kunene AMCG Complex

The Kunene AMCG Complex (KC) is huge (>18,000 km^2) and it contains the largest known examples of Proterozoic massif-type anorthosites on Earth. The KC is located at the southwestern margin of the Congo craton and extends ~300 km north-south from southwestern Angola (hosting ~80% of the total extension of the KC) to northwestern Namibia (Figs. 1 and 2) (Simpson and Otto, 1960; Silva, 1990; Ashwal and Twist, 1994; Bybee et al., 2019). The eastern extent of the KC is not fully known due to the Kalahari sediment cover of Quaternary age. The KC possibly has a total areal extent of ~36,000 km^2 based on subsurface geophysical data (Rey-Moral et al., 2022), which would almost certainly make it the largest known AMCG Complex on Earth. Like other Proterozoic massif-type anorthosites, the KC comprises predominantly anorthosite *senso stricto* with intermediate plagioclase compositions (molar % An_{48-73}: Ashwal, 1993; An_{40-60}: Hill, 2017). There are also leucotroctolite, leucogabbronorite and leuconorite lithologies and even lesser amounts of MUM rocks mostly located at the southwestern margins of the KC (Silva, 1990; Ashwal and Twist, 1994; Drüppel, 2007; Maier et al., 2013; Bybee et al., 2019). Maier et al. (2013) reports that the leucotroctolites of the KC are among the least evolved leucotroctolites in massif anorthosite complexes globally with olivine and plagioclase mineral compositions of Fo_{59-77} and An_{56-70}, respectively. The KC anorthosite suite has been precisely age dated to between 1500 and 1360 Ma, demonstrating the extremely long duration nature of these magmatic systems (Bybee et al., 2019). The Red Granite Suite (RGS) is a volumetrically major component of the KC and has a similar age range to the anorthosite suite (Milani et al., 2022).

An earlier hypothesis suggested that the KC was a layered mafic intrusion and there are past geochemical characterisation studies that suggested it had compositional zones similar to the Critical and Main Zones of the Bushveld Complex in South Africa (Silva, 1990). This suggestion was based on features of magmatic layering observed locally,

especially in the central part of the Angolan portion of the KC and in the Zebra Mountains in the Namibian portion of the KC (Fig. 2) (Silva, 1990). Furthermore, it was proposed by Maier et al. (2013) that the Zebra Mountain anorthosites are layered with distinct mineral compositional trends observed. However, the layered intrusion hypothesis of Silva (1990) was abandoned after detailed field observations revealed little compositional and textural variations throughout most of the KC anorthosites, and along with other features such as 'block structures', indicated that the KC anorthosites are more typical of a composite Proterozoic massif-type anorthosite (Ashwal and Twist, 1994; Maier et al., 2013; Bybee et al., 2019).

Publications on field observations and mineral compositions report that the anorthosite suite of the KC can be broadly referred to as the white anorthosite suite and the dark anorthosite suite (Simpson and Otto, 1960; Silva, 1990; Drüppel et al., 2007; Maier et al., 2013; Bybee et al., 2019). The white anorthosite suite is a pyroxene-bearing anorthosite/leucogabbronorite that was intruded by the dark anorthosite, an olivine-bearing anorthosite/leucotroctolite and in the Zebra Mountains region of Namibia these two units are interlayered (Maier et al., 2013). The white anorthosite is altered whereas the dark anorthosite is less altered. The explanation for the dichotomy of white and dark anorthosites is that the early mantle-derived parental magma to the white anorthosite was affected by lower crustal contamination which led to these magmas crystallising orthopyroxene instead of olivine. Subsequently, the parent magmas to the dark anorthosites were intruded through the same conduit systems and did not interact with the crust (because of shielding) and hence crystallised olivine instead of orthopyroxene (e.g., Bybee et al., 2019). Field evidence for this emplacement history includes the presence of sharp contacts between the layered dark and white anorthosites, a white anorthosite that is progressively enriched in orthopyroxene at the contact between white anorthosite and granite-gneiss country rocks, and basement xenocrysts in the white anorthosites (e.g., Maier et al., 2008; Drüppel, 2003). Moreover, an innovative remote sensing and geological investigation of the KC by Lehmann et al. (2023) suggests the presence of lithological regions and boundaries

(Fig. 3). Based on the report, KC anorthosite suite has been divided into six domains that were identified based on distinct internal spectral response and architecture (Fig. 3). The report also suggests that the KC anorthosite suite comprises at least four distinct magmatic plutons with a timeframe > 60 Myr based on high-precision geochronological data published in Bybee et al. (2019). The work broadly showed a northern pluton (1380 Ma) of domain 1 that comprises massive olivine-bearing anorthosite, and the central pluton (1412-1400 Ma) of domain 2 with interlayered olivine-bearing and olivine-poor anorthosite with a belt of the Red Granite Suite trending NE-SW that separates the northern pluton from the central pluton. The southern central pluton (1390 Ma) consists of domains 3 and 4 (Fig. 3). The southern central pluton is layered and comprises olivine-bearing anorthosite that forms ridges and metasomatized olivine-poor and pyroxene-bearing anorthosite that forms valleys (Fig. 3). The southernmost pluton (1363-1377 Ma) is similarly layered trending E-W that consists of domain 6 and includes the Zebra Mountains in the Namibian KC and southeasternmost Angolan KC, and it is separated from the southern central pluton by a thrust zone (Fig. 3). A small pluton (1438-1434 Ma) known as domain 5 is also located southeast of the main KC in Angola, and it comprises olivine-bearing anorthosite *sensu lato*. This study supports the previous work by Ashwal and Twist (1994) in the KC anorthosite suite. Based on detailed field and laboratory study, Ashwal and Twist (1994) suggested that the KC anorthosite suite is analogous to composite, massif-type anorthosite complexes (as mentioned previously) and, with the support of satellite images, several individual plutons were also outlined in the KC anorthosite suite.

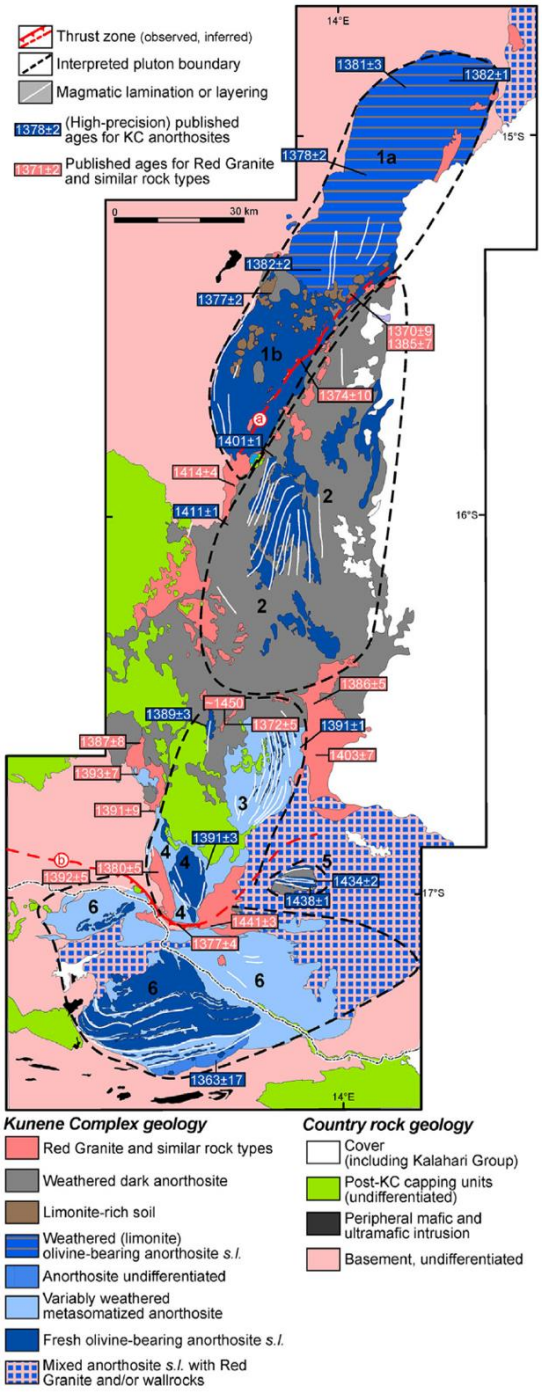


Figure 3: Geological map of the Kunene Complex highlighting the six domains (demarcated by black-dashed lines) based on remote sensing data and high-precision geochronological data (Lehmann et al., 2023).

The KC was emplaced into the Palaeoproterozoic Regional Granite that comprises biotite granites, granodiorites and tonalites of the Eburnean basement (2000-1950 Ma: McCourt et al., 2013; Jelsma et al., 2018; Lehmann et al., 2020) (Fig. 2, Table 1). The Eburnean basement rocks were themselves emplaced into the Archaean granitic-tonalitic gneisses and migmatites which are mainly preserved in the northern parts of the KC (2680-2520 Ma: McCourt et al., 2013) (Table 1). It is also important to mention another old basement rock unit which is comprised of the pre-Eburnean (~2300 Ma) Schist-Quartzite-Amphibolite-Marble (±metapelite) Complex (SQAMC) (also referred as the Ovipaca Schist by Smuts, 1998) (Fig. 2, Table 1). The SQAMC represents low-grade metasediments interbedded with lenses of chert and marble (de Carvalho, 1984; Silva, 1990; McCourt et al., 2013). Some authors seem to equate the SQAMC with the early-Palaeoproterozoic metamorphosed supracrustal volcano-sedimentary sequences collectively referred to as the Chivanda Group and which comprises quartzite, conglomerate, sandstone, pillow lava, felsic volcanic rocks, and schist (2149±83 Ma: Silva, 1990; McCourt et al, 2013; Lehmann et al., 2020). However, recent report also regards the SQAMC as the Namibe Group which is part of the Namibe Zone (Ferreira et al., 2024). In their report, they highlight that the Namibe Group comprise metapelite, felsic metavolcanoclastite, metagreywacke along and intercalation of marble and amphibolite with an age of emplacement of 1.8 Ga. Other older rocks at the margins of the KC consist of the relatively undeformed Palaeoproterozoic Chela Group on the Humpata Plateau, which is mostly found in Angola, and the pre-Regional Granite metamorphosed supracrustal unit (Chivanda Group) along the western side of the KC (McCourt et al., 2013; Lehmann et al., 2020) (Table 1). The Epupa Metamorphic Complex (EMC) is the dominant basement rock to the Zebra Mountain anorthosites (Fig. 2, Table 1). The EMC is a high-grade unit comprised of meta- to peraluminous calc-alkaline granitoid gneisses (1760-1860 Ma: McCourt et al., 2013; Bybee, et al., 2019; Lehmann et al., 2020) (Fig. 2, Table 1). The supracrustal gneisses of the EMC are divided to the south of the Zebra Mountains into the granulite facies Epembe Unit and the amphibolite facies Orue Unit. The Epembe Unit comprises felsic-mafic granulites with intercalated paragneisses, felsic-mafic granulites and minor

amphibolite facies shear zones. The Orue Unit comprises migmatitic granitic orthogneisses and lenses of paragneisses and amphibolite (Brandt et al., 2007; Drüppel et al., 2007).

Table 1: Lithostratigraphic units surrounding the Kunene AMCG Complex (the data are from compilations of authors cited in the Comments).

	Lithostratigraphic Unit	**Main Rock types**	**Age (Ma)**	**Comments**
Neoproterozoic	Damara Supergroup	Quartzite, conglomerate, marble, amphibolite and schist	No published age	Probably an extension of Nosib Group in northern Namibia (compiled from McCourt el al., 2013; Jelsma et al., 2018)
Mesoproterozoic	Red Granite	Granite, granodiorite, syenite and rhyolitic porphyry	1411 ± 24 to 1302 ± 20	Intruded the KC anorthosite suite; Rb-Sr ages (compiled from McCourt et al., 2013; Jelsma et al., 2018)
	KC anorthosite suite	Massive anorthosite, leucotroctolite, leucogabbro, mangerite and syenodiorite	1500 ± 1 to 1377 ± 2	U-Pb ages (compiled from Bybee et al., 2019)
Palaeoproterozoic	Chela group	Conglomerates, quartzites, sandstones, felsic volcanic rocks, and argillites	1798 ± 11 to >1500	U-Pb ages (compiled from Jelsma et al., 2018; Ferreira et al., 2024)
	Epupa Metamorphic Complex	Metapelites, metagreywackes and amphibolites, metapelites, granitic gneisses, migmatites and anatectic granites	1808 ± 12 to 1757 ± 4	U-Pb ages (compiled from Jelsma et al., 2018; Ferreira et al., 2024)
	Regional Granite	Biotite, granite, granodiorite and tonalite, felsic volcanic and volcaniclastic rocks	2038 ± 28 to 1954 ± 6	U-Pb ages (compiled from McCourt et al., 2013; Jelsma et al., 2018)
	Chivanda Group	Quartzite, conglomerate, sandstone, pillow lava, felsic volcanic rocks and schist	2149 ± 83 to 1915 ± 58	Rb-Sr ages (compiled from McCourt et al., 2013; Jelsma et al., 2018)
	SQAMC-Schist, Quartzite, Amphibolite, Marble Complex or Namibe Group	Chert, schist, quartzite, amphibolite and marble	<2300 to >1811 Ma	U-Pb ages (compiled from McCourt et al., 2013; Ferreira et al., 2024)
Archaean	Archean granitic-tonalitic gneisses	Orthogneiss amphibolite, granitic-tonalitic gneisses, migmatite, granite and quartz diorite	2680 ± 5 to 2519 ± 5	U-Pb ages (compiled from McCourt et al., 2013; Jelsma et al., 2018)

Recent detailed structural work in the southwestern part of the KC in Angola revealed two important deformation events, referred to as D_1 and D_2 (Lehmann et al., 2020; Hayes et al., 2022) (Fig. 2: the area demarcated with a black outline). In this work, the authors report the absence of D_1 fabrics in the KC anorthosite suite and RGS. On the other hand, D_2 fabrics are present in the basement rocks as well as the KC anorthosite suite and RGS and it is interpreted to represent progressive, eastward ductile thrusting in a convergent margin setting (Lehmann et al., 2020). The findings suggest that the KC may have been formed in a continental arc setting in accordance with the petrogenesis of such anorthosites elsewhere (e.g., Bybee et al., 2014; Ashwal & Bybee, 2017).

Proterozoic AMCG Complexes, including the KC and Nain Plutonic Suite (NPS) of eastern Canada, host volumetrically small mafic-ultramafic intrusions (MUM). In the KC, the known MUM intrusions are preferentially localised at the southwestern margins of the KC and are composed of peridotites, pyroxenites, troctolites and gabbros (Fig. 2). Some of these MUM intrusions contain sulphide mineralisation that has been previously reported (Smuts, 1998; Maier et al., 2013). There is also a suite of MUM intrusions located further north in the KC, to the west of the northern domain of leucotroctolites (Lehmann et al., 2023). This suite includes the Palaeoproterozoic Hamutenha intrusion (Campeny et al., 2023) (Fig. 2). The geology of some of the main MUM intrusions around the southwestern margins of the KC, which are the focus of this project, are described in section 2.2.

In a study conducted by Maier et al. (2013), in the Namibian part of the KC, they suggested that the MUM intrusions were derived from a mantle source and the magmas were emplaced at the margins of the KC anorthosite suite. A mantle source for the MUM intrusions was supported by the relative enrichment in MgO, Ni and Cr, as well as the mantle-like isotopic characteristics of the dark anorthosite suite of the Zebra Mountains with $\delta^{18}O$ (5 to 7), $\delta^{34}S$ (+0.4 to +3), and ε_{NdT} (+0.9 to +1.8 at 1370 Ma). The ε_{NdT} compositions of the dark anorthosite in the Zebra Mountains contrasts with the ε_{NdT} values obtained by Slejko et al. (2002) for two samples from the Angolan KC

that gave more negative ε_{NdT} values (-5.7 to -6.4). In the petrogenetic model of Maier et al. (2013), it is suggested that there were successive mantle upwellings (plumes?) which resulted in the magmatism that produced the MUM intrusions. However, Maier et al. (2013) suggested that more isotopic and geochronological data are needed to constrain the petrogenetic relationship of the MUM bodies with the main KC anorthosite suite.

2.2 MUM Intrusions of the Kunene Complex

As described in the section 2.1, there is a suite of mafic-ultramafic (MUM) intrusions located around the margins of the KC (Fig. 2). These intrusions are the primary focus of this MSc research project because they are the best exploration targets for Ni-Cu-(Co-PGE) (± Cr) mineralisation. The studied intrusions include the following, from the north in the Angolan KC to the south in the Namibian KC: Oncócua, Ombuku North and South, Ohamaremba and Otjijanjasemo. However, Hamutenha, in the Angolan KC, and Onyokohe, in the Namibian KC, were later added to the set of studied intrusions in this project (Fig. 2). The age relations of these MUM intrusions, as well as their genetic links to the KC, are still poorly known at the time of submission of this thesis. Therefore, it cannot yet be explicitly stated if these MUM intrusions are coeval (and therefore cogenetic) to the KC. This section (section 2.2) provides details about the geology of some of the MUM intrusions located at the southwestern margin of the KC, which have been studied in this project.

2.2.1 Oncócua Intrusion

The Oncócua intrusion is situated a few kilometres south of Oncócua village in the municipality of Curoca, in the Cunene Province, which is one of the southernmost provinces of Angola (Fig. 2). The Oncócua intrusion is approximately 9 km long and it strikes NW-SE at the southwestern margin of the Angolan KC. The main lithologies of the intrusion comprise medium to coarse-grained apatite-bearing pyroxenite with dominant clinopyroxene (up to 80 vol%), minor plagioclase and Fe-rich olivine in places (Maier et al., 2013; Selfe, 2003; Vale's report, pers. comm.) (Fig. 4). Other

lithologies in the intrusion include gabbro, anorthosite, and red granite. The gabbro (including leucogabbro and olivine gabbro variants) is predominantly present along the western side of the intrusion while anorthosites are on the eastern side – and may share affinities with the KC anorthosite suite. Troctolites are also present, and they mainly intruded into the anorthosite, as well as close to the contact of the gabbro and anorthosite (Fig. 4). Magnetite is associated with the anorthosite where troctolite is more predominant than gabbro. Gossans are mainly present at the contact of gabbro and anorthosite and, to a lesser extent, in the gabbro itself, and are rare in the anorthosite. The red granites are in contact with the anorthosite in the north and again in the south where they are in contact with the anorthosite plus gabbro.

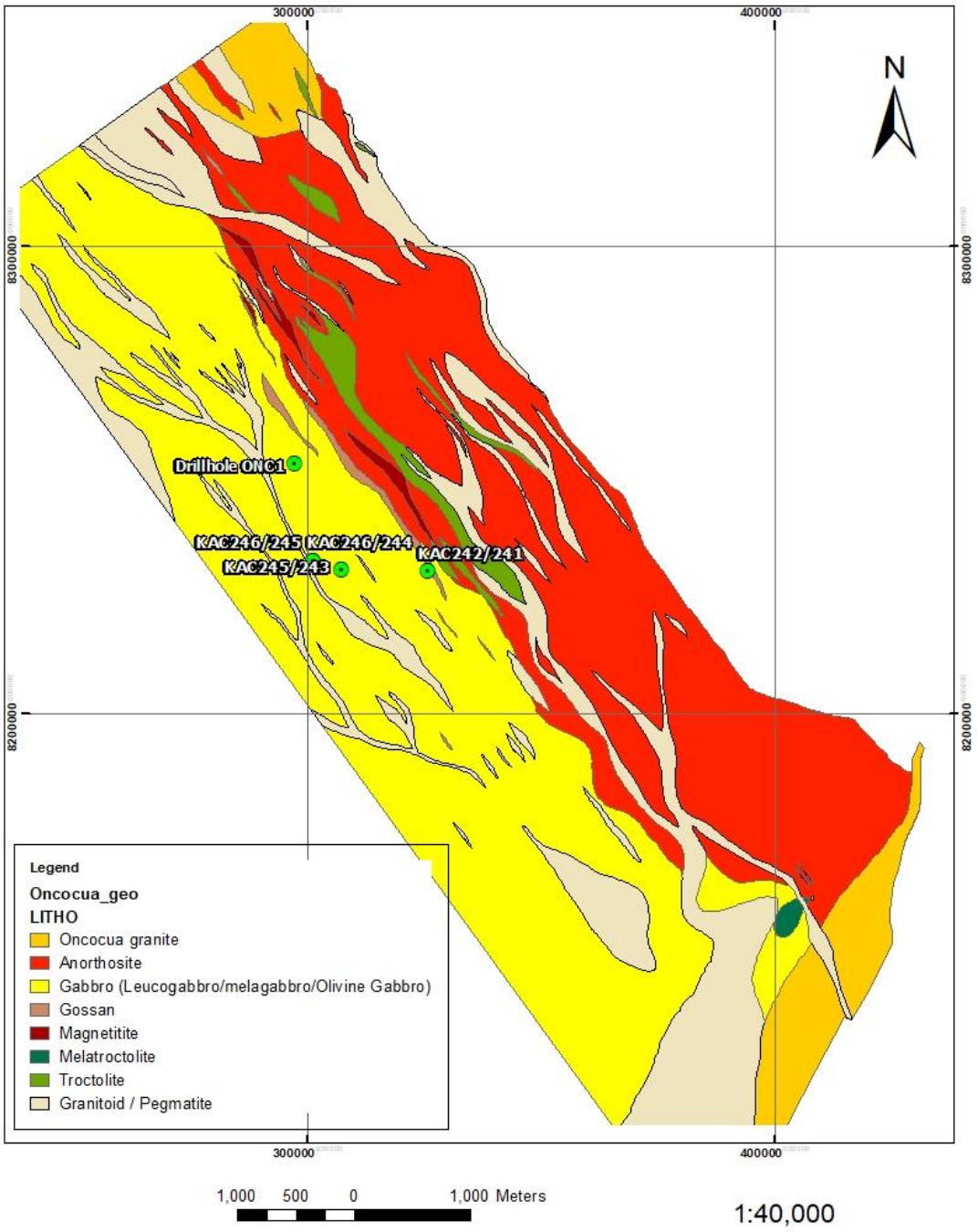


Figure 4: A geological map of the Oncócua Intrusion showing the main lithologies and sample locations (VALE report, pers comm).

The Oncócua intrusion intruded the Palaeoproterozoic Regional Granite and the Palaeoproterozoic (pre-Eburnean) Schist-Quartzite-Amphibolite-Marble Complex (SQAMC) unit in the western and southwestern parts of the intrusion (Colin Nash's report, pers. comm.; Silva, 1990; Ferreira et al., 2024) (Fig. 2, Table 1). Age dating on apatite in gabbros of the Oncócua intrusion has given an age range of ~1400 -1300 Ma which may indicate that the intrusion is coeval with the KC (van Zyl, 2022). Unpublished age dates of zircon from surface hand samples of the Oncócua intrusion collected near the contact with the SQAMC give a large age range of ~1400 - 2100 Ma (Hayes, pers comm). Such a large age range may mean that Oncócua is Palaeoproterozoic in age and has been reset to younger ages or Oncócua is the same age as the KC, but it has undergone significant inheritance of old zircon from the adjacent basement rocks. This is yet to be resolved at the time of submission of this thesis (Hayes pers. comm.) and has implications for the age correction of some of the radiogenic isotope data presented here.

Oncócua was drilled by Anglo-American in the 1990s and Vale in 2009 (Smuts, 1997; Selfe, 2003; Vale report, pers. comm.). According to Smuts (1997) and Selfe (2003), Anglo-American drilled a total of 13 drill holes with a total combined depth of 2553 m to test magnetic, and soil geochemistry anomalies and gossans. The drill holes were oriented NW-SE along strike and were collared in anorthosite, troctolite, norite and granite gneiss lithologies. The hole ONC1 (Fig. 4) intersected a 4.25 m thick zone of mineralisation with 35 modal % disseminated sulphide in norite and a 6.0 m thick zone of mineralisation with 45 modal % disseminated sulphide which also contained local 30 cm thick intercalated bands of massive sulphide. ONC1 gave the best Ni-Cu grades of 0.32% Ni and 0.41% Cu over 1.26 m in the mineralised zones. The sulphide phases are dominantly pyrrhotite and minor chalcopyrite (Smuts, 1998; Selfie, 2003). According to the Vale report (pers. comm.), Vale drilled a total of 5 holes with a total combined depth of 1459 m. The drill holes were oriented NE-SW along strike and were collared in anorthosite, gabbro and troctolite. Drill holes DH01 and DH02 gave the best grades of 0.12% Ni and 0.27% Cu over 2.90 m within leopard-textured sulphide hosted

in troctolitic unit, and 0.12% Ni and 0.22% Cu over 12.50 m with massive sulphide associated within the troctolitic unit. The sulphide assemblage consisted of pyrrhotite (48-84 %), chalcopyrite (2-7 %), pentlandite (2-2.5%), magnetite (2-27%) and ilmenite (1-20%).

2.2.2 Ohamaremba Intrusion

The Ohamaremba intrusion is located 2 km south of the Zebra Lobe (Fig. 2), and it is approximately 10 km long and strikes E-W and is in contact with the Epupa Metamorphic Complex (EMC: Fig. 5, Table 1). The intrusion comprises mostly medium-grained troctolites (with an average of 50 vol% olivine and 50 vol% plagioclase, with locally up to 75 vol% olivine) as well as less abundant fine-grained melatroctolites, anorthosite and olivine gabbronorite (Fig. 5). The Ohamaremba intrusion is spatially related to amphibolite and granulite gneisses of the Orue and Epembe units of the EMC (Brandt et al., 2007; Drüppel et al., 2007) (Table 1). The contact between the intrusion and the EMC is suggested to be tectonic which makes it difficult to interpret the original shape of the intrusion although some reports suggest a dyke-like shape (Maier et al., 2013).

Maier et al. (2013) published a baddeleyite age of 1220 ± 15 Ma for Ohamaremba which is significantly younger than the ages of the adjacent KC anorthosite suite published by the same workers (1363 ± 17 Ma) and reported by Drüppel et al. (2007) (1385 ± 25 Ma). Zircon grains had been extracted from Ohamaremba samples and yielded ages ranging between 1400 and 1800 Ma (van Zyl, 2022). This presents a similar problem to Oncócua in terms of interpreting the age data (Hayes, pers comm).

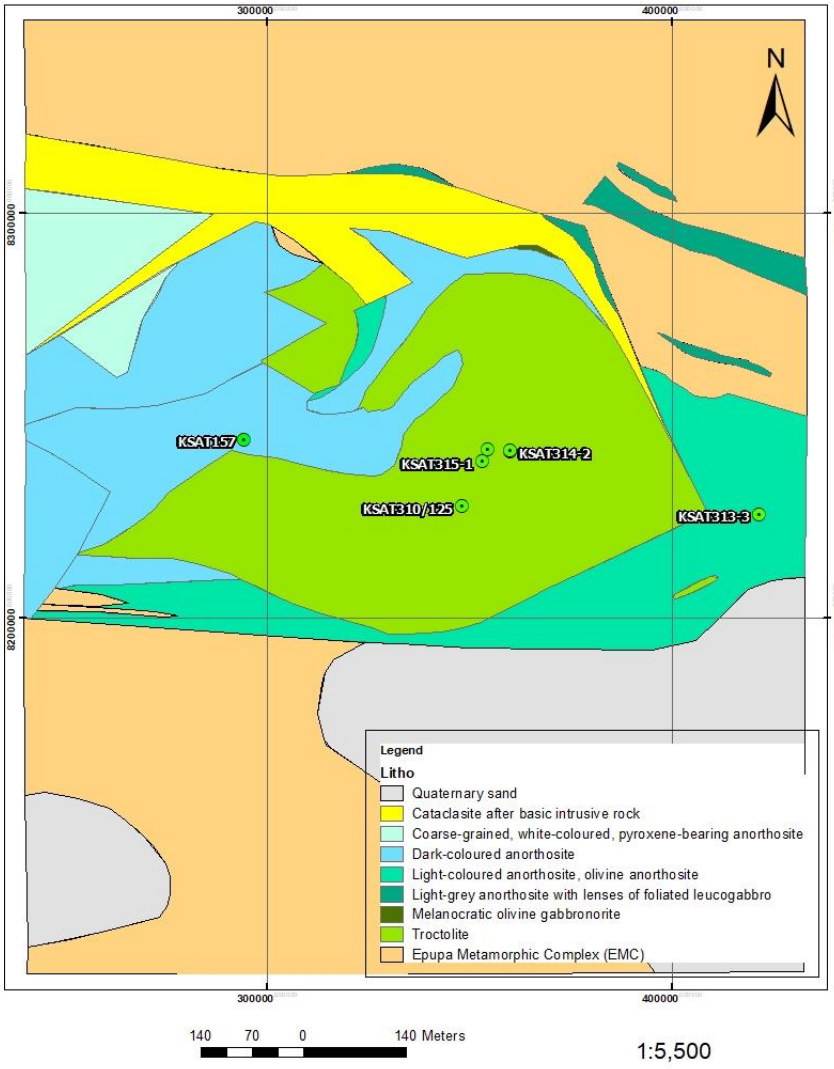


Figure 5: A geological map of the Ohamaremba intrusion showing the major lithologies and sample locations (Naumov, 2008).

Olivine in troctolite from drillcore samples at Ohamaremba shows compositions of Fo_{68-74} with low NiO contents (0.053-0.132 wt%) but with no clear trend between olivine Fo composition and depth (Maier et al., 2008). There are reports that a drilling program was conducted at Ohamaremba in 2000 that consisted of 14 drill holes (4 diamond cores and 10 reverse circulations) with a total combined depth of 2924 m drilled (Freyer, 2004). The drilling program was based on encouraging results from geophysical and soil geochemistry surveys. The diamond drill holes were collared in

anorthosite, leucotroctolite, troctolite and melatroctolite. The sulphide mineralisation was mainly associated with troctolites. HRDD03 contained the best mineralised intersection with grades of 0.14% Ni and 0.11% Cu over 24 m in a total drill hole depth of 325 m.

2.2.3 Otjijanjasemo Intrusion

A previous study referred to Otjijanjasemo and Okanguati interchangeably (Maier et al., 2013). In this study, we refer to it as the Otjijanjasemo intrusion in reference to the closest township of the same name and for consistency with van Zyl (2022) as the Okanguati (also referred as Okongwati) is located farther NE to the intrusion studied here (Fig. 6). The Otjijanjasemo intrusion is a troctolitic body located approximately 11 km from the southwest margin of the Zebra Lobe and it strikes 6 km W-E and is 1 km wide. The predominant basement rocks to the Otjijanjasemo intrusion are granitic gneisses of the EMC (Table 1). Kröner et al. (2010) described the basement samples collected in the Otjijanjasemo area as comprising granite gneiss, coarse-grained granitic augen-gneiss, and aplite veins.

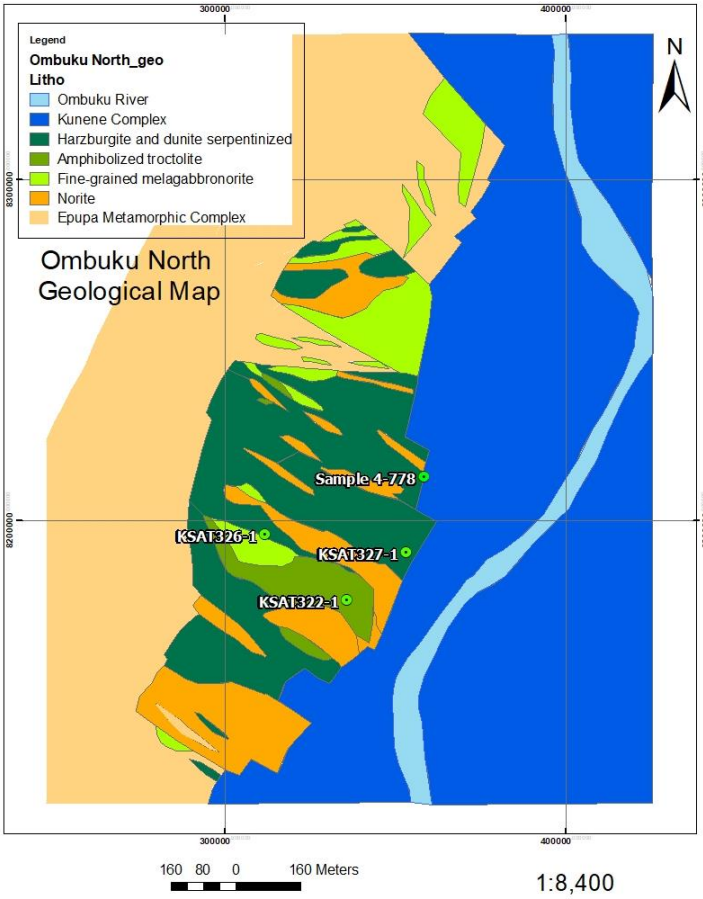
Otjijanjasemo consists of similar lithologies to Ohamaremba with troctolite as the dominant lithology, along with gabbro and norite (Maier et al., 2013). Olivine mineral compositional data reported by Maier et al. (2013) are also similar to Ohamaremba but with relatively narrow variabilities in olivine Fo (68-71) and NiO (0.0827-0.125 wt%) contents. Age dating of two zircons from an Otjijanjasemo troctolite gave an age of 1762 Ma (van Zyl, 2022). However, van Zyl (2022) suggested that these zircon grains were inherited from the EMC basement as they showed oscillatory zoning cores with bright recrystallisation rims and thus they do not give a reliable crystallisation age for the intrusion.



Figure 6: Google Earth satellite image of the Otjijanjasemo intrusion showing the outcrop samples collected by the Kunene Team and past Otjijanjasemo drillholes.

2.2.4 Ombuku North & South Intrusions

The Ombuku intrusions (North & South) are located less than 250 m from the western margin of Zebra Lobe anorthosite suite (Freyer, 2004) (Fig. 2). Ombuku North and Ombuku South strike NE-SW and are approximately 2.5 km and 8 km long, respectively. Both intrusions comprise mainly olivine-magnetite fine-grained gabbronorite, olivine norite, massive fine- to coarse-grained troctolite, fine-grained and porphyritic harzburgites and fine-grained dunite, pyroxenite, layered gabbroic rocks, feldspathic harzburgite (Fig. 7). Ombuku North mostly comprises altered ultramafic rocks in which some are present at the contact with gneissic country rocks of the EMC (Maier et al., 2013) and Ombuku South is more mafic in composition. The geology around the Ombuku intrusions includes the KC anorthosite suite with leucotroctolites to the east and felsic and mafic orthogneiss of the EMC (with locally disseminated sulphide) to the west (Fig. 6). There are some magnetite-bearing quartzites and iron-banded metasedimentary rocks to the north of Ombuku North. Amphibole-granites of the EMC completely host Ombuku South (Maier *et al.,* 2013) (Table 1).


Legend
Ombuku North_geo
Litho
Ombuku River
Kunene Complex
Harzburgite and dunite serpentinized
Amphibolized troctolite
Fine-grained melagabbronorite
Norite
Epupa Metamorphic Complex
Ombuku North
Geological Map
N
300000
400000
8300000
8200000
Sample 4-778
KSAT326-1
KSAT327-1
KSAT322-1
160 80 0 160 Meters
1:8,400

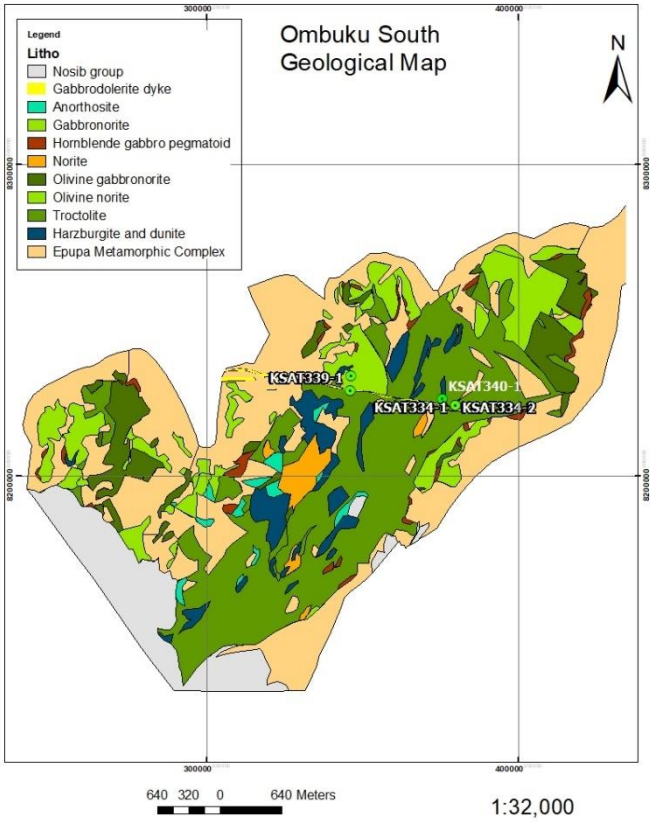


Figure 7: Geological maps of the Ombuku intrusions. Ombuku North (top) and Ombuku South bottom) showing the major lithologies and their sample locations (Naumov, 2008).

van Zyl (2022) reports in-situ age dating of two zircons of a dunite from a sample of Ombuku North which gave a U-Pb zircon age of 1356 Ma, suggesting a very late-stage emplacement of the Ombuku North intrusion relative to KC magmatism. Further geochronological data for Ombuku South range from 1800 to 1400 Ma based on U-Pb dating of zircon from a diorite sample (Hayes, pers. comm.). This is similar to the results produced for Oncócua and Ohamaremba. Maier et al. (2013) report on two drill holes (KNBD001 and KNBD002) at Ombuku North that were conducted by African Nickel Limited in 2008. The drill holes intersected a zone of disseminated sulphide enriched in Ni and PGE in harzburgite and pyroxenite. KNBD002 intersected a 4.2 m wide vein of semi-massive sulphide with grades of 0.53% Ni and 0.72 g/t PGE + Au.

2.2.5 Other Peripheral MUM Intrusions of the KC

Hamutenha is one of the MUM intrusions that was not initially included in this study and a summary based on a recent publication by Campeny et al. (2023) is highlighted here. Hamutenha is the northernmost MUM intrusion in this study area (Fig. 2). The intrusion is 3 km long and is located approximately 10–15 km away from the northwestern Angolan KC in Huile Province. The intrusion consists of a northern unit of dunite intercalated with olivine gabbro and a southern unit of amphibole diorite hosted in the granitoids of the EMC (Table 1). The dunite comprises subhedral fractured cumulus olivine. The olivine gabbros comprise subhedral, cumulus olivine and interstitial augite. The amphibole diorites comprise mainly plagioclase with subhedral hornblende, with clinochlore alteration, and accessory quartz and magnetite. The olivine grains in the dunite and olivine gabbro have Fo molar percentages ranging $Fo_{81\text{-}84}$ and 1728.86–2671.87 ppm Ni. Campeny et al. (2023) suggest that crustal contamination was minimal based on positive ε_{Nd} values at ~1.8 Ga (5.44 to 6.65) and trace element ratios (Nb/Th and Th/Yb). They also suggested that there was no segregation of immiscible sulphide liquid. Like the other peripheral MUM intrusions, the intrusion was spatially associated to the KC, however, a well constrained U-Pb zircon date from an amphibole diorite yielded an age of 1844 ± 14 Ma suggesting Hamutenha is part of the Palaeoproterozoic basement (Campeny et al., 2023). Campeny et al. (2023) also highlights the presence of minor disseminated sulphides reported as secondary sulphides, mainly associated with magnetite and ilmenite.

Onyokohe is another intrusive body that was not initially part of this study. The intrusion is 6 km long striking NE-SW located south of the Zebra Mountains and approximately 6 km north of Ombuku North (van Zyl, 2022; Oosthuizen, 2023) (Fig. 2). The area is characterised by a system of cross-cuting faults (Oosthuizen, 2023). The intrusion is divided into structural parts in which one part is represented by two mafic-ultramafic intrusions in the north-western and southern parts, and the other part comprise a central linear zone of cataclased and migmatised rocks also referred as the Onyokohe Fault (van Zyl, 2022). The intrusion shows a variety of lithologies and

comprises norite, troctolite, harzburgite, fine- to medium-grained magnetic, melanocratic, thin-banded and foliated olivine gabbronorite and minor pyroxenite (van Zyl, 2022; Oosthuizen, 2023). The intrusion has faulted boundaries with the KC that is hosted in migmatitic gneisses of the EMC (Table 1). Sulphides consist mostly of finely disseminated blebs and locally semi-massive to massive pyrrhotite and pyrite with rare chalcopyrite (van Zyl, 2022).

2.3 Nain Plutonic Suite and Voisey's Bay/Other Intrusions

The Nain Plutonic Suite (NPS) in northern Labrador (eastern Canada) has an areal extent of 19,000 km² and comprises anorthosite *senso stricto*, granitoid, charnockite and mangerite, and is collectively regarded as an AMCG complex (Emslie et al., 1994) (Fig.1). The anorthosite suite of the NPS is typical of Proterozoic massif-type anorthosites although the molar An contents of plagioclase are moderately high and range between An_{65-70} (Scoates and Mitchell, 2000). The magmatism responsible for the NPS lasted from 1363 to 1289 Ma with the magmas emplaced along an old collisional boundary striking N-S between a Palaeoproterozoic province in the west and an Archean province in the east (Myers et al., 2001) (Fig. 8).

The NPS also hosts many MUM intrusions including the Voisey's Bay Intrusion (VBI) which is well known for its world-class magmatic Ni-sulphide deposit (Ryan, 2000). The VBI is located in the central part of the NPS in northern Labrador (Fig. 8). The VBI has a volumetric size of 10 km^3, and the intrusion overlaps the Palaeoproterozoic province and the Archean province in a E-W sinistral strike-slip fault zone (Lightfoot and Evans-Lamswood, 2015; Saumur and Cruden, 2016) (Fig. 8). It is composed of olivine gabbro, troctolite, ferrodiorite, ferrogabbro and it has basal breccias (Lightfoot and Naldrett, 1999). The troctolite and the olivine gabbro contain 5–11 wt% MgO and high HILE (highly incompatible lithophile elements: Th-Nb-Ta-LREE) relative to MILE (moderately incompatible lithophile elements: Zr-Hf-Ti-MREE-Y). The mineral chemistry of the normal troctolite (medium-grained uniform texture troctolite) and varied-textured troctolite (blotchy sulphides and variable amounts of gneissic inclusions and discrete intercumulus minerals) shows plagioclase compositions that

range from An_{40} in normal troctolite to An_{67} in varied-textured troctolite (Sappin et al., 2021; Li et al., 2000; Li and Naldrett, 1999). The VBI has initial isotopic compositions (at 1.32 Ga) which suggest a mantle-like magma source with minor contamination with slightly negative ε_{Nd_T} values that range from –1 to –2, and initial $^{87}Sr/^{86}Sr$ values that range from 0.7034 to 0.7038 (Amelin et al., 2000). The intrusion has S/Se ratios ranging from 3482-7083 and $\delta^{34}S$ of -1.52 (Queffurus and Barnes, 2015). These are values departing from mantle-like values and suggest that the magma had some interaction with crustal sulphur-source component as it ascended to the upper levels of the crust to the deposition site (mantle values: S/Se = 2850-4350 and $\delta^{34}S = 0 \pm 2‰$) (Rai and Thiemens, 2007; Labidi et al., 2014; Queffurus and Barnes, 2015). Olivine mineral chemistry of the feeder gabbro (similar to olivine gabbro but contains relatively more intercumulus minerals), basal breccia and normal troctolite have a large range of Fo_{42-83} (Sappin et al., 2021; Li and Naldrett, 1999). The VBI has a U-Pb baddeleyite age (for the troctolite and gabbro) of 1332.7±1 Ma which is interpreted as the age of emplacement (Amelin et al., 1999) making it one of the oldest MUM intrusions in the NPS (Ryan, 2000). The magmatic Ni-sulphide deposit in the VBI was discovered in 1993 and by 1996 a resource of 124.4 million tonnes had been defined with grades of 1.66 wt% Ni, 0.88 wt% Cu and 0.09 wt% Co (Lightfoot and Naldrett, 1999). The deposit is associated with troctolitic rocks of the VBI (Lightfoot and Naldrett, 1999).

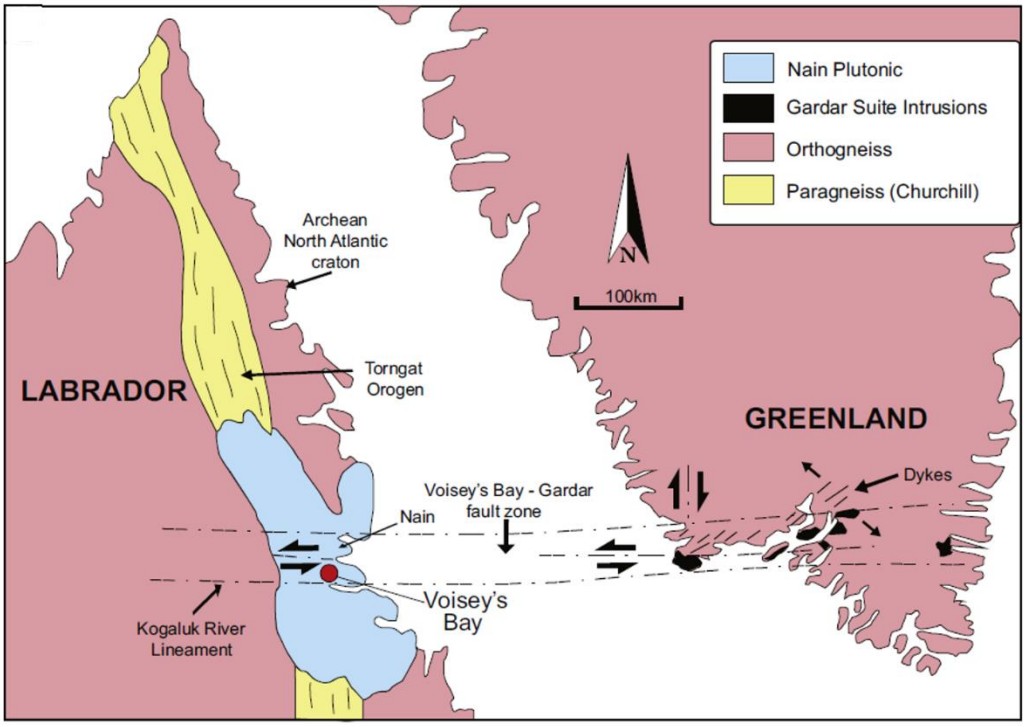


Figure 8: Regional structural map highlighting the Nain Plutonic Suite location associated with trans-lithospheric structural controls. The location of Voisey's Bay is also shown (Lightfoot and Ivans-Lamswood, 2015).

2.3.1 Nain Plutonic Suite and Voisey's Bay

The NPS, as previously mentioned, is a Proterozoic massif-type anorthosite with an age constrained between 1363 Ma and 1289 Ma (Saumur and Cruden, 2000; Myers et al., 2008) (Fig. 1). The NPS is located on the 50 km wide Voisey's Bay-Gardar fault zone that extends 1000 km east-to-west from Greenland to Labrador where it intersects an old continental suture (Saumur et al., 2015) (Fig. 8). The NPS 'stitches' the 1.85 Ga collisional boundary that separates the Palaeoproterozoic Churchill Province Tasiuyak paragneiss and Enderbitic orthogneiss in the west from the Archean Nain Province orthogneiss at the western margin of the North Atlantic Craton in the east (Li et al., 2000; Lightfoot & Evans-Lamswood, 2015; Saumur et al., 2015) (Figs. 8). The Torngat orogen occurred between 1.87 and 1.85 Ga because of the collision of the Archean province with the Palaeoproterozoic province (Saumur et al., 2015) (Fig. 8). There is geological evidence to support subduction between 1.91 and 1.89 Ga around the time

the Tasiuyak sediments were deposited, particularly in the northern part of the Torngat orogen, approximately 400 km north of the VBI where the Churchill province subducted easterly under the Nain province. It is difficult to resolve if this either continues or if there was westerly subduction of the Nain province under the Churchill province about 100 km north of the VBI (Saumur et al., 2015). The collisional event produced crustal thickening resulting in a 1.85 Ga collisional suture, a phase of sinistral transpression between 1.84 to 1.82 Ga along the collisional suture that formed the Abloviak shear zone (10-15 km wide mylonite) in the Tasiuyak gneiss. Subsequently, the uplifting of the Churchill province segment of the orogen resulted in brittle faulting between 1.79 and 1.71 Ga (Saumur et al., 2015).

The NPS contains several large anorthosite (*senso stricto*) intrusions with plagioclase compositions of An_{65-70} (Scoates and Mitchell, 2000; Ashwal, 1993), as well as granites, ferrodiorites, and a volumetrically small suite of troctolites and gabbros (Li et al., 2000) (Fig. 9). The granite bodies are mostly exposed in the western parts of the NPS and less so in the eastern parts. The erosional history suggests that the granitoid rocks, which once formed a sheath above and around the anorthositic and mafic rocks, underwent erosion to remove the granitic roof. This resulted in exposing some anorthositic rocks in the west, while the eastern portion was affected by an intense erosional process that resulted in large exposure of the anorthosite (Kerr and Smith, 2000). The Tasiuyak gneiss in the west consists of interbanded garnet-sillimanite and is sulphide- and graphite-bearing feldspathic paragneiss (Fig. 9), whereas the 1.89-1.88 Ga Enderbitic orthogneiss located in the central part is a pyroxene-bearing and biotite-rich dioritic orthogneiss, both collectively referred to as the Palaeoproterozoic Churchill province (Fig. 9) (Li and Naldrett, 1999; Lightfoot and Naldrett, 1999). In the east, the Archean Nain orthogneiss consists of well-banded quartzofeldspathic and mafic orthogneisses (2.84 Ma) (Li et al., 2000; Saumur et al., 2015) (Fig. 9). Field and petrographical work done by Xue and Morse (1993) on different intrusions in the NPS showed that there are spatially dichotomous lithologies (troctolitic and noritic suites) divided by the so-called N-S olivine-boundary. The authors suggested that the

dichotomy is a result of the crystallisation of the early olivine phase in some intrusions for the troctolitic suite (also referred 'dark facies'), and pyroxene crystallisation without the early olivine phase in others for the noritic suite (also referred as 'pale facies') possibly related to different proportions of crustal contamination during magmatism.

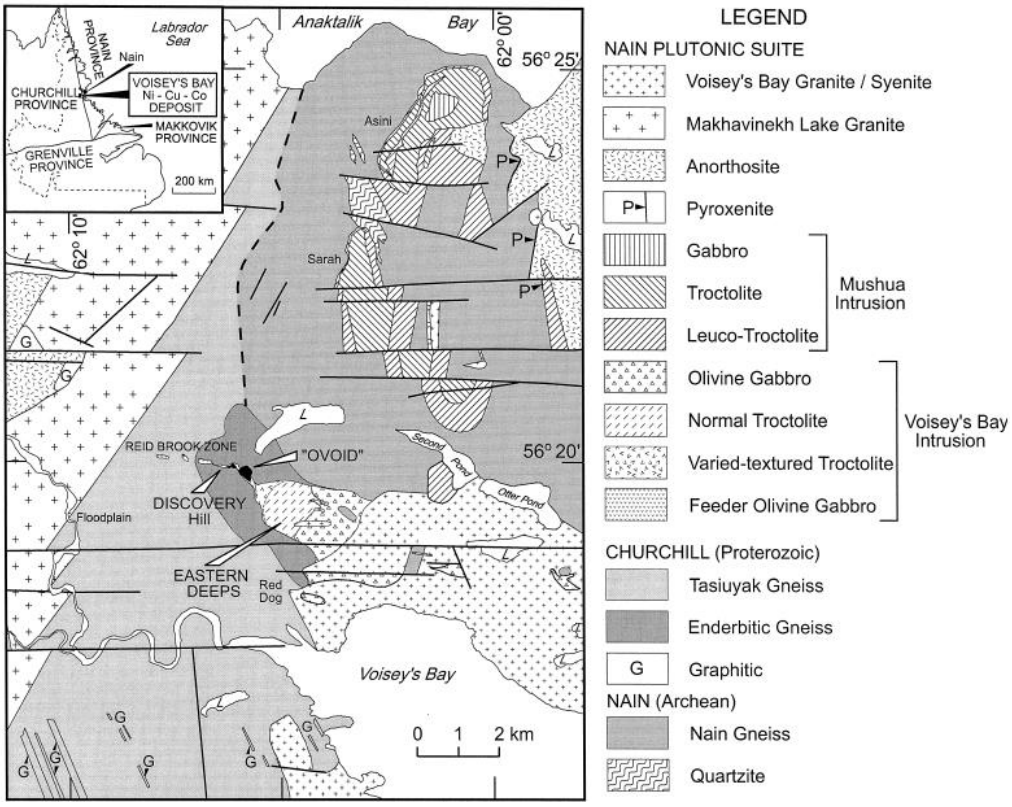


Figure 9: Geological map of the Nain Plutonic Suite (NPS) showing Voisey's Bay and the Mushuau intrusions as well as the surrounding basement rocks (Li and Naldrett, 1999).

The NPS hosts several MUM intrusions, one of which hosts the world-class Voisey's Bay Ni-Cu-(Co-PGE) magmatic sulphide deposit (VBI) (Fig. 9). The VBI is currently the only known mineralised Ni-Cu-PGE sulphide MUM intrusion that is associated with a Proterozoic AMCG Complex. As previously highlighted above, the NPS shows similarities to the Kunene AMCG Complex and, therefore, it is critical to provide a thorough understanding of the geological, petrological and geochemical characteristics

of the VBI to assess the presence of similar ore-forming processes in the peripheral MUM intrusions of the KC.

The VBI is approximately 7 km long and about 10 km³ in volume and strikes E-W close to the central part of the NPS (Li et al, 2000; Lightfoot and Evans-Lamswood, 2015; Sappin et al, 2021) (Fig. 9). The VBI has an age of 1.33 Ga (Amelin et al., 1999) and was emplaced in the central part of the NPS, where it transgresses the 1.85 Ga suture between the Palaeoproterozoic Churchill Province and the Archean Nain Province (Figs. 8, 9). The intrusion consists of the mineralised lower Reid Brook chamber on the western end and the upper Eastern Deeps chamber on the eastern end that are connected by feeder dyke-like conduits (Fig. 10). Along the feeder dykes are dilated portions of mineralised zones that include, from the west to the east, the Discovery Hill, Mini-Ovoid and Ovoid ore deposits (Amelin et al., 2000; Lightfoot et al., 2012) (Fig. 10). The intrusion crops out at the Discovery Hill and Eastern Deep chamber and extends sub-vertically to the west where it is cut by Rapaviki-textured granite (Lightfoot and Naldrett, 1999; Ryan, 2000).

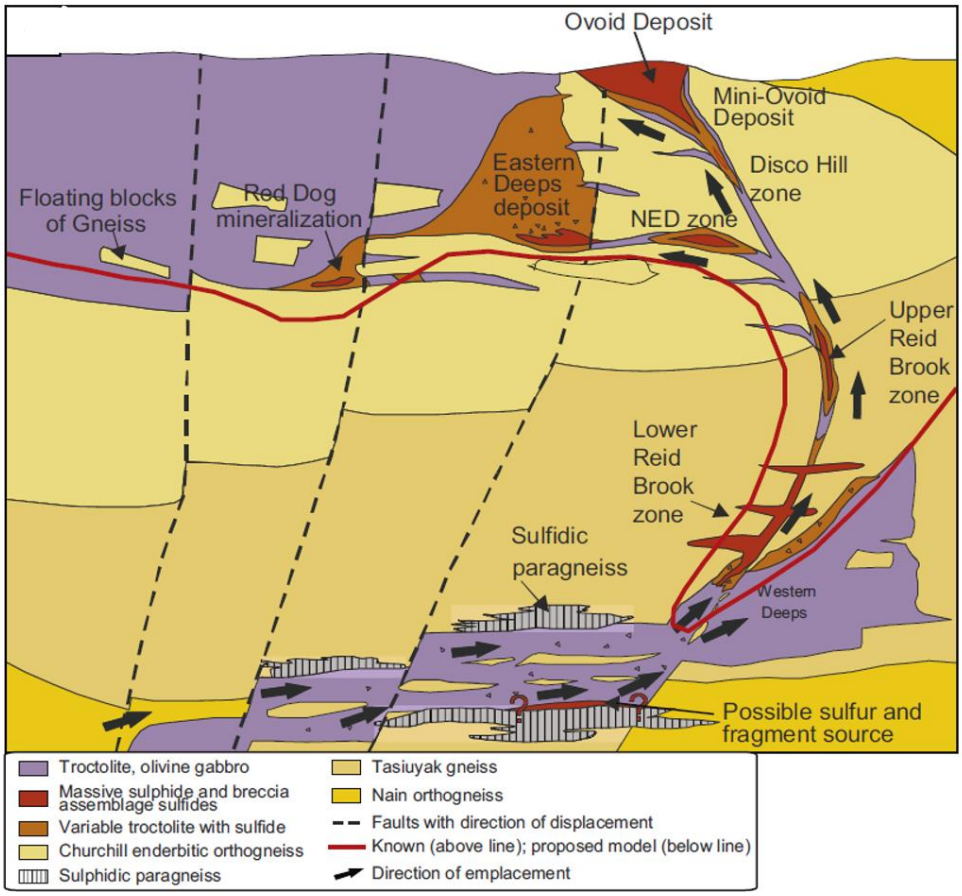


Figure 10: Genetic model of the Voisey's Bay deposit looking-west section and showing the mineralised zones and loci for magma interaction with basement rocks (Lightfoot and Ivans-Lamswood, 2015).

The petrography of the rocks at VBI are described by Li et al. (2000), and to a lesser extent, by Lightfoot and Naldrett (1999). The lithologies comprise the following (Fig. 9, 10): basal breccia sequence hosts minor ultramafic, olivine gabbro fragments and abundant gneissic inclusions; varied-textured troctolite shows pegmatitic to medium-grained texture and variable contents of disseminated sulphide, inclusions of gneiss with overgrowths of hypersthene and intercumulus biotite; leopard troctolite has black spots olivine oikocrysts or augite enclosing plagioclase and olivine in a yellowish interstitial matrix of sulphides and is referred to as variable troctolite when < 25% sulphide is present; normal troctolite shows a uniformly medium-grained texture and consists of cumulus olivine and plagioclase with plagioclase enclosing olivine and

vice-versa, along with reaction rims of granular hypersthene around olivine grains that in turn is surrounded by biotite + plagioclase and fine-granular hypersthene; feeder olivine gabbro is a weakly mineralised zone with small amount of cumulus plagioclase and olivine within the upper part of conduit; olivine gabbro contains more cumulus plagioclase and olivine in the upper part of the Eastern Deeps relative to the feeder olivine gabbro; and ferrogabbro and ferrodiorite are typically unmineralised chilled margins (Li and Naldrett, 1999; Li et al, 2000; Lightfoot, 2007, Lightfoot and Evans-Lamswood, 2015; Sappin et al., 2021) (Fig. 10). The spatially dichotomous olivine-line in the NPS reported by Xue and Morse (1993) positions the VBI in the noritic suite, close to the southernmost boundary of the olivine-line. The position of the VBI intrusion is fortuitous as it enabled the sulphide-bearing paragneissic crust to play an important role in the development of sulphide mineralisation as is discussed in the next section (Naldrett, 2010; Saumur & Cruden, 2016; Barnes et al., 2017) (Fig. 9, 10). Most of the VBI is hosted in paragneiss and enderbitic orthogneiss of the Churchill province in the west (Lightfoot and Ivan-Lamswood, 2015). The VBI ore deposit is hosted in feeder dyke networks and two chambers (the Reid Brook lower chamber and the Eastern Deeps upper chamber) (Fig. 10). The feeder dykes delivered magma into two-layered troctolite-gabbronorite chambers. The lower Reid Brook chamber, hosted by the paragneiss of the Churchill province, received the initial influx of magma that underwent cooling, differentiation and segregated immiscible sulphides resulting in depleted chalcophile metals in the residual melt. Subsequent chalcophile-undepleted influxes of fresh magma entered the chamber through the same conduit system and these increased the metal tenor of the pre-existing sulphides, which were then remobilised (along with the cumulates) and carried up to the Eastern Deeps upper chamber through feeder dykes where they were deposited (Lightfoot, 2007). The mineralisation in the feeder dykes and the two chambers consists of massive sulphides, leopard-textured sulphides, basal breccia sequence sulphides and disseminated sulphides in vari-textured troctolites (Lightfoot & Naldrett, 1999; Naldrett et al., 2000) (Fig. 10).

Lightfoot et al. (2012) reports on the different compositions of the VBI ore zones and highlights they are the result of variation in parental magma compositions and R-factor regimes. For instance, the sulphides of the Ovoid have a higher metal tenor than the sulphides in the dykes and Eastern Deeps ore zones and it is attributed to segregation of sulphides from a more primitive magma of the Ovoid. In contrast, the relative low metal tenors of the dyke-hosted sulphides are attributed to lesser amounts of silicate magma being available to upgrade the metal concentration of the sulphides (Lightfoot et al., 2012) (Fig. 10). The Eastern Deeps sulphides have intermediate metal tenors relative to the Ovoid and dyke-hosted sulphides. The intermediate metal tenor in the Eastern Deeps sulphides is suggested to be the result of a relatively higher R-factor produced by more silicate magma available to upgrade the sulphides. In addition, the Ovoid orebody fractionated from sulphide melt that resulted in the residual melt becoming increasingly enriched in Cu and PGE (Platinum Group Elements). These melts formed small pods of exsolved pentlandite and chalcopyrite from the monosulphide solution (MSS) in which Pd preferentially followed the Ni into pentlandite. The Ir and Rh would be distributed in different sulphide phases (Lightfoot et al., 2012).

2.3.2 Ore-forming Processes in the Voisey's Bay Intrusion (VBI)

The ore-forming processes in the VBI have been well-characterised by multiple authors using a combination of field observations, petrological information and geochemical data (e.g., Naldrett, 1999, 2010; Li et al., 2000; Lightfoot, 2007; Barnes et al., 2016). Broadly, the ore-forming process can be summarised in 7 steps (after Naldrett, 2010): (1) Partial melting of the mantle to produce a komatiitic-basalt to basaltic magma; (2) A translithospheric fault zone (e.g., a suture-collisional boundary) that facilitates magma ascent from the mantle to the crust as well as an environment that is conducive to magma mixing and crustal contamination; (3) Interaction between the magma and S-bearing basement rocks (e.g., the sulphide-bearing Palaeoproterozoic Churchill-Tasiuyak paragneiss in the vicinity of the VBI) as external sulphur addition in this way

may lead to sulphur saturation and the formation of immiscible sulphide liquids; (4) The magma and the entrained immiscible sulphide liquids ascend to upper levels in the crust; (5) The immiscible sulphides are concentrated during magma flow into a hydraulic trap (e.g., dilatational zones or the entry point of the magma conduit); (6) Successive influxes of fresh magma flow through the same conduit system, upgrading the metal tenors of the pre-existing sulphides (i.e., high R-factor: a high ratio of silicate melt to sulphide liquid); (7) finally, the magma, and the upgraded sulphides, are cooled and crystallised to form the ore deposit.

Past workers have suggested that mafic-ultramafic intrusions hosting magmatic sulphide ores are associated with high-temperature parent magmas that have the potential to crystallise a high proportion of olivine (Naldrett, 1999; Barnes et al., 2016; Barnes, 2023). The source of the parent magma has implications for the compositions of ore-forming silicate magmas, and the Ni contents of olivine has been used as a petrogenetic indicator of mantle magma sources of mafic-ultramafic intrusions associated with magmatic sulphides (Barnes et al, 2023; Barnes, 2023; Barnes et al, 2016; Lightfoot and Naldrett, 1999). Mantle sources have a high potential to crystallise olivine that is generally elevated in Ni content. Olivine is crystallised from the magma as early phase with Ni preferentially partitioning into the olivine. However, Ni partitioning is also controlled by the Fo content of the olivine, and whether the magma has become depleted in chalcophile elements (Naldrett, 1999). Mantle-derived magmas are usually associated with higher MgO and thus hotter than normal ambient mantle melting products. According to Sappin et al. (2021), the VBI rock types contained 5–11 wt% MgO, 0.6–3.9 wt% TiO_2 and 31–46 wt% SiO2 and likely derived from a parent magma that contained approximately 8 wt% MgO (i.e., a tholeiitic basalt). Olivine in the normal troctolite (and ultramafic fragments in the varied-textured troctolite and basal breccia and melatroctolite horizon within the normal troctolite) has compositions of Fo_{83} and olivine in the feeder gabbro and basal breccia is significantly more Fe-rich with compositions of Fo_{42} and suggest wide variability in Fo compositions (Sappin et al., 2021; Bulle and Layne, 2015; Li and Naldrett, 1999). Clinopyroxene in the varied-

textured troctolites has compositions of $Mg\#_{72-84}$ and clinopyroxene in the olivine gabbros has compositions of $Mg\#_{76-79}$ (Sappin et al., 2021). Naldrett (1999) reported a moderate olivine Fo content for the feeder olivine gabbro and Eastern Deeps olivine gabbro of Fo_{50-65}. Barnes et al. (2016) reported that the olivine with compositions of Fo_{70-80} in the VBI crystallised from a parent magma with less than 6 wt% MgO content (and 250–300 ppm Ni) suggesting that the parent magma was of a basaltic composition. The VBI is one of the larger world-class magmatic Ni-sulphide deposits with the least forsteritic olivine (with a lower limit of $<Fo_{50}$: Barnes, 2023). This questions the principle that magmatic Ni-sulphide ores are associated with rocks of high-MgO content that were fractionated from high-temperature magmas. High-temperature magmas, however, are better able to promote crustal assimilation, which may be an important factor in producing immiscible sulphide liquids (Barnes, 2023).

The structural controls on magma emplacement define the intrusion geometry and deposition of solid phases from the magma. Most magmatic Ni-sulphide deposits are associated with structures, either within or adjacent to them (Lightfoot and Evans-Lamswood, 2015; Barnes et al., 2016). The VBI was tectonically controlled by the western portion of the W-E translithospheric-scale Gardar-Voisey's Bay fault zone with a sinistral strike-slip displacement located at the margin of the North Atlantic Craton (Lightfoot and Evan-Lamswood, 2015) (Fig. 8). The intrusion straddles the N-S suture-collisional boundary along the Churchill province to the west and the Nain province to the east (Figs. 8, 9). The fault structures are mostly contained within the N-S dimension of the corridor (Lightfoot and Evans-Lamswood, 2015). This fault zone is associated with the NPS and the VBI (Lightfoot and Evans-Lamswood, 2015). The importance of magma ascent to the crust is twofold: (i) it allows the parent magma to escape from the mantle to the surface, and (ii) it promotes magma mixing and crustal contamination in long-lived transcrustal conduit systems, which are critical for the formation of magmatic Ni-sulphide deposits (Barnes et al., 2016). Therefore, the presence of translithospheric structures provides the long-lived transport pathway for the basaltic mantle-derived magmas from the mantle to the crust.

The interaction of mantle-derived basaltic magma with S-bearing basement rock is regarded as a critical process for sulphur saturation and for the segregation of immiscible sulphide liquids in some magmatic nickel sulphide deposits (e.g., Naldrett, 2010; Barnes et al. 2016). For the formation of the VBI ore deposit, there is field, petrological, and geochemical evidence that indicates that the Tasiuyak paragneiss promoted sulphur saturation in the VBI magmas (Li et al., 2000; Mariga et al., 2006) (Fig. 10). The lower Reid Brook chamber in the west is hosted by the Tasiuyak paragneiss which comprises sillimanite-garnet, sulphide-, and graphite-bearing quartzite feldspathic paragneiss (Lightfoot and Evans-Lamswood, 2015) (Fig. 10). The magma in this chamber interacted with this S-bearing basement rock, and the magma was transported to the upper chamber in the east via a dyke-like conduit (Fig. 10). Petrological studies of the mineralised VBI basal breccias also showed that there were Tasiuyak paragneiss xenoliths and xenocrysts in the breccias (Lightfoot and Naldrett, 1999; Li et al, 2000; Mariga et al, 2006; Lightfoot and Evans-Lamswood, 2015) (Fig. 10). Moreover, sulphur isotopes and trace element ratios (e.g., Th/Nb and La/Sm) for the VBI show trends towards the Tasiuyak paragneiss (Smith, 2006; Li et al., 2000). The presence of Tasiuyak paragneiss xenoliths and their trace element ratio signatures associated with mineralised lithologies is critical evidence that assimilation of crustal sulphur from the basement rocks played an important role in the ore-forming event (Lightfoot and Evans-Lamswood, 2012).

The magma and entrained immiscible liquid sulphide then ascended to the upper crust and was emplaced into a hydraulic trap. In this open conduit system, the immiscible sulphides were concentrated and further upgraded by fresh chalcophile-undepleted magmas (Barnes et al., 2016). Ore formation in mafic magmatic systems like the VBI takes place during magma transport along the vertical and horizontal transport networks and as a result, mafic systems are subjected to gravitational and thermal potential energy. Gravitation potential energy drives the deposition of the dense sulphide liquid into dilatational zones and the entry points of the magma conduit (Fig. 10). At the same time, mafic magma exploited the existing fractures and created other

fractures by thermal stress on the wallrock while ascending to the upper crust which resulted in conduit widening during the incorporation of country rock into the magma (Barnes et al, 2016). The evidence of a dynamic open conduit system in the VBI includes the fragments of country rock in the basal breccia sequences and variable-textured contaminated mafic rocks at the contact with the country rock (Fig. 10). This indicates that there was significant magma flow in a relatively long-lived magmatic system which facilitated metal tenor upgrading of the sulphides by fresh magmas in the same conduit system (Barnes et al, 2016).

2.3.3 Other Mafic-Ultramafic Intrusions

There are other mafic-ultramafic intrusions in the NPS and other plutonic complexes that are unmineralized. They were also studied during the literature review, so that the magmatic processes of the unmineralised intrusions could be characterised. This allows for a better understanding of which processes are critical in the formation of nickel sulphide mineralisation in the VBI, and in the NPS as a whole. Other mafic-ultramafic intrusions that have been investigated include the Mushuau intrusion (MI) in the northeastern part of the NPS and the intrusions in the Harp Lake Intrusive Suite (HLIS) located south of the NPS.

The MI is in the central part of the NPS, like the VBI. It is located approximately 4 km north of the VBI and is 10 km long, striking in a N-S direction (Fig. 9). The intrusion has an emplacement age of 1.313 Ga and is therefore about 20 Myr younger than the VBI. The MI lithologies comprise mainly fine to medium-grained cumulate melatroctolite at the margin with modal layering and fine lamination, fine to medium-grain leucotroctolite towards its middle, a core of olivine gabbro with equigranular to mottled fabrics and massive troctolite with localised pegmatoidal units that intruded and brecciated the melatroctolite (Li et al., 2000) (Fig. 9). The intrusion hosts only minor amounts of sulphide mineralisation and failed to become an economic deposit. The disseminated blebby sulphide mineralisation is mainly associated with troctolites at the basal contact. This is cut by centimetre-wide massive sulphide veins and locally centimetre-wide leopard texture sulphides similar to those found in the VBI (Li et al.,

2000). The MI was emplaced almost entirely on the eastern side of the ~1.85 Ga boundary between the Churchill and Nain provinces and, therefore, it is hosted by the Archean-aged Nain province basement rocks (Li et al., 2000). Fragments of gneiss were also observed in the troctolite. Although there are fragments of paragneiss in the variable troctolites, Th/Nb and La/Sm systematics and Nd-Pb-Sr isotopes suggest that the MI parent magmas interacted with the Nain Province which is consistent with the spatial location of the intrusion. Like the VBI, the MI has relatively low MgO contents (<8.5 wt%). However, the MI cumulates are more olivine-enriched with higher MgO contents relative to the VBI. Melatroctolite is a predominant lithology in the MI, whereas melatroctolite is found as fragments in the basal breccia of the VBI, interpreted as disrupted early cumulus layers in the conduit system. This lithology has lower olivine Fo compositions in the MI (Fo_{70}) compared with the fragments of similar rock in basal breccia in VBI (Fo_{81}) (Li et al., 2000) with Sappin et al. (2021) and Bulle and Layne (2015) reporting olivine Fo compositions as low as Fo_{42}. Olivine Fo compositions in the MI are also less Ni-depleted relative to the VBI (Li et al., 2000). In general, several ore-forming processes appear to have been absent in the MI, resulting in subeconomical sulphide mineralisation. The MI is younger than the VBI and it has been suggested, by some, that the older intrusions are better prospects for ore deposits because they more readily interact with crustal material along the channelized conduit system (Li et al., 2000; Barnes et al, 2016). Younger magma injections using the same structural pathways may not interact with the crust because the conduits are coated by solidified basaltic material from earlier pulses, shielding subsequent magma pulses from crustal interaction. Furthermore, the MI was emplaced in the sulphur barren orthogneiss, and shows minimal trace element and isotopic evidence of interaction with its basement, which is unfavourable for sulphur saturation. MI olivines are also not depleted in Ni, which suggests the magma did not equilibrate with a sulphide liquid. Therefore, the available evidence suggests that the MI failed to produce an economic deposit on the scale of the VBI.

The HLIS is a Proterozoic massif type anorthosite located approximately 20 km south of the NPS, and it covers an area of about 10,000 km^2 (Ashwal, 1993; Kerr and Smith, 2000; Smith, 2006). The HLIS has an emplacement age of 1.45 Ga and is about 100 Myr older than the NPS, (Kerr and Smith, 2000). However, they intruded the same basement rocks (Fig. 11). The HLIS has an almost elliptical geometry, and it hosts predominantly anorthosite *senso lato* (80% proportion) that includes anorthosite (plagioclase molar % of An_{49-59}: Ashwal, 1993) and outer rings of leucotroctolitic and leucogabbroic rocks, granitoids as marginal discrete bodies around the main anorthosite, and late minor mafic rocks (include marginal gabbroic rocks) (Fig. 11). Small mafic intrusions are also present and comprise gabbro and troctolite in different locations within the main anorthosite (Fig. 11). Generally, sulphide mineralisation in most of the intrusions is associated with the leucotroctolitic and anorthositic rocks (Kerr and Smith, 2000). There are major differences between the HLIS and the NPS in terms of their geological setting. For instance, the HLIS contains less granitoid and these are mainly found around the margins of the main anorthosite relative to the NPS. There is a continuous outer ring of gabbroic rocks in the HLIS. There is the absence of layered troctolitic intrusions in the HLIS and there is abundant olivine-anorthosite and leucotroctolite in the HLIS relative to the NPS. Finally, the HLIS is a more deeply eroded plutonic suite relative to the NPS which would suggest that prospective mafic rocks possibly exist at depth as deep-penetrative geophysics techniques had not been used at the time of the publication by Kerr and Smith (2000).

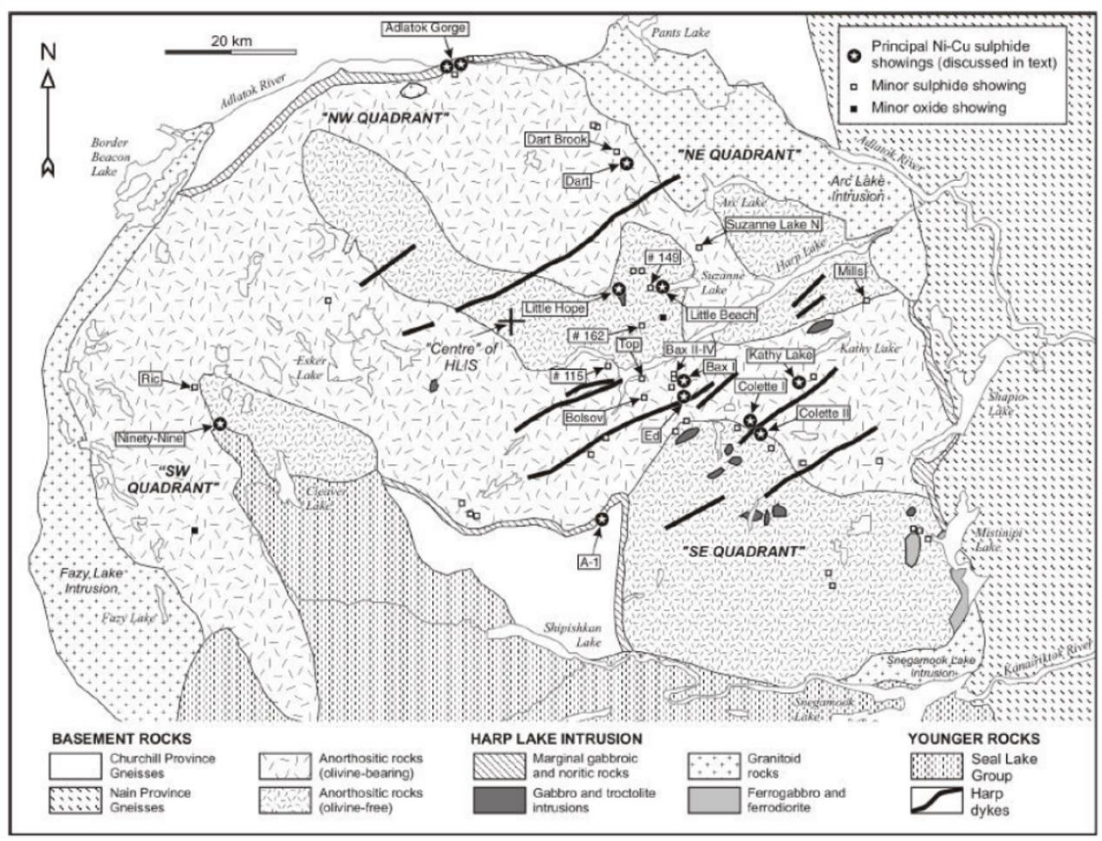


Figure 11: Geological map of the Harp Lake Intrusive Suite showing the several intrusions and associated sulphide mineral occurrences (Kerr and Smith, 2000).

Like the NPS, the HLIS straddles the Churchill-Nain province suture. According to Ryan (1996), Tasiuyak paragneiss is absent in the HLIS area. Although the search for magmatic Ni sulphides in the mafic intrusions of the HLIS started in the 1970s, no significant mineralisation discovery has been made to date. After the discovery of the VBI deposit, mineral exploration continued in the HLIS, but only disseminated and interstitial sulphides (with local semi-massive sulphides, but with low metal tenor) are the most common sulphide mineralisation (main pyrrhotite and chalcopyrite) hosted mainly in leucotroctolites and anorthosites and to a lesser extent in gabbroic and troctolitic units (Kerr and Smith, 2000; Smith, 2006). The geochemistry of the HLIS suggests that the most mafic rocks were not fractionated from primary mantle-derived melts, and they are likely to represent cumulates fractionated from residual basaltic liquids. Plagioclase accumulated to form the leucotroctolite, leuconorite and

anorthosite with olivine and orthopyroxene forming late, interstitially to the plagioclase. Olivine has moderate forsterite compositions (Fo_{59-68}) and low Ni contents (16–59 ppm Ni) (Kerr and Smith, 2000). The disseminated sulphide mineralisation is syngenetic to the host rocks and possibly formed from the same late residual liquid that was trapped (Kerr and Smith, 2000; Smith, 2006). The syngenetic disseminated sulphide is the most common style of mineralisation in the mafic intrusions of the HLIS and it is hosted mainly in leucotroctolite and anorthosite. The syngenetic disseminated sulphide has high metal contents (up to 6.5% Ni and up to 3.15% Cu) but expresses an absolute low grade because of the low total sulphide contents (<5%). This style of mineralisation only represents <1% of the mineralisation in NPS and is associated with mafic veins and gabbronoritic segregations. These rocks or equivalent mafic rocks with the same style of mineralisation and range of metal contents have not been found in the HLIS. This suggests that these rocks resemble the original silicate magmas from which the sulphides separated. Kerr and Smith (2000) explain that gravity and fluid dynamics were not efficient in this style of mineralisation in the HLIS partly because of the high concentrations of plagioclase (i.e., too mushy). This created an unconducive magmatic environment to concentrate enough of the sulphide liquids to become economical because of the lack of effective separation of enough sulphide liquids from the cumulates. The small available sulphide liquid was able to interact with the interstitial Ni- and Cu-rich residual liquid trapped in the cumulate rocks to form the disseminated mineralisation that is present. The other, and less common, style of mineralisation in the HLIS is semi-massive to massive sulphide that postdates the crystallisation of the host rocks, but it is the most common in the NPS. However, the metal contents of this type of sulphide are low (<0.5% Ni and up to 5.3% Cu) in the HLIS. Kerr and Smith (2000) associated this style of mineralisation with the anorthosite and likely represents the fractionation and dispersal of the sulphide liquid. This is the result of late-stage sulphur saturation after the crystallisation of the mafic silicate phases (olivine and pyroxene) which removed substantial Ni leaving a Ni-Cu poor residual liquid in equilibrium with the sulphide liquid.

The most common style of mineralisation in the HLIS is different from the VBI-style of mineralisation. Most of the mineralisation is hosted in plagioclase-dominated lithologies (leucotroctolite and olivine-bearing anorthosite) in which Ni contents for a given Fo contents are very low, whereas in the VBI, the mineralisation is hosted in olivine-dominated lithologies (troctolites). The intrusions in the HLIS host mostly syngenetic disseminated sulphide mineralisation with high Ni and Cu contents as a result of a late-stage fractional crystallisation of mafic phases (olivine and pyroxene) postdating cumulus plagioclase. The crystallisation of plagioclase cumulates produced metal-rich interstitial residual liquid which crystallised sulphide prior to the crystallisation of the mafic silicate phases.

Chapter 3: Methods

A series of methods were used to collect the data presented in this study. They include (i) fieldwork and sampling of the peripheral mafic-ultramafic (MUM) intrusions of the KC to understand the field relationships, (ii) petrography on thin sections to understand the mineral assemblages and textural relationships, (iii) bulk rock major oxide and trace element data to compare the geochemistry of the MUM intrusions to the anorthosite suite and to the basement rocks to draw insights into their petrogenesis, (iv) microprobe analyses of olivine and pyroxene grains in selected samples to determine the molar Fo and Ni compositions of the olivine and quantify any chemical zonation in pyroxene and/or plagioclase that can be used to trace ore-forming processes (explained below), (v) bulk rock Sr-Nd radiogenic isotopes to determine any evidence of crustal contamination and the nature of the magma sources for the MUM intrusions, and (vi) S isotope analyses of the MUM intrusions (and basement rocks) to determine if their magmas interacted with S-bearing crustal reservoirs. The data produced will allow a study of the ore-forming processes present in the MUM intrusions in the KC which can be compared with Voisey's Bay.

3.1 Sampling and Fieldwork

No fieldwork was directly conducted in this MSc project, partly due to the difficulties in arranging access to Angola for fieldwork during the Covid-19 global pandemic. However, a large database of existing field samples and observations, as well as old detailed exploration reports, were available for this study. Samples of the MUM intrusions were selected (Table 2) from the existing KC rock database which contains a total of 517 samples (503 samples are in Table III.1 in Appendix III), collected between 2015 and 2021. In addition, five drillcore samples (3 for Oncócua, 1 Ombuku North and 1 for Ohamaremba) were obtained from a collaboration with the University of Pretoria (UP) and were used for petrographical observations and microprobe analysis.

Table 2: List of samples used in this study along with summary of the data collected for each sample in this MSc.

Sample ID	Intrusion	Sample Type	Thin Section	Petrography	Major Oxides	CIPW Norm	Trace Elements	Mineral Chemistry	Sr-Nd Isotopes	Sulphur Isotopes
KSAT306/123	Ohamaremba	Field			x	X	x			
KSAT306-1	Ohamaremba	Field	X	X	x	X	x	x		
KSAT308/124	Ohamaremba	Field			x	X	x			x
KSAT310/125	Ohamaremba	Field	X		x	X	x		x	x
KSAT313-1	Ohamaremba	Field	X		x	X	x			
KSAT313-2	Ohamaremba	Field	X		x	X	x			
KSAT313-3	Ohamaremba	Field	x		x	X	x		x	x
KSAT314-1	Ohamaremba	Field	x		x	X	x			
KSAT314-2	Ohamaremba	Field	x		x	X	x			
KSAT315-1	Ohamaremba	Field	x		x	X	x			x
KSAT 157	Ohamaremba	Drillcore	x	X				x		
KSAT301/118	Otjijanjasemo	Field	x	X	x	X	x	x		
KSAT301/119	Otjijanjasemo	Field			x	X	x			
KSAT303/120	Otjijanjasemo	Field			x	X	x			
KSAT305/122	Otjijanjasemo	Field	X	X	x	X	x	X	x	x
KSAT333-1	Ombuku South	Field	X		x	X	x			
KSAT333-2	Ombuku South	Field	X		x	X	x			
KSAT334-1	Ombuku South	Field	X		x	X	x			
KSAT334-2	Ombuku South	Field	X		x	X	x			
KSAT338-1	Ombuku South	Field	X		x	X	x		x	x
KSAT339-1	Ombuku South	Field	X		x	X	x			
KSAT340-1	Ombuku South	Field			x	X	x			
KSAT322-1	Ombuku North	Field	X	X	x	X	x	x		
KSAT326-1	Ombuku North	Field	X	X	x	X	x		x	x
KSAT327-1	Ombuku North	Field	X	X	x	X	x			x
4-778	Ombuku North	Drillcore	X					x		
KSAT330-1	Onyokohe	Field	X		x	X	x			
KAC241/240	Oncócua	Field			x	X	x			
KAC242/241	Oncócua	Field			x	X	x		x	x
KAC245/243	Oncócua	Field			x	X	x		x	x
KAC246/244	Oncócua	Field			x	X	x		x	x
KAC246/245	Oncócua	Field			x	X	x			
ONC-1-35	Oncócua	Drillcore	X	X				x		
ONC-1-55	Oncócua	Drillcore	X	X				x		
ONC-1-59	Oncócua	Drillcore	X	X				x		
KSAT049/032	Hamutenha	Field			x	X	x		X	x
KSAT051/033	Hamutenha	Field			x	X	x			
KSAT052/034	Hamutenha	Field			x	X	x			

During previous field campaigns by researchers at Wits, UJ and UP, the field relationships of the MUM intrusions were described and samples collected. This reservoir of information was used and a summary of the key findings are presented in section 4.1. The samples were carefully prepared (cutting, washing, thin sectioning and pulverisation) in the School of Geosciences at the University of the Witwatersrand. From this collection, samples were selected for petrographical study (25 samples), major and trace element whole rock analysis (517 samples), electron probe microanalysis (10 samples), radiogenic isotope analysis (28 samples) and stable isotope

analysis (20 samples). A suite of the same MUM samples was also sent to the Pacific Centre of Isotope and Geochemical Research (PCIGR) at the University of British Columbia for age dating at the beginning of this MSc project. The intention here was for precise age dates to be determined for the MUM intrusions early on during this MSc study so that a mineral system model could be better developed. However, as of the time of the writing and submission of this thesis, we are still waiting for a full suite of age data for the MUM intrusions. This limits some of the interpretations that can be made in this study, as elaborated on in the discussion chapter.

3.2 Petrography

Petrographical observations using transmitted and reflected light microscopy were completed on 25 thin sections. The thin sections were studied using an Olympus BX-41 microscope in the WIMLab at the School of Geosciences at the University of the Witwatersrand. Each polished thin section was 30 mm thick. The aim here was to describe the textural relationships and mineral assemblages of the rocks to allow classification of the intrusions and elucidate any evidence of magma replenishment – an important part of the ore-forming process (see section 4.2). Point counting was also done on thin section photomicrographs to determine modal abundances for formal rock classification. Photomicrographs were collected of representative textures for report purposes (shown in section 4.2).

3.3 Bulk Rock Major and Trace Element Database

The entire KC rock database (517 samples in total) was sent to Bureau Veritas Mineral Laboratories in British Columbia (Canada) where samples were analysed for major, trace element and platinum group elements. The sample pulps were dried at 105 ºC prior to the digestion methods. Different digestion methods and analytical determinations were used. $LiBO_2/LiB_4O_7$ fusion was used to digest 0.2 g aliquot of each pulp sample and ICP-OES was used for the major oxides (in weight %) and the minor elements (in ppm), and ICP-MS was used for the trace elements (concentrations in ppm). The 0.5 g aliquot of each pulp sample was digested in a 4-acid solution with the base metal contents (in weight %) determined by ICP-OES. Aqua regia digestion

was used to determine “ultra-trace elements” in which 30 g aliquot was digested and the content (in ppm or ppb) determined by ICP-MS. Au, Pt and Pd were measured by fire assay fusion on a 30 g aliquot of each pulp sample and the concentration (in ppb) was determined by ICP-MS. Carbon and sulphur were determined by total Leco furnace on 0.1 g aliquot while the loss of ignition (LOI) was determined on a 1 g aliquot, all in weight %. For data processing, it is important to highlight that the analytical values below the lower detection limits (<LOD) were multiplied by ½ LOD. The quality assurance and quality control (QAQC) of the data were also assessed by plotting MgO, Ni and Nd data (Table IV.1 and Fig. IV.1 in Appendix IV). The LOD was 0.01 wt% for MgO, 10 ppm for Ni and 0.3 ppm for Nd. The 30 blank samples generally passed QAQC, except for Nd, in which 7% of the samples failed (2 samples in total) (Fig. IV.1 A-C). The duplicates inserted in the sample batches by the analytical lab passed QAQC within ± 10% MPD (Mean Percentage Difference) (Fig. IV.1 D, E). However, the Nd plot also shows that some samples did not pass, particularly those approaching the LOD. As the data approach the LOD, the ability of the method to determine measurements with precision is reduced and the data start to spread out to give a ‘peacock-like tail’ feature. OREAS30A was used by the analytical lab as the Certified Reference Material (CRM) with an expected MgO value of 4.69 ± 0.091 wt% (Fig. IV.1 F). The CRM plot shows that while most samples passed at 2 x standard deviation (Std), some samples only passed at 3 x Std.

3.4 Electron Probe Microanalysis

Silicate phases in 10 thin sections were analysed using a Cameca SX-100 Electron Probe Microanalyser (EPMA) at Spectrau at the University of Johannesburg. EPMA is an analytical technique that allows for the non-destructive quantification of chemical compositions (major and minor elements as oxides) of rock-forming minerals. The primary aim here was to determine the molar Fo (forsterite) and nickel compositions in olivine to track melt evolution and sulphide paragenesis in the MUM intrusions. An additional objective of this method was to determine Cr_2O_3 zonation (rim-core-rim) in clinopyroxene and orthopyroxene. The thin sections were carbon coated (25 nm thick) before the analyses. Glass_Ni1 was the method file used and the calibration was done

by using LLIF crystals as the standard to calibrate for NiO, FeO, MnO and Cr_2O_3 which were analysed in spectrometer 3 (Fig. I.1 in Appendix I). Calibration for MgO was done using TAP crystal and analysed in spectrometer 2. Other crystals were also analysed for K_2O, CaO, TiO_2, Na_2O, Al_2O_3 and SiO_2 in spectrometers (1, 2 and 4). The data on the standard showed little variation range throughout the analysis on most of the oxides with Cr_3O_2, NiO and MnO ranging < 2 wt%. FeO showed the widest variation range up to 34 wt%. Each analysis had a duration of ~3 minutes with the column conditions of 20 kV accelerating potential, 20 nA current and spot size of 1 µm. The results are in section 4.2.

3.5 Radiogenic (Sr-Nd) Isotope Analyses

A total of 28 samples were processed in four sets (batches) for Sr-Nd isotope analyses in the School of Geosciences at Wits. The main aim was to further understand what interaction with the crust these magmas may have had and to distinguish possible contaminants (e.g., Amelin et al., 2000). Samples were digested with a combination of Nitric acid and Hydrofluoric acid. The separation/extraction of the isotopes was done with Fe-resin chromatography columns with 1.5 M HCl for Sr and Rb, and with 6 M HCl for the LREE to be used for the separation/extraction of Nd and Sm done with Ln-Spac resin chromatography columns with 0.2 M HCl and 0.4 M HCl, respectively. All processes of separation/extraction were done at the state-of-the-art ultraclean lab facility at Wits. Sr and Nd were loaded into degassed zone refined Re filaments in which 1 µL 0.5N HNO_3 and 1 µL 0.5N TaF5 activator were used for Sr and 1 µL 0.5N HNO_3 and 1 µL 1N H_3PO_4 activator were used for Nd between two Parafilm strips. The sample filaments were heated slowly to 2400-3000 mA for Sr filament and 1400-1800 mA for Nd to obtain stable signals. A blank ionizer filament was also heated to 4200-4400 mA for Nd. Sr and Nd isotopic compositions were determined using a Thermal Ionisation Mass Spectrometer (NuTIMS) analytical instrument at Wits. This instrument has 16 fixed Faraday detectors and a zoom lens system capable of alignment of isotopes into adjacent collectors. The isotope ratios were collected in 3-line dynamic measurements with time drift corrections. Faraday detectors were connected to

amplifiers with 10^{11} Ω resistors during the isotope analyses. Using the normal $^{87}Rb/^{85}Rb$ ratio of 0.3857, the ^{85}Rb signal was used to correct for the isobaric interference of ^{87}Rb on ^{87}Sr. For Sr isotope measurements, a $^{86}Sr/^{88}Sr$ value of 0.1194 was used to account for the instrumental mass fractionation while for Nd, a $^{146}Nd/^{144}Nd$ ratio of 0.7219 was used to account for the instrumental mass fractionation. For Rb and Sm, the Rb and Sm were in 5 mL 2% HNO_3 and analysed using an Apex desolvating nebuliser with conditions such as coolant Ar flow at 18L/min, auxiliary Ar flow at 0.9–1.2 L/min. In addition, the nebulizer has of Ar flow 1.15–1.2 L/min and apex with Ar flow 3.81–3.89 L/min for Rb and nebuliser Ar pressure 31.9 psi, apex with Ar flow 4.1–4.2 L/min for Sm. The Rb and Sm isotopes were determined using a NuSapphire MC-ICP-MS at Wits. This instrument is also equipped with 16 fixed Faraday detectors connected to amplifiers with 10^{11} Ω resistors, and a zoom lens system. The ratios were collected during static measurements of 50 cycles. With sample-standard bracketing, the mass fractionation of a natural Rb solution was corrected using the standard $^{87}Rb/^{85}Rb$ ratio of 0.38571, while the mass fractionation was corrected using a $^{147}Sm/^{154}Sm$ ratio of 0.65918. QAQC data show that the SRM987 Reference Material has an average measured $^{87}Sr/^{86}Sr$ value isotope value of 0.710251 ± 0.00014 based on 29 repeats from August 2022 to February 2023, compared to the accepted value of 0.710340 ± 0.00052 (at 2 x Standard Error). QAQC data show that the JNdi Reference Material has an average measured $^{143}Nd/^{144}Nd$ isotope value of 0.512092 ± 0.000042 based on 18 repeats from October 2022 to May 2023, compared to the accepted value of 0.512099 ± 0.00001 (at 2 x Standard Error) (Fig. III.2 in Appendix III). Three standards (BHVO2, BCR2 and TPB2) were also inserted in the batches. The collected data, so far, only include BHVO2 as the majority of the remaining data is pending analysis. Measurement of BHVO2 returned values for $^{87}Sr/^{86}Sr$ of 0.703584 ± 0.000082 and for $^{143}Nd/^{144}Nd$ of 0.5129633 ± 0.000005 and are generally within the range of accepted values reported by Fuenlabrada (2023) (Table III.1). The data gathered by Fuenlabrada (2023) on BHVO2 between 2015 and July 2023 yielded an average Sr isotopic ratio of 0.703485 ± 0.000024 from 88 replica analyses and an

average Nd isotopic ratio of 0.512978 ± 0.000012 from 62 replica analyses. The results are in section 4.4.

3.6 Sulphur Isotope Analyses

Twenty samples were analysed for $\delta^{34}S$ in collaboration with the Jan Veizer Stable Isotope Laboratory at the University of Ottawa, Canada. The primary aim was to use sulphur isotope ratios to detect evidence of assimilation of possible sulphur-bearing basement rock sources. The samples were first submitted for sulphur concentration (%S) determination by using Elementar Isotope Cube which is a method capable of analyzing concentrations down to 0.01% by combustion. The analytical precision is ±0.2% (2 standard deviation). Based on the %S concentration, a minimum weight of 50µg of S was targeted and about 1mg was added to the tin capsule (8x11 mm Sn). 150mg sulphur-free WO_3 additive was added to bind the alkalis (Na, Ca, and K) to prevent oxide formation that may interfere with the combustion zone. The samples were then loaded into the Elemental Analyser (EA) Isotope Cube in S mode (Elementar) to be flash combusted at 1800 ºC. Ultra-pure He was used to carry the released gas through the EA where water was chemically removed and the SO_2 was separated from CO_2 and N_2 by a trap and purge column. The SO_2 analyte was carried into the Thermo Finnigan DeltaPlus XP IRMS via a Conflo IV for the analytical determination of $\delta^{34}S$ in each sample at an analytical precision of ±0.3 ‰ and the data were standardised to Vienna-Canon Diablo Troilite (VCDT). S-6 (an argentite) was the in-house standard inserted in the batch while two pulp duplicates of the routine samples were inserted also for QAQC. Three measurements of the S-6 standard returned an average $\delta^{34}S$ value of -1 ± 0.2‰. At 2std, the range varied between -1.4 and -0.6‰ and the current expected value for the S-6 is -0.7‰. For the two duplicates, one sample passed at ± 10% MPD (Fig. II.1 in Appendix II). The $\delta^{34}S$ results are presented in section 4.3.

Chapter 4: Results

4.1 Fieldwork

Fieldwork was done by the Kunene Team between 2015 and 2021. For detailed field relationship descriptions of the KC anorthosite suite and basement rocks, see the recent publications by Bybee et al. (2019) and Lehmann et al. (2020). Field observations at the Oncócua, Ohamaremba, and Ombuku North show that they comprise massive outcrops of coarse-grained and orthopyroxene-rich mafic-ultramafic lithologies (Figs 12A-M). Troctolite with wehrlite bands and plagioclase-rich and plagioclase-poor zonation is observed at Ombuku North (Fig. 12A). An orthopyroxene-rich outcrop is observed with autoliths (or xenoliths) of coarse-grained orthopyroxenite at Oncócua (Fig. 12B). Massive outcrops of feldspathic pyroxenite show coarse-grained upper parts and brecciated margins, and plagioclase- with fine-scale layering, and anorthosite veins crosscutting blocks of gabbro that seem to interact with the interstitial plagioclase in the pyroxenite at Oncócua (Figs 12C & E). Massive olivine anorthosite is observed at Ohamaremba (Fig. 12D). Oncócua gabbroic-gabbronoritic lithologies are crosscut by leuconoritic-anorthositic dykes/veins with some gabbroic-gabbronoritic outcrops hosting rounded blocks of finer-grained mafic rocks (dolerite and/or basalt) while others show coarse plagioclase crystals in the gabbroic matrix (Figs. 12G-H). Magmatic layering of leucogabbro and troctolite is observed in the drillcore of Oncócua (Fig. 12I). There are calc-silicate xenolith in the western parts of Oncócua near its contact with the Regional Granite basement (Fig. 12F). Minor phases include phlogopite associated with pyroxenitic, troctolitic, gabbroic and anorthositic lithologies while magnetite is usually associated with the boundaries of olivine grains and interstices in troctolite as well as gabbroic rocks observed in the drillcores of Oncócua (Figs. 12J-K). Mineralisation includes mainly disseminated blebs of sulphide that locally grade into net-textured (some leopard textured) and semi-massive sulphides of pyrrhotite, and minor chalcopyrite and pyrite are observed in the Oncócua drillcores (Figs. 12J-K). Leucotroctolite is observed with feldspathic veins in different locations,

and are parallel to each other as well as the magnetite-bearing layered leucotroctolite with pyroxenitic veins in Ohamaremba (Figs. 12L-M).

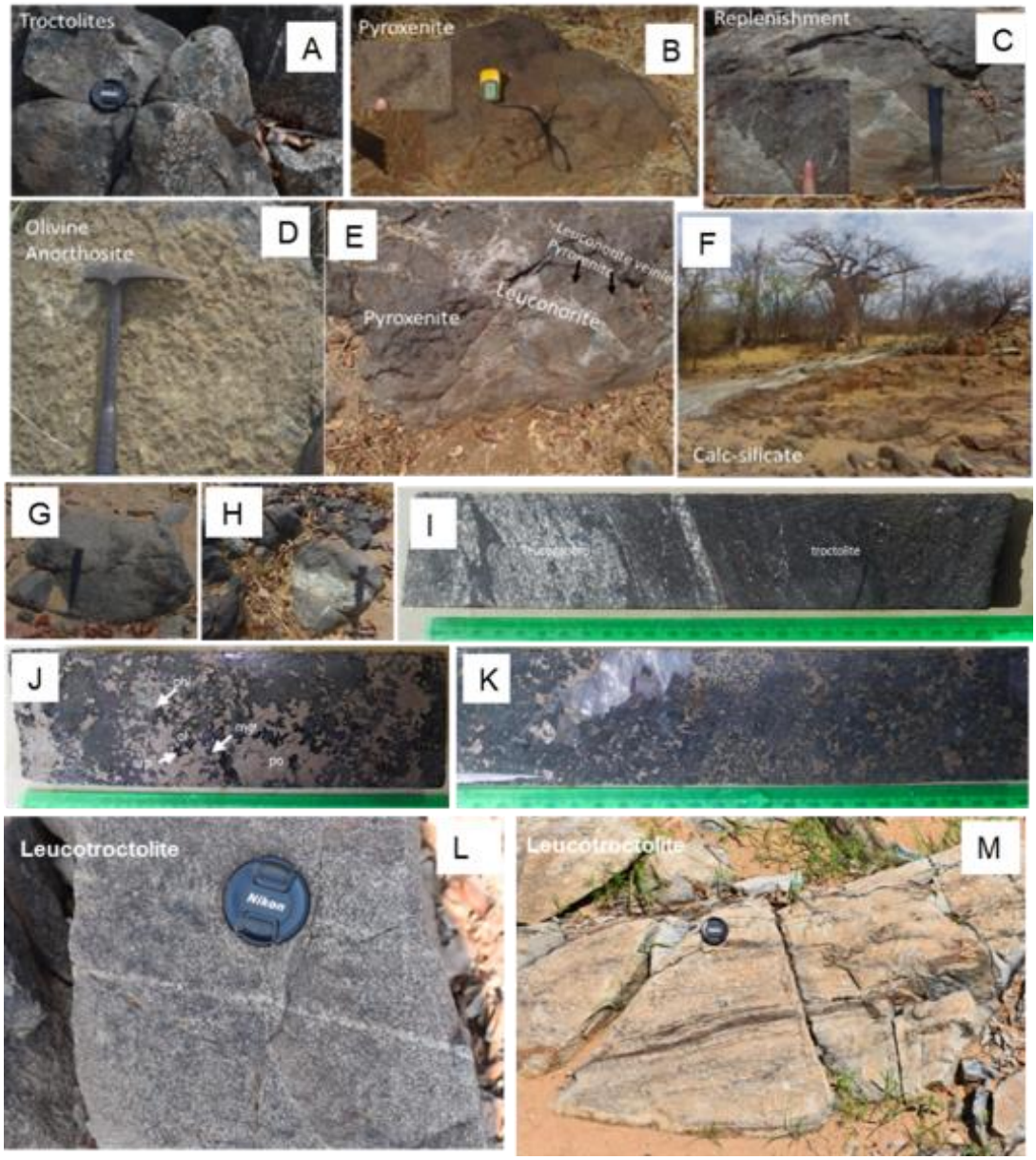


Figure 12: Photographs of outcrops (A-H & L-M) and drillcores (I-K) taken during fieldwork in the Mafic-Ultramafic intrusions (mainly Oncócua intrusion) of the Kunene Complex that show a range of mafic to ultramafic lithologies and textures. A) Troctolite at Ombuku North with wehrlite bands showing plagioclase-rich and plagioclase-poor zonation; B) Orthopyroxene-rich outcrop at Oncócua intrusion with coarse-grained orthopyroxenite xenoliths/autoliths; C & E) Feldspathic pyroxenite at Oncócua in contact with leuconoritic vein and veinlets connected to the interstitial plagioclase of the pyroxenite; D) Olivine anorthosite at Ohamaremba; F) Calc-silicate at the contact between the basement rock in

Oncócua; G) Gabbronorite hosting rounded blocks of fine-grained gabbro or norite at Oncócua; H) Anorthosite dyke crosscutting the gabbroic and pyroxenitic lithologies at Oncócua; I) Leucogabbro and troctolite showing magmatic layering in drillcore from Oncócua; J-K) Semi-massive and net-textured sulphides in magnetite-rich pyroxenites in drillcore from Oncócua; L) Leucotroctolite with feldspathic veins at Ohamaremba; M) Magnetite-bearing layered leucotroctolite with pyroxenitic veins at Ohamaremba.

4.2 Petrography and *in situ* Mineral Compositions of the Mafic-Ultramafic Intrusions

The MUM samples have been lithologically classified using the IUGS classification of Strekeisen (1976) on the basis of the modal abundances as determined by the petrographic observations (Fig. 13).). The samples of Ohamaremba and Otjijanjasemo plot in the troctolitic field, and some samples of Ohamaremba also plot in the intermediate gabbroic and troctolitic fields. The samples of Ombuku North plot in the pyroxenitic and intermediate gabbroic fields. Samples of Oncócua plot in the peridotitic and olivine gabbroic field.

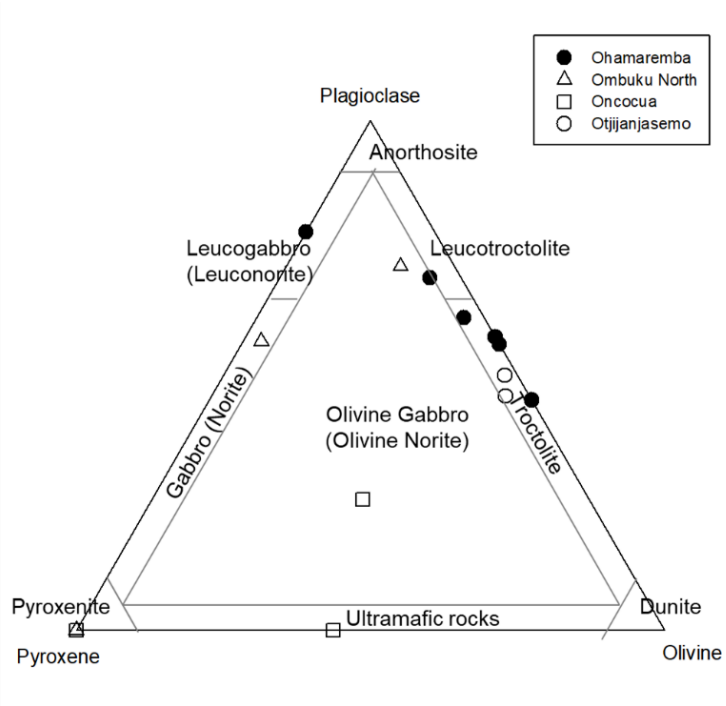


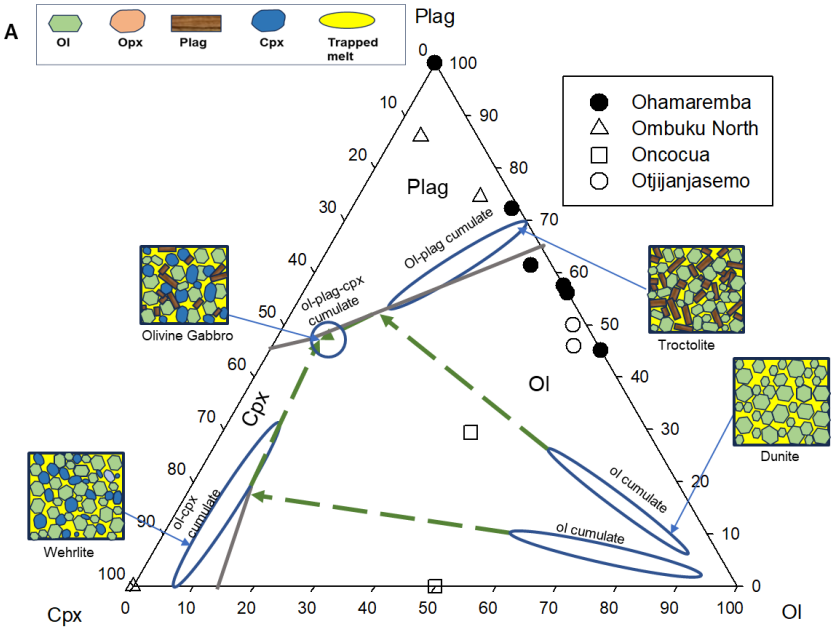
Figure 13: Lithological variation and classification of the MUM intrusions.

Petrographical observations for the MUM intrusions are summarised in Table I.1 of Appendix I and representative textures (including the mineral compositions) are shown in the photomicrographs in subsections 4.2.1, 4.2.2, 4.2.3 and 4.2.4. It is also important to note that several other thin sections of the intrusions were also observed petrographically, but due to intense serpentinisation, amphibolisation, and sericitisation, they were not described and instead, CIPW (Cross, Iddings, Pirsson and Washington) norms were calculated using the bulk rock major oxide data.

The MUM intrusions range in composition from ultramafic to mafic to intermediate. The samples comprise leucotroctolite, gabbronorite, troctolite, pyroxenite, websterite and lherzolite. The grain size generally ranges from coarse (6 mm) to fine (0.2 mm) with olivine and pyroxene (clinopyroxene and orthopyroxene) and plagioclase as the major phases. Accessory phases include biotite, Fe-Ti oxides (mainly magnetite) and apatite, although some of the Oncócua drillcore samples contain up to 30% apatite. Cumulate, ophitic, sub-ophitic, cumulophyric, and poikilitic are the most common textures. Other features such as resorbed-looking grains, corona and peritectic reaction rim textures, and symplectitic textures, along with fractures and deformation features, are also observed. Detail descriptions for each intrusion are given in the subsequent subsections (see subsections 4.2.1, 4.2.2, 4.2.3 and 4.2.4).

The modal abundances of olivine, clinopyroxene, orthopyroxene, and plagioclase, as well as the silica (SiO_2) contents, are plotted on two tetrahedra phase diagrams that depict the crystallisation pathways of basaltic liquids (Figs. 14A & B). The silica contents on the diagram are obtained from the whole rock major oxide analysis of the respective sample or recalculated a ratio 100Y/(Y+Z) to find the X-axis on ternary rock classification plot (Winter, 2001). In Figure 14A, Oncócua shows a crystallisation pathway of olivine ± clinopyroxene ± plagioclase, whereas Ohamaremba, Otjijanjasemo and Ombuku North, in general, show crystallisation pathways of olivine-plagioclase and plagioclase ± olivine ± clinopyroxene. One sample of Ombuku North also is adjacent to olivine–clinopyroxene cumulate. In Figure 9B, orthopyroxene is included as in the olivine–plagioclase–silica phase diagram. Most samples from

Ohamaremba show a crystallisation pathway of olivine–plagioclase. Otjijanjasemo shows a crystallisation pathway of olivine–orthopyroxene–plagioclase. Also, two samples from Ombuku North and 1 sample from Ohamaremba follow the same crystallisation pathway but are more evolved compositions. Two samples from Oncócua also show a crystallisation pathway towards olivine–orthopyroxene ± plagioclase, however, they are relatively more silica-rich with minor to no plagioclase. Two samples (from Oncócua and Ombuku North) plot at the silica-rich end-member.



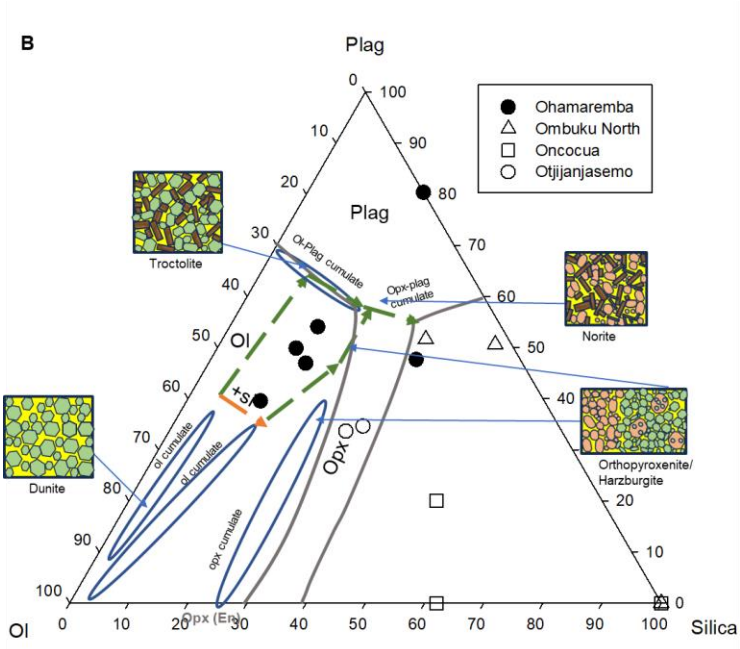


Figure 14: The modal abundances of the MUM intrusions plotted on mineral ternary plots (A, Ol-Plag-Cpx; B, Ol-Plag-Silica) modified from Barnes (2023). This plot included only samples that were relatively unaltered and described petrographically. These ternary diagrams show the crystalllisation sequences of basaltic liquids. The ellipse-like shapes are zones of cumulates (dark blue). The MUM intrusions are plotted (Ohamaremba, Otjijanjasemo, Oncócua and Ombuku North). Ol=Olivine, Plag=Plagioclase, Cpx=Clinopyroxene and Opx=Orthopyroxene.

The *in situ* mineral chemical data are reported in Table I.2 in Appendix I. TAP and LLIF crystals were used as the standards for MgO, NiO, FeO, MnO and Cr_2O_3 and a plot to assess the quality of the data is in the appendix I (Fig. I.1). Olivine compositions range between 23.25–43.04 wt% MgO, 16.84–42.78 wt% FeO, 0.23–0.56 wt% MnO and 28.80–41.86 wt% SiO_2 and contain up to 0.27 wt% NiO. Oncócua has the highest MnO content in olivine and Ombuku North has the lowest MnO content in olivine. Olivine in the Oncócua feldspathic peridotite and the Ohamaremba and Otjijanjasemo troctolites has the same range of SiO_2 (35.58–38.06 wt%). Olivine in an Ombuku North gabbro has the highest SiO_2 contents (39.40–39.79 wt%). Clinopyroxene contains 13.02–17.67 wt% MgO, 3.75–16.54 wt% FeO, 10.52–22.89 wt% CaO, 0.01–0.87 wt% Cr_2O_3, 2.24–7.95 wt% Al_2O_3, 45.90–51.81 wt% SiO_2 with molar Mg# between 66–87. Orthopyroxene contains 19.56–33.75 wt% MgO, 7.42–24.62 wt% FeO, 0.02–3.46 wt%

CaO, up to 0.43 wt% Cr_2O_3, up to 4.72 wt% Al_2O_3, and 41.86–55.77 wt% SiO_2 with molar Mg# between 59–89. The molar Mg# (molar proportions of the oxides) for clinopyroxene and orthopyroxene was calculated as follows:

$$Mg\# = [(MgO/40.32) / ((MgO/40.32) + (FeO/71.85))] \times 100$$

where MgO and FeO are the oxides in weight % determined by the analytical method above, and 40.32 and 71.85 are the molecular weights of MgO and FeO, respectively (Gill, 2010).

The olivine compositions for the samples are plotted in Figures 15 and 16 as molar % Fo and NiO variations (the plots used the converted Ni content in ppm, with the conversion factor = 0.785845). The forsterite (Fo) is the Mg-endmember of olivine and was calculated as follows:

$$Fo = [(Mg)/(Mg + Fe + Mn)] \times 100,$$

where the atoms were calculated from the oxide data. Fo and Ni contents show a positive correlation and the Fo contents range between 54–81 and Ni contents up to 2122 ppm. Oncócua contains the most Fe-rich olivines (and lowest Ni contents) and Ombuku North has the most Mg-rich olivine (and highest Ni contents). In general, the samples of each intrusion show narrow variabilities in Fo content, particularly Ombuku North that shows similar Fo, while the other intrusions show some variability. Their Ni contents show some variability in all intrusions (Fig. 15).

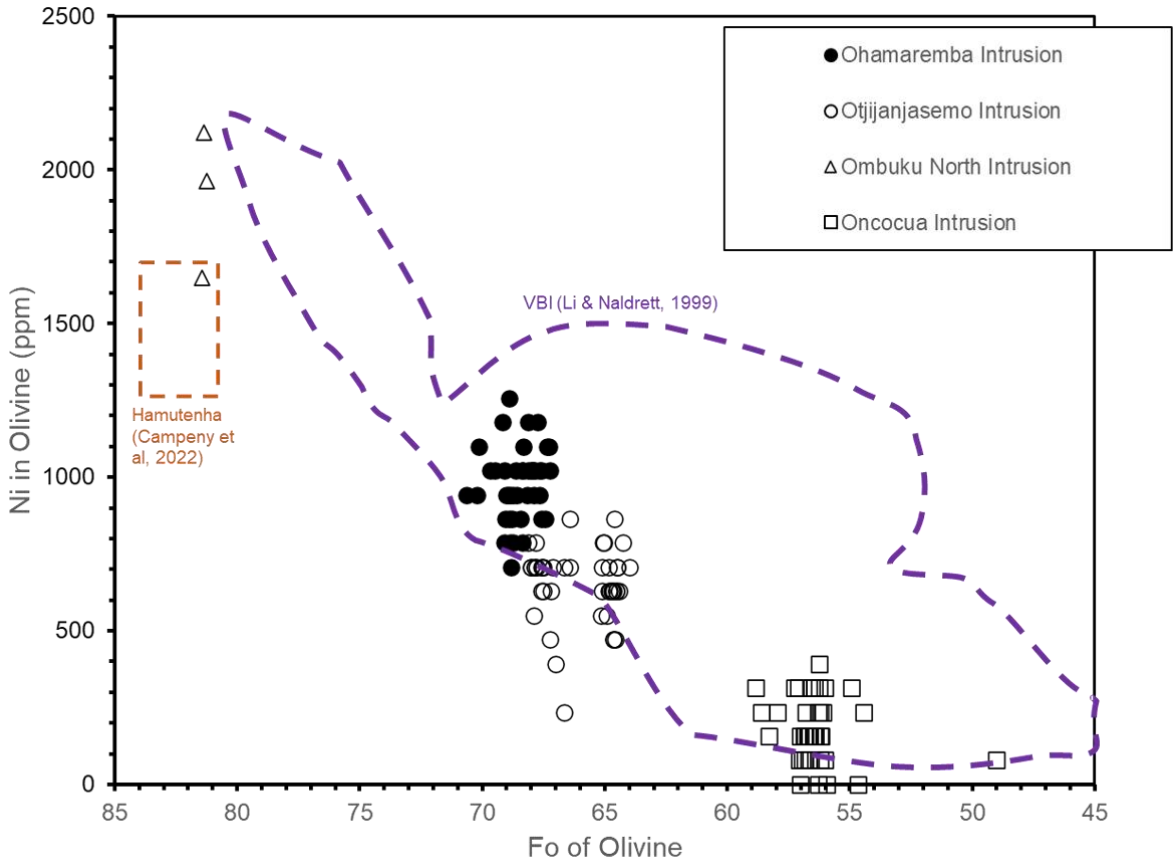


Figure 15: Molar Fo-Ni (ppm) compositions of olivine for Ohamaremba, Otjijanjasemo, Ombuku North, and Oncócua. Data for the Voisey's Bay intrusion (VBI) are from Li and Naldrett (1999) and data for Hamutenha are from Campeny et al. (2023).

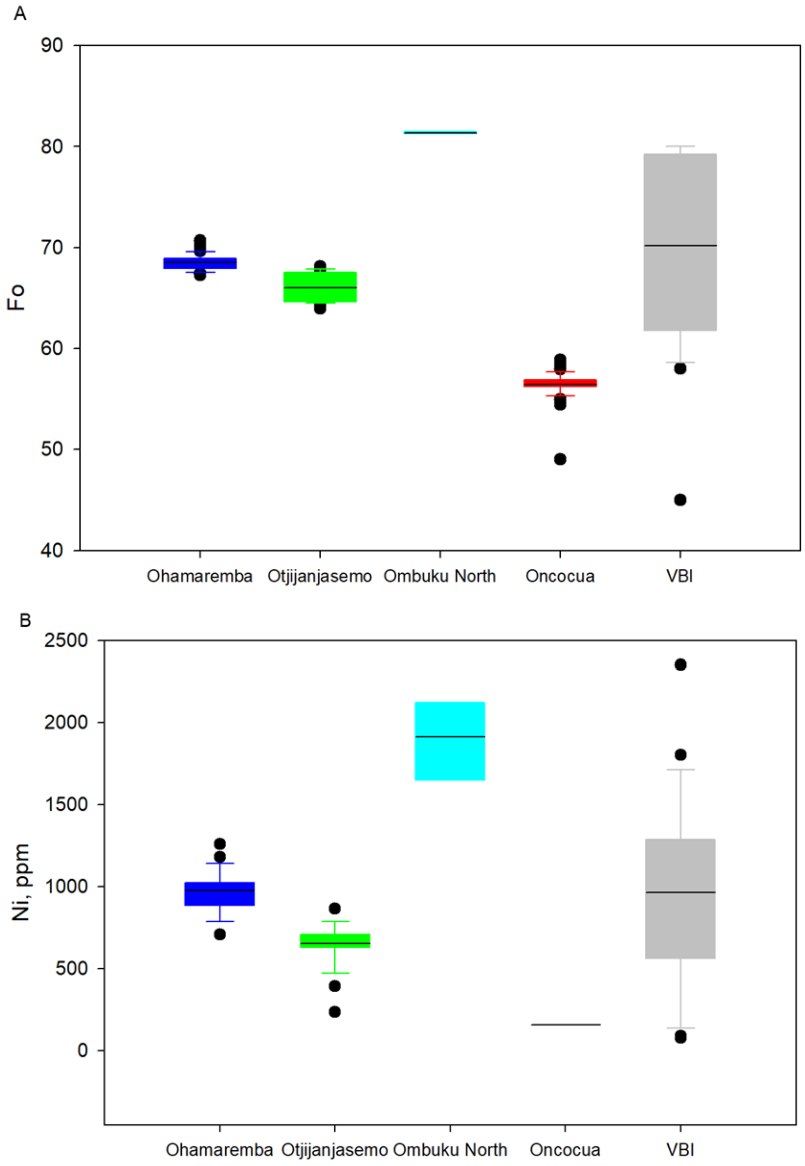


Figure 16: Boxplots showing the range of the Fo composition of olivine (A, Molar Fo; B, Ni in ppm) with outliers (black dots). Olivine Fo-Ni data from the Voisey's Bay intrusion (VBI) are shown for comparison (these data are from Bulle & Layne, 2015).

Cr_2O_3 profiles (Fig. 32; Figs. I.2A & B in the Appendix I) for the pyroxene grains from each intrusion are plotted to assess the nature of any chromium-zoning. No immediate trends are observed due to the very low Cr_2O_3 contents in the pyroxene grains. A ternary plot showing the pyroxene endmember compositions is shown in Figure 17. Pyroxene plots in the fields of enstatite, pigeonite, augite and diopside (Fig. 17).

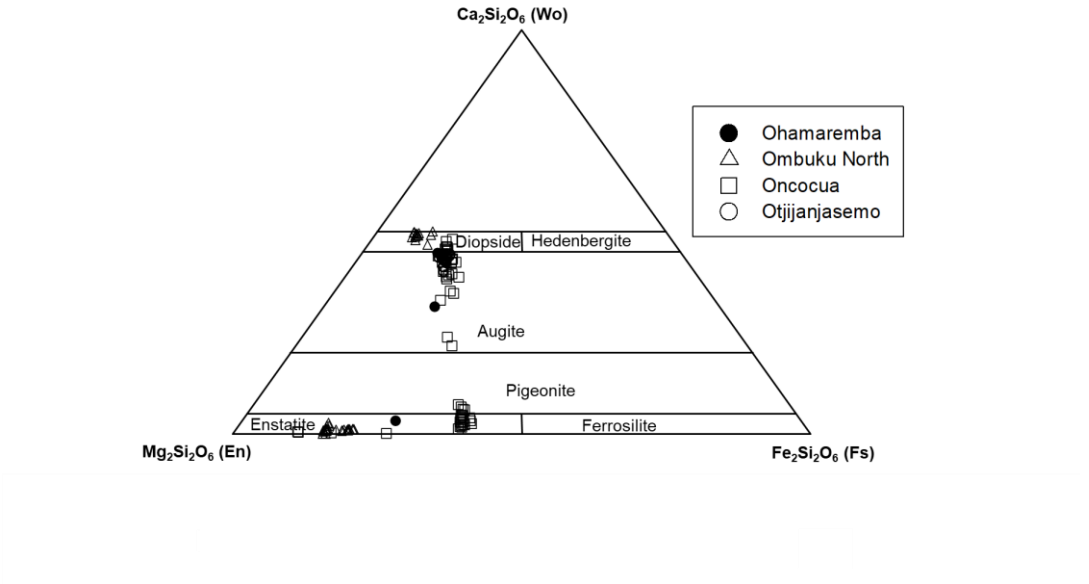


Figure 17: Ternary composition diagram for pyroxene with the mineral compositions of pyroxene plotted for Oncócua, Otjijanjasemo, Ombuku North, and Ohamaremba.

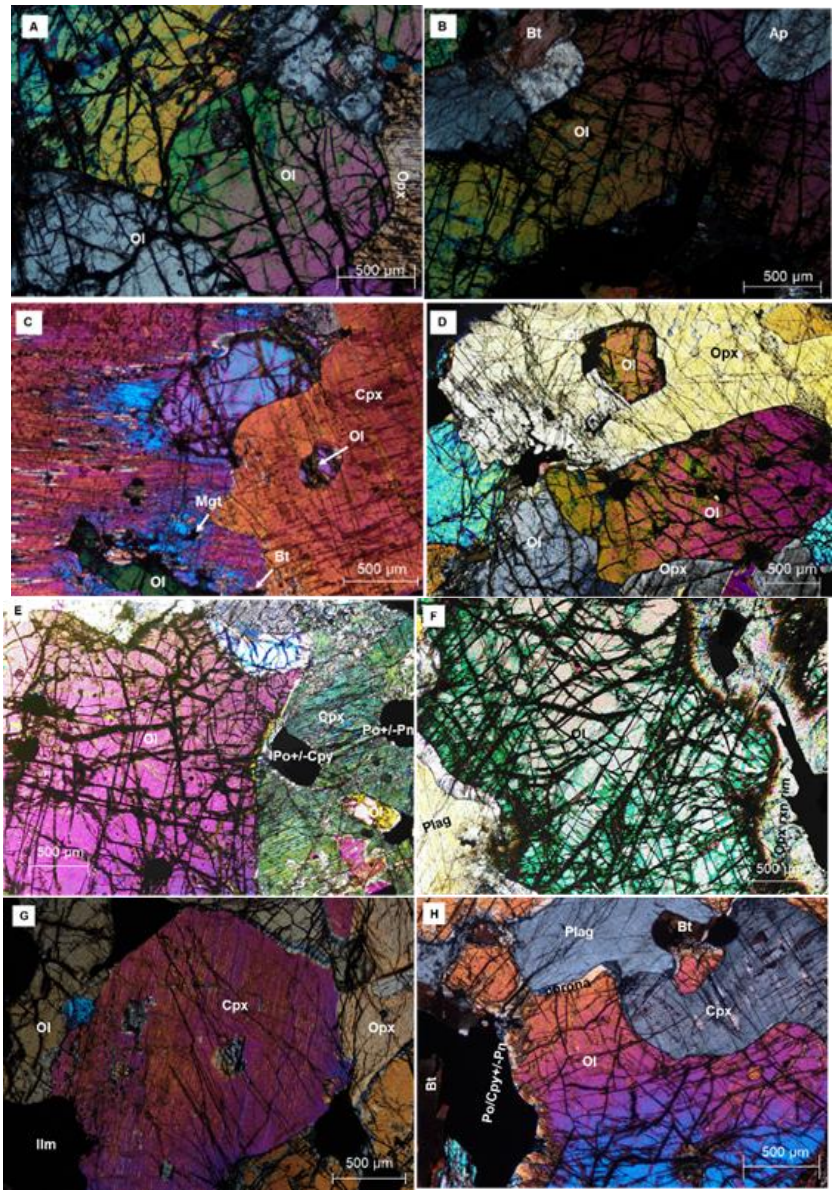
4.2.1 Oncócua Intrusion

ONC-1-55: Olivine Websterite

ONC-1-55 is an olivine websterite consisting of cumulus olivine (39%) and pyroxene (11% orthopyroxene and 39% clinopyroxene) as the major phases. There are 10% opaque phases (magnetite, pyrrhotite and chalcopyrite), 1% biotite, and very local minor interstitial plagioclase (Figs. 18A, C-E, G, I & M). Olivine is subhedral to anhedral and ranges in size from coarse-grained (5 mm) to medium-grained (<5 mm) to fine-grained (0.2 mm). The fine-grained olivine is mostly interstitial but is also present as resorbed-looking chadacrysts in large altered clinopyroxene and orthopyroxene oikocrysts (Fig. 18C-E and M). Some resorbed olivine chadacrysts also have orthopyroxene rims with symplectite textures (Fig. 18M). Pyroxene oikocrysts are anhedral and are mostly coarse-grained (up to 6 mm) and medium-grained (1 mm) with the clinopyroxene oikocrysts showing orthopyroxene exsolution lamellae (Figs. 18C, D, I). The Fe-Ti oxides form medium to fine-grained blebs and stringers, and,

together with the sulphides, and biotite, are interstitial in texture and locally occur as inclusions in the pyroxene oikocrysts (Fig. 18C & E).

Olivine compositions range between Fo_{54-58} and Fa_{41-45} with up to 393 ppm Ni in sample ONC-1-55 (Figs. 15, 16). The resorbed-looking olivine chadacrysts are the most Fe-rich (Fo_{54-55}) (Fig. 15, 18M). The clinopyroxene oikocrysts have molar Mg# compositions of 66–75 and low Cr_2O_3 contents of 0.02–0.06 wt% (Table I.2 and Figs. I.2A, B in Appendix I). The pyroxene ternary diagram shows compositions of pigeonite, augite and diopside (Fig. 17).



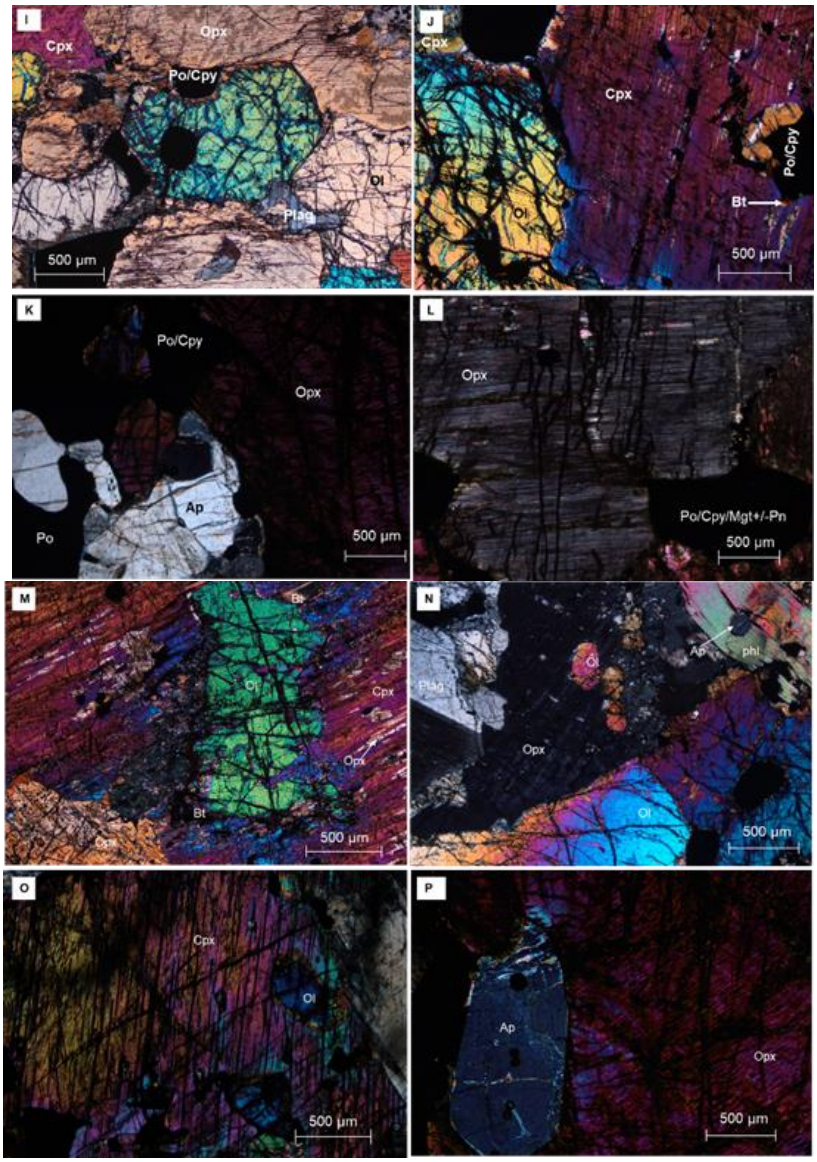


Figure 18: Transmitted light photomicrographs (all XPL; 4x magnification) of three samples from Oncócua. A) Medium- to fine-grained subhedral cumulus olivine with altered clinopyroxene in the olivine websterite. B) Medium-grained subhedral to anhedral cumulus olivine with minor apatite and biotite in the feldspathic peridotite. C) Resorbed interstitial olivine and resorbed chadacrystic olivine in coarse-grained altered clinopyroxene in the olivine websterite. D) Interstitial olivine and resorbed olivine in coarse-grained orthopyroxene in the olivine websterite. E) Coarse-grained olivine, interstitial olivine and resorbed chadacrystic olivine in coarse-grained, altered clinopyroxene in the olivine websterite. F) Coarse-grained olivine with corona in contact with plagioclase and an orthopyroxene rim in contact with opaque phases in feldspathic peridotite. G) Coarse-grained clinopyroxene with exsolution lamellae and fined-grained, anhedral olivine and orthopyroxene in olivine websterite. H) Coarse-grained and fine-grained olivine with corona in contact with plagioclase and fine-grained olivine with resorbed textures and anhedral medium-grained

clinopyroxene in feldspathic peridotite. I) Interstitial olivine in altered clinopyroxene and orthopyroxene in olivine websterite. J) Clinopyroxene with exsolution lamellae, medium-grained olivine and fined-grained olivine showing resorbed textures in feldspathic peridotite. K) Coarse-grained orthopyroxene with interstitial apatite in the apatite orthopyroxenite. L) Fractured orthopyroxene in apatite orthopyroxenite. M) Angular resorbed olivine chadacrysts in clinopyroxene with orthopyroxene exsolution lamellae in the olivine websterite. N) Olivine, plagioclase and orthopyroxene that encloses fine-grained resorbed olivine in the feldspathic peridotite. O) Clinopyroxene with exsolution lamellae and resorbed olivine chadacrysts in feldspathic peridotite. P) Coarse-grained orthopyroxene with medium-grained apatite. Ol (Olivine), Cpx (Clinopyroxene), Opx (Orthopyroxene), Plag (Plagioclase), Bt (Biotite), Ap (Apatite), Mgt (Magnetite), Ilm (Ilmenite), Cpy (Chalcopyrite), Po (Pyrrhotite), Pn (Pentlandite).

ONC-159: Feldspathic Peridotite

ONC-159 is a feldspathic peridotite consisting of 28% olivine, 20% clinopyroxene, 20% plagioclase and 10% orthopyroxene. There are 17% opaque phases and 5% biotite in ONC-159. Olivine is anhedral (and locally subhedral) and is both coarse-grained (5 mm) and fine-grained (0.2 mm) (Fig. 18B, F & H). Fine-grained interstitial olivine shows resorbed-looking textures in both clinopyroxene and orthopyroxene oikocrysts (Fig. 18H, N, O). Olivine shows orthopyroxene rims and symplectite textures containing magnetite locally (Fig. 18F). Pyroxene is anhedral and is coarse-grained (5 mm) to fine-grained (0.6 mm) with orthopyroxene exsolution lamellae in clinopyroxene. Plagioclase is anhedral and coarse-grained (6 mm) to fine-grained (0.5 mm) and is closely associated with olivine (Fig. 18F, H). Biotite is typically associated with the opaque minerals (magnetite and sulphide) in the interstices (Fig. 18H, J).

Olivine compositions range between $Fo_{56\text{-}59}$ and $Fa_{41\text{-}59}$ with up to 314 ppm Ni in ONC-159 (Figs. 15, 16). The clinopyroxene oikocrysts have molar Mg# compositions between 68–76 with low Cr_2O_3 contents of 0.03–0.07 wt%. The orthopyroxene oikocrysts have molar Mg# compositions between 73–89 and low Cr_2O_3 contents of up to 0.01 wt%. The pyroxene ternary diagram shows that ONC-159 consists of enstatite, augite and diopside (Fig. 17).

ONC-1-35: Apatite Orthopyroxenite

ONC-1-35 is an apatite orthopyroxenite consisting of ~60% orthopyroxene and 20–30% apatite. There are 7-10% opaque phases in the interstices, and which partly replace

orthopyroxene and apatite (Fig. 18K, L, P). Orthopyroxene is anhedral and is coarse-grained (6 mm) to fine-grained (0.5 mm). Neoblasts of fine-grained orthopyroxene grains are typically present at the boundaries of the orthopyroxene oikocrysts and exsolution lamellae of orthopyroxene endmembers are also present (Fig. 18L). Apatite is euhedral to anhedral and is medium-grained (~1.7 mm) to fine-grained (0.2 mm) and is typically interstitial to the main phases and as inclusions in the opaque minerals, which include sulphide and local magnetite. There is also locally net-textured sulphide typically associated with the apatite.

The orthopyroxene oikocrysts have Mg# between 59–62 and up to 0.04 wt% Cr_2O_3. The pyroxene ternary diagram shows that ONC1-35 consists of enstatite and pigeonite compositions (Fig. 17).

In general, the samples of olivine websterite and feldspathic peridotite have similar mineral composition (± plagioclase), textures, and olivine compositions. The range of clinopyroxene Mg# compositions are also similar for the feldspathic peridotite and the olivine websterite, as are the clinopyroxene endmember composition (augite and diopside). Cumulus orthopyroxene in the apatite orthopyroxenite shows a lower range Mg# relative to the orthopyroxene rims in olivine in the feldspathic peridotite. The orthopyroxene endmember compositions of the apatite orthopyroxenite varies from enstatite to pigeonite whereas the feldspathic peridotite only consists of enstatite.

4.2.2 Ohamaremba Intrusion

KSAT 306-1: Orthopyroxene-bearing Leucotroctolite

KSAT306-1 is an orthopyroxene-bearing leucotroctolite consisting of 65% plagioclase and 27% olivine (Figs. 19A-C & G). Minor phases include 4% orthopyroxene (± rare clinopyroxene), 3% biotite, and 1% opaque phases. Plagioclase forms euhedral laths that are medium-grained (2 mm) and fine-grained (0.2 mm). The plagioclase laths show Carlsbad, albite and pericline twinning. Plagioclase is locally partially enclosed by orthopyroxene, giving sub-ophitic textures (Fig. 19G). Olivine grains form clusters in places to give glomeroporphyritic textures (Fig. 19B). Olivine is euhedral-anhedral and

ranges in size from medium-grained (~2 mm) to fine-grained (~0.7 mm). Olivine may be enclosed in orthopyroxene to give ophitic textures (Fig. 19G). Orthopyroxene is interstitial, forming oikocrysts, as well as peritectic rims around olivine (Figs. 19B, G). The biotite is interstitial and is closely related to plagioclase and fine-grained disseminated opaque minerals (sulphide and magnetite) (Figs. 19C, G).

Olivine compositions range between $Fo_{67\text{-}71}$ and $Fa_{29\text{-}32}$ with Ni contents between 786–1179 ppm (Figs. 15, 16). The interstitial orthopyroxene has molar Mg# compositions of 73 with Cr_2O_3 contents of 0.01 wt%. The pyroxene ternary diagram shows that KSAT306-1 contains enstatite (Fig. 17).

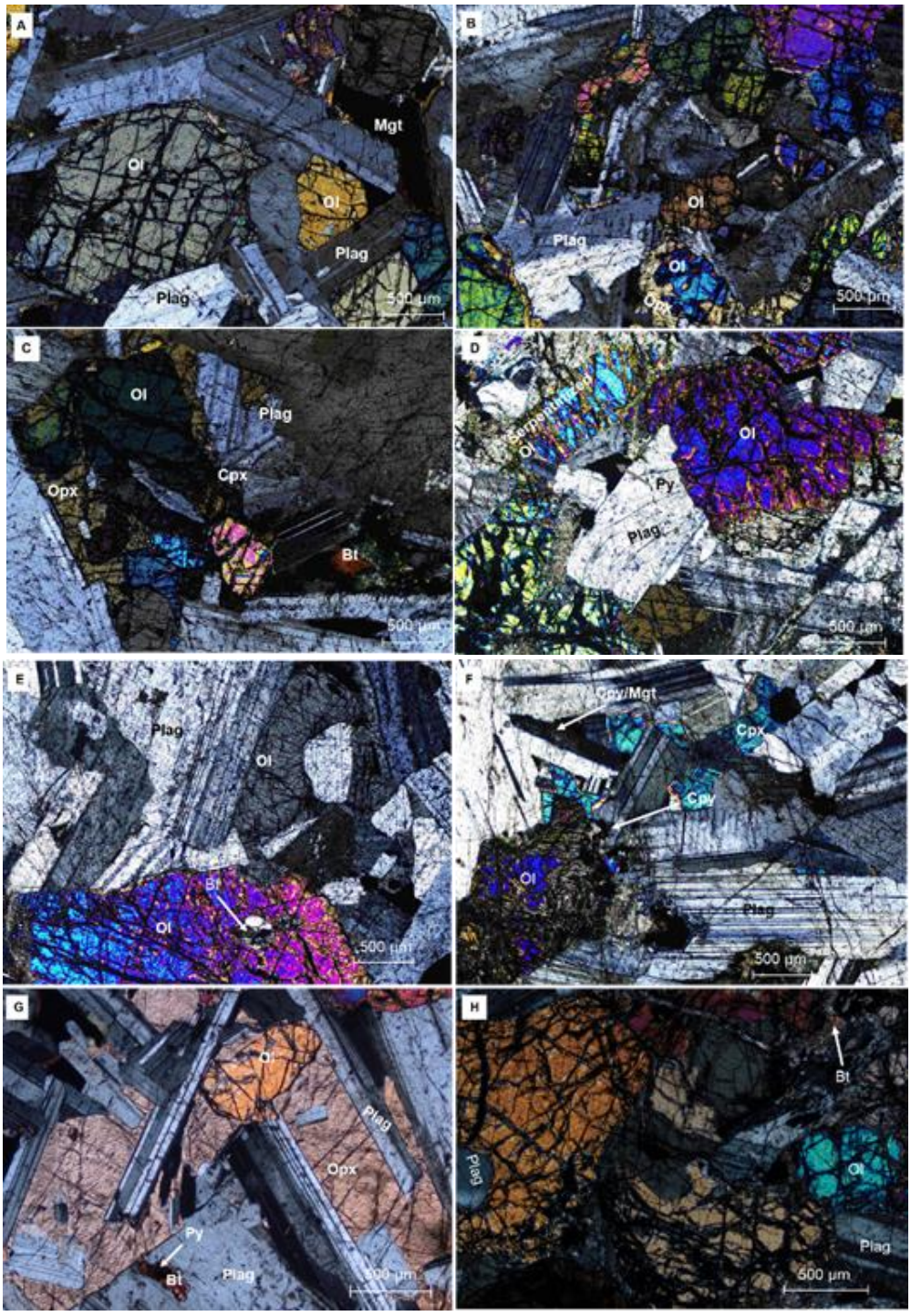


Figure 19: Transmitted-Light Photomicrographs (all XPL; 4x magnification) of two samples from Ohamaremba. A) Fine- to medium- grained and subhedral to anhedral olivine and subhedral to anhedral plagioclase laths to give a cumulate texture in the leucotroctolite. B) Fine-grained subhedral to anhedral olivine and mainly anhedral, partially enclosed plagioclase, with olivine showing orthopyroxene reaction rims. C)

Fine-grained subhedral to anhedral olivine and medium- to fine-grained plagioclase with interstitial olivine and pyroxene enclosing olivine and plagioclase in the leucotroctolite. D) Medium- to fine-grained anhedral olivine partially enclosing anhedral plagioclase and olivine showing serpentinisation in the leucotroctolite. E) Fine- to medium-grained anhedral olivine and fine- to medium-grained anhedral plagioclase with interstitial olivine in the leucotroctolite. F) Altered fine-grained olivine and fine- to medium-grained plagioclase with interstitial clinopyroxene in the leucotroctolite. G) Fine-grained subhedral olivine together with medium- to fined-grained plagioclase enclosed in orthopyroxene in the leucotroctolite. H) Medium- to fine-grained olivine partially enclosing plagioclase. Ol (Olivine), Cpx (Clinopyroxene), Opx (Orthopyroxene), Plag (Plagioclase), Bt (Biotite), Mgt (Magnetite), Cpy (Chalcopyrite), Po (Pyrrhotite), Py (Pyrite).

KSAT-157: Clinopyroxene-bearing (Leuco) Troctolite

KSAT-157 is a clinopyroxene-bearing (leuco)-troctolite (Table I.1 of Appendix I) consisting of 56% plagioclase, and 33% olivine (Fig. 19D-F & H). Minor phases include 5% opaque minerals, 3% clinopyroxene and 2% biotite. Plagioclase is present as subhedral to anhedral laths and is coarse-grained (5 mm) to fine-grained (0.3 mm). The plagioclase laths show Carlsbad, albite and pericline twinning (Figs. 19D-F & H). Olivine is mostly anhedral and locally subhedral and is medium-grained (3 mm) to fine-grained (0.5 mm) (Figs. 19D, E & H). Olivine locally partially encloses plagioclase to give a sub-ophitic texture and olivine is locally serpentinised (Figs. 19D). Clinopyroxene is interstitial and is associated with plagioclase and olivine (Fig. 14F). Biotite is interstitial and is associated with the opaque minerals, as well as olivine and plagioclase (Fig. 19H). The opaque minerals consist of sulphide and Fe-oxides (1%), and they are in close association with biotite, plagioclase and olivine.

Olivine compositions range between Fo_{68-70} and Fa_{29-31} with Ni contents of 707–1257 ppm (Figs. 15, 16). The interstitial clinopyroxene has molar Mg# compositions between 72–77 with Cr_2O_3 contents between 0.01–0.34 wt% (Table I.2 in Appendix I). The pyroxene ternary diagram shows that KSAT-157 contains augite to diopside compositions (Fig. 17).

Both leucotroctolite and (leuco) troctolite show similar mineral compositions and textures, although the leucotroctolite also shows peritectic orthopyroxene textures. The

samples show similar Fo and Ni contents with a slightly wide range in Fo composition (Fo_{67-71}) in the leucotroctolite.

4.2.3 Otjijanjasemo Intrusion

KSAT 301/118: Serpentinised Clinopyroxene-bearing Troctolite

KSAT301-118 is a serpentinised clinopyroxene-bearing troctolite consisting of 50% olivine and 46% plagioclase (Figs. 20A-C). Minor phases include 4% clinopyroxene as well as <1% opaque phases (pyrite ± chalcopyrite) and rare biotite. Olivine (typically serpentinised) is euhedral to anhedral and is medium-grained (3 mm) to fine-grained (0.1 mm). Plagioclase is euhedral to anhedral and is coarse-grained (6 mm) to fine-grained (0.8 mm) (Figs. 20A-C). Olivine grains are enclosed by clinopyroxene, and locally by plagioclase laths, to give a poikilitic texture (Fig. 20B). A large olivine grain also partially encloses plagioclase laths to give a sub-ophitic texture (Figs. 20A). Plagioclase shows mainly Carlsbad and albite twinning. The opaque minerals consist of magnetite and sulphide and are mostly associated with the grain boundaries of the silicate minerals.

Olivine compositions in KSAT301-118 range between Fo_{67-68} with Ni contents of 236–864 ppm (Figs. 15, 16). The interstitial clinopyroxene has molar Mg# compositions that range between 74–75 with Cr_2O_3 contents between 0.37–0.43 wt% (Table I.2 in Appendix I). The pyroxene ternary diagram shows KSAT301/118 contains augite to diopside compositions (Fig. 17).



Figure 20: Transmitted light photomicrographs (all XPL; 4x magnification) of two samples from Otjijanjasemo. A) Medium-grained anhedral olivine partially enclosing plagioclase to give a sub-ophitic texture locally in the serpentinised troctolite. B) euhedral fine-grained olivine enclosed by clinopyroxene to give a poikilitic texture and locally by plagioclase laths in serpentinised troctolite. C) Medium- to fine-grained plagioclase laths and fine-grained subhedral olivine in the serpentinised troctolite. D) euhedral olivine and plagioclase laths in the troctolite. E) Subhedral to euhedral medium- to fine-grained olivine and medium-grained plagioclase with interstitial clinopyroxene and locally fine-grained olivine enclosed by plagioclase. F) Medium- to fine-grained olivine and medium-grained plagioclase with interstitial magnetite in the troctolite. Ol (Olivine), Cpx (Clinopyroxene), Opx (Orthopyroxene), Plag (Plagioclase), Bt (Biotite), Ap (Apatite), Mgt (Magnetite), Cpy (Chalcopyrite), Po (Pyrrhotite).

KSAT305/122: Troctolite

KSAT305-122 is a troctolite consisting of 47% plagioclase and 45% olivine (Figs. 20D-F). Minor phases include 4% opaque minerals, 2% clinopyroxene, and 2% biotite. Plagioclase is euhedral and is coarse-grained (6 mm) to fine-grained (0.6 mm) (Fig. 15D-F). Olivine is euhedral-subhedral and is medium-grained (1.7 mm) to fine- grained

(0.4 mm). Fine-grained olivine is locally enclosed by plagioclase laths (Figs. 15D-E). Plagioclase shows Carlsbad, albite, and pericline twinning (Figs. 20D-F). Plagioclase laths show local evidence of deformation (bent twins). Clinopyroxene is interstitial and is associated with olivine and plagioclase (Fig. 20E). Biotite is associated with olivine and plagioclase as well as the opaque phases (Fig. 20D). The opaque minerals comprise sulphide (1%) and magnetite (4%). The interstitial sulphide is fine-grained and disseminated and is mostly associated with olivine and plagioclase. Magnetite is interstitial (Figs. 20D & F).

Olivine compositions in KSAT305-122 range from between Fo_{64-65} with NiO contents of 0.06–0.11 wt% (Figs. 15, 16). The interstitial clinopyroxene has molar Mg# compositions of 72–74 with Cr_2O_3 contents of 2.5–3.7 wt% (Table I.2 in Appendix I). The pyroxene ternary diagram shows that KSAT305-122 contains augite to diopside compositions (Fig. 17).

Both troctolitic samples at Otjijanjasemo have the same mineral assemblages consisting of olivine and plagioclase. However, the serpentinised troctolite sample has more fine-grained olivine and plagioclase relative to the troctolite sample. The serpentinised troctolite sample also has poikilitic clinopyroxene enclosing fine euhedral olivine grains and sub-ophitic olivine partially enclosing plagioclase laths. The samples have similar pyroxene endmember compositions. The olivine Fo and clinopyroxene Mg# contents of the samples do not show large ranges, however, the serpentinised troctolite has higher ranges of Fo and clinopyroxene Mg# relative to the troctolite. The NiO contents of olivine are similar although the serpentinised troctolite has a wider and lower range of NiO contents.

4.2.4 Ombuku North Intrusion

KSAT 322-1: Pyroxene-bearing Leucotroctolite

KSAT 322-1 is a pyroxene-bearing leucotroctolite that consists of plagioclase (70%), olivine (20%) and minor phases that include pyroxene (5% clinopyroxene and 4% orthopyroxene) (Figs. 21C-D). There is also <1% sulphide present (Figs. 21C-D).

Plagioclase is medium-grained (1.8 mm) to fine-grained (0.2 mm) forming granular anhedral grains. Plagioclase grains show Carlsbad, albite and pericline twinning. Anhedral olivine is medium-grained (3.0 mm) to fine-grained (0.3 mm) with medium-grained olivine showing some alteration and fractures. Subhedral to anhedral orthopyroxene is medium-grained (1.0 mm) to fine-grained (0.3 mm). Clinopyroxene, and most of orthopyroxene, are fine-grained and are interstitially associated with plagioclase and, to a lesser extent, olivine. Some large orthopyroxene grains are well-preserved cumulus grains (Fig. 21D). The fine pyroxene grains (orthopyroxene and clinopyroxene) show annealed textures (Fig. 21C). A vein rich in altered orthopyroxene and clinopyroxene cuts across the thin section and the surrounding phases are also altered.

KSAT322-1 contains olivine with compositions of Fo_{81} and Fa_{18} with Ni contents ranging between 2122–1650 ppm (Figs. 15, 16). Clinopyroxene has Mg# compositions of 81 with Cr_2O_3 contents ranging between 0.41–0.44 wt% (Table I.2 in Appendix I). Orthopyroxene Mg# compositions range between 79 compositions 81 with Cr_2O_3 contents ranging between 0.01–0.16 wt%. Pyroxene compositions are enstatite to diopside (Fig. 17).

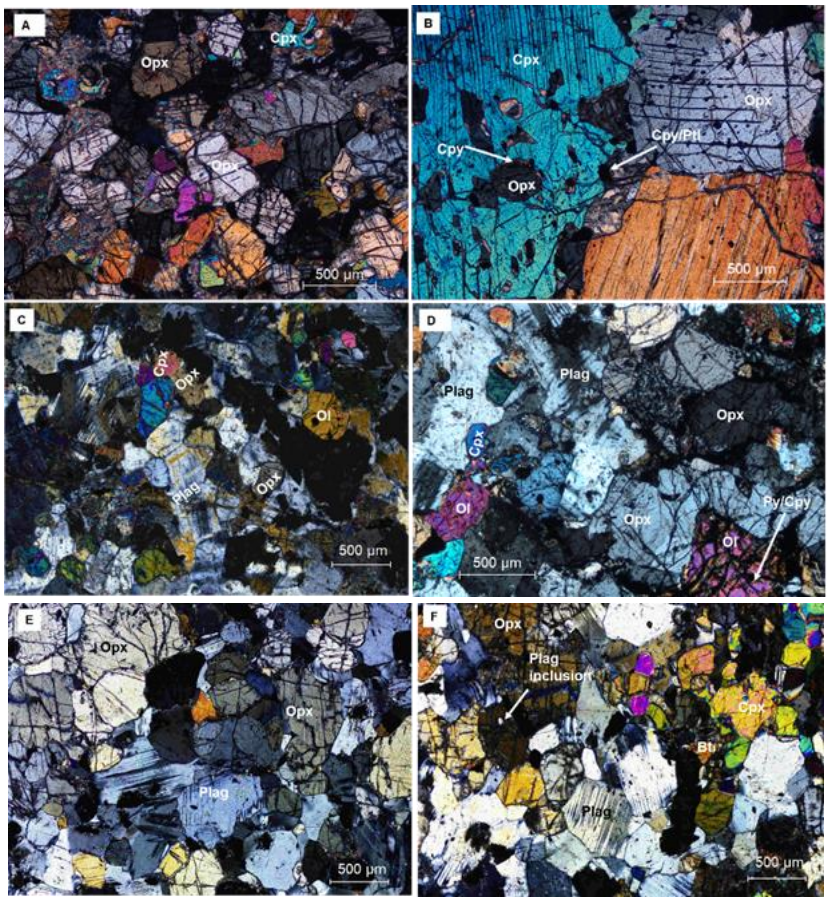


Figure 21: Transmitted-Light Photomicrographs (all XPL; 4x magnification) of three samples from Ombuku North and South. A) Fine-grained subhedral to anhedral orthopyroxene and interstitial clinopyroxene in serpentinised websterite. B) Coarse-grained clinopyroxene and orthopyroxene with clinopyroxene showing orthopyroxene exsolution lamellae and orthopyroxene enclosed by clinopyroxene oikocrysts in serpentinised websterite. C) Subhedral to anhedral fine-grained olivine and fine-grained orthopyroxene, clinopyroxene and fine-grained granular plagioclase in the leucotroctolite. E) Fine-grained olivine, subhedral to anhedral fine-grained orthopyroxene and granular fine-grained plagioclase with interstitial clinopyroxene and a larger olivine grain associated with a larger orthopyroxene in the leucotroctolite. E) Subhedral to anhedral orthopyroxene and granular plagioclase in the (leuco) norite. F) Fine-grained orthopyroxene, granular plagioclase and fine-grained clinopyroxene with clinopyroxene mainly interstitial in the (leuco) norite. Ol (Olivine), Cpx (Clinopyroxene), Opx (Orthopyroxene), Plag (Plagioclase), Bt (Biotite), Mgt (Magnetite), Cpy (Chalcopyrite), Pn (Pentlandite).

4-778: Serpentinised Websterite

4-778 is a serpentinised websterite that comprises clinopyroxene (52%), orthopyroxene (46%) and minor sulphide (<2%) (Figs. 21A-B). Clinopyroxene is anhedral to subhedral and coarse-grained (5.0 mm) to fine-grained (0.2 mm). Orthopyroxene is

anhedral to subhedral and medium-grained (2.4 mm) to fine-grained (0.2 mm) with most of the fine-grains being subhedral. Clinopyroxene oikocrysts locally show orthopyroxene exsolution lamellae (Fig. 21B). Fine-grained clinopyroxene has also exsolved from the fine-grained orthopyroxene (Fig. 21A). Serpentinisation, and carbonate alteration, are typically present in places. Carbonate-rich veins cut across the mineral assemblage. Clinopyroxene and orthopyroxene oikocrysts locally show deformation features (Fig. 21B). Sulphide phases form fine-grained disseminated stringers and blebs and is typically interstitial in texture, associated locally with alteration (but not associated with the carbonate veins). Sulphide also rarely infills the exsolution lamellae of coarse-grained pyroxene.

Clinopyroxene oikocrysts have Mg# compositions of 85–87 with Cr_2O_3 contents ranging between 0.60–0.82 wt%. Orthopyroxene oikocrysts have Mg# compositions of 82–85 with Cr_2O_3 contents ranging between 0.14–0.43 wt% (Table I.2 in Appendix I). Sample 4-778 contains enstatite to diopside compositions (Fig. 17).

KSAT 326-1: (Leuco) Norite

KSAT 326-1 is a (leuco) norite consisting of plagioclase (55%), orthopyroxene (33%) and minor phases that include clinopyroxene (6%), olivine (3%), biotite (<2%) and opaque minerals (<1%, mainly magnetite) (Figs. 21E, F). Orthopyroxene is subhedral to anhedral and medium-grained (~2.0 mm) to fine-grained (0.2 mm) with local oikocrysts hosting plagioclase inclusions. Plagioclase is anhedral and medium-grained (1.6 mm) to fine-grained (0.2 mm) and is usually granular with Carlsbad, albite and pericline twinning. Olivine is anhedral and fine-grained (0.1-0.5 mm) and it is typically interstitial. Clinopyroxene is also anhedral and fine-grained (Fig. 21F). Opaque minerals consist of interstitial disseminated magnetite. Biotite is interstitial and is locally associated with orthopyroxene (Fig. 21F).

In summary, these samples for Ombuku North exhibit cumulate textures. The orthopyroxene grains are euhedral to anhedral, and the plagioclase grains are granular. The websterite shows clinopyroxene exsolution and gradational variations in grain size. Clinopyroxene shows annealed textures in the leucotroctolite and (leuco) norite.

Olivine in the leucotroctolite shows no variability in Fo composition, but there is variability in the Ni contents, as well as the Mg# and Cr_2O_3 composition of clinopyroxene and orthopyroxene.

4.2.5 Sulphides of the MUM Intrusions

Sulphides in the surface samples of the MUM intrusions are generally in trace amounts and only the drillcore samples here are used to highlight the sulphide assemblage and textures (Fig. 22A-C).

Sulphide in Ohamaremba consists of 35% modal pyrrhotite and minor chalcopyrite. Pyrrhotite is fine-grained, and forms angular blebs and stringers (Fig. 22A). The sulphide is mainly interstitial and is present at the boundaries of the silicate phases. Chalcopyrite is at the boundary of pyrrhotite–silicate phases. Chalcopyrite also appears to replace pyrrhotite, and is also locally finely disseminated (± pyrrhotite) in altered silicate phases. However, interstitial trace pyrite is also observed locally associated with silicate phases.

Oncócua sulphide comprises 7–10% pyrrhotite and minor chalcopyrite with locally net-textured to semi-massive sulphide (Fig. 22B). Anhedral to subhedral blebs of pyrrhotite are medium- to fine-grained. Chalcopyrite is mainly present in fine-grained stringers associated with pyrrhotite. The sulphide is mainly interstitial to the silicate phases, fills fractures in the silicate minerals and is associated with the altered rims of the silicate minerals. Magnetite, and locally chalcopyrite, appears to replace pyrrhotite. Other samples (i.e., apatite orthopyroxenite) also locally show net-textured sulphide typically associated with the apatite. Trace pentlandite is also observed locally and appears associated with chalcopyrite and pyrrhotite.

Sulphide in Ombuku North comprises <1 disseminated, fine-grained, anhedral-subhedral blebs and stringers of chalcopyrite and pyrrhotite (Fig. 22C). The sulphide appears to be associated with zones of alteration at the boundaries of the silicate minerals. Fine, disseminated sulphide is also interstitially present in zones with less alteration and fills in the exsolution lamellae of some of the coarse-grained silicate

minerals. However, there are also trace pentlandite associated with interstitial chalcopyrite in places and trace pyrite associated with chalcopyrite in fracture of locally large olivine grain.

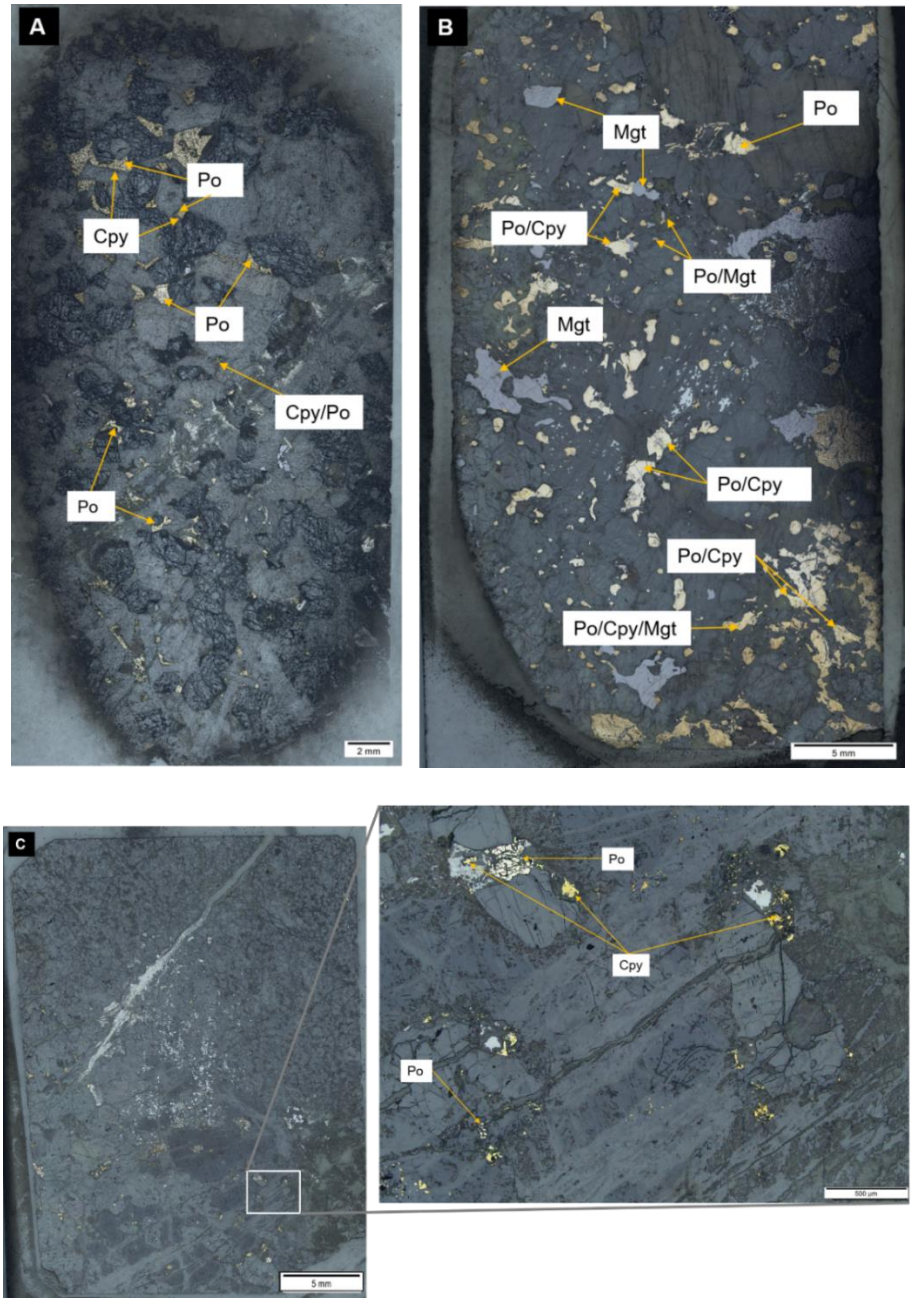


Figure 22: Reflected-Light Photomicrographs (all PPL; 4x magnification) of three drillcore samples from Ohamaremba (KSAT-157), Oncocua (ONC1-59) and Ombuku North (4-778). A) (Leuco) troctolite from Ohamaremba with 3–5% fine-grained anhedral pyrrhotite and minor subhedral blebs/stringers of chalcopyrite; B) Feldspathic

peridotite from Oncocua with 7–10% medium- to fine-grained, anhedral-subhedral pyrrhotite and minor blebs and stringers of chalcopyrite. Chalcopyrite (and magnetite) appears to replace pyrrhotite locally; C) Serpentinised websterite from Ombuku North with 1% fine-grained, anhedral blebs/stringers of chalcopyrite and subhedral pyrrhotite. Cpy (Chalcopyrite), Po (Pyrrhotite), Mgt (Magnetite)

4.3 Major Oxide and Trace Element Geochemistry

The whole rock geochemical data (Table IV.1 in Appendix IV) was used to create several plots to help identify the magmatic evolution and potential sulphide-related ore-forming processes in the MUM intrusions. Figure 23 shows the FeO*-MgO (FeO* = total ferrous iron) compositions of the MUM intrusions compared to well-known magmatic nickel sulphide deposits globally. Figure 24 is an Al_2O_3-Mg# diagram that allows for the discrimination of the cumulate rocks. Figure 25 is a basaltic tetrahedron plot that allows the "crystallisation pathways" of the parent basaltic liquids to be determined. Figure 26 is an Mg-Fe, Al, and Si ternary plot that discriminates between orthopyroxene- and olivine-dominant cumulates. Figure 27 includes AFM and Th/Yb-Zr/Y diagrams to assess the magmatic series affinity. Figures 28A-D are trace ratio-ratio and ratio-major oxide diagrams to assess the degree of partial-melting, magma evolution and magma sources associated with different tectonic settings. Figure 29A-H shows primitive-mantle normalised REE and multi-element diagrams and Table 2 shows the average trace element ratio values. Figure 30 includes Pearce ratio-ratio and La/Sm-Th/Yb diagrams that assess magma-crust interaction, magma sources and tectonic setting. Figures 31 includes diagrams of primitive-mantle normalised PGE to assess for the enrichment in PGE relative to primitive mantle and Cu vs Zr to constrain sulphide liquid addition/extraction. Figure 32 is a Cu vs Ni diagram to assess base metal enrichment.

The MUM intrusions are compared to the parental magmas of world-class magmatic nickel sulphide deposits (Fig. 23). The MUM intrusions plot above and below the 'fertile magma' line. The samples with the lowest MgO and FeO* contents are generally anorthositic in composition, emphasising the strong modal plagioclase control on these compositions. Some samples plot closer to the 'fertile magma' line, including the 2 troctolite-gabbro samples from Ohamaremba, 2 samples from Oncócua,

1 sample from Hamutenha and 1 sample from Ombuku South. These samples are similar in composition to Voisey's Bay, Noril'sk, Midcontinent Rift, H'Shandong, and Savannah. The two Ohamaremba troctolites also plot close to Tamarack. Melatroctolitic samples from Onyokohe (1 sample) and Hamutenha (2 samples) plot outside of the diagram as indicated by the blue dashed arrow. Two troctolitic samples from Otjijanjasemo plot near the Pechenga field. Three samples of Ombuku North and five samples of Ombuku South plot below the 'fertile magma' line.

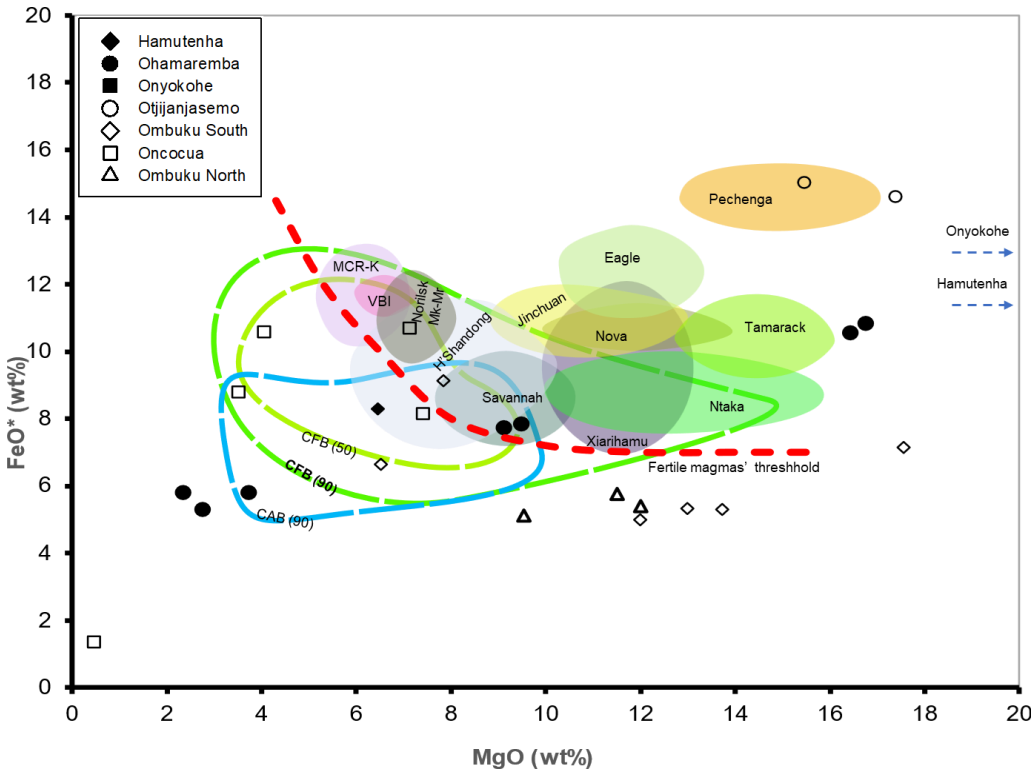


Figure 23: A FeO-MgO (wt%) diagram that includes the parent magma compositions of world-class magmatic Nickel sulphide mineralised intrusions globally. The MUM intrusions associated with the KC are also plotted for comparison (1 sample of Onyokohe and 2 samples of Hamutenha plot outside the diagram as indicated by blue dashed arrow). The liquid composition curve (red dashed line) is the empirical threshold for 'fertile magma' with most Ni-enriched deposits plotting above this line. MCR = Mid-Continent Rift; VBI = Voisey's Bay Intrusion. The circled fields (dashed lines) represent the MgO and FeO* compositional fields of Continental Flood Basalts (CFB) and Continental Arc Basalts (CAB). The plot is modified from Barnes (2023). FeO* represents the total ferrous iron content which was calculated from the total iron content (assuming a ferrous iron proportion of 0.9 in the total iron content).*

Figure 24 allows the compositions of the MUM intrusions (and KC anorthosite suite) to be classified as either cumulates or non-cumulates. Ohamaremba plots in all three cumulate fields, whereas Ombuku North and Ombuku South plot in the mafic and anorthositic cumulate fields only. Ombuku North and South have the highest Mg# of the mafic cumulates ($Mg\#_{83-79}$). Some Ombuku South samples plot in the non-cumulate field and above the anorthositic cumulate field. Otjijanjasemo plots in the mafic and ultramafic cumulate fields. Hamutenha plots in the ultramafic cumulate field and in the mafic non-cumulate field. Oncócua plots above and below the olivine-liquid mixing line in the mafic non-cumulate field. Onyokohe plots in the ultramafic cumulate field with Mg#81.

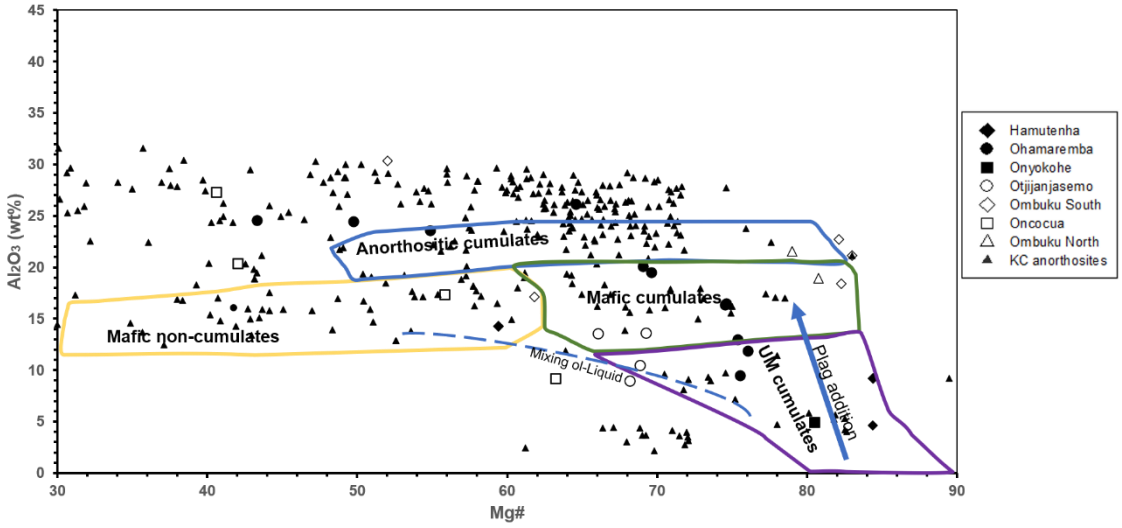
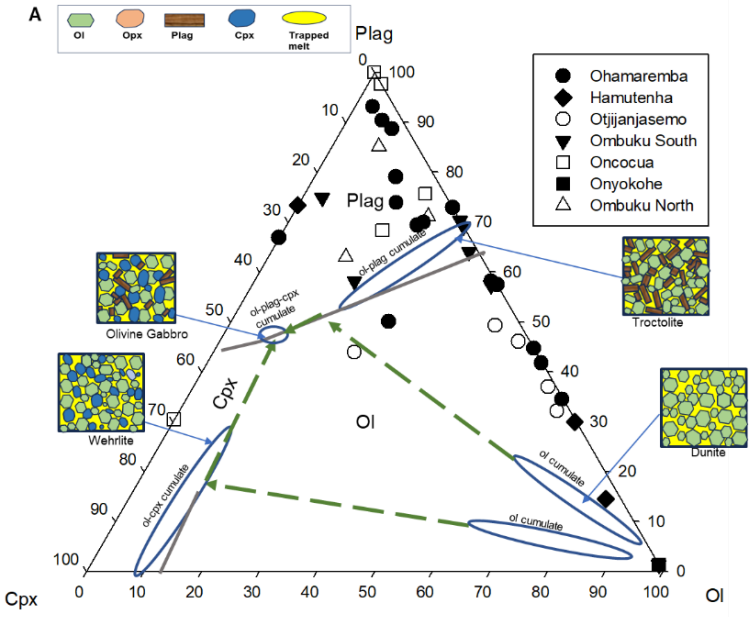


Figure 24: Mg# vs Al_2O_3 plot to discriminate the compositions of cumulate and non-cumulate rocks (from Barnes, 2022). A curve showing the mixing of olivine ("ol") with liquid is shown (dashed blue line). An arrow pointing towards plagioclase addition is also shown. UM = Ultramafic.

CIPW norms were calculated using the whole rock major element oxide data to identify the lithologies of the samples that were not described using the microscope due to their intense alteration. The normative minerals of the samples are plotted on two ternary plots that show the crystallisation sequences of basaltic liquids (Figs. 25A-B), similar to what is done with the modal abundances in section 4.2 (Figs. 14A-B). In Fig. 19A,

the plot shows that most samples follow olivine-plagioclase and plagioclase ± olivine ± clinopyroxene crystallisation pathways. A sample from Oncócua shows a pathway of olivine-clinopyroxene close to the olivine-clinopyroxene cumulate field. The Onyokohe sample is adjacent to the olivine cumulate field. One Hamutenha sample plots close to the olivine cumulate field. In Figure 18B, the Onyokohe sample, Hamutenha (2 samples), Ombuku South (2 samples), Ohamaremba (5 samples) and Otjijanjasemo (4 samples) show olivine-orthopyroxene ± plagioclase crystallisation pathways. Ombuku South (3 samples), Ombuku North (3 samples), Oncócua (5 samples) and Hamutenha (1 sample), together with other samples from Ohamaremba (5 samples), may follow the same crystallisation path, but with more evolved compositions with minor to no olivine. One sample of Ombuku South has a crystallisation pathway of olivine ± orthopyroxene with almost no plagioclase and minor silica. All intrusions show different proportions of silica addition.



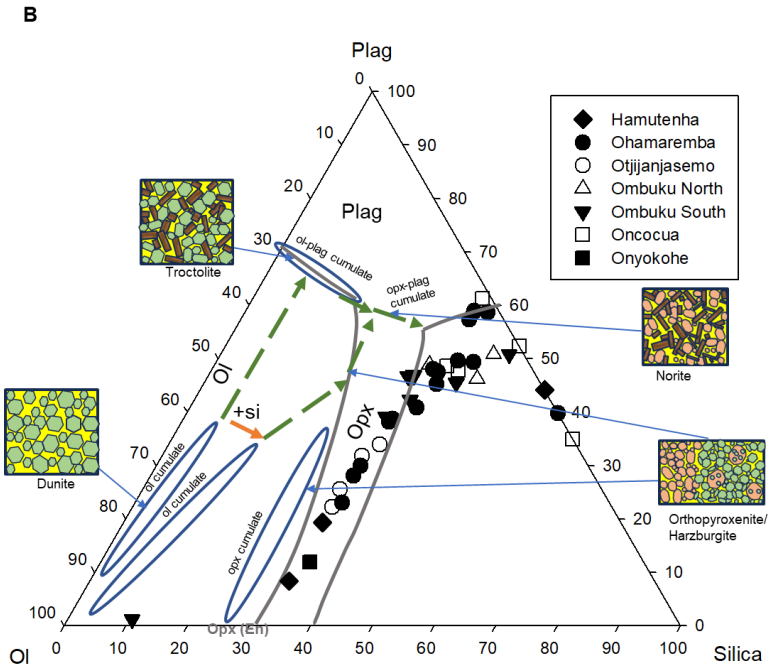


Figure 25: Whole rock data of the MUM intrusions used to determine the normative mineralogy of the samples by CIPW(Cross, Iddings, Pirsson and Washington) Norm and plotted in the ternary plots of crystallisation sequences of basaltic liquids modified from Barnes (2023) (A and B). The ellipsoidal circles are zones of cumulates (dark blue). A) Basalt Tetrahedron System of Ol-Plag-Cpx following a normal pathway of crystallisation sequences; B) Basalt Tetrahedron System Ol-Plag-Silica (silica includes Opx) of crystallisation sequences after addition of silica (e.g., Crustal input). Ol= Olivine, Plag=Plagioclase. Cpx=Clinopyroxene and Opx=Orthopyroxene.

Figure 26 allows the MUM samples to be compared to various ultramafic-mafic cumulate and non-cumulate fields. Samples from Hamutenha (2 samples), Onyokohe, and, to a lesser extent Ohamaremba (1 sample) and Otjijanjasemo (1 sample), plot in the olivine cumulate field and extend towards Si-enrichment. Some samples from Ohamaremba and Otjijanjasemo plot in the mafic cumulate field together with a sample from Ombuku South. Some samples of Ombuku South and Ohamaremba, together with a sample from Oncócua, and all samples of Ombuku North, plot between the mafic cumulate and non-cumulate fields. Three samples of Oncócua, three samples of Ohamaremba and one sample of Hamutenha plot below the non-cumulate and mafic cumulate fields. None of the sample plots in the orthopyroxene-rich cumulate field,

although there are samples that plot in the mafic cumulate and non-cumulate fields on the extended orthopyroxene + liquid mixing line.

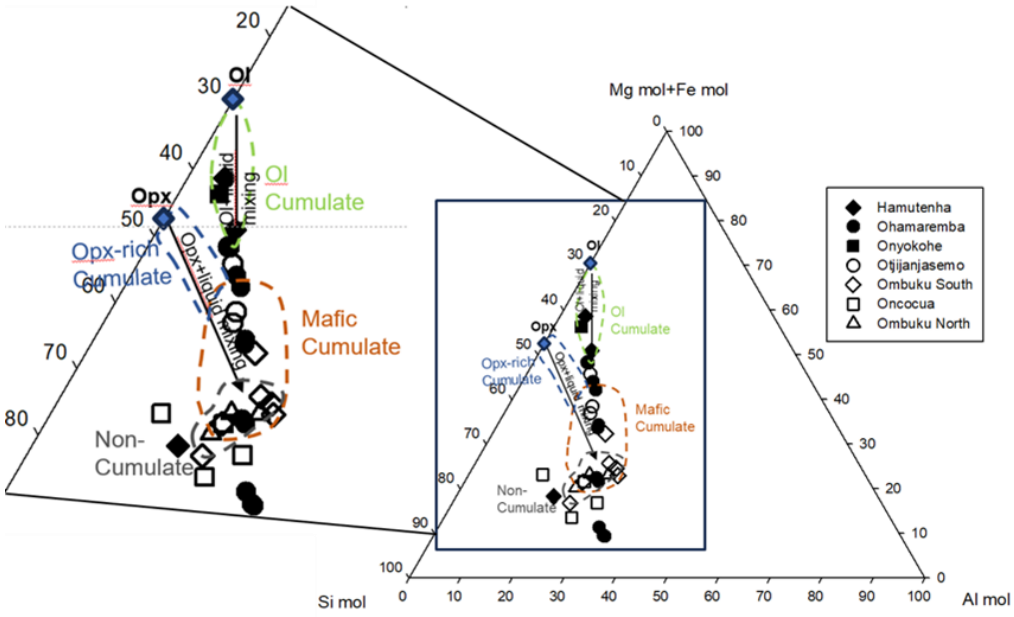
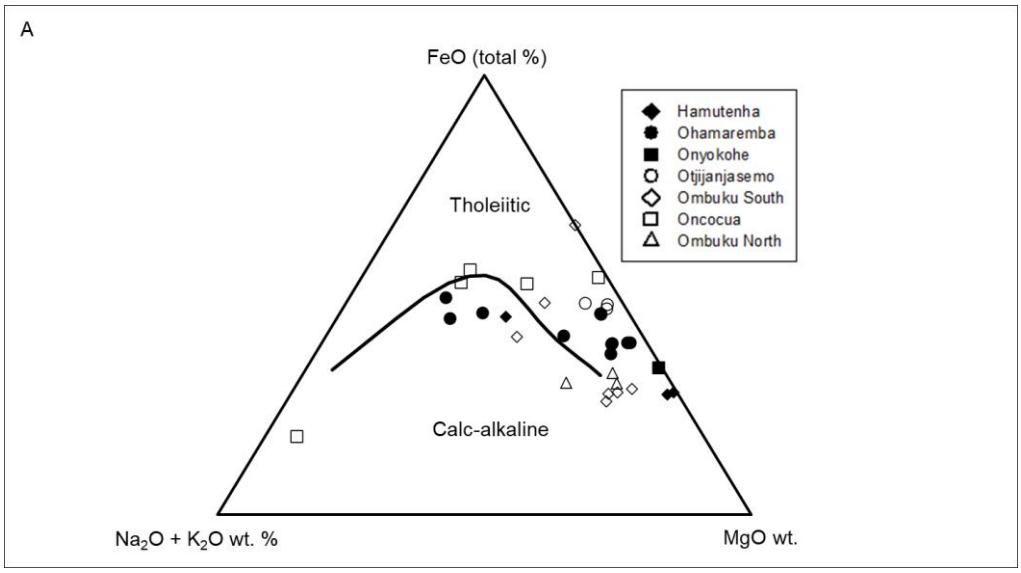


Figure 26: Whole rock data of the MUM intrusions plotted in a Ternary Si-Al-Mg+Fe diagram. The delimited fields (fields with blue outlines) represent areas of olivine- and orthopyroxene-dominated cumulates as well as mafic cumulates and non-cumulate gabbros. The arrows represent the trend of evolved liquid with olivine and evolved liquid with orthoproxene. The plot is modified from Barnes (2023).

Figure 27 provides constraints on the magmatic affinity and evolution of the MUM intrusions. The ternary AFM diagram shows that some samples are classified as calc-alkaline whilst others extend towards Fe-enrichment (tholeiitic), even within the same intrusion (Fig. 27A). A sample from Oncócua shows very high Na_2O+K_2O and low MgO and FeO (total). A discrimination plot showing ratios of immobile incompatible trace elements is shown in Figure 27B (Zr/Y vs Th/Yb: Sappin et al., 2022) considering many of the samples are altered and it is likely that their major oxide compositions are no longer primary. Most samples show a positive correlation towards high Zr/Y (>2) and Th/Yb (>0.3) and are located in the transitional and calc-alkaline fields. One sample from Ombuku South plost at low Zr/Y and Th/Yb in the tholeiitic field.



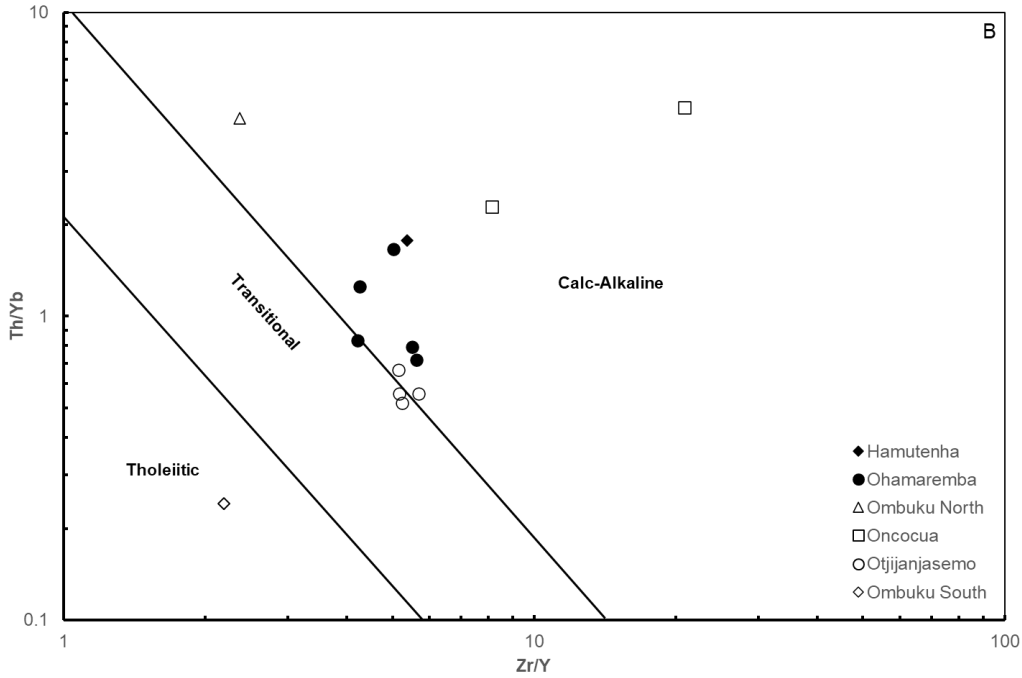


Figure 27: Major oxides and trace element ratio diagrams to assess the magmatic affinity of the MUM intrusions. A) Ternary AFM diagram (after Irvine and Baragar, 1971) shows that most of the MUM samples follow a calc-alkaline trend, towards alkali-enrichment whereas some plot on a tholeiitic trend, towards Fe-enrichment. B) A Zr/Y vs Th/Yb diagram (e.g., Ross and Bédard, 2008; Sappin et al., 2022) showing that most of the MUM samples plot in the transitional and calc-alkaline fields. AFM: A(Na_2O+K_2O); F($FeO+Fe_2O_3$); M(MgO).

Figure 28A shows that most of the intrusions cluster together towards high Ce/Zr and moderate Ce/Nb and seem to positively correlate, although three Ombuku South samples, one Oncócua sample, and, to a lesser extent, one Ohamaremba sample are outside of the main cluster. Figures 28B-C show that samples from Ombuku North, Onyokohe, together with two samples from Ombuku South, have low Ce/Yb (< 10) with high Cr_2O_3 and low TiO_2. Samples of Oncócua, Ohamaremba, Otjijanjasemo and Hamutenha, together with some samples of Ombuku South, have high Ce/Yb (>10) with low Cr_2O_3 and high TiO_2. Oncócua also shows scattered data points. Figure 28D shows that most of the intrusions have Zr/Nb values between 10-30 and two samples from Ombuku South have Zr/Nb values >30 and are in the field of N-MORB. Two samples from Oncócua and one sample from Ombuku South have Zr/Nb values of <10 and are in the field of the OIB. The reference Zr/Nb values are from Winter (2001).

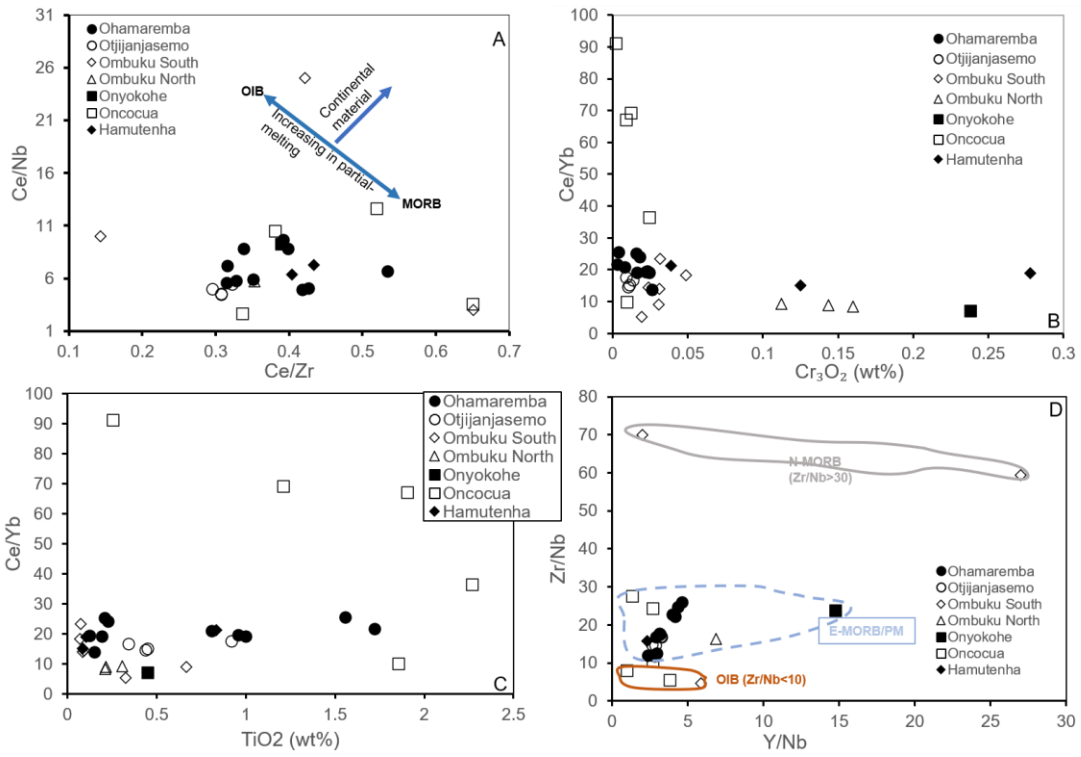
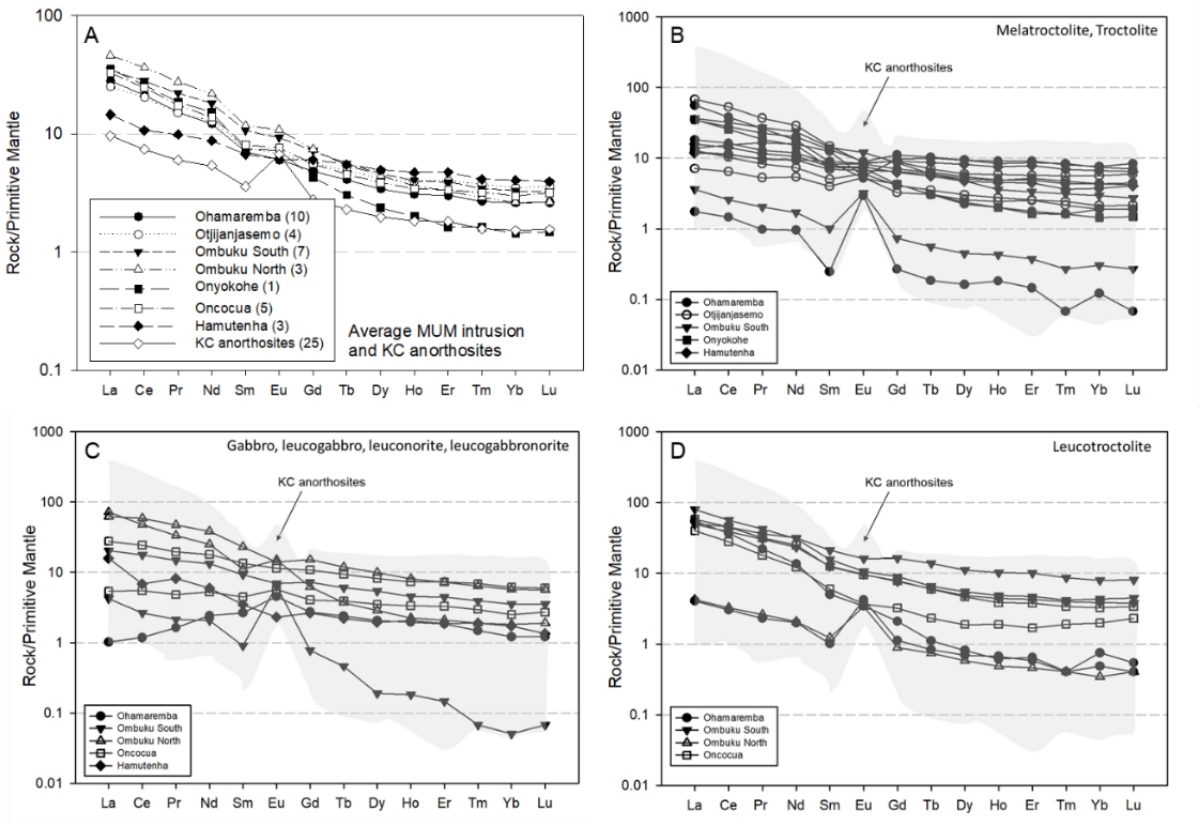


Figure 28: Trace element ratios and major oxides of the MUM intrusions to assess magma sources and magma evolution in the crust. A) Ce/Zr vs Ce/Nb evaluates the degree of partial-melting (negative blue double-arrow line) with two possible end-member sources (OIB = Ocean Island Basalt and MORB = Mid-Ocean Ridge Basalt),

continental material involvement (positive blue arrow). B) Ce/Yb vs Cr_3O_2 evaluates the degree of parental magma evolution. C) Ce/Yb vs TiO_2 evaluates the degree of parental magma evolution and assimilation-fractional crystallisation. D) Y/Nb vs Zr/Nb identifies possible magma sources. Endmember values and trends are from Winter (2001).

All trace element data were normalised to Primitive Mantle values taken from Sun and McDonough (1989) (Figs. 29A-H). Table 3 shows average values of trace element ratios that were used to quantify the patterns in the diagrams. In general, the MUM intrusions, and the KC anorthosite suite, show gentle enrichment in LREE over HREE (Figs. 29A-D). The average Ce/Yb_N and La/Yb_N values of the MUM intrusions range between 5–25 and 3–18, respectively, with Hamutenha and Otjijanjasemo showing the lowest Ce/Yb_N and La/Yb_N values and Ombuku South, Ohamaremba and Onyokohe showing the highest values. The melatroctolite, troctolite, leucotroctolite, gabbro, leucogabbro, leuconorite and leucogabbronorite of the intrusions overlap with the KC anorthosite suite (range based 25 anorthosite samples). However, two samples from Ombuku South (dunite) and Ohamaremba (troctolite) are less LREE-enriched with HREE-depletion. These samples show moderately high to moderate positive Eu-anomalies. The other troctolite and melatroctolite are closely spaced relative to one another. The gabbro, leucogabbro, leuconorite and leucogabbronorite show a gentle pattern of LREE-enrichment relative to HREE and some samples are almost flat (i.e., the Oncócua gabbro and Hamutenha gabbro and to lesser extent Ombuku South leucogabbro) (Fig. 29C). Ombuku North leucogabbro and leuconorite show the greatest enrichment in LREE/HREE. An Ohamaremba leuconorite shows the least LREE-enrichment, and is relatively enriched in MREE, with low values of La/Yb_N (0.84), La/Sm_N (0.383), Gd/Lu_N (2.24) and Eu/Eu* (1.68). An Ombuku South leucogabbronorite shows depletion in HREE with a moderate positive Eu-anomaly. The leucotroctolites show REE-enrichment in general with the exception of two Ohamaremba samples and one Ombuku North sample that show HREE-depletion with least LREE-enrichment (Fig. 29D).


A
Rock/Primitive Mantle
100
10
1
0.1
La Ce Pr Nd Sm Eu Gd Tb Dy Ho Er Tm Yb Lu
Ohamaremba (10)
Otjijanjasemo (4)
Ombuku South (7)
Ombuku North (3)
Onyokohe (1)
Oncocua (5)
Hamutenha (3)
KC anorthosites (25)
Average MUM intrusion and KC anorthosites
B
Melatroctolite, Troctolite
KC anorthosites
1000
100
10
1
0.1
0.01
Ohamaremba
Otjijanjasemo
Ombuku South
Onyokohe
Hamutenha
C
Gabbro, leucogabbro, leuconorite, leucogabbronorite
KC anorthosites
Ohamaremba
Ombuku South
Ombuku North
Oncocua
Hamutenha
D
Leucotroctolite
KC anorthosites
Ohamaremba
Ombuku South
Ombuku North
Oncocua

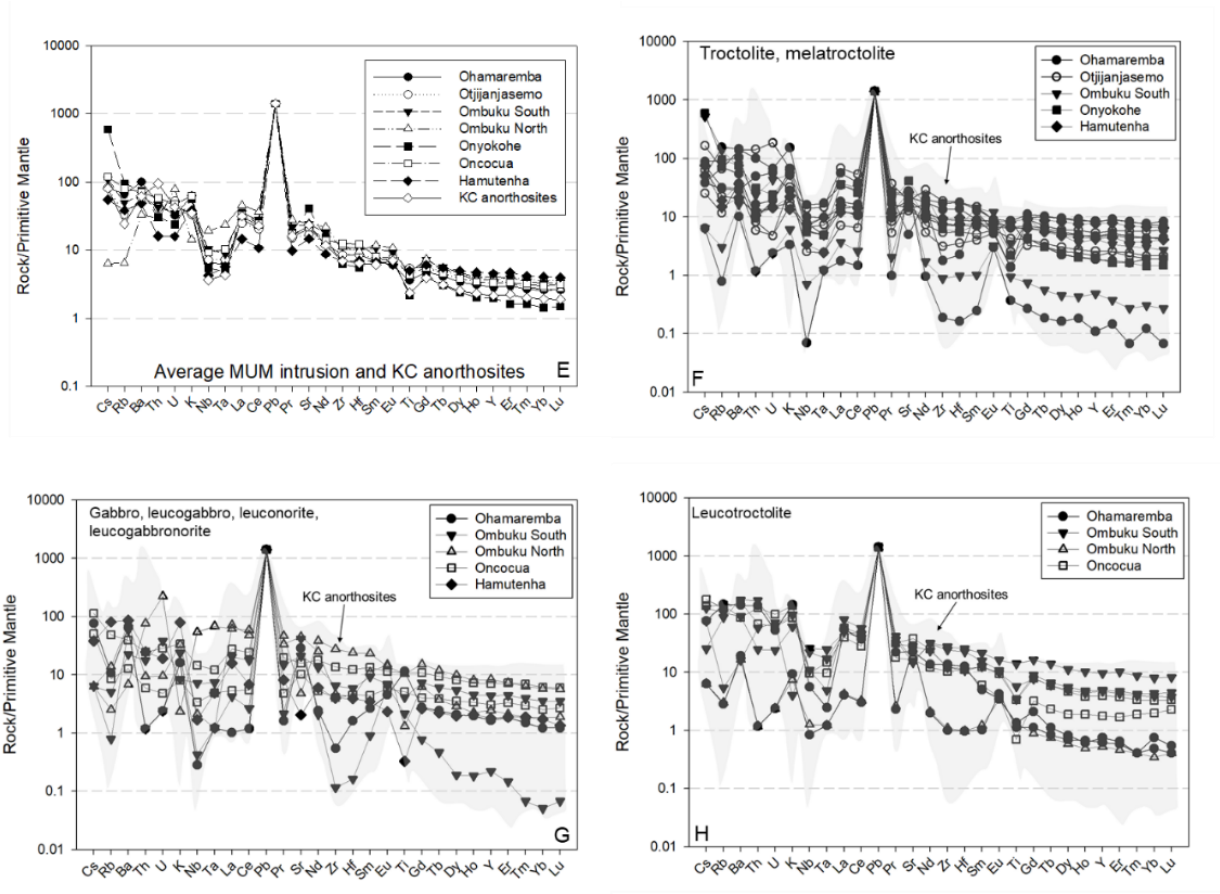


Figure 29: Primitive mantle normalised multi-element diagrams of the MUM intrusions (average values for particular rock types from each intrusion are shown in each diagram) and the KC anorthosite suite. A-D) Primitive Mantle normalised Rare Earth Element (REE) diagrams of selected samples of the MUM intrusions. E-H) Primitive Mantle normalised multi-element diagrams of selected samples of the MUM intrusions. The numbers in brackets represent the number of samples in the calculated average. The grey shaded area in each rock-type represents the range of the 25 KC anorthosite suite samples. Primitive Mantle values are from Sun & McDonough (1989).

Table 3: Average primitive mantle normalised trace element ratios of the MUM intrusions and the KC anorthosite suite. Hamutenha and Otjijanjasemo intrusion show the lowest LREE/HREE values (La/Yb_N and Ce/Yb_N) while Onyokohe, Ohamaremba and Ombuku South show the highest. Ombuku North and to a lesser extent, Hamutenha, show the lowest LILE (Large Ion Lithophile Elements)/HFSE (High Field Strength Elements) values (Rb/Sr_N and Th/Y_N), while Oncocua and Ohamaremba show the highest LILE/HFSE. Hamutenha shows the lowest Eu/Eu values whereas Ohamaremba and Ombuku South show the highest Eu/Eu* values. Eu/Eu* was calculated using the formula: $Eu/Eu^* = Eu_N/\sqrt{[(Sm_N)(Gd_N)]}$ (Rollinson, 1993).*

Normalised ratio	*Oncócua*	*Ohamaremba*	*Ombuku North*	*Onyokohe*	*Ombuku South*	*Otjijanjasemo*	*Hamutenha*	*KC anorthosite suite*
La/Yb_N	15.08	22.25	20.72	24.56	21.57	6.17	5.07	18.33
Ce/Yb_N	10.57	15.41	15.24	17.88	15.07	5.09	3.14	12.52
Eu/Eu*	1.39	3.89	1.94	1.28	2.30	1.14	0.93	5.62
Rb/Sr_N	3.71	3.72	0.26	2.30	2.04	1.93	2.61	1.05
Th/Y_N	33.90	34.30	7.69	15.46	10.47	11.49	3.55	44.08

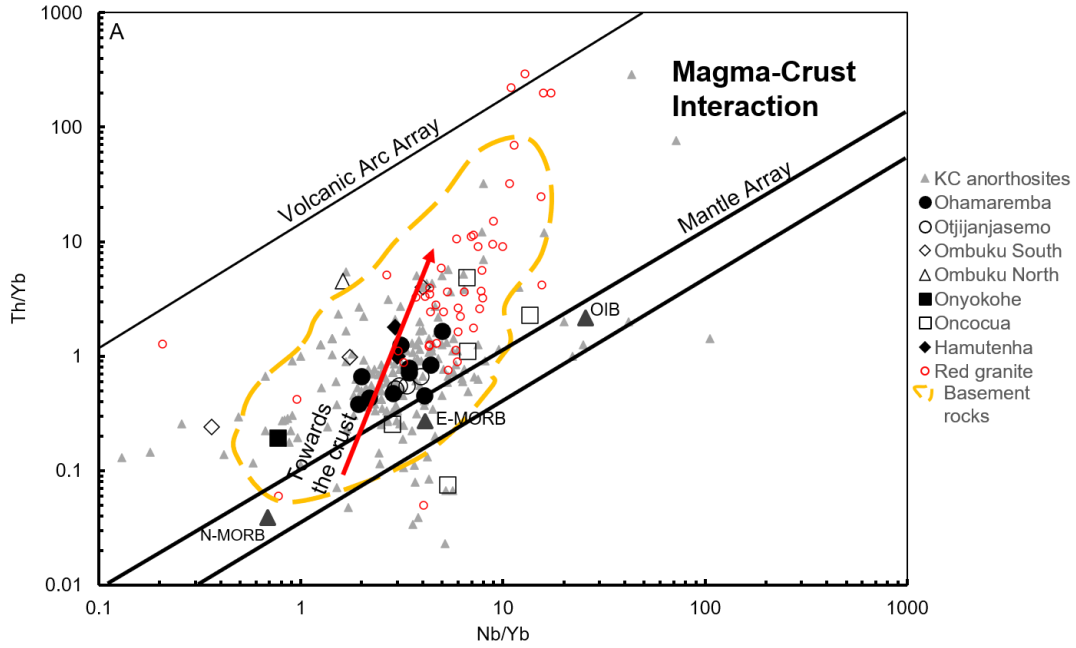
The multi-element diagrams show enrichment Large Ion Lithophile Elements (LILE) and High Field Strength Elements (HFSE), with Th/Y_N and Rb/Sr_N values ranging between 3–34 and 0.3–4, respectively (Fig. 29E-H, Table 3). Hamutenha shows the lowest Th/Y_N values whereas Ohamaremba and Oncócua show the highest Th/Y_N values. The MUM intrusions (and KC anorthosite suite) show generally similar patterns and show moderately high to moderately small negative Nb-Ta ± Th-U anomalies and moderately small negative Ti anomalies (Fig. 29E). The intrusions also show moderately small positive Sr anomalies. However, Ombuku North shows the least Cs-, Rb-, Ba-and K-enrichment while Onyokohe shows the most Cs- and Rb-enrichment with the least HFSE-enrichment. The KC anorthosite suite (average based on 25 samples) show the most negative Nb-Ta and Ti anomalies with the most positive Th anomalies in comparison to the MUM intrusions (Fig. 29E). The intrusions plot inside the field of the KC anorthosite suite (Fig. 29F-H). The troctolite and melatroctolite show moderately high to moderately small negative Nb-Ta ± Th-U anomalies, high to slightly negative Zr ± Nd ± Hf ± Sm anomalies and slight negative Ti anomalies with moderate positive Sr anomalies (Fig. 29F). However, two samples from Ombuku South and Ohamaremba show also moderately high to moderate positive

Eu anomalies, and they show the least LILE-enrichment (Rb-depletion in Ohamaremba troctolite) and the most HFSE-depletion. One Otjijanjasemo troctolite also shows a slight positive Th-U anomaly. An Ohamaremba troctolite and an Ombuku South dunite are the least LILE-enriched with depletion in Rb, Nb and most of the least incompatible elements. The gabbro, leuconorite, leucogabbro and leucogabbronorite show moderate to small negative Nb-Ta, Th-U anomalies, moderate to slight negative Zr-Hf anomalies and moderately small to slight negative Ti anomalies with moderately to slight positive Sr anomalies (Fig. 29G). However, the Ombuku North leucogabbro shows a moderate positive Nb-Ta anomaly, and moderate positive Th-U anomalies with a small negative Sr anomaly. An Ombuku South leucogabbro shows depletion in Rb, Nb and most of the least incompatible elements. The Hamutenha gabbro and Ombuku South leucogabbronorite show slight negative Sr anomalies and the Hamutenha gabbro also shows depletion in Ti. The leucotroctolites show moderate to moderately small negative Nb-Ta anomalies, moderate to slight positive Th-U anomalies and moderately small to slight positive Ti anomalies (Fig. 29H). Two leucotroctolites from Ohamaremba (1) and Ombuku North (1) show positive Sr anomalies with negative Nb-Zr-Hf-Sm anomalies and moderately small negative Eu anomalies. These samples, together with another Ohamaremba sample and Ombuku North, also show depletions in some of the least incompatible elements. The Oncócua leucotroctolite shows the most Cs and Sr-enrichment and least Ti-enrichment. The Pb-enrichment in all of the MUM intrusions is matched by the high lower detection limit (Figs 29E-H, Table IV.1).

The Nb/Yb vs Th/Yb plot demonstrates that most samples of the MUM intrusions and the KC anorthosite suite (including the Red Granite Suite) plot in the magma-crust interaction field, close and perpendicular to a mantle array (Fig. 30A). Most of the MUM intrusions and the KC anorthosite suite also plot inside the basement rock field. Some samples from the KC anorthosite suite and one sample from Oncócua plot below the mantle array.

In Figure 30B, Oncócua and Ohamaremba show moderate enrichment in Th/Nb and La/Sm. Otjijanjasemo (4 samples) and Onyokohe shows low Th/Nb and moderately

low La/Sm. Hamutenha (2 samples) shows moderate Th/Nb values and moderately low La/Sm values. Ombuku South (2 samples) shows a trend towards moderate Th/Nb enrichment and low La/Sm. Ombuku North (1 sample) plots at very high Th/Nb and low La/Sm values. Although the KC anorthosite suite is scattered throughout the plot, the majority of the anorthosite samples have moderate to low Th/Nb-La/Sm values. The Red Granite Suite shows a similar trend to Oncócua.



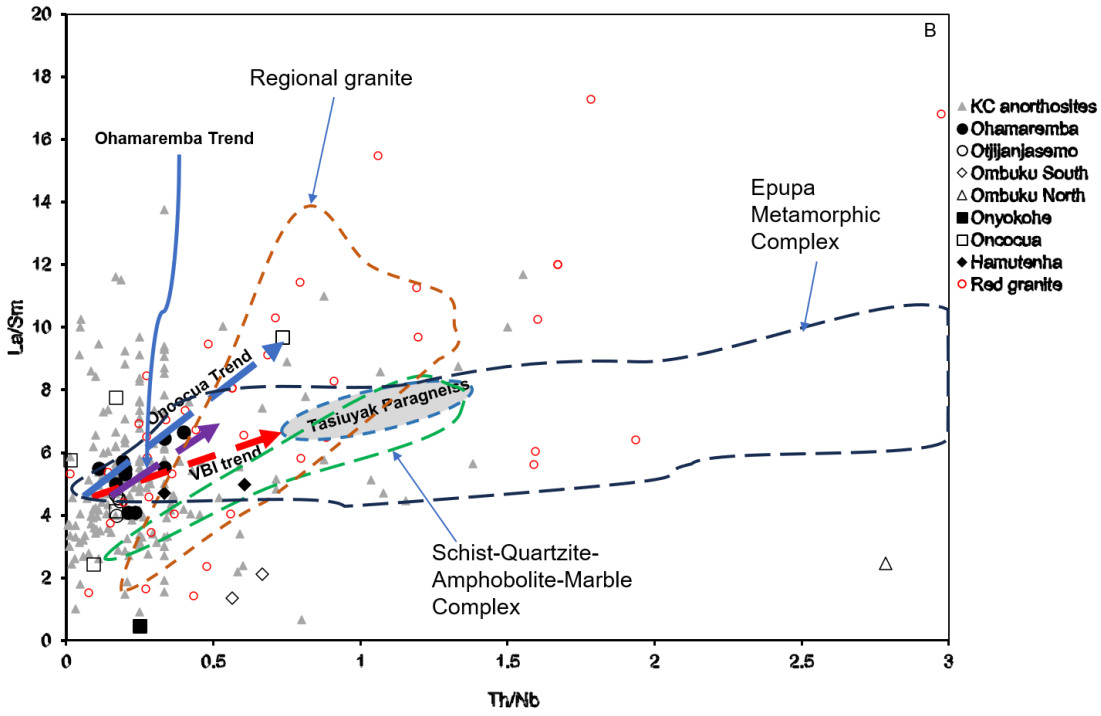
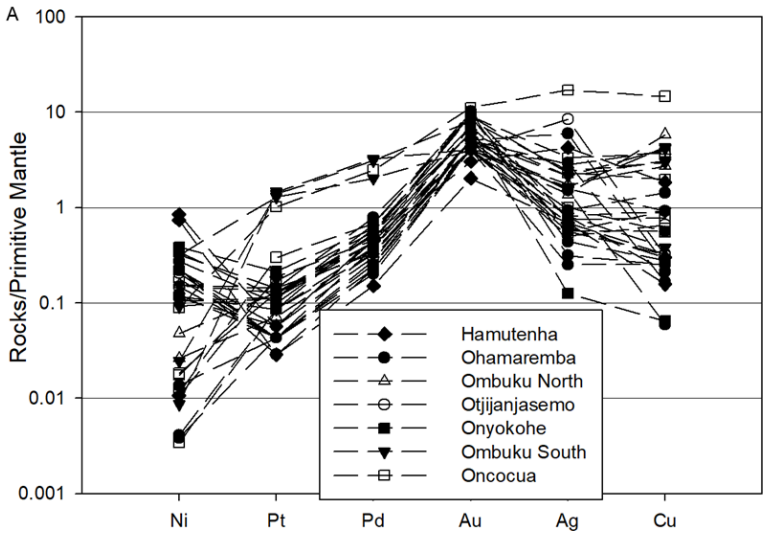


Figure 30: Trace element ratio diagrams to assess magma sources and magma-crust interaction for the MUM intrusions. A) The MUM intrusions plotted on a Th-Yb vs Nb/Yb diagram showing various mantle reservoirs (modified from Pearce, 2008; Sappin et al., 2022); and B) The MUM intrusions plotted on a La/Sm vs Th/Nb diagram that assesses the evidence of crustal contamination. The Regional Granite and Schist-Quartzite-Amphibolite-Marble Complex (SQAMC: green dashed circle) are the basement rocks surrounding Oncócua. The Epupa Metamorphic Complex (EMC: dark blue dashed circle) is the basement rock surrounding Ohamaremba. The Voisey's Bay intrusion contamination trajectory (VBI) towards the Tasiuyak paragneiss is shown for comparison (modified from Li et al., 2000).

The normalised primitive mantle diagram of base metals and PGE shows that all of the MUM intrusions are slightly enriched in PGE (Au ± Ag) (Fig. 31A). Three samples of Ombuku South (a leucogabbro, leucogabbronorite and dunite) and one sample of Oncócua (a leucotroctolite) show slight PGE-enrichment (Pt and Pd). The MUM intrusions show both enrichment and depletion in Cu and depletion in Ni. Ombuku North only shows Cu-enrichments and Ni-depletion.

The plot of Zr versus Cu allows the assessment of sulphide liquid addition or extraction from magma (Fig. 31B). This is because Cu is a highly incompatible chalcophile

element during the crystallisation of cumulus silicate phases. The result is a constant Cu/Zr composition of the residual magma. But, when there is the extraction of cumulus sulphide, Cu becomes depleted relative to Zr (Maier et al, 2013; Barnes, 2022). Cu/Zr values less than the Primitive Mantle value (Cu/Zr < 5) indicate there was the early extraction of sulphide liquid from the magma, whereas Cu/Zr values greater than the Primitive Mantle value (Cu/Zr >5) indicate a magma enriched due to the addition of sulphide liquid. Figure 24B shows that Ohamaremba and Hamutenha, as well as the majority of Oncócua and Otjijanjasemo, and three samples from Ombuku South, plot in the field of sulphide liquid extraction. Ombuku North (3) and other samples from Ombuku South (4), and Oncócua (1) plot in the field of sulphide liquid addition. Two subgroups can be defined within the sulphide liquid extraction field in which a lower subgroup associated with olivine-rich samples (< 60 ppm Zr) and an upper subgroup associated with olivine-poor samples (>60 ppm Zr; the exception is one Otjijanjasemo troctolite). This olivine-based sub-division includes samples of Ohamaremba (9), Oncócua (1), Ombuku South (3), Otjijanjasemo (3), Hamutenha (1) and Onyokohe (1) and is characterised by lower Zr-Cu. The Olivine-poor subgroup includes samples of Otjijanjasemo (1), Hamutenha (1), Oncócua (3), and Ohamaremba (2) and is characterised by higher Zr-Cu.



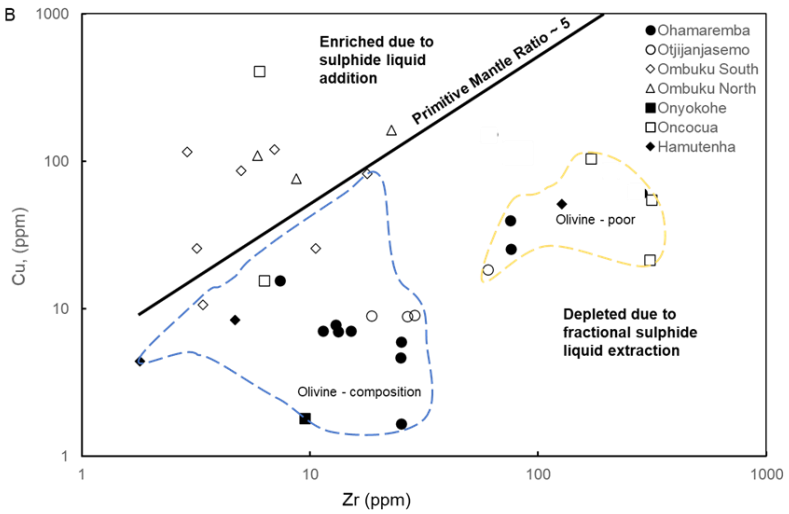


Figure 31: Diagrams of primitive mantle normalised PGE (Platinum Group Elements) and some base metals. A) Plot of Primitive Mantle normalised PGE. B) Plot showing Zr vs Cu to assess evidence of sulphide liquid addition or extraction from sulphur-undersaturated magmas in the MUM intrusions. Primitive Mantle values are from Barnes and Maier (1999). The dashed fields represent clusters of high Zr (> 60 ppm) of olivine-poor rocks and low Zr (< 60 ppm) of olivine-rich rocks. The Cu-Zr plot is modified from Barnes (2023) and Li and Naldrett (1999).

A Ni/Cu ratio plot is shown to assess the base metal enrichment of the MUM intrusions (Fig. 32). The plot shows that Oncócua and Ombuku North have Ni/Cu ratios of 1. Ohamaremba and Ombuku South have Ni/Cu ratios ranging between 1 to 10. Hamutenha, Onyokohe and Otjijanjasemo have Ni/Cu ratios of 10.

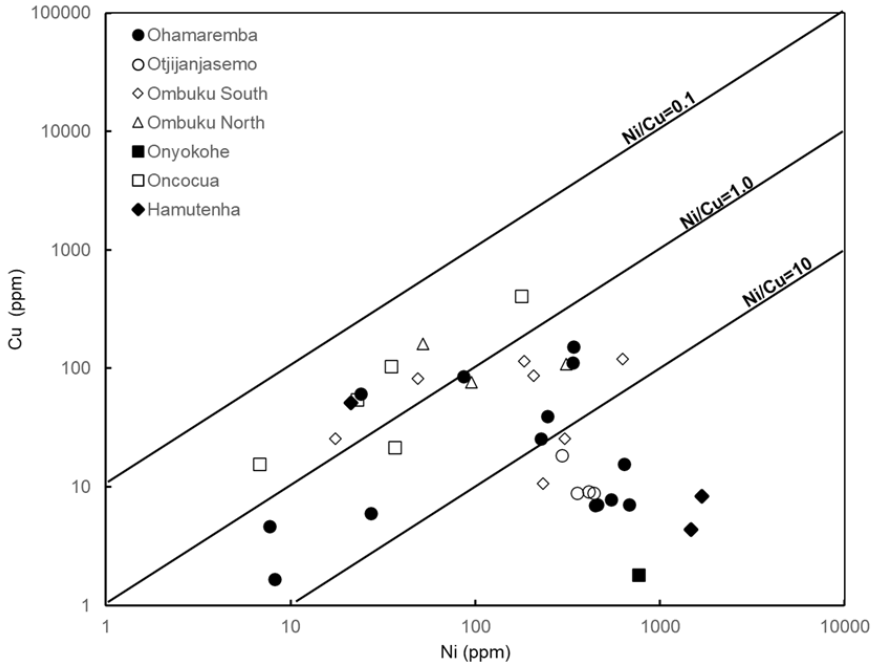


Figure 32: Plot of Ni vs Cu to assess metal enrichment in the MUM intrusions showing which intrusions are likely to be Ni enriched over Cu.

4.4 Sulphur Isotopes

Figure 27 shows the sulphur isotope ($\delta^{34}S$) compositions of the MUM intrusions and their associated basement rocks relative to a mantle $\delta^{34}S$ composition of 0 ± 2‰ (dashed blackline = mantle mean value and pale light blue field = mantle deviation) (Rai and Thiemens, 2007; Libidi et al., 2014; Queffurus and Barnes, 2015). The full dataset is in the Table II.1 in Appendix II. The samples have either negative or positive $\delta^{34}S$ values. Two basement rocks (at Oncócua and Ohamaremba) were not analysed for $\delta^{34}S$ as their sulphur concentrations were too low. Hamutenha has a $\delta^{34}S$ value of +3.11‰ and its associated basement rock has a $\delta^{34}S$ value of -1.64‰. Oncócua has a narrow range of $\delta^{34}S$ values from -0.96 to +0.99‰ while its basement rocks have a relatively wider range of $\delta^{34}S$ values from -0.66 to +2.73‰. Ombuku North has a $\delta^{34}S$ value of -0.05‰, close to the typical mantle value, whereas Ombuku South has a $\delta^{34}S$ value of +1.18‰. Ohamaremba has a wide range of $\delta^{34}S$ values from +2.04 to +6.49‰ and its associated basement rocks have a similar range of $\delta^{34}S$ values from +1.92 to

+6.62‰. Ohamaremba and the associated basement rocks have a wider variability of $\delta^{34}S$ values relative to Oncócua and its associated basement rocks. Otjijanjasemo has a $\delta^{34}S$ value of +1.17‰. Note that Otjijanjasemo and Ohamaremba (the southernmost intrusions) intruded the same basement rocks.

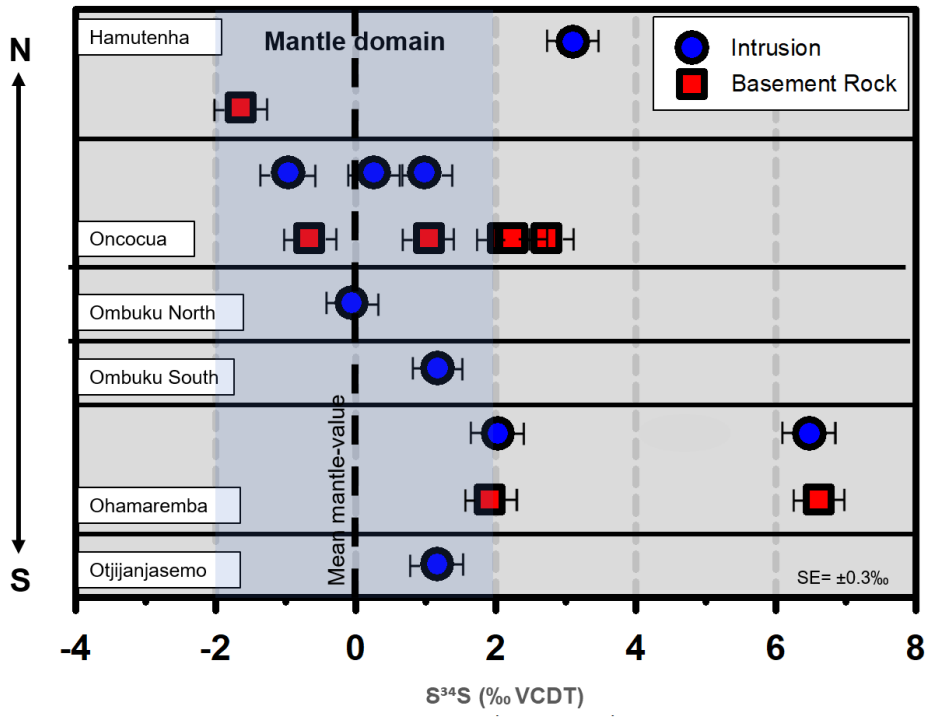


Figure 33: $\delta^{34}S$ values from the MUM intrusions and their associated basement rocks from north to south across the entire western and southern margin of the Kunene Complex. VCDT was used to standardise $\delta^{34}S$. Mantle $\delta^{34}S$ value of 0 ± 2‰ (mean value represented by the dashed blackline and mantle deviation range represented by the pale light blue field) is from Rai and Thiemens (2007), Labidi et al. (2014) and Queffurus and Barnes (2015). VCDT= Vienna-Canyon Diablo Troilite.

4.5 Radiogenic Sr-Nd Isotopes

A total of 28 samples were initially selected and submitted for high-precision radiogenic Sr-Nd isotopic analyses (Table 2). The selection comprises samples of the intrusions and their respective basement rocks to constrain magma sources and

potential contamination sources. Due to severe disruption and delays caused by building renovation work and instrument setup, only six samples were fully analysed for Oncócua at the time this thesis was compiled (Fig 34; Table 4). The collected Sr-Nd isotopic data were age corrected at both 1.4 Ga and 1.8 Ga because the age at which Oncócua crystallised is unclear at the time of this submission.

The initial Sr-Nd radiogenic isotopic compositions are shown in Figure 34 (Table 4, Fig. III.1 in Appendix III). Most of the Oncócua intrusion and the basement rocks plot in the enriched source field (initial $^{87}Sr/^{86}Sr$ values >0.703 and $\varepsilon_{Nd(t)}$ <0) demarcated by CHUR (Chondritic Uniform Reservoir) when Oncócua is considered to be 1.4 Ga (Fig. 34A). At 1.8 Ga, most samples plot in the depleted mantle source field demarcated by initial $^{87}Sr/^{86}Sr$ values <0.703 and $\varepsilon_{Nd(t)}$ >0 (Fig. 34B). Oncócua, at 1.4 Ga, shows values of initial $^{87}Sr/^{86}Sr$ between 0.702442 and 0.705612, initial $^{143}Nd/^{144}Nd$ between 0.51057 and 0.51068 with corresponding $\varepsilon_{Nd(t)}$ between -2.86 and -5.03. The basement rocks west of Oncócua, at 1.4 Ga, show initial $^{87}Sr/^{86}Sr$ between 0.704007 and 0.711739, initial $^{143}Nd/^{144}Nd$ between 0.510599 and 0.510988 with corresponding $\varepsilon_{Nd(t)}$ between -3.28 and -4.36. Oncócua, at 1.8 Ga, shows initial $^{87}Sr/^{86}Sr$ between 0.701570 and 0.705255, initial $^{143}Nd/^{144}Nd$ between 0.51025 and 0.51039 with corresponding $e_{Nd(t)}$ between -1.11 and 1.75. The basement rocks west of Oncócua, at 1.8 Ga, show initial $^{87}Sr/^{86}Sr$ between 0.699195 and 0.702515, initial $^{143}Nd/^{144}Nd$ between 0.51031 and 0.51053 with corresponding $\varepsilon_{Nd(t)}$ between 0.09 and 4.37.

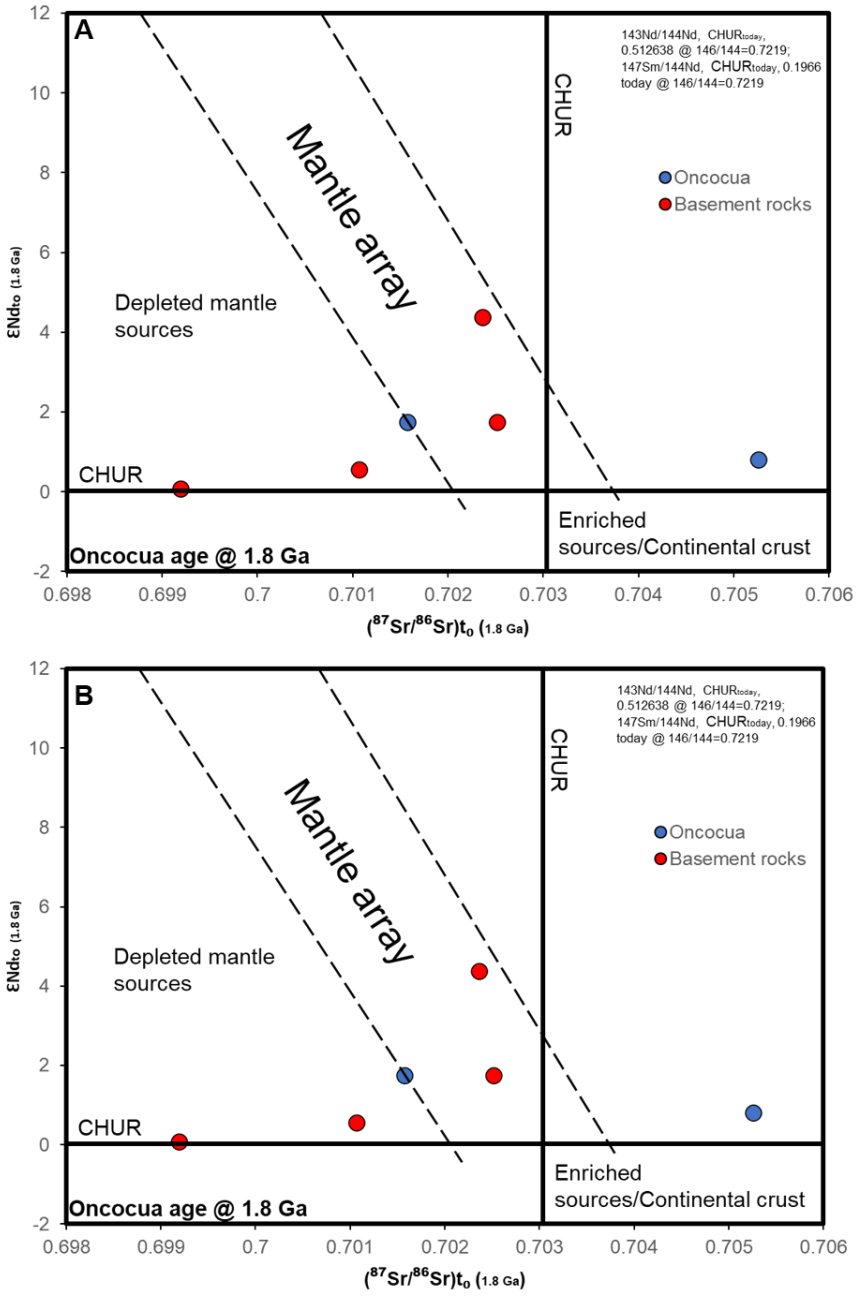


Figure 34: Initial Sr-Nd isotopic compositions of Oncócua and basement rocks. A) Initial $^{87}Sr/^{86}Sr$ and ε_{Nd} for Oncócua and the surrounding basement rocks corrected to 1.4 Ga. B) Initial $^{87}Sr/^{86}Sr$ and ε_{Nd} for Oncócua and the surrounding basement rocks corrected to 1.8 Ga. The 2SE's in initial $^{87}Sr/^{86}Sr$ ratios vary from ± 0.000006 to ± 0.000038. The 2SE's initial $^{143}Nd/^{144}Nd$ used to calculate the initial ε_{Nd} values vary from ± 0.000003 to ± 0.000019. CHUR values are from Gleißner et al. (2011). CHUR = Chondritic Uniform Reservoir and SE= Standard Error.

Table 4: Radiogenic Sr-Nd Isotopic Data for Oncócua and its basement rocks including a BHVO2 standard measurement.

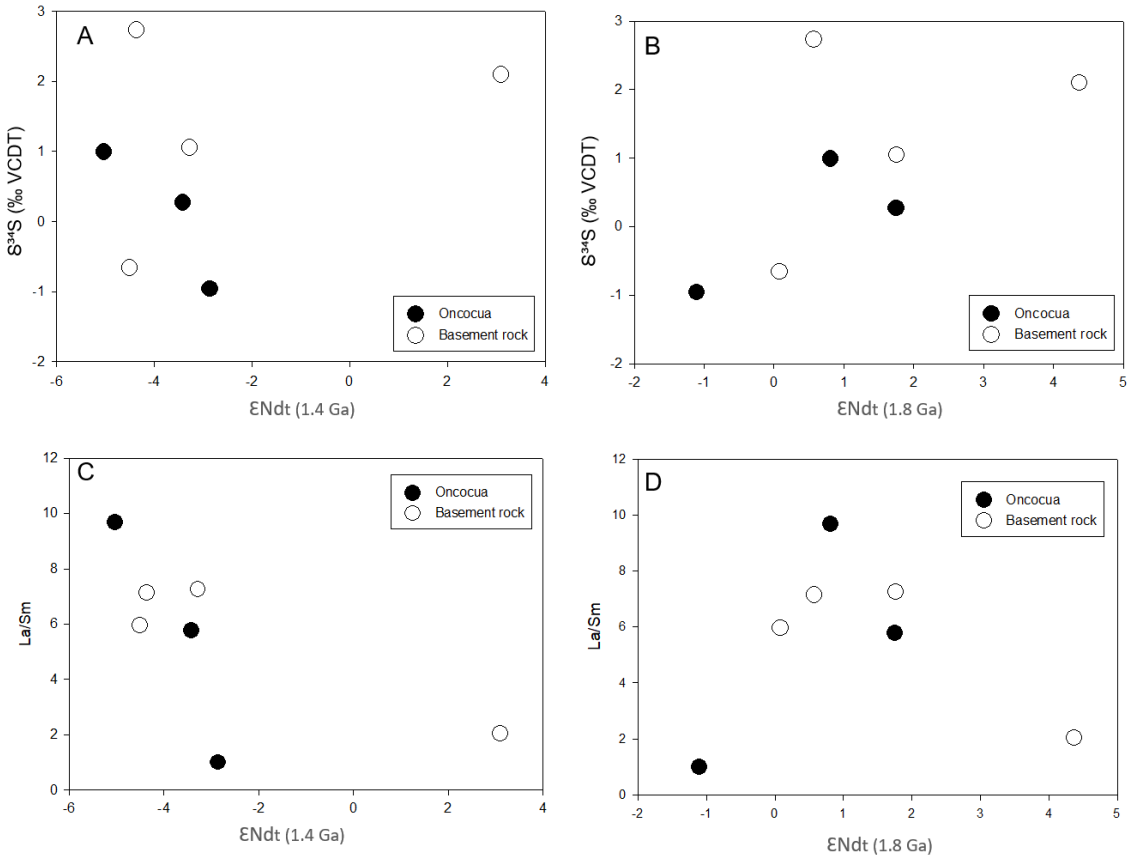
SAMPLEID	Lithology	Setting	Rb (ppm)	Sr (ppm)	$^{87}Rb/^{86}Sr$	Measured $^{87}Sr/^{86}Sr$	Initial $^{87}Sr/^{86}Sr$ at 1.4 Ga	Initial $^{87}Sr/^{86}Sr$ at 1.8 Ga	Sm (ppm)	Nd (ppm)	$^{147}Sm/^{144}Nd$	Measured $^{143}Nd/^{144}Nd$	$^{143}Nd/^{144}Nd$ at 1.4 Ga	Initial εNd ± 2SE(%) at 1.4 Ga	$^{143}Nd/^{144}Nd$ at 1.8 Ga	Initial εNd ± 2SE(%) at 1.8 Ga
KAC242/241	Clinopyroxene Leucotroctolite	Oncócua Intrusion							1.12	4.13	0.164543 ± 7	0.512190 ± 5	0.510684 ± 5	-2.860 ± 001	0.510253 ± 5	-1.114 ± 0.001
KAC245/243	K-feldspar-bearing Leucotroctolite	Oncócua Intrusion	60.63	1141.54	0.15	0.705497 ± 7	0.702442 ± 7	0.701570 ± 7	7.45	46.13	0.09760 ± 28	0.51155 ± 20	0.51065 ± 19	-3.432 ± 0.005	0.51039 ± 19	1.746 ± 0.005
KAC246/244	K-feldspar-bearing Norite	Oncócua Intrusion	14.27	656.91	0.06	0.70686 ± 19	0.70561 ± 19	0.70526 ± 19	7.28	52.13	0.084471 ± 9	0.511346 ± 6	0.510573 ± 6	-5.034 ± 0.002	0.510351 ± 6	0.815 ± 0.002
KAC346	Granodiorite	Basement	66.62	734.15	0.26	0.709227 ± 9	0.704007 ± 9	0.702515 ± 9	8.02	48.35	0.10027 ± 13	0.51158 ± 12	0.51066 ± 12	-3.281 ± 0.003	0.510399 ± 12	1.759 ± 0.003
KAC356-2	Garnet-Amphibole-White Mica	Basement	122.56	189.47	1.87	0.749095 ± 9	0.711739 ± 8	0.701065 ± 8	7.47	44.16	0.102327 ± 6	0.511544 ± 3	0.510607 ± 3	-4.3637 ± 0.0009	0.510339 ± 3	0.57061 ± 0.0009
KAC357-1	Micaschist	Basement	190.28	267.37	2.07	0.752052 ± 6	0.710942 ± 5	0.699195 ± 5	8.82	48.91	0.109005 ± 5	0.511597 ± 3	0.510599 ± 3	-4.5067 ± 0.0007	0.510314 ± 3	0.0851 ± 0.0007
KAC358	Foliated Amphibolite	Basement	34.06	232.24	0.42	0.71321 ± 39	0.70477 ± 38	0.70236 ± 38	2.88	10.01	0.173943 ± 7	0.512581 ± 5	0.510988 ± 4	3.103 ± 0.001	0.510533 ± 4	4.374 ± 0.001
BHVO2 Standard	Hawaiian Basalt		8.74	379.57	0.07	0.70358 ± 82			6.16	25.90	0.143691 ± 7	0.512963 ± 5				

Obs: The samples were corrected to 1.4 Ga and 1.8 Ga

2SE= 2 Standard Error

2SE on $^{87}Sr/^{86}Sr$ and $^{143}Nd/^{144}Nd$ included errors obtained the analytical runs; SE on $^{87}Rb/^{86}Sr$ and $^{147}Sm/^{144}Nd$ ratios and the Rb, Sr, Sm and Nd concentrations from analytical runs and corrected for the blanks; Initial $^{87}Sr/^{86}Sr$ and εNd included propagated uncertainties in measured $^{87}Sr/^{86}Sr$, and measured $^{143}Nd/^{144}Nd$ and initial $^{143}Nd/^{144}Nd$, respectively.

The $\varepsilon_{Nd(t)}$ values are also plotted with sulphur isotopic data and whole rock trace elements (Figs. 35A-H). $\varepsilon_{Nd(t)}$ vs $\delta^{34}S$ diagrams show that Oncócua and its basement rocks correlate negatively and positively at 1.4 Ga and 1.8 Ga, respectively (Figs 35A, B). The basement amphibolite shows $\varepsilon_{Nd(t)}$ and $\delta^{34}S$ values that do not negatively correlate at 1.4 Ga and the values positively correlate at 1.8 Ga (Figs 35A, B). $\varepsilon_{Nd(t)}$ vs La/Sm show that Oncócua correlates negatively and positively at 1.4 Ga and 1.8 Ga, respectively (Figs 35C, D). The amphibolite does not appear to be part of the positive correlation trend that is exhibited with the Oncócua samples and the other basement rocks at 1.8 Ga. $\varepsilon_{Nd(t)}$ vs Th/Yb shows a negative correlation at 1.4 Ga (Fig. 35E). While the basement rock samples show a negative correlation, the samples of Oncócua do not show a clear correlation at 1.8 Ga (Figs. 35F). However, the Oncócua norite appears to have broadly similar values to the basement rock garnet-amphibole-white mica at 1.4 Ga and at 1.8 Ga. $\varepsilon_{Nd(t)}$ vs. Ce/Yb shows a negative correlation at 1.4 Ga and a positive correlation at 1.8 Ga (Figs. 35G-H). One Oncócua troctolitic sample, together with the garnet-amphibole-white mica and micaschist, shows decoupling between Th/Yb and Ce/Yb (Figs. 35E-H). Oncócua appears to have higher Ce/Yb ratios relative to its basement rocks.


A
B
C
D
Oncocua
Basement rock
δ³⁴S (‰ VCDT)
εNdt (1.4 Ga)
εNdt (1.8 Ga)
La/Sm

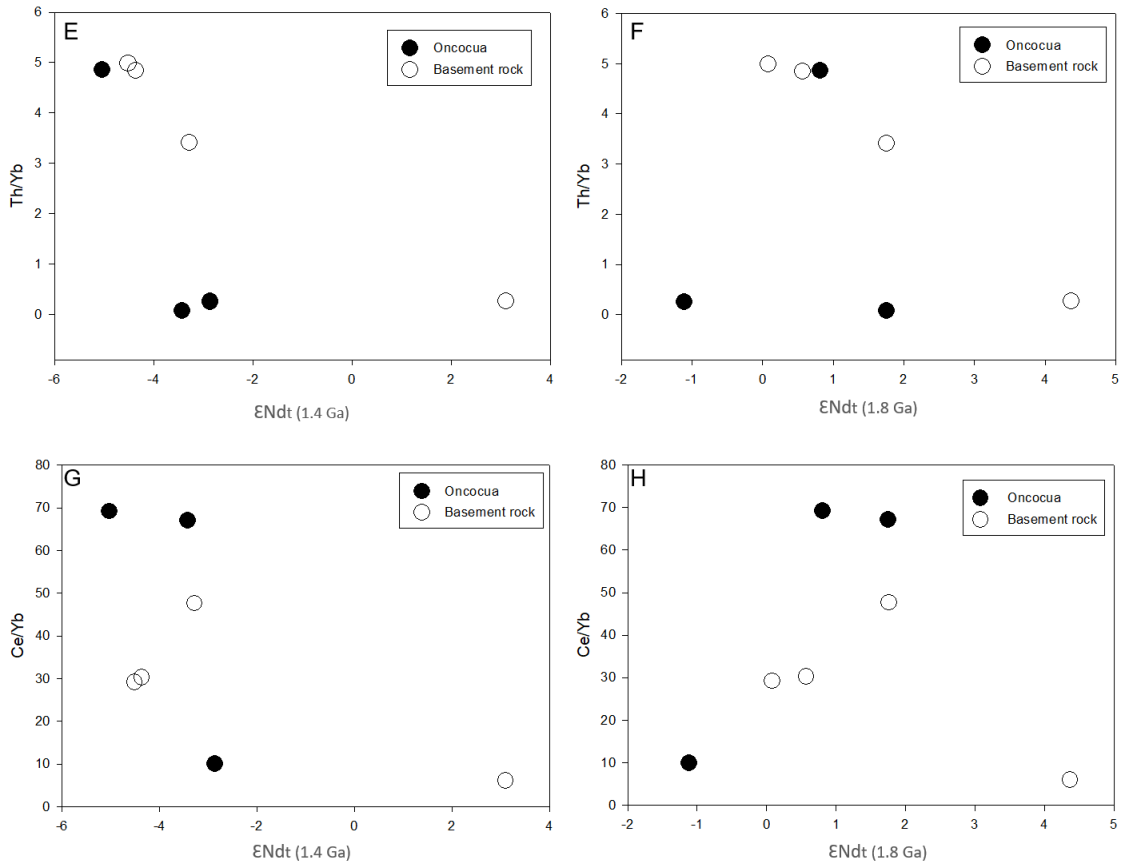


Figure 35: Covariant plots of $\varepsilon_{Nd(t)}$ for Oncócua and its basement rocks (corrected at 1.4 Ga and 1.8 Ga) versus $\delta^{34}S$ and selected trace element ratios. A-B) ε_{Ndt} vs $\delta^{34}S$ showing negative correlation at 1.4 Ga and positive correlation at 1.8 Ga. C-D) ε_{Ndt} vs La/Sm showing negative correlation at 1.4 Ga and positive correlation at 1.8 Ga. E-F) ε_{Ndt} vs Th/Yb showing negative correlation at 1.4 Ga and the basement rocks showing negative correlation at a 1.8 Ga. G-H) ε_{Ndt} vs Ce/Yb showing negative correlation at 1.4 Ga and positive correlation at 1.8 Ga.

Chapter 5: Discussion

The petrological and geochemical data presented in this study provide the basis for a discussion about the possible genetic relationships between the mafic-ultramafic (MUM) intrusions and the Kunene AMCG Complex (KC) while attempting to characterise the evidence of ore-forming processes using the mineral system approach and a table below summarises the results in section 4 (Table 5). This will allow for some conclusions about the potential of the KC to host economic Ni-Cu-(Co-PGE) mineralisation and for guiding future mineral exploration in this region. However, before proceeding with the discussion, it is important to revisit certain elements of the MUM intrusions at the western margin of the KC that were highlighted in the literature review section to assist in contextualising the discussion.

Table 5: Summary result of the data of the MUM intrusions.

	HAMUTENHA	ONCOCUA	OHAMAREMBA	OMBUKU NORTH	OMBUKU SOUTH	OTJIJANJASEMO	ONYOKOHE
Location	Northwesern margin of Angolan KC	Southwestern margin of Angolan KC	South margin of Namibian KC	Southwestern margin of Namibian KC	Southwestern margin of Namibian KC	Southwestern margin of Namibian KC	Southwestern margin of Namibian KC
Age (published age interpreted as crystallisation age)	1800 Ma by Campeny et al., 2023	1400 Ma (apatite age dating) by van Zyl, 2022	1407 Ma (zircon age dating) by van Zyl (2022); 1200 Ma (baddeleyite age dating) by Maier et al. (2013)	1353 Ma (zircon age dating) by van Zyl (2022)		1762 Ma (zircon age dating) by van Zyl (2022)	
Size	3 Km long	9 Km long striking NW-SE	10 Km long striking E-W	2.5 Km long striking NE-SW	8 Km long striking NE-SW	6 Km long striking E-W	6 Km long striking NE-SW
Basement rock: Fieldwork relationship	Granitoid of the ENMC	ENMC and Regional Granite	Granitic gneiss and amphibolite granulite of the ENMC	Granitic gneiss and amphibolite granulite of the ENMC	Amphibolite granulite of the ENMC	Granitic gneiss of ENMC	Migmatitic gneiss of the ENMC
Fieldwork Observations		Pyroxenite with anorthositic/leuconoritic veins, pyroxenitic/basaltic autholiths, magmatic layering	Layered leucotroctolite with pyroxenitic veins	Troctolite with wehrlite bands showing Plag-rich and -poor zonations			
Lithology: Petrography, fieldwork observations	Dunite, Ol gabbro and amphibole diorite (Campeny et al., 2023)	Pyroxenite, feldspathic peridotite, gabbro, Ol gabbro, leuconorite, troctolite, minor melatroctolite	Troctolite, Ol gabbro, melatroctolite, leucotroctolite, norite, leuconorite	Gabbronorite, olivine norite, troctolite, harzburgite, dunite, pyroxenite and websterite	Gabbronorite, olivine norite, troctolite, harzburgite, dunite and pyroxenite	Troctolite	Harzburgite, troctolite and norite
Igneous mineralogy: Petrography and fieldwork observations	Ol, Plag, Cpx, Hbl Campeny et al., 2023)	Ol, Plag, Cpx and Opx, Ap and minor Bt, Fe-oxides	Ol, Plag, Opx, Cpx and minor Bt Fe-oxides	Ol, Plag, Opx, Cpx	Ol, Plag, Opx and Cpx	Ol, Plag and minor Cpx	Ol, Plag and Opx

Igneous texture: Petrography and fieldwork observation	Cumulus and subhedral olivine with interstitial augite and plagioclase and subhdral hornblende	Cumulus olivine and pyroxene; fine- to medium-grained and subhedral to anhedral olivine; orthopyroxene reaction rims; resorbing chadacrystic olivine enclosed by coarse-grainded altered pyroxene oikocrysts; interstial olivine; clinopyroxene with exsolution lamellae; minor interstitial apatite but can be abundant when associated with pyroxene-dominant lithology	Cumulus olivine, plagioclase and pyroxene; fine- to medium-grained and subhedral to anhedral olivine and plagioclase; pyroxene is mainly interstitial intercumulus and encloses olivine and plagioclase laths; orthopyroxene reaction rim around olivine; serpentinisation in olivine-dominant lithology	Cumulus olivine, pyroxene and plagioclase; fine-grained subhdral to anhedral orthopyroxene; fine-grained subhedral to anhedral olivine; coarse-grained orthopyroxene and clinopyroxene with exsolution lamellae; medium-grained olivine associated with coarse-grained orthopyroxene; plagioclase is mainly fine- to medium- grained granular; interstitial clinopyroxene; serpentinisation and amphibolitisation	Samples largely affected by amphibolitisation and serpentinization	Cumulus olivine and plagioclase with interstitial intercumulus pyroxene (mainly clinopyroxene); medium-grained subhedral to anhedral olivine partially enclosing plagioclase; fine-grained olivine enclosed by clinopyroxene; serpentinisation	sample largely affected by serpentinisation
Crustal contamination: Sulphur isotope signatures, trace element ratios, Sr-Nd radiogenic isotope composition	Crustal contamination, but yet to resolve the source of contamination	Crustal contamination by ENMC and Regional Granite	Crustal contamination by granitic gneiss and amphibolite granulite of ENMC	minimal no crustal contamination	Some crustal contamination, but yet to resolve the source of contamination	Some crustal contamination, but yet to resolve the source of contamination	
Sulphide: Petrography observation	< 1% secondary sulphide (godlevskite and putoranite by *Campeny et al., 2023*)	7-10% pyrrhotite-chalcopyrite ± pentlandite	3-5% pyrrhotite-chalcopyrite ± pentlandite	<2% chalcopyrite-pentlandite	1% disseminated pyrrhotite-pyrite-chalcopyrite	<1% pyrrhotite ± chalcopyrite *(van Zyl, 2022)*	
<u>Geochemistry - bulk rock major Oxide</u>							
Parental magma's similarity of world class sulphide deposit-hosted intrusions by Barnes (2023): MgO vs FeO*	H'Shandong	Norislk Mk-Mr, H'Shandong, MCR-K and Voisey's Bay, Savannah	Savannah, H'Shandong and Tamarack, Xiarihamu		Savannah, H'Shandong	Pechenga	
Cumulate evidence by Barnes (2023): Mg# vs Al2O3, Si-Al-Mg+Fe and crystallisation sequence of basaltic liquid (CIPW Norms)	Ultramafic	Mafic noncumulate	Ultramafic, Mafic and anorthositic	Mafic and anorthositic	Mafic and anorthositic	Mafic and Ultramafic	Ultramafic
<u>Geochemistry - bulk rock trace element</u>	Troctolitic and gabbroic rocks	Gabbroic and troctolitic rocks	Troctolitic and gabbroic rocks	Troctolitic and gabbroic rocks	Gabbroic, troctolitic and dunitic rocks	Troctolitic rocks	Troctolitic rock

Magmati series affinity: Immobile trace element ratio (Zr/Y vs Th/Yb diagram)	Calc-alkaline	Calc-alkaline	Calc-alkaline	Calc-alkaline	Tholeiitic	Calc-alkaline	Calc-alkaline
Parental magma source: Trace element ratios (Ce/Zr vs Ce/Nb; Y/Nb vs Zr/Nb; Nb/Yb vs Th/Yb)	E-MORB/PM	E-MORB/PM and OIB	E-MORB/PM	E-MORB/PM	N-MORB and OIB	E-MORB/PM	E-MORB/PM
Magma evolution: Trace element ratios and major oxides Ce/Yb vs Cr_3O_2 and TiO_2)	Ce/Yb >10	Ce/Yb ≥10	Ce/Yb >10	Ce/Yb <10	<10 Ce/Yb >10	Ce/Yb >10	Ce/Yb <10
LREE/HREE: La/Yb_N	5.07	15.08	22.25	20.72	21.57	6.17	24.56
LILE/HFSE: Th/Y_N	3.55	33.9	34.3	7.69	10.47	11.49	15.46
Eu/Eu*	<1	1.39	3.89	1.94	2.3	1.14	1.28
Sulphide liquid extraction: Cu/Zr (PM ~ 5)	Fractional sulphide liquid extraction/sulphide liquid addition	Fractional sulphide liquid extraction	Fractional sulphide liquid extraction	Sulphide liquid addition	Fractional sulphide liquid extraction and sulphide liquid addition	Fractional sulphide liquid extraction	Fractional sulphide liquid extraction
$\delta^{34}S$ of the MUM intrusions (Mantle-value = 0.00‰)	+3.11	-96 to +99	+2.4 to +6.49	-0.05	+1.18	+1.17	
$\delta^{34}S$ of the basement rocks (Mantle-value = 0.00‰)		-0.66 to +2.73	+1.92 to +6.62				
Magma source and crustal contamination: Initial Sr-Nd isotopic composition		$(^{87}Sr/^{86}Sr$ = 0.702442 to 0.705612, $^{143}Nd/^{144}Nd$ 0.51057 to 0.51068, $\varepsilon_{Nd(t)}$ = -2.86 to -5.03 corrected at 1.4 Ga; $^{87}Sr/^{86}Sr$ = 0.701570 to 0.705255, $^{143}Nd/^{144}Nd$ = 0.51025 to 0.51039, $\varepsilon_{Nd(t)}$ = -1.11 to 1.75.corrected at 1.8 Ga					
Mineral composition							
Ol		Fo_{54-58} in olivine websterite; Fo_{56-59} in feldspathic peridotite	Fo_{67-71} in two troctolitic rocks	Fo_{81} in troctolitic rock		Fo_{64-68} in troctolitic rocks	
Opx		$Mg\#_{73-89}$ in olivine websterite; $Mg\#_{59-62}$ in apatite pyroxenite	$Mg\#_{73}$ in troctolitic sample	$Mg\#_{79-81}$ in troctolitic sample; $Mg\#_{82-85}$ in websterite		$Mg\#_{80}$ in troctolite	

Cpx		$Mg\#_{66-75}$ in olivine websterite; $Mg\#_{68-76}$ in Feldspathic peridotite	$Mg\#_{72-77}$ in troctotic sample	$Mg\#_{81}$ in troctolitic sample; $Mg\#_{85-87}$ in Websterite		$Mg\#_{72-75}$ in troctolite	
Parental magma	Mantle-derived basalt	Mantle-derived basalt	Mantle-derived basalt	Mantle-derived basalt	Mantle-derived basalt	Mantle-derived high MgO-FeO basalt	Mantle-derived basalt

Obs: Ol (olivine); Cpx (clinopyroxene); Opx (orthopyroxene); Plag (plagioclase); Bt (biotite); Ap (apatite); Hbl (Hornblende)
ENMC (Epupa Namibe Metamorphic Complex); PM (Primitive Mantle)

The MUM intrusions were emplaced into a wide range of Palaeoproterozoic basement rocks (Figs. 2, 4, 5, 7, 8, 36 and Table 1). Hamutenha consists of a dunite unit intercalated with olivine gabbro and an amphibole diorite unit, and it is hosted in the Eburnean basement (2040 – 1954 Ma) comprising amphibolite-facies granitoids, ortho- and paragneisses at the periphery of the northern Angolan KC (Campeny et al., 2023). Oncócua comprises pyroxenite and olivine gabbros and is hosted by the ENMC (1861–1757 Ma) in the southern Angolan KC. Oncócua is also in contact with the RGS in the north and south, and the KC anorthosite suite to the east. Ombuku North and Ombuku South are located at the western margin of the Zebra Mountains of the Namibian KC, and comprise similar lithologies including gabbronorite, olivine norite, troctolite, porphyritic harzburgites and dunite, pyroxenite, layered gabbroic rocks and feldspathic harzburgite. However, Ombuku North differs by its abundance of altered ultramafic rock whereas Ombuku South comprises mostly troctolites. While Ombuku North is in contact with the KC in the east, the ENMC in the west and metasedimentary rocks in the north, Ombuku South is completely hosted by the ENMC. Ohamaremba is located in the southern margin of the Zebra Mountains, and consists of troctolite, melatroctolite and olivine gabbronorite. Ohamaremba intruded the amphibolite and granulite gneisses of the ENMC. Otjijanjasemo is a dominantly troctolitic body in the southwestern margin of the Zebra Mountains and it intruded granitic gneisses of the ENMC.

5.1 The Genetic Relationship of the Mafic-Ultramafic Intrusions to the KC Anorthosite Suite

The possible genetic relationships between the MUM intrusions and the KC anorthosite suite have been reported by many workers and, to date, interpretations have mostly been made on the basis of spatial and lithological evidence (e.g., Simpson, 1960; Simpson, 1970; Maier et al., 2013; Rey-Moral et al., 2023). The data presented in this MSc project show that the MUM intrusions are genetically linked to one another broadly based on field relationships and petrological observations as well as geochemical and mineralogical proxies. Spatially, the MUM intrusions are located approximately 0.3 to 15 km away from the western margin of the KC anorthosite suite

and have therefore been referred to as 'satellite' bodies to the KC anorthosite suite (i.e., implying a genetic connection). Ombuku North and Oncócua are the most proximal intrusions to the KC anorthosite suite and are practically in contact with it, while Hamutenha and Otjijanjasemo are the most distal intrusions (Simpson, 1970; Ashwal and Twist, 1994; Maier et al., 2013, van Zyl, 2022; Campeny et al., 2023) (Figs. 2-8).

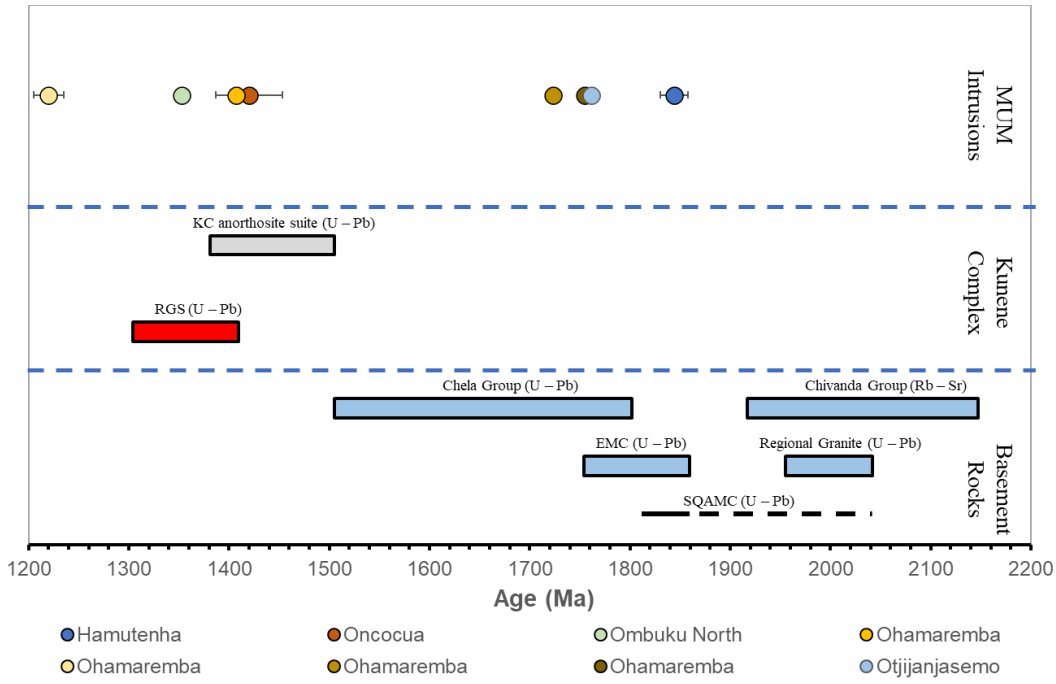


Figure 36: A Timeline showing the published geochronological data for the MUM intrusions, KC and basement rocks. The MUM intrusions have been dated using U-Pb LA-ICP-MS in zircon, with the exception of Oncócua that was dated using U-Pb LA-ICP-MS in apatite (1400 Ma: van Zyl, 2022) and Ohamaremba (the age at 1220 Ma: Maier et al. 2013) that was dated using U-Pb SHRIMP in baddeleyite. van Zyl (2022) obtained the zircon ages for Ohamaremba at 1407 Ma, 1723 Ma and 1755 Ma, Ombuku North at 1353 Ma, Otjijanjasemo at 1762 Ma. Campeny et al. (2022) obtained the zircon age for Hamutenha at 1844 Ma by LA-ICP-MS. The ages of the KC anorthosite suite were obtained from Bybee et al. (2019) and the ages of the Red Granite Suite were obtained from Milani et al. (2022). The ages of basement rocks were compiled from McCourt et al. (2013), Jelsma et al. (2018), Lehmann et al. (2020) and Kunene Team's map (pers. comm.).

The simplest way of testing a possible genetic link between the MUM intrusions and the KC is to precisely date the rocks. The KC anorthosite suite and RGS have both been

well age-constrained in the literature to between 1.5 and 1.37 Ga (Bybee et al., 2019; Milani et al., 2022) (Figs. 2, 36 and Table 1). Such a study to precisely date the MUM intrusions was initiated at the start of this project, however, due to various non-scientific and scientific factors, there are still no firm age constraints on the ages of the MUM intrusions at the time of submission of this thesis. However, during the MSc project, some ages for these rocks have been published (Fig. 36). For example, Campeny et al. (2023) published an age of 1844 ± 14 Ma for a diorite sample from Hamutenha. This is similar to the age of 1803 ± 1.1 Ma for Caongoquepia that was studied in Langa (2019). These two ages suggest that there is mafic magmatism related to the c. 1.8 Ga "Namibe event" which is substantially older than the KC. van Zyl (2022) was able to date zircons from Ohamaremba, Otjijanjasemo and Ombuku North that gave ages ranging between 1800 and 1350 Ma. van Zyl (2022) interpreted the oldest ages to inheritance of older ENMC basement material and suggested that the crystallisation age of these intrusions was around 1400 Ma, which is within the age range of the KC. The U-Pb zircon age dates by LA-ICP-MS of van Zyl (2022) for Ohamaremba (1407 Ma, 1723 Ma and 1755 Ma) are substantially older than the age of 1220 ± 15 Ma that was published by Maier et al. (2013). The date of 1407 Ma was interpreted to represent the crystallisation age of Ohamaremba while the 1723 Ma and 1755 Ma dates were interpreted to represent xenocrysts inherited from the basement rocks into which the intrusions we emplaced. The 1220 Ma age obtained from *in situ* SHRIMP U-Pb dating of baddeleyite grains was interpreted to be the crystallisation age of Ohamaremba (Maier et al., 2013). Maier et al. (2013) suggested that Ohamaremba is part of a late episode of magmatism to the main KC and that at least two distinct generations of troctolite are present in the KC. van Zyl (2022) also reported ages of ~1400 Ma for apatite in drillcore samples from Oncócua and they were interpreted to represent the crystallisation age of Oncócua. The age dating study that ran concurrently with this MSc project has so far yielded similar results to van Zyl (2022) with zircon dates for Oncócua and Ombuku South ranging between 2100 and 1400 Ma (Hayes, pers. comm.). This is ongoing research. At the time of the submission of this thesis, the author of this study cannot confidently conclude whether the MUM

intrusions studied are coeval with the KC. However, the author has been able to test a genetic connection using the trace element and isotopic data presented in the results chapter, and which will be discussed here.

The MUM intrusions are generally small (<10 km in length) and field and petrographical observations show that they comprise mostly ultramafic to mafic to intermediate cumulates (Figs. 13, 14, 18-21). The AFM diagram shows these intrusions correspond to both tholeiitic and calc-alkaline lineages with some samples particularly enriched in MgO (Fig. 27A). These samples appear to have been crystallised from the least evolved magmas (Fig. 27A). As highlighted in the previous section, the AFM trends may be affected by the level of alteration, therefore, a Zr/Y vs Th/Yb plot is used, and these elements are generally immobile (Fig. 27B). This plot shows that most of the intrusions have transitional to calc-alkaline magma series characteristics with the exception of Ombuku South which appears to be part of a tholeiitic magma series (Irvine and Baragar, 1971; Ross and Bédard, 2008) (Fig. 27B). The tholeiitic magma affinity of Ombuku South suggests that the parental magma was produced from an OIB-source. Another hypothesis is that the parental magma was contaminated by a tholeiitic crustal component as it ascended to the upper level of the crust (Sappin et al., 2021).

Barnes et al. (2016) and Barnes (2023) reported that the parental magmas to the majority of intrusions that host magmatic Ni-sulphide deposits are derived by a high degree of partial melting of mantle-like sources, particularly, magmas with trace element compositions similar to primitive mantle field (Pearce, 2008). The whole rock trace element diagrams show that the MUM intrusions are likely to be the result of different degrees of partial melting of multiple mantle sources (Figs. 28A, D and 30A-B). The parental magmas to Ohamaremba, Otjijanjasemo, Ombuku South, Ombuku North, Oncócua, Hamutenha and Onyokohe generally represent a high degree of partial melting (Table 3: La/Yb_N = 5.07 –24.56 and Ce/Yb_N = 3.14 – 17.88) of mantle sources although there is variation between the intrusions and within individual intrusions (Fig. 28A). The parent magma to Ombuku South may have been derived from a low degree

of partial melting. Otjijanjasemo defines its own cluster suggesting that it is probably the result of less variation in the degree of partial melting in the source or that it is derived from a relatively homogeneous source compared to the other intrusions. The Y/Nb vs Zr/Nb relations show that most of the intrusions have been derived from magmas with MORB-like sources (PM or E-MORB) while the magmas that formed Ombuku South (2 samples) may be from N-MORB-like sources (Zr/Nb values for N-MORB > 30 and OIB <10 from Winter, 2001; Rollinson, 1993) (Fig. 28D). Otjijanjasemo, again, defines its own cluster in the PM/E-MORB field. Other samples of Oncócua (2 samples) and Ombuku South (1 sample) show OIB-like compositions, in agreement with the multiple sources indicated in Figure 28A. The Pearce diagram further supports a mantle-like source for the MUM intrusions (Fig. 30). The samples plot in the crust-magma interaction field, and they are perpendicular to, and in, the mantle array field. Ombuku South appears to have tapped multiple sources of the mantle array from N-MORB to OIB. Oncócua appears also to tap multiple MORB sources in the mantle array (possibly PM or E-MORB) and OIB. The OIB source is associated with a low degree of partial melting (Winter, 2001) and this supports a low degree of partial melting observed also in some samples as well as multiple sources as shown in Figures 28A and 27B.

The REE are used to provide insights into the genetic relationships of the MUM intrusions to the KC anorthosite suite and generally establish the nature of its magma sources. In general, the Primitive Mantle normalised REE diagrams show that the MUM intrusions and KC anorthosite suite are L/HREE-enriched (Figs. 29A-D). This suggests either, or a combination of, melting of enriched mantle sources, relatively low degrees of partial melting, the mixing of magmas in relative disequilibrium to one another, and/or crustal contamination, as crust is enriched in L/HREE. Ombuku South, Ohamaremba and Onyokohe show some of the greatest degrees of L/HREE-enrichment (e.g., La/Yb = 15.08 to 24.56 and Ce/Yb = 10.57 to 17.88) whereas Hamutenha and Otjijanjasemo show the lowest degrees of L/HREE-enrichment (La/Yb = 5.07 to 6.17 and Ce/Yb = 3.14 to 5.09). This may be because the parent magmas to

Hamutenha and Otjijanjasemo originated from relatively higher degrees of partial melting and/or from a less enriched source (Table 3). Average Eu/Eu* values are also highest in Ohamaremba and Ombuku South while Eu/Eu* values are lowest in Hamutenha and Otjijanjasemo (Table 3). This suggests that plagioclase crystallisation had a control on the magmatic evolution of these intrusions. The rock type-specific REE diagrams show that some samples from Ohamaremba, Ombuku South and Ombuku North, with pronounced positive Eu anomalies, also show depletion in HREE and this suggests there was a high degree of plagioclase accumulation in the intrusions and that there was garnet retention in the magma sources (Pearce, 2008). The Onyokohe melatroctolite shows REE and multi-element (e.g., LILE) patterns similar to an Ombuku South troctolite. Both samples are subject to high degrees of amphibolitisation and serpentinisation based on the field and petrographical observations. These two samples also show moderate to high LOI contents (3–6 wt%) and it is likely the LILE in these samples were affected by late alteration events (Table IV.1 of Appendix IV). The KC anorthosite suite shows similar REE and multi-element patterns to the MUM intrusions although with less enrichment in REE (and incompatible elements overall) except for Hamutenha which is slightly less enriched in HREE and incompatible elements (Figs. 29A & E). REE ratios for the KC anorthosite suite (La/Yb = 18.33 and Ce/Yb = 12.52) are also similar to the MUM intrusions, with the exception of Hamutenha and Otjijanjasemo (Table 3). This suggests that most of the MUM intrusions and KC anorthosite suite crystallised from magmas derived by similar degrees of partial melting. Therefore, the parent magmas to these intrusions may likely be genetically linked to the KC anorthosite suite. However, they also suggest that Hamutenha and Otjijanjasemo are not cogenetic to the other MUM intrusions, as well as to the KC anorthosite suite. The consistently similar L/HREE enrichment (La/Yb and Ce/Yb) and Eu/Eu* values between Hamutenha and Otjijanjasemo suggest that these intrusions are likely cogenetic to one another. The report on Hamutenha by Campeny et al. (2023) suggests that this intrusion is related to magmatic events associated with the Palaeoproterozoic basement (ENMC) based on the geochronology data (Fig. 36). The ENMC is the dominant basement rock in the

Namibian portion of the KC, and, on that basis, it is likely that Otjijanjasemo is related to the same magmatic event that produced Hamutenha. However, it is worth noting that Hamutenha and Otjijanjasemo are around 300 km apart. A precise age for Otjijanjasemo would help to constrain this hypothesis. van Zyl (2022) recovered zircon dates of ~1800 Ma for Otjijanjasemo, but this age was interpreted to be representative of the basement which was inherited during emplacement and favoured a 1400 Ma crystallisation age, similar to Ohamaremba which is nearby.

The Sr-Nd isotope compositions for Oncócua suggest its parental magma was derived by the partial melting of an enriched mantle-like source when corrected to 1.4 Ga (initial $^{87}Sr/^{86}Sr$ = 0.702442 to 0.705612 and $\varepsilon_{Nd(t)}$ = -5.03 to -2.86) with the olivine-bearing rocks displaying lower initial $^{87}Sr/^{86}Sr$ and higher $\varepsilon_{Nd(t)}$ than the pyroxene-bearing rock from this intrusion (Fig. 34A). As highlighted above, the age of Oncócua is still unclear. Therefore, the Sr-Nd isotope compositions are corrected to 1.8 Ga, the alternate crystallisation age for this intrusion. When these samples are age corrected at 1.8 Ga, they are more primitive, suggesting Oncócua is derived from the partial melting of a depleted mantle-like source (initial $^{87}Sr/^{86}Sr$ = 0.701570 to 0.705255 and $\varepsilon_{Nd(t)}$ = -1.11 to 1.75: Fig. 28B). Gleiβner et al. (2011) reported initial Sr-Nd isotopic compositions (initial $^{87}Sr/^{86}Sr$ = 0.7028 to 0.7042 and $\varepsilon_{Nd(t)}$ = -3.1 to 2.1 at 1.38 Ga) in the Namibian KC anorthosite suite. Slejko et al. (2002) also reported initial Nd isotopic compositions ($\varepsilon_{Nd(t)}$ = -6.36 to -5.72 at 1.37 Ga) in the northern part of the Angolan KC anorthosite suite. The $\varepsilon_{Nd(t)}$ values of Oncócua appear to 'fill in the isotopic gap' between the Angolan and Namibian KC anorthosites when Oncócua is corrected to 1.4 Ga. It is, therefore, likely that Oncócua crystallised from a magma that is genetically related to the magmas that produced the Angolan KC anorthosites. Another possible interpretation is that the $\varepsilon_{Nd(t)}$ values of Oncócua at 1.4 Ga are the result of contamination by the older (1.8 Ga) basement rocks.

Although precise geochronological constraints on the age of the MUM intrusions is ongoing research, the petrological and geochemical data presented here give important insights. In general, the MUM intrusions appear to be cogenetic with one another and

their magmas are derived, mostly, from the high degree partial melting of mantle-like sources (from N-MORB to OIB) with some minor variation in the degree of partial-melting between the different intrusions. Some intrusions (particularly Ombuku South and possibly Oncócua) appear to be derived from multiple mantle sources while others (i.e., Otjijanjasemo and Hamutenha) appear to be the result of higher degree of partial melting of their sources. Hamutenha and Otjijanjasemo are the exception as they appear to be non-cogenetic to the other intrusions based on normalised primitive mantle REE patterns and they are likely related to relatively higher degrees of partial melting of mantle-like sources. It is also possible that Ohamaremba, Ombuku North and South, Onyokohe and Oncócua are cogenetic to the KC anorthosite suite (1.35–1.5 Ga) based also on similar REE systematics and preliminary Sr-Nd isotopic data for Oncócua.

5.2 Evidence of Ore-forming Processes in the Mafic-Ultramafic Intrusions to the KC

Several reports have highlighted evidence of critical ore-forming processes in the formation of world-class Ni-deposits like Voisey's Bay (Naldrett, 1999; Li et al., 2000; Kerr and Smith, 2001; Lightfoot, 2007; Naldrett, 2010; Barnes et al., 2016; Barnes, 2023). In this section, the petrological and geochemical evidence of potentially similar types of processes in the MUM intrusions at the periphery of the KC are discussed. This relates to the literature review in section 2.3.2.

5.2.1 Cumulate Rocks in the MUM Intrusions and Fo-Ni Relationships in Olivine

A critical aspect of the ore-forming processes of magmatic Ni-sulphide deposits is the source of the magma of the host intrusion because this has implications for the compositions of the parent silicate magmas (Lightfoot and Naldrett, 1999; Arndt et al., 2005; Barnes et al., 2016; Barnes, 2023). However, it is important to mention that the MUM intrusions are generally cumulate in nature and are not therefore representative of liquid compositions. In fact, almost no chilled margins or fine-grained rocks have been sampled from these intrusions. This places difficulty in determining the parental

magma as the compositions of cumulates, by definition, differ from the composition of their parental magma (e.g., Barnes et al., 2016; Barnes, 2023). However, the fact that these small sized intrusions are dominantly cumulate in nature is promising as this is indicative of a hot, dynamic and open-system magmatic environment, which is conducive for the formation of a Ni-sulphide deposit (e.g., Barnes, 2023). Here, the author tries to have an insight into the nature of the parental magmas to the MUM intrusions and compares these with the parental magmas associated with magmatic intrusions hosting world-class Ni-sulphide mineralisation.

The olivine compositions (i.e., Fo-Ni) of the MUM intrusions were used to help constrain the composition of the parental magmas to the MUM intrusions (Figs. 15, 16; Table I.2 in Appendix I). On the regional-scale, the intrusions show a range of Fo and Ni compositions in olivine, and the trends suggest fractional crystallisation processes in which Ombuku North (and Hamutenha based on published data in Campeny et al., 2023) crystallised from the most primitive (high-Mg) basaltic parental magma (a near primary magma composition with olivine compositions of ~Fo_{81}). In contrast, Oncócua crystallised from the most evolved parental magma (olivine compositions of ~Fo_{59-54}). Ohamaremba and Otjijanjasemo also have olivine Fo compositions (Fo_{67-71} and Fo_{64-68}, respectively) that suggest basaltic parental magmas although they are more evolved than Ombuku North. The similar Fo compositions in Ohamaremba and Otjijanjasemo suggest a similar degree of fractional crystallisation.

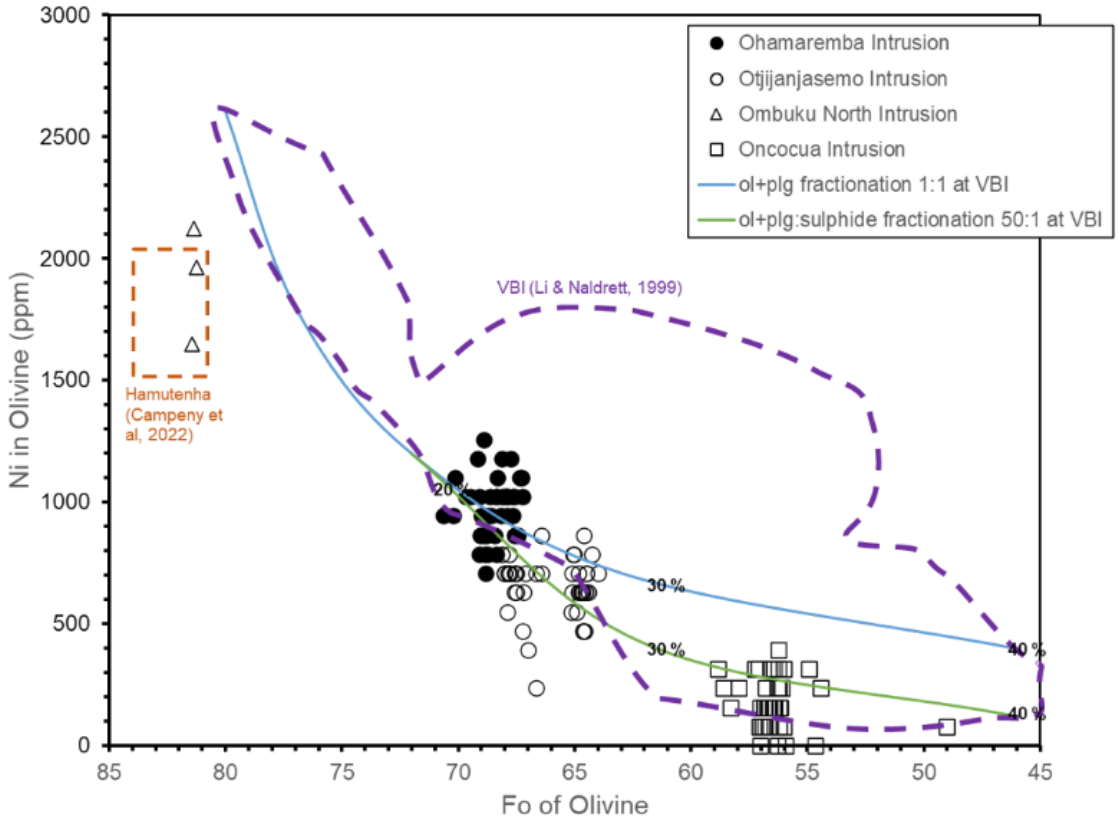


Figure 37: Molar Fo-Ni (ppm) compositions of olivine for Ohamaremba, Otjijanjasemo, Ombuku North, and Oncócua showing the model fractionation curves for Voisey's Bay (Li and Naldrett, 1999). The data for Hamutenha are from Campeny et al. (2023).

Figure 37 shows the olivine Fo-Ni compositions, for Ohamaremba, Otjijanjasemo, Ombuku North and Oncócua and includes modelled fractional crystallisation curves for Voisey's Bay from Li and Naldrett (1999). The Fo-Ni compositions of olivine generally show similarities to Voisey's Bay. Ohamaremba and Otjijanjasemo fall on a normal fractional crystallisation curve (1:1 olivine/plagioclase crystallisation). The Fo-Ni compositions of olivine at Oncócua are very low for these ultramafic rocks. Similar low Fo-Ni compositions of olivine were also observed in the feeder olivine gabbro, olivine gabbro and leucotroctolite at Voisey's Bay at between 30% to 40% crystallisation (Li and Naldrett, 1999). The evolved Fo-Ni compositions may be the result of re-equilibration of existing olivine with residual melt and sulphide, with the parent magma following a fractionation curve consisting of olivine-

plagioclase:sulphide crystallisation at a ratio of 50:1 (Fig. 37). The process may be the result of a fractionating magma becoming sulphur-saturated through interaction with an external sulphur source. After the fractionation of olivine, plagioclase and sulphide (at a ratio of 50:1 silicate to sulphide), the existing olivine interacted with trapped intercumulus liquid with olivine nucleating on the core of the existing olivine. Because the trapped liquid fractionated olivine rapidly, the olivine became Fa-rich (particularly at the rim) due to relative rapid rates of diffusion that favoured high Fe/Mg in the olivine structure at magmatic temperatures (Roeder and Emslie, 1970; Li and Naldrett, 1999). Similarly, the process also modified the Ni content as the olivine crystallising from the intercumulus liquid became Ni-poor (Li and Naldrett, 1999; Barnes et al., 2023). However, low Ni in olivine can also be caused by olivine co-crystallising with sulphide or olivine that crystallised from a magma that was subjected to the segregation of sulphide liquid. A second hypothesis to explain the low Fo-Ni contents of olivine in Oncócua is the entrainment of layered intrusion components transported to an upper level of the crust by influxes of fresh magmas in a dynamic open system. The disrupted Fa-rich component layers would have interacted with silica-rich crust to produce the textures (e.g., orthopyroxene rim reaction around olivine) observed petrographically in the samples of these intrusions (Figs. 18C–F, H). In addition, the plots of whole rock trace element ratios with major oxides also support the Fo-Ni compositional evolution of the MUM intrusions in which Ombuku North crystallised from the least evolved magma (Ce/Yb < 10) together with Onyokohe and, to lesser extent, Ombuku South and Hamutenha while Oncócua crystallised from the most evolved magma (Ce/Yb > 10) (Fig. 28B-C). The data for Oncócua appear to be scattered which suggests Oncócua is also likely to have been affected by the process of assimilation with fractional crystallisation (AFC) (e.g., Pearce, 2008; Gill, 2010).

Several publications associate magmatic Ni-sulphide deposit-hosted-intrusions with cumulate rocks as they are recognised as favourable zones of deposition, particularly those formed in dynamic open-systems (Li et al., 2000; Barnes et al., 2016; Barnes, 2023). Barnes (2023) states that most small mafic-ultramafic magmatic sulphide

deposit-hosted intrusions are associated with cumulus olivine by itself or with cumulus pyroxene (predominantly orthopyroxene). Orthopyroxene-dominant cumulate rocks (i.e., harzburgite and olivine orthopyroxenite) are the most common host rocks in small intrusions, although there is also less common olivine–clinopyroxene cumulate-hosted intrusions as well as more evolved phases of olivine ± orthopyroxene–clinopyroxene–plagioclase. Petrographical observations show that the MUM intrusions consist dominantly of cumulus phases (Figs. 14, 18-21). The petrographical observations are further supported by the discriminant cumulate plots which show that the whole rock geochemical data plot in the cumulate fields (Figs. 24-26). Ohamaremba plots in the ultramafic to mafic to anorthositic cumulate fields, Otjijanjasemo in the ultramafic to mafic cumulate fields, Ombuku North in the mafic and anorthositic cumulate fields, Ombuku South in the mafic cumulate field, and Hamutenha in the ultramafic cumulate field (Fig. 24). Moreover, Figure 26 shows that Hamutenha, Onyokohe and some samples of Ohamaremba are ultramafic olivine-dominant cumulates and that Ombuku North, Ombuku South, Otjijanjasemo, other samples of Ohamaremba and, to a lesser extent, Oncócua, are broadly mafic-dominant cumulates. This further demonstrates that the parental magmas of the MUM intrusions are high-Mg basalt to basalt in composition. Also, the modal abundances obtained from the petrographical observations and the CIPW norms obtained from the whole rock major oxide data were plotted in separate basaltic liquid crystallisation pathway diagrams modelled by Barnes (2023) and they show broadly similar trends (Figs. 14, 25). The diagrams show that the MUM intrusions follow similar crystallisation pathways of basaltic magmas with trends towards crystallisation of ultramafic to mafic to intermediate cumulate rocks. The trend towards the crystallisation of ultramafic cumulates suggests that it is likely that the basaltic magmas had not initially evolved too far from their original compositions (Barnes, 2023).

The MgO-FeO* diagram (Fig. 23) allows inferences to be made about the composition of the parental magmas of world-class magmatic sulphide ore deposits because deposit-hosted intrusions are associated with cumulate rocks. Most of the samples of the

peripheral MUM intrusions to the KC are also cumulate rocks as highlighted above. Figure 23 shows that some of the MUM intrusions plot in the same fields as magmatic intrusions that host world-class Ni-sulphide deposits and near the 'fertile magma threshold'. They also plot inside the Continental Flood Basalts (CFB) and Continental Arc Basalts (CAB) fields. These intrusions include Ohamaremba (2 samples) and Ombuku South (1 sample) in the Savannah and H'Shandong ore camps, and Oncócua (2 samples) in the H'Shandong, Norilsk Mr-Mk and MCR-K ore camps. Hamutenha (1 sample) is also in the H'Shandong ore camp. Otjijanjasemo (2 samples) are in and close to the Pechenga ore camp far above the 'fertile magma threshold'. The parental magmas of these ore intrusions are broadly basaltic in composition (Lightfoot and Evans-Lamswood, 2015; Le Vaillant et al., 2020; Barnes, 2023) and suggest that the MUM intrusions probably have parental magma compositions similar to these world-class deposit-hosted intrusions. The exception is Otjijanjasemo which appears to have parental magma compositions similar to Pechenga ore camp which itself is picrite in composition. The high MgO-FeO contents of Pechenga have been suggested to be associated with a high melting temperatures, greater depths of magma generation and high pressures for a similar degree of partial melting (Barnes, 2023).

In general, the parental magmas of the MUM intrusions show many characteristics that are similar to the magmatic intrusions that host world-class Ni sulphide deposits. The MUM intrusions from the periphery of the KC comprise ultramafic to mafic to intermediate cumulates derived from broadly basaltic parental magmas of mantle-like sources. Ombuku North, Hamutenha, Ohamaremba and, to a lesser extent, Otjijanjasemo crystallised from primary magmas while Oncócua crystallised from the most evolved parental magma of all intrusions based on its olivine Fo-Ni compositions. The whole range of olivine Fo-Ni compositions in all MUM intrusions is similar to the VBI and they appear to follow similar fractional crystallisation curves (i.e., Ohamaremba, Otjijanjasemo and Oncócua). Whole rock Ce/Yb vs major oxide plots support the fractional crystallisation evolution of the magmas of these intrusions. The plots include Onyokohe, Ombuku South and, to a lesser extent, Hamutenha to likely

have been crystallised from least evolved parental magmas, whereas Oncócua appears to be the most evolved intrusion with AFC processes possibly involved. The presence of cumulate rocks in the MUM intrusions and similar parental magma compositions to world-class ore camps suggest that these intrusions are fertile with respect to their potential to host a magmatic sulphide deposit.

5.2.2 Crustal Contamination

Magma interaction with sulphur-bearing country rock was a critical process in the formation of many types of magmatic Ni sulphide deposits (e.g., Smuts, 1998; Lightfoot and Naldrett, 1999; Li et al, 2000; Naldrett, 2010; Barnes et al, 2016; Barnes, 2023). In this study, field relationships with basement rocks (i.e., Oncócua), trace elements ratios, and $\delta^{34}S$ (in ‰) isotope signatures attest to the evidence of crustal contamination during the petrogenesis of the MUM intrusions (Figs. 12F, 30, 33, Table 3). Preliminary Sr-Nd isotopic composition data obtained for Oncócua constrain the evidence of crustal contamination by the surrounding basement rocks, particularly at 1.4 Ga (Figs. 34). The radiogenic isotopic data further support the evidence of crustal contamination when plotted together with $\delta^{34}S$ and whole rock trace element ratios (Fig. 35). Figure 36 is a timeline of the MUM intrusions and the basement rocks that are potential contaminants (in section 5.1).

The Primitive Mantle normalised multi-element patterns and ratios suggest that the MUM intrusions were contaminated by continental crustal components (Fig. 29). The average Rb/Sr_N and Th/Y_N ratios suggest enrichment in LILE and HFSE (Fig. 29E-H, Table 3). In general, the intrusions show negative Nb-Ta, Th ± U and Ti anomalies. The Pb enrichment exhibited by the intrusions resulted from the limitation of the analytical method in determining Pb concentrations. The Rb/Sr_N and Th/Y_N ratios show that Ombuku North and, to a lesser extent, Hamutenha are the least enriched in LILE, whereas Ohamaremba and Oncócua are the most enriched in LILE. This is also observed in the multi-element patterns that show Ombuku North and Hamutenha have the least Cs-, Ba- and Rb-enrichment coupled with the least negative Nb-Ta anomalies.

This suggests that the parent magmas of Ombuku North and Hamutenha had minimal interaction with the crust, and is in agreement with the findings of Campeny et al. (2023). Although the multi-element patterns show that Onyokohe has the most Cs- and Ba enrichment and relatively high Rb/Sr_N, the alteration observed in this sample, together with its high LOI value (6 wt%), suggests it was affected by fluid metasomatism. Another sample of Ombuku South showed a similar pattern and is also highly altered with a moderately high LOI value (3 wt%) suggesting that Ombuku South was probably also affected by fluid metasomatism (Table IV.1 of Appendix IV). The Nb/Yb vs Th/Yb diagram shows that most of the MUM intrusions plot in the crust-magma interaction field and within the basement rock field, close to the mantle array (Fig. 30A). The Th/Nb vs La/Sm diagram also shows evidence of magma-crust interaction, particularly for Oncócua and Ohamaremba as they trend towards the basement rocks. The basement Regional Granite together with the ENMC appears to have Th/Nb and La/Sm signatures comparable to upper crustal compositions (Th/Nb = 0.89 and La/Sm = 6.66: McLennan, 2001). However, the basement amphibolites associated with the ENMC have Th/Nb (0.03 – 0.38) and La/Sm (2.03 – 4.35) signatures that are comparable to lower crustal compositions (Th/Nb = 0.30 and La/Sm = 3.47: McLennan, 2001). Ombuku North and, to a lesser extent, Onyokohe and Ombuku South, plot outside the compositional range defined by the basement rocks (Fig. 30B). This suggests that the parent magma to Ombuku North had the least interaction with the basement rocks while Onyokohe and Ombuku South magmas had relatively more interaction with the basement, but still significantly less than Ohamaremba and Oncócua. The parent magmas of Otjijanjasemo and Hamutenha have consistently low La/Sm and Th/Yb, with high Nb/Th, that are not similar to bulk continental crust (La/Sm = 5.1, Th/Yb = 3.0, Nb/Th = 1.4: Sappin et al., 2022) (Fig. 30). This suggests that the magmas of Otjijanjasemo and Hamutenha also had minimal interaction with the crust. The TiO_2-Ce/Yb values of Oncócua are widely distributed which suggests there was AFC processes in the evolution of this intrusion. Oncócua and Ohamaremba appear to have the highest Rb/Sr_N and Th/Y_N suggesting crustally contaminated magmas and/or derivation from an enriched source. Field observations

at Oncócua shows that there was interaction of magma and calc-silicate-bearing basement rocks lending further support to the conclusions drawn from the geochemistry that these intrusions were heavily influenced by crustal contamination (Figs. 12F, 29E-H; Table 3). In addition, CIPW norm determinations for an Oncócua sample (KAC246/245) collected not far from the contact of intrusion with the basement reported wollastonite in its mineral composition (just enough to assign the name of wollastonite gabbro for this sample). This suggests the possibility of the presence of carbonate basement rocks in the vicinity of Oncócua that reacted with magma, adding Ca, and triggering the crystallisation of Ca-rich pyroxene.

The intrusions have S/Se ratios similar to the mantle domain that suggest less contamination of mantle-derived magmas by S-rich crustal sources with Ohamaremba in the upper end of the S/Se mantle domain (2850-4350: Queffurus and Barnes, 2015) (Fig. IV.2 and Table IV.1 in Appendix IV). Another suggestion is that these S/Se ratios are the result of late to post-magmatic crystallisation processes associated with the breakdown of sulphides due to alteration, high-grade metamorphism and supergene weathering which would considerably lower the S/Se ratios below the mantle domain range. However, Oncócua shows S/Se ratios (10000–10333) above the mantle domain suggesting its mantle-derived magma were contaminated by S-rich crustal sources or other magmatic processes (e.g., depletion of the silicate magma in Se or variation in R-factor) (Queffures and Barnes, 2015).

Figure 33 shows that Oncócua shares similar $\delta^{34}S$ signatures with a granodiorite from the Regional Granite as well as a mica-schist which is part of the ENMC. A $\delta^{34}S$ value of 2‰ was reported for Oncócua by Maier et al. (2013), similar to the amphibolite basement rock (Fig. 33). The initial Sr-Nd isotopic data for Oncócua suggests its magma incorporated basement material (initial $^{87}Sr/^{86}Sr$ = 0.7024 to 0.7056 and $\varepsilon_{Nd(t)}$ = -5.03 to -2.86 at 1.4 Ga) (Fig. 34 and Table III.1 of Appendix III). Plots of $\varepsilon_{Nd(t)}$, $\delta^{34}S$ and trace element ratios show negative correlation when corrected to 1.4 Ga and positive correlation when corrected to 1.8 Ga (Fig. 35). The ε_{Nd} vs $\delta^{34}S$ diagram at 1.4 Ga suggests crustal sulphur was added to Oncócua (Fig. 35A). At 1.4 Ga, the basement

rocks (granodiorite, micaschist and garnet-amphibole-white mica) near an Oncócua K-feldspar-bearing troctolitic sample (based on CIPW Norm) shows moderately high La/Sm and Th/Yb ratios that suggest that Oncócua had multiple contaminants (Figs. 35C). High Th/Yb ratios of the micaschist and garnet-amphibole-white mica basement rocks also suggest contamination without the involvement of the granodiorite (Fig. 35G). The Oncócua troctolitic sample shows decoupled Ce/Yb and Th/Yb (Figs. 35E, G), which is associated with the micaschist and garnet-amphibole-mica basement rocks. Furthermore, the two Oncócua K-feldspar-bearing samples highlighted above show higher Ce/Yb ratios than the basement rocks. There is tonalite and migmatite in the vicinity of Oncócua with similarly high Ce/Yb ratios (63 and 68, respectively) that may represent the contaminants.

The report by Smuts (1998) described xenoliths of hydrous sulphide-bearing schist embedded in a hybrid anatectic rock in the Oncócua intrusion. The assemblage of schists consists of metasediments with mafic and felsic schists and tuffs, together with some intercalations of chert and marble, which is part of the ENMC. This anatectic rock is the reaction product at the contact between basement rock and the intrusive anorthositic magma. This interaction is responsible for the formation of immiscible sulphide liquid and consequentially the contact-style sulphide mineralisation highlighted in the report (Smuts, 1998). Petrographical observations of drillcore samples of Oncócua show the presence of 7–10% sulphides (Fig. 22B). Ohamaremba shows wide variability in its $\delta^{34}S$ signatures with its granitic gneiss and amphibolite granulite basement rocks of the ENMC (Fig. 33). The wide variability of $\delta^{34}S$ signatures at Ohamaremba suggests external heterogeneous S-bearing sources were involved in its petrogenesis. Maier et al. (2013) also reported $\delta^{34}S$ values of 1.6 to 2.4‰ for Ohamaremba. Petrographical observations of drillcore samples of Ohamaremba show also the presence of 3–5% sulphides (Fig. 22A). Ombuku North has a mantle-like $\delta^{34}S$ signature of 0.05‰ that suggests little to no crustal sulphur involvement (Labidi et al., 2014; Quefffurus and Barnes, 2015). Ombuku South and Otjijanjasemo have $\delta^{34}S$ signatures departing from the mantle-like signature that suggests minor

crustal contamination or that their magmas interacted with crust that had unfractionated S isotope which is common in areas predominantly made up of granulite (Maier et al., 2013). It may also suggest that Ombuku South intruded a spatially different basement rock that is devoid of sulphur relative to the other intrusions. This is similar to the Voisey's Bay and Mushuau intrusions in the Nain Plutonic Suite. Voisey's Bay intruded a sulphide-bearing paragneiss (the Tasiuyak paragneiss) of the Palaeoproterozoic Churchill province whereas the Mushuau intrusion, only ~4 km away, intruded into the Nain province that is devoid of sulphide (Fig. 9). Maier et al. (2013) reported $\delta^{34}S$ signatures of 0.4 to 3‰ for Ombuku (with no reference as to either Ombuku North or Ombuku South) and suggested some assimilation of basement amphibolite and quartzite. Drillcore samples of Ombuku North contain <2% sulphides (Fig. 22C). Hamutenha also has a $\delta^{34}S$ signature that differs from mantle values and its neighbouring basement rocks, and this suggests that its magmas did not interact with this particular basement rock, but likely with other basement rocks in the vicinity of this intrusion. It may also suggest that Hamutenha inherited sulphur isotope signature from deep level crust material before its emplacement. Campeny et al. (2023) reported disseminated secondary sulphides up to 1% in outcrop at Hamutenha. Initial Sr-Nd radiogenic isotope composition data are not currently available for Ohamaremba, Ombuku North, Ombuku South, Otjijanjasemo and Hamutenha.

Another way to attain sulphide saturation in the absence of external sulphur addition is by magma mixing and it could likely be the case of intrusions with minimal crustal sulphur input (Ripley and Li, 2013). However, Ripley and Li (2013) also question whether the end-member magmas carry enough sulphur content to trigger the formation of an immiscible sulphide liquid. The authors also suggest that mantle-like $\delta^{34}S$ values, like those reported at Ombuku North, can also be the result of homogenisation in the magma or by accumulation of sulphide from uncontaminated magma in the chamber.

In summary, the petrological and geochemical data show evidence that the MUM intrusions had different degrees of crustal contamination. Ombuku North, Onyokohe and to lesser extent, Hamutenha, appear to be the least crustally contaminated

intrusions whereas Ohamaremba and Oncócua appear to be the most crustally contaminated intrusions. In addition, the Sr-Nd radiogenic isotopic compositions corrected at 1.4 Ga suggests that Oncócua was emplaced synchronously with the KC anorthosite suite.

5.2.3 Subsequent Magma Influxes and Upgrading of Sulphide

It is well-accepted that world-class magmatic Ni-Cu-(Co-PGE) sulphide-hosted intrusions are spatially associated with the margins of ancient Archaean cratonic blocks as these sites comprise deep lithospheric structures that facilitate the transportation of mantle-derived magma to the crust (Lightfoot and Evans-Lamswood, 2015; Barnes et al., 2016; Augustin et al., 2022). The KC is associated with the southwestern margin of the Congo craton and its magmatism may have been facilitated by translithospheric structures (Maier et al., 2013; Jelsma et al., 2018; Bybee et al., 2019; Lehmann et al., 2020; Rey-Morals et al., 2022). Long-lived magma pathways at craton margins allowed magma to be focused through conduit-like magmatic systems in which large volumes of magma pass through a relatively small intrusion (Barnes et al., 2016). A long-lived magma pathway is also critical to allow for the replenishment and mixing of successive fresh silicate magmas that have chalcophile-undepleted characteristics (Naldrett, 2010). The presence of breccias, varied-textured contaminated mafic rocks in contact with the basement rocks in these small intrusions suggests large volume influxes of magma and protracted magma flow (Barnes et al., 2016). Barnes (2023) reports that cumulate rocks can either form in a closed-system (e.g., layered Skaergaard and Kiglapait intrusions) or an open-system (e.g., VBI, Jinchuan and Bushveld) and in small or large intrusions. However, for the formation of magmatic Ni-Cu-(Co-PGE) sulphide deposit, as highlighted in section 5.2.1, cumulate rocks are best as they form in dynamic open-systems that allow for the continuous flux and replenishment of fresh magma. This is also critical for metal enrichment of the existing sulphide liquids by inducing a high R-factor. It is best if the fresh magma interacts with the sulphide liquid before it fractionates olivine and, to a lesser extent, pyroxene, also. Work done by van Zyl (2022) from drillcores reports that the MUM intrusions exhibit low R-factors based

on the PGE tenors of the sulphides. The whole rock data obtained for this study show very low base metal and PGE contents in the outcrop samples (Table IV.1 in Appendix IV). The low R-factors postulated by van Zyl (2022) suggest that the sulphides have a low metal tenor and that could be the result of either the source being PGE-depleted or that there was early segregation of sulphide liquid and the removal of the PGE, as suggested by the Pd contents and Cu/Pd ratios. Nevertheless, some of the lithologies of Ombuku North have R-factors of 1000 to 10000 with some samples consisting of very high Pd contents (up to 670 ppb) in the magma that equilibrated with 1% to 10% sulphide liquid (van Zyl, 2022). The data provided in this study shows that Ombuku North interacted with very little crustal material and likely did not receive any external sulphur. This could suggest that Ombuku North received fresh influxes of undepleted chalcophile magma in a dynamic open system and interacted with small volumes of sulphide liquid segregated from the magma source. Similar situations have been reported in sub-economic mafic-ultramafic intrusions in the HLIS in eastern Canada and it may be the case that the peripheral MUM intrusions in the KC have a similar metallogenetic history. van Zyl (2022) highlights that the high metal tenors in Ombuku North are associated with metasomatised altered host rocks and that it is likely that the mineralisation is the result of rock-fluid interaction and not necessarily orthomagmatic processes. Naumov (2008) also reports the presence of chalcopyrite-dominant secondary sulphide mineralisation at Ombuku North.

Oncócua, Ohamaremba and Ombuku North show some insightful relationships indicative of magma replenishment (Fig. 12). Possible magma mingling is observed in the feldspathic pyroxenite by the presence of anorthositic and leuconoritic veins at Oncócua. The pyroxenitic and basaltic autoliths in gabbro and gabbronorite, along with magmatic layering in leucogabbro and troctolite at Oncócua, are also indicative of replenishment. Ohamaremba shows magnetite-bearing layered leucotroctolite with pyroxenitic veins. Ombuku North shows also troctolite with wehrlite bands showing plagioclase-rich and plagioclase-poor zonation. All these features suggest that possibly there are influxes of fresh magma in the Oncócua and Ohamaremba systems. Autoliths

are also observed at Voisey's Bay with ultramafic fragments in varied-textured troctolite and basal breccia sequences interpreted to be part of early magmatism in the conduit that was transported to the upper levels by fresh magmas (Li and Naldrett, 1999; Bulle and Layne, 2015). One method of tracking whether a magmatic conduit was a dynamic open system and whether economic grades of mineralisation were formed is by assessing the zonation of chromium in pyroxene (e.g., Schoneveld et al., 2020). In this study, the author attempted to assess chromium zonation in pyroxene for several MUM intrusions (Fig. I.2 and Table II.1 in Appendix I). Although petrographical observations show that the intrusions comprise cumulus orthopyroxene with resorbed olivine chadacrysts (e.g., Oncócua), the pyroxene mineral compositional profiles do not show clear indications of complex chromium zoning (Fig. 38).

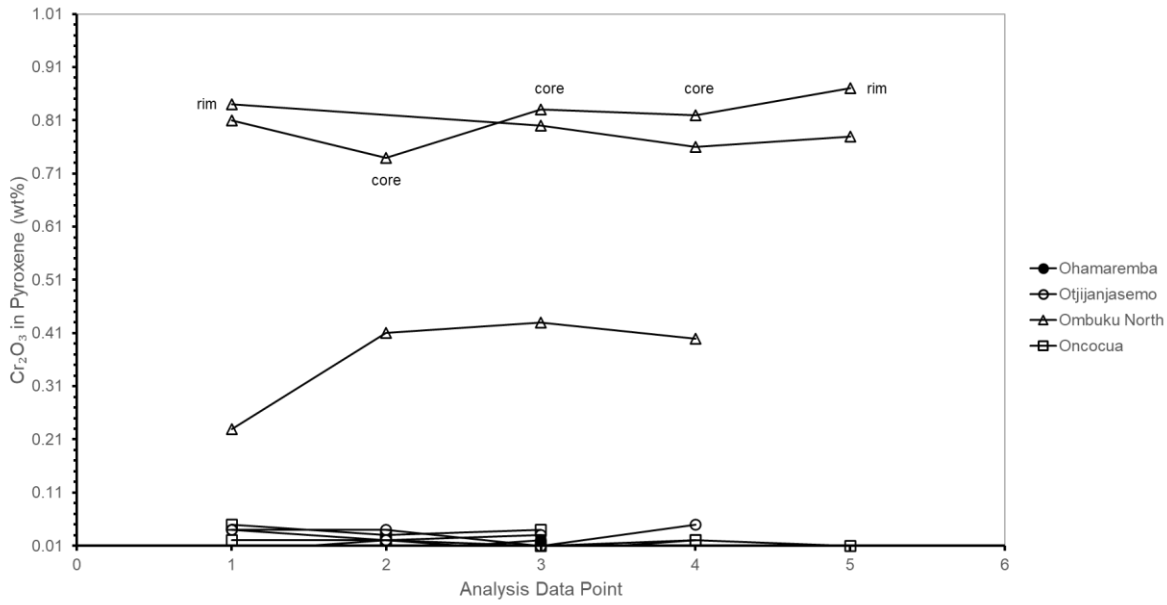


Figure 38: Chromium profiles in pyroxene grains of the MUM intrusions for chromium zoning.

Ohamaremba contains 3–5% sulphide consisting of pyrrhotite-chalcopyrite ± pentlandite ± pyrite. Oncócua contains 7–10% consisting of pyrrhotite-chalcopyrite ± pentlandite. Ombuku North contains <2% chalcopyrite-pentlandite ± pyrite. Otjijanjasemo contains <1% pyrrhotite ± chalcopyrite (Figs. 18-22). The sulphide contents in Ohamaremba, and to a lesser extent, Ombuku North and Otjijanjasemo, are similar to the total sulphide contents found in the Harp Lake Intrusive Intrusion (<5%).

However, the sulphides in the KC MUM intrusions are mainly hosted in mafic to ultramafic lithologies whereas sulphides in the Harp Lake Intrusive Suite are hosted mainly in intermediate lithologies (Kerr and Smith, 2000). This suggests that the KC MUM intrusions are more olivine-rich than the Harp Lake Intrusive Suite. The whole rock metal contents vary from sample to sample of the same intrusion although all intrusions show Ni-Cu depletion with slight enrichment in these elements when normalised to primitive mantle values (Fig. 31A). All intrusions show depletion in Pt and Pd. Whole rock Zr vs Cu plot also indicates that immiscible sulphide liquids were formed (Fig. 31B) and therefore the parent magmas to these intrusions were subjected to early sulphide liquid extraction that removed the metals prior to their emplacement in the crust (Li and Naldrett, 1999; Maier et al., 2013; Barnes, 2023). However, Ombuku North shows Cu-enrichment and it is the only intrusion showing no geochemical evidence of equilibration with sulphide liquid. This may be the result of limited available immiscible sulphide liquid that resulted from the small amounts of crustal contamination. In addition, olivine at Ombuku North shows the highest Ni contents of all olivine suggesting that early olivine crystallisation possibly removed the Ni from the magma before it became sulphur-saturated. Ombuku South also shows many samples with Cu-enrichment, and sulphur isotope signature departs from the mantle-like values (Figs 31, 36). Although petrographical observation of samples of Ombuku South did not show sulphide, van Zyl (2022) reported up to 1% disseminated pyrrhotite-pyrite-chalcopyrite in drillcore samples. All these factors suggest that the magma of Ombuku was contaminated with some crustal sulphur-source component and equilibrated with immiscible sulphide liquid at deposition site. It is likely that sulphur saturation, and the segregation of sulphide liquids in these MUM intrusions, happened at a deeper level in the crust as there is evidence of early sulphide liquid extraction before emplacement as most samples show depletion in Ni-Cu-PGE (Fig. 31). This hypothesis was also suggested at Kiglapait in the NPS by Scoates and Mitchell (2000).

Based on the petrological and geochemical evidence presented here, the MUM intrusions from the margins of the KC show critical processes for the development of magmatic Ni-Cu-(Co-PGE) sulphide deposits. There is evidence that suggests that these MUM intrusions crystallised from parental magmas that are basaltic in composition and are derived from high degrees of partial melting of a mantle source. There is evidence that the magmas ascended through the crust at the margin of Congo craton. On the ascendence to the crust, magmas of some of the MUM intrusions in this study, particularly Ohamaremba and Oncócua, interacted and assimilated crustal sulphur that triggered the formation of immiscible sulphide liquids. The immiscible sulphide interacted and equilibrated with silicate magmas, and possibly in the presence of subsequent fresh influxes of magma (i.e., Ohamaremba and Oncocua) in a dynamic conduit system. These are critical ore-forming processes investigated in world-class magmatic sulphide deposit-hosted intrusions (e.g., Naldrett, 2010; Barnes et al., 2016). Therefore, the MUM intrusions at the periphery of the KC have the potential to host economic magmatic Ni-Cu-(Co-PGE) sulphide deposits.

These intrusions are conducive to hosting a magmatic sulphide deposit as there is evidence of presence of the ore-forming processes. However, the intrusions show generally low sulphide mineralisation. Based on Lehmann et al. (2020), the KC shows evidence of deformation that is syntectonic to the KC magmatism and that could affect the preservation and detectability of a mineralised intrusion and subsequently the trap (i.e., Oncocua area). This would cause strain that leads to displacement (possibly on hundreds of meters) of the main orebody from its original location as a massive sulphide ore is easily deformed relative to disseminated ore (Barnes et al., 2016). In addition, the geochemical evidence from these intrusions suggests there was the early extraction of sulphide liquid that probably occurred at depth in the crust before reaching their deposition site. This further limits the possibility of finding a nickel sulphide deposit at the current level of exposure of the KC. Magmatic sulphide deposits can form in a wide range of crustal levels and erosional events bring to the surface in some cases (Fig. 31). Therefore, while it critical to apply the proxies used in this study

together with a larger dataset of Fo-Ni compositions it is also critical to understand deformation and erosional histories of these intrusions to find an ore deposit.

5.3 Limitations and Suggestions

The following limitations in this MSc study are important to be highlighted and some future suggestions are made on what could be done next. More detailed work on these MUM intrusions is needed to further enhance future Ni-PGE exploration targeting in the KC:

- The lack of precise age data for the MUM intrusions created interpretative difficulties during this MSc project. Voisey's Bay unequivocally overlaps in age with the Nain Plutonic Suite (Amelin et al., 2000), and this first-order chronological constraint is missing between the peripheral MUM intrusions and the KC. The ages of these intrusions must be constrained before further detailed geological and geochemical work is done to test their genetic relations to the KC.
- The fieldwork at the Oncócua intrusion in southwestern Angola was cancelled due to the logistics around the COVID pandemic in 2021–2022. This would have enabled a better understanding of the field relationships and for the systematic sampling of the lithologies to provide a detailed geological and geochemical study of this sulphide-mineralised intrusion.
- The lack of lithological diversity in each intrusion as well as the number of samples available put constraints on the interpretations. Some intrusions were represented by < 3 samples while other intrusions had more samples (>10). This affects the real variability in the dataset and subsequently the conclusions drawn from the study.
- Although 28 samples were selected for radiogenic Sr-Nd isotopes, only 7 samples were completed. This was the result of the expansion of the lab facilities that is still ongoing at the School of Geosciences. Additional

radiogenic isotopic data would help to constrain the magma source(s) and allow for a more detailed assessment of the genetic relationships between the MUM intrusions and the KC.

- An improved lithological map of the basement rock is needed. This will allow the identification of suitable contaminants that may have provided crustal sulphur.
- Detailed studies of individual MUM intrusions that include mapping and sampling. The study would also need to consider structural fabrics as tectonic deformation is common in magmatic Ni-sulphide ores (e.g., Thompson deposit in Manitoba, Canada) and it would result in the dislocation of the primary magmatic ore deposit (Franchuk, 2014; Lightfoot and Evans-Lamswood, 2015).
- A large olivine Fo-Ni composition database is needed for exploration targeting and it will allow us to better constrain fractionation trends and melt evolution. While wide variability in Fo and Ni is important between related intrusions on a regional scale, targeting priority is given to similar olivine Fo compositions with wide variation in olivine Ni contents (Barnes et al., 2023). High and low Ni in olivine are equally important signals as the presence of high Ni olivine indicate that there are rocks in the system that crystallised from Ni-enriched magmas, while low Ni olivine indicates that possibly the magma interacted with sulphide prior to olivine crystallisation in the same system.

Chapter 6: Conclusion

The aim of this study was to utilise a mineral system approach to assess the magmatic Ni-Cu-(Co-PGE) sulphide potential of the mafic-ultramafic (MUM) intrusions associated with the Kunene Complex (KC) in southern Angola and northern Namibia. Much like the Nain Plutonic Suite, which is host to the world-class Voisey's Bay nickel sulphide deposit (VBI), the KC is a Proterozoic massif-type anorthosite that shows geological and geochemical similarities to Nain. Overall, the geological, petrological, and geochemical evidence presented in this thesis suggests that the MUM intrusions at the periphery of the KC appear to be broadly cogenetic with one another (with exception of the Otjijanjasemo and Hamutenha) and that similar ore-forming processes responsible for the formation of world-class magmatic Ni-Cu-(Co-PGE) sulphide-hosted intrusions are also present in the KC MUM intrusions.

While reliable ages for the MUM intrusions are critical to further understand their temporal and genetic relationships to the KC anorthosite suite, the Primitive Mantle normalised REE patterns and trace element ratios suggest that the parent magmas of the MUM intrusions are cogenetic and were derived from high degrees of partial melting of a heterogeneous mantle source (Fig. 29 and Table 3). The exceptions are Otjijanjasemo and Hamutenha with lower La/Yb and Ce/Yb ratios relative to the other intrusions.

Olivine Fo-Ni compositions and whole rock trace element ratios of the MUM intrusions suggest that the parental magmas were high-Mg basalt to basalt in composition (Figs. 15, 16, 28, 30). The parent magmas fractionated ultramafic and mafic cumulate rocks rich in olivine, pyroxene and plagioclase, together with sulphide, based on the field, petrographic and geochemical data (Figs. 12, 13, 14, 18-22, 24-26). Moreover, the whole rock major oxides show that some of the MUM intrusions (i.e., Ohamaremba, Oncócua, Ombuku South and, to a lesser extent, Hamutenha) have parental magma signatures similar to world-class ore camps such as the Savannah, H'Shandong, Noril'sk Mk-Mr and MCR-K (Fig. 23). Otjijanjasemo shows parental

magma signatures similar to Pechenga. In addition, the KC MUM intrusions have olivine Fo-Ni compositions in the range of the VBI and have a similar fractional crystallisation evolution on the regional-scale (Fig. 15, 16, 37). The olivine Fo-Ni compositions also show that Ombuku North formed from the least evolved parent magma and Oncócua from the most evolved magma, which is supported by the trace element data (Figs. 28B, C).

Previous regional geology studies show that the KC and the MUM intrusions are spatially associated with the southwestern margins of the Congo craton (Figs. 1, 2). The general consensus is that world-class magmatic Ni-Cu-(Co-PGE) sulphide-hosted intrusions are closely associated with the margins of cratons. Craton margins provide favourable structural controls for ore forming mantle-derived magmas to ascend and interact with the basement rocks on its way to the upper crust. In addition, they focus subsequent fresh mantle-derived magmas in a dynamic conduit system that increase the metal tenor of sulphide.

The KC MUM intrusions experienced different proportions of crustal contamination during emplacement (Fig. 30A). Ombuku North and, to a lesser extent, Ombuku South, show the least amounts of crustal contamination by the surrounding basement rocks (Fig. 30B). Ombuku North shows mantle-like sulphur isotope compositions whereas Ohamaremba and Oncócua have non-zero sulphur isotopic compositions indicative of interaction with the regional basement rocks they were emplaced into (Fig. 33). Otjijanjasemo, Hamutenha and Ombuku South also have sulphur isotope values departing from mantle values. Initial Sr-Nd isotopic compositions for Oncócua further show there is evidence of crustal contamination, if the intrusion was emplaced synchronously with the KC anorthosite suite at 1.4 Ga (Fig. 34). This is consistent with the geochemical, petrological and geological evidence of crustal contamination in Oncócua (Figs. 12, 29, 30, 33, 34). Therefore, this suggests that Oncócua was emplaced at 1.4 Ga and contaminated with 1.8 Ga basement rocks. This also suggests that Oncócua is likely to be part of KC.

Ohamaremba, Oncócua, Otjijanjasemo, Hamutenha and, to lesser extent, Ombuku South show evidence for the extraction of sulphide liquids (Fig. 31). This resulted in the depletion of chalcophile elements. Ombuku North, however, does not show early extraction of sulphide and did not therefore equilibrate with enough immiscible sulphide liquid due to limited available sulphide liquids that would be promoted in the presence of sufficient magma-crust interaction (Figs. 30, 33). In addition, field observations show textures indicating significant magma flux and replenishment in a dynamic open system, (i.e., Ohamaremba and Oncócua). This is important as fresh influxes of undepleted chalcophile magma interacted with the available immiscible sulphide liquid which has the potential to upgrade the metal tenors and produce an economic deposit.

The MUM intrusions of the KC have the potential to host a VBI-type magmatic Ni-Cu-(Co-PGE) sulphide deposit as shown on a regional-scale. To determine the potential at the intrusion-scale and to create exploration targets, similar, but more detailed scientific studies are required, including: (i) the establishment of a larger database of olivine Fo-Ni compositions to pinpoint ore-forming processes with priority to those intrusions showing a wide variability of low and high Ni contents at similar Fo content (e.g., Barnes et al, 2023); (ii) further detailed mapping, sampling and structural studies of the intrusions to constrain the relative timing of their emplacement and morphology; and (iii) geophysical studies to improve the understanding and delineating of potential ore deposits in the region, particularly on the eastern side of the KC which is covered in Kalahari sediments.

Chapter 7: References

Abily, B., Boudreau, A.E., Blanchette, F., Bush, J.W.M. Igneous Layering in Magma Chamber. 2015.

Amelin, Y., Li, C., Naldrett, A.J., 1999. Geochronology of the Voisey's Bay intrusion, RoLabrador, Canada, by precise U–Pb dating of coexisting baddeleyite, zircon, and apatite. *Lithos*, Vol. 47, pp. 33-51.

Amelin, Y., Li, C., Valeyev, O., Naldrett, A.J., 2000. Nd-Pb-Sr Isotope Systematics of Crustal Assimilation in Voisey's Bay and Mushuau Intrusions, Labrador, Canada. *Economic Geology*, Vol. 95, pp. 815-830.

Arndt, N.T., Lesher, C.M., Czamanske, G.K., 2005. Mantle-derived magmas and magmatic Ni-Cu-(PGE) Deposits. *Economic Geology*, 100th Aniversary, pp. 5-24. hal-00016864

Ashwal, L.D., Bybee, G.M., 2017. Crustal evolution and the temporality of anorthosites. *Earth-Sciences Reviews*, Vol. 173, pp. 307-330.

Ashwal, L. Anorthosites, 1993 Springer-Verlag.

Ashwal, L.D. and Twist, D., 1994. The Kunene complex, Angola/Namibia: a composite massif-type anorthosite complex. *Geological Magazine*, Vol. 131(5), pp.579-591.

Barnes, J.R., Hauck, S.A, Morton, P., Strommer, J., 1990. Geology and Mineralization of a Cyclic Layered Series, Water Hen Intrusion, St. Louis County, Minnesota. Technical Report. The University of Minnesota. 1990. 39 p. NRRI\GMIN-TR-89-17.

Barnes, S.J., Le Vaillant, M., Lightfoot, P.C., 2017. Textural Development in Sulfide-matrix Ore Breccias in the Voisey's Bay Ni-Cu-Co Deposit, Labrador, Canada. *Ore Geology Reviews*, Vol. 90, pp. 414-438.

Barnes, S.J., Maier, W.D., 1999. The Fractionation of Ni, Cu and the Noble Metals in Silicate and Sulphide Liquids. Geol. Assoc. Can. Short Course Notes 13, 69–106.

Barnes, S.J., 2022. Whole-rock geochemistry for intrusion-hosted magmatic Ni-Cu-Co exploration: identifying prospective host rocks. *Explore Newsletter*, Vol. 195, pp. 1-13.

Barnes, S.J., 2023. Lithogeochemistry in exploration for intrusion-hosted magmatic Ni–Cu–Co deposits. *Geochemistry: Exploration, Environment, Analysis*, Vol. 23, pp. 1-17.

Brandt, S., Will, T.M., Klemd, R., 2007. Magmatic loading in the Proterozoic Epupa Complex, NW Namibia, as evidenced by ultrahigh-temperature sapphirine-bearing orthopyroxene–sillimanite–quartz granulites. *Precambr. Res*. Vol. 153 (3–4), 143–178.

Bedard, J.H., 2001. Parental magmas of the Nain Plutonic Suite anorthosites and mafic cumulates: a trace element modelling approach. *Contrib. Mineral Petrol.,* Vol. 141, pp. 747-771.

Bulle, F., Layne, G.D., 2015. Multi-element variations in olivine as geochemical signatures of Ni-Cu sulfide mineralization in mafic magma systems—examples from Voisey's Bay and Pants Lake intrusions, Labrador, Canada. *Miner Deposita,* Vol. 51, pp. 49-69.

Bybee, G.M., Hayes, B., Owen-Smith, T.M., Lehmann, J., Ashwal, L.D., Brower, A.M., Hill, C.M., Corfu, F. & Manga, M., 2019. Proterozoic massif-type anorthosites as the archetypes of long-lived (≥ 100 Myr) magmatic systems—New evidence from the Kunene Anorthosite Complex (Angola). *Precambrian Research,* Vol. 332, pp. 105-393.

Campeny, M., Proenza, J.A., Castillo-Oliver, M., Torró, L., Villanova-de-Benavent, C., Melgarejo, J.C., Gonçalves, A.O., Román-Alpiste, M.J., Blanco-Quintero, I.F., Llovet, X. and Farré-de-Pablo, J., 2023. Petrology, metallogeny and U-Pb geochronology of the palaeoproterozoic mafic-ultramafic Hamutenha intrusion, Angolan Shield. *Journal of African Earth Sciences*, Vol. 197, pp.1-33.

Drüppel, K., Littmann, S., Romer, R.L., Okrusch, M., 2007. Petrology and Isotope Geochemistry of the Mesoproterozoic Anorthosite and Related Rocks of the Kunene Intrusive Complex, NW Namibia. *Precambrian Research,* Vol. 156, pp.1-31.

Dobson, D.P., Crichton, W.A., Vocadlo, L., Jones, A.P., Wang, Y., Uchida, T., Rivers, M., Sutton, S., Brodholt, J.P., 2000. In situ measurement of viscosity of liquids in the Fe–FeS system at high pressures and temperatures. *Am. Mineral.* Vol. 85, pp.1838–1842.

Franchuk, A. High Tenor Ni-PGE Sulfide Mineralization of South Manasan Ultramafic Intrusion, Thompson Nickel Belt, Manitoba. MSc Thesis, School of Graduate Studies at Laurentian University, 2014.

Freyer, E.E. Nambia Kunene Project: Status Report, Namibia. Status Report, 2004.

Fuenlabrada, J.M., 2023. High-precision Sr and Nd isotope characterization of BHVO-2 reference material by thermal ionization mass spectrometry. *Rapid Communications in Mass Spectrometry*. https://doi.org/10.1002/rcm.9632

Gill, R. Igneous Rocks and processes: A Pratical Guide. 2010. Wiley-Blackwell.

Gleißner, P., Drüppel, K., Romer, R.L., 2011. The role of crustal contamination in massif-type anorthosites, new evidence from Sr–Nd–Pb isotopic composition of the Kunene Intrusive Complex, NW Namibia. Precambrian Research, Vol. 185, pp. 18-36.

Goode, A., 1974. Oxidation of natural olivines. *Nature*, Vol. 248, 500–501 https://doi.org/10.1038/248500a0

Hayes, B., Bédard, J.H., J., Hryciuk, M., Wing, B., Nabelek, P., MacDonald, W.D., Lissenberg, C.J., 2015. Sulfide Immiscibility Induced by Wall-Rock Assimilation in a Fault-Guided Basaltic Feeder System, Franklin Large Igneous Province, Victoria Island (Arctic Canada). *Economic Geology*, Vol. 110, pp. 1697-1717.

Hayes, B., Lehmann, J., Bybee, G.M., Owen-Smith, T.M., 2021. Crystal transfer from magma to wallrock during syntectonic granite emplacement. Journal of the Geological Society, Vol. 179, pp. 1-16.

Hill, C.M. Experimental Constraints on Crustal Contamination in Proterozoic Anorthosite Petrogenesis. MSc Thesis, School of Geosciences at University of the Witwatersrand, 2017.

Jelsma, H.A., McCourt, S., Perritt, S.H., Armstrong, R.A. (2018). The Geology and Evolution of the Angolan Shield, Congo Craton. *Regional Geology Reviews.* Vol. pp 217–239.

Kerr, A., Smith, J.L., 2000. Magmatic Ni-Cu Sulphide Mineralization in Harp Lake Intrusive Suite, Central Labrador. *Current Research Report 2000-1 Newfoundland Department of Mines and Energy*, Vol. pp. 311-334.

Kröner, A., Rojas-Agramonte, Y., Hegner, E., Hoffmann, K.-H., Wingate, M.T.D., 2010. SHRIMP zircon dating and Nd isotopic systematics of Palaeoproterozoic migmatitic orthogneisses in the Epupa Metamorphic Complex of northwestern Namibia. *Precambr. Res*. Vol. 183 (1), 50–69.

Labidi, J., Cartigny, P., Hamelin C., Moreira, M., Dosso, L., 2014. Sulfur isotope budget (32S, 33S, 34S and 36S) in Pacific–Antarctic ridge basalts: A record of mantle source heterogeneity and hydrothermal sulfide assimilation. *Geochemica et Cosmochimica Acta*, Vol. 133, 47–67.

Langa, W.M. The Petrology and Economic Potential of Mafic-ultramafic Intrusions West of the Kunene Anorthosite Complex, SW Angola. MSc Thesis, School of Geosciences at University of Johannesburg, 2019.

Lehmann, J., Bybee, G.M., Hayes, B., Owen-Smith, T.M., 2020. Emplacement of the giant Kunene AMCG complex into a contractional ductile shear zone and implications for the Mesoproterozoic tectonic evolution of SW Angola. *International Journal of Earth Sciences*, Vol. 109, pp. 1453-1485.

Lehmann, J., Brower, A., Owen-Smith, T., Bybee, G., Hayes, B., 2023. Landsat 8 and ALOS DEM geological mapping reveals the architecture of the giant Mesoproterozoic Kunene Complex anorthosite suite (Angola/Namibia). Geoscience Frontiers, https://doi.org/10.1016/j.gsf.2023.101620.

Le Vaillant, M., Barnes, S.J., Mole, D.R., Fiorentine, M.L., 2020. Multidisciplinary Study of a Complex Magmatic System: The Savannah Ni-Cu-Co Camp, Western Australia. *Ore Geology Reviews*, Vol. 117, pp. 1-26.

Li, C., Naldrett, A.J., 1999. Geology and petrology of the Voisey's Bay intrusion: reaction of olivine with sulfide and silicate liquids. Lithos, Vol. 47, pp. 1-31.

Li, C., Lightfoot, P.C., Emelin, Y., Naldrett, A.J., 2000. Contrasting Petrological and Geochemical Relationships in the Voisey's Bay and Mushuau Intrusions, Labrador, Canada: Implications for Ore Genesis. *Economic Geology*, Vol. 95, pp. 771-799.

Lightfoot, P.C., 2007. Advances in Ni-Cu-PGE Sulphide Deposit Models and Implications for Exploration Technologies. Ore Deposits and Exploration Technology: In Proceedings of Exploration 07. Paper 44. pp. 629-646.

Lightfoot, P.C., Keays, R.R., Evans-Lamswood, D., Wheeler, R., 2012. S saturation history of Nain Plutonic Suite mafic intrusions: origin of the Voisey's Bay Ni–Cu–Co sulfide deposit, Labrador, Canada. *Miner Deposita*, Vol. 47, pp. 23-20.

Lightfoot, P.C., Evans-Lamswood, D., 2015. Structural controls on the primary distribution of mafic–ultramafic intrusions containing Ni–Cu–Co–(PGE) sulfide mineralization in the roots of large igneous provinces. *Ore Geology Reviews*, Vol. 64, pp. 354-386.

Lightfoot, P.C., Naldrett, A.J., 1999. Geological and Geochemical Relationships in the Voisey's Bay Intrusion, Nain Plutonic Suite, Labrador, Canada. *Short Course Notes*, Vol. 13, pp. 1-30.

Maier, W.D., Teigler, B., Miller, R.M., 2008. The Kunene Anorthosite Complex and Its Satellite Intrusions.

Maier, W.D., Rasmussen, B., Fletcher, I.R., Barnes, S.J., Huhma, H., 2013. The Kunene Anorthosite Complex, Namibia, and Its Satellite Intrusions: Geochemistry, Geochronology, and Economic Potential. *Society of Economic Geology*, Vol. 108, pp. 953-986.

McBirney, A.R., Murase, T., 1984. Rheological Properties of Magmas. Annul, Rev. Earth Planet. Sci., Vol. 12, pp. 337-357.

McCourt, S., Armstrong, R.A., Jelsma, H., Mapeo, R.B.M., 2013. New U–Pb SHRIMP Ages from the Lubango Region, SW Angola: Insights into the Palaeoproterozoic Evolution of the Angolan Shield, Southern Congo Craton, Africa. *Journal of the Geological Society*, Vol. 170, pp. 353-363.

McLennan, S.M., 2001. Relationships between the trace element composition of sedimentary rocks and upper continental crust. *AGU and the Geochemical Society*, Vol. 2, paper number 2000GC000109.

Milani, L., Lehmann, J., Bybee, G.M., Hayes, B., Owen-Smith, T.M., Oosthuizen, L., Delport, P.W., Ueckermann, H., 2022. Geochemical and geochronological constraints on the Mesoproterozoic Red Granite Suite, Kunene AMCG omplex of Angola and Namibia. *Precambrian Research*, Vol. 379, p.1-21.

Misra, K.C. Understanding Mineral Deposits, 2000. Springer-Science+Business Media, B.V, Vol. I

Naldrett, A.J., 2010. From the Mantle to the Bank: The Life of a Ni-Cu-(PGE) Sulphide Deposit. *South African Journal of Geology*, Vol. 113, pp. 1-32.

Naldrett, A.J., Asif, M., Krstic, S., Li, Chusi, 2000. The Composition of Mineralization at Voisey's Bay Ni-Cu Sulfide Deposit, with Special Reference to Platinum-Group Elements. *Economic Geology*, Vol. 95, pp. 845-865.

Naumov, M.V., 2008. Geology and Sulfide Mineralization of the Ombuku North Prospect and Adjacent Areas (Kunene Region, Northern Namibia) Internal report, African Nickel Limited.

Oosthuizen, L. In-situ trace element characterisation of Fe(-Ti)-oxides of the peripheral intrusions of the Kunene Anorthosite Complex. MSc Thesis, Department of Geology at University of Pretoria, 2023.

Pearce, J.A., 2008. Geochemical Fingerprints of Oceanic Basalts with Applications to Ophiolite Classification and the Search for Arechean Oceanic Crust. *Lithos*, Vol. 100, pp. 14-48.

Rai, V.K., Thiemens, M.H., 2007. Mass Independently Fractionated Sulfur Components in Chondrites. *Geochimica et Cosmochimica Acta*, Vol. 71, pp. 1341-1354.

Rey-Moral, C., Mochales, T., Martinez, E.M., Lobon, J.L.G., Bahut, M.T.L., Martin-Banda, R., Feria, M.C., Ballesteros, D., Machadinho, A., Alves, D., 2022.

Recording the Largest Gabbro-Anorthositic Complex Worldwide: The Kunene Complex (KC), SW Angola. *Precambrian Research,* Vol. 379, pp. 1-22.

Ripley, E.M., Park, Y., Li, C., Naldrett, A.J., 1999. Sulfur and Oxygen Isotopic Evidence of Country Rock Contamination in the Voisey's Bay Ni–Cu–Co deposit, Labrador, Canada. *Lithos*, Vol. 47, pp. 53-68.

Ripley, E.M., Li, C., 2013. Sulfide Saturation in Mafic Magmas: Is External Sulfur Required for Magmatic Ni-Cu-(PGE) Ore Genesis?. *Economic Geology*, Vol. 108, pp. 45-58.

Rollinson, H.R. Using Geochemical Data: Evaluation, Presentation, Interpretation. 1993. Pearson Prentice Hall. Harlow.

Roeder, P.L., Emslie, R.F., 1970. Olivine-Liquid Equilibrium. *Contr. Mineral. and Petrol.,* Vol. 29, pp. 275-289.

Ryan, B., 2000. Nain-Churchill Boundary and Nain Plutonic Suite: A Regional Perspective on the Geologic Setting of the Voisey's Bay Ni-Cu-Co Deposit. *Economic Geology*, Vol. 95, pp. 703-724.

Saumur, B.M., Cruden, A.R., Evan-Lamswood, D., Lightfoot, P.C., 2015. Wall-Rock Structural Controls on the Genesis of the Voisey's Bay Intrusion and its Ni-Cu-Co Magmatic Sulfide Mineralization (Labrador, Canada). *Economic Geology*, Vol. 110, pp. 691-711.

Saumur, B.M., Cruden, A.R., 2016. On the Emplacement of the Voisey's Bay Intrusion (Labrador, Canada). *Geological Society of American Bulletin,* Vol. 128, pp. 147-168.

Scoates, J.S., Mitchell, J.N., 2000. The Evolution of Troctolitic and High Al Basaltic Magmas in Proterozoic Anorthosite Plutonic Suites and Implications for the Voisey's Bay Massive Ni-Cu Sulfide Deposit. *Economic Geology,* Vol. 95, pp. 677-701.

Schoneveld, L., Barnes, S.J., Makkonen, H.V., Le Vaillant, M., Paterson, D.J., Taranovic, V., Wang, K., Mao, Y., 2020. Zoned Pyroxenes as Prospectivity Indicators for Magmatic Ni-Cu Sulphide Mineralization. *Frontiers in Earth Sciences,* Vol. 8 (256), pp. 1-19.

Sheth, H.C., Torres-Alvarado, I., Verma, S.P., 2002. What is the "Calc-alkaline Rock Series"?. *International Geology Review*, Vol. 44, pp. 686-701.

Silva, Z.C.G., 1990. Geochemistry of the Gabbro-Anorthosite Complex of Southwest Angola. *Journal of African Earth Sciences,* Vol. 10, pp. 683-692.

Simpson, E. S. W., Otto, J. D. T., 1960. On the Precambrian anorthosite mass of southern Angola. 21st International Geological Congress, Copenhagen 13, 216–27.

Simpson, E. S. W., 1970. The anorthosite of Southern Angola: A review of present data. In African Magmatism and Tectonics (eds Clifford, T. N. and Gass, I. G.), pp. 89–96. Edinburgh: Oliver & Boyd.

Slejko, F.F., Demarchi, G., Morais, E., 2011. Mineral chemistry and Nd isotopic composition of two anorthositic rocks from the Kunene complex (South Western Angola). *Journal of African Earth Sciences*, Vol. 35, pp. 77-88.

Smith, R.L. The Basal Gabbro Subdivision and Associated Magmatic Nickel-Copper Sulphide Mineralization of the Pants Lake Intrusion, Labrador, Canada: A Combined Geological, Petrological, Geochemical, and Metallogenic Study, MSc Thesis, Department of Earth Sciences at Memorial University, 2006.

Smut, J., 1998. Oncócua Project Situation Report. 13/103/504a/UNI/98/0317.

Streckeisen, A., 1976. To each plutonic rock its proper name. *Earth-Science Reviews*, Vol. 12, pp.1-33.

Taranovic, V., Barnes, S.J., Baublys, K., Bathgate, K., Fiorentine, M.L., 2022. Isotopic Investigations of the Nova-Bollinger Ni-Cu-Co deposit in the Fraser Zone, Albany-Fraser Orogen, Western Australia. *Australian Journal of Earth Sciences*, https://doi.org/10.1080/08120099.2022.2076741

Taylors Jr., H.P., 1968. The Oxygen Isotope Geochemistry of Igneous Rocks. *Contributions Mineralogy Petrology*, Vol. 19, pp.1-71.

Thode, H.G., Monster, J., Dunford, H.B., 1961 Jr., H.P., 1968. Sulfur isotope geochemistry. *Geochimica et Cosmochimica Acta*, Vol. 25, pp.150-174.

Torres-Rodriguez, N., Barnes, J.B., Taranovic, V., Pearce, M.A., Verral, M., Schoneveld, L.E., 2021. Reaction Coronas at Olivine–Plagioclase Contacts in Host Rocks from the Nova–Bollinger Ni–Cu–Co Deposit, Albany–Fraser Orogen, Western Australia: Evidence of a Magmatic to Metamorphic *Continuum. Journal of Petrology*, Vol. 62 (9), pp.1-24.doi: 10.1093/petrology/egab055

Ueki, K., Inui, M., Mutsunaga, K., Okamoto, N., Oshio, K., 2020. Oxidation during magma mixing recorded by symplectites at Kusatsu–Shirane Volcano, Central Japan. *Earth, Planets and Space*, Vol. 72 (68) https://doi.org/10.1186/s40623-020-01192-4.

van Zyl, A.C. Geochemistry and geochronology of the peripheral intrusions to the Kunene Anorthosite Complex in southern Angola and northern Namibia. MSc Thesis, Department of Geology at University of Pretoria, 2022.

Winter, J.D. Introduction to Igneous and Metamorphic Petrology. 2001. Prentice Hall. New Jersey.

Xue, S., Morse, S.A., 1993. Geochemistry of Nain massif anorthosite, Labrador: Magma diversity in five Intrusions. *Geochimica et Cosmochimica Acta*, Vol. 57, pp.3925-3948.

Chapter 8: Appendices

Appendix I – Petrography and Mineral Compositions of the MUM Intrusions

Table I.1-Petrographical Observations of the Thin Sections of Representative Samples from the MUM Intrusions in the KC.

Intrusion	Sample #	Sampletype	Lat/Long	Thin Section Description	Modal Abundances	Mineral Textures Relationships	Rocktype
Oncócua	ONC-1-35	DRILLCORE (@ 121.77 m depthin Drillhole ONC-1)	-16.713089/13.441456	Opx: Coarse- (6.0 mm) to fine- (0.5 mm) grained subhedral to anhedral; coarse grains are fractured and deformed, whereas the fine-grained fills the boundary spaces between the same mineral phases (microstructure texture) and also minerals Ap: Medium- (1.7 mm) to fine- (0.2 mm) grained euhedral to anhedral associated with both opq and opx; some fine grains appear as inclusion in the opq and vice versa Opq: usually in between Opx and the ap but also as inclusions in Opx and ap; the consist medium to fine-grained magnetite (2%) and pyrrhotite - chalcopyrite ± pentlandite (8%) blebs, stringers, and silicate fracture infills; the chalcopyrite appears to grow out of the pyrrhotite; locally net-textured sulphide	Opx (60%); Ap (30%); opq (10%)	Cumulus phases and deformation and fractures	Apatite Orthopyroxenite
	ONC-1-59	DRILLCORE (@ 157 m depth in Drillhole ONC-1)	-16.713089/13.441456	Ol: coarse (5.0 mm) to fine- (0.2 mm) grained subhedral to anhedral; clusters of medium-grained subhedral in places; all with cracks/fractures that are filled with Fe-rich due serpentinisation; corona around it when in contact with plag and mgt ± px coronas; chadacrysts in contact and enclosed by plag seems to cause cracks in plag probably due to serpentinisation fluid; some grains are almost completely altered or replaced to another mineral with lower relief (opx); resorbed textures (dissolution of crystals, usually fine around residual olivine) in large px (cpx and opx)	Ol (28%); Plg (20%); Opx (10%); Cpx (20%); Bt (5%); Opq (17%)	Cumulus phases; Ol resorbed olivine chadacryst in poikilitic cpx and opx; px exsolution texture; opx reaction rims around ol; strain is shown in plag; corona at the contact of ol/plag; two blocks: large ol + cpx with very little presence of plag and block of relatively small	Feldspathic Peridotite

				Px: Coarse- (5.0 mm) to fine- (0.6 mm) grained mainly anhedral; coarse oikocrysts having ol and plag chadacrysts; chadacrysts enclosed by ol oikocrysts locally; some coarse and medium grains show exsolution and sieving textures; opx mostly as reaction rims around olivine and some large altered poikilitic with resorbed ol chadacryst and exsolution; while cpx is mostly as large altered poikilitic with resorbed ol chadacryst Plagioclase:cumulus coarse- (6.0 mm) to interstitial fine- (0.5 mm) grained elongated and anhedral; inclusions to px; core-mantle microstructure (?) that suggest some strains; corona with Ol and the large crystals are being consumed in this reaction Biotite: fine-grained and mainly anhedral associated with opaque minerals mainly; Opaque: mainly pyrrhotite - chalcopyrite ± pentlandite (14%) stringers and blebs and Fe-Ti oxides (3%); chalcopyrite appears to grow out of pyrrhotite.		ol +cpx+interstitial plag and ap and opx rim reaction around ol; the two blocks are separated by large cumulus plag in which the large ol + cpx is surrounded by the plag; opx exsolving out of cpx	
	ONC-1-55	DRILLCORE (@ 145.49 m depth in Drillhole ONC-1)	-16.713089/13.441456	Olivine: coarse- (5.0 mm) to mainly medium- (5.0 mm) to fine- (0.1 mm) grained subhedral to anhedral and some elongated; clusters of medium-grained subhedral in places; the fine grains are either interstitial and resorbed chadacrysts to poikilitic cpx and opx; cracks/fractures in all grains; locally ophitic texture in which px grains are partially enveloped in olivine; olivine with orthopyroxene rim reaction; locally angular olivine chadacryst in cpx oikocrysts Pyroxene: Coarse- (5.0 mm) to medium- (1.0 mm) anhedral grains mainly; some large-grained opx and cpx are altered and show sieving and mainly opx exsolution in cpx (and vice-versa also occurs); poikilitic cpx and opx with ol chadacrysts and other inclusions especially in px large grains with some sort of alteration; fractures infilled with opq minerals; opx reaction rim around ol and opq (pyrrhotite and chalcopyrite growing out the pyrrhotite)	Ol (39%); Opx (11%); Cpx (39%); Opq (10% Fe-Ti oxide, po - cpy ± ptl); Bt (1%)	Cumulus phases; ol generations: subhedral and anhedral as well as chadacrysts (usually round resorbed texture, and scarce angular); opx and cpx poikilitic texture with resorbed ol; opx exsolving out of the cpx	Olivine websterite

				Bt: associated mainly with px, some as inclusions and others interstitially; opq: mainly Fe-Ti Oxide, pyrrhotite - chalcopyrite ± pentlandite (5%) in which Fe-Ti oxides (5%) and chalcopyrite appear to grow out of the pyrrhotite, associated mainly with px and bt and interstitially with ol; minor interstitial fine-grained anhedral plag locally			
Ohamaremba	KSAT 306-1	ROCK	-17.46517/13.407565	Plag: euhedral to anhedral medium- (2 mm) to fine- (0.15 mm) (latter, interstitial, and inclusion) laths to granular (stubby) with mainly simple, albite and minor pericline twinnings and some no twinning; inclusions in Ti-Fe oxide and ol in places; very few normal and oscillatory (?) zonings; some are poikilitic to ol/px chadacryst; no preferable orientation but some laths show ophitic texture in place in px Ol: euhedral to anhedral primocrysts mainly cumulate, medium- (1.8 mm) to v. fine- (0.7 mm) grained (some in inclusions in plag and px and other interstitially); cracks in all directions; it is locally surrounded by px and in some place inclusion in px; hosts inclusion of fine-grained Plg in places; bt and Ti-Fe oxide in the peripheral and also Ti-Fe oxides fill the cracks; some px seems to grow from ol Px (Px): rarely euhedral but mostly anhedral, and elongated around the ol; medium- (1.4 mm) to fine-grained (some in inclusion in plag); mainly opx Bt: appears throughout in interstitial but often surrounding magnetite; opaque: disseminated chalcopyrite growing out of pyrrhotite and magnetite all mainly interstitially but also some inclusions associated with bt, ol and px	Plag (65%); Ol (27%); Opx (4%); Cpx (1%); Bt (3%); Fe-Ti Oxide (1%)	Cumulus phases; poikilitic; ophitic texture of opx and cpx enclosing ol and plag; sub-ophitic; plag inclusion in ol and in opx	Orthopyroxene-bearing Leucotroctolite
	KSAT-157	DRILLCORE (@397 m depth in Drillhole KNAD001)	-17.460024/13.38688	Plag: coarse- (5.0 mm) to fine- (0.3 mm) grained subhedral to anhedral laths with some partially enveloped in ol in places and fine grains inclusions in ol as well; no preferential orientation; enclose chadacrysts in ol in places; the general texture plag laths seem to segregate the olivine grains	Plag (56%); Ol (33%); Bt (3%); Opq (5%); Cpx (3%)	Cumulus phases; ophitic texture of oli enclosing plag; plag inclusion in ol; serpentinisation+ other alteration	Clinopyroxene-bearing (Leuco) Troctotolite

				Ol: medium- (3.0 mm) to fine-(0.5 mm) grained, mainly anhedral but few subhedral; olivine enclosing plag to give ophitic texture in places; some grains are serpentinised and others are in early alteration stage; another alteration is related to probable carbonate material; one grain seems to alter from inside out leaving a formation of ol rim and altered core. Bt: associated with opq in places and associated with olivine and plag in places; px: minor mainly intercumulus cpx in the interstices of plag laths, but also locally intercumulus opx in the intertices of olivine and plag ; opq: mainly medium to fine-grained stringers and blebs of pyrrhotite and chalcopyrite and, to a lesser extent, magnetite (1%) mainly interstitially associated with olivine and plag boundaries			
Ombuku North	KSAT 322-1	ROCK	-17.25245/13.319049	Plag: medium- (1.8 mm) to fine- (0.2 mm) grained mainly granular anhedral with albite, Carlsbad, and minor pericline twinnings and other no twinnings; annealed texture Ol: medium- (3.0 mm) to fine- (0.5 mm) grained anhedral, highly fractured, associated with plag and surrounded by opx in place; the fine-grained is mainly interstitial to plag Px: mostly opx medium- (1.0 mm) to fine- (0.3 mm) grained subhedral to anhedral most well-preserved cumulates; opx+cpx vein crosscut the short dimension of the thin section and as moving towards the vein the mineral phases become deformed; some medium grains at lower & upper parts of the thin section are being altered and rims (coronas) are observed; opx inclusions in Plag in places; cpx is mostly interstitial of plag Opq: mainly fine-grained disseminated chalcopyrite ± pentlandite interstices and in fractures (cracks); bt: in places associated with altered px and to a lesser extent with the opq	Plag (70%); Opx (4%); Cpx (5%); Ol (20%); opaque (<<1%)	Cumulus phases; annealed texture	pyroxene-bearing Leucotroctolite
	KSAT 326-1	ROCK	-17.25039/13.31579	Plag: cumulus medium- (1.6 mm) to very fine- (0.16 mm) grained mainly granular anhedral	Plag (55%); Opx (33%); Cpx (6%);	Cumulus phases; fined-grained with annealing	Ol-bearing (Leuco) norite

				Px: mostly opx, medium- (1.0 mm) to fine- (0.2 mm) grained euhedral to anhedral mostly well-preserved cumulus; opx inclusions in plag in places; cpx is mainly fine-grained interstitial anhedral Bt: fills interstitial between plag and px; ol: fine- (0.5 mm) to very fine- (0.1 mm) grained anhedral interstitial and fractured surrounded by opx grains; opq: fine and disseminated and stringers of pyrrhotite ± pentlandite ± chalcopyrite and magnetite fill interstitial and fractures (cracks)	Ol (3%); Bt (2%); opq (<<1%)		
	4-778	DRILLCORE (@ in Drillhole KNBD002	-17.249135/13.319482	Opx: medium- (2.4 mm) to fine- (0.15 mm) grained, subhedral (mainly lower grain-size) to anhedral (the medium grain-size); zones of predominantly medium grain-size and also zones of predominantly fine grains; some elongated in which some probably fill veining-lets vein; oikocrysts with opx chadacrysts; some grains show sieve texture or opx growing out of ol; locally mild-strong serpentinised; strains in some coarse grains; some grains are cut by carbonate (?) veins that shows some shearing stress Cpx: mainly medium- (3 mm) to very fine- (0.16 mm) grained anhedral (some elongated) though some subhedral; places opx exsolution growing out of cpx; ol: fine (0.8 mm) to very fine (0.15 mm) grained anhedral mainly surrounded by opx grains; opq: chalcopyrite and pentlandite interstices and as infills in fractures of silicate phases	Cpx (46%); Opx (52%); Opq(<2%)	Cumulus phases; locally serpentinisation and an altered matrix (carbonate?) in other places; opx exsolution growing out of cpx; zones of large to very fine in which medium size are mostly subhedral; gradational grainsize	serpentinised Olivine-bearing Websterite
Otjijanjasemo	KSAT 305/122	ROCK	-17.45554/13.20294	Ol: medium- (1.7 mm) to fine (0.4 mm) euhedral to anhedral (this elongated); very coarse seems to be ophitic with Plag partially enveloped and the other way around is also true particularly ol fine grains; anhedral (likely interstitially) have some euhedral ol grains suggesting probably two generations; weakly serpentinised in places, but generally fresh grains Plag: coarse (6 mm) to fine (0.6 mm) euhedral mainly to anhedral laths; oikocryst to ol chadacrysts, but also partially enveloped by ol elsewhere; it also shows bends and cracks, especially in places associated with olivine (probably due to serpentinisation) and fractures not necessarily related to serpentinisation	Ol (45%); Plag (47%); Cpx(2%) Bt (2%); Opq (4%)	Cumulus phases; ophitic of intercumulus opx enclosing ol and sub-ophitic of plag enclosing ol; ol inclusions in plag and vice-versa	Clinopyroxene-bearing Troctolite

				Bt: associated mainly with opq forming the rim but also ol in some places; opq: interstitial disseminated chalcopyrite ± pentlandite blebs and stringers (1%) and magnetite (3%) associated with bt; px: minor amount locally interstitially between ol and to a lesser degree between ol and plag			
	KSAT 301/118	ROCK	-17.45837/13.20522	Ol: isolated medium- (2.8 mm) grained to fine- (1.0-0.1 mm) grained euhedral to subhedral mainly but some anhedral also; chads to plag and px oikocrysts; large grain partially enveloping plag laths locally (subophitic); clusters of fine olivine grains segregated by plag laths. Weakly serpentinised in places and the plag laths seem to crack in these places including where chadacrysts seem to serpentinise Plag: coarse- (6.0 mm) to fine- (0.8 mm) grained clusters to very fine (0.2 mm) euhedral to anhedral laths and stubby; locally one stubby grain partially envelops another plag laths Opx: medium- to fine - grained anhedral; elongated anhedral mainly interstitially and enveloping several fine olivine grains to give ophitic textures; though subhedral in place with some plag inclusion; opq: mainly interstitial pyrite and to a lesser chalcopyrite along the silicate phase boundaries	Ol (50%); Plag (46%); Cpx (4%); Opq (1%)	Cumulus phases; weakly to moderately serpentinised in places with fine olivine clusters throughout and ophitic texture of interstitial clinopyroxene enclosing olivine and large olivine enclosing plag (ol and plag locally; locally fine plag show preferred orientation; olivine inclusions in plag	Serpentinised Clinopyroxene-bearing Troctotolite
Plag= Plagioclase; Ol= Olivine; Px= Pyroxene; Opx= Orthopyroxene; Cpx=Clinopyroxene, Bt= Biotite; Ap= Apatite; Opq= Opaque; Mgt= Magnetite; Py=Pyrite; Cpy=Chalcopyrite							

Table I.2- In situ mineral compositional data of Olivine, Clinopyroxene and Orthopyroxene for the MUM intrusions in the KC.

Olivine																		
SAMPLEID	**Lithology**	**Intrusion**	**SiO2 (wt%)**	**TiO2 (wt%)**	**Al2O3 (wt%)**	**FeO (wt%)**	**MnO (wt%)**	**MgO (wt%)**	**CaO (wt%)**	**Na2O (wt%)**	**K2O (wt%)**	**Cr2O3 (wt%)**	**NiO (wt%)**	**Total (wt%)**	**Mg#**	**Fo (molar %)**	**Fa (molar %)**	**Ni (ppm)**
ONC-1-55	Olivine Websterite	Oncócua	35.94	0.00	0.00	37.04	0.50	26.77	0.03	0.00	0.00	0.01	0.00	100.29	56	56	43	0.00
			35.69	0.00	0.00	36.83	0.52	26.95	0.03	0.01	0.00	0.00	0.01	100.04	57	56	43	78.58
			35.79	0.01	0.00	36.72	0.52	27.15	0.03	0.01	0.00	0.01	0.02	100.25	57	56	43	157.17
			39.26	0.00	0.16	27.05	0.48	26.46	0.09	0.01	0.02	0.00	0.01	93.54	64	63	36	78.58

			36.00	0.02	0.00	36.61	0.49	27.28	0.03	0.00	0.00	0.00	0.01	100.45	57	57	43	78.58
			35.94	0.04	0.00	36.95	0.51	27.08	0.03	0.02	0.00	0.01	0.05	100.63	57	56	43	392.92
			35.84	0.00	0.00	36.68	0.52	27.13	0.03	0.01	0.01	0.00	0.02	100.26	57	56	43	157.17
			35.73	0.00	0.00	36.85	0.53	26.96	0.02	0.01	0.00	0.00	0.02	100.12	57	56	43	157.17
			35.88	0.00	0.00	36.75	0.51	27.07	0.03	0.00	0.01	0.02	0.02	100.28	57	56	43	157.17
			35.71	0.00	0.00	36.88	0.52	26.94	0.03	0.02	0.00	0.00	0.02	100.12	57	56	43	157.17
			35.84	0.01	0.00	36.80	0.49	26.95	0.02	0.00	0.00	0.00	0.04	100.16	57	56	43	314.34
			35.83	0.00	0.00	36.60	0.51	26.86	0.03	0.00	0.00	0.01	0.03	99.87	57	56	43	235.75
			35.71	0.01	0.00	37.05	0.50	26.89	0.03	0.01	0.00	0.00	0.04	100.24	56	56	43	314.34
			35.89	0.07	0.00	36.77	0.49	27.14	0.03	0.00	0.01	0.00	0.04	100.44	57	56	43	314.34
			35.71	0.03	0.01	36.35	0.48	27.11	0.03	0.00	0.00	0.00	0.02	99.76	57	57	43	157.17
			35.81	0.01	0.00	36.19	0.51	27.22	0.03	0.00	0.00	0.00	0.02	99.79	57	57	42	157.17
			35.94	0.00	0.00	35.58	0.48	27.95	0.02	0.00	0.01	0.01	0.03	100.02	58	58	41	235.75
			35.57	0.00	0.00	37.98	0.53	26.09	0.03	0.01	0.00	0.01	0.00	100.21	55	55	45	0.00
			35.55	0.01	0.00	38.06	0.54	25.91	0.02	0.00	0.00	0.00	0.03	100.13	55	54	45	235.75
			35.63	0.01	0.01	37.71	0.56	26.21	0.01	0.00	0.00	0.00	0.04	100.2	55	55	44	314.34
			35.92	0.00	0.01	36.85	0.52	26.75	0.03	0.03	0.01	0.00	0.01	100.13	56	56	43	78.58
			35.58	0.00	0.00	36.82	0.50	27.18	0.02	0.00	0.00	0.00	0.02	100.12	57	56	43	157.17
			35.61	0.01	0.01	37.05	0.51	26.96	0.03	0.01	0.00	0.00	0.03	100.21	56	56	43	235.75
ONC-1-59	Feldspathic Peridotite	Oncócua	36.03	0.00	0.00	36.56	0.50	27.20	0.02	0.00	0.00	0.00	0.02	100.33	57	57	43	157.17
			36.03	0.00	0.00	36.33	0.50	27.47	0.02	0.00	0.00	0.01	0.01	100.38	57	57	42	78.58
			36.02	0.00	0.00	36.26	0.46	27.41	0.04	0.00	0.01	0.00	0.02	100.22	57	57	42	157.17
			35.96	0.00	0.00	36.66	0.52	27.31	0.01	0.00	0.01	0.00	0.02	100.5	57	57	43	157.17
			35.90	0.00	0.01	36.42	0.51	27.29	0.03	0.01	0.00	0.00	0.03	100.2	57	57	43	235.75
			35.93	0.01	0.00	36.66	0.53	27.21	0.03	0.00	0.00	0.00	0.04	100.42	57	57	43	314.34
			35.87	0.00	0.01	36.21	0.48	27.64	0.02	0.01	0.00	0.01	0.04	100.28	58	57	42	314.34
			35.83	0.00	0.01	36.47	0.50	27.64	0.02	0.00	0.00	0.00	0.04	100.51	57	57	42	314.34

			35.60	0.01	0.01	36.75	0.52	27.42	0.02	0.00	0.00	0.00	0.02	100.36	57	57	43	157.17
			36.02	0.00	0.00	36.45	0.53	27.57	0.05	0.01	0.00	0.00	0.00	100.62	57	57	42	0.00
			36.13	0.01	0.00	36.54	0.49	27.39	0.04	0.01	0.00	0.01	0.02	100.65	57	57	43	157.17
			36.08	0.00	0.00	36.49	0.50	27.37	0.02	0.01	0.00	0.02	0.01	100.51	57	57	43	78.58
			35.97	0.00	0.01	36.52	0.53	27.51	0.03	0.00	0.01	0.00	0.01	100.58	57	57	42	78.58
			36.97	0.00	0.00	35.10	0.48	28.01	0.06	0.00	0.01	0.01	0.02	100.65	59	58	41	157.17
			36.53	0.00	0.00	34.35	0.51	27.74	0.02	0.01	0.00	0.00	0.03	99.19	59	59	41	235.75
			28.80	0.00	0.01	42.78	0.23	23.25	0.09	0.03	0.02	0.01	0.01	95.23	49	49	51	78.58
			36.28	0.01	0.00	35.48	0.48	28.91	0.04	0.02	0.01	0.00	0.04	101.26	59	59	41	314.34
			35.84	0.01	0.00	36.71	0.50	27.37	0.02	0.01	0.00	0.00	0.02	100.49	57	57	43	157.17
			35.97	0.01	0.00	36.69	0.50	27.30	0.02	0.01	0.00	0.00	0.01	100.51	57	57	43	78.58
KSAT 322-1	Pyroxene-bearing Leucotroctolite	Ombuku North	39.79	0.00	0.00	16.84	0.23	42.54	0.00	0.00	0.00	0.00	0.21	99.62	82	81	18	1650.27
			39.33	0.00	0.00	17.12	0.24	42.85	0.01	0.02	0.00	0.00	0.25	99.82	82	81	18	1964.61
			39.40	0.01	0.00	17.04	0.25	43.04	0.00	0.00	0.00	0.00	0.27	100.02	82	81	18	2121.78
KSAT 157-1	Pyroxene-bearing (Leuco) Troctolite	Ohamaremba	37.29	0.04	0.03	27.40	0.35	34.64	0.09	0.01	0.00	0.00	0.09	99.94	69	69	31	707.26
			36.72	0.03	0.03	27.45	0.36	34.59	0.10	0.01	0.00	0.00	0.12	99.4	69	69	31	943.01
			37.57	0.03	0.02	27.51	0.35	34.07	0.10	0.00	0.00	0.00	0.13	99.78	69	68	31	1021.60
			37.51	0.04	0.02	27.65	0.37	34.25	0.12	0.01	0.01	0.00	0.10	100.09	69	68	31	785.85
			36.29	0.02	0.02	27.51	0.35	34.55	0.11	0.01	0.00	0.00	0.13	99	69	69	31	1021.60
			37.70	0.01	0.02	27.34	0.38	34.73	0.10	0.01	0.00	0.00	0.12	100.41	69	69	30	943.01
			36.39	0.13	0.01	27.25	0.38	34.83	0.11	0.02	0.00	0.01	0.12	99.23	70	69	30	943.01
			37.55	0.03	0.01	27.47	0.37	34.09	0.07	0.01	0.00	0.01	0.11	99.71	69	68	31	864.43
			37.44	0.04	0.02	27.17	0.38	34.80	0.09	0.01	0.00	0.00	0.10	100.05	70	69	30	785.85
			37.29	0.04	0.02	27.60	0.34	34.17	0.10	0.01	0.00	0.00	0.13	99.72	69	68	31	1021.60
			37.09	0.04	0.03	27.30	0.36	34.65	0.09	0.00	0.00	0.00	0.11	99.68	69	69	30	864.43
			36.80	0.04	0.02	27.00	0.35	35.22	0.08	0.01	0.00	0.00	0.13	99.66	70	69	30	1021.60
			36.97	0.01	0.01	26.62	0.35	35.87	0.07	0.00	0.01	0.01	0.14	100.08	71	70	29	1100.18

			36.16	0.03	0.02	27.12	0.36	35.69	0.08	0.00	0.00	0.00	0.13	99.59	70	70	30	1021.60
			37.35	0.03	0.02	27.16	0.37	34.77	0.09	0.01	0.00	0.00	0.11	99.91	70	69	30	864.43
			36.78	0.04	0.02	27.40	0.40	34.92	0.10	0.01	0.00	0.00	0.16	99.83	69	69	30	1257.35
			38.06	0.05	0.00	26.92	0.37	34.47	0.07	0.00	0.00	0.00	0.13	100.07	70	69	30	1021.60
			35.85	0.00	0.01	26.48	0.38	35.84	0.08	0.00	0.00	0.01	0.12	98.77	71	70	29	943.01
			37.44	0.03	0.01	27.29	0.39	34.47	0.09	0.00	0.00	0.00	0.11	99.83	69	69	31	864.43
			37.28	0.04	0.02	27.38	0.39	34.56	0.10	0.01	0.01	0.00	0.10	99.88	69	69	31	785.85
			37.53	0.02	0.02	27.28	0.37	34.17	0.11	0.01	0.00	0.00	0.12	99.64	69	69	31	943.01
KSAT 306-1	Leucotroctolite	Ohamaremba	37.64	0.02	0.02	27.30	0.38	34.62	0.09	0.01	0.00	0.00	0.10	100.19	69	69	30	785.85
			37.77	0.03	0.01	27.33	0.37	34.76	0.08	0.01	0.01	0.00	0.12	100.5	69	69	30	943.01
			37.29	0.04	0.02	27.13	0.40	34.93	0.07	0.01	0.00	0.00	0.15	100.04	70	69	30	1178.77
			37.32	0.03	0.03	28.14	0.39	34.28	0.05	0.01	0.00	0.01	0.13	100.38	68	68	31	1021.60
			37.43	0.03	0.01	28.19	0.39	34.27	0.08	0.01	0.00	0.00	0.13	100.54	68	68	31	1021.60
			37.36	0.02	0.00	28.29	0.40	34.24	0.08	0.01	0.00	0.01	0.13	100.54	68	68	31	1021.60
			37.34	0.04	0.01	28.09	0.40	34.07	0.08	0.02	0.00	0.00	0.12	100.18	68	68	31	943.01
			37.43	0.02	0.01	28.17	0.41	33.80	0.08	0.00	0.00	0.00	0.13	100.07	68	68	32	1021.60
			37.42	0.04	0.03	28.37	0.41	33.92	0.07	0.01	0.00	0.01	0.13	100.41	68	68	32	1021.60
			37.38	0.06	0.01	27.51	0.40	34.08	0.09	0.00	0.00	0.00	0.14	99.67	69	68	31	1100.18
			30.82	0.03	0.03	27.40	0.38	37.79	0.06	0.01	0.00	0.01	0.12	96.65	71	71	29	943.01
			37.54	0.01	0.01	28.60	0.39	33.64	0.07	0.01	0.00	0.01	0.13	100.41	68	67	32	1021.60
			37.76	0.04	0.01	28.51	0.39	33.74	0.08	0.01	0.01	0.00	0.14	100.69	68	67	32	1100.18
			36.75	0.04	0.01	28.18	0.41	34.32	0.07	0.01	0.00	0.00	0.13	99.91	68	68	31	1021.60
			37.21	0.03	0.01	28.07	0.38	34.44	0.10	0.00	0.00	0.00	0.15	100.39	69	68	31	1178.77
			37.38	0.03	0.02	28.14	0.42	34.19	0.08	0.02	0.01	0.00	0.13	100.42	68	68	31	1021.60
			37.18	0.04	0.01	28.57	0.40	33.70	0.10	0.00	0.00	0.00	0.14	100.15	68	67	32	1100.18
			37.42	0.01	0.01	28.37	0.41	33.71	0.11	0.00	0.00	0.01	0.11	100.17	68	67	32	864.43
			37.48	0.03	0.03	28.35	0.39	34.00	0.08	0.00	0.00	0.01	0.12	100.49	68	68	32	943.01

			37.94	0.04	0.02	27.75	0.39	33.98	0.06	0.00	0.01	0.00	0.13	100.33	69	68	31	1021.60
			37.22	0.01	0.02	28.17	0.38	33.92	0.09	0.00	0.00	0.01	0.15	99.97	68	68	32	1178.77
			37.18	0.05	0.02	28.20	0.37	33.67	0.07	0.02	0.01	0.00	0.11	99.7	68	68	32	864.43
			37.51	0.05	0.02	27.87	0.39	34.18	0.05	0.00	0.00	0.00	0.12	100.19	69	68	31	943.01
KSAT 301-118	Serpentinised Pyroxene-bearing Troctolite	Otjijanjasemo	37.48	0.02	0.02	28.08	0.35	33.83	0.11	0.00	0.00	0.01	0.09	99.99	68	68	32	707.26
			37.58	0.03	0.01	27.98	0.36	33.75	0.09	0.00	0.01	0.00	0.10	99.9	68	68	32	785.85
			37.46	0.05	0.01	27.94	0.36	33.99	0.09	0.01	0.00	0.02	0.09	100.02	68	68	31	707.26
			37.38	0.03	0.02	28.14	0.35	33.91	0.06	0.00	0.00	0.01	0.09	99.99	68	68	32	707.26
			37.02	0.05	0.01	28.61	0.38	33.61	0.10	0.00	0.00	0.02	0.06	99.86	68	67	32	471.51
			37.25	0.00	0.01	28.61	0.38	33.48	0.11	0.02	0.00	0.01	0.09	99.98	68	67	32	707.26
			37.07	0.09	0.00	29.10	0.37	33.01	0.12	0.00	0.01	0.01	0.11	99.89	67	66	33	864.43
			37.28	0.04	0.02	28.28	0.40	33.73	0.13	0.01	0.00	0.02	0.09	99.98	68	68	32	707.26
			37.37	0.04	0.01	28.38	0.35	33.85	0.10	0.00	0.00	0.00	0.09	100.2	68	68	32	707.26
			37.15	0.05	0.01	28.16	0.40	33.59	0.09	0.01	0.01	0.00	0.09	99.56	68	68	32	707.26
			37.48	0.04	0.02	28.37	0.41	33.83	0.12	0.00	0.00	0.00	0.08	100.36	68	68	32	628.68
			37.16	0.06	0.02	28.37	0.36	33.82	0.07	0.01	0.00	0.00	0.08	99.96	68	68	32	628.68
			37.14	0.04	0.01	28.48	0.40	33.44	0.09	0.01	0.01	0.00	0.08	99.7	68	67	32	628.68
			37.29	0.06	0.01	28.02	0.36	33.86	0.07	0.00	0.02	0.00	0.07	99.75	68	68	32	550.09
			37.35	0.06	0.02	28.94	0.40	33.60	0.09	0.00	0.00	0.00	0.05	100.49	67	67	32	392.92
			37.20	0.03	0.01	28.95	0.38	33.08	0.08	0.00	0.00	0.00	0.09	99.83	67	67	33	707.26
			37.23	0.04	0.00	29.10	0.41	33.24	0.06	0.01	0.00	0.00	0.03	100.11	67	67	33	235.75
			37.18	0.04	0.02	27.86	0.36	34.05	0.05	0.00	0.01	0.02	0.10	99.69	69	68	31	785.85
			37.41	0.02	0.02	27.85	0.36	33.87	0.06	0.01	0.00	0.00	0.09	99.67	68	68	31	707.26
			37.14	0.05	0.02	29.15	0.38	32.97	0.08	0.00	0.00	0.00	0.09	99.87	67	66	33	707.26
			37.56	0.04	0.02	28.11	0.38	33.98	0.07	0.00	0.00	0.00	0.09	100.25	68	68	32	707.26
KSAT 305-122	Troctolite	Otjijanjasemo	36.75	0.03	0.00	30.57	0.44	31.98	0.10	0.00	0.00	0.00	0.06	99.93	65	65	35	471.51
			36.97	0.05	0.01	30.36	0.42	32.44	0.07	0.02	0.00	0.00	0.07	100.42	66	65	34	550.09

			36.82	0.03	0.00	30.64	0.43	31.95	0.11	0.00	0.00	0.00	0.08	100.07	65	65	35	628.68
			37.03	0.06	0.00	30.53	0.39	31.95	0.11	0.00	0.01	0.00	0.06	100.14	65	65	35	471.51
			37.22	0.02	0.02	30.41	0.39	32.10	0.09	0.01	0.00	0.01	0.09	100.36	65	65	34	707.26
			36.85	0.04	0.00	30.62	0.41	32.32	0.09	0.00	0.00	0.01	0.08	100.42	65	65	34	628.68
			36.90	0.04	0.02	30.60	0.42	32.01	0.10	0.00	0.00	0.00	0.08	100.17	65	65	35	628.68
			36.93	0.04	0.02	30.68	0.43	31.94	0.07	0.01	0.00	0.01	0.08	100.2	65	65	35	628.68
			36.78	0.06	0.02	30.64	0.45	31.76	0.10	0.01	0.01	0.00	0.08	99.9	65	64	35	628.68
			36.86	0.04	0.01	30.62	0.43	32.05	0.11	0.00	0.00	0.00	0.11	100.23	65	65	35	864.43
			36.75	0.07	0.02	30.77	0.41	32.01	0.10	0.00	0.00	0.01	0.09	100.22	65	65	35	707.26
			36.85	0.03	0.02	30.71	0.43	32.01	0.07	0.00	0.00	0.00	0.06	100.18	65	65	35	471.51
			36.98	0.05	0.02	30.68	0.42	31.23	0.12	0.01	0.01	0.01	0.09	99.61	64	64	35	707.26
			37.01	0.06	0.02	30.55	0.41	31.99	0.07	0.00	0.00	0.00	0.08	100.18	65	65	35	628.68
			37.06	0.05	0.02	30.31	0.36	32.03	0.11	0.01	0.00	0.01	0.07	100.01	65	65	34	550.09
			36.82	0.03	0.02	30.56	0.40	32.02	0.06	0.00	0.00	0.02	0.08	99.99	65	65	35	628.68
			37.01	0.04	0.00	30.32	0.42	32.38	0.06	0.01	0.00	0.02	0.08	100.33	66	65	34	628.68
			36.88	0.05	0.02	30.40	0.44	32.02	0.07	0.00	0.00	0.01	0.08	99.98	65	65	35	628.68
			36.75	0.06	0.01	30.21	0.41	32.18	0.06	0.00	0.00	0.00	0.10	99.79	66	65	34	785.85
			36.91	0.04	0.02	30.99	0.44	31.89	0.07	0.00	0.00	0.00	0.10	100.45	65	64	35	785.85
			36.81	0.05	0.02	30.12	0.40	32.14	0.06	0.00	0.00	0.00	0.09	99.68	66	65	34	707.26
			36.82	0.04	0.01	30.29	0.44	32.29	0.08	0.01	0.00	0.00	0.10	100.09	66	65	34	785.85
			37.00	0.07	0.02	30.63	0.43	31.87	0.08	0.01	0.00	0.00	0.09	100.19	65	65	35	707.26

Clinopyroxene

SAMPLEID	Lithology	Intrusion	SiO2 (wt%)	TiO2 (wt%)	Al2O3 (wt%)	FeO (wt%)	MnO (wt%)	MgO (wt%)	CaO (wt%)	Na2O (wt%)	K2O (wt%)	Cr2O3 (wt%)	NiO (wt%)	Total (wt%)	Mg#	Cr (ppm)	Wo	En	Fs
		Oncócua	50.81	0.83	3.2	8.73	0.25	14.01	20.98	0.44	0.00	0.06	0.00	99.32	74	410.52	44	41	14

0.00ONC-1-55	Olivine Websterite		51.57	0.64	2.9	15.29	0.34	17.44	11.38	0.37	0.01	0.03	0.00	99.97	67	205.26	24	51	25
			51.02	0.94	3.26	9.12	0.25	14.53	20.22	0.45	0.01	0.04	0.00	99.84	74	273.68	43	43	15
			50.45	1.07	3.61	8.22	0.22	13.36	21.7	0.52	0.00	0.04	0.01	99.2	74	273.68	42	40	14
			50.84	0.92	3.5	10.63	0.27	14.89	18.49	0.42	0.00	0.04	0.02	100.01	71	273.68	39	44	17
			50.37	0.97	3.58	8.81	0.23	13.82	21.11	0.45	0.00	0.05	0.01	99.4	74	342.10	45	41	15
			50.97	0.73	3.1	10.75	0.29	14.88	18.16	0.43	0.01	0.03	0.01	99.37	71	205.26	38	44	18
			50.49	0.98	3.7	8.3	0.25	13.38	21.68	0.55	0.00	0.04	0.02	99.39	74	273.68	46	40	14
			50.95	0.91	3.5	7.93	0.23	13.34	22.53	0.46	0.01	0.05	0.00	99.9	75	342.10	48	39	13
			49.74	1.43	2.67	11.87	0.29	14.04	18.32	0.35	0.00	0.03	0.01	98.76	68	205.26	39	41	20
			50.56	0.92	3.72	9.67	0.26	13.39	20.07	0.56	0.00	0.05	0.00	99.2	71	342.10	43	40	16
			51.3	0.67	2.99	8.19	0.25	13.54	22.24	0.45	0.00	0.05	0.01	99.71	75	342.10	47	37	13
			50.26	0.94	3.78	9.89	0.27	13.76	19.88	0.56	0.00	0.06	0.02	99.42	71	410.52	43	41	17
			50.96	0.83	3.2	8.33	0.22	13.6	21.89	0.48	0.00	0.04	0.02	99.56	74	273.68	46	40	14
			50.83	0.9	3.27	8.65	0.24	13.44	21.24	0.48	0.00	0.04	0.01	99.11	73	273.68	45	40	14
			51.58	0.44	2.7	16.54	0.37	17.67	10.52	0.26	0.00	0.04	0.03	100.14	66	273.68	22	51	27
			50.5	1.01	3.66	8.78	0.25	13.76	20.93	0.48	0.00	0.02	0.01	99.41	74	136.84	45	41	15
ONC-1-59	Feldspathic Peridotite	Oncócua	50.65	1.05	3.51	9.8	0.26	13.67	20.17	0.45	0.00	0.04	0.00	99.59	71	273.68	43	41	16
			50.67	1.02	3.55	10.2	0.26	14.63	18.92	0.47	0.01	0.06	0.00	99.79	72	410.52	40	43	17
			51.09	0.95	2.83	11.83	0.32	16.32	15.86	0.34	0.00	0.07	0.03	99.64	71	478.94	33	48	19
			50.46	0.9	4.07	8.01	0.19	14.17	20.46	0.83	0.00	0.04	0.00	99.14	76	273.68	44	42	13
			45.9	1.92	7.95	9.81	0.18	13.46	17.19	1.96	0.24	0.06	0.01	98.7	71	410.52	39	43	18
			51.07	0.88	3.54	8.31	0.22	13.61	21.51	0.45	0.00	0.05	0.00	99.63	75	342.10	46	40	14
			50.72	0.98	3.33	8.46	0.24	13.45	21.75	0.5	0.01	0.04	0.01	99.47	74	273.68	46	40	14
			50.84	0.92	3.2	9.99	0.25	13.9	19.96	0.56	0.00	0.05	0.00	99.68	71	342.10	42	41	17
			50.48	1.15	3.69	10.35	0.27	13.42	19.77	0.51	0.00	0.04	0.01	99.69	70	273.68	43	40	17
			51.25	0.73	3.18	12.68	0.35	15.25	16.65	0.35	0.01	0.04	0.01	100.49	68	273.68	35	44	21
			50.46	1.28	3.39	11.96	0.29	15.14	16.68	0.4	0.01	0.03	0.00	99.64	69	205.26	35	45	20

			50.65	1.13	3.6	10.88	0.28	14.35	18.76	0.42	0.00	0.04	0.00	100.12	70	273.68	40	42	18
			51.22	0.9	3.22	9.97	0.25	14.9	19.18	0.42	0.00	0.04	0.00	100.12	73	273.68	40	43	16
KSAT 322-1	Pyroxene-bearing Leucotroctolite	Ombuku North	48.77	1.43	6.81	5.47	0.13	13.02	22.43	0.95	0.00	0.44	0.04	99.5	81	3010.49	50	40	10
			48.99	1.38	6.68	5.96	0.13	13.9	21.17	0.95	0.00	0.41	0.04	99.6	81	2805.23	47	43	10
			48.69	1.42	6.83	5.52	0.14	13.19	22	1.03	0.00	0.43	0.02	99.28	81	2942.07	49	41	10
4-778	Serpentinised Websterite	Ombuku North	51.03	0.81	4.9	3.77	0.11	14.49	22.89	0.96	0.00	0.6	0.04	99.62	87	4105.21	50	44	6
			51.02	0.8	5.02	3.9	0.13	14.75	22.41	0.98	0.00	0.66	0.01	99.69	87	4515.73	49	45	7
			50.72	0.83	5.3	3.75	0.11	14.21	22.62	1.04	0.01	0.66	0.00	99.24	87	4515.73	50	44	6
			50.47	0.88	5.63	4.34	0.13	14.1	22.25	0.98	0.00	0.84	0.03	99.64	85	5747.30	49	43	7
			50.2	0.98	5.74	4.29	0.12	13.95	22.42	0.96	0.01	0.8	0.01	99.47	85	5473.62	50	43	7
			50.62	0.87	5.38	4.11	0.13	14.29	22.28	1.02	0.00	0.76	0.03	99.48	86	5199.94	49	44	7
			50.37	0.88	5.58	4.11	0.12	14.26	22.62	1.02	0.00	0.78	0.03	99.78	86	5336.78	50	43	7
			50.42	0.85	5.65	4.24	0.1	14.04	22.09	1.1	0.00	0.81	0.01	99.3	86	5542.04	49	43	7
			50.5	0.86	5.44	4.17	0.13	14.32	22.13	1.03	0.00	0.74	0.03	99.36	86	5063.09	49	44	7
			50.63	0.99	5.47	4.07	0.09	14.17	22.52	1.01	0.00	0.83	0.00	99.78	86	5678.88	50	43	7
			50.12	0.89	5.55	4.29	0.12	14.25	22.34	1	0.00	0.82	0.01	99.37	86	5610.46	49	44	7
			50.43	0.87	5.72	4.46	0.13	14.49	21.84	0.96	0.00	0.87	0.03	99.8	85	5952.56	48	44	8
KSAT 157	Pyroxene-bearing (Leuco) Troctolite	Ohamaremba	49.81	1.19	3.07	7.87	0.2	14.39	21.22	0.51	0.00	0.34	0.01	98.61	77	2326.29	45	42	13
			50.76	1.11	2.94	8.65	0.23	14.02	20.98	0.42	0.00	0.04	0.03	99.17	74	273.68	44	41	14
			51.81	0.87	2.24	12	0.3	17.33	15.44	0.32	0.01	0.01	0.03	100.36	72	68.42	32	49	19
KSAT 301-118	Serpentinised Pyroxene-bearing Troctolite	Otjijanjasemo	49.84	1.62	3.6	8.62	0.19	14.21	20.61	0.53	0.01	0.39	0.01	99.65	75	2668.39	44	42	14
			49.6	1.67	3.86	8.49	0.2	13.92	20.9	0.58	0.00	0.38	0.02	99.62	75	2599.97	45	41	14
			50.65	1.39	3.14	8.41	0.19	14.46	20.63	0.5	0.00	0.37	0.04	99.8	75	2531.55	44	43	14

			49.18	1.8	3.93	8.76	0.19	13.98	19.94	0.55	0.00	0.43	0.01	98.78	74	2942.07	43	42	15
KSAT 305-122	Troctolite	Otjijanjasemo	49.46	1.89	3.74	9.25	0.18	13.79	20.45	0.51	0.00	0.06	0.04	99.37	73	410.52	44	41	15
			49.04	1.93	3.73	8.89	0.21	13.74	21.02	0.48	0.00	0.07	0.03	99.14	73	478.94	45	41	15
			49.09	1.93	3.68	9.47	0.21	14.11	19.84	0.47	0.00	0.07	0.02	98.89	73	478.94	42	42	16
			50.35	1.38	2.82	9.24	0.21	14.22	20.16	0.5	0.00	0.03	0.02	98.93	73	205.26	43	42	15
			50.62	1.29	2.59	8.62	0.2	14.1	20.9	0.49	0.00	0.04	0.00	98.86	74	273.68	44	41	14
			50.69	1.33	2.62	9.63	0.19	14.86	19.84	0.45	0.01	0.04	0.02	99.68	73	273.68	41	43	16
			50.2	1.55	3.15	9.29	0.21	14.12	20.24	0.51	0.01	0.01	0.00	99.29	73	68.42	43	42	15
			50.44	1.41	2.76	9.17	0.2	14.25	20.24	0.49	0.00	0.05	0.02	99.03	73	342.10	43	42	15
			51.15	1.31	2.51	10.04	0.22	14.95	19.27	0.48	0.00	0.04	0.02	99.99	73	273.68	40	43	16
			50.33	1.35	2.94	9.56	0.18	14.26	20.21	0.47	0.00	0.02	0.01	99.33	73	136.84	42	41	16
			50.35	1.34	2.94	9.39	0.19	14.21	20.21	0.51	0.00	0.03	0.01	99.18	73	205.26	42	41	15
			49.11	1.81	3.56	9.29	0.18	13.57	20.55	0.49	0.00	0.05	0.02	98.64	72	342.10	44	40	15
			49.34	1.86	3.69	8.78	0.18	13.56	20.93	0.49	0.00	0.06	0.03	98.93	73	410.52	44	40	15
			50.21	1.49	2.98	9.58	0.21	14.61	19.57	0.45	0.00	0.06	0.01	99.18	73	410.52	41	42	16
			49.7	1.79	3.52	9.11	0.17	14.09	20.05	0.48	0.00	0.06	0.01	98.98	73	410.52	42	41	15

Orthopyroxene																			
SAMPLEID	**Lithology**	**Intrusion**	**SiO2 (wt%)**	**TiO2 (wt%)**	**Al2O3 (wt%)**	**FeO (wt%)**	**MnO (wt%)**	**MgO (wt%)**	**CaO (wt%)**	**Na2O (wt%)**	**K2O (wt%)**	**Cr2O3 (wt%)**	**NiO (wt%)**	**Total (wt%)**	**Mg #**	**Cr (ppm)**	**En**	**Fs**	**Wo**
ONC-1-59	Feldspathic Peridotite	Oncócua	45.59	0.00	0.04	11.75	0.19	32.49	0.13	0.06	0.05	0.00	0.03	90.34	83	0.00	82.94	16.83	0.24
			45.45	0.02	0.00	7.42	0.27	33.6	0.27	0.01	0.05	0.00	0.00	87.09	89	0.00	88.52	10.97	0.51
			45.67	0.00	0.00	7.54	0.24	33.75	0.22	0.02	0.07	0.00	0.01	87.53	89	0.00	88.49	11.09	0.41
			41.86	0.03	0.1	20.07	0.37	31.18	0.1	0.03	0.03	0.01	0.00	93.8	73	68.42	73.35	26.48	0.17
ONC-1-35	Olivine-bearing	Oncócua	50.8	1.79	1.45	24.2	0.55	19.87	1.93	0.04	0.00	0.02	0.02	100.67	59	136.84	57.04	38.97	3.98

	Apatite Pyroxenite		51.56	0.21	1.6	22.78	0.54	19.58	2.85	0.08	0.00	0.02	0.00	99.22	61	136.84	56.91	37.14	5.95
			51.97	0.21	1.55	23.47	0.55	20.21	1.79	0.03	0.00	0.01	0.00	99.79	61	68.42	58.3	37.98	3.71
			52.06	0.2	1.43	23.84	0.58	20.73	1.01	0.03	0.00	0.02	0.00	99.91	61	136.84	59.52	38.4	2.08
			52.36	0.21	1.52	23.23	0.55	20.42	1.91	0.04	0.00	0.01	0.00	100.26	61	68.42	58.64	37.42	3.94
			52	0.19	1.67	21.58	0.53	19.67	3.46	0.09	0.01	0.03	0.02	99.24	62	205.26	57.41	35.33	7.26
			52.33	0.25	1.44	23.89	0.55	20.87	0.93	0.00	0.00	0.02	0.03	100.31	61	136.84	59.73	38.36	1.91
			51.81	0.18	1.48	23.75	0.56	20.96	0.62	0.01	0.00	0.04	0.00	99.42	61	273.68	60.35	38.36	1.28
			51.96	0.23	1.52	23.94	0.54	20.68	0.8	0.02	0.00	0.02	0.02	99.72	61	136.84	59.62	38.72	1.66
			52.04	0.22	1.64	23	0.52	20.07	2.22	0.06	0.00	0.01	0.01	99.79	61	68.42	58.06	37.33	4.62
			52.14	0.17	1.71	23.3	0.53	20.32	1.67	0.03	0.00	0.02	0.00	99.9	61	136.84	58.74	37.79	3.47
			52.04	0.21	1.78	22.26	0.51	19.76	3.24	0.08	0.00	0.00	0.00	99.88	61	0.00	57.15	36.12	6.73
			51.28	1.55	1.47	24.5	0.57	19.93	1.56	0.04	0.00	0.02	0.01	100.93	59	136.84	57.28	39.5	3.22
			51.73	0.16	1.73	22.42	0.52	19.56	2.96	0.11	0.00	0.00	0.00	99.2	61	0.00	57.09	36.71	6.21
			52.08	0.22	1.61	22.94	0.57	20.08	2.3	0.04	0.00	0.02	0.02	99.88	61	136.84	58.03	37.19	4.78
			51.96	0.3	1.41	24	0.55	20.36	1.11	0.04	0.01	0.02	0.01	99.77	60	136.84	58.81	38.89	2.3
			51.77	0.37	1.54	23.66	0.54	20.31	1.47	0.02	0.01	0.01	0.03	99.73	61	68.42	58.63	38.32	3.05
			52.01	0.35	1.52	23.6	0.53	20.51	1.35	0.03	0.01	0.03	0.00	99.94	61	205.26	59.07	38.13	2.79
			52.32	0.16	1.45	23.48	0.54	20.63	1.47	0.02	0.01	0.03	0.00	100.11	61	205.26	59.18	37.79	3.03
			50.86	2.63	1.05	24.62	0.57	19.81	1.21	0.02	0.00	0.00	0.04	100.82	59	0.00	57.44	40.04	2.52
			52.15	0.25	1.44	23.84	0.54	20.44	1.14	0.02	0.00	0.01	0.00	99.84	60	68.42	59.02	38.62	2.37
KSAT 322-1	Pyroxene-bearing Leucotroctolite	Ombuku North	54.24	0.07	2.61	12.17	0.27	29.68	0.33	0.03	0.00	0.01	0.07	99.49	81	68.42	80.77	18.58	0.65
			54.43	0.11	3.23	12.12	0.25	29.16	0.49	0.02	0.01	0.02	0.04	99.87	81	136.84	80.29	18.74	0.97
			53.53	0.15	4.29	12.5	0.24	28.58	0.43	0.02	0.00	0.08	0.06	99.89	80	547.36	79.61	19.53	0.86

			54.13	0.13	3.77	12.57	0.27	28.57	0.57	0.02	0.01	0.05	0.04	100.12	80	342.10	79.29	19.57	1.14
			53.98	0.08	3.48	12.56	0.27	28.85	0.43	0.02	0.01	0.05	0.05	99.8	80	342.10	79.69	19.46	0.85
			54.87	0.12	2.63	12.04	0.26	29.34	0.4	0.01	0.00	0.00	0.05	99.8	81	478.94	80.64	18.56	0.79
			53.55	0.16	4.06	12.49	0.24	28.69	0.54	0.03	0.00	0.00	0.05	99.88	80	547.36	79.51	19.42	1.08
			54.22	0.15	3.39	12.46	0.26	28.84	0.45	0.01	0.00	0.00	0.06	99.92	81	547.36	79.77	19.33	0.89
			53.2	0.16	4.26	12.72	0.25	28.65	0.53	0.02	0.00	0.00	0.05	99.93	80	547.36	79.22	19.73	1.05
			53.3	0.21	4.5	12.88	0.28	28.11	0.56	0.00	0.00	0.00	0.07	100.05	80	957.88	78.66	20.22	1.13
			52.7	0.25	4.72	12.86	0.27	28.06	0.57	0.02	0.01	0.16	0.05	99.66	80	1094.72	78.63	20.22	1.15
			53.04	0.19	4.34	12.98	0.27	28.04	0.54	0.01	0.00	0.00	0.04	99.54	79	547.36	78.52	20.39	1.09
4-778	Serpentinised Websterite	Ombuku North	54.86	0.18	3.4	10.17	0.24	30.39	0.53	0.00	0.00	0.26	0.05	100.08	84	1778.93	81.331	15.64	1.04
			54.7	0.19	3.51	10.11	0.22	30.44	0.53	0.03	0.01	0.29	0.04	100.07	84	1984.19	83.41	15.54	1.04
			55.05	0.16	3.1	9.97	0.22	30.67	0.43	0.01	0.00	0.22	0.05	99.89	85	1505.24	83.86	15.29	0.85
			54.32	0.15	3.5	10.03	0.27	30.44	0.02	0.02	0.02	0.27	0.01	99.86	84	1847.35	84.37	15.59	0.04
			54.51	0.24	3.57	9.91	0.24	29.99	1.36	0.09	0.01	0.35	0.04	100.3	84	2394.71	82.1	15.22	2.68
			54.72	0.22	3.67	9.93	0.22	30.11	0.99	0.05	0.01	0.31	0.03	100.24	84	2121.03	82.74	15.31	1.96
			54.84	0.17	3.13	10.24	0.23	30.49	0.53	0.02	0.00	0.28	0.04	99.97	84	1915.77	83.27	15.69	1.04
			54.55	0.22	3.45	10.1	0.23	30.27	0.62	0.03	0.00	0.34	0.03	99.85	84	2326.29	83.2	15.57	1.22
			54.92	0.16	2.99	10.29	0.24	30.58	0.43	0.01	0.01	0.23	0.05	99.92	84	1573.66	83.41	15.75	0.84
			54.19	0.19	3.63	10.31	0.24	30.19	0.02	0.02	0.00	0.41	0.03	99.68	84	2805.23	83.89	16.07	0.04
			54.49	0.19	3.77	10.3	0.23	30.12	0.49	0.03	0.01	0.43	0.07	100.15	84	2942.07	83.09	15.94	0.97
			54.14	0.25	3.84	10.16	0.26	29.98	0.98	0.06	0.00	0.4	0.04	100.11	84	2736.81	82.4	15.67	1.94
			55.77	0.15	1.96	10.14	0.23	31	0.33	0.00	0.01	0.14	0.05	99.77	85	957.88	83.95	15.4	0.64
			54.8	0.18	3.45	10.23	0.23	30.23	0.45	0.04	0.01	0.36	0.06	100.03	84	2463.13	83.3	15.81	0.89

			54.91	0.17	3.1	10.3	0.23	30.45	0.37	0.02	0.00	0.33	0.05	99.94	84	2257.87	83.44	15.83	0.73
			54.11	0.2	3.85	11.21	0.26	29.5	0.5	0.02	0.00	0.3	0.02	99.97	82	2052.61	81.61	17.4	0.99
KSAT 306-1	Leucotroctolite	Ohamaremba	52.6	0.54	1.52	16.86	0.38	25.12	1.63	0.03	0.00	0.01	0.02	98.7	73	68.42	70.27	26.46	3.28

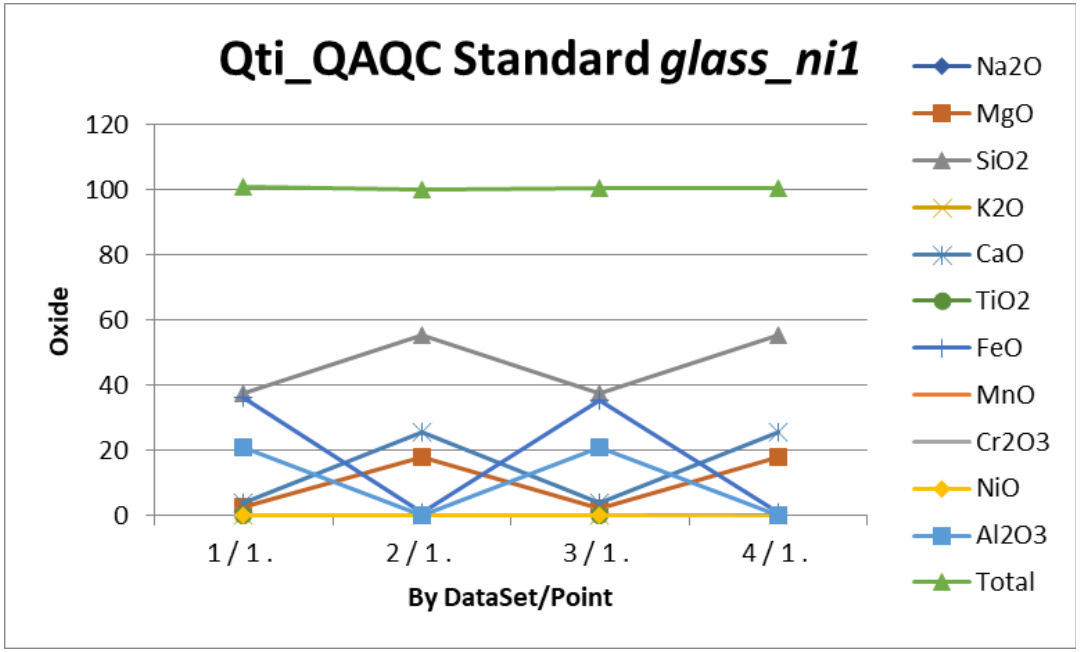


Figure I.1- Plot of the standard used to assess the in situ mineral chemistry data.

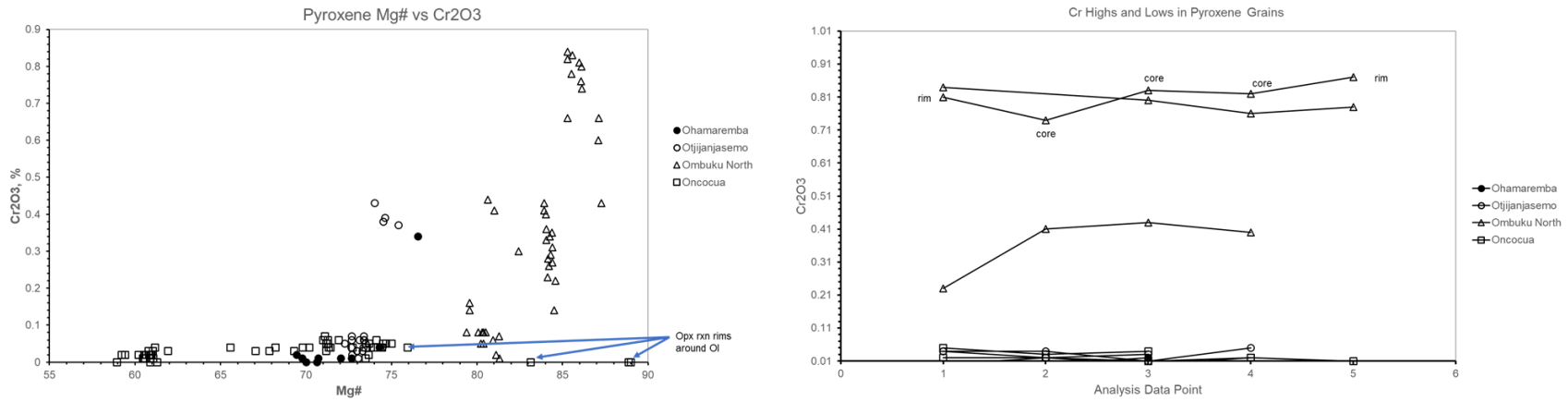


Figure I.2: A)Plot to assess Mg# and Cr_2O_3; B) Cr_2O_3 profiles in pyroxene.

Appendix II- Sulphur Isotopes of the MUM Intrusions and their Basement Rocks.

Table II.1: $\delta^{34}S$ value data of the MUM intrusions and surrounding Basement rocks.

SampleID	Locality	Lithology	Group	Weight_S Concentration (mg)	S Concentration (%)	Weight_ S Isotope (mg)	$\delta^{34}S$ (‰ VCDT)	Mass Fraction S (%)
KAC242/241	Oncócua	Leucotroctoltite	Oncócua Intrusion	56.564	0.235	22.105	-0.96	0.35
KAC245/243	Oncócua	K-feldspar-bearing Leucotroctolite	Oncócua Intrusion	58.249	0.071	70.235	0.27	0.10
KAC246/244	Oncócua	Lueconorite	Oncócua Intrusion	44.185	0.090	58.179	0.99	0.12
KAC346	Oncócua	Granodiorite	Basement rock	48.96	0.007	202.007	1.05	0.02
KAC356-2	Oncócua	Garnet-Amphibole-White Mica	Basement rock	44.493	<0.005	200.737	2.73	0.01
KAC357-1	Oncócua	Micaschist	Basement rock	44.24	<0.005	204.278	-0.66	0.00

KAC358	Oncócua	Foliated Amphibolite	Basement rock	47.525	<0.005	201.285	2.1	0.01
KAC369-2	Oncócua	Migmatite/Granodiorite	Basement rock	45.641	0.025	200.239	2.24	0.04
KAC384-3	Otjijanjasemo/Ohamaremba	Amphibolite/Qtz-Feld Gneiss	Basement rock	46.706	<0.005	203.305	1.92	0.00
KAC385-1	Otjijanjasemo/Ohamaremba	Qtz-Feldspathic Gneiss	Basement rock	48.438	<0.005	201.488	6.62	0.01
KAC422-1	Ohamaremba	Granitoid Gneiss	Basement rock	45.136	<0.005	198.303	S peak too small for data	
KSAT028/015	Oncócua	Pyroxenite	Basement rock	46.314	<0.005	199.062	S peak too small for data	
KSAT049/032	Hamutenha	Gabbro	Hamutenha Intrusion	45.119	<0.005	197.965	3.11	0.01
KSAT127/058B	Hamutenha	Diorite + granite	Basement rock	50.013	0.024	218.901	-1.64	0.04
KSAT305/122	Otjijanjasemo	Troctolite	Otjijanjasemo Intrusion	45.043	0.015	197.93	1.17	0.03
KSAT310/125	Ohamaremba	Troctolite	Ohamaremba Intrusion	49.478	<0.005	200.34	2.04	0.01
KSAT313-3	Ohamaremba	Olivine-bearing anorthosite	Ohamaremba Intrusion	42.665	<0.005	208.51	6.49	0.00
KSAT317-1	Ohamaremba	Olivine-bearing Leuconorite	Ohamaremba Intrusion	43.101	0.079	65.38	4.65	0.09
KSAT326-1	Ombuku North	Mgt leuconorite	Umbuku North Intrusion	46.564	0.053	97.85	-0.05	0.07
KSAT338-1	Ombuku South	Olivine leucogabbro	Ombuku South Intrusion	45.358	0.034	151.88	1.18	0.06

Appendix III- Radiogenic Sr-Nd Isotopes

Table III.1: QAQC Data of the Radiogenic Sr-Nd isotope Analysis.

Rb-Sr Systematic QAQC Data

Order	Analysis name	measured 87Sr/86Sr	spike-corrected 87Sr/86Sr	in-run 1SE
0	SRM987 Accepted value	0.71034		0.00026
-0.75	SRM987; Luu et al., 2022 Chem Geol; n = 38	0.7102467		0.0000043
-0.5	SRM987; Zhang and Hu 2020 Atomic Spec	0.710248		0.000012
-1	Bulk Silicate Earth	0.7045		
0.5	Wits SRM987 Mean (n = 29: Aug22-Feb23)	0.7102509		0.000068
	BHVO2 Standard (Hawaiian Basalt)	0.70342842	0.703584268	0.0000409

Sample	85Rb (V)	87Rb/85Rb	87Rb/85Rb (Sr corrected)	in-run 1SE	in-run 1SE ppm	deviation from normal ratio*
		Normal ratio = 0.38571				
Rb 50 ppb	3.459684	0.408467	0.4084649	0.000205	501.8791088	0.944291664
Rb 50 ppb	3.417975	0.4065444	0.4065425	0.000065	159.8848829	0.948756895
Rb 50 ppb	3.37098	0.4056017	0.4055999	0.0000571	140.7791274	0.950961773
Rb 50 ppb	2.198863	0.413065	0.413064	0.000431	1043.421843	0.933777817
Rb 50 ppb	1.923577	0.4092799	0.4092793	0.000186	454.457384	0.942412675
Rb 50 ppb	1.879007	0.4073326	0.4073321	0.000139	341.2448957	0.946917761

Sm-Nd Systematic QAQC Data

Order	Analysis name	measured 143Nd/144Nd	spike-corrected 143Nd/144Nd	in-run 1SE
-1.5	JNdi (Tanaka et al., 2000)	0.512115		0.000007
-1	JNdi (BSU Measured)	0.512102		
-0.75	JNdi (Luu et al., 2022 Chem Geol) n = 9	0.5120941		0.0000011

-0.5	JNdi (Zhang and Hu 2020, Atomic Spec.)	0.512107		0.000012		
0	Garcon et al., 2018, Chem Geol	0.512099		0.000005		
0.25	CHUR Nd (Bouvier et al., 2008)	0.51263				
0.5	MORB Nd (Gale et al., 2013)	0.513074				
0.75	Wits Mean (n = 18; Oct22-May23)	0.512092		2.08889E-05		
	BHVO2 Standard (Hawaiian Basalt)	0.51302803	0.512963294	0.00000255		

	Sample	**total Sm (V)**	**147Sm/152Sm**	**in-run 1SE**	**in-run 1SE ppm**	**deviation from normal ratio***
			Normal ratio = 0.560666			
	Sm std 10 ppb	6.567525	0.5608219	0.0000036	6.419150179	0.999722933
	Sm std 10 ppb	6.515841	0.5608117	0.00000349	6.223122663	0.999741116
	Sm std 10 ppb	8.206862	0.5608181	0.00000334	5.955585242	0.999729707
	Sm std 10 ppb	8.267264	0.5608205	0.00000328	5.848573652	0.999725428

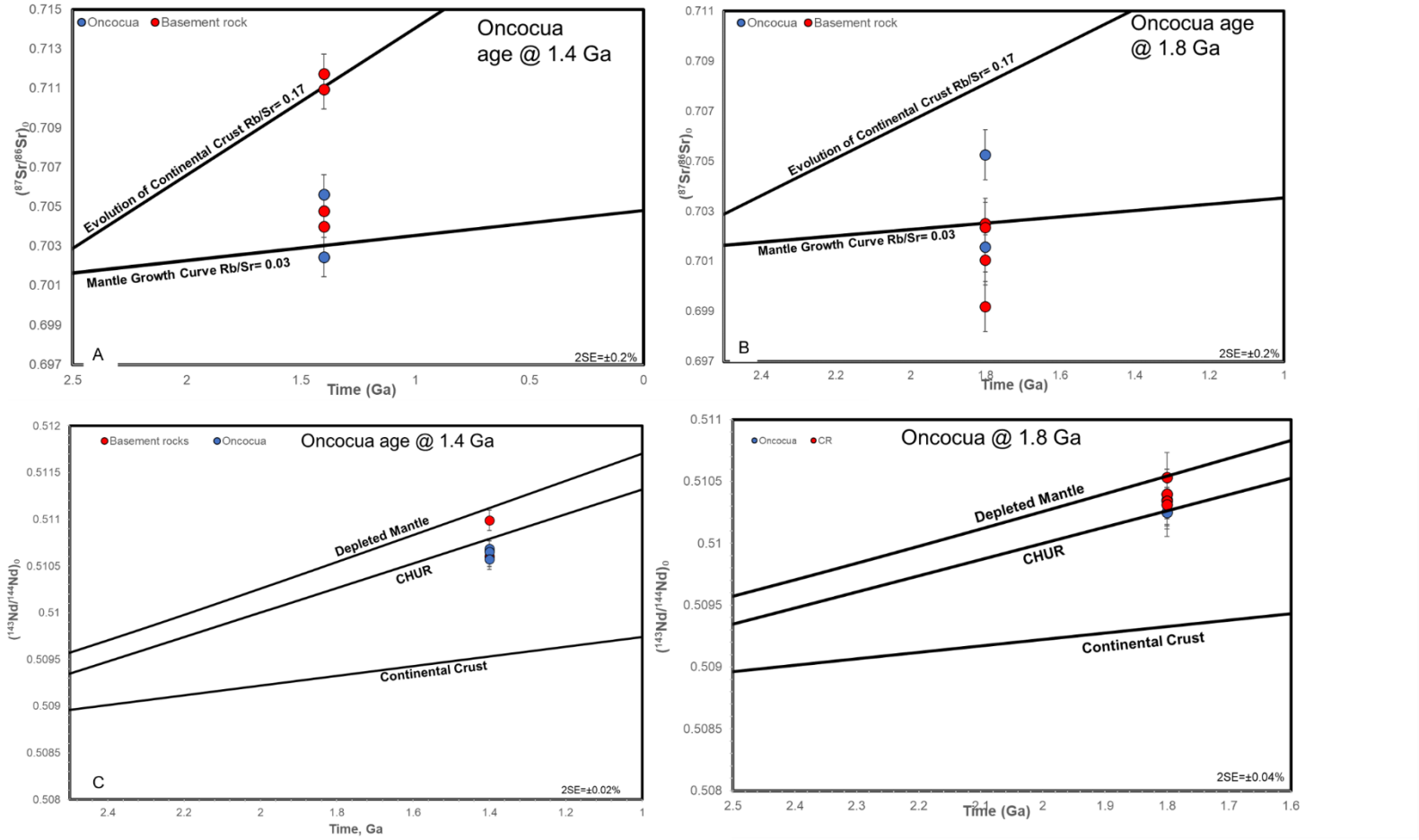


Figure III.1: Sr-Nd isotope composition data for Oncocua and its basement rocks. A-B) Initial $^{87}Sr/^{86}Sr$ Isotopic Compositions corrected to 1.4 Ga and 1.8 Ga. C-D) Initial $^{143}Nd/^{144}Nd$ Isotopic Compositions corrected to 1.4 Ga and 1.8 Ga.

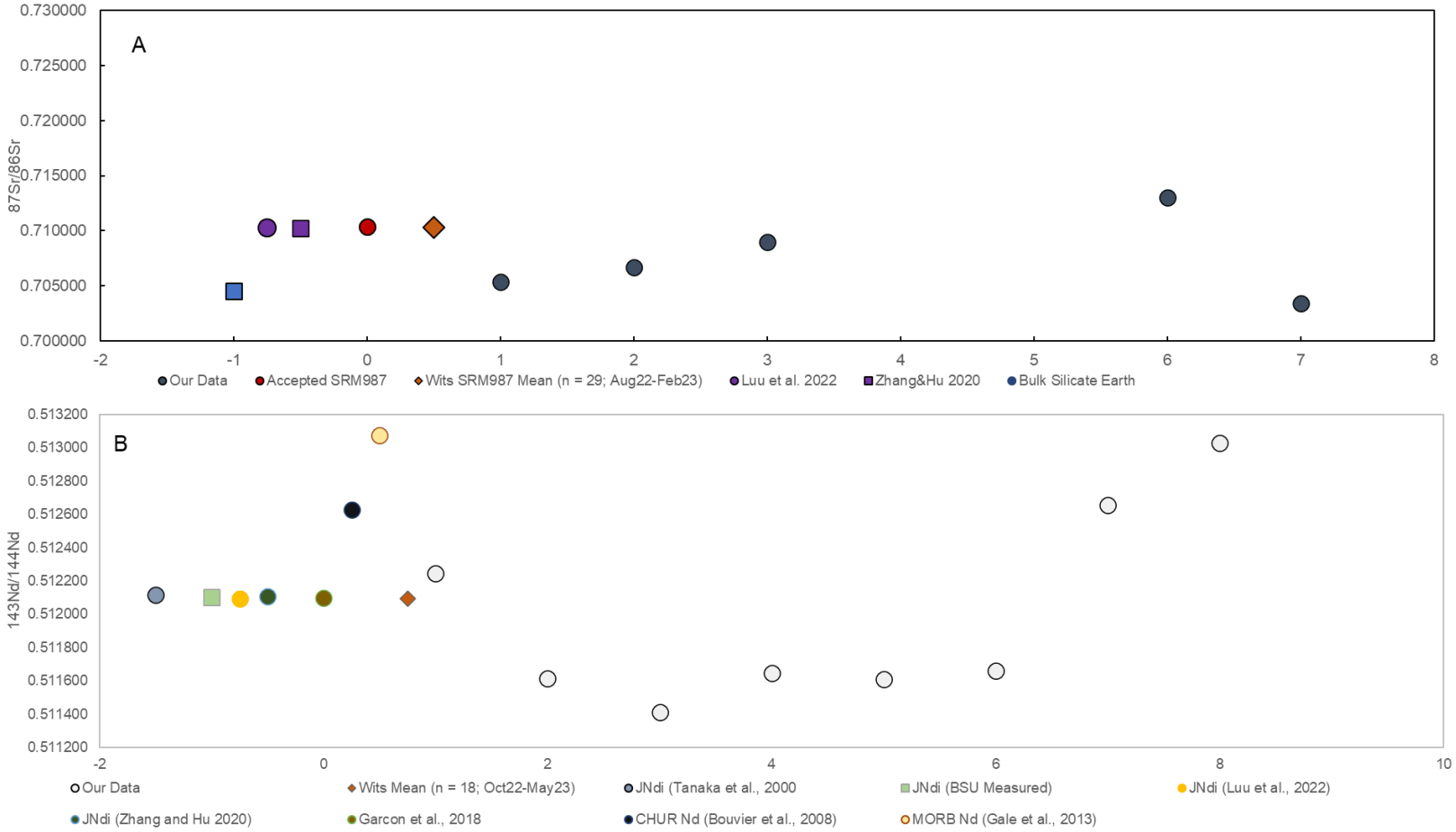


Figure III.2: Performance of standards and reference materials durning the Sr-Nd isotope measurements in the lab at Wits. A) $^{87}Sr/^{86}Sr$; B) $^{143}Nd/^{144}Nd$.

Appendix IV- Whole rock major oxides and trace elements

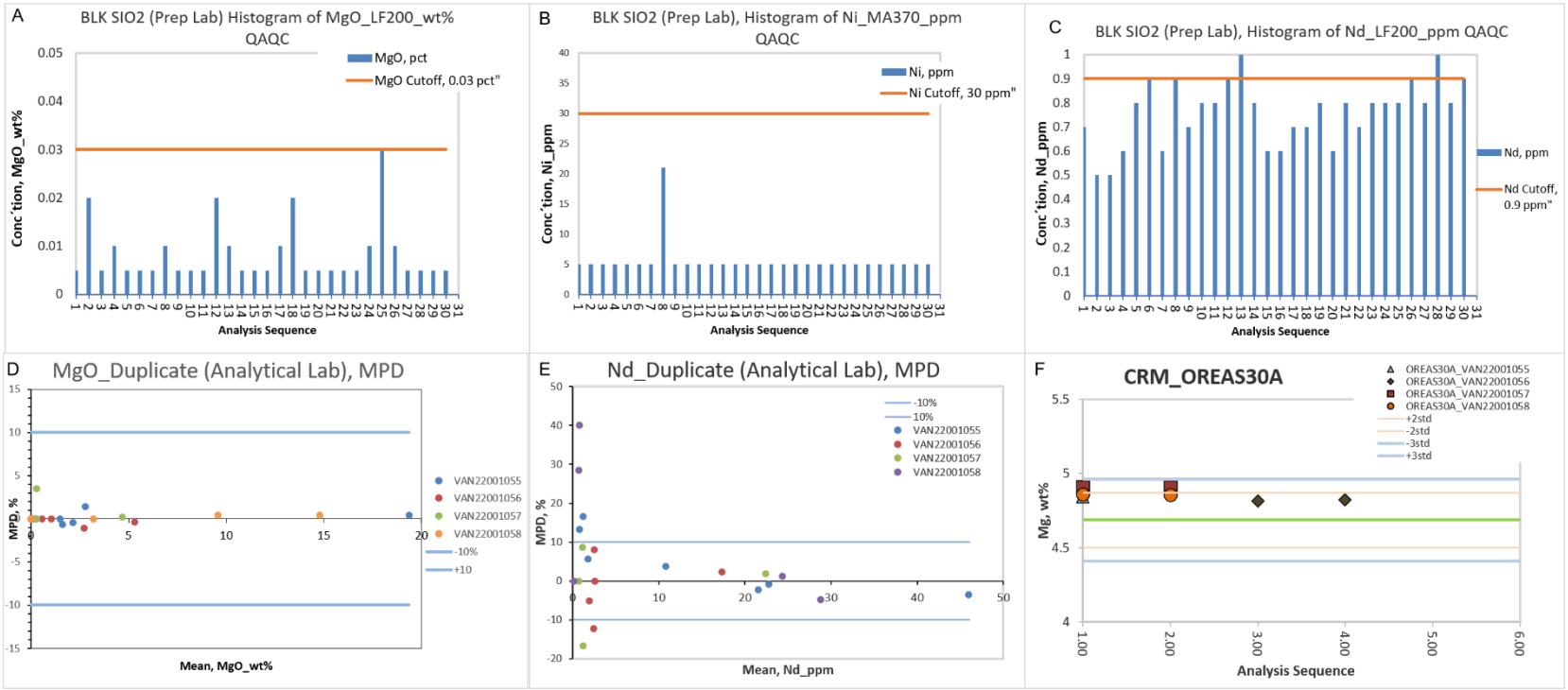


*Figure IV.1: QAQC of the samples analysed for major oxides and trace elements at Bureau Veritas. A-C) Blank QAQC samples inserted in the sample batches with approximately 98.76 wt% SiO_2 to assess the level and source of introduced contamination in the method; D-E) Duplicates of routine samples inserted in the sample batches by the lab to assess the precision of the analytical method; F) Certified Reference Material (CRM: OREAS30A) inserted in the sample batches to assess the accuracy of the analytical method. The Mg concentration was converted from MgO (0.6031*MgO) to standardise with the OREAS30A certificate. MPD = Mean Percentage Differences.*

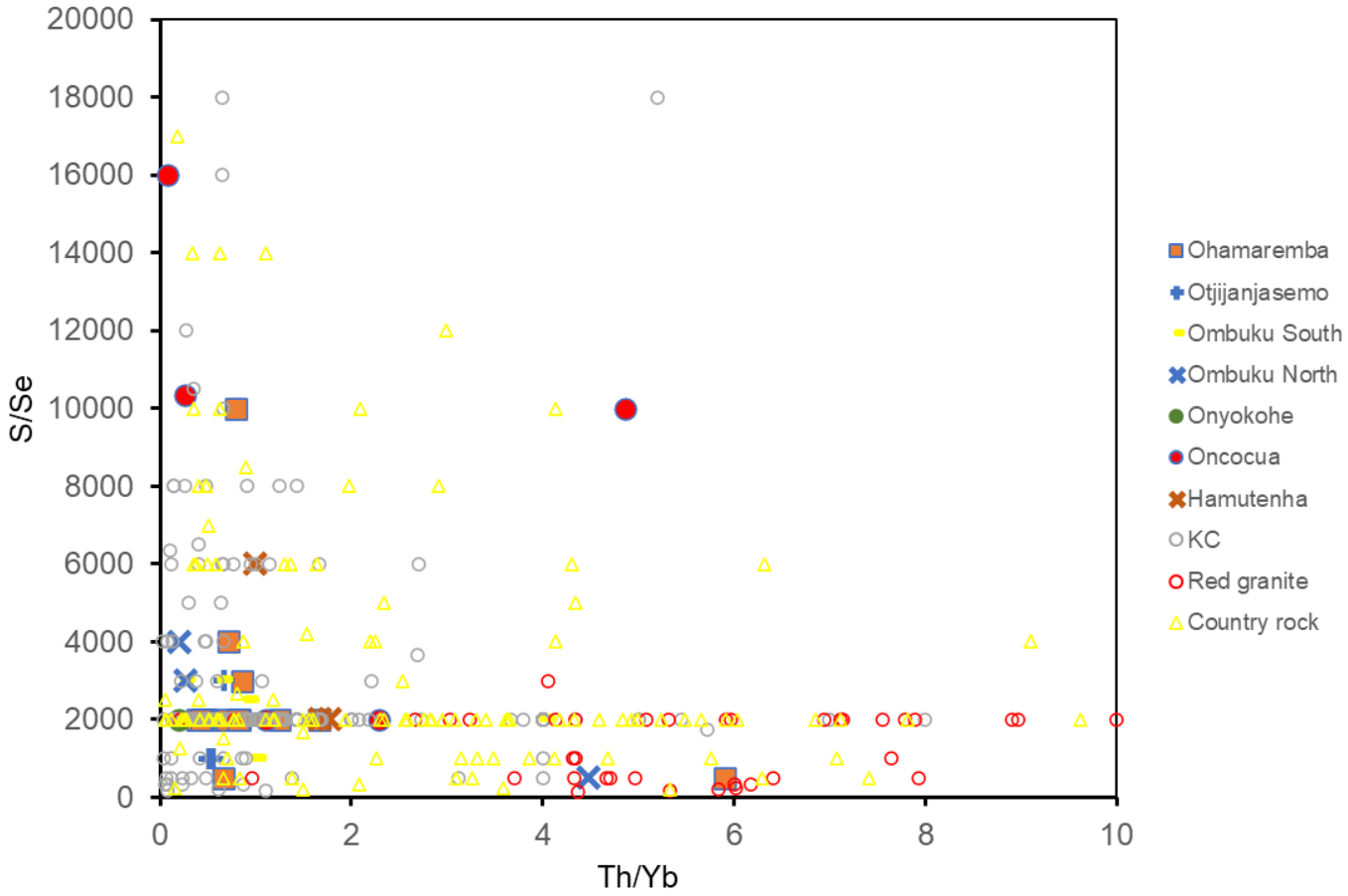


Figure IV.2- Whole rock trace elemental ratios of Th/Yb vs S/Se to assess possible sources of contamination.

Table IV.1- Whole rock major oxides and trace elements of the MUM intrusions, KC anorthosite suite and the basement rocks.

Sample_ID	KSAT049/032	KSAT051/033	KSAT052/034	KAC241/240	KAC242/241	KAC245/243	KAC246/244	KAC246/245	KSAT330-1	KSAT322-1	KSAT326-1	KSAT327-1
Lat_S	-15.4384	-15.4100	-15.4095	-16.7151	-16.7215	-16.7214	-16.7206	-16.7206	-17.2209	-17.2519	-17.2504	-17.2508
Long_E	13.6132	13.6146	13.6169	13.4610	13.4521	13.4452	13.4428	13.4428	13.3271	13.3177	13.3158	13.3191
Rocktype	Luecogabbronorite	Melatroctolite	Melatroctolite	Olivine-bearing anorthosite	Pyroxene leucotroctolite	K feldspar-bearing leucotroctolite	Leuconorite	Wollastonite-bearing gabbro	Orthopyroxene-bearing meltroctolite	Pyroxene-bearing leucotroctolite	Leuconorite	Orthopyroxene-bearing olivine leucogabbro
Group	Hamutenha Intrusion	Hamutenha Intrusion	Hamutenha Intrusion	Oncócua Intrusion	Oncócua Intrusion	Oncócua Intrusion	Oncócua Intrusion	Oncócua Intrusion	Onyokohe Intrusion	Ombuku North Intrusion	Ombuku North Intrusion	Ombuku North Intrusion
SiO2_pct	54.57	38.04	39.42	53.53	47.89	46.72	54.75	46.30	38.40	45.57	50.10	50.84
TiO2_pct	0.82	0.10	0.08	0.25	1.83	1.89	1.20	2.23	0.42	0.21	0.21	0.30
Al2O3_pct	14.01	4.36	8.55	26.75	17.07	20.19	18.67	9.03	4.59	21.06	18.70	16.70
Fe2O3t_pct	9.05	13.31	11.11	1.44	11.68	11.64	9.66	8.88	15.43	6.25	5.92	5.55
MnO_pct	0.14	0.18	0.13	0.02	0.15	0.12	0.13	0.11	0.20	0.09	0.11	0.12
MgO_pct	6.33	34.30	28.74	0.47	7.04	4.03	3.50	7.29	30.39	11.23	11.85	9.32
CaO_pct	8.23	2.79	4.30	9.16	9.36	8.51	5.74	23.76	3.21	11.10	9.69	11.21
Na2O_pct	2.73	0.20	0.69	5.23	3.03	3.69	3.83	0.21	0.24	1.74	1.81	2.70
K2O_pct	2.00	0.07	0.10	0.90	0.48	1.50	1.28	0.07	0.02	0.16	0.21	0.95
Cr2O3_pct	0.04	0.26	0.12	0.00	0.01	0.01	0.01	0.02	0.22	0.14	0.16	0.11
P2O5_pct	0.26	0.02	0.02	0.10	0.03	0.76	0.12	0.41	0.01	<0.01	<0.01	<0.01
Normalised *	98.24	93.88	93.48	97.99	98.68	99.20	99.14	98.36	93.26	97.65	98.84	97.87
SiO2_pct*	55.55	40.52	42.17	54.63	48.53	47.10	55.22	47.07	41.18	46.67	50.69	51.95
TiO2_pct*	0.84	0.10	0.08	0.26	1.88	1.94	1.23	2.29	0.43	0.22	0.22	0.31

Al2O3_pct*	55.55	40.52	42.17	54.63	48.53	47.10	55.22	47.07	41.18	46.67	50.69	51.95
Fe2O3t_pct*	9.21	14.18	11.88	1.47	11.84	11.73	9.74	9.03	16.55	6.40	5.99	5.67
FeO_pct*	7.83	12.05	10.10	1.25	10.06	9.97	8.28	7.67	14.06	5.44	5.09	4.82
Fe2O3_pct*	1.38	2.13	1.78	0.22	1.78	1.76	1.46	1.35	2.48	0.96	0.90	0.85
FeO*_pct	8.29	12.76	10.70	1.32	10.65	10.56	8.77	8.13	14.89	5.76	5.39	5.10
MnO_pct*	0.14	0.18	0.13	0.02	0.15	0.12	0.13	0.11	0.21	0.09	0.11	0.12
MgO_pct*	6.44	36.54	30.74	0.48	7.13	4.06	3.53	7.41	32.59	11.50	11.99	9.52
CaO_pct*	8.44	2.86	4.41	9.39	9.60	8.72	5.88	24.36	3.29	11.38	9.93	11.49
Na2O_pct*	2.80	0.21	0.71	5.36	3.11	3.78	3.93	0.22	0.25	1.78	1.86	2.77
K2O_pct*	2.05	0.07	0.10	0.92	0.49	1.54	1.31	0.07	0.02	0.16	0.22	0.97
Cr2O3_pct*	0.04	0.27	0.12	0.00	0.01	0.01	0.01	0.02	0.23	0.14	0.16	0.11
P2O5_pct*	0.27	0.02	0.02	0.10	0.03	0.78	0.12	0.42	0.01	N/A	N/A	N/A
Mg#	59.45	84.38	84.43	40.63	55.82	42.06	43.17	63.25	80.50	79.02	80.76	77.88
Mo_pct	<0.001	<0.001	<0.001	<0.001	<0.001	<0.001	<0.001	<0.001	<0.001	<0.001	<0.001	<0.001
Cu_pct	0.01	<0.001	<0.001	0.00	0.04	0.01	0.01	0.00	<0.001	0.01	0.01	0.02
Pb_pct	<0.02	<0.02	<0.02	<0.02	<0.02	<0.02	<0.02	<0.02	<0.02	<0.02	<0.02	<0.02
Zn_pct	<0.01	<0.01	<0.01	<0.01	<0.01	0.01	0.01	<0.01	<0.01	<0.01	<0.01	<0.01
Ag_ppm	<2	<2	<2	<2	<2	<2	<2	<2	<2	<2	<2	<2
Ni_ppm	45.00	1931.00	1616.00	<10	214.00	44.00	33.00	136.00	1082.00	472.00	234.00	173.00
Mo_ppm	0.13	0.22	0.48	0.73	0.29	0.29	0.97	0.83	0.05	0.18	0.19	0.14
Cu_ppm	51.35	8.38	4.39	15.55	410.08	104.62	54.96	21.54	1.80	109.35	76.14	162.23
Pb_ppm	4.44	0.28	0.26	0.79	1.17	1.40	2.72	1.77	0.30	0.43	0.54	13.60
Zn_ppm	30.10	57.80	50.80	8.40	54.60	68.20	38.60	13.10	18.60	2.90	5.80	5.50
Ag_ppb	68.00	10.00	11.00	16.00	272.00	53.00	37.00	12.00	2.00	45.00	28.00	22.00
Ni_ppm	21.30	1689.50	1478.80	6.80	177.20	35.00	22.90	36.60	766.80	309.80	95.60	52.10

Co_ppm	15.00	144.10	127.00	4.70	45.10	22.90	12.10	7.60	91.20	26.20	9.70	6.60
Mn_ppm	317.00	1255.00	992.00	102.00	573.00	176.00	157.00	82.00	756.00	178.00	80.00	128.00
As_ppm	0.20	<0.1	0.20	<0.1	<0.1	<0.1	<0.1	0.40	0.40	<0.1	0.10	0.50
Au_ppb	<0.2	<0.2	<0.2	<0.2	4.50	1.60	1.10	0.20	<0.2	1.00	0.30	0.30
Cd_ppm	0.06	0.02	<0.01	0.02	0.05	0.02	0.02	0.09	<0.01	<0.01	<0.01	0.01
Sb_ppm	<0.02	<0.02	<0.02	<0.02	<0.02	<0.02	<0.02	<0.02	<0.02	<0.02	<0.02	0.02
Bi_ppm	<0.02	<0.02	<0.02	<0.02	0.03	<0.02	<0.02	<0.02	<0.02	<0.02	<0.02	0.06
Cr_ppm	75.10	92.80	88.90	11.00	25.50	51.10	24.70	32.90	410.20	134.40	136.90	90.60
Hg_ppb	<5	<5	<5	<5	<5	<5	<5	<5	<5	<5	<5	<5
Se_ppm	<0.1	<0.1	<0.1	<0.1	0.30	<0.1	0.10	<0.1	<0.1	0.20	0.20	0.20
Te_ppm	<0.02	<0.02	<0.02	<0.02	0.09	<0.02	0.04	0.04	<0.02	0.03	<0.02	<0.02
Ge_ppm	<0.1	0.20	0.20	<0.1	<0.1	<0.1	<0.1	<0.1	<0.1	<0.1	<0.1	<0.1
In_ppm	<0.02	<0.02	<0.02	<0.02	<0.02	0.02	<0.02	<0.02	<0.02	<0.02	<0.02	<0.02
Re_ppb	<1	<1	<1	<1	<1	<1	1.00	<1	<1	<1	<1	<1
Be_ppm	0.40	<0.1	<0.1	0.10	<0.1	0.20	<0.1	0.30	<0.1	<0.1	<0.1	0.30
Li_ppm	13.00	8.00	1.50	4.50	3.00	6.40	4.50	2.20	0.70	1.00	0.60	2.20
Pd_ppb	<10	<10	<10	<10	<10	<10	<10	<10	<10	<10	<10	<10
Pt_ppb	<2	<2	<2	<2	6.00	<2	<2	<2	<2	<2	<2	<2
Au_ppb	3.00	6.00	2.00	7.00	11.00	9.00	9.00	10.00	7.00	5.00	4.00	4.00
Pt_ppb	1.30	0.40	0.20	0.60	7.10	1.20	2.10	0.90	1.50	1.00	0.90	0.50
Pd_ppb	1.80	1.90	0.60	1.50	9.80	2.20	2.70	1.70	2.40	1.30	1.40	1.30
B_ppm	<1	5.00	1.00	1.00	<1	<1	<1	1.00	<1	4.00	1.00	5.00
Tl_ppm	0.03	<0.02	<0.02	<0.02	<0.02	0.07	<0.02	<0.02	<0.02	0.04	0.05	0.02
LOI_pct	1.50	5.50	6.00	1.90	1.00	0.50	0.60	1.40	6.20	2.10	0.90	1.90
TOT/C_TC000_pct	0.04	0.06	0.12	0.06	0.07	<0.02	0.07	0.04	0.15	0.07	0.03	<0.02

TOT/S_pct	<0.02	0.03	<0.02	<0.02	0.31	0.08	0.10	<0.02	<0.02	0.06	0.08	<0.02
Ba_ppm	600.00	38.00	17.00	820.00	473.00	805.00	1887.00	48.00	13.00	71.00	78.00	262.00
Sc_ppm	24.00	5.00	4.00	<1	24.00	15.00	22.00	13.00	14.00	11.00	20.00	30.00
Sum_pct	99.74	99.38	99.48	99.89	99.68	99.70	99.74	99.76	99.46	99.75	99.74	99.77
Cs_ppm	0.70	0.20	<0.1	2.40	0.40	0.20	0.10	<0.1	0.20	0.70	0.40	1.70
Ga_ppm	14.70	2.60	3.40	20.80	17.00	23.30	18.50	12.60	4.90	11.00	11.60	11.70
Hf_ppm	3.60	0.20	<0.1	0.10	0.30	4.10	7.60	7.40	0.40	0.20	0.30	0.90
Nb_ppm	7.60	0.30	<0.1	0.60	1.10	7.00	11.40	38.50	0.40	<0.1	<0.1	1.40
Rb_ppm	49.70	1.30	0.30	7.70	1.30	29.00	9.00	1.60	0.20	2.60	4.20	28.00
Sn_ppm	<1	<1	<1	<1	<1	2.00	<1	3.00	<1	<1	<1	<1
Sr_ppm	611.50	164.20	199.60	803.70	922.90	1111.30	664.30	100.80	51.00	364.60	361.60	312.60
Ta_ppm	0.40	<0.1	<0.1	<0.1	<0.1	0.30	0.30	2.80	<0.1	<0.1	<0.1	0.10
Th_ppm	4.60	<0.2	<0.2	<0.2	<0.2	<0.2	8.40	6.50	<0.2	<0.2	<0.2	3.90
U_ppm	1.20	<0.1	<0.1	<0.1	<0.1	<0.1	0.70	4.70	<0.1	<0.1	<0.1	1.50
V_ppm	192.00	32.00	22.00	<8	218.00	208.00	185.00	127.00	103.00	68.00	92.00	144.00
W_ppm	0.70	<0.5	1.00	1.60	0.90	1.40	1.00	2.70	<0.5	1.10	<0.5	0.80
Zr_ppm	127.30	4.70	1.80	6.30	6.00	170.40	314.70	308.00	9.50	5.90	8.70	22.70
Y_ppm	23.70	0.70	0.50	1.60	4.20	18.80	15.10	37.90	5.90	3.80	4.00	9.60
La_ppm	26.10	0.80	0.40	4.50	2.00	41.80	66.40	42.40	0.60	1.80	1.70	3.20
Ce_ppm	55.20	1.90	0.90	8.20	3.90	88.50	119.70	103.60	3.70	3.30	4.10	8.00
Pr_ppm	6.49	0.17	0.08	0.94	0.56	10.62	12.99	12.93	0.77	0.44	0.42	1.03
Nd_ppm	25.00	0.80	0.40	3.80	3.00	42.90	47.20	51.90	4.90	2.10	1.80	4.70
Sm_ppm	5.23	0.17	0.06	0.58	0.82	7.24	6.86	10.21	1.35	0.46	0.38	1.30
Eu_ppm	1.30	0.08	0.11	1.68	1.06	2.53	3.02	2.34	0.45	0.37	0.34	0.49
Gd_ppm	4.83	0.17	0.11	0.45	0.93	5.92	5.01	9.01	1.41	0.63	0.57	1.49

Tb_ppm	0.75	0.02	<0.01	0.06	0.13	0.70	0.58	1.28	0.19	0.11	0.09	0.26
Dy_ppm	4.38	0.13	0.08	0.28	0.80	3.56	3.04	7.28	1.20	0.68	0.63	1.49
Ho_ppm	0.87	0.03	<0.02	0.05	0.16	0.67	0.58	1.32	0.21	0.16	0.15	0.33
Er_ppm	2.62	0.10	0.04	0.13	0.47	1.74	1.63	3.49	0.59	0.42	0.46	0.95
Tm_ppm	0.36	0.01	<0.01	0.02	0.07	0.23	0.25	0.47	0.08	0.06	0.06	0.14
Yb_ppm	2.59	0.10	0.06	0.09	0.39	1.32	1.73	2.84	0.52	0.37	0.49	0.87
Lu_ppm	0.35	0.01	<0.01	0.01	0.06	0.19	0.28	0.42	0.08	0.05	0.06	0.13

Sample_ID	KSAT333-1	KSAT333-2	KSAT334-1	KSAT334-2	KSAT338-1	KSAT339-1	KSAT340-1	KSAT306-1	KSAT306/123	KSAT308/124	KSAT310/125	KSAT313-1
Lat_S	-17.2900	-17.2900	-17.2898	-17.2898	-17.2882	-17.2869	-17.2891	-17.4652	-17.4652	-17.4602	-17.4609	-17.4610
Long_E	13.2734	13.2734	13.2713	13.2713	13.2612	13.2612	13.2701	13.4076	13.4076	13.3900	13.3897	13.3935
Rocktype	K feldspar-bearing leucotroctolite	Leucotroctolite	K feldspar-bearing leucotroctolite	Troctolite	Olivine leucogabbro	K feldspar-bearing leucogabbronorite	Magnetite-bearing corundum dunite	Leucotroctolite	Leucotroctolite	Melatroctolite	Troctolite	Lueconorite
Group	Ombuku South Intrusion	Ombuku South Intrusion	Ombuku South Intrusion	Ombuku South Intrusion	Ombuku South Intrusion	Ombuku South Intrusion	Ombuku South Intrusion	Ohamaremba Intrusion	Ohamaremba Intrusion	Ohamaremba Intrusion	Ohamaremba Intrusion	Ohamaremba Intrusion
SiO2_pct	43.08	42.66	44.39	43.55	47.17	52.73	6.74	47.21	47.52	39.34	40.96	50.59
TiO2_pct	0.07	0.08	0.07	0.09	0.65	0.32	1.08	0.99	0.95	0.14	0.12	0.80
Al2O3_pct	22.13	21.32	20.29	17.78	16.67	16.97	27.68	19.95	19.39	8.78	11.32	23.42
Fe2O3t_pct	5.24	5.55	5.65	7.66	9.87	7.21	28.71	8.51	8.64	15.84	14.31	6.36
MnO_pct	0.07	0.07	0.08	0.11	0.15	0.16	0.44	0.11	0.11	0.19	0.17	0.10
MgO_pct	11.36	12.17	13.16	16.96	7.62	6.38	14.84	9.05	9.44	23.32	21.68	3.69
CaO_pct	10.17	9.61	9.13	8.28	12.05	9.87	0.16	9.89	9.96	4.11	5.18	10.40
Na2O_pct	1.64	1.84	1.68	1.63	2.56	3.38	<0.01	2.65	2.52	0.82	1.12	3.24
K2O_pct	0.85	0.37	1.44	0.50	0.42	0.84	<0.01	0.62	0.63	0.11	0.13	0.55

Cr2O3_pct	0.03	0.03	0.05	0.02	0.03	0.02	11.51	0.02	0.02	0.02	0.02	0.01
P2O5_pct	<0.01	<0.01	<0.01	<0.01	0.01	<0.01	<0.01	0.17	0.16	0.03	0.02	0.03
Normalised *	94.76	93.74	96.01	96.69	97.24	97.90	91.26	99.24	99.44	92.76	95.09	99.18
SiO2_pct*	45.46	45.51	46.23	45.04	48.51	53.86	7.39	47.57	47.79	42.41	43.07	51.01
TiO2_pct*	0.07	0.08	0.07	0.09	0.67	0.33	1.11	1.01	0.97	0.14	0.12	0.82
Al2O3_pct*	45.46	45.51	46.23	45.04	48.51	53.86	7.39	47.57	47.79	42.41	43.07	51.01
Fe2O3t_pct *	5.53	5.92	5.88	7.92	10.15	7.36	31.46	8.58	8.69	17.08	15.05	6.41
FeO_pct*	4.70	5.03	5.00	6.73	8.63	6.26	26.74	7.29	7.39	14.51	12.79	5.45
Fe2O3_pct *	0.83	0.89	0.88	1.19	1.52	1.10	4.72	1.29	1.30	2.56	2.26	0.96
FeO*_pct	4.98	5.33	5.30	7.13	9.14	6.63	28.31	7.72	7.82	15.37	13.54	5.77
MnO_pct*	0.07	0.07	0.08	0.11	0.15	0.16	0.45	0.11	0.11	0.19	0.17	0.10
MgO_pct*	11.99	12.98	13.71	17.54	7.84	6.52	16.26	9.12	9.49	25.14	22.80	3.72
CaO_pct*	10.43	9.85	9.36	8.49	12.35	10.12	0.16	10.14	10.21	4.21	5.31	10.66
Na2O_pct*	1.68	1.89	1.72	1.67	2.62	3.47	#VALUE!	2.72	2.58	0.84	1.15	3.32
K2O_pct*	0.87	0.38	1.48	0.51	0.43	0.86	#VALUE!	0.64	0.65	0.11	0.13	0.56
Cr2O3_pct *	0.03	0.03	0.05	0.02	0.03	0.02	11.80	0.02	0.02	0.02	0.02	0.01
P2O5_pct*	N/A	N/A	N/A	N/A	0.01	N/A	N/A	0.17	0.16	0.03	0.02	0.03
Mg#	81.97	82.13	83.00	82.28	61.81	64.98	52.01	69.04	69.61	75.53	76.05	54.88
Mo_pct	<0.001	<0.001	<0.001	<0.001	<0.001	<0.001	<0.001	<0.001	<0.001	<0.001	<0.001	<0.001
Cu_pct	0.00	0.00	0.01	0.01	0.01	0.00	0.01	0.00	0.01	<0.001	0.00	<0.001
Pb_pct	<0.02	<0.02	<0.02	<0.02	<0.02	<0.02	<0.02	<0.02	<0.02	<0.02	<0.02	<0.02
Zn_pct	<0.01	<0.01	<0.01	<0.01	<0.01	<0.01	0.10	<0.01	<0.01	0.01	<0.01	<0.01
Ag_ppm	<2	<2	<2	<2	<2	<2	<2	<2	<2	<2	<2	<2
Ni_ppm	368.00	420.00	310.00	421.00	72.00	48.00	1408.00	269.00	287.00	803.00	738.00	51.00
Mo_ppm	0.06	0.09	0.14	0.18	0.07	0.43	0.38	0.45	0.40	0.19	0.05	0.31

Cu_ppm	10.65	25.69	115.70	86.72	82.65	25.69	120.14	25.46	39.73	7.06	15.60	5.96
Pb_ppm	2.98	22.29	4.25	1.17	0.84	4.35	1.22	0.75	0.77	0.25	0.28	1.68
Zn_ppm	23.60	24.00	13.40	14.80	41.20	20.30	30.70	43.50	42.30	75.50	70.90	15.10
Ag_ppb	13.00	13.00	34.00	34.00	39.00	25.00	26.00	9.00	15.00	5.00	9.00	13.00
Ni_ppm	233.80	306.10	183.30	207.70	48.80	17.40	627.10	226.30	244.70	681.40	639.10	27.10
Co_ppm	31.00	37.80	32.70	32.60	28.00	10.30	31.10	43.80	45.20	125.30	114.10	8.90
Mn_ppm	242.00	318.00	173.00	228.00	431.00	304.00	640.00	560.00	570.00	1140.00	1015.00	127.00
As_ppm	0.40	0.80	1.30	0.90	0.30	1.10	0.30	<0.1	0.10	<0.1	0.20	<0.1
Au_ppb	<0.2	<0.2	1.10	0.50	4.80	0.70	1.50	<0.2	0.30	<0.2	<0.2	<0.2
Cd_ppm	0.02	0.02	0.01	<0.01	0.02	0.01	<0.01	0.02	0.02	0.01	0.01	0.01
Sb_ppm	<0.02	<0.02	<0.02	<0.02	<0.02	0.06	<0.02	<0.02	<0.02	<0.02	<0.02	<0.02
Bi_ppm	0.02	<0.02	0.03	0.03	<0.02	0.10	0.03	<0.02	<0.02	<0.02	<0.02	<0.02
Cr_ppm	79.90	104.60	73.00	46.70	143.50	57.10	2750.10	12.80	32.30	44.10	40.40	27.70
Hg_ppb	<5	<5	<5	<5	<5	<5	<5	<5	<5	<5	<5	<5
Se_ppm	<0.1	<0.1	0.20	0.10	0.20	0.10	<0.1	0.10	<0.1	<0.1	<0.1	<0.1
Te_ppm	<0.02	<0.02	<0.02	0.02	<0.02	<0.02	<0.02	<0.02	<0.02	<0.02	<0.02	<0.02
Ge_ppm	<0.1	<0.1	<0.1	<0.1	<0.1	<0.1	0.10	<0.1	<0.1	<0.1	<0.1	<0.1
In_ppm	<0.02	<0.02	<0.02	<0.02	<0.02	<0.02	<0.02	<0.02	<0.02	<0.02	<0.02	<0.02
Re_ppb	<1	<1	<1	<1	<1	<1	<1	<1	<1	<1	<1	<1
Be_ppm	<0.1	<0.1	<0.1	<0.1	<0.1	0.20	<0.1	0.10	0.10	<0.1	<0.1	0.40
Li_ppm	21.10	26.40	17.20	17.40	6.40	3.90	2.50	2.20	2.30	1.40	1.80	4.10
Pd_ppb	<10	<10	<10	<10	10.00	11.00	13.00	<10	<10	<10	<10	<10
Pt_ppb	<2	<2	<2	<2	6.00	5.00	12.00	<2	<2	<2	<2	<2
Au_ppb	6.00	4.00	6.00	5.00	8.00	4.00	4.00	4.00	5.00	10.00	9.00	4.00
Pt_ppb	0.60	0.90	0.80	0.80	9.60	10.20	9.00	0.40	0.30	0.80	1.00	0.30

Pd_ppb	2.40	2.00	2.10	1.70	12.30	12.80	8.00	1.80	1.50	2.60	3.10	0.80
B_ppm	5.00	4.00	9.00	8.00	2.00	3.00	24.00	<1	<1	<1	<1	<1
Tl_ppm	0.04	<0.02	0.11	0.07	0.03	0.05	<0.02	0.02	0.02	<0.02	<0.02	0.02
LOI_pct	5.00	6.00	3.70	3.00	2.50	1.90	1.30	0.50	0.30	6.80	4.50	0.70
TOT/C_TC000_pct	0.12	0.19	0.08	0.03	0.04	0.04	<0.02	0.04	0.04	0.09	0.04	0.04
TOT/S_pct	<0.02	<0.02	0.05	0.03	0.06	<0.02	<0.02	0.04	0.05	<0.02	<0.02	<0.02
Ba_ppm	195.00	87.00	564.00	262.00	228.00	350.00	84.00	351.00	346.00	104.00	114.00	298.00
Sc_ppm	3.00	4.00	6.00	7.00	35.00	33.00	4.00	12.00	15.00	6.00	6.00	9.00
Sum_pct	99.76	99.74	99.71	99.69	99.74	99.80	92.56	99.74	99.74	99.56	99.59	99.88
Cs_ppm	2.10	1.30	2.40	1.40	0.50	1.00	0.10	<0.1	0.10	<0.1	<0.1	0.30
Ga_ppm	11.30	10.40	10.70	9.60	14.90	15.40	69.90	14.50	15.20	5.00	6.70	21.30
Hf_ppm	<0.1	<0.1	0.10	0.10	0.70	0.70	0.20	1.90	1.80	0.30	0.20	0.70
Nb_ppm	<0.1	<0.1	<0.1	<0.1	0.30	2.30	0.10	4.30	4.30	0.50	0.30	2.00
Rb_ppm	30.10	11.80	52.90	17.30	10.00	21.60	2.00	11.30	10.20	1.20	1.30	6.80
Sn_ppm	<1	<1	<1	<1	<1	<1	<1	<1	<1	<1	<1	<1
Sr_ppm	388.00	382.10	361.60	106.40	623.60	540.90	4.50	501.80	495.20	211.70	284.50	306.40
Ta_ppm	<0.1	<0.1	<0.1	<0.1	<0.1	0.20	<0.1	0.20	0.20	<0.1	<0.1	0.10
Th_ppm	<0.2	<0.2	<0.2	<0.2	0.20	1.30	<0.2	0.90	1.00	<0.2	<0.2	0.80
U_ppm	<0.1	<0.1	<0.1	0.10	<0.1	1.00	<0.1	0.20	0.30	<0.1	<0.1	0.10
V_ppm	24.00	25.00	26.00	42.00	263.00	140.00	859.00	114.00	119.00	34.00	27.00	53.00
W_ppm	0.60	0.60	0.60	0.70	<0.5	1.10	3.10	0.90	1.20	<0.5	<0.5	0.80
Zr_ppm	3.40	3.20	2.90	5.00	17.80	10.60	7.00	76.00	75.30	11.40	7.40	25.10
Y_ppm	1.10	1.40	1.30	1.50	8.10	13.50	0.20	13.50	13.70	2.00	1.30	5.90
La_ppm	1.20	1.20	1.00	1.10	3.20	2.70	0.60	11.10	11.10	1.70	1.60	7.40
Ce_ppm	2.10	2.10	2.00	2.30	7.50	6.90	1.00	23.90	24.70	3.60	2.90	13.40

Pr_ppm	0.23	0.25	0.20	0.23	1.14	1.22	0.09	2.89	2.84	0.43	0.33	1.46
Nd_ppm	0.90	1.10	0.80	1.00	6.00	6.90	<0.3	12.70	11.90	1.60	1.30	5.80
Sm_ppm	0.14	0.20	0.14	0.18	1.51	2.01	0.06	2.72	2.72	0.32	0.29	1.11
Eu_ppm	0.24	0.26	0.24	0.25	0.72	0.89	0.06	0.97	1.09	0.26	0.29	1.21
Gd_ppm	0.19	0.28	0.21	0.31	1.76	2.54	<0.05	2.75	2.81	0.42	0.30	1.21
Tb_ppm	0.02	0.04	0.03	0.04	0.29	0.41	<0.01	0.42	0.42	0.06	0.04	0.19
Dy_ppm	0.17	0.21	0.21	0.29	1.55	2.75	<0.05	2.44	2.41	0.35	0.20	1.11
Ho_ppm	0.04	0.04	0.05	0.06	0.32	0.55	<0.02	0.45	0.55	0.07	0.06	0.20
Er_ppm	0.13	0.13	0.15	0.19	0.96	1.60	<0.03	1.51	1.43	0.19	0.13	0.67
Tm_ppm	0.01	0.01	0.01	0.02	0.15	0.21	<0.01	0.19	0.19	0.03	0.02	0.10
Yb_ppm	0.09	0.15	0.11	0.16	0.83	1.32	<0.05	1.25	1.26	0.26	0.15	0.64
Lu_ppm	0.01	0.02	0.01	0.02	0.12	0.20	<0.01	0.18	0.20	0.04	0.02	0.09

Sample_ID	KSAT313-2	KSAT313-3	KSAT314-1	KSAT314-2	KSAT315-1	KSAT301/118	KSAT301/119	KSAT303/120	KSAT305/122	KAC003/001	KAC003/002	KAC004/003
Lat_S	-17.4610	-17.4610	-17.4602	-17.4602	-17.4603	-17.4584	-17.4584	-17.4567	-17.4555	-17.3321	-17.3321	-17.3316
Long_E	13.3935	13.3935	13.3903	13.3903	13.3899	13.2052	13.2052	13.2039	13.2029	13.9563	13.9563	13.9581
Rocktype	Olivine-bearing anorthosite	Olivine-bearing anorthosite	Orthopyroxene-bearing troctolite	Orthopyroxene-bearing troctolite	Orthopyroxene-bearing troctolite	Melatroctolite	Orthopyroxene-bearing melatroctolite	Troctolite	Troctolite	Anorthosite	Anorthosite	Anorthosite
Group	Ohamaremba Intrusion	Ohamaremba Intrusion	Ohamaremba Intrusion	Ohamaremba Intrusion	Ohamaremba Intrusion	Otjijanjasemo Intrusion	Otjijanjasemo Intrusion	Otjijanjasemo Intrusion	Otjijanjasemo Intrusion	KC	KC	KC
SiO2_pct	48.92	49.19	43.25	43.38	40.45	40.35	40.78	42.60	44.05	53.37	50.69	54.68
TiO2_pct	1.69	1.52	0.22	0.20	0.18	0.44	0.43	0.33	0.92	0.41	1.38	1.24
Al2O3_pct	24.12	23.92	15.69	15.75	12.22	8.76	10.25	13.17	13.57	24.88	25.04	18.38
Fe2O3t_pct	6.31	5.72	11.52	11.21	13.83	21.13	19.43	15.69	16.67	2.4	4.27	9.52

MnO_pct	0.08	0.08	0.14	0.13	0.16	0.24	0.23	0.18	0.20	0.18	0.16	0.32
MgO_pct	2.30	2.70	16.09	15.73	20.19	21.63	20.51	16.86	15.49	0.48	0.93	1
CaO_pct	10.48	10.09	6.94	7.13	5.51	4.24	4.70	6.15	6.58	8.11	8.3	5.42
Na2O_pct	3.47	3.40	1.76	1.76	1.12	1.13	1.32	1.61	1.98	5.38	4.91	4.98
K2O_pct	0.70	0.97	0.21	0.21	0.15	0.21	0.23	0.22	0.46	2.03	1.73	3.19
Cr2O3_pct	0.00	0.00	0.02	0.02	0.02	0.01	0.01	0.01	0.01	0.002	0.013	0.006
P2O5_pct	0.04	0.03	0.04	0.03	0.04	0.07	0.07	0.04	0.16	0.21	0.47	0.33
Normalised*	98.15	97.67	95.97	95.68	94.01	98.28	97.99	96.96	100.15	97.54	98.06	99.47
SiO2_pct*	49.84	50.36	45.07	45.34	43.03	41.06	41.62	43.94	43.98	54.72	51.69	54.97
TiO2_pct*	1.73	1.56	0.23	0.21	0.18	0.45	0.44	0.34	0.94	0.42	1.41	1.27
Al2O3_pct*	49.84	50.36	45.07	45.34	43.03	41.06	41.62	43.94	43.98	25.51	51.69	54.97
Fe2O3t_pct*	6.43	5.86	12.00	11.72	14.71	21.50	19.83	16.18	16.65	2.46	4.35	9.57
FeO_pct*	5.46	4.98	10.20	9.96	12.50	18.27	16.85	13.75	14.15	2.09	3.70	8.14
Fe2O3_pct*	0.96	0.88	1.80	1.76	2.21	3.22	2.97	2.43	2.50	0.37	0.65	1.44
FeO*_pct	5.79	5.27	10.80	10.54	13.24	19.35	17.85	14.56	14.98	2.21	3.92	8.61
MnO_pct*	0.08	0.08	0.14	0.13	0.16	0.25	0.24	0.18	0.21	0.18	0.16	0.33
MgO_pct*	2.34	2.76	16.77	16.44	21.48	22.01	20.93	17.39	15.47	0.49	0.95	1.01
CaO_pct*	10.74	10.34	7.12	7.31	5.65	4.35	4.82	6.31	6.75	8.31	8.51	5.56
Na2O_pct*	3.56	3.49	1.80	1.80	1.15	1.16	1.35	1.65	2.03	5.52	5.03	5.11
K2O_pct*	0.72	0.99	0.22	0.22	0.15	0.22	0.24	0.23	0.47	2.08	1.77	3.27
Cr2O3_pct*	0.00	0.00	0.02	0.02	0.02	0.01	0.01	0.01	0.01	0.00	0.01	0.01
P2O5_pct*	0.04	0.03	0.04	0.03	0.04	0.07	0.07	0.04	0.16	0.22	0.48	0.34
Mg#	43.32	49.74	74.54	74.63	75.37	68.21	68.88	69.26	66.08	29.54	31.35	18.05
Mo_pct	<0.001	<0.001	<0.001	<0.001	<0.001	<0.001	<0.001	<0.001	<0.001	<0.001	<0.001	<0.001
Cu_pct	<0.001	<0.001	<0.001	<0.001	<0.001	0.00	0.00	0.00	0.00	0.00	0.00	<0.001

Pb_pct	<0.02	<0.02	<0.02	<0.02	<0.02	<0.02	<0.02	<0.02	<0.02	<0.02	<0.02	<0.02
Zn_pct	<0.01	<0.01	<0.01	<0.01	<0.01	0.01	0.01	<0.01	0.01	<0.01	<0.01	0.01
Ag_ppm	<2	<2	<2	<2	<2	<2	<2	<2	<2	<2	<2	<2
Ni_ppm	11.00	11.00	500.00	487.00	647.00	490.00	463.00	389.00	320.00	<10	11.00	<10
Mo_ppm	0.11	0.20	0.06	0.08	0.09	0.58	0.15	0.49	0.86	0.72	0.83	0.91
Cu_ppm	4.65	1.66	7.06	7.04	7.79	8.88	9.09	8.94	18.37	19.99	12.57	5.59
Pb_ppm	4.14	3.71	0.35	0.40	0.35	0.49	0.37	0.38	0.46	2.69	1.54	0.51
Zn_ppm	28.10	24.20	60.10	59.10	66.60	113.80	106.80	83.70	94.10	22.70	25.10	35.60
Ag_ppb	47.00	24.00	4.00	95.00	7.00	134.00	11.00	9.00	8.00	12.00	16.00	16.00
Ni_ppm	7.70	8.20	457.20	446.60	544.80	439.20	411.70	355.10	295.30	5.00	10.30	5.20
Co_ppm	16.80	15.30	88.40	84.50	98.60	143.20	136.60	111.80	99.00	3.90	7.90	4.10
Mn_ppm	168.00	193.00	978.00	963.00	851.00	1701.00	1610.00	1291.00	1355.00	1423.00	651.00	1386.00
As_ppm	0.20	<0.1	0.20	0.10	<0.1	0.10	<0.1	0.20	<0.1	0.10	<0.1	<0.1
Au_ppb	<0.2	<0.2	0.30	<0.2	<0.2	<0.2	<0.2	0.40	<0.2	1.10	0.80	<0.2
Cd_ppm	0.05	0.03	0.01	0.01	0.01	0.02	0.02	0.02	0.03	0.04	0.02	0.03
Sb_ppm	<0.02	<0.02	<0.02	<0.02	<0.02	<0.02	<0.02	<0.02	<0.02	<0.02	<0.02	<0.02
Bi_ppm	<0.02	<0.02	<0.02	<0.02	<0.02	<0.02	<0.02	<0.02	<0.02	<0.02	<0.02	<0.02
Cr_ppm	14.40	17.80	30.90	28.90	42.30	36.20	37.50	35.00	23.50	7.50	47.80	33.00
Hg_ppb	<5	<5	<5	<5	<5	<5	<5	<5	<5	<5	<5	<5
Se_ppm	<0.1	<0.1	<0.1	<0.1	<0.1	<0.1	0.10	0.10	0.10	<0.1	<0.1	<0.1
Te_ppm	<0.02	<0.02	<0.02	<0.02	<0.02	<0.02	<0.02	<0.02	<0.02	<0.02	<0.02	<0.02
Ge_ppm	<0.1	<0.1	<0.1	<0.1	<0.1	<0.1	<0.1	<0.1	0.10	<0.1	<0.1	<0.1
In_ppm	<0.02	<0.02	<0.02	<0.02	<0.02	<0.02	<0.02	<0.02	<0.02	<0.02	<0.02	<0.02
Re_ppb	<1	<1	<1	<1	<1	<1	<1	<1	<1	<1	<1	<1
Be_ppm	0.20	0.20	<0.1	<0.1	<0.1	<0.1	<0.1	<0.1	<0.1	0.30	0.10	<0.1

Li_ppm	4.10	5.20	1.60	1.60	1.30	2.60	2.80	3.00	2.70	2.10	3.50	0.60
Pd_ppb	<10	<10	<10	<10	<10	<10	<10	<10	<10	<10	<10	<10
Pt_ppb	<2	<2	<2	<2	<2	<2	<2	<2	<2	<2	<2	<2
Au_ppb	4.00	5.00	4.00	5.00	9.00	4.00	4.00	5.00	4.00	3.00	2.00	2.00
Pt_ppb	0.30	0.60	0.20	0.30	0.70	0.40	0.30	0.30	0.30	0.30	0.30	0.20
Pd_ppb	0.90	1.30	0.90	1.00	2.10	1.20	1.00	1.10	1.00	0.60	0.60	0.50
B_ppm	<1	<1	<1	<1	<1	<1	<1	<1	<1	5.00	4.00	2.00
Tl_ppm	<0.02	<0.02	<0.02	<0.02	<0.02	<0.02	<0.02	<0.02	<0.02	<0.02	<0.02	<0.02
LOI_pct	1.70	2.20	3.70	4.00	5.60	1.30	1.60	2.70	-0.50	2.30	1.80	0.40
TOT/C_TC000_pct	0.02	0.14	0.08	0.10	0.04	0.08	0.04	0.03	0.03	0.08	0.15	0.16
TOT/S_pct	<0.02	<0.02	<0.02	<0.02	<0.02	<0.02	<0.02	<0.02	0.03	<0.02	0.05	0.04
Ba_ppm	393.00	620.00	164.00	168.00	118.00	130.00	147.00	160.00	260.00	1056.00	1132.00	3309.00
Sc_ppm	13.00	13.00	5.00	5.00	6.00	10.00	10.00	8.00	12.00	4.00	7.00	25.00
Sum_pct	99.85	99.87	99.67	99.68	99.61	99.58	99.59	99.66	99.65	99.84	99.86	99.87
Cs_ppm	0.60	0.30	<0.1	<0.1	<0.1	<0.1	0.10	<0.1	0.20	0.20	0.10	<0.1
Ga_ppm	22.30	20.40	9.20	9.70	7.20	7.50	8.70	10.20	13.10	19.00	17.80	22.70
Hf_ppm	0.70	0.70	0.40	0.30	0.30	0.70	0.70	0.60	1.70	1.20	1.80	5.10
Nb_ppm	2.10	2.10	0.90	0.60	0.50	1.80	1.70	1.10	4.10	2.70	5.50	1.70
Rb_ppm	11.10	15.40	2.00	2.10	1.70	2.70	3.00	2.90	7.40	24.00	18.90	11.00
Sn_ppm	<1	<1	<1	<1	<1	<1	<1	<1	<1	<1	<1	<1
Sr_ppm	557.00	480.20	390.20	389.30	297.70	216.10	257.00	331.30	345.20	1146.80	829.50	571.90
Ta_ppm	0.20	0.20	<0.1	<0.1	<0.1	0.10	0.10	0.10	0.20	0.20	0.30	<0.1
Th_ppm	0.40	0.70	<0.2	<0.2	<0.2	0.30	0.30	0.20	0.70	0.80	0.50	<0.2
U_ppm	<0.1	0.10	<0.1	<0.1	<0.1	<0.1	<0.1	<0.1	0.10	0.20	0.10	<0.1
V_ppm	236.00	172.00	36.00	36.00	38.00	65.00	66.00	56.00	104.00	25.00	60.00	22.00

W_ppm	0.60	0.80	<0.5	<0.5	0.70	0.80	<0.5	1.00	1.70	2.60	1.20	1.20
Zr_ppm	24.90	25.10	15.10	13.30	13.00	26.70	28.80	18.60	60.20	50.50	85.60	256.10
Y_ppm	5.90	5.00	2.60	2.50	2.30	4.70	5.50	3.60	11.70	7.30	10.90	8.90
La_ppm	5.50	6.00	2.80	2.50	2.30	4.00	4.20	2.90	8.90	12.70	12.10	6.90
Ce_ppm	10.40	10.70	5.30	5.30	4.40	8.20	8.50	6.00	18.50	23.80	25.50	13.30
Pr_ppm	1.11	1.19	0.60	0.59	0.52	0.96	0.99	0.74	2.29	2.85	3.27	2.00
Nd_ppm	4.80	4.50	2.80	2.70	2.40	4.10	4.20	3.10	9.90	11.70	14.70	10.70
Sm_ppm	0.96	0.93	0.51	0.50	0.42	0.86	0.92	0.65	2.23	2.02	3.09	2.57
Eu_ppm	0.82	0.85	0.47	0.45	0.34	0.50	0.55	0.53	1.01	2.30	2.25	5.67
Gd_ppm	1.05	0.98	0.60	0.48	0.44	0.95	0.95	0.70	2.44	2.07	2.73	2.72
Tb_ppm	0.16	0.14	0.07	0.07	0.07	0.15	0.15	0.10	0.38	0.28	0.38	0.35
Dy_ppm	0.88	0.95	0.48	0.41	0.41	0.90	1.07	0.59	2.23	1.49	2.03	1.91
Ho_ppm	0.18	0.19	0.10	0.09	0.08	0.19	0.21	0.12	0.45	0.28	0.39	0.33
Er_ppm	0.55	0.54	0.25	0.24	0.25	0.52	0.53	0.39	1.23	0.78	0.99	0.81
Tm_ppm	0.08	0.07	0.05	0.03	0.03	0.09	0.09	0.05	0.18	0.10	0.14	0.11
Yb_ppm	0.48	0.42	0.22	0.21	0.23	0.54	0.58	0.36	1.05	0.70	0.76	0.70
Lu_ppm	0.09	0.07	0.03	0.03	0.04	0.09	0.09	0.06	0.16	0.10	0.12	0.13

Sample_ID	KAC005/004	KAC005/005a	KAC005/005b	KAC006/007	KAC006/008	KAC012/014	KAC012/014a	KAC012/017	KAC013/018	KAC016/020	KAC017/022	KAC018/023
Lat_S	-17.3318	-17.3318	-17.3318	-17.3263	-17.3263	-16.9913	-16.9913	-16.9913	-16.9854	-16.9323	-16.9314	-16.9071
Long_E	13.9607	13.9607	13.9607	13.9413	13.9413	13.9144	13.9144	13.9144	13.9131	13.6330	13.6343	13.6036
Rocktype	Norite?	Leuconorite	Leuconorite	Anorthosite	Anorthosite	Leuconorite	Foliated Pl in 012/014	Autolith within 012/014	Leuconorite	Anorthosite	Anorthosite	Leuconorite/ leucotroctolite
Group	KC	KC	KC	KC	KC	KC	KC	KC	KC	KC	KC	KC

SiO2_pct	48.87	51.14	51.1	49.54	51.8	48.13	47.94	51.51	47.16	51.65	49.17	48.54
TiO2_pct	2.51	2.05	2.14	1.75	0.55	0.72	1.05	0.16	0.44	0.14	0.25	0.11
Al2O3_pct	15.68	16.35	16.34	24.14	24.66	17.92	19.34	27.44	20.13	27.97	26.74	27.38
Fe2O3t_pct	15.51	13.4	13.37	4.96	3.79	12.1	9.60	1.33	9.41	1.37	2.99	2.77
MnO_pct	0.28	0.27	0.24	0.07	0.09	0.16	0.13	0.03	0.13	0.03	0.05	0.05
MgO_pct	2.54	2.25	1.94	1.65	0.8	8.91	7.22	0.58	8.70	0.69	3.59	3.88
CaO_pct	7.47	6.63	6.28	9.6	10.09	7.41	10.56	9.39	9.62	11.92	12.82	12.81
Na2O_pct	4.1	4.11	4.09	4.2	4.63	3.11	2.97	4.34	2.83	4.33	3.03	3.00
K2O_pct	1.46	2.38	2.49	0.65	0.86	0.81	0.39	2.15	0.36	0.25	0.19	0.13
Cr2O3_pct	0.004	0.003	<0.002	0.002	0.006	0.012	0.02	<0.002	0.02	0.01	0.01	0.12
P2O5_pct	0.91	1.04	1.05	0.26	0.2	0.08	0.07	0.01	0.06	0.01	0.03	<0.01
Normalised*	99.63	99.85	99.35	96.86	97.48	99.44	99.35	97.04	98.94	98.39	98.96	98.78
SiO2_pct*	49.05	51.22	51.43	51.15	53.14	48.40	48.25	53.08	47.67	52.50	49.69	49.14
TiO2_pct*	2.57	2.10	2.19	1.79	0.56	0.74	1.08	0.16	0.45	0.14	0.26	0.11
Al2O3_pct*	49.05	51.22	51.43	51.15	53.14	48.40	48.25	53.08	47.67	52.50	49.69	49.14
Fe2O3t_pct*	15.57	13.42	13.46	5.12	3.89	12.17	9.66	1.37	9.51	1.39	3.02	2.80
FeO_pct*	13.23	11.41	11.44	4.35	3.30	10.34	8.21	1.16	8.08	1.18	2.57	2.38
Fe2O3_pct*	2.34	2.01	2.02	0.77	0.58	1.83	1.45	0.21	1.43	0.21	0.45	0.42
FeO*_pct	14.01	12.08	12.11	4.61	3.50	10.95	8.70	1.23	8.56	1.25	2.72	2.52
MnO_pct*	0.29	0.28	0.25	0.07	0.09	0.16	0.13	0.03	0.13	0.03	0.05	0.05
MgO_pct*	2.55	2.25	1.95	1.70	0.82	8.96	7.27	0.60	8.79	0.70	3.63	3.93
CaO_pct*	7.66	6.80	6.44	9.84	10.34	7.60	10.83	9.63	9.86	12.22	13.14	13.13
Na2O_pct*	4.20	4.21	4.19	4.31	4.75	3.19	3.04	4.45	2.90	4.44	3.11	3.08
K2O_pct*	1.50	2.44	2.55	0.67	0.88	0.83	0.40	2.20	0.37	0.26	0.19	0.13
Cr2O3_pct*	0.00	0.00	N/A	0.00	0.01	0.01	0.02	N/A	0.02	0.01	0.01	0.12

P2O5_pct*	0.93	1.07	1.08	0.27	0.21	0.08	0.07	0.01	0.06	0.01	0.03	#VALUE!
Mg#	25.56	26.04	23.32	41.09	30.68	60.69	61.19	47.76	65.97	51.36	71.57	74.60
Mo_pct	<0.001	<0.001	<0.001	<0.001	<0.001	<0.001	<0.001	<0.001	<0.001	<0.001	<0.001	<0.001
Cu_pct	0.00	0.00	0.00	0.00	<0.001	0.01	0.01	<0.001	0.01	0.00	0.00	0.00
Pb_pct	<0.02	<0.02	<0.02	<0.02	<0.02	<0.02	<0.02	<0.02	<0.02	<0.02	<0.02	<0.02
Zn_pct	0.02	0.02	0.02	<0.01	<0.01	<0.01	<0.01	<0.01	<0.01	<0.01	<0.01	<0.01
Ag_ppm	<2	<2	<2	<2	<2	<2	<2	<2	<2	<2	<2	<2
Ni_ppm	<10	<10	<10	13.00	13.00	191.00	190.00	11.00	287.00	14.00	122.00	124.00
Mo_ppm	1.61	1.62	1.34	0.47	0.43	0.75	0.57	0.43	0.65	1.25	0.29	0.44
Cu_ppm	15.87	15.58	14.10	22.70	4.01	54.90	83.99	4.83	89.97	15.47	22.36	15.83
Pb_ppm	0.26	0.63	0.53	0.61	0.78	0.90	0.83	0.42	0.73	0.58	0.28	0.33
Zn_ppm	40.40	55.70	30.20	46.70	26.00	74.20	45.10	7.20	54.30	6.30	10.80	10.70
Ag_ppb	10.00	21.00	7.00	16.00	2.00	45.00	24.00	2.00	28.00	9.00	11.00	8.00
Ni_ppm	2.50	4.20	2.50	12.40	11.70	159.40	151.20	9.40	256.70	9.80	90.70	98.40
Co_ppm	7.90	8.70	10.70	17.20	8.30	60.80	40.90	3.70	56.60	2.50	13.30	17.00
Mn_ppm	772.00	375.00	419.00	405.00	354.00	1052.00	627.00	163.00	889.00	193.00	211.00	252.00
As_ppm	<0.1	<0.1	<0.1	<0.1	<0.1	<0.1	<0.1	<0.1	<0.1	<0.1	<0.1	<0.1
Au_ppb	0.30	0.30	<0.2	<0.2	<0.2	0.40	0.60	0.30	1.00	<0.2	0.50	0.40
Cd_ppm	0.03	0.04	0.05	0.02	0.02	0.02	0.01	<0.01	0.02	0.01	<0.01	<0.01
Sb_ppm	<0.02	<0.02	<0.02	<0.02	<0.02	<0.02	<0.02	<0.02	<0.02	<0.02	<0.02	<0.02
Bi_ppm	<0.02	<0.02	<0.02	<0.02	<0.02	<0.02	<0.02	<0.02	<0.02	<0.02	<0.02	<0.02
Cr_ppm	11.60	18.50	3.80	5.80	40.10	62.80	100.60	6.10	83.50	26.50	30.80	52.30
Hg_ppb	<5	<5	<5	<5	<5	<5	<5	<5	<5	<5	<5	<5
Se_ppm	0.10	0.20	0.20	<0.1	<0.1	<0.1	<0.1	<0.1	<0.1	<0.1	<0.1	<0.1
Te_ppm	<0.02	<0.02	<0.02	<0.02	<0.02	<0.02	<0.02	<0.02	<0.02	0.02	<0.02	<0.02

Ge_ppm	<0.1	<0.1	<0.1	<0.1	<0.1	<0.1	<0.1	<0.1	<0.1	<0.1	<0.1	<0.1
In_ppm	0.02	0.04	0.05	<0.02	<0.02	<0.02	<0.02	<0.02	<0.02	<0.02	<0.02	<0.02
Re_ppb	<1	<1	<1	<1	<1	<1	<1	<1	<1	<1	<1	<1
Be_ppm	<0.1	<0.1	<0.1	<0.1	<0.1	0.10	0.10	<0.1	0.10	<0.1	0.10	<0.1
Li_ppm	0.80	0.60	0.60	5.60	3.10	4.50	3.70	3.20	2.60	0.90	0.70	0.90
Pd_ppb	<10	<10	<10	<10	<10	<10	<10	<10	<10	<10	<10	<10
Pt_ppb	<2	<2	<2	<2	<2	<2	<2	<2	<2	<2	<2	<2
Au_ppb	2.00	3.00	2.00	3.00	2.00	4.00	I.S.	3.00	3.00	3.00	2.00	2.00
Pt_ppb	0.10	0.10	0.10	0.20	0.20	0.70	I.S.	0.20	0.30	0.30	0.20	0.20
Pd_ppb	<0.5	<0.5	0.50	0.50	<0.5	1.60	I.S.	1.10	1.10	2.10	0.90	0.90
B_ppm	1.00	1.00	<1	1.00	3.00	<1	<1	<1	<1	<1	<1	<1
Tl_ppm	<0.02	<0.02	<0.02	<0.02	<0.02	0.05	<0.02	<0.02	<0.02	<0.02	<0.02	<0.02
LOI_pct	0.20	-0.10	0.40	3.00	2.40	0.30	0.40	2.80	0.80	1.50	0.90	1.10
TOT/C_TC000_pct	0.04	0.07	0.04	0.24	0.04	0.11	0.08	0.03	0.04	0.04	0.02	0.02
TOT/S_pct	<0.02	0.08	<0.02	0.03	<0.02	0.03	0.04	<0.02	0.03	<0.02	<0.02	<0.02
Ba_ppm	2498.00	2008.00	2545.00	472.00	538.00	330.00	264.00	876.00	210.00	207.00	121.00	57.00
Sc_ppm	35.00	23.00	24.00	7.00	6.00	9.00	23.00	1.00	10.00	2.00	5.00	2.00
Sum_pct	99.83	99.75	99.75	99.86	99.88	99.74	99.75	99.84	99.74	99.89	99.86	99.88
Cs_ppm	<0.1	<0.1	<0.1	0.40	0.40	0.20	<0.1	<0.1	<0.1	<0.1	0.20	<0.1
Ga_ppm	20.80	20.80	21.20	17.00	19.30	15.30	17.20	16.70	14.70	17.10	14.40	13.20
Hf_ppm	3.10	12.00	13.50	1.80	1.10	2.00	1.30	0.20	0.80	0.10	0.30	0.10
Nb_ppm	10.50	22.50	25.50	5.80	1.40	4.20	2.90	0.40	1.40	0.20	1.20	0.20
Rb_ppm	3.80	11.10	14.20	3.70	6.50	18.80	3.30	47.70	4.40	2.30	1.40	1.10
Sn_ppm	<1	<1	<1	<1	<1	<1	<1	<1	1.00	<1	<1	<1
Sr_ppm	463.70	496.20	511.90	642.50	741.40	517.40	624.70	1242.70	627.80	798.10	575.10	492.90

Ta_ppm	0.50	1.10	1.30	0.40	<0.1	0.20	0.20	<0.1	<0.1	<0.1	0.20	<0.1
Th_ppm	<0.2	<0.2	0.30	0.70	0.30	1.80	0.60	<0.2	0.50	<0.2	<0.2	<0.2
U_ppm	<0.1	0.10	0.30	0.10	<0.1	0.30	0.10	<0.1	0.10	<0.1	<0.1	<0.1
V_ppm	84.00	79.00	76.00	66.00	59.00	97.00	175.00	14.00	73.00	27.00	43.00	29.00
W_ppm	1.80	<0.5	1.10	1.50	0.90	1.90	1.70	1.10	2.50	2.50	1.10	1.50
Zr_ppm	127.60	600.40	683.30	93.60	47.80	82.20	52.70	8.20	32.40	6.70	16.40	5.50
Y_ppm	39.50	47.30	50.00	6.80	7.50	10.40	13.30	1.70	7.20	1.70	3.50	1.80
La_ppm	33.60	45.20	47.70	8.20	8.30	11.70	8.00	2.80	5.70	2.60	2.50	1.30
Ce_ppm	79.50	101.80	107.40	16.70	16.40	23.50	16.40	5.10	12.40	4.80	5.70	2.50
Pr_ppm	11.38	13.58	14.32	2.08	2.14	2.68	2.24	0.58	1.54	0.48	0.67	0.30
Nd_ppm	54.10	60.50	62.90	9.20	9.10	11.30	9.80	2.40	7.00	2.00	2.90	1.30
Sm_ppm	11.18	12.26	12.87	1.86	1.79	2.16	2.45	0.49	1.31	0.35	0.67	0.23
Eu_ppm	6.09	4.73	4.92	1.50	1.75	0.97	1.25	0.57	0.82	0.68	0.47	0.32
Gd_ppm	11.57	12.15	12.49	1.79	1.84	1.94	2.63	0.45	1.43	0.32	0.74	0.31
Tb_ppm	1.49	1.66	1.75	0.24	0.26	0.30	0.41	0.06	0.22	0.05	0.11	0.05
Dy_ppm	8.14	9.41	9.99	1.35	1.52	1.80	2.46	0.28	1.24	0.28	0.62	0.31
Ho_ppm	1.52	1.77	1.91	0.27	0.28	0.35	0.50	0.05	0.27	0.04	0.13	0.05
Er_ppm	3.96	5.02	5.25	0.67	0.81	1.12	1.47	0.20	0.75	0.19	0.40	0.16
Tm_ppm	0.48	0.68	0.71	0.09	0.10	0.15	0.19	0.02	0.10	0.02	0.05	0.02
Yb_ppm	2.94	4.36	4.53	0.61	0.67	1.08	1.25	0.13	0.65	0.13	0.32	0.15
Lu_ppm	0.47	0.69	0.70	0.08	0.10	0.16	0.19	0.02	0.10	0.02	0.05	0.02

Sample_ID	KAC019/024	KAC021/026	KAC022/027ab	KAC023/029	KAC024/030a	KAC024/030b	KAC028/032	KAC031/034	KAC033/036	KAC047/047	KAC048/048a	KAC049/049	KAC050/050a	KAC050/050b
Lat_S	-16.8851	-16.8561	-16.8341	-16.7813	-16.8697	-16.8697	-16.9082	-16.9415	-16.7696	-16.5860	-16.5971	-16.6108	-16.6285	-16.6285
Long_E	13.5404	13.5121	13.4903	13.4858	13.4799	13.4799	13.4656	13.4700	13.4912	13.8040	13.8094	13.8122	13.8147	13.8147

Rocktype	Anorthosite	Anorthosite	Anorthosite (green, altered)	Anorthosite/ Leuconorite	Anorthosite	Anorthosite	Anorthosite	Anorthosite	Anorthosite	Anorthosite	Opx megacryst + host anorthosite	Anorthosite	Opx megacryst in 50b	Anorthosite (host to 050/050a)
Group	KC	KC	KC	KC	KC	KC	KC	KC	KC	KC	KC	KC	KC	KC
SiO2_pct	47.01	48.48	49.54	52.35	50.02	50.07	49.51	44.18	47.88	50.27	51.66	51.91	51.57	52.64
TiO2_pct	0.11	0.11	0.31	0.86	1.93	1.97	0.78	0.60	0.26	0.10	0.34	0.10	0.53	0.20
Al2O3_pct	28.69	23.32	26.52	23.76	21.45	20.46	21.40	19.84	20.82	26.02	16.05	27.47	3.59	27.92
Fe2O3t_pct	3.61	4.26	2.28	4.26	8.90	8.75	6.09	7.49	5.87	3.72	11.05	1.88	19.00	1.26
MnO_pct	0.05	0.08	0.05	0.06	0.15	0.14	0.14	0.12	0.10	0.05	0.20	0.03	0.32	0.02
MgO_pct	2.86	6.41	1.02	1.37	1.61	1.71	3.73	4.79	7.13	3.75	10.23	1.57	22.73	0.31
CaO_pct	13.97	12.57	12.78	8.38	7.99	9.02	10.73	10.87	10.17	10.92	6.65	11.49	1.54	11.56
Na2O_pct	2.42	2.60	3.96	4.65	3.97	3.75	3.62	3.33	3.09	3.59	2.53	4.06	0.04	4.40
K2O_pct	0.17	0.14	0.63	1.49	1.66	1.25	1.10	0.34	0.66	0.30	0.23	0.34	<0.01	0.41
Cr2O3_pct	0.02	0.05	0.01	0.01	0.01	0.00	0.02	0.01	0.10	0.00	0.04	<0.002	0.19	<0.002
P2O5_pct	0.02	<0.01	0.03	0.37	0.22	0.26	0.09	0.04	0.01	0.03	0.03	0.01	0.01	0.05
Normalised*	98.89	98.03	97.21	97.58	97.95	97.45	97.24	91.62	96.10	98.74	99.05	98.87	99.57	98.79
SiO2_pct*	47.54	49.45	50.96	53.65	51.07	51.38	50.92	48.22	49.82	50.91	52.16	52.50	51.79	53.28
TiO2_pct*	0.11	0.11	0.32	0.88	1.98	2.02	0.80	0.62	0.27	0.10	0.35	0.10	0.54	0.21
Al2O3_pct*	47.54	49.45	50.96	53.65	51.07	51.38	50.92	48.22	49.82	50.91	52.16	52.50	51.79	53.28
Fe2O3t_pct*	3.65	4.35	2.35	4.37	9.09	8.98	6.26	8.18	6.11	3.77	11.16	1.90	19.08	1.28
FeO_pct*	3.10	3.69	1.99	3.71	7.72	7.63	5.32	6.95	5.19	3.20	9.48	1.62	16.22	1.08
Fe2O3_pct*	0.55	0.65	0.35	0.65	1.36	1.35	0.94	1.23	0.92	0.57	1.67	0.29	2.86	0.19
FeO*_pct	3.29	3.91	2.11	3.93	8.18	8.08	5.64	7.36	5.50	3.39	10.04	1.71	17.17	1.15

MnO_pct*	0.05	0.08	0.05	0.06	0.15	0.14	0.14	0.12	0.10	0.05	0.21	0.03	0.33	0.02
MgO_pct*	2.89	6.54	1.05	1.40	1.64	1.75	3.84	5.23	7.42	3.80	10.33	1.59	22.83	0.31
CaO_pct*	14.32	12.89	13.10	8.59	8.19	9.25	11.00	11.14	10.43	11.20	6.82	11.78	1.58	11.85
Na2O_pct*	2.48	2.67	4.06	4.77	4.07	3.84	3.71	3.41	3.17	3.68	2.59	4.16	0.04	4.51
K2O_pct*	0.17	0.14	0.65	1.53	1.70	1.28	1.13	0.35	0.68	0.31	0.24	0.35	#VALUE!	0.42
Cr2O3_pct*	0.02	0.05	0.01	0.01	0.01	0.00	0.02	0.01	0.11	0.00	0.04	#VALUE!	0.20	#VALUE!
P2O5_pct*	0.02	#VALUE!	0.03	0.38	0.23	0.27	0.09	0.04	0.01	0.03	0.03	0.01	0.01	0.05
Mg#	62.42	75.93	48.40	40.27	27.50	29.06	56.22	57.28	71.80	67.88	66.00	63.65	71.49	34.03
Mo_pct	<0.001	<0.001	<0.001	<0.001	<0.001	<0.001	<0.001	<0.001	<0.001	<0.001	<0.001	<0.001	<0.001	<0.001
Cu_pct	0.00	0.00	0.00	0.00	0.01	0.01	0.00	0.01	0.01	0.00	<0.001	<0.001	0.00	0.00
Pb_pct	<0.02	<0.02	<0.02	<0.02	<0.02	<0.02	<0.02	<0.02	<0.02	<0.02	<0.02	<0.02	<0.02	<0.02
Zn_pct	<0.01	<0.01	<0.01	<0.01	<0.01	<0.01	<0.01	<0.01	<0.01	<0.01	<0.01	<0.01	0.02	<0.01
Ag_ppm	<2	<2	<2	<2	<2	<2	<2	<2	<2	<2	<2	<2	<2	<2
Ni_ppm	84.00	168.00	17.00	21.00	20.00	21.00	23.00	92.00	101.00	122.00	86.00	45.00	304.00	10.00
Mo_ppm	0.66	0.58	0.33	0.65	1.03	1.01	0.36	0.32	0.19	0.73	0.42	0.75	0.40	0.69
Cu_ppm	11.30	28.58	11.16	17.02	51.36	52.28	25.77	125.92	41.97	11.39	6.54	7.75	6.63	12.76
Pb_ppm	0.48	0.18	0.70	5.71	3.50	2.26	1.60	0.70	0.45	0.29	0.36	0.30	0.18	1.05
Zn_ppm	18.20	14.20	12.90	30.50	36.40	46.50	33.00	46.00	26.90	15.00	12.80	6.70	18.20	5.30
Ag_ppb	39.00	10.00	46.00	56.00	33.00	43.00	16.00	35.00	17.00	17.00	3.00	5.00	<2	6.00
Ni_ppm	68.50	122.30	14.50	17.90	16.50	14.90	15.30	84.50	77.80	107.30	16.80	32.10	45.20	9.40
Co_ppm	18.60	24.90	6.10	11.30	13.70	15.20	13.40	41.30	31.10	22.50	7.80	8.90	13.90	2.30
Mn_ppm	334.00	343.00	259.00	230.00	354.00	304.00	539.00	815.00	442.00	271.00	178.00	136.00	261.00	109.00
As_ppm	<0.1	<0.1	<0.1	<0.1	<0.1	<0.1	<0.1	<0.1	<0.1	<0.1	0.20	<0.1	0.10	0.20
Au_ppb	<0.2	0.30	0.20	0.90	1.50	1.10	0.50	1.70	0.20	0.60	1.10	0.70	0.40	0.50

Cd_ppm	0.02	0.01	0.02	0.05	0.07	0.06	0.06	0.05	0.02	<0.01	<0.01	<0.01	0.01	0.01
Sb_ppm	<0.02	<0.02	<0.02	<0.02	<0.02	<0.02	<0.02	<0.02	<0.02	<0.02	<0.02	<0.02	<0.02	<0.02
Bi_ppm	<0.02	<0.02	<0.02	0.03	<0.02	<0.02	<0.02	<0.02	<0.02	<0.02	<0.02	<0.02	<0.02	<0.02
Cr_ppm	7.20	38.10	33.90	45.30	50.40	25.70	56.10	37.40	236.40	11.90	69.50	9.40	307.20	10.40
Hg_ppb	<5	<5	<5	<5	8.00	<5	<5	<5	<5	<5	<5	<5	<5	<5
Se_ppm	<0.1	<0.1	<0.1	<0.1	<0.1	<0.1	<0.1	<0.1	<0.1	<0.1	<0.1	<0.1	<0.1	<0.1
Te_ppm	0.03	<0.02	<0.02	<0.02	<0.02	<0.02	<0.02	<0.02	<0.02	<0.02	<0.02	<0.02	<0.02	<0.02
Ge_ppm	<0.1	<0.1	<0.1	<0.1	<0.1	<0.1	<0.1	0.10	<0.1	<0.1	<0.1	<0.1	<0.1	<0.1
In_ppm	<0.02	<0.02	<0.02	<0.02	<0.02	<0.02	<0.02	<0.02	<0.02	<0.02	<0.02	<0.02	<0.02	<0.02
Re_ppb	<1	<1	<1	<1	<1	<1	<1	<1	<1	<1	<1	<1	<1	<1
Be_ppm	0.10	<0.1	0.20	0.40	0.50	0.30	0.30	0.30	<0.1	<0.1	<0.1	<0.1	<0.1	<0.1
Li_ppm	1.20	0.90	2.80	21.10	7.30	7.90	4.00	5.90	9.60	1.90	4.60	2.10	5.20	1.60
Pd_ppb	<10	<10	<10	<10	<10	<10	<10	<10	<10	<10	<10	<10	<10	<10
Pt_ppb	<2	<2	<2	<2	<2	<2	<2	<2	<2	<2	<2	<2	<2	<2
Au_ppb	2.00	3.00	3.00	2.00	3.00	3.00	2.00	2.00	2.00	1.00	2.00	3.00	2.00	3.00
Pt_ppb	0.20	0.20	0.20	0.20	0.20	0.20	0.20	0.20	0.20	0.10	0.20	0.10	0.20	0.20
Pd_ppb	0.70	0.70	0.60	0.60	0.70	0.60	0.60	0.80	0.80	0.70	0.80	0.60	0.80	1.00
B_ppm	<1	<1	2.00	6.00	8.00	7.00	5.00	<1	1.00	<1	<1	<1	<1	<1
Tl_ppm	<0.02	<0.02	<0.02	0.03	0.03	0.02	<0.02	<0.02	<0.02	<0.02	<0.02	<0.02	<0.02	<0.02
LOI_pct	1.00	1.80	2.70	2.30	1.90	2.40	2.60	8.20	3.70	1.10	0.70	1.00	0.00	1.10
TOT/C_TC000_pct	0.04	0.04	0.13	0.02	0.05	0.03	0.17	1.37	0.03	0.03	0.03	0.04	0.03	0.03
TOT/S_pct	<0.02	<0.02	<0.02	<0.02	<0.02	<0.02	<0.02	<0.02	<0.02	<0.02	<0.02	<0.02	<0.02	<0.02
Ba_ppm	87.00	57.00	255.00	354.00	406.00	323.00	346.00	156.00	251.00	195.00	170.00	224.00	22.00	268.00
Sc_ppm	2.00	13.00	4.00	2.00	16.00	15.00	29.00	12.00	28.00	1.00	19.00	<1	44.00	1.00

Sum_pct	99.89	99.83	99.91	99.88	99.85	99.85	99.84	99.82	99.80	99.84	99.75	99.87	99.57	99.89
Cs_ppm	<0.1	<0.1	1.30	0.70	1.50	1.20	1.40	0.20	2.10	<0.1	<0.1	<0.1	<0.1	<0.1
Ga_ppm	14.80	11.70	19.70	18.40	21.20	20.10	18.20	17.50	14.80	15.80	13.00	16.60	7.50	18.20
Hf_ppm	0.10	0.10	0.30	0.60	4.60	4.00	1.20	0.60	0.50	<0.1	0.30	<0.1	0.40	0.40
Nb_ppm	0.40	<0.1	0.60	4.00	9.70	8.50	3.50	1.10	0.40	0.60	0.50	0.10	0.20	1.00
Rb_ppm	1.60	0.40	10.70	52.00	41.40	32.80	24.10	4.80	13.70	0.90	1.30	1.00	0.20	1.70
Sn_ppm	<1	<1	<1	<1	3.00	1.00	<1	<1	<1	<1	<1	<1	<1	<1
Sr_ppm	506.80	401.10	553.60	625.50	340.10	341.80	454.20	433.90	498.20	820.70	479.10	868.10	7.50	868.50
Ta_ppm	<0.1	<0.1	<0.1	0.30	0.60	0.50	0.20	<0.1	<0.1	<0.1	<0.1	<0.1	<0.1	<0.1
Th_ppm	<0.2	<0.2	<0.2	1.00	4.10	2.90	0.80	0.50	<0.2	<0.2	<0.2	<0.2	<0.2	0.20
U_ppm	<0.1	<0.1	<0.1	0.60	1.10	0.80	0.20	0.10	<0.1	<0.1	<0.1	<0.1	<0.1	<0.1
V_ppm	27.00	83.00	49.00	87.00	213.00	222.00	176.00	150.00	99.00	9.00	89.00	9.00	205.00	12.00
W_ppm	2.10	1.10	1.10	1.50	1.10	1.60	0.70	0.80	1.10	3.30	2.20	1.90	2.50	2.10
Zr_ppm	6.20	3.40	12.20	22.60	174.40	150.70	40.40	21.90	11.80	3.10	12.30	4.40	9.80	20.60
Y_ppm	1.50	2.30	3.30	9.20	27.40	21.40	14.40	6.10	5.20	0.80	4.30	0.70	5.20	2.80
La_ppm	2.20	0.60	3.90	11.20	20.10	16.10	11.00	4.10	2.20	2.90	2.70	2.80	0.40	5.10
Ce_ppm	4.50	1.50	7.70	23.20	43.70	35.20	23.50	8.50	3.80	4.60	5.30	4.60	0.80	10.20
Pr_ppm	0.52	0.16	0.89	2.86	5.38	4.34	2.91	1.05	0.52	0.50	0.62	0.44	0.11	1.13
Nd_ppm	2.20	1.10	3.80	12.30	22.70	19.00	12.40	4.70	2.30	1.90	2.40	2.00	0.60	4.70
Sm_ppm	0.38	0.25	0.78	2.16	4.98	4.10	2.77	1.02	0.72	0.25	0.42	0.29	0.23	0.79
Eu_ppm	0.51	0.34	0.91	1.31	1.63	1.59	1.28	0.88	0.58	0.61	0.57	0.69	0.09	0.82
Gd_ppm	0.37	0.36	0.73	2.16	5.44	4.40	3.07	1.28	0.96	0.27	0.57	0.28	0.48	0.71
Tb_ppm	0.05	0.06	0.10	0.29	0.82	0.68	0.47	0.17	0.15	0.03	0.10	0.02	0.09	0.10
Dy_ppm	0.25	0.43	0.62	1.66	5.03	4.07	2.81	1.08	0.87	0.15	0.63	0.11	0.67	0.64

Ho_ppm	0.05	0.08	0.11	0.32	1.05	0.78	0.58	0.23	0.21	0.03	0.15	0.03	0.15	0.10
Er_ppm	0.14	0.26	0.29	0.81	2.93	2.28	1.59	0.61	0.54	0.07	0.49	0.06	0.67	0.30
Tm_ppm	0.01	0.03	0.04	0.11	0.35	0.30	0.22	0.10	0.07	0.01	0.07	<0.01	0.11	0.03
Yb_ppm	0.11	0.21	0.24	0.76	2.42	1.81	1.41	0.54	0.45	0.08	0.52	<0.05	0.69	0.21
Lu_ppm	0.02	0.03	0.04	0.12	0.38	0.29	0.20	0.07	0.07	<0.01	0.09	<0.01	0.13	0.03

Sample_ID	KAC051/051	KAC054/053	KAC055/054	KAC060/057	KAC063/060	KAC064/061	KAC065/062	KAC066/063	KAC067/064	KAC067/065a	KAC067/065b	KAC068/066a	KAC068/066b	KAC069/067a
Lat_S	-16.6502	-16.6572	-16.6592	-16.5686	-16.3843	-16.3652	-16.3303	-16.2939	-16.2581	-16.2581	-16.2581	-16.1828	-16.1828	-16.1503
Long_E	13.8209	13.8277	13.8366	13.9266	13.9522	13.9470	13.9105	13.8753	13.8613	13.8613	13.8613	13.8545	13.8545	13.8813
Rocktype	Leuconorite	Leuconorite	Leuconorite	Leuconorite	Anorthosite/leuconorite	Anorthosite	Mag anorthosite	Anorthosite	Leuconorite	Pegmatitic patch	Anorthosite; host to 067/065a.	Opx megacryst	Host anorthosite to 068/066a	Opx megacryst
Group	KC	KC	KC	KC	KC	KC	KC	KC	KC	KC	KC	KC	KC	KC
SiO2_pct	48.66	50.20	48.95	57.50	55.68	55.44	51.68	53.85	51.97	52.86	53.31	50.75	53.01	48.33
TiO2_pct	0.09	0.11	0.09	1.05	0.10	0.10	1.14	0.46	0.20	0.21	0.15	0.58	0.21	1.20
Al2O3_pct	22.59	24.70	23.48	17.34	26.62	26.92	26.38	27.44	21.79	23.79	25.54	3.04	22.94	4.33
Fe2O3t_pct	6.51	4.79	5.37	8.27	0.76	0.68	4.42	0.83	6.14	4.40	2.85	21.55	4.73	14.63
MnO_pct	0.08	0.06	0.06	0.17	0.01	<0.01	0.02	<0.01	0.09	0.07	0.04	0.34	0.07	0.29
MgO_pct	7.06	4.89	6.31	0.68	0.09	0.07	0.91	0.06	6.79	4.25	2.78	21.81	4.45	13.77
CaO_pct	9.55	10.28	9.87	3.80	9.85	10.03	9.29	10.47	8.79	9.28	9.98	1.93	9.14	16.03
Na2O_pct	3.27	3.27	3.27	5.11	5.29	5.04	4.65	4.97	3.15	3.80	4.13	0.08	3.94	0.53
K2O_pct	0.30	0.31	0.26	4.55	0.47	0.88	0.59	0.71	0.33	0.48	0.50	<0.01	0.47	<0.01
Cr2O3_pct	0.01	0.00	0.01	0.00	0.01	<0.002	0.04	<0.002	0.02	0.02	0.01	0.07	0.02	0.11
P2O5_pct	0.02	0.02	0.01	0.44	0.02	0.02	<0.01	0.30	<0.01	0.04	0.01	0.01	0.02	0.01

Normalised*	98.20	98.63	97.71	99.21	99.00	99.29	99.15	99.10	99.31	99.25	99.38	100.19	99.04	99.26
SiO2_pct*	49.55	50.90	50.10	57.96	56.24	55.84	52.12	54.34	52.33	53.26	53.64	50.65	53.52	48.69
TiO2_pct*	0.09	0.11	0.09	1.08	0.10	0.10	1.17	0.47	0.21	0.22	0.15	0.59	0.22	1.23
Al2O3_pct*	49.55	50.90	50.10	57.96	56.24	55.84	52.12	54.34	52.33	53.26	53.64	50.65	53.52	48.69
Fe2O3t_pct*	6.63	4.86	5.50	8.34	0.77	0.68	4.46	0.84	6.18	4.43	2.87	21.51	4.78	14.74
FeO_pct*	5.63	4.13	4.67	7.09	0.65	0.58	3.79	0.71	5.26	3.77	2.44	18.28	4.06	12.53
Fe2O3_pct*	0.99	0.73	0.82	1.25	0.12	0.10	0.67	0.13	0.93	0.66	0.43	3.23	0.72	2.21
FeO*_pct	5.97	4.37	4.95	7.50	0.69	0.62	4.01	0.75	5.56	3.99	2.58	19.36	4.30	13.27
MnO_pct*	0.08	0.06	0.06	0.17	0.01	N/A	0.02	N/A	0.09	0.07	0.04	0.35	0.07	0.30
MgO_pct*	7.19	4.96	6.46	0.69	0.09	0.07	0.92	0.06	6.84	4.28	2.80	21.77	4.49	13.87
CaO_pct*	9.79	10.54	10.12	3.90	10.10	10.28	9.52	10.73	9.01	9.51	10.23	1.98	9.37	16.43
Na2O_pct*	3.35	3.35	3.35	5.24	5.42	5.17	4.77	5.10	3.23	3.90	4.23	0.08	4.04	0.54
K2O_pct*	0.31	0.32	0.27	4.66	0.48	0.90	0.60	0.73	0.34	0.49	0.51	N/A	0.48	N/A
Cr2O3_pct*	0.01	0.00	0.01	0.00	0.01	N/A	0.04	N/A	0.02	0.02	0.01	0.08	0.02	0.12
P2O5_pct*	0.02	0.02	0.01	0.45	0.02	0.02	N/A	0.31	N/A	0.04	0.01	0.01	0.02	0.01
Mg#	69.45	68.16	71.13	14.70	19.89	17.75	30.15	13.16	69.87	66.94	67.16	67.97	66.36	66.37
Mo_pct	<0.001	<0.001	<0.001	<0.001	<0.001	<0.001	<0.001	<0.001	<0.001	<0.001	<0.001	<0.001	<0.001	<0.001
Cu_pct	<0.001	<0.001	<0.001	0.00	<0.001	0.00	<0.001	<0.001	0.00	0.00	<0.001	0.00	<0.001	0.02
Pb_pct	<0.02	<0.02	<0.02	<0.02	<0.02	<0.02	<0.02	<0.02	<0.02	<0.02	<0.02	<0.02	<0.02	<0.02
Zn_pct	<0.01	<0.01	<0.01	<0.01	<0.01	<0.01	<0.01	<0.01	<0.01	<0.01	<0.01	0.02	<0.01	0.01
Ag_ppm	<2	<2	<2	<2	<2	<2	<2	<2	<2	<2	<2	<2	<2	<2
Ni_ppm	182.00	119.00	184.00	<10	<10	18.00	66.00	<10	124.00	64.00	46.00	338.00	81.00	224.00
Mo_ppm	0.63	0.38	0.27	1.50	0.37	0.51	0.44	0.79	0.29	0.71	0.35	0.61	0.34	0.82
Cu_ppm	6.42	4.50	4.77	11.26	7.83	29.06	5.03	2.54	4.67	4.11	3.60	15.48	3.65	145.19
Pb_ppm	0.33	0.29	0.28	0.39	0.18	0.16	1.56	0.13	0.28	0.31	0.27	0.11	0.23	0.16

Zn_ppm	25.90	14.50	22.00	64.50	1.50	1.10	5.40	0.50	6.60	7.80	4.70	12.40	6.20	32.30
Ag_ppb	4.00	3.00	5.00	12.00	3.00	4.00	3.00	<2	2.00	2.00	<2	7.00	3.00	4.00
Ni_ppm	160.30	90.20	164.60	1.90	6.00	16.10	47.20	4.40	30.70	16.50	16.20	44.50	22.30	81.80
Co_ppm	42.70	23.50	36.70	2.40	0.80	1.40	11.30	1.10	5.60	4.00	3.10	10.50	4.50	22.60
Mn_ppm	507.00	218.00	419.00	778.00	72.00	43.00	81.00	34.00	95.00	112.00	59.00	175.00	114.00	304.00
As_ppm	0.20	<0.1	<0.1	<0.1	<0.1	<0.1	<0.1	<0.1	<0.1	<0.1	<0.1	<0.1	<0.1	<0.1
Au_ppb	0.70	0.50	0.30	0.30	<0.2	0.20	0.30	<0.2	0.30	<0.2	<0.2	0.70	<0.2	<0.2
Cd_ppm	0.02	<0.01	<0.01	0.04	<0.01	<0.01	<0.01	<0.01	<0.01	<0.01	<0.01	<0.01	<0.01	0.02
Sb_ppm	<0.02	<0.02	<0.02	<0.02	<0.02	<0.02	<0.02	<0.02	<0.02	<0.02	<0.02	<0.02	<0.02	<0.02
Bi_ppm	<0.02	<0.02	<0.02	<0.02	<0.02	<0.02	<0.02	<0.02	<0.02	<0.02	<0.02	<0.02	<0.02	<0.02
Cr_ppm	17.30	10.30	37.90	4.60	30.20	4.50	169.90	8.80	84.30	62.60	47.20	120.20	71.90	228.20
Hg_ppb	<5	<5	<5	<5	<5	<5	<5	<5	<5	<5	<5	<5	<5	<5
Se_ppm	<0.1	<0.1	<0.1	0.20	<0.1	<0.1	<0.1	<0.1	<0.1	<0.1	<0.1	<0.1	<0.1	<0.1
Te_ppm	<0.02	<0.02	<0.02	<0.02	<0.02	<0.02	<0.02	<0.02	<0.02	<0.02	<0.02	<0.02	<0.02	<0.02
Ge_ppm	<0.1	<0.1	<0.1	<0.1	<0.1	<0.1	<0.1	<0.1	<0.1	<0.1	<0.1	<0.1	<0.1	<0.1
In_ppm	<0.02	<0.02	<0.02	0.02	<0.02	<0.02	<0.02	<0.02	<0.02	<0.02	<0.02	<0.02	<0.02	<0.02
Re_ppb	<1	<1	<1	<1	<1	<1	<1	<1	<1	<1	<1	<1	<1	<1
Be_ppm	<0.1	0.10	<0.1	<0.1	<0.1	<0.1	<0.1	<0.1	<0.1	<0.1	<0.1	<0.1	<0.1	<0.1
Li_ppm	1.90	2.70	2.00	1.70	0.70	0.60	1.80	0.70	1.90	1.70	1.50	1.20	0.90	0.50
Pd_ppb	<10	<10	<10	<10	<10	<10	<10	<10	<10	<10	<10	<10	<10	<10
Pt_ppb	<2	<2	<2	<2	<2	<2	<2	<2	<2	<2	<2	<2	<2	<2
Au_ppb	3.00	2.00	2.00	2.00	2.00	2.00	1.00	4.00	4.00	3.00	3.00	8.00	3.00	3.00
Pt_ppb	0.20	0.10	0.20	0.10	0.20	1.70	0.40	0.20	0.40	0.30	0.30	1.10	0.30	0.40
Pd_ppb	1.10	1.00	0.80	0.60	0.70	1.10	0.70	0.80	1.90	1.10	1.20	1.40	0.80	1.00
B_ppm	<1	<1	<1	<1	<1	<1	<1	<1	<1	<1	<1	<1	<1	<1

Tl_ppm	<0.02	<0.02	<0.02	<0.02	<0.02	<0.02	<0.02	<0.02	<0.02	<0.02	<0.02	<0.02	<0.02	<0.02
LOI_pct	1.60	1.20	2.10	0.70	0.90	0.60	0.70	0.80	0.50	0.60	0.50	-0.60	0.80	0.40
TOT/C_TC000_pct	0.03	0.03	0.02	<0.02	<0.02	<0.02	0.04	<0.02	0.02	<0.02	0.03	0.03	0.11	0.03
TOT/S_pct	<0.02	<0.02	<0.02	<0.02	<0.02	<0.02	<0.02	<0.02	<0.02	<0.02	<0.02	<0.02	<0.02	<0.02
Ba_ppm	186.00	199.00	191.00	3029.00	488.00	575.00	455.00	411.00	194.00	248.00	258.00	19.00	246.00	13.00
Sc_ppm	2.00	1.00	1.00	24.00	<1	<1	<1	<1	9.00	8.00	5.00	40.00	8.00	82.00
Sum_pct	99.80	99.83	99.81	99.91	99.90	99.89	99.85	99.90	99.81	99.85	99.88	99.59	99.84	99.66
Cs_ppm	<0.1	<0.1	<0.1	0.10	<0.1	<0.1	<0.1	<0.1	<0.1	<0.1	<0.1	<0.1	<0.1	<0.1
Ga_ppm	13.90	14.70	13.80	25.60	18.40	18.70	20.00	17.40	13.80	14.60	15.40	6.50	13.70	9.00
Hf_ppm	<0.1	0.20	<0.1	2.10	<0.1	<0.1	<0.1	<0.1	<0.1	0.30	<0.1	0.50	0.10	1.90
Nb_ppm	<0.1	0.20	<0.1	13.90	0.10	<0.1	<0.1	0.30	0.20	0.20	0.20	0.20	0.20	0.20
Rb_ppm	1.20	0.90	1.00	36.60	0.60	0.40	0.60	0.50	1.00	2.10	1.60	0.30	1.60	0.20
Sn_ppm	<1	<1	<1	<1	<1	<1	<1	<1	<1	<1	<1	<1	<1	<1
Sr_ppm	638.20	714.60	680.30	282.00	892.10	880.60	920.60	867.40	597.60	655.30	675.40	6.90	647.40	24.90
Ta_ppm	<0.1	<0.1	<0.1	0.80	<0.1	<0.1	<0.1	<0.1	<0.1	<0.1	<0.1	<0.1	<0.1	<0.1
Th_ppm	<0.2	<0.2	<0.2	1.00	<0.2	<0.2	<0.2	<0.2	<0.2	<0.2	<0.2	<0.2	<0.2	<0.2
U_ppm	<0.1	<0.1	<0.1	0.30	<0.1	<0.1	<0.1	<0.1	<0.1	<0.1	<0.1	<0.1	<0.1	<0.1
V_ppm	<8	9.00	9.00	9.00	<8	<8	166.00	17.00	50.00	40.00	25.00	208.00	44.00	403.00
W_ppm	1.90	2.00	1.00	2.00	1.10	1.80	1.60	2.80	0.90	2.20	8.10	2.00	1.10	2.50
Zr_ppm	2.50	6.40	2.10	101.50	2.50	0.70	2.20	1.30	3.40	11.10	2.20	11.90	3.80	44.30
Y_ppm	0.60	0.90	0.50	23.40	0.70	0.20	<0.1	1.00	1.50	1.50	0.90	5.10	1.20	27.20
La_ppm	2.30	2.80	2.30	32.90	3.20	2.60	1.60	2.90	2.10	2.50	2.30	0.40	2.20	2.90
Ce_ppm	3.80	4.70	3.80	69.90	5.20	4.30	2.20	4.70	3.40	4.50	3.40	1.10	3.30	10.00
Pr_ppm	0.36	0.51	0.39	8.46	0.51	0.37	0.13	0.59	0.37	0.47	0.37	0.17	0.37	1.96
Nd_ppm	1.60	1.80	1.40	35.80	1.80	1.60	0.40	2.80	1.60	1.80	1.30	1.00	1.50	11.80

Sm_ppm	0.20	0.24	0.25	7.27	0.24	0.13	<0.05	0.40	0.16	0.27	0.11	0.31	0.20	3.97
Eu_ppm	0.54	0.59	0.58	8.07	1.11	1.19	1.07	1.08	0.51	0.64	0.62	0.11	0.61	1.25
Gd_ppm	0.16	0.27	0.17	6.48	0.26	0.14	<0.05	0.46	0.26	0.34	0.18	0.59	0.25	5.24
Tb_ppm	0.02	0.03	0.01	0.87	0.02	<0.01	<0.01	0.05	0.04	0.04	0.02	0.11	0.03	0.82
Dy_ppm	0.09	0.16	0.09	4.94	0.14	0.06	<0.05	0.14	0.25	0.28	0.12	0.81	0.18	5.16
Ho_ppm	<0.02	0.04	<0.02	0.92	<0.02	<0.02	<0.02	0.03	0.06	0.06	0.03	0.20	0.05	1.06
Er_ppm	0.05	0.08	0.05	2.49	0.05	<0.03	<0.03	0.07	0.20	0.17	0.10	0.73	0.15	3.12
Tm_ppm	<0.01	<0.01	<0.01	0.31	<0.01	<0.01	<0.01	<0.01	0.03	0.03	0.01	0.11	0.02	0.40
Yb_ppm	0.06	0.08	<0.05	2.06	<0.05	<0.05	<0.05	<0.05	0.21	0.20	0.10	0.81	0.18	2.59
Lu_ppm	<0.01	<0.01	<0.01	0.34	<0.01	<0.01	<0.01	<0.01	0.04	0.03	0.02	0.14	0.03	0.39

Sample_ID	KAC069/067c	KAC069/067d	KAC070/068a	KAC070/068b	KAC070/069	KAC072/070b	KAC081/075	KAC083/076	KAC084/077	KAC085/078	KAC087/079	KAC089/080	KAC090/081	KAC090/082
Lat_S	-16.1503	-16.1503	-16.1133	-16.1133	-16.1133	-16.0114	-15.7331	-15.7644	-15.6094	-15.7455	-15.5471	-15.3800	-15.3645	-15.3645
Long_E	13.8813	13.8813	13.8913	13.8913	13.8913	13.9394	13.9506	14.0827	14.0554	14.0031	14.0525	13.9715	13.9466	13.9466
Rocktype	Anorthosite host to 067b	Opx megacryst	Opx megacryst	Host anorthosite to 070/068a	Mylonitised anorthosite	Anorthosite + Mylonite	Anorthosite	Leuconorite	Opx megacryst	Anorthosite/ Leuconorite/ Leucotroctolite/ Megacryst	Anorthosite	Anorthosite	Leucotroctolite/ anorthosite next to megacryst in 090/082	Opx megacryst
Group	KC	KC	KC	KC	KC	KC	KC	KC	KC	KC	KC	KC	KC	KC
SiO2_pct	52.36	50.44	48.91	53.84	52.35	52.91	50.03	53.89	50.63	42.58	52.23	48.73	50.48	48.09
TiO2_pct	0.23	0.60	0.99	0.10	0.27	0.18	1.34	0.13	0.68	1.90	0.55	0.11	0.35	1.51
Al2O3_pct	23.79	3.65	4.40	28.00	20.71	24.50	24.20	27.95	4.15	2.44	27.36	28.32	27.10	3.93
Fe2O3t_pct	4.39	20.84	21.45	0.68	6.80	3.68	4.95	0.76	19.07	21.73	2.30	2.62	2.41	11.09

MnO_pct	0.07	0.32	0.32	<0.01	0.10	0.06	0.04	<0.01	0.30	0.58	0.02	0.03	0.04	0.22
MgO_pct	4.70	22.14	20.85	0.19	7.36	3.77	1.69	0.17	22.28	16.35	0.29	2.81	1.39	13.58
CaO_pct	9.36	1.77	2.27	10.79	8.11	9.97	10.37	10.58	2.39	8.69	10.82	13.09	12.83	20.04
Na2O_pct	3.70	0.06	0.26	4.82	3.14	3.73	4.63	5.06	0.24	0.33	4.92	3.03	3.62	0.42
K2O_pct	0.40	<0.01	0.03	0.64	0.42	0.45	0.69	0.52	0.03	0.05	0.64	0.15	0.38	<0.01
Cr2O3_pct	0.03	0.10	0.10	0.01	0.04	0.03	<0.002	0.01	0.10	0.01	0.01	0.00	0.01	0.00
P2O5_pct	0.02	0.01	0.07	0.02	0.02	0.01	1.32	0.02	0.04	4.84	0.30	<0.01	0.18	<0.01
Normalised*	99.04	99.95	99.68	99.10	99.40	99.35	99.34	99.08	99.97	99.52	99.47	98.89	98.76	98.88
SiO2_pct*	52.87	50.47	49.07	54.33	52.67	53.26	50.36	54.39	50.65	42.79	52.51	49.28	51.11	48.63
TiO2_pct*	0.24	0.62	1.01	0.10	0.28	0.18	1.37	0.13	0.70	1.95	0.56	0.11	0.36	1.55
Al2O3_pct*	52.87	50.47	49.07	54.33	52.67	53.26	50.36	54.39	50.65	42.79	52.51	49.28	51.11	48.63
Fe2O3t_pct*	4.43	20.85	21.52	0.69	6.84	3.70	4.98	0.77	19.08	21.83	2.31	2.65	2.44	11.22
FeO_pct*	3.77	17.72	18.29	0.58	5.81	3.15	4.24	0.65	16.21	18.56	1.97	2.25	2.07	9.53
Fe2O3_pct*	0.66	3.13	3.23	0.10	1.03	0.56	0.75	0.12	2.86	3.28	0.35	0.40	0.37	1.68
FeO*_pct	3.99	18.77	19.37	0.62	6.16	3.33	4.48	0.69	17.17	19.65	2.08	2.38	2.20	10.09
MnO_pct*	0.07	0.33	0.33	#VALUE!	0.10	0.06	0.04	#VALUE!	0.31	0.59	0.02	0.03	0.04	0.23
MgO_pct*	4.75	22.15	20.92	0.19	7.40	3.79	1.70	0.17	22.29	16.43	0.29	2.84	1.41	13.73
CaO_pct*	9.60	1.81	2.33	11.06	8.31	10.22	10.63	10.85	2.45	8.91	11.09	13.42	13.15	20.55
Na2O_pct*	3.79	0.06	0.27	4.94	3.22	3.82	4.75	5.19	0.25	0.34	5.04	3.11	3.71	0.43
K2O_pct*	0.41	N/A	0.03	0.66	0.43	0.46	0.71	0.53	0.03	0.05	0.66	0.15	0.39	#VALUE!
Cr2O3_pct*	0.03	0.10	0.10	0.01	0.04	0.03	#VALUE!	0.01	0.10	0.01	0.01	0.00	0.01	0.00
P2O5_pct*	0.02	0.01	0.07	0.02	0.02	0.01	1.35	0.02	0.04	4.96	0.31	#VALUE!	0.18	#VALUE!
Mg#	69.18	69.01	67.08	36.94	69.41	68.23	41.72	31.92	71.01	61.20	20.91	69.22	54.73	71.97

Mo_pct	<0.001	<0.001	<0.001	<0.001	<0.001	<0.001	<0.001	<0.001	<0.001	<0.001	<0.001	<0.001	<0.001	<0.001
Cu_pct	0.00	0.02	0.00	0.00	0.00	0.00	0.00	0.00	0.00	0.01	0.00	0.00	0.01	0.00
Pb_pct	<0.02	<0.02	<0.02	<0.02	<0.02	<0.02	<0.02	<0.02	<0.02	<0.02	<0.02	<0.02	<0.02	<0.02
Zn_pct	<0.01	0.02	0.02	<0.01	<0.01	<0.01	<0.01	<0.01	0.01	0.03	<0.01	<0.01	<0.01	<0.01
Ag_ppm	<2	<2	<2	<2	<2	<2	<2	<2	<2	<2	<2	<2	<2	<2
Ni_ppm	76.00	410.00	356.00	20.00	129.00	71.00	12.00	12.00	279.00	115.00	14.00	103.00	70.00	131.00
Mo_ppm	0.44	0.79	0.49	0.34	0.73	0.56	0.42	0.37	0.47	0.30	0.38	0.30	0.40	0.36
Cu_ppm	8.04	205.77	32.30	28.21	10.75	8.63	14.85	18.52	18.80	29.16	10.34	10.24	102.96	17.71
Pb_ppm	0.43	0.52	0.18	0.24	0.27	0.45	0.15	0.35	0.39	1.04	0.27	0.38	0.62	0.15
Zn_ppm	6.80	10.60	16.40	1.50	5.40	2.40	21.10	2.10	9.80	70.80	8.70	12.60	15.00	10.30
Ag_ppb	4.00	833.00	65.00	2.00	3.00	6.00	2.00	5.00	5.00	5.00	3.00	32.00	11.00	3.00
Ni_ppm	29.30	98.90	79.60	15.40	32.00	23.80	10.80	8.80	39.10	36.40	9.50	88.00	58.60	23.60
Co_ppm	5.30	13.40	15.20	1.60	4.90	3.00	15.70	0.90	9.60	21.00	3.40	16.70	9.80	8.40
Mn_ppm	92.00	186.00	173.00	41.00	73.00	75.00	190.00	31.00	137.00	957.00	51.00	190.00	107.00	218.00
As_ppm	<0.1	<0.1	<0.1	<0.1	<0.1	0.10	<0.1	<0.1	<0.1	0.50	<0.1	<0.1	0.20	<0.1
Au_ppb	<0.2	3.30	0.20	<0.2	<0.2	0.20	<0.2	0.30	0.30	0.40	0.20	1.30	1.00	0.90
Cd_ppm	<0.01	<0.01	<0.01	<0.01	<0.01	<0.01	<0.01	<0.01	<0.01	0.08	<0.01	0.03	0.02	0.03
Sb_ppm	<0.02	<0.02	<0.02	<0.02	<0.02	<0.02	<0.02	<0.02	<0.02	<0.02	<0.02	<0.02	<0.02	<0.02
Bi_ppm	<0.02	0.04	<0.02	<0.02	<0.02	<0.02	<0.02	<0.02	<0.02	<0.02	<0.02	<0.02	<0.02	<0.02
Cr_ppm	106.30	120.90	325.90	40.60	91.60	111.50	5.50	36.10	181.70	40.70	41.20	8.10	30.20	16.40
Hg_ppb	<5	<5	<5	<5	<5	<5	<5	<5	<5	<5	<5	<5	6.00	<5
Se_ppm	<0.1	0.20	<0.1	<0.1	<0.1	<0.1	0.10	<0.1	<0.1	0.90	<0.1	<0.1	<0.1	<0.1
Te_ppm	<0.02	0.05	<0.02	<0.02	<0.02	<0.02	<0.02	<0.02	<0.02	<0.02	<0.02	<0.02	<0.02	<0.02
Ge_ppm	<0.1	<0.1	<0.1	<0.1	<0.1	<0.1	<0.1	<0.1	<0.1	<0.1	<0.1	<0.1	<0.1	<0.1
In_ppm	<0.02	<0.02	<0.02	<0.02	<0.02	<0.02	<0.02	<0.02	<0.02	0.04	<0.02	<0.02	<0.02	<0.02

Re_ppb	<1	<1	<1	<1	<1	<1	<1	<1	<1	<1	<1	<1	<1	<1
Be_ppm	<0.1	<0.1	<0.1	<0.1	<0.1	0.10	<0.1	<0.1	<0.1	0.20	<0.1	0.10	0.20	<0.1
Li_ppm	1.40	0.20	1.70	0.80	1.30	0.70	2.30	1.20	2.10	3.60	1.10	2.10	2.10	0.90
Pd_ppb	<10	<10	<10	<10	<10	<10	<10	<10	<10	<10	<10	<10	<10	<10
Pt_ppb	<2	2.00	<2	<2	<2	<2	<2	<2	<2	<2	<2	<2	<2	<2
Au_ppb	4.00	8.00	4.00	3.00	3.00	4.00	4.00	3.00	3.00	5.00	3.00	3.00	4.00	4.00
Pt_ppb	0.30	2.50	0.40	0.30	0.50	0.30	0.20	0.30	0.30	0.50	0.20	3.20	0.40	0.30
Pd_ppb	1.60	3.50	1.20	0.90	1.20	1.00	<0.5	0.50	0.90	1.10	0.70	0.70	1.00	1.20
B_ppm	<1	<1	<1	<1	<1	<1	<1	<1	<1	<1	<1	1.00	<1	<1
Tl_ppm	<0.02	<0.02	<0.02	<0.02	<0.02	<0.02	<0.02	<0.02	<0.02	<0.02	<0.02	<0.02	<0.02	<0.02
LOI_pct	0.80	-0.40	-0.10	0.80	0.40	0.50	0.50	0.80	-0.40	0.00	0.40	1.00	1.10	0.80
TOT/C_TC000_pct	0.05	0.02	<0.02	<0.02	<0.02	0.04	0.02	0.03	0.03	0.06	0.03	<0.02	0.13	0.22
TOT/S_pct	<0.02	<0.02	<0.02	<0.02	<0.02	<0.02	0.03	<0.02	<0.02	0.03	<0.02	<0.02	0.09	<0.02
Ba_ppm	210.00	34.00	71.00	304.00	280.00	176.00	469.00	285.00	19.00	59.00	425.00	91.00	172.00	6.00
Sc_ppm	8.00	38.00	36.00	<1	12.00	6.00	2.00	<1	42.00	42.00	<1	1.00	8.00	150.00
Sum_pct	99.84	99.55	99.58	99.90	99.80	99.85	99.84	99.88	99.57	99.52	99.87	99.89	99.86	99.68
Cs_ppm	<0.1	<0.1	<0.1	<0.1	<0.1	<0.1	<0.1	<0.1	<0.1	<0.1	<0.1	<0.1	<0.1	<0.1
Ga_ppm	13.60	6.80	8.50	16.10	13.00	13.20	19.40	18.80	5.80	6.10	18.30	15.50	18.30	6.90
Hf_ppm	0.10	2.10	1.00	<0.1	0.20	0.30	0.20	0.20	0.50	2.40	0.50	0.10	1.30	3.00
Nb_ppm	0.30	0.50	1.70	0.10	0.20	1.60	1.60	0.40	1.00	19.10	1.10	0.20	2.40	0.50
Rb_ppm	1.40	0.40	1.00	2.00	2.10	4.30	1.80	1.90	0.40	1.20	2.10	0.80	3.70	0.60
Sn_ppm	<1	<1	<1	<1	<1	<1	<1	<1	<1	<1	<1	<1	<1	<1
Sr_ppm	625.10	10.30	39.50	764.10	549.90	683.30	915.90	959.00	53.70	115.90	925.10	526.00	686.60	39.30
Ta_ppm	<0.1	<0.1	<0.1	<0.1	<0.1	<0.1	0.10	<0.1	<0.1	0.90	<0.1	<0.1	0.10	<0.1

Th_ppm	<0.2	<0.2	0.30	<0.2	<0.2	0.30	<0.2	<0.2	0.40	2.60	0.40	<0.2	0.80	0.40
U_ppm	<0.1	<0.1	<0.1	<0.1	<0.1	<0.1	<0.1	<0.1	<0.1	0.40	<0.1	<0.1	0.10	0.10
V_ppm	42.00	201.00	254.00	<8	69.00	39.00	96.00	<8	235.00	112.00	56.00	11.00	25.00	421.00
W_ppm	1.40	2.50	1.70	1.30	2.30	2.60	1.70	1.20	1.60	0.60	1.50	0.90	0.90	1.40
Zr_ppm	3.40	90.20	36.80	1.70	6.80	12.40	10.70	7.60	17.10	82.00	17.20	5.00	41.10	69.20
Y_ppm	1.30	5.30	9.00	0.40	2.50	2.40	9.50	1.10	5.10	134.80	5.40	0.90	12.50	31.10
La_ppm	1.90	0.50	2.20	2.80	2.20	5.30	12.50	4.10	2.30	170.00	8.20	2.00	7.10	3.20
Ce_ppm	3.50	1.50	4.90	4.50	3.90	9.60	28.90	7.40	5.00	380.20	16.10	3.30	15.80	12.50
Pr_ppm	0.34	0.20	0.66	0.45	0.42	1.01	3.89	0.76	0.58	50.43	2.03	0.35	2.01	2.38
Nd_ppm	1.50	1.20	3.20	1.60	1.80	3.80	18.50	3.00	2.70	217.70	8.90	1.20	9.60	13.50
Sm_ppm	0.09	0.34	0.76	0.16	0.20	0.46	3.72	0.45	0.55	42.03	1.77	0.22	2.15	4.85
Eu_ppm	0.59	0.11	0.26	0.74	0.60	0.55	2.11	0.77	0.16	5.38	1.58	0.53	0.91	1.17
Gd_ppm	0.29	0.55	1.25	0.21	0.37	0.46	3.56	0.32	0.75	38.15	1.63	0.27	2.38	6.37
Tb_ppm	0.03	0.11	0.21	0.02	0.05	0.06	0.41	0.04	0.13	5.04	0.20	0.03	0.38	1.05
Dy_ppm	0.20	0.76	1.31	0.07	0.35	0.37	2.01	0.20	0.88	27.04	0.97	0.18	2.20	6.09
Ho_ppm	0.05	0.23	0.33	<0.02	0.10	0.07	0.32	0.04	0.20	5.11	0.19	0.03	0.51	1.30
Er_ppm	0.16	0.69	1.13	<0.03	0.26	0.23	0.87	0.10	0.65	13.64	0.47	0.09	1.42	3.42
Tm_ppm	0.02	0.11	0.17	<0.01	0.04	0.04	0.09	0.02	0.11	1.84	0.06	0.01	0.17	0.48
Yb_ppm	0.13	0.86	1.25	<0.05	0.28	0.27	0.45	0.07	0.67	11.34	0.31	<0.05	1.22	2.78
Lu_ppm	0.03	0.14	0.21	<0.01	0.04	0.04	0.06	0.01	0.13	1.69	0.05	<0.01	0.17	0.44

Sample_ID	KAC090/084	KAC090/085	KAC090/086	KAC099/093	KAC100/094	KAC101/095	KAC103/096	KAC105/097	KAC107/098	KAC108/099	KAC109/100	KAC110/101a	KAC110/101b	KAC111/102
Lat_S	-15.3645	-15.3645	-15.3645	-14.9424	-14.9385	-14.9338	-14.9265	-14.8959	-14.8819	-14.8789	-14.9233	-14.8643	-14.8643	-14.8643

Long_E	13.9466	13.9466	13.9466	14.0441	14.0543	14.0670	14.1028	14.1453	14.1718	14.1827	14.1962	14.2218	14.2218	14.2218
Rocktype	Foliated Anorthosite (SM2)	Foliated anorthosite (SM1 + SM2)	Opx megacryst + host	Leuconorite	Leuconorite/troctolite	Olivine-bearing leuconorite	Leuconorite / leucotroctolite	Leuconorite / leucotroctolite	Leuconorite/ leucotroctolite	Leucotroctolite	Leucotroctolite	Leucotroctolite	Leucotroctolite/ anorthosite	Leuconorite/ leucotroctolite
Group	KC	KC	KC	KC	KC	KC	KC	KC	KC	KC	KC	KC	KC	KC
SiO2_pct	50.72	50.32	46.91	45.97	47.46	49.66	47.03	47.04	48.61	47.00	46.53	48.20	50.12	49.15
TiO2_pct	0.12	0.11	2.77	0.26	0.26	0.13	0.16	0.11	0.08	0.21	0.16	0.12	0.13	0.13
Al2O3_pct	30.15	28.69	4.31	24.20	26.20	28.68	26.38	27.26	31.24	27.48	27.46	28.00	25.55	29.39
Fe2O3t_pct	0.84	2.10	12.53	6.49	4.73	1.90	4.74	3.92	0.83	3.90	3.87	3.17	3.75	2.13
MnO_pct	<0.01	0.02	0.24	0.08	0.06	0.02	0.06	0.05	<0.01	0.05	0.05	0.05	0.06	0.03
MgO_pct	0.25	1.52	13.22	7.72	4.86	1.64	5.49	4.53	0.22	3.75	4.67	3.50	4.06	1.48
CaO_pct	13.24	12.82	18.52	12.00	12.92	13.58	13.19	13.74	15.10	13.54	13.82	13.40	12.00	14.04
Na2O_pct	3.57	3.42	0.53	2.07	2.46	3.19	2.12	2.13	2.67	2.37	1.97	2.31	2.90	2.63
K2O_pct	0.25	0.25	0.05	0.16	0.17	0.19	0.11	0.12	0.17	0.13	0.09	0.13	0.17	0.14
Cr2O3_pct	<0.002	0.01	0.00	0.01	0.01	0.01	0.01	0.01	<0.002	0.01	<0.002	0.01	0.02	0.01
P2O5_pct	<0.01	<0.01	0.07	0.01	0.02	<0.01	0.02	<0.01	<0.01	0.02	<0.01	<0.01	<0.01	<0.01
Normalised*	99.22	99.29	99.17	99.00	99.15	99.01	99.34	98.97	98.93	98.48	98.66	98.87	98.76	99.10
SiO2_pct*	51.12	50.68	47.30	46.43	47.87	50.16	47.34	47.53	49.14	47.73	47.16	48.75	50.75	49.60
TiO2_pct*	0.12	0.11	2.84	0.27	0.27	0.13	0.16	0.11	0.08	0.22	0.16	0.12	0.13	0.13
Al2O3_pct*	51.12	50.68	47.30	46.43	47.87	50.16	47.34	47.53	49.14	47.73	47.16	48.75	50.75	49.60
Fe2O3t_pct*	0.85	2.12	12.63	6.56	4.77	1.92	4.77	3.96	0.84	3.96	3.92	3.21	3.80	2.15
FeO_pct*	0.72	1.80	10.74	5.57	4.05	1.63	4.06	3.37	0.71	3.37	3.33	2.73	3.23	1.83
Fe2O3_pct*	0.13	0.32	1.90	0.98	0.72	0.29	0.72	0.59	0.13	0.59	0.59	0.48	0.57	0.32
FeO*_pct	0.76	1.90	11.37	5.90	4.29	1.73	4.29	3.56	0.76	3.56	3.53	2.89	3.42	1.93
MnO_pct*	N/A	0.02	0.25	0.08	0.06	0.02	0.06	0.05	N/A	0.05	0.05	0.05	0.06	0.03

MgO_pct*	0.25	1.53	13.33	7.80	4.90	1.66	5.53	4.58	0.22	3.81	4.73	3.54	4.11	1.49
CaO_pct*	13.57	13.14	18.99	12.30	13.25	13.92	13.52	14.09	15.48	13.88	14.17	13.74	12.30	14.39
Na2O_pct*	3.66	3.51	0.54	2.12	2.52	3.27	2.17	2.18	2.74	2.43	2.02	2.37	2.97	2.70
K2O_pct*	0.26	0.26	0.05	0.16	0.17	0.19	0.11	0.12	0.17	0.13	0.09	0.13	0.17	0.14
Cr2O3_pct*	#VALUE!	0.01	0.00	0.01	0.01	0.01	0.01	0.01	#VALUE!	0.01	#VALUE!	0.01	0.02	0.01
P2O5_pct*	#VALUE!	#VALUE!	0.07	0.01	0.02	#VALUE!	0.02	#VALUE!	#VALUE!	0.02	#VALUE!	#VALUE!	#VALUE!	#VALUE!
Mg#	38.42	60.28	68.87	71.38	68.30	64.41	70.83	70.78	35.72	66.84	71.67	69.83	69.42	59.29
Mo_pct	<0.001	<0.001	<0.001	<0.001	<0.001	<0.001	<0.001	<0.001	<0.001	<0.001	<0.001	<0.001	<0.001	<0.001
Cu_pct	<0.001	<0.001	0.00	0.00	0.00	0.01	0.02	<0.001	<0.001	<0.001	0.00	<0.001	0.01	0.00
Pb_pct	<0.02	<0.02	<0.02	<0.02	<0.02	<0.02	<0.02	<0.02	<0.02	<0.02	<0.02	<0.02	<0.02	<0.02
Zn_pct	<0.01	<0.01	<0.01	<0.01	<0.01	<0.01	<0.01	<0.01	<0.01	<0.01	<0.01	<0.01	<0.01	<0.01
Ag_ppm	<2	<2	<2	<2	<2	<2	<2	<2	<2	<2	<2	<2	<2	<2
Ni_ppm	<10	46.00	132.00	276.00	125.00	34.00	160.00	125.00	<10	96.00	144.00	94.00	100.00	16.00
Mo_ppm	0.48	0.30	0.38	0.33	0.33	0.62	0.26	0.42	0.53	0.38	0.37	0.33	0.26	0.33
Cu_ppm	4.92	7.34	21.73	27.46	22.60	61.59	137.60	14.49	3.51	16.62	21.78	18.89	65.34	16.01
Pb_ppm	0.33	0.37	0.22	0.64	0.45	0.41	0.47	0.31	0.39	0.42	0.36	0.50	0.62	0.41
Zn_ppm	3.20	8.80	10.20	35.10	21.10	6.50	23.20	18.40	3.70	18.20	18.60	11.00	5.40	5.50
Ag_ppb	4.00	5.00	38.00	13.00	10.00	16.00	34.00	8.00	6.00	13.00	10.00	9.00	30.00	10.00
Ni_ppm	3.90	41.50	29.70	267.90	108.80	28.70	143.60	115.20	3.40	92.80	128.10	75.00	65.60	8.90
Co_ppm	1.20	10.90	9.90	47.30	26.20	7.40	33.70	26.30	0.80	22.60	26.20	14.40	6.30	2.60
Mn_ppm	43.00	135.00	192.00	566.00	316.00	82.00	369.00	307.00	53.00	252.00	289.00	187.00	65.00	59.00
As_ppm	0.20	<0.1	<0.1	0.20	0.30	0.30	0.50	0.20	0.20	0.30	0.20	<0.1	0.10	0.20
Au_ppb	<0.2	<0.2	<0.2	<0.2	<0.2	<0.2	0.40	<0.2	<0.2	<0.2	0.50	<0.2	2.60	2.90
Cd_ppm	0.02	<0.01	0.02	0.03	0.02	0.01	0.01	<0.01	0.01	0.02	0.02	0.01	0.02	<0.01
Sb_ppm	<0.02	<0.02	<0.02	<0.02	<0.02	<0.02	<0.02	<0.02	<0.02	<0.02	<0.02	<0.02	<0.02	<0.02

Bi_ppm	<0.02	<0.02	<0.02	<0.02	<0.02	<0.02	<0.02	<0.02	<0.02	<0.02	<0.02	<0.02	<0.02	<0.02
Cr_ppm	4.80	37.70	9.10	48.00	41.10	19.80	38.50	18.80	5.10	50.10	9.10	58.20	62.50	21.10
Hg_ppb	<5	<5	<5	<5	<5	<5	<5	<5	<5	<5	<5	<5	<5	<5
Se_ppm	<0.1	<0.1	<0.1	<0.1	<0.1	<0.1	<0.1	<0.1	<0.1	<0.1	<0.1	<0.1	<0.1	<0.1
Te_ppm	<0.02	<0.02	<0.02	<0.02	<0.02	<0.02	<0.02	<0.02	<0.02	<0.02	<0.02	0.05	0.02	<0.02
Ge_ppm	<0.1	<0.1	<0.1	0.10	<0.1	<0.1	<0.1	<0.1	<0.1	<0.1	<0.1	<0.1	<0.1	<0.1
In_ppm	<0.02	<0.02	<0.02	<0.02	<0.02	<0.02	<0.02	<0.02	<0.02	<0.02	<0.02	<0.02	<0.02	<0.02
Re_ppb	<1	<1	<1	<1	<1	<1	<1	<1	<1	<1	<1	<1	<1	<1
Be_ppm	0.10	0.20	<0.1	<0.1	0.10	<0.1	<0.1	<0.1	0.10	0.20	<0.1	0.20	0.20	0.20
Li_ppm	2.20	1.90	0.90	2.80	1.70	1.50	1.90	1.60	2.00	1.70	1.40	1.90	1.70	1.40
Pd_ppb	<10	<10	<10	<10	<10	<10	<10	<10	<10	<10	<10	<10	<10	<10
Pt_ppb	<2	<2	<2	<2	<2	<2	<2	<2	<2	<2	<2	<2	6.00	<2
Au_ppb	3.00	3.00	7.00	3.00	3.00	2.00	3.00	2.00	3.00	3.00	3.00	10.00	7.00	6.00
Pt_ppb	0.20	0.20	0.60	0.60	0.50	0.30	0.40	0.20	0.20	0.30	0.60	1.20	6.70	0.30
Pd_ppb	0.60	0.90	2.50	1.50	1.00	1.10	0.70	1.20	0.70	1.00	1.40	5.60	8.20	1.40
B_ppm	<1	<1	<1	<1	<1	<1	<1	<1	<1	<1	<1	<1	<1	<1
Tl_ppm	<0.02	<0.02	<0.02	<0.02	<0.02	<0.02	<0.02	<0.02	<0.02	<0.02	<0.02	<0.02	<0.02	<0.02
LOI_pct	0.70	0.60	0.50	0.80	0.70	0.90	0.50	0.90	1.00	1.40	1.20	1.00	1.10	0.80
TOT/C_TC000_pct	0.02	0.07	0.15	0.04	0.03	0.02	0.04	0.04	<0.02	0.03	0.05	0.03	0.04	0.03
TOT/S_pct	<0.02	<0.02	<0.02	0.02	<0.02	<0.02	<0.02	<0.02	<0.02	<0.02	<0.02	<0.02	0.04	<0.02
Ba_ppm	133.00	143.00	20.00	72.00	79.00	90.00	59.00	62.00	77.00	66.00	49.00	90.00	117.00	115.00
Sc_ppm	<1	1.00	133.00	5.00	5.00	3.00	5.00	4.00	<1	4.00	3.00	2.00	7.00	3.00
Sum_pct	99.92	99.89	99.67	99.80	99.85	99.91	99.84	99.87	99.93	99.88	99.86	99.87	99.86	99.90
Cs_ppm	<0.1	<0.1	0.40	<0.1	<0.1	<0.1	<0.1	<0.1	<0.1	<0.1	<0.1	<0.1	<0.1	<0.1
Ga_ppm	19.50	18.00	8.10	15.10	15.20	19.10	14.70	15.10	18.40	15.30	14.10	16.80	18.60	18.20

Hf_ppm	<0.1	<0.1	5.50	0.30	0.40	0.20	0.20	0.10	<0.1	0.40	0.30	0.10	0.10	0.10
Nb_ppm	0.20	0.20	6.40	0.60	0.90	0.20	0.60	0.20	0.10	0.60	0.40	0.10	<0.1	0.30
Rb_ppm	1.10	1.30	5.10	1.50	1.40	0.80	1.00	0.70	1.40	1.10	0.80	0.70	1.00	0.90
Sn_ppm	<1	<1	<1	<1	<1	<1	<1	<1	<1	<1	<1	<1	<1	<1
Sr_ppm	705.40	666.40	57.70	450.50	468.80	523.90	431.00	455.00	563.50	478.40	459.60	544.10	536.10	615.80
Ta_ppm	<0.1	<0.1	0.40	<0.1	<0.1	<0.1	<0.1	<0.1	<0.1	<0.1	<0.1	<0.1	<0.1	<0.1
Th_ppm	<0.2	<0.2	1.60	<0.2	<0.2	<0.2	0.30	<0.2	<0.2	<0.2	<0.2	<0.2	<0.2	<0.2
U_ppm	<0.1	<0.1	0.50	<0.1	<0.1	<0.1	<0.1	<0.1	<0.1	<0.1	<0.1	<0.1	<0.1	<0.1
V_ppm	<8	<8	386.00	39.00	47.00	19.00	33.00	23.00	10.00	32.00	23.00	17.00	27.00	21.00
W_ppm	1.80	0.60	1.20	0.70	1.20	1.90	1.60	1.10	2.00	1.10	1.30	0.90	1.20	1.50
Zr_ppm	2.90	3.60	169.10	10.00	15.30	4.90	13.10	5.00	3.10	14.10	7.50	4.00	3.90	5.80
Y_ppm	0.80	1.10	44.20	2.40	3.30	1.30	2.10	1.30	0.80	2.30	1.90	1.00	0.60	1.20
La_ppm	2.40	2.80	6.00	2.30	2.50	1.90	1.60	1.30	1.70	2.00	1.70	2.40	2.00	2.30
Ce_ppm	4.30	5.20	20.00	4.30	5.50	3.10	3.60	2.50	2.90	4.20	3.20	4.30	2.90	4.00
Pr_ppm	0.46	0.52	3.57	0.54	0.67	0.42	0.45	0.30	0.31	0.51	0.38	0.48	0.30	0.44
Nd_ppm	1.80	2.00	19.90	2.50	2.80	1.90	2.00	1.20	1.40	2.10	1.60	1.80	1.20	1.40
Sm_ppm	0.20	0.22	6.58	0.43	0.60	0.29	0.40	0.20	0.26	0.50	0.32	0.23	0.20	0.27
Eu_ppm	0.68	0.65	1.23	0.48	0.49	0.47	0.40	0.41	0.45	0.46	0.34	0.42	0.39	0.45
Gd_ppm	0.25	0.31	8.45	0.50	0.74	0.34	0.49	0.32	0.22	0.51	0.36	0.32	0.16	0.30
Tb_ppm	0.04	0.03	1.43	0.07	0.11	0.05	0.07	0.04	0.03	0.08	0.06	0.03	0.02	0.04
Dy_ppm	0.14	0.13	8.39	0.46	0.75	0.30	0.41	0.25	0.17	0.47	0.34	0.21	0.12	0.20
Ho_ppm	0.02	0.02	1.81	0.09	0.14	0.06	0.08	0.04	0.02	0.10	0.09	0.04	0.02	0.05
Er_ppm	0.07	0.08	5.03	0.22	0.40	0.15	0.26	0.15	0.09	0.20	0.18	0.09	0.08	0.12
Tm_ppm	<0.01	<0.01	0.66	0.03	0.05	0.01	0.03	0.02	<0.01	0.03	0.03	0.01	0.01	0.02
Yb_ppm	<0.05	<0.05	4.25	0.21	0.31	0.10	0.19	0.11	0.07	0.24	0.19	0.08	0.11	0.14

Lu_ppm	<0.01	<0.01	0.63	0.04	0.05	0.02	0.03	0.02	<0.01	0.04	0.02	0.02	0.02	0.02

Sample_ID	KAC113/103	KAC114/104	KAC115/105	KAC116/106	KAC117/107	KAC122/111	KAC123/112	KAC124/113	KAC126/114	KAC128/116	KAC128/117a	KAC129/118	KAC130/119	KAC131/120
Lat_S	-14.8637	-14.8596	-14.8501	-14.8378	-14.8336	-15.0816	-15.1110	-15.1044	-15.1346	-15.1530	-15.1683	-15.2267	-15.2400	-15.2599
Long_E	14.2955	14.3169	14.3704	14.3948	14.4162	14.0308	14.0695	14.0815	14.0844	14.0933	14.0941	14.1095	14.1231	14.1164
Rocktype	Leuconorite/leucotroctolite	Leuconorite/leucotroctolite	Leuconorite/troctolite	Anorthosite	Leuconorite	Anorthosite	Leuconorite/leucotroctolite	Leucotroctolite	Leuconorite/troctolite	Anorthosite/Leucotroctolite	Opx megacryst	Leuconorite/troctolite	Leuconorite/troctolite	Leuconorite/troctolite
Group	KC	KC	KC	KC	KC	KC	KC	KC	KC	KC	KC	KC	KC	KC
SiO2_pct	48.87	47.48	45.87	48.75	48.65	46.58	48.28	49.25	49.07	50.65	51.65	48.60	47.95	49.36
TiO2_pct	0.21	0.16	0.17	0.18	0.29	0.13	0.17	0.14	0.10	0.12	0.64	0.20	0.11	0.13
Al2O3_pct	27.32	28.02	26.69	29.88	28.72	27.03	25.57	26.21	25.78	29.39	2.71	26.36	24.53	28.35
Fe2O3t_pct	3.81	4.04	5.71	1.50	2.76	4.47	5.68	4.67	4.85	1.22	18.28	4.30	6.83	2.74
MnO_pct	0.05	0.05	0.07	0.02	0.04	0.06	0.07	0.05	0.06	0.01	0.32	0.06	0.08	0.03
MgO_pct	3.31	3.54	5.28	0.64	1.43	5.20	5.29	3.96	4.59	0.74	22.26	4.02	5.93	2.07
CaO_pct	12.74	13.44	12.82	14.73	13.67	13.29	11.63	11.77	11.83	13.47	3.11	12.61	10.93	13.35
Na2O_pct	2.85	2.22	2.09	2.82	2.82	2.17	2.93	3.23	2.82	3.45	0.15	2.87	2.92	2.91
K2O_pct	0.16	0.15	0.11	0.15	0.23	0.12	0.20	0.25	0.22	0.24	<0.01	0.18	0.21	0.20
Cr2O3_pct	0.00	0.01	0.01	0.01	0.01	0.01	0.01	0.00	0.00	0.00	0.16	0.01	0.01	0.00
P2O5_pct	0.02	<0.01	0.02	<0.01	0.02	<0.01	<0.01	<0.01	<0.01	<0.01	0.03	0.01	<0.01	<0.01
Normalised*	99.38	99.17	98.84	98.71	98.60	99.05	99.85	99.57	99.36	99.32	99.38	99.27	99.55	99.20
SiO2_pct*	49.17	47.88	46.41	49.39	49.34	47.03	48.35	49.46	49.39	51.00	51.97	48.96	48.17	49.76
TiO2_pct*	0.22	0.16	0.17	0.18	0.30	0.13	0.17	0.14	0.10	0.12	0.66	0.21	0.11	0.13
Al2O3_pct*	49.17	47.88	46.41	49.39	49.34	47.03	48.35	49.46	49.39	51.00	51.97	48.96	48.17	49.76

Fe2O3t_pct*	3.83	4.07	5.78	1.52	2.80	4.51	5.69	4.69	4.88	1.23	18.39	4.33	6.86	2.76
FeO_pct*	3.26	3.46	4.91	1.29	2.38	3.84	4.84	3.99	4.15	1.04	15.63	3.68	5.83	2.35
Fe2O3_pct*	0.58	0.61	0.87	0.23	0.42	0.68	0.85	0.70	0.73	0.18	2.76	0.65	1.03	0.41
FeO*_pct	3.45	3.67	5.20	1.37	2.52	4.06	5.12	4.22	4.39	1.11	16.55	3.90	6.17	2.49
MnO_pct*	0.05	0.05	0.07	0.02	0.04	0.06	0.07	0.05	0.06	0.01	0.33	0.06	0.08	0.03
MgO_pct*	3.33	3.57	5.34	0.65	1.45	5.25	5.30	3.98	4.62	0.75	22.40	4.05	5.96	2.09
CaO_pct*	13.06	13.78	13.14	15.10	14.01	13.63	11.92	12.07	12.13	13.81	3.19	12.93	11.21	13.69
Na2O_pct*	2.92	2.28	2.14	2.89	2.89	2.22	3.00	3.31	2.89	3.54	0.15	2.94	2.99	2.98
K2O_pct*	0.16	0.15	0.11	0.15	0.24	0.12	0.21	0.26	0.23	0.25	N/D	0.18	0.22	0.21
Cr2O3_pct*	0.00	0.01	0.01	0.01	0.01	0.01	0.01	0.00	0.00	0.00	0.16	0.01	0.01	0.00
P2O5_pct*	0.02	N/D	0.02	N/D	0.02	N/D	N/D	N/D	N/D	N/D	0.03	0.01	N/D	N/D
Mg#	64.56	64.75	65.97	47.22	52.07	70.92	66.13	64.00	66.49	55.98	71.85	66.22	64.54	61.30
Mo_pct	<0.001	<0.001	<0.001	<0.001	<0.001	<0.001	<0.001	<0.001	<0.001	<0.001	<0.001	<0.001	<0.001	<0.001
Cu_pct	<0.001	<0.001	0.00	<0.001	0.00	0.00	<0.001	<0.001	<0.001	<0.001	0.00	<0.001	<0.001	<0.001
Pb_pct	<0.02	<0.02	<0.02	<0.02	<0.02	<0.02	<0.02	<0.02	<0.02	<0.02	<0.02	<0.02	<0.02	<0.02
Zn_pct	<0.01	<0.01	<0.01	<0.01	<0.01	<0.01	<0.01	<0.01	<0.01	<0.01	0.01	<0.01	<0.01	<0.01
Ag_ppm	<2	<2	<2	<2	<2	<2	<2	<2	<2	<2	<2	<2	<2	<2
Ni_ppm	64.00	85.00	116.00	15.00	21.00	148.00	133.00	96.00	131.00	16.00	337.00	95.00	146.00	56.00
Mo_ppm	0.43	0.32	0.37	0.35	0.65	0.60	0.20	0.43	0.15	0.34	0.27	0.37	0.21	0.16
Cu_ppm	18.11	15.42	24.23	15.01	29.33	24.21	8.74	13.24	6.13	12.22	47.81	13.56	6.23	9.05
Pb_ppm	0.61	0.71	0.45	0.52	0.43	0.36	0.25	0.29	0.36	0.33	0.29	0.83	0.22	0.35
Zn_ppm	16.40	16.40	32.20	7.10	11.40	19.40	28.70	23.00	21.40	4.90	14.60	20.10	36.90	12.70
Ag_ppb	11.00	15.00	15.00	12.00	7.00	11.00	5.00	11.00	5.00	8.00	12.00	11.00	5.00	5.00
Ni_ppm	57.00	75.80	107.60	13.60	15.50	142.90	137.60	93.90	107.20	14.00	77.10	84.50	147.90	45.90

Co_ppm	19.00	20.40	34.70	2.60	6.90	27.30	37.20	28.80	28.40	2.90	14.80	23.10	43.80	13.00
Mn_ppm	214.00	180.00	482.00	77.00	106.00	323.00	504.00	371.00	345.00	55.00	307.00	315.00	668.00	188.00
As_ppm	0.20	0.20	0.30	0.20	0.20	<0.1	<0.1	<0.1	0.10	0.30	0.20	<0.1	0.20	0.20
Au_ppb	0.40	1.00	<0.2	<0.2	0.40	0.60	<0.2	<0.2	<0.2	<0.2	0.30	0.20	<0.2	<0.2
Cd_ppm	0.02	0.02	0.03	<0.01	0.01	0.01	0.01	<0.01	<0.01	<0.01	<0.01	0.01	<0.01	<0.01
Sb_ppm	<0.02	<0.02	<0.02	<0.02	<0.02	<0.02	<0.02	<0.02	<0.02	<0.02	<0.02	<0.02	<0.02	<0.02
Bi_ppm	<0.02	<0.02	<0.02	<0.02	<0.02	<0.02	<0.02	<0.02	<0.02	<0.02	<0.02	<0.02	<0.02	<0.02
Cr_ppm	12.80	36.20	15.30	42.30	21.70	22.60	27.60	13.20	19.60	11.10	296.60	37.40	30.70	20.70
Hg_ppb	<5	<5	<5	<5	<5	<5	<5	<5	<5	<5	<5	<5	<5	<5
Se_ppm	<0.1	<0.1	<0.1	<0.1	<0.1	0.10	<0.1	<0.1	<0.1	<0.1	<0.1	<0.1	<0.1	<0.1
Te_ppm	<0.02	<0.02	<0.02	0.02	0.03	0.04	0.02	<0.02	0.02	0.02	<0.02	0.03	<0.02	0.03
Ge_ppm	<0.1	<0.1	<0.1	<0.1	<0.1	<0.1	<0.1	<0.1	<0.1	<0.1	<0.1	<0.1	<0.1	<0.1
In_ppm	<0.02	<0.02	<0.02	<0.02	<0.02	<0.02	<0.02	<0.02	<0.02	<0.02	<0.02	<0.02	<0.02	<0.02
Re_ppb	<1	<1	<1	<1	<1	<1	<1	<1	<1	<1	<1	<1	<1	<1
Be_ppm	<0.1	0.20	<0.1	<0.1	0.10	0.10	<0.1	<0.1	0.10	0.10	<0.1	0.10	<0.1	0.10
Li_ppm	2.20	2.00	2.80	1.20	2.70	2.20	2.00	2.00	1.70	2.70	0.90	1.80	1.70	2.00
Pd_ppb	<10	<10	<10	<10	<10	<10	<10	<10	<10	<10	<10	<10	<10	<10
Pt_ppb	<2	<2	<2	<2	<2	<2	<2	<2	<2	<2	<2	<2	<2	<2
Au_ppb	4.00	4.00	3.00	3.00	7.00	3.00	3.00	4.00	3.00	3.00	3.00	3.00	3.00	4.00
Pt_ppb	0.40	0.50	0.60	0.20	0.40	0.80	0.30	0.30	0.30	0.30	0.40	0.20	0.20	0.20
Pd_ppb	1.60	2.50	3.30	1.60	1.80	1.40	1.00	1.00	1.60	0.70	1.10	1.30	0.70	1.10
B_ppm	<1	<1	<1	<1	<1	<1	<1	<1	<1	<1	<1	<1	<1	<1
Tl_ppm	<0.02	<0.02	<0.02	<0.02	<0.02	<0.02	<0.02	<0.02	<0.02	<0.02	<0.02	<0.02	<0.02	<0.02
LOI_pct	0.50	0.70	1.00	1.20	1.30	0.80	0.00	0.30	0.50	0.60	0.20	0.60	0.30	0.70
TOT/C_TC000_pct	<0.02	0.03	0.02	0.03	<0.02	0.03	0.03	0.04	<0.02	0.03	0.13	<0.02	<0.02	0.04

TOT/S_pct	<0.02	0.03	<0.02	<0.02	<0.02	<0.02	<0.02	<0.02	<0.02	<0.02	0.03	<0.02	<0.02	<0.02
Ba_ppm	93.00	124.00	68.00	83.00	115.00	58.00	87.00	113.00	111.00	141.00	13.00	107.00	97.00	105.00
Sc_ppm	4.00	3.00	3.00	4.00	4.00	3.00	3.00	2.00	1.00	1.00	52.00	5.00	2.00	1.00
Sum_pct	99.88	99.87	99.84	99.91	99.90	99.85	99.85	99.87	99.86	99.92	99.58	99.87	99.85	99.90
Cs_ppm	<0.1	<0.1	<0.1	<0.1	<0.1	<0.1	<0.1	<0.1	<0.1	<0.1	<0.1	<0.1	<0.1	<0.1
Ga_ppm	18.20	16.00	14.00	15.70	15.50	13.50	14.90	16.80	15.90	18.70	4.50	16.50	16.70	17.20
Hf_ppm	0.40	0.30	0.20	0.30	0.50	0.10	0.30	0.10	<0.1	<0.1	0.60	0.30	<0.1	0.10
Nb_ppm	0.60	0.60	0.50	0.50	1.20	0.20	0.30	0.10	0.10	0.10	0.90	0.40	<0.1	0.30
Rb_ppm	1.80	1.00	1.40	2.00	4.50	1.00	1.10	1.20	1.00	0.70	0.40	1.30	0.70	0.90
Sn_ppm	<1	<1	<1	<1	<1	<1	<1	<1	<1	<1	<1	<1	<1	<1
Sr_ppm	538.10	557.60	525.90	614.20	608.80	458.00	481.90	495.10	509.00	561.70	24.00	488.30	476.60	576.40
Ta_ppm	<0.1	<0.1	<0.1	<0.1	<0.1	<0.1	<0.1	<0.1	<0.1	<0.1	<0.1	<0.1	<0.1	<0.1
Th_ppm	<0.2	<0.2	<0.2	<0.2	0.30	<0.2	<0.2	<0.2	<0.2	<0.2	<0.2	<0.2	<0.2	<0.2
U_ppm	<0.1	<0.1	<0.1	<0.1	<0.1	<0.1	<0.1	<0.1	<0.1	<0.1	<0.1	<0.1	<0.1	<0.1
V_ppm	31.00	24.00	23.00	31.00	38.00	24.00	21.00	18.00	11.00	11.00	222.00	43.00	13.00	15.00
W_ppm	1.70	0.90	1.60	1.40	1.40	1.50	1.20	0.70	1.10	1.20	0.90	0.70	0.80	0.80
Zr_ppm	13.10	11.00	11.10	10.30	16.40	5.50	10.40	5.10	3.00	4.30	21.90	9.70	2.40	5.40
Y_ppm	2.90	1.80	2.00	2.50	4.10	1.60	1.50	0.80	0.60	1.10	6.00	2.10	0.80	1.40
La_ppm	2.60	2.50	2.40	2.00	3.30	1.50	2.10	1.80	1.90	2.20	1.60	2.10	1.90	2.00
Ce_ppm	5.30	5.10	4.00	4.60	6.20	3.00	4.00	3.80	3.40	4.10	3.80	4.20	3.60	3.90
Pr_ppm	0.60	0.52	0.47	0.50	0.77	0.36	0.45	0.39	0.35	0.40	0.44	0.48	0.34	0.42
Nd_ppm	2.70	1.90	2.20	2.40	3.40	1.60	2.10	1.60	1.40	1.50	2.70	2.20	1.40	1.70
Sm_ppm	0.46	0.45	0.38	0.50	0.67	0.35	0.34	0.27	0.26	0.26	0.61	0.38	0.17	0.23
Eu_ppm	0.52	0.57	0.48	0.55	0.56	0.38	0.67	0.65	0.61	0.57	0.18	0.53	0.61	0.59
Gd_ppm	0.61	0.42	0.44	0.55	0.81	0.36	0.38	0.27	0.21	0.24	0.88	0.44	0.19	0.31

Tb_ppm	0.09	0.06	0.06	0.08	0.11	0.04	0.05	0.03	0.02	0.03	0.16	0.07	0.03	0.04
Dy_ppm	0.53	0.32	0.42	0.50	0.68	0.31	0.31	0.20	0.12	0.22	1.14	0.43	0.11	0.22
Ho_ppm	0.11	0.07	0.08	0.10	0.14	0.05	0.06	0.03	0.04	0.04	0.27	0.10	0.03	0.05
Er_ppm	0.34	0.18	0.20	0.31	0.37	0.17	0.16	0.09	0.07	0.10	0.80	0.22	0.07	0.13
Tm_ppm	0.04	0.03	0.03	0.04	0.06	0.02	0.02	0.01	<0.01	0.01	0.13	0.03	<0.01	0.01
Yb_ppm	0.33	0.15	0.25	0.22	0.38	0.15	0.14	0.10	0.07	0.07	0.90	0.20	0.07	0.10
Lu_ppm	0.04	0.03	0.04	0.03	0.05	0.02	0.02	0.01	<0.01	<0.01	0.13	0.03	<0.01	0.01

Sample_ID	KAC132/121	KAC133/122	KAC134/123	KAC135/124	KAC136/125	KAC138/126	KAC139/127	KAC140/128	KAC141/129	KAC142/130	KAC142/131	KAC142/132a	KAC142/132b	KAC142/133
Lat_S	-15.2911	-15.1598	-15.1306	-15.1133	-15.0703	-15.3138	-15.3389	-15.3633	-15.3911	-15.7915	-15.7915	-15.7915	-15.7915	-15.7915
Long_E	14.1147	14.1569	14.1809	14.2057	14.2225	14.1275	14.1023	14.0723	14.0439	13.8453	13.8453	13.8453	13.8453	13.8453
Rocktype	Leuconorite/troctolite	Leuconorite/troctolite	Leucotroctolite	Leucotroctolite	Leucotroctolite	Leuconorite/troctolite	Leuconorite/troctolite	Leuconorite/troctolite	Leuconorite/troctolite	Olivine/ Apatite ? in Leucotroctolite	Leucotroctolite	Pl autolith	Pl autolith	Leucotroctolite
Group	KC	KC	KC	KC	KC	KC	KC	KC	KC	KC	KC	KC	KC	KC
SiO2_pct	49.05	46.75	48.51	47.93	46.51	48.44	49.13	47.71	50.30	48.74	46.85	48.28	48.95	49.85
TiO2_pct	0.25	0.30	0.14	0.16	0.12	0.24	0.24	0.08	0.41	0.13	0.28	0.18	0.25	0.12
Al2O3_pct	27.15	25.21	29.24	28.43	28.08	27.06	28.48	28.80	28.27	26.38	22.04	24.44	26.03	27.03
Fe2O3t_pct	3.72	5.99	2.17	2.96	3.64	3.81	2.66	2.77	2.07	4.66	9.21	6.87	4.92	3.58
MnO_pct	0.05	0.07	0.03	0.04	0.04	0.05	0.03	0.03	0.03	0.05	0.11	0.09	0.06	0.04
MgO_pct	3.11	5.86	1.64	3.06	4.06	3.52	1.23	2.81	0.65	4.20	8.23	5.18	4.02	2.80
CaO_pct	12.96	12.48	14.47	14.21	14.03	12.90	14.06	13.86	13.76	12.07	10.06	10.96	11.90	12.26
Na2O_pct	2.94	2.32	2.66	2.19	2.08	2.87	2.90	2.63	3.26	3.04	2.63	2.92	3.16	3.31
K2O_pct	0.19	0.16	0.16	0.10	0.08	0.18	0.28	0.10	0.35	0.23	0.22	0.31	0.28	0.31

Cr2O3_pct	0.01	0.01	0.00	0.01	<0.002	0.01	0.01	0.01	<0.002	0.00	<0.002	0.00	<0.002	0.00
P2O5_pct	0.01	0.02	<0.01	<0.01	<0.01	0.02	0.01	<0.01	0.08	<0.01	0.03	0.02	0.04	<0.01
Normalised*	99.47	99.23	99.00	99.08	98.67	99.08	99.10	98.78	99.21	99.55	99.69	99.33	99.65	99.37
SiO2_pct*	49.31	47.11	49.00	48.38	47.14	48.89	49.58	48.30	50.70	48.96	47.00	48.61	49.12	50.17
TiO2_pct*	0.26	0.31	0.14	0.16	0.12	0.25	0.25	0.08	0.42	0.13	0.29	0.18	0.26	0.12
Al2O3_pct*	49.31	47.11	49.00	48.38	47.14	48.89	49.58	48.30	50.70	48.96	47.00	48.61	49.12	50.17
Fe2O3t_pct*	3.74	6.04	2.19	2.99	3.69	3.85	2.68	2.80	2.09	4.68	9.24	6.92	4.94	3.60
FeO_pct*	3.18	5.13	1.86	2.54	3.14	3.27	2.28	2.38	1.77	3.98	7.85	5.88	4.20	3.06
Fe2O3_pct*	0.56	0.91	0.33	0.45	0.55	0.58	0.40	0.42	0.31	0.70	1.39	1.04	0.74	0.54
FeO*_pct	3.37	5.43	1.97	2.69	3.32	3.46	2.42	2.52	1.88	4.21	8.31	6.22	4.44	3.24
MnO_pct*	0.05	0.07	0.03	0.04	0.04	0.05	0.03	0.03	0.03	0.05	0.11	0.09	0.06	0.04
MgO_pct*	3.13	5.91	1.66	3.09	4.11	3.55	1.24	2.84	0.66	4.22	8.26	5.21	4.03	2.82
CaO_pct*	13.29	12.79	14.83	14.57	14.38	13.23	14.41	14.21	14.11	12.37	10.31	11.24	12.20	12.57
Na2O_pct*	3.01	2.38	2.73	2.25	2.13	2.94	2.97	2.70	3.34	3.12	2.70	2.99	3.24	3.39
K2O_pct*	0.19	0.16	0.16	0.10	0.08	0.18	0.29	0.10	0.36	0.24	0.23	0.32	0.29	0.32
Cr2O3_pct*	0.01	0.01	0.00	0.01	#VALUE!	0.01	0.01	0.01	#VALUE!	0.00	#VALUE!	0.00	#VALUE!	0.00
P2O5_pct*	0.01	0.02	N/D	N/D	#VALUE!	0.02	0.01	#VALUE!	0.08	#VALUE!	0.03	0.02	0.04	#VALUE!
Mg#	63.67	67.22	61.31	68.43	70.05	65.95	49.22	68.02	39.70	65.39	65.20	61.25	63.14	62.12
Mo_pct	<0.001	<0.001	<0.001	<0.001	<0.001	<0.001	<0.001	<0.001	<0.001	<0.001	<0.001	<0.001	<0.001	<0.001
Cu_pct	0.00	0.00	0.00	<0.001	0.00	0.00	0.00	<0.001	0.00	<0.001	0.00	<0.001	0.00	<0.001
Pb_pct	<0.02	<0.02	<0.02	<0.02	<0.02	<0.02	<0.02	<0.02	<0.02	<0.02	<0.02	<0.02	<0.02	<0.02
Zn_pct	<0.01	<0.01	<0.01	<0.01	<0.01	<0.01	<0.01	<0.01	<0.01	<0.01	<0.01	<0.01	<0.01	<0.01
Ag_ppm	<2	<2	<2	<2	<2	<2	<2	<2	<2	<2	<2	<2	<2	<2
Ni_ppm	72.00	168.00	44.00	71.00	112.00	92.00	17.00	78.00	<10	112.00	218.00	131.00	107.00	71.00

Mo_ppm	0.30	0.15	0.26	0.14	0.25	0.17	0.26	0.22	0.47	0.19	0.36	0.19	0.30	0.18
Cu_ppm	17.33	12.27	9.58	9.74	19.25	11.91	19.27	6.66	16.39	5.11	19.06	7.29	8.01	4.24
Pb_ppm	0.48	0.38	0.35	0.33	0.28	0.36	0.51	0.56	0.66	0.30	0.40	0.54	0.45	0.43
Zn_ppm	17.90	30.30	8.90	10.20	14.80	16.50	7.60	13.60	9.80	21.10	47.90	35.60	23.30	17.40
Ag_ppb	8.00	8.00	6.00	7.00	9.00	7.00	10.00	8.00	11.00	4.00	60.00	5.00	4.00	5.00
Ni_ppm	66.80	154.20	35.00	56.10	90.70	72.20	9.70	60.00	4.30	104.10	205.60	114.80	94.80	65.10
Co_ppm	19.40	33.90	8.90	11.20	20.20	18.80	4.00	16.30	2.50	28.40	59.80	35.40	27.90	20.00
Mn_ppm	278.00	487.00	128.00	141.00	269.00	251.00	57.00	229.00	57.00	351.00	778.00	535.00	354.00	261.00
As_ppm	<0.1	0.10	<0.1	<0.1	<0.1	0.20	<0.1	0.10	<0.1	<0.1	<0.1	<0.1	<0.1	<0.1
Au_ppb	<0.2	<0.2	<0.2	<0.2	0.70	<0.2	<0.2	<0.2	1.10	<0.2	0.40	0.20	0.20	0.50
Cd_ppm	<0.01	0.01	0.01	<0.01	0.01	<0.01	<0.01	<0.01	0.04	0.01	0.01	0.02	0.02	0.02
Sb_ppm	<0.02	<0.02	<0.02	<0.02	<0.02	<0.02	<0.02	<0.02	<0.02	<0.02	<0.02	0.04	<0.02	<0.02
Bi_ppm	<0.02	<0.02	<0.02	<0.02	<0.02	<0.02	<0.02	<0.02	<0.02	<0.02	<0.02	<0.02	<0.02	<0.02
Cr_ppm	26.20	20.30	13.30	19.10	12.30	23.80	18.70	35.80	9.10	18.00	12.20	21.60	10.90	16.30
Hg_ppb	<5	<5	<5	<5	<5	<5	<5	<5	9.00	<5	<5	<5	<5	<5
Se_ppm	<0.1	<0.1	<0.1	<0.1	<0.1	<0.1	0.10	<0.1	<0.1	<0.1	<0.1	<0.1	<0.1	<0.1
Te_ppm	0.02	<0.02	0.04	0.03	0.03	0.03	0.04	0.05	0.03	<0.02	<0.02	<0.02	<0.02	<0.02
Ge_ppm	<0.1	<0.1	<0.1	<0.1	<0.1	<0.1	<0.1	<0.1	0.10	<0.1	<0.1	<0.1	0.10	<0.1
In_ppm	<0.02	<0.02	<0.02	<0.02	<0.02	<0.02	<0.02	<0.02	<0.02	<0.02	<0.02	<0.02	<0.02	<0.02
Re_ppb	<1	<1	<1	<1	<1	<1	<1	<1	<1	<1	<1	<1	<1	<1
Be_ppm	0.10	0.10	0.10	0.10	<0.1	0.10	0.20	0.10	0.20	0.20	<0.1	0.30	0.10	0.10
Li_ppm	1.90	1.80	1.30	1.20	1.40	2.00	1.90	1.30	1.90	1.90	2.90	1.90	2.30	2.40
Pd_ppb	<10	<10	<10	<10	<10	<10	<10	<10	<10	<10	<10	<10	<10	<10
Pt_ppb	<2	<2	<2	<2	<2	<2	<2	<2	<2	<2	<2	<2	<2	<2
Au_ppb	3.00	3.00	3.00	<1	3.00	2.00	3.00	4.00	3.00	3.00	5.00	3.00	3.00	4.00

Pt_ppb	0.20	0.20	0.20	0.10	0.20	0.10	0.20	0.30	0.20	0.20	0.40	0.20	0.20	0.30
Pd_ppb	0.70	<0.5	<0.5	<0.5	<0.5	<0.5	0.60	1.70	0.60	0.60	0.90	0.70	0.60	0.90
B_ppm	<1	<1	<1	<1	<1	<1	<1	<1	<1	<1	<1	<1	<1	<1
Tl_ppm	<0.02	<0.02	<0.02	<0.02	<0.02	<0.02	<0.02	<0.02	<0.02	<0.02	<0.02	<0.02	<0.02	<0.02
LOI_pct	0.40	0.60	0.90	0.80	1.20	0.80	0.80	1.10	0.70	0.30	0.10	0.50	0.20	0.50
TOT/C_TC000_pct	0.04	<0.02	0.02	0.02	0.02	0.03	<0.02	<0.02	<0.02	0.10	0.11	0.11	0.11	0.10
TOT/S_pct	<0.02	<0.02	<0.02	<0.02	<0.02	<0.02	<0.02	<0.02	<0.02	<0.02	<0.02	<0.02	<0.02	<0.02
Ba_ppm	104.00	73.00	96.00	68.00	55.00	90.00	133.00	71.00	155.00	119.00	116.00	155.00	141.00	154.00
Sc_ppm	4.00	6.00	3.00	4.00	2.00	4.00	5.00	2.00	6.00	1.00	3.00	2.00	3.00	1.00
Sum_pct	99.87	99.83	99.90	99.88	99.87	99.88	99.90	99.88	99.91	99.85	99.79	99.83	99.85	99.87
Cs_ppm	<0.1	<0.1	<0.1	<0.1	<0.1	<0.1	<0.1	<0.1	<0.1	<0.1	<0.1	<0.1	<0.1	<0.1
Ga_ppm	17.20	15.80	18.70	16.10	15.00	16.30	18.50	17.10	19.10	17.40	15.10	16.60	16.70	17.70
Hf_ppm	0.30	0.50	0.20	0.20	0.20	0.40	0.30	<0.1	1.10	0.20	0.30	0.30	0.60	0.20
Nb_ppm	0.70	0.90	0.20	0.40	0.20	0.70	0.60	<0.1	1.90	0.30	0.90	1.10	1.10	0.50
Rb_ppm	1.50	1.90	1.00	1.10	0.90	1.80	1.80	0.50	4.50	1.90	1.90	2.00	3.00	2.00
Sn_ppm	<1	<1	<1	<1	<1	<1	<1	<1	<1	<1	<1	<1	<1	<1
Sr_ppm	542.90	466.50	540.70	467.20	447.20	480.30	576.90	587.00	530.10	619.90	528.10	565.20	623.20	634.60
Ta_ppm	<0.1	<0.1	<0.1	<0.1	<0.1	<0.1	<0.1	<0.1	0.10	<0.1	<0.1	<0.1	<0.1	<0.1
Th_ppm	<0.2	0.20	<0.2	<0.2	<0.2	<0.2	<0.2	<0.2	0.50	<0.2	<0.2	<0.2	0.30	<0.2
U_ppm	<0.1	<0.1	<0.1	<0.1	<0.1	<0.1	<0.1	<0.1	<0.1	<0.1	<0.1	<0.1	<0.1	<0.1
V_ppm	33.00	42.00	17.00	28.00	19.00	28.00	36.00	<8	45.00	18.00	33.00	20.00	29.00	14.00
W_ppm	1.00	0.70	0.80	0.70	1.20	1.30	0.70	0.90	1.30	0.90	1.00	1.30	0.90	0.60
Zr_ppm	13.40	17.80	7.70	7.50	4.90	16.20	11.20	2.10	47.50	7.60	12.20	12.00	23.90	8.30
Y_ppm	2.60	3.70	1.50	2.00	1.30	2.90	2.80	0.50	7.30	1.10	2.40	2.60	3.30	1.40
La_ppm	2.80	2.80	2.10	2.50	1.70	2.60	2.80	1.20	6.20	2.40	2.90	3.90	3.80	2.90

Ce_ppm	5.50	5.90	3.60	4.50	3.00	5.20	5.40	2.60	13.00	3.90	5.80	7.00	7.00	5.20
Pr_ppm	0.67	0.74	0.45	0.50	0.37	0.63	0.64	0.27	1.64	0.50	0.72	0.87	0.92	0.57
Nd_ppm	2.80	3.60	1.90	2.20	1.50	2.80	2.70	1.30	7.00	1.60	2.80	3.30	3.80	2.40
Sm_ppm	0.54	0.73	0.34	0.34	0.29	0.60	0.45	0.11	1.57	0.33	0.54	0.63	0.78	0.41
Eu_ppm	0.61	0.62	0.52	0.43	0.33	0.56	0.71	0.50	0.87	0.58	0.57	0.78	0.70	0.71
Gd_ppm	0.68	0.86	0.36	0.37	0.27	0.67	0.67	0.16	1.70	0.26	0.53	0.66	0.77	0.39
Tb_ppm	0.09	0.13	0.05	0.05	0.04	0.10	0.09	0.02	0.24	0.04	0.08	0.09	0.11	0.05
Dy_ppm	0.51	0.67	0.36	0.30	0.24	0.54	0.51	0.12	1.50	0.20	0.43	0.47	0.67	0.25
Ho_ppm	0.11	0.14	0.05	0.07	0.04	0.11	0.11	0.03	0.28	0.05	0.08	0.09	0.13	0.05
Er_ppm	0.31	0.39	0.14	0.18	0.10	0.29	0.28	0.07	0.77	0.10	0.22	0.26	0.35	0.12
Tm_ppm	0.03	0.06	0.02	0.02	0.02	0.04	0.03	<0.01	0.11	0.02	0.03	0.04	0.05	0.01
Yb_ppm	0.22	0.34	0.13	0.18	0.10	0.30	0.24	0.06	0.60	0.09	0.17	0.27	0.25	0.12
Lu_ppm	0.04	0.05	0.02	0.03	0.02	0.04	0.03	<0.01	0.10	0.01	0.03	0.04	0.04	0.01

Sample_ID	KAC142/134	KAC143/136	KAC144/139	KAC145/140	KAC146/141a	KAC146/141b	KAC146/141c	KAC147/142	KAC149/143	KAC150/144	KAC151/145a	KAC151/145b	KAC152/146a	KAC152/146b
Lat_S	-15.7915	-15.3635	-15.8475	-15.8800	-15.8790	-15.8790	-15.8790	-15.9000	-15.7503	-15.3729	-15.4222	-15.4222	-15.4155	-15.4155
Long_E	13.8453	13.9465	13.8143	13.8123	13.8111	13.8111	13.8111	13.8069	13.8196	13.9042	13.9014	13.9014	13.8169	13.8169
Rocktype	Leucotroctolite	Pl megacryst fr pegmatoidal anorthosite dyke	Anorthosite/ Leuconorite	Leuconorite	Felsic band	Felsic band + leuconorite host	Leuconorite	Leuconorite	Leuconorite	Leucotroctolite	Leucotroctolite	Leucotroctolite	Leucotroctolite	Leucotroctolite
Group	KC	KC	KC	KC	KC	KC	KC	KC	KC	KC	KC	KC	KC	KC
SiO2_pct	50.59	63.20	51.05	50.95	52.86	52.17	51.73	50.60	46.82	48.45	47.76	46.53	51.96	51.51
TiO2_pct	0.12	<0.01	0.17	0.24	0.12	0.29	0.47	0.51	0.20	0.12	0.45	0.24	0.58	0.59
Al2O3_pct	29.72	19.17	24.47	24.39	26.92	26.85	25.82	23.30	26.01	25.77	27.22	23.88	26.00	25.79

Fe2O3t_pct	1.21	0.16	4.90	4.80	1.59	2.40	3.49	6.47	4.93	4.76	4.18	7.34	3.70	4.06
MnO_pct	0.02	<0.01	0.05	0.05	0.02	0.02	0.04	0.06	0.06	0.05	0.05	0.09	0.04	0.05
MgO_pct	0.56	0.04	4.62	4.09	0.94	1.34	1.87	4.59	5.02	5.33	2.99	6.88	1.23	1.53
CaO_pct	13.14	0.33	9.84	9.49	10.71	9.99	10.49	8.98	12.47	11.86	13.48	11.65	11.26	11.28
Na2O_pct	3.47	2.97	3.83	4.11	4.68	4.71	4.36	4.15	2.54	2.81	2.61	2.10	4.08	4.03
K2O_pct	0.24	11.50	0.33	0.21	0.55	0.37	0.30	0.46	0.18	0.15	0.20	0.14	0.41	0.41
Cr2O3_pct	<0.002	<0.002	0.01	0.01	0.00	0.00	0.05	0.04	0.01	0.00	0.01	0.01	0.01	<0.002
P2O5_pct	<0.01	0.01	0.02	0.02	0.05	0.02	0.04	0.02	0.03	<0.01	0.04	0.02	0.03	0.02
Normalised*	99.11	99.14	99.34	98.34	98.50	98.19	98.67	99.23	98.25	99.35	98.97	98.92	99.28	99.27
SiO2_pct*	51.04	63.75	51.39	51.81	53.66	53.13	52.43	50.99	47.65	48.77	48.26	47.04	52.34	51.89
TiO2_pct*	0.12	N/D	0.17	0.25	0.12	0.30	0.48	0.52	0.21	0.12	0.46	0.25	0.59	0.60
Al2O3_pct*	51.04	63.75	51.39	51.81	53.66	53.13	52.43	50.99	47.65	48.77	48.26	47.04	52.34	51.89
Fe2O3t_pct*	1.22	0.16	4.93	4.88	1.61	2.44	3.54	6.52	5.02	4.79	4.22	7.42	3.73	4.09
FeO_pct*	1.04	0.14	4.19	4.15	1.37	2.08	3.01	5.54	4.27	4.07	3.59	6.31	3.17	3.48
Fe2O3_pct*	0.18	0.02	0.74	0.73	0.24	0.37	0.53	0.98	0.75	0.72	0.63	1.11	0.56	0.61
FeO*_pct	1.10	0.15	4.44	4.39	1.45	2.20	3.18	5.87	4.52	4.31	3.80	6.68	3.35	3.68
MnO_pct*	0.02	N/D	0.05	0.05	0.02	0.02	0.04	0.06	0.06	0.05	0.05	0.09	0.04	0.05
MgO_pct*	0.57	0.04	4.65	4.16	0.95	1.36	1.90	4.63	5.11	5.36	3.02	6.96	1.24	1.54
CaO_pct*	13.47	0.34	10.09	9.73	10.98	10.24	10.75	9.21	12.78	12.16	13.82	11.94	11.54	11.56
Na2O_pct*	3.56	3.04	3.93	4.21	4.80	4.83	4.47	4.25	2.60	2.88	2.68	2.15	4.18	4.13
K2O_pct*	0.25	11.79	0.34	0.22	0.56	0.38	0.31	0.47	0.18	0.15	0.21	0.14	0.42	0.42
Cr2O3_pct*	N/D	N/D	0.01	0.01	0.00	0.00	0.05	0.04	0.01	0.00	0.01	0.01	0.01	N/D
P2O5_pct*	N/D	0.01	0.02	0.02	0.05	0.02	0.04	0.02	0.03	N/D	0.04	0.02	0.03	0.02
Mg#	49.25	34.39	66.41	64.11	55.35	53.93	52.90	59.80	68.10	70.13	59.99	66.27	41.07	44.14

Mo_pct	<0.001	<0.001	<0.001	<0.001	<0.001	<0.001	<0.001	<0.001	<0.001	<0.001	<0.001	<0.001	<0.001	<0.001
Cu_pct	<0.001	<0.001	<0.001	0.00	<0.001	<0.001	<0.001	0.00	<0.001	<0.001	0.00	<0.001	0.00	0.00
Pb_pct	<0.02	<0.02	<0.02	<0.02	<0.02	<0.02	<0.02	<0.02	<0.02	<0.02	<0.02	<0.02	<0.02	<0.02
Zn_pct	<0.01	<0.01	<0.01	<0.01	<0.01	<0.01	<0.01	<0.01	<0.01	<0.01	<0.01	<0.01	<0.01	<0.01
Ag_ppm	<2	<2	<2	<2	<2	<2	<2	<2	<2	<2	<2	<2	<2	<2
Ni_ppm	15.00	<10	124.00	106.00	12.00	24.00	55.00	135.00	124.00	145.00	86.00	161.00	17.00	13.00
Mo_ppm	0.34	0.17	0.77	0.39	0.83	0.55	0.35	0.41	0.20	0.32	0.30	0.31	0.37	0.43
Cu_ppm	4.63	6.95	8.48	10.49	6.13	4.30	9.98	6.74	9.07	8.48	15.37	10.68	28.86	30.72
Pb_ppm	0.37	4.02	0.38	0.49	0.68	0.41	0.46	0.19	0.53	0.60	0.54	0.48	0.59	0.38
Zn_ppm	4.40	2.00	25.50	21.00	8.50	15.30	7.00	24.80	25.20	26.60	18.70	40.70	10.80	12.70
Ag_ppb	4.00	6.00	17.00	8.00	4.00	5.00	7.00	3.00	7.00	9.00	10.00	7.00	7.00	6.00
Ni_ppm	15.70	5.60	117.00	80.00	13.10	25.00	48.90	120.60	108.20	149.50	73.90	152.50	14.60	9.30
Co_ppm	4.40	0.90	31.70	26.00	5.50	10.70	11.90	33.00	31.00	38.90	18.90	45.50	8.50	9.00
Mn_ppm	115.00	51.00	361.00	262.00	83.00	157.00	84.00	376.00	377.00	439.00	237.00	623.00	65.00	78.00
As_ppm	<0.1	<0.1	<0.1	0.10	<0.1	0.30	0.20	<0.1	<0.1	0.20	0.10	<0.1	0.20	<0.1
Au_ppb	0.30	0.30	0.20	0.30	<0.2	<0.2	<0.2	0.30	<0.2	<0.2	0.20	<0.2	<0.2	<0.2
Cd_ppm	0.02	<0.01	<0.01	0.01	<0.01	<0.01	<0.01	<0.01	0.02	<0.01	0.02	0.02	<0.01	<0.01
Sb_ppm	<0.02	<0.02	<0.02	<0.02	<0.02	<0.02	<0.02	<0.02	<0.02	<0.02	<0.02	<0.02	<0.02	<0.02
Bi_ppm	<0.02	<0.02	<0.02	<0.02	<0.02	<0.02	<0.02	<0.02	<0.02	<0.02	<0.02	<0.02	<0.02	<0.02
Cr_ppm	17.10	36.30	32.60	78.00	13.50	20.10	270.40	204.60	26.00	18.30	39.70	18.20	34.70	13.90
Hg_ppb	<5	<5	<5	<5	<5	<5	<5	<5	<5	<5	<5	<5	<5	<5
Se_ppm	<0.1	<0.1	<0.1	<0.1	<0.1	<0.1	<0.1	<0.1	<0.1	<0.1	<0.1	<0.1	<0.1	<0.1
Te_ppm	<0.02	<0.02	<0.02	<0.02	<0.02	<0.02	<0.02	<0.02	<0.02	<0.02	<0.02	0.03	<0.02	<0.02
Ge_ppm	<0.1	<0.1	<0.1	<0.1	<0.1	<0.1	<0.1	<0.1	<0.1	<0.1	<0.1	<0.1	<0.1	<0.1
In_ppm	<0.02	<0.02	<0.02	<0.02	<0.02	<0.02	<0.02	<0.02	<0.02	<0.02	<0.02	<0.02	<0.02	<0.02

Re_ppb	<1	<1	<1	<1	<1	<1	<1	<1	<1	<1	<1	<1	<1	<1
Be_ppm	<0.1	0.10	<0.1	<0.1	<0.1	<0.1	0.10	<0.1	0.10	<0.1	0.20	0.10	0.10	<0.1
Li_ppm	1.80	0.40	2.60	2.50	2.70	4.20	2.70	1.40	2.40	1.90	1.80	2.60	2.50	2.30
Pd_ppb	<10	<10	<10	<10	<10	<10	<10	<10	<10	<10	<10	<10	<10	<10
Pt_ppb	<2	<2	<2	<2	<2	<2	<2	<2	<2	<2	<2	<2	<2	<2
Au_ppb	3.00	3.00	3.00	3.00	3.00	4.00	4.00	3.00	3.00	3.00	3.00	3.00	2.00	2.00
Pt_ppb	0.20	0.20	0.20	0.30	0.20	0.20	0.30	0.20	0.20	0.20	0.30	0.20	0.20	0.20
Pd_ppb	0.60	0.70	0.70	0.70	0.70	0.70	1.00	0.70	0.60	0.70	0.70	0.80	0.50	0.60
B_ppm	<1	<1	<1	1.00	<1	<1	<1	<1	<1	<1	<1	<1	<1	<1
Tl_ppm	<0.02	0.02	<0.02	<0.02	<0.02	<0.02	<0.02	<0.02	<0.02	<0.02	<0.02	<0.02	<0.02	<0.02
LOI_pct	0.80	0.80	0.50	1.50	1.40	1.70	1.20	0.60	1.60	0.50	0.90	0.90	0.60	0.60
TOT/C_TC000_pct	<0.02	0.06	0.02	0.02	0.04	0.03	0.04	<0.02	0.02	0.06	0.07	0.06	0.04	0.03
TOT/S_pct	<0.02	<0.02	<0.02	<0.02	<0.02	<0.02	<0.02	<0.02	<0.02	<0.02	0.04	<0.02	<0.02	<0.02
Ba_ppm	150.00	15819.00	196.00	199.00	276.00	231.00	215.00	234.00	114.00	99.00	119.00	90.00	214.00	209.00
Sc_ppm	<1	<1	1.00	2.00	<1	1.00	3.00	2.00	3.00	2.00	6.00	4.00	7.00	8.00
Sum_pct	99.91	99.94	99.84	99.84	99.90	99.89	99.87	99.83	99.85	99.85	99.87	99.82	99.88	99.87
Cs_ppm	<0.1	2.60	<0.1	<0.1	<0.1	<0.1	<0.1	<0.1	<0.1	<0.1	<0.1	<0.1	<0.1	<0.1
Ga_ppm	19.60	16.10	15.90	17.60	17.30	17.50	17.30	16.80	16.00	15.10	16.30	14.00	21.50	21.20
Hf_ppm	<0.1	<0.1	0.20	0.20	0.20	0.20	0.40	0.20	0.30	0.10	0.60	0.30	0.40	0.50
Nb_ppm	1.00	0.10	0.40	0.70	0.40	0.90	0.70	0.50	0.50	0.10	1.20	0.50	0.60	0.80
Rb_ppm	1.40	355.90	1.40	1.20	2.90	2.10	1.60	1.90	1.90	0.70	1.90	1.40	2.00	2.30
Sn_ppm	<1	<1	<1	<1	<1	<1	<1	<1	<1	<1	<1	<1	<1	<1
Sr_ppm	715.80	535.00	679.30	726.00	766.70	769.30	720.70	677.70	529.70	555.40	614.60	526.00	678.00	670.20
Ta_ppm	<0.1	<0.1	<0.1	<0.1	<0.1	<0.1	<0.1	<0.1	<0.1	<0.1	<0.1	<0.1	<0.1	<0.1
Th_ppm	<0.2	<0.2	<0.2	<0.2	<0.2	<0.2	0.20	<0.2	<0.2	<0.2	<0.2	<0.2	<0.2	<0.2

U_ppm	<0.1	<0.1	<0.1	<0.1	<0.1	<0.1	<0.1	<0.1	<0.1	<0.1	<0.1	<0.1	<0.1	<0.1
V_ppm	14.00	<8	19.00	34.00	11.00	23.00	73.00	83.00	23.00	18.00	52.00	28.00	135.00	132.00
W_ppm	1.30	1.40	2.30	1.10	1.60	1.40	1.40	1.50	1.20	0.90	1.30	1.20	1.80	1.10
Zr_ppm	2.40	2.40	9.60	6.40	8.30	11.00	15.60	7.40	9.90	4.80	20.50	11.80	13.50	16.50
Y_ppm	0.80	0.30	1.00	1.30	1.60	1.40	3.20	1.00	2.20	1.00	4.60	2.40	3.10	3.60
La_ppm	2.70	1.00	2.60	2.80	3.60	3.50	3.50	2.40	2.50	1.80	3.90	2.50	3.70	4.10
Ce_ppm	4.40	1.00	4.70	4.90	6.10	5.80	6.10	4.30	4.60	3.20	7.90	4.80	7.00	7.90
Pr_ppm	0.50	0.04	0.48	0.54	0.73	0.66	0.74	0.42	0.56	0.37	0.94	0.63	0.82	0.93
Nd_ppm	1.90	<0.3	2.00	2.20	3.00	2.80	3.20	2.00	2.30	1.70	4.50	2.60	3.60	4.10
Sm_ppm	0.32	<0.05	0.31	0.38	0.47	0.37	0.61	0.26	0.45	0.29	0.98	0.55	0.71	0.77
Eu_ppm	0.72	2.46	0.64	0.65	0.78	0.76	0.71	0.66	0.54	0.49	0.72	0.58	1.02	0.98
Gd_ppm	0.26	0.19	0.30	0.39	0.45	0.38	0.69	0.29	0.44	0.27	0.99	0.49	0.76	0.77
Tb_ppm	0.03	<0.01	0.03	0.04	0.06	0.04	0.09	0.03	0.06	0.02	0.14	0.07	0.09	0.11
Dy_ppm	0.18	0.19	0.17	0.26	0.31	0.25	0.50	0.18	0.33	0.18	0.79	0.47	0.55	0.69
Ho_ppm	0.02	<0.02	0.04	0.05	0.06	0.04	0.11	0.04	0.07	0.03	0.18	0.09	0.10	0.13
Er_ppm	0.06	<0.03	0.10	0.15	0.17	0.13	0.32	0.11	0.18	0.09	0.46	0.23	0.31	0.39
Tm_ppm	<0.01	<0.01	0.01	0.02	0.02	0.02	0.04	0.01	0.02	0.01	0.06	0.03	0.04	0.05
Yb_ppm	0.05	<0.05	0.09	0.12	0.13	0.11	0.29	0.11	0.15	0.08	0.39	0.22	0.26	0.30
Lu_ppm	<0.01	<0.01	0.01	0.02	0.01	0.01	0.04	0.01	0.02	0.01	0.06	0.03	0.03	0.05

Sample_ID	KAC170/159	KAC172/160	KAC084/174B	KAC090/175A	KAC090/175B	KAC146/259	KAC151/179	KAC151/180	KAC151/181	KAC183/182	KAC184/183	KAC187/189	KAC188/190	KAC206/201
Lat_S	-15.1785	-15.6936	-15.6094	-15.3645	-15.3645	-15.8790	-15.4222	-15.4222	-15.4222	-15.4417	-15.4402	-15.4251	-15.4715	-16.9121
Long_E	13.9877	14.0912	14.0554	13.9466	13.9466	13.8111	13.9014	13.9014	13.9014	13.8765	13.8769	14.0598	14.0925	13.4725

Rocktype	Leucotroctolite	Anorthosite	Opx megacryst + Pl blebs and veins	Leucotroctolite	Leucotroctolite	olivine-bearing anorthosite	Anorthosite block within noritic framework	Weakly foliated leuconorite and pegmatitic norite	Foliated leuconorite	Leucotroctolite/leuconorite	Leucotroctolite/leuconorite	Sheared anorthosite/granite?	Fe-Ti oxide rock	Foliated leucotroctolite
Group	KC	KC	KC	KC	KC	KC	KC	KC	KC	KC	KC	KC	KC	KC
SiO2_pct	52.88	48.59	51.17	51.43	48.40	51.74	46.50	48.31	48.79	47.53	47.99	58.07	1.71	47.22
TiO2_pct	0.14	0.12	0.47	0.16	0.25	0.53	0.18	0.34	0.10	0.25	0.34	0.71	20.22	1.86
Al2O3_pct	27.84	27.83	3.48	28.79	26.27	26.02	26.18	28.44	31.36	25.23	24.14	18.07	5.69	19.11
Fe2O3t_pct	1.28	3.28	18.86	1.39	4.92	3.21	5.49	2.89	0.78	6.37	6.76	6.06	68.78	10.65
MnO_pct	0.01	0.04	0.29	0.02	0.06	0.04	0.07	0.03	<0.01	0.08	0.08	0.12	0.24	0.12
MgO_pct	0.68	3.25	23.20	0.89	3.91	1.81	5.29	2.21	0.16	5.45	5.78	1.87	1.31	3.88
CaO_pct	11.21	13.34	2.08	12.68	12.13	10.40	12.63	13.87	15.35	11.73	11.05	3.17	0.03	10.98
Na2O_pct	4.72	2.71	0.16	3.76	2.93	4.40	2.29	2.66	2.67	2.57	2.90	4.94	<0.01	3.15
K2O_pct	0.43	0.15	<0.01	0.37	0.24	0.40	0.15	0.19	0.13	0.17	0.20	5.02	<0.01	0.96
Cr2O3_pct	0.00	0.01	0.10	0.01	0.00	0.03	0.01	0.01	0.00	0.01	0.01	0.03	0.12	0.11
P2O5_pct	0.01	<0.01	<0.01	0.08	0.02	0.02	0.01	0.02	<0.01	0.02	0.03	0.27	0.01	0.08
Normalised*	99.19	99.38	99.87	99.59	99.15	98.58	98.84	98.98	99.41	99.44	99.34	98.73	98.17	98.17
SiO2_pct*	53.31	48.89	51.24	51.64	48.81	52.49	47.05	48.81	49.08	47.80	48.31	58.82	1.74	48.10
TiO2_pct*	0.14	0.12	0.48	0.16	0.26	0.54	0.18	0.35	0.10	0.26	0.35	0.73	20.73	1.91
Al2O3_pct*	53.31	48.89	51.24	51.64	48.81	52.49	47.05	48.81	49.08	47.80	48.31	58.82	1.74	48.10
Fe2O3t_pct*	1.29	3.30	18.88	1.40	4.96	3.26	5.55	2.92	0.78	6.41	6.80	6.14	70.06	10.85
FeO_pct*	1.10	2.81	16.05	1.19	4.22	2.77	4.72	2.48	0.67	5.44	5.78	5.22	59.55	9.22
Fe2O3_pct*	0.19	0.50	2.83	0.21	0.74	0.49	0.83	0.44	0.12	0.96	1.02	0.92	10.51	1.63
FeO*_pct	1.16	2.97	17.00	1.26	4.47	2.93	5.00	2.63	0.71	5.77	6.12	5.52	63.06	9.76

MnO_pct*	0.01	0.04	0.30	0.02	0.06	0.04	0.07	0.03	N/D	0.08	0.08	0.12	0.25	0.12
MgO_pct*	0.69	3.27	23.23	0.89	3.94	1.84	5.35	2.23	0.16	5.48	5.82	1.89	1.33	3.95
CaO_pct*	11.49	13.68	2.13	13.00	12.44	10.66	12.95	14.22	15.74	12.03	11.33	3.25	0.03	11.26
Na2O_pct*	4.84	2.78	0.16	3.85	3.00	4.51	2.35	2.73	2.74	2.63	2.97	5.06	N/D	3.23
K2O_pct*	0.44	0.15	N/D	0.38	0.25	0.41	0.15	0.19	0.13	0.17	0.21	5.15	N/D	0.98
Cr2O3_pct*	0.00	0.01	0.10	0.01	0.00	0.03	0.01	0.01	0.00	0.01	0.01	0.03	0.12	0.12
P2O5_pct*	0.01	N/D	N/D	0.08	0.02	0.02	0.01	0.02	N/D	0.02	0.03	0.28	0.01	0.08
Mg#	52.69	67.50	72.06	57.31	62.49	54.17	66.89	61.59	30.07	64.20	64.19	39.28	3.84	43.30
Mo_pct	<0.001	<0.001	<0.001	<0.001	<0.001	<0.001	<0.001	<0.001	<0.001	<0.001	<0.001	<0.001	<0.001	<0.001
Cu_pct	<0.001	0.00	<0.001	0.00	0.00	<0.001	<0.001	0.00	<0.001	0.00	0.00	0.00	0.00	0.01
Pb_pct	<0.02	<0.02	<0.02	<0.02	<0.02	<0.02	<0.02	<0.02	<0.02	<0.02	<0.02	<0.02	<0.02	<0.02
Zn_pct	<0.01	<0.01	0.01	<0.01	<0.01	<0.01	<0.01	<0.01	<0.01	<0.01	<0.01	<0.01	0.05	<0.01
Ag_ppm	<2	<2	<2	<2	<2	<2	<2	<2	<2	<2	<2	<2	<2	<2
Ni_ppm	12.00	90.00	328.00	22.00	99.00	37.00	147.00	71.00	<10	105.00	109.00	42.00	312.00	40.00
Mo_ppm	0.52	0.20	0.43	0.19	0.32	0.55	0.28	0.28	0.24	0.53	0.24	0.53	<0.01	0.48
Cu_ppm	7.89	13.47	7.61	19.64	11.58	9.88	8.39	15.54	3.36	11.22	17.50	14.53	4.87	107.02
Pb_ppm	0.32	0.37	0.09	0.73	0.39	0.30	0.41	0.55	0.42	0.39	0.33	0.99	0.07	0.62
Zn_ppm	3.80	14.20	8.90	9.50	18.30	8.20	27.70	12.00	3.20	33.40	37.40	38.10	162.60	32.20
Ag_ppb	5.00	7.00	<2	10.00	77.00	4.00	5.00	5.00	3.00	8.00	5.00	16.00	<2	46.00
Ni_ppm	8.90	75.70	26.40	14.60	75.20	25.00	130.60	53.80	3.30	90.60	103.20	39.40	109.40	23.70
Co_ppm	2.10	18.40	7.90	2.50	23.20	8.90	31.90	11.90	1.00	37.50	42.40	8.30	66.30	24.70
Mn_ppm	47.00	220.00	129.00	56.00	284.00	88.00	440.00	157.00	43.00	544.00	575.00	442.00	531.00	187.00
As_ppm	<0.1	<0.1	<0.1	<0.1	<0.1	<0.1	<0.1	0.10	0.40	0.20	<0.1	<0.1	<0.1	<0.1
Au_ppb	<0.2	<0.2	<0.2	<0.2	<0.2	<0.2	<0.2	<0.2	<0.2	<0.2	0.40	0.50	<0.2	<0.2

Cd_ppm	<0.01	<0.01	<0.01	0.01	<0.01	<0.01	0.02	<0.01	<0.01	0.01	0.02	0.05	0.01	0.05
Sb_ppm	0.16	<0.02	<0.02	<0.02	<0.02	<0.02	<0.02	<0.02	<0.02	<0.02	<0.02	<0.02	<0.02	<0.02
Bi_ppm	<0.02	<0.02	<0.02	<0.02	<0.02	<0.02	<0.02	<0.02	<0.02	<0.02	<0.02	<0.02	<0.02	<0.02
Cr_ppm	10.30	25.90	104.00	18.80	10.80	114.00	13.00	40.10	5.90	20.70	33.00	41.70	286.90	9.90
Hg_ppb	<5	<5	<5	<5	<5	<5	<5	<5	<5	<5	<5	<5	<5	<5
Se_ppm	<0.1	<0.1	<0.1	<0.1	<0.1	<0.1	<0.1	0.10	<0.1	<0.1	<0.1	<0.1	<0.1	<0.1
Te_ppm	<0.02	0.03	<0.02	0.02	0.02	<0.02	0.04	0.03	0.04	0.03	0.03	<0.02	<0.02	<0.02
Ge_ppm	<0.1	<0.1	<0.1	<0.1	<0.1	<0.1	<0.1	<0.1	<0.1	<0.1	<0.1	<0.1	<0.1	<0.1
In_ppm	<0.02	<0.02	<0.02	<0.02	<0.02	<0.02	<0.02	<0.02	<0.02	<0.02	<0.02	0.04	0.04	<0.02
Re_ppb	<1	<1	<1	<1	<1	<1	<1	<1	<1	<1	<1	<1	<1	<1
Be_ppm	<0.1	0.10	<0.1	0.20	0.10	<0.1	0.10	0.10	0.10	0.10	0.10	<0.1	<0.1	0.10
Li_ppm	2.40	1.60	2.50	3.80	1.50	2.90	2.30	2.20	1.30	2.20	2.30	2.10	4.40	5.30
Pd_ppb	<10	<10	<10	<10	<10	<10	<10	<10	<10	<10	<10	<10	<10	<10
Pt_ppb	<2	<2	<2	<2	<2	<2	<2	<2	<2	<2	<2	<2	<2	<2
Au_ppb	3.00	3.00	3.00	4.00	3.00	4.00	4.00	4.00	3.00	5.00	4.00	4.00	9.00	3.00
Pt_ppb	0.20	0.30	0.30	0.30	0.20	0.30	0.20	0.30	0.20	0.30	0.30	0.40	0.80	0.70
Pd_ppb	0.60	0.80	0.80	1.00	0.70	0.90	1.00	0.60	0.70	1.20	1.10	0.80	2.50	0.80
B_ppm	<1	<1	<1	<1	<1	<1	<1	<1	<1	<1	<1	<1	2.00	3.00
Tl_ppm	<0.02	<0.02	<0.02	<0.02	<0.02	<0.02	<0.02	<0.02	<0.02	<0.02	<0.02	<0.02	<0.02	<0.02
LOI_pct	0.70	0.50	-0.30	0.30	0.70	1.30	1.00	0.90	0.50	0.40	0.50	1.10	1.30	1.60
TOT/C_TC000_pct	0.07	0.02	<0.02	0.08	0.10	0.04	0.05	0.05	0.02	<0.02	0.02	0.04	<0.02	<0.02
TOT/S_pct	<0.02	<0.02	<0.02	<0.02	<0.02	<0.02	0.02	0.03	<0.02	<0.02	<0.02	<0.02	0.04	<0.02
Ba_ppm	247.00	92.00	12.00	208.00	137.00	236.00	104.00	122.00	104.00	96.00	104.00	3183.00	31.00	215.00
Sc_ppm	<1	2.00	42.00	2.00	4.00	3.00	3.00	5.00	<1	3.00	6.00	17.00	16.00	35.00

Sum_pct	99.89	99.88	99.57	99.89	99.85	99.88	99.84	99.88	99.91	99.84	99.84	99.83	99.47	99.77
Cs_ppm	<0.1	<0.1	<0.1	<0.1	0.20	<0.1	<0.1	<0.1	<0.1	<0.1	<0.1	<0.1	<0.1	0.60
Ga_ppm	19.50	16.40	6.40	20.90	18.50	16.50	15.40	18.30	19.10	16.40	17.40	24.40	52.70	20.90
Hf_ppm	<0.1	0.10	0.20	1.30	0.40	0.20	0.10	0.30	<0.1	0.40	0.50	9.00	2.00	1.10
Nb_ppm	0.30	0.30	0.20	1.30	0.70	1.20	0.30	0.80	<0.1	1.10	1.10	3.60	7.40	1.80
Rb_ppm	1.30	1.10	0.20	3.90	2.90	2.20	1.00	1.50	0.50	2.20	1.90	27.50	0.20	20.10
Sn_ppm	<1	<1	<1	<1	<1	<1	<1	6.00	<1	<1	<1	<1	2.00	<1
Sr_ppm	906.10	555.60	28.20	729.50	660.20	747.00	583.90	664.90	739.60	478.10	470.50	347.20	16.60	446.70
Ta_ppm	<0.1	<0.1	<0.1	<0.1	<0.1	<0.1	<0.1	<0.1	<0.1	<0.1	<0.1	0.20	0.50	0.10
Th_ppm	<0.2	<0.2	<0.2	0.50	0.50	<0.2	<0.2	<0.2	<0.2	<0.2	<0.2	0.40	<0.2	0.50
U_ppm	<0.1	<0.1	<0.1	<0.1	<0.1	<0.1	<0.1	<0.1	<0.1	<0.1	<0.1	<0.1	0.10	0.10
V_ppm	<8	17.00	213.00	11.00	29.00	47.00	31.00	28.00	<8	26.00	49.00	9.00	2621.00	586.00
W_ppm	1.40	1.00	1.40	1.10	1.00	1.60	0.90	1.10	1.00	1.60	1.30	<0.5	1.80	4.00
Zr_ppm	4.00	4.60	7.10	63.20	15.80	9.20	6.10	12.70	2.10	14.60	16.10	590.60	76.10	34.80
Y_ppm	0.90	1.10	3.80	6.10	2.60	1.40	1.70	3.30	0.70	2.40	3.80	12.60	0.80	9.60
La_ppm	3.10	1.90	0.60	8.70	2.80	3.10	2.60	3.10	2.20	2.50	2.80	27.40	3.70	4.90
Ce_ppm	4.70	3.60	0.60	16.40	5.70	5.50	5.00	6.20	4.50	5.10	5.90	54.20	4.10	11.50
Pr_ppm	0.54	0.39	0.08	2.04	0.66	0.59	0.57	0.73	0.43	0.57	0.71	7.14	0.92	1.46
Nd_ppm	1.90	1.60	0.50	8.30	2.80	2.20	2.60	3.30	1.80	2.70	3.20	30.50	4.10	7.30
Sm_ppm	0.33	0.33	0.29	1.52	0.58	0.36	0.48	0.60	0.33	0.54	0.67	5.52	0.63	1.78
Eu_ppm	0.74	0.54	0.07	1.03	0.67	0.76	0.57	0.71	0.61	0.56	0.62	8.06	0.20	0.90
Gd_ppm	0.29	0.28	0.41	1.55	0.55	0.34	0.43	0.67	0.28	0.55	0.78	4.32	0.49	1.94
Tb_ppm	0.03	0.03	0.07	0.20	0.07	0.04	0.05	0.10	0.02	0.07	0.12	0.53	0.05	0.33
Dy_ppm	0.18	0.22	0.56	1.18	0.49	0.27	0.34	0.56	0.17	0.46	0.68	2.81	0.25	1.90
Ho_ppm	0.03	0.03	0.13	0.21	0.09	0.06	0.06	0.10	<0.02	0.09	0.13	0.49	0.03	0.40

Er_ppm	0.08	0.11	0.46	0.59	0.27	0.16	0.16	0.30	0.04	0.26	0.38	1.37	0.09	1.21
Tm_ppm	0.01	0.01	0.08	0.07	0.04	0.02	0.02	0.04	<0.01	0.03	0.06	0.17	<0.01	0.16
Yb_ppm	0.07	0.12	0.54	0.45	0.24	0.16	0.15	0.27	<0.05	0.22	0.37	1.20	0.07	0.94
Lu_ppm	<0.01	0.02	0.10	0.06	0.04	0.02	0.03	0.04	<0.01	0.03	0.05	0.21	<0.01	0.14

Sample_ID	KAC206/202	KAC217/213	KAC224/223	KAC229/232	KAC238/238	KAC258/251	KAC258/252	KAC259/253	KAC261/255	KAC261/256	KAC262/257	KAC263/261	KAC264/262	KAC264/263
Lat_S	-16.9121	-16.9982	-16.9365	-16.7660	-16.7725	-16.2691	-16.2691	-16.0197	-15.9271	-15.9271	-15.9517	-15.8727	-15.8729	-15.8729
Long_E	13.4725	13.4520	13.4682	13.4766	13.4919	13.4836	13.4836	13.6854	13.8044	13.8044	13.7992	13.8116	13.8112	13.8112
Rocktype	Foliated leucotroctolite	Anorthosite	Sheared leuconorite	Foliated anorthosite	Sheared anorthosite	Metasomatised leuconorite	Foliated leuconorite	Leuconorite	Mortarised leuconorite	Foliated leuconorite	Metasomatised anorthosite	non-olivine-bearing anorthosite	olivine-bearing anorthosite	olivine-bearing anorthosite
Group	KC	KC	KC	KC	KC	KC	KC	KC	KC	KC	KC	KC	KC	KC
SiO2_pct	47.86	48.56	44.32	49.29	40.85	51.74	50.91	51.48	51.25	51.49	52.16	52.36	50.08	50.91
TiO2_pct	1.63	0.08	1.10	1.14	0.13	1.08	1.54	0.90	1.49	1.00	1.33	0.11	0.23	0.23
Al2O3_pct	19.93	25.13	14.45	20.41	22.35	24.39	22.53	24.09	25.12	25.59	26.48	27.75	24.56	24.28
Fe2O3t_pct	9.68	0.67	8.34	8.18	4.24	4.45	5.78	4.95	4.58	4.95	2.89	1.35	4.92	4.62
MnO_pct	0.11	0.01	0.14	0.10	0.06	0.05	0.10	0.06	0.04	0.03	0.02	0.01	0.05	0.05
MgO_pct	3.42	0.39	5.81	3.02	3.64	1.73	2.57	2.05	1.82	1.10	0.25	0.82	4.21	4.21
CaO_pct	10.68	17.66	10.76	8.44	22.48	8.96	9.96	9.39	9.55	9.34	9.64	10.84	9.77	9.81
Na2O_pct	3.41	3.39	2.25	4.41	0.08	4.59	4.11	4.15	4.61	4.76	4.99	4.64	3.96	4.00
K2O_pct	1.07	0.14	0.24	1.26	<0.01	0.73	0.74	0.65	0.54	0.49	0.81	0.31	0.28	0.36
Cr2O3_pct	0.01	0.03	0.21	0.03	0.01	0.01	0.00	0.01	0.01	0.02	0.01	<0.002	0.01	0.00
P2O5_pct	0.09	0.01	0.04	0.29	<0.01	0.04	0.02	0.06	<0.01	0.01	0.03	<0.01	0.01	<0.01
Normalised*	97.96	96.03	87.70	96.64	93.82	97.87	98.34	97.78	99.07	98.77	98.68	98.20	98.14	98.54

SiO2_pct*	48.86	50.57	50.54	51.00	43.54	52.87	51.77	52.65	51.73	52.13	52.86	53.32	51.03	51.66
TiO2_pct*	1.67	0.08	1.13	1.17	0.13	1.11	1.58	0.92	1.53	1.03	1.36	0.11	0.24	0.24
Al2O3_pct*	48.86	50.57	50.54	51.00	43.54	52.87	51.77	52.65	51.73	52.13	52.86	53.32	51.03	51.66
Fe2O3t_pct*	9.88	0.70	9.51	8.46	4.52	4.55	5.88	5.06	4.62	5.01	2.93	1.37	5.01	4.69
FeO_pct*	8.40	0.59	8.08	7.19	3.84	3.86	5.00	4.30	3.93	4.26	2.49	1.17	4.26	3.99
Fe2O3_pct*	1.48	0.10	1.43	1.27	0.68	0.68	0.88	0.76	0.69	0.75	0.44	0.21	0.75	0.70
FeO*_pct	8.89	0.63	8.56	7.62	4.07	4.09	5.29	4.56	4.16	4.51	2.64	1.24	4.51	4.22
MnO_pct*	0.11	0.01	0.14	0.10	0.06	0.05	0.10	0.06	0.04	0.03	0.02	0.01	0.05	0.05
MgO_pct*	3.49	0.41	6.62	3.13	3.88	1.77	2.61	2.10	1.84	1.11	0.25	0.84	4.29	4.27
CaO_pct*	10.95	18.11	11.03	8.65	23.05	9.19	10.21	9.63	9.79	9.58	9.88	11.11	10.02	10.06
Na2O_pct*	3.50	3.48	2.31	4.52	0.08	4.71	4.21	4.25	4.73	4.88	5.12	4.76	4.06	4.10
K2O_pct*	1.10	0.14	0.25	1.29	N/D	0.75	0.76	0.67	0.55	0.50	0.83	0.32	0.29	0.37
Cr2O3_pct*	0.01	0.03	0.22	0.03	0.01	0.01	0.00	0.01	0.01	0.02	0.01	N/D	0.01	0.00
P2O5_pct*	0.09	0.01	0.04	0.30	N/D	0.04	0.02	0.06	N/D	0.01	0.03	N/D	0.01	N/D
Mg#	42.55	54.96	59.36	43.63	64.28	44.90	48.24	46.47	45.45	31.78	15.35	56.01	64.21	65.64
Mo_pct	<0.001	<0.001	<0.001	<0.001	<0.001	<0.001	<0.001	<0.001	<0.001	<0.001	<0.001	<0.001	<0.001	<0.001
Cu_pct	0.02	<0.001	0.01	0.01	0.00	0.00	0.00	0.00	<0.001	0.00	0.00	<0.001	0.00	0.00
Pb_pct	<0.02	<0.02	<0.02	<0.02	<0.02	<0.02	<0.02	<0.02	<0.02	<0.02	<0.02	<0.02	<0.02	<0.02
Zn_pct	<0.01	<0.01	<0.01	<0.01	<0.01	<0.01	<0.01	<0.01	<0.01	<0.01	<0.01	<0.01	<0.01	<0.01
Ag_ppm	<2	<2	<2	<2	<2	<2	<2	<2	<2	<2	<2	<2	<2	<2
Ni_ppm	37.00	<10	70.00	26.00	78.00	34.00	30.00	34.00	55.00	55.00	22.00	21.00	129.00	124.00
Mo_ppm	0.33	0.18	0.10	0.21	0.38	0.43	0.45	0.50	0.26	0.49	0.27	0.46	0.21	0.38
Cu_ppm	154.03	6.10	86.28	40.37	35.36	21.22	13.45	22.27	4.59	15.76	3.67	4.75	9.32	11.04
Pb_ppm	0.84	3.50	1.04	3.89	1.96	0.76	0.56	0.53	0.30	0.46	0.44	0.40	0.45	0.42
Zn_ppm	28.70	4.70	43.00	63.30	20.80	21.60	22.50	26.90	14.90	16.60	7.90	6.00	16.80	22.30

Ag_ppb	65.00	41.00	32.00	56.00	26.00	13.00	9.00	5.00	3.00	8.00	4.00	10.00	7.00	7.00
Ni_ppm	25.50	4.20	55.70	19.80	66.70	28.60	22.40	27.90	43.30	44.80	17.40	17.60	85.90	99.40
Co_ppm	21.10	1.10	31.60	22.20	24.30	14.60	15.20	14.80	14.20	15.70	5.70	5.50	23.00	25.90
Mn_ppm	193.00	53.00	1048.00	416.00	372.00	141.00	159.00	202.00	146.00	116.00	49.00	79.00	202.00	300.00
As_ppm	<0.1	0.20	<0.1	<0.1	<0.1	<0.1	<0.1	<0.1	<0.1	<0.1	<0.1	0.40	0.30	0.30
Au_ppb	<0.2	<0.2	0.30	1.10	<0.2	<0.2	<0.2	<0.2	<0.2	<0.2	<0.2	0.80	0.50	0.40
Cd_ppm	0.06	0.02	0.08	0.02	0.04	<0.01	0.02	0.01	<0.01	<0.01	<0.01	<0.01	<0.01	<0.01
Sb_ppm	<0.02	<0.02	<0.02	<0.02	<0.02	<0.02	<0.02	<0.02	<0.02	<0.02	<0.02	<0.02	<0.02	<0.02
Bi_ppm	<0.02	<0.02	<0.02	<0.02	<0.02	<0.02	<0.02	<0.02	<0.02	<0.02	<0.02	<0.02	<0.02	<0.02
Cr_ppm	28.00	20.80	281.00	22.00	51.80	46.80	24.80	38.40	64.40	114.90	55.50	8.20	41.50	14.80
Hg_ppb	<5	<5	<5	<5	<5	<5	<5	<5	<5	<5	<5	<5	<5	<5
Se_ppm	<0.1	<0.1	0.10	0.50	<0.1	<0.1	<0.1	<0.1	<0.1	<0.1	<0.1	<0.1	<0.1	<0.1
Te_ppm	<0.02	<0.02	<0.02	<0.02	<0.02	<0.02	<0.02	<0.02	<0.02	<0.02	<0.02	<0.02	<0.02	<0.02
Ge_ppm	<0.1	<0.1	<0.1	<0.1	0.30	<0.1	<0.1	<0.1	<0.1	<0.1	<0.1	<0.1	<0.1	<0.1
In_ppm	<0.02	<0.02	0.04	<0.02	<0.02	<0.02	<0.02	<0.02	<0.02	<0.02	<0.02	<0.02	<0.02	<0.02
Re_ppb	<1	<1	<1	<1	<1	<1	<1	<1	<1	<1	<1	<1	<1	<1
Be_ppm	0.10	<0.1	0.20	0.40	0.20	<0.1	<0.1	0.10	<0.1	<0.1	<0.1	<0.1	<0.1	<0.1
Li_ppm	5.10	0.40	4.40	44.20	10.30	8.20	8.60	6.40	3.30	3.80	1.80	2.10	2.80	2.80
Pd_ppb	<10	<10	<10	<10	<10	<10	<10	<10	<10	<10	<10	<10	<10	<10
Pt_ppb	<2	<2	<2	<2	<2	<2	<2	<2	<2	<2	<2	<2	<2	<2
Au_ppb	4.00	3.00	4.00	3.00	7.00	8.00	7.00	8.00	3.00	3.00	4.00	8.00	7.00	7.00
Pt_ppb	0.30	0.30	0.20	0.20	0.60	0.50	0.40	0.40	0.20	0.20	0.10	0.60	0.60	0.50
Pd_ppb	0.80	0.90	0.60	0.80	1.20	1.40	1.40	1.00	<0.5	<0.5	<0.5	1.40	1.50	1.70
B_ppm	3.00	6.00	<1	5.00	5.00	<1	<1	<1	<1	<1	<1	2.00	1.00	2.00
Tl_ppm	<0.02	<0.02	<0.02	0.02	<0.02	<0.02	<0.02	<0.02	<0.02	<0.02	<0.02	<0.02	<0.02	<0.02

LOI_pct	1.80	3.90	12.10	3.20	6.10	2.00	1.50	2.10	0.80	1.10	1.20	1.70	1.70	1.30
TOT/C_TC000_pct	<0.02	<0.02	2.45	0.06	0.16	0.05	0.04	0.18	0.03	<0.02	<0.02	0.05	0.04	0.03
TOT/S_pct	0.03	<0.02	0.06	<0.02	<0.02	0.04	<0.02	<0.02	<0.02	<0.02	<0.02	<0.02	0.03	<0.02
Ba_ppm	222.00	73.00	89.00	364.00	15.00	546.00	547.00	312.00	314.00	303.00	412.00	198.00	191.00	204.00
Sc_ppm	31.00	<1	50.00	14.00	5.00	2.00	16.00	6.00	3.00	<1	1.00	<1	1.00	2.00
Sum_pct	99.76	99.93	99.80	99.84	99.92	99.87	99.84	99.88	99.87	99.87	99.88	99.90	99.84	99.84
Cs_ppm	0.80	0.40	0.40	0.90	0.10	0.50	0.60	0.40	<0.1	<0.1	<0.1	<0.1	<0.1	<0.1
Ga_ppm	22.50	17.70	15.60	19.10	19.30	18.10	18.60	18.10	16.30	18.40	18.60	16.90	16.80	16.00
Hf_ppm	1.50	<0.1	1.40	2.30	0.20	0.40	0.80	0.40	0.40	0.10	0.40	<0.1	0.10	0.20
Nb_ppm	3.10	<0.1	2.40	4.90	0.40	2.00	2.30	1.20	2.20	0.30	2.10	<0.1	0.30	0.40
Rb_ppm	24.20	3.20	5.40	41.60	0.30	3.80	4.50	6.70	2.10	1.80	3.30	0.90	1.50	1.70
Sn_ppm	<1	<1	<1	<1	<1	<1	<1	<1	<1	<1	<1	<1	<1	<1
Sr_ppm	455.00	468.80	214.00	412.50	44.20	761.30	681.80	588.80	717.80	777.00	864.50	789.60	716.80	688.70
Ta_ppm	0.20	<0.1	0.20	0.30	<0.1	0.20	0.10	<0.1	0.10	<0.1	0.20	<0.1	<0.1	<0.1
Th_ppm	0.80	<0.2	0.50	0.80	<0.2	<0.2	<0.2	0.30	<0.2	<0.2	<0.2	<0.2	<0.2	<0.2
U_ppm	0.30	<0.1	0.10	0.10	<0.1	<0.1	<0.1	<0.1	<0.1	<0.1	<0.1	<0.1	<0.1	<0.1
V_ppm	522.00	<8	316.00	156.00	31.00	73.00	143.00	84.00	92.00	144.00	94.00	<8	21.00	16.00
W_ppm	1.60	1.40	<0.5	0.80	1.50	1.40	1.30	2.30	1.40	1.50	1.50	1.40	1.00	1.80
Zr_ppm	53.30	2.40	45.40	94.40	6.40	14.10	26.30	13.20	16.00	5.60	13.90	4.40	5.20	8.70
Y_ppm	12.70	0.50	13.80	13.90	1.50	1.00	5.90	2.80	1.20	0.40	0.70	0.80	1.30	1.50
La_ppm	7.20	1.70	3.70	19.80	3.10	4.00	3.90	5.10	3.10	3.30	4.00	2.40	2.70	2.70
Ce_ppm	16.40	3.20	9.70	42.40	4.80	6.50	8.00	9.20	5.50	5.30	6.50	3.90	4.90	5.10
Pr_ppm	2.13	0.33	1.33	5.04	0.54	0.75	1.09	1.06	0.57	0.53	0.68	0.38	0.54	0.53
Nd_ppm	9.40	1.40	7.10	21.80	1.80	2.90	5.10	4.10	2.30	2.00	2.60	1.60	1.90	2.40
Sm_ppm	2.18	0.20	1.98	3.82	0.32	0.39	1.25	0.67	0.34	0.24	0.40	0.22	0.29	0.38

Eu_ppm	0.99	0.48	0.96	1.86	0.71	1.33	1.44	1.05	0.91	0.92	1.09	0.66	0.66	0.66
Gd_ppm	2.52	0.16	2.41	3.74	0.37	0.37	1.43	0.76	0.34	0.18	0.31	0.20	0.33	0.37
Tb_ppm	0.39	0.02	0.42	0.48	0.05	0.04	0.19	0.09	0.04	0.01	0.03	0.02	0.04	0.04
Dy_ppm	2.26	0.10	2.59	2.72	0.30	0.21	1.19	0.57	0.23	0.09	0.16	0.12	0.23	0.27
Ho_ppm	0.51	<0.02	0.55	0.54	0.06	0.03	0.21	0.11	0.05	<0.02	0.03	0.02	0.03	0.05
Er_ppm	1.38	0.04	1.58	1.47	0.15	0.10	0.59	0.33	0.13	0.04	0.08	0.05	0.10	0.14
Tm_ppm	0.21	<0.01	0.22	0.21	0.03	0.01	0.09	0.04	0.02	<0.01	<0.01	<0.01	0.02	0.02
Yb_ppm	1.23	0.06	1.24	1.32	0.14	0.08	0.50	0.28	0.10	<0.05	0.05	0.06	0.10	0.12
Lu_ppm	0.20	<0.01	0.20	0.19	0.03	0.01	0.07	0.04	0.01	<0.01	<0.01	<0.01	0.01	0.01

Sample_ID	KAC265/264	KAC266/266	KAC267/267	KAC268/275	KAC268/276	KAC268/278	KAC269/271	KAC269/272	KAC027/230	KAC272/274	KAC090/177	KAC090/178	KAC288	KAC300-2
Lat_S	-15.8731	-15.8685	-15.8662	-15.6131	-15.6131	-15.6131	-15.5956	-15.5956		-15.5439			-17.0926	-17.0713
Long_E	13.8107	13.8146	13.8141	13.8900	13.8900	13.8900	13.8898	13.8898		13.8908			13.5310	13.5391
Rocktype	non-olivine-bearing anorthosite	non-olivine-bearing anorthosite	olivine-bearing anorthosite	anorthosite	anorthosite	anorthosite	anorthosite	anorthosite		leucoctroctolite				sheared anorthosite
Group	KC	KC	KC	KC	KC	KC	KC	KC	KC	KC	KC	KC	KC	KC
SiO2_pct	50.18	52.20	50.36	49.87	49.23	49.25	52.87	52.67	56.68	49.02	48.86	49.81	53.08	41.78
TiO2_pct	0.59	0.32	0.27	0.19	0.53	0.26	0.13	0.19	1.59	0.28	0.55	0.23	1.26	0.40
Al2O3_pct	26.64	27.55	23.62	27.30	25.32	27.43	27.44	27.17	15.38	27.09	25.63	27.04	21.72	23.34
Fe2O3t_pct	3.70	1.64	5.97	2.95	5.28	3.25	1.54	1.91	8.71	3.37	5.13	3.79	4.94	4.50
MnO_pct	0.04	0.01	0.06	0.04	0.06	0.04	0.02	0.02	0.14	0.04	0.06	0.04	0.06	0.07
MgO_pct	1.72	0.47	5.15	2.08	2.40	2.41	0.45	0.49	3.41	2.71	3.32	2.70	1.33	1.48
CaO_pct	10.76	11.01	9.48	12.32	11.13	12.51	10.91	10.91	4.76	12.99	11.94	12.15	7.14	23.36
Na2O_pct	4.24	4.74	3.89	3.36	3.46	3.16	4.64	4.65	4.97	3.12	3.25	3.24	6.15	0.35

K2O_pct	0.26	0.55	0.37	0.18	0.32	0.24	0.51	0.33	0.29	0.26	0.29	0.25	0.87	<0.01
Cr2O3_pct	0.02	0.01	0.01	0.01	0.01	0.01	0.00	0.01	0.01	0.01	0.01	0.02	0.01	0.01
P2O5_pct	0.08	0.04	<0.01	<0.01	0.05	0.02	<0.01	<0.01	0.79	0.04	0.07	<0.01	0.14	0.04
Normalised*	98.27	98.59	99.23	98.29	97.77	98.59	98.55	98.44	96.78	98.97	99.15	99.27	96.74	95.28
SiO2_pct*	51.06	52.95	50.75	50.74	50.35	49.95	53.65	53.50	58.57	49.53	49.28	50.18	54.87	43.85
TiO2_pct*	0.60	0.33	0.28	0.19	0.54	0.27	0.13	0.19	1.63	0.29	0.56	0.24	1.29	0.41
Al2O3_pct*	51.06	52.95	50.75	50.74	50.35	49.95	53.65	53.50	58.57	49.53	49.28	50.18	54.87	43.85
Fe2O3t_pct*	3.77	1.66	6.02	3.00	5.40	3.30	1.56	1.94	9.00	3.41	5.17	3.82	5.11	4.72
FeO_pct*	3.20	1.41	5.11	2.55	4.59	2.80	1.33	1.65	7.65	2.89	4.40	3.25	4.34	4.01
Fe2O3_pct*	0.56	0.25	0.90	0.45	0.81	0.49	0.23	0.29	1.35	0.51	0.78	0.57	0.77	0.71
FeO*_pct	3.39	1.50	5.41	2.70	4.86	2.97	1.41	1.75	8.10	3.06	4.66	3.44	4.60	4.25
MnO_pct*	0.04	0.01	0.06	0.04	0.06	0.04	0.02	0.02	0.14	0.04	0.06	0.04	0.06	0.07
MgO_pct*	1.75	0.48	5.19	2.12	2.45	2.44	0.46	0.50	3.52	2.74	3.35	2.72	1.37	1.55
CaO_pct*	11.03	11.29	9.72	12.63	11.41	12.83	11.19	11.19	4.88	13.32	12.24	12.46	7.32	23.95
Na2O_pct*	4.35	4.86	3.99	3.44	3.55	3.24	4.76	4.77	5.10	3.20	3.33	3.32	6.31	0.36
K2O_pct*	0.27	0.56	0.38	0.18	0.33	0.25	0.52	0.34	0.30	0.27	0.30	0.26	0.89	N/D
Cr2O3_pct*	0.02	0.01	0.01	0.01	0.01	0.01	0.00	0.01	0.01	0.01	0.01	0.02	0.01	0.01
P2O5_pct*	0.08	0.04	N/D	N/D	0.05	0.02	N/D	N/D	0.81	0.04	0.07	N/D	0.14	0.04
Mg#	49.36	37.53	64.39	59.65	48.80	60.86	37.99	34.97	45.08	62.77	57.57	59.90	36.08	40.81
Mo_pct	<0.001	<0.001	<0.001	<0.001	<0.001	<0.001	<0.001	<0.001	<0.001	<0.001	<0.001	<0.001	<0.001	<0.001
Cu_pct	<0.001	0.00	0.00	<0.001	0.00	0.00	0.05	0.06	0.00	0.00	0.00	0.00	0.05	0.00
Pb_pct	<0.02	<0.02	<0.02	<0.02	<0.02	<0.02	<0.02	<0.02	<0.02	<0.02	<0.02	<0.02	<0.02	<0.02
Zn_pct	<0.01	<0.01	<0.01	<0.01	<0.01	<0.01	<0.01	<0.01	<0.01	<0.01	<0.01	<0.01	<0.01	<0.01
Ag_ppm	<2	<2	<2	<2	<2	<2	<2	<2	<2	<2	<2	<2	<2	<2
Ni_ppm	44.00	18.00	157.00	46.00	31.00	79.00	256.00	308.00	37.00	85.00	97.00	75.00	36.00	32.00

Mo_ppm	0.26	0.60	0.37	0.20	0.24	0.18	0.44	0.85	0.23	0.29	0.27	0.47	1.22	0.31
Cu_ppm	2.30	10.03	10.82	8.67	10.61	16.20	542.56	497.74	10.32	19.26	20.10	6.42	461.89	14.39
Pb_ppm	0.59	0.58	0.28	0.87	0.57	0.42	1.32	2.13	3.35	0.64	0.52	0.74	13.37	2.22
Zn_ppm	13.80	6.10	26.10	11.70	22.40	14.30	13.30	11.70	95.60	16.70	20.00	18.70	68.80	22.10
Ag_ppb	9.00	13.00	6.00	6.00	7.00	11.00	359.00	219.00	36.00	15.00	5.00	13.00	273.00	32.00
Ni_ppm	34.80	13.90	124.60	28.70	22.40	53.60	185.30	194.40	35.40	71.90	91.70	68.40	33.50	29.50
Co_ppm	10.30	3.70	32.30	9.20	15.50	13.90	5.30	6.10	23.10	17.10	24.60	20.30	27.30	12.80
Mn_ppm	140.00	56.00	380.00	138.00	237.00	164.00	77.00	70.00	953.00	218.00	302.00	238.00	180.00	319.00
As_ppm	0.30	0.40	0.20	0.30	0.40	0.30	0.40	0.50	0.20	0.60	0.50	0.50	0.40	0.20
Au_ppb	1.50	0.90	0.30	<0.2	<0.2	0.40	0.90	1.40	0.80	<0.2	<0.2	<0.2	0.90	<0.2
Cd_ppm	0.01	<0.01	<0.01	<0.01	<0.01	<0.01	0.09	0.08	0.02	0.02	<0.01	0.02	0.13	<0.01
Sb_ppm	<0.02	<0.02	<0.02	<0.02	<0.02	<0.02	<0.02	<0.02	<0.02	<0.02	<0.02	<0.02	0.04	<0.02
Bi_ppm	<0.02	<0.02	<0.02	<0.02	<0.02	<0.02	0.21	0.21	<0.02	<0.02	<0.02	<0.02	<0.02	<0.02
Cr_ppm	129.80	54.00	48.90	23.90	57.00	21.30	24.90	17.50	47.50	26.10	32.80	63.70	24.50	58.90
Hg_ppb	<5	<5	<5	<5	<5	<5	<5	<5	<5	<5	<5	6.00	<5	<5
Se_ppm	<0.1	<0.1	<0.1	<0.1	<0.1	<0.1	<0.1	<0.1	<0.1	<0.1	<0.1	<0.1	0.40	<0.1
Te_ppm	<0.02	<0.02	<0.02	<0.02	<0.02	<0.02	0.15	0.10	0.03	<0.02	<0.02	<0.02	0.02	<0.02
Ge_ppm	<0.1	<0.1	<0.1	<0.1	<0.1	<0.1	<0.1	<0.1	0.20	<0.1	<0.1	<0.1	<0.1	0.20
In_ppm	<0.02	<0.02	<0.02	<0.02	<0.02	<0.02	<0.02	<0.02	0.04	<0.02	<0.02	<0.02	<0.02	<0.02
Re_ppb	<1	<1	<1	<1	<1	<1	<1	<1	<1	<1	<1	<1	<1	<1
Be_ppm	0.10	0.20	<0.1	0.20	0.20	<0.1	0.20	0.30	1.10	0.30	<0.1	0.10	0.80	0.30
Li_ppm	6.10	1.80	1.70	2.00	2.20	1.80	9.80	12.50	16.00	2.10	2.20	1.80	16.20	11.70
Pd_ppb	<10	<10	<10	<10	<10	<10	<10	<10	10.00	<10	<10	<10	<10	<10
Pt_ppb	<2	<2	<2	<2	<2	<2	<2	<2	<2	<2	<2	<2	<2	<2
Au_ppb	8.00	8.00	8.00	6.00	6.00	7.00	7.00	9.00	5.00	5.00	7.00	5.00	3.00	3.00

Pt_ppb	0.80	0.50	0.40	0.60	0.70	0.60	2.60	2.10	1.00	0.30	1.00	0.50	0.10	0.20
Pd_ppb	1.50	1.40	1.10	1.10	1.50	1.50	3.60	3.00	1.80	1.20	1.40	1.20	0.60	0.80
B_ppm	<1	2.00	<1	<1	<1	<1	<1	1.00	2.00	<1	<1	<1	4.00	2.00
Tl_ppm	<0.02	<0.02	<0.02	<0.02	<0.02	<0.02	0.02	0.04	<0.02	<0.02	<0.02	<0.02	0.07	<0.02
LOI_pct	1.60	1.30	0.60	1.60	2.10	1.30	1.30	1.40	3.00	0.90	0.70	0.60	3.00	4.60
TOT/C_TC000_pct	<0.02	0.03	<0.02	<0.02	<0.02	<0.02	<0.02	<0.02	0.08	0.02	0.09	0.08	0.12	<0.02
TOT/S_pct	<0.02	<0.02	<0.02	<0.02	<0.02	<0.02	0.03	<0.02	<0.02	<0.02	0.03	<0.02	0.07	<0.02
Ba_ppm	192.00	242.00	218.00	180.00	243.00	151.00	340.00	417.00	101.00	145.00	156.00	152.00	199.00	17.00
Sc_ppm	3.00	1.00	2.00	1.00	8.00	2.00	<1	2.00	21.00	4.00	5.00	2.00	6.00	7.00
Sum_pct	99.87	99.89	99.83	99.89	99.87	99.89	99.85	99.84	99.78	99.87	99.85	99.87	99.74	99.88
Cs_ppm	<0.1	<0.1	<0.1	<0.1	<0.1	<0.1	0.90	1.30	0.50	<0.1	<0.1	<0.1	0.80	<0.1
Ga_ppm	17.60	17.30	16.40	19.10	18.20	17.30	17.00	17.50	20.50	18.10	18.80	18.80	19.10	25.00
Hf_ppm	0.80	0.50	0.40	0.40	0.80	0.40	0.40	0.30	5.70	0.50	0.90	0.20	8.80	0.60
Nb_ppm	2.50	0.70	0.30	0.50	1.70	0.60	1.70	0.60	15.70	1.30	2.00	0.40	18.00	2.10
Rb_ppm	1.40	3.60	1.70	0.90	3.40	2.20	31.90	14.20	4.70	2.50	3.30	1.60	41.00	0.70
Sn_ppm	<1	<1	<1	<1	<1	<1	<1	<1	1.00	<1	<1	<1	<1	<1
Sr_ppm	735.70	789.60	658.70	618.10	627.30	531.50	641.20	668.70	457.50	600.80	635.20	663.00	495.40	613.50
Ta_ppm	0.20	<0.1	<0.1	<0.1	<0.1	<0.1	0.10	<0.1	1.10	<0.1	0.20	<0.1	1.00	<0.1
Th_ppm	0.30	<0.2	<0.2	<0.2	0.60	<0.2	1.00	<0.2	7.20	0.30	0.50	<0.2	19.20	0.30
U_ppm	<0.1	<0.1	<0.1	<0.1	<0.1	<0.1	0.20	<0.1	2.20	<0.1	<0.1	<0.1	2.00	<0.1
V_ppm	62.00	31.00	27.00	19.00	80.00	30.00	13.00	27.00	165.00	29.00	69.00	37.00	103.00	96.00
W_ppm	1.00	1.30	2.20	2.00	2.30	1.50	1.20	3.70	2.30	1.00	0.90	2.40	1.10	1.40
Zr_ppm	30.60	17.60	13.40	17.10	33.60	17.10	11.70	11.30	239.50	22.30	35.90	6.60	353.00	23.10
Y_ppm	4.40	3.00	1.40	2.30	6.50	2.90	4.40	3.40	42.20	4.00	6.30	1.10	28.50	5.20
La_ppm	5.00	4.10	2.90	2.70	5.30	3.00	3.10	4.20	63.20	4.00	5.30	2.90	68.50	3.50

Ce_ppm	9.20	7.80	4.80	5.30	11.30	5.60	4.40	5.40	122.60	8.10	10.70	5.40	133.40	7.50
Pr_ppm	1.12	0.91	0.53	0.62	1.36	0.70	0.62	0.79	15.81	1.00	1.35	0.57	13.68	0.94
Nd_ppm	4.70	4.00	2.20	2.60	6.30	2.80	2.50	3.60	60.90	4.50	6.00	2.30	48.60	4.40
Sm_ppm	0.96	0.68	0.32	0.51	1.27	0.64	0.56	0.68	11.11	0.82	1.27	0.35	7.99	0.98
Eu_ppm	0.82	0.75	0.64	0.76	1.00	0.69	0.50	0.63	2.71	0.68	0.81	0.68	1.70	0.67
Gd_ppm	0.97	0.74	0.35	0.49	1.39	0.64	0.68	0.65	9.63	0.79	1.34	0.32	6.33	1.12
Tb_ppm	0.13	0.09	0.04	0.07	0.19	0.09	0.10	0.10	1.35	0.12	0.20	0.04	0.97	0.17
Dy_ppm	0.78	0.55	0.24	0.41	1.16	0.51	0.64	0.56	7.81	0.72	1.23	0.27	5.61	0.90
Ho_ppm	0.16	0.10	0.05	0.07	0.24	0.10	0.15	0.11	1.40	0.14	0.25	0.04	1.16	0.19
Er_ppm	0.45	0.27	0.14	0.24	0.71	0.30	0.44	0.31	3.97	0.38	0.70	0.13	3.31	0.59
Tm_ppm	0.05	0.04	0.02	0.02	0.08	0.04	0.06	0.04	0.54	0.05	0.09	0.02	0.47	0.08
Yb_ppm	0.39	0.22	0.11	0.20	0.54	0.28	0.37	0.26	3.29	0.33	0.53	0.08	3.36	0.54
Lu_ppm	0.06	0.03	0.02	0.03	0.09	0.03	0.05	0.03	0.51	0.05	0.08	0.01	0.52	0.08

Sample_ID	KAC323	KAC327	KAC328	KAC329	KAC339-1	KAC339-2	KAC340-1	KAC340-2	KAC377	KAC378-1	KAC381-1	KAC382-1	KAC393-1	KAC399-1
Lat_S	-17.0276	-16.8726	-16.8723	-16.8714	-16.5917	-16.5917	-16.5914	-16.5914	-16.8407	-17.4245	-17.3940	-17.4085	-17.3776	-17.3741
Long_E	13.5040	13.4702	13.4692	13.4682	13.4670	13.4670	13.4650	13.4650	13.5125	13.4329	13.6039	13.4011	13.3037	13.3037
Rocktype	Schistosed anorthosite	anorthosite	pegmatitic anorthosite	leuconorite	metasomatised anorthosite	metasomatised anorthosite	Anorthosite	Anorthosite	Anorthosite	Leucotrocolite	Anorthosite	Pegmatoidal leuconorite	Pegmatoidal leuconorite	Norite with magmatic foliation
Group	KC	KC	KC	KC	KC	KC	KC	KC	KC	KC	KC	KC	KC	KC
SiO2_pct	50.15	46.03	42.75	50.44	59.98	57.03	51.25	64.72	45.02	49.62	51.66	51.14	50.96	47.75
TiO2_pct	0.35	0.07	0.07	0.17	0.21	0.27	0.41	0.65	0.17	0.11	0.08	0.14	0.26	0.09
Al2O3_pct	22.30	22.91	15.79	20.61	21.46	21.65	26.62	16.43	18.93	24.21	29.17	28.82	17.58	24.22
Fe2O3t_pct	5.36	7.20	14.08	4.48	2.33	2.95	1.58	4.08	12.05	5.64	0.81	1.27	8.02	5.60

MnO_pct	0.07	0.09	0.17	0.08	0.04	0.09	0.02	0.05	0.15	0.07	<0.01	0.02	0.13	0.06
MgO_pct	4.19	8.55	16.09	4.07	1.07	0.33	0.50	1.21	10.36	5.52	0.29	0.77	10.28	5.81
CaO_pct	9.37	10.83	7.18	13.54	3.70	8.07	9.98	1.69	9.16	10.40	12.67	13.04	8.08	10.17
Na2O_pct	4.21	2.23	1.70	3.53	8.29	7.46	4.20	5.23	2.26	3.37	3.95	3.60	2.37	2.29
K2O_pct	1.01	0.13	0.15	0.20	0.84	0.05	2.27	3.62	0.32	0.30	0.27	0.31	0.22	0.11
Cr2O3_pct	0.04	0.01	0.01	0.03	0.00	0.00	0.01	0.00	0.01	0.00	0.01	0.01	0.04	0.01
P2O5_pct	0.04	<0.01	<0.01	<0.01	0.06	0.03	0.06	0.13	0.01	<0.01	<0.01	<0.01	<0.01	0.01
Normalised*	97.17	98.10	98.08	97.16	97.98	97.93	97.00	97.99	98.44	99.34	98.93	99.12	97.97	96.15
SiO2_pct*	51.61	46.92	43.59	51.91	61.22	58.24	52.84	66.05	45.73	49.95	52.22	51.59	52.02	49.66
TiO2_pct*	0.36	0.07	0.07	0.17	0.22	0.28	0.42	0.67	0.17	0.11	0.08	0.14	0.27	0.09
Al2O3_pct*	51.61	46.92	43.59	51.91	61.22	58.24	52.84	66.05	45.73	49.95	52.22	51.59	52.02	49.66
Fe2O3t_pct*	5.52	7.34	14.36	4.61	2.38	3.01	1.63	4.16	12.24	5.68	0.82	1.28	8.19	5.82
FeO_pct*	4.69	6.24	12.20	3.92	2.02	2.56	1.38	3.54	10.40	4.83	0.70	1.09	6.96	4.95
Fe2O3_pct*	0.83	1.10	2.15	0.69	0.36	0.45	0.24	0.62	1.84	0.85	0.12	0.19	1.23	0.87
FeO*_pct	4.96	6.61	12.92	4.15	2.14	2.71	1.47	3.75	11.02	5.11	0.74	1.15	7.37	5.24
MnO_pct*	0.07	0.09	0.17	0.08	0.04	0.09	0.02	0.05	0.15	0.07	N/D	0.02	0.13	0.06
MgO_pct*	4.31	8.72	16.40	4.19	1.09	0.34	0.52	1.23	10.52	5.56	0.29	0.78	10.49	6.04
CaO_pct*	9.61	11.10	7.36	13.88	3.79	8.27	10.23	1.73	9.39	10.66	12.99	13.37	8.28	10.43
Na2O_pct*	4.32	2.29	1.74	3.62	8.50	7.65	4.31	5.36	2.32	3.45	4.05	3.69	2.43	2.35
K2O_pct*	1.04	0.13	0.15	0.21	0.86	0.05	2.33	3.71	0.33	0.31	0.28	0.32	0.23	0.11
Cr2O3_pct*	0.04	0.01	0.01	0.03	0.00	0.00	0.01	0.00	0.01	0.00	0.01	0.01	0.04	0.01
P2O5_pct*	0.04	N/D	N/D	N/D	0.06	0.03	0.06	0.13	0.01	N/D	N/D	N/D	N/D	0.01
Mg#	62.10	71.34	70.55	65.57	49.05	19.00	39.88	38.34	64.32	67.23	42.88	55.97	72.88	68.50
Mo_pct	<0.001	<0.001	<0.001	<0.001	<0.001	<0.001	<0.001	<0.001	<0.001	<0.001	<0.001	<0.001	<0.001	<0.001
Cu_pct	0.00	<0.001	<0.001	<0.001	<0.001	<0.001	0.00	<0.001	0.01	<0.001	<0.001	0.00	0.00	0.00

Pb_pct	<0.02	<0.02	<0.02	<0.02	<0.02	<0.02	<0.02	<0.02	<0.02	<0.02	<0.02	<0.02	<0.02	<0.02
Zn_pct	<0.01	<0.01	<0.01	<0.01	<0.01	<0.01	<0.01	<0.01	<0.01	<0.01	<0.01	<0.01	<0.01	<0.01
Ag_ppm	<2	<2	<2	<2	<2	<2	<2	<2	<2	<2	<2	<2	<2	<2
Ni_ppm	57.00	265.00	414.00	85.00	19.00	<10	25.00	<10	249.00	168.00	10.00	14.00	140.00	180.00
Mo_ppm	0.11	0.33	0.27	0.22	0.15	0.32	0.20	0.19	0.12	0.18	0.20	0.29	0.10	0.18
Cu_ppm	8.37	5.50	5.91	2.63	2.22	2.90	18.36	3.57	61.31	4.86	1.90	7.32	22.65	9.51
Pb_ppm	0.80	0.41	0.25	0.29	1.34	2.31	4.96	5.99	0.45	0.24	0.25	0.45	0.22	0.25
Zn_ppm	28.30	35.20	69.50	13.10	18.80	9.50	6.30	56.30	67.50	13.80	3.30	5.90	16.80	30.30
Ag_ppb	197.00	16.00	134.00	11.00	24.00	31.00	19.00	29.00	21.00	8.00	6.00	8.00	14.00	102.00
Ni_ppm	44.00	239.40	377.60	52.20	18.30	5.00	21.20	7.20	220.00	133.20	8.50	8.80	41.60	153.90
Co_ppm	23.60	54.60	103.40	14.90	6.60	3.10	4.90	7.80	74.90	30.10	1.50	2.50	15.40	36.70
Mn_ppm	321.00	585.00	1182.00	206.00	214.00	438.00	85.00	335.00	1017.00	372.00	40.00	80.00	290.00	351.00
As_ppm	<0.1	<0.1	<0.1	<0.1	<0.1	0.30	0.20	<0.1	<0.1	0.10	<0.1	0.20	<0.1	<0.1
Au_ppb	<0.2	<0.2	<0.2	<0.2	<0.2	<0.2	0.30	0.20	<0.2	0.50	0.20	0.20	<0.2	0.30
Cd_ppm	<0.01	0.01	0.02	0.03	<0.01	0.01	0.03	<0.01	0.02	<0.01	<0.01	<0.01	<0.01	<0.01
Sb_ppm	0.02	<0.02	<0.02	<0.02	<0.02	<0.02	<0.02	<0.02	<0.02	<0.02	<0.02	<0.02	<0.02	<0.02
Bi_ppm	<0.02	<0.02	<0.02	<0.02	<0.02	<0.02	<0.02	<0.02	<0.02	<0.02	<0.02	<0.02	<0.02	<0.02
Cr_ppm	94.70	37.80	24.90	49.10	17.20	5.10	41.80	16.80	23.60	11.50	24.00	18.30	61.00	23.10
Hg_ppb	<5	<5	<5	<5	<5	<5	<5	<5	<5	<5	<5	<5	<5	<5
Se_ppm	<0.1	<0.1	<0.1	<0.1	<0.1	<0.1	0.10	<0.1	<0.1	<0.1	<0.1	<0.1	<0.1	<0.1
Te_ppm	<0.02	0.02	<0.02	<0.02	<0.02	0.04	<0.02	<0.02	<0.02	<0.02	<0.02	<0.02	<0.02	<0.02
Ge_ppm	<0.1	<0.1	<0.1	<0.1	<0.1	<0.1	<0.1	<0.1	<0.1	<0.1	<0.1	<0.1	<0.1	<0.1
In_ppm	<0.02	<0.02	<0.02	<0.02	<0.02	<0.02	<0.02	0.03	<0.02	<0.02	<0.02	<0.02	<0.02	<0.02
Re_ppb	<1	<1	<1	<1	<1	<1	<1	<1	<1	<1	<1	<1	<1	<1
Be_ppm	0.10	<0.1	<0.1	<0.1	0.30	0.30	0.10	0.90	0.10	<0.1	<0.1	0.10	<0.1	<0.1

Li_ppm	16.40	1.80	2.80	2.00	9.40	1.00	6.50	13.80	3.50	1.00	0.40	1.20	0.60	1.40
Pd_ppb	<10	<10	<10	<10	<10	<10	<10	<10	<10	<10	<10	<10	<10	<10
Pt_ppb	<2	<2	<2	<2	<2	3.00	<2	<2	<2	<2	<2	<2	<2	<2
Au_ppb	3.00	3.00	2.00	3.00	2.00	2.00	2.00	3.00	3.00	3.00	3.00	3.00	2.00	4.00
Pt_ppb	0.20	0.20	0.20	0.50	1.10	2.80	0.20	0.20	0.20	0.20	0.30	0.40	0.20	0.40
Pd_ppb	1.00	0.80	0.60	1.10	0.80	0.50	<0.5	<0.5	<0.5	<0.5	<0.5	0.70	0.90	0.90
B_ppm	<1	<1	<1	<1	1.00	1.00	5.00	1.00	3.00	1.00	<1	<1	2.00	1.00
Tl_ppm	<0.02	<0.02	<0.02	<0.02	<0.02	<0.02	0.04	0.03	<0.02	<0.02	<0.02	<0.02	<0.02	<0.02
LOI_pct	2.70	1.70	1.60	2.70	1.90	1.60	2.90	1.80	1.30	0.50	1.00	0.80	1.80	3.70
TOT/C_TC000_pct	0.04	0.04	0.02	0.06	0.02	0.04	0.05	0.07	<0.02	0.04	<0.02	0.02	0.07	0.08
TOT/S_pct	<0.02	<0.02	<0.02	<0.02	<0.02	<0.02	0.03	<0.02	<0.02	<0.02	<0.02	<0.02	<0.02	<0.02
Ba_ppm	399.00	66.00	68.00	83.00	176.00	100.00	774.00	1178.00	158.00	159.00	159.00	159.00	122.00	70.00
Sc_ppm	9.00	3.00	5.00	11.00	2.00	3.00	3.00	7.00	7.00	3.00	<1	4.00	21.00	2.00
Sum_pct	99.87	99.80	99.68	99.86	99.88	99.53	99.90	99.79	99.74	99.84	99.93	99.92	99.77	99.85
Cs_ppm	0.40	0.30	<0.1	0.10	0.30	<0.1	2.80	0.80	0.20	<0.1	<0.1	<0.1	0.40	0.20
Ga_ppm	16.00	14.50	10.50	14.90	10.80	20.50	17.00	17.10	14.60	16.60	17.70	17.10	13.30	14.80
Hf_ppm	0.50	<0.1	<0.1	0.20	1.50	18.00	0.60	10.70	0.20	<0.1	<0.1	0.20	0.20	0.10
Nb_ppm	1.00	<0.1	<0.1	<0.1	2.40	3.70	1.00	16.50	0.50	0.10	<0.1	0.30	0.20	0.20
Rb_ppm	36.30	1.00	1.70	3.10	15.90	1.10	43.60	61.50	3.60	1.50	1.30	1.50	3.80	1.00
Sn_ppm	<1	<1	<1	<1	<1	<1	<1	<1	<1	<1	<1	<1	<1	<1
Sr_ppm	405.70	436.20	303.80	506.10	677.50	2208.30	688.90	286.90	440.10	507.00	566.50	573.80	321.60	384.60
Ta_ppm	<0.1	<0.1	<0.1	<0.1	0.10	0.20	<0.1	0.70	<0.1	<0.1	<0.1	<0.1	<0.1	<0.1
Th_ppm	<0.2	<0.2	<0.2	<0.2	2.10	12.10	0.30	25.60	<0.2	<0.2	<0.2	<0.2	<0.2	<0.2
U_ppm	<0.1	<0.1	<0.1	<0.1	0.50	1.70	<0.1	2.50	<0.1	<0.1	<0.1	<0.1	<0.1	<0.1
V_ppm	69.00	18.00	22.00	61.00	17.00	39.00	43.00	44.00	22.00	13.00	<8	21.00	125.00	16.00

W_ppm	0.60	1.30	1.10	3.10	2.70	18.60	8.50	0.90	0.60	<0.5	1.00	0.50	<0.5	0.90
Zr_ppm	19.80	3.30	2.30	7.90	55.30	650.10	21.60	455.20	7.50	2.30	2.00	6.10	5.10	5.20
Y_ppm	4.40	0.70	0.50	3.00	7.80	18.40	3.60	22.30	1.50	0.90	0.40	1.90	2.20	0.90
La_ppm	3.40	1.00	0.70	1.40	39.20	209.20	6.40	144.10	1.70	1.70	1.60	2.20	0.90	1.40
Ce_ppm	6.70	1.90	1.60	3.30	60.70	402.60	11.30	267.90	3.20	2.90	2.80	3.90	1.70	2.30
Pr_ppm	0.81	0.19	0.12	0.36	6.75	42.01	1.29	27.30	0.32	0.31	0.28	0.46	0.19	0.24
Nd_ppm	3.90	0.70	0.80	2.10	22.90	139.50	5.20	89.30	1.60	1.30	1.10	2.10	1.00	1.20
Sm_ppm	0.80	0.13	0.09	0.49	3.57	16.72	0.87	12.33	0.29	0.20	0.13	0.36	0.17	0.19
Eu_ppm	0.61	0.41	0.28	0.63	0.91	1.31	0.98	1.92	0.46	0.55	0.54	0.65	0.36	0.47
Gd_ppm	0.99	0.17	0.14	0.57	2.55	9.89	0.86	8.70	0.40	0.20	0.17	0.38	0.30	0.19
Tb_ppm	0.13	0.02	0.01	0.09	0.35	1.00	0.12	0.99	0.05	0.02	0.02	0.05	0.06	0.03
Dy_ppm	0.90	0.08	0.11	0.52	1.81	4.51	0.63	4.71	0.30	0.18	0.12	0.35	0.39	0.11
Ho_ppm	0.18	0.02	<0.02	0.11	0.33	0.74	0.14	0.84	0.07	0.02	<0.02	0.07	0.10	0.04
Er_ppm	0.47	0.08	0.07	0.39	0.84	1.91	0.35	2.50	0.18	0.09	0.04	0.20	0.37	0.07
Tm_ppm	0.06	<0.01	<0.01	0.04	0.13	0.29	0.05	0.33	0.02	0.01	<0.01	0.02	0.04	0.01
Yb_ppm	0.40	0.10	0.10	0.29	0.77	2.22	0.28	2.10	0.17	0.08	<0.05	0.14	0.34	0.09
Lu_ppm	0.05	<0.01	0.01	0.04	0.14	0.38	0.04	0.34	0.03	0.01	<0.01	0.02	0.06	0.01
Sample_ID	KAC402-1	KAC403-1	KAC404-1	KAC404-2	KAC405-1	KAC407-1	KAC408-1	KAC409-1	KAC410-1	KAC411-1	KAC411-2	KAC412-1	KAC415-1	KAC416-1
Lat_S	-17.3641	-17.3614	-17.3580	-17.3580	-17.3589	-17.3512	-17.3484	-17.3476	-17.3459	-17.3443	-17.3443	-17.3414	-17.3747	-17.3747
Long_E	13.3024	13.3014	13.3009	13.3009	13.3011	13.2982	13.3062	13.3079	13.3118	13.3116	13.3116	13.3126	13.2672	13.2669
Rocktype	Olivine-bearing anorthosite	Leucotroctolite	Leuconorite	lamination in leuconorite	red material replacing opx	Leucotroctolite	Leucotroctolite	Leuconorite	Leuconorite	Leuconorite with lamination	Leuconorite	Metasomatised anorthosite s.s.	Leuconorite	Mylonite
Group	KC	KC	KC	KC	KC	KC	KC	KC	KC	KC	KC	KC	KC	KC

SiO2_pct	49.54	48.59	52.44	50.14	50.88	48.26	49.76	51.86	48.57	50.10	50.05	53.19	45.48	44.86
TiO2_pct	0.15	0.10	0.09	0.10	0.11	0.13	0.33	0.10	0.10	0.09	0.24	0.10	0.30	0.22
Al2O3_pct	25.68	23.12	27.66	26.84	27.46	23.60	21.99	27.94	22.61	26.41	23.73	28.42	14.87	21.51
Fe2O3t_pct	3.85	6.25	1.44	3.07	2.07	6.23	5.30	1.41	7.52	3.79	4.90	0.63	9.85	5.09
MnO_pct	0.05	0.07	0.02	0.02	0.03	0.07	0.09	0.02	0.08	0.04	0.05	<0.01	0.13	0.08
MgO_pct	3.77	6.68	1.13	3.64	1.95	6.38	5.71	0.93	6.32	2.76	3.60	0.28	10.07	8.41
CaO_pct	11.56	10.11	11.63	9.44	11.72	10.10	12.34	11.60	9.29	10.44	11.10	11.36	12.39	12.89
Na2O_pct	3.41	3.15	3.95	3.65	3.76	3.24	2.86	4.33	3.49	3.49	3.16	4.46	1.97	2.11
K2O_pct	0.19	0.20	0.25	0.21	0.17	0.23	0.17	0.26	0.25	0.24	0.22	0.49	0.07	0.55
Cr2O3_pct	0.01	0.01	0.01	0.00	0.01	0.01	0.04	0.00	0.01	0.00	0.03	0.01	0.03	0.12
P2O5_pct	<0.01	<0.01	<0.01	<0.01	<0.01	<0.01	<0.01	<0.01	<0.01	<0.01	<0.01	<0.01	<0.01	<0.01
Normalised *	98.17	98.32	98.62	97.08	98.20	98.33	98.62	98.42	98.24	97.39	97.07	99.03	95.21	95.89
SiO2_pct*	50.46	49.42	53.17	51.65	51.81	49.08	50.46	52.69	49.44	51.44	51.56	53.71	47.77	46.78
TiO2_pct*	0.15	0.10	0.09	0.10	0.11	0.13	0.34	0.10	0.10	0.09	0.25	0.10	0.31	0.23
Al2O3_pct*	50.46	49.42	53.17	51.65	51.81	49.08	50.46	52.69	49.44	51.44	51.56	53.71	47.77	46.78
Fe2O3t_pct *	3.92	6.36	1.46	3.16	2.11	6.34	5.37	1.43	7.65	3.89	5.05	0.64	10.35	5.31
FeO_pct*	3.33	5.40	1.24	2.69	1.79	5.39	4.57	1.22	6.51	3.31	4.29	0.54	8.79	4.51
Fe2O3_pct*	0.59	0.95	0.22	0.47	0.32	0.95	0.81	0.21	1.15	0.58	0.76	0.10	1.55	0.80
FeO*_pct	3.53	5.72	1.31	2.85	1.90	5.70	4.84	1.29	6.89	3.50	4.54	0.57	9.31	4.78
MnO_pct*	0.05	0.07	0.02	0.02	0.03	0.07	0.09	0.02	0.08	0.04	0.05	N/D	0.13	0.08
MgO_pct*	3.84	6.79	1.15	3.75	1.99	6.49	5.79	0.94	6.43	2.83	3.71	0.28	10.58	8.77
CaO_pct*	11.85	10.36	11.92	9.68	12.02	10.35	12.65	11.89	9.52	10.70	11.38	11.65	12.70	13.22
Na2O_pct*	3.50	3.23	4.05	3.74	3.85	3.32	2.93	4.44	3.58	3.58	3.24	4.57	2.02	2.16
K2O_pct*	0.19	0.21	0.26	0.22	0.17	0.24	0.17	0.27	0.26	0.25	0.23	0.50	0.07	0.56
Cr2O3_pct*	0.01	0.01	0.01	0.00	0.01	0.01	0.04	0.00	0.01	0.00	0.03	0.01	0.03	0.12

P2O5_pct*	N/D	N/D	N/D	N/D	N/D	N/D	N/D	N/D	N/D	N/D	N/D	N/D	N/D	N/D
Mg#	67.24	69.14	62.19	71.31	66.39	68.22	69.31	58.03	63.79	60.42	60.63	48.23	68.19	77.60
Mo_pct	<0.001	<0.001	<0.001	<0.001	<0.001	<0.001	<0.001	<0.001	<0.001	<0.001	<0.001	<0.001	<0.001	<0.001
Cu_pct	0.00	0.00	0.00	<0.001	<0.001	0.00	0.00	<0.001	0.00	0.00	0.00	<0.001	0.04	0.01
Pb_pct	<0.02	<0.02	<0.02	<0.02	<0.02	<0.02	<0.02	<0.02	<0.02	<0.02	<0.02	<0.02	<0.02	<0.02
Zn_pct	<0.01	<0.01	<0.01	<0.01	<0.01	<0.01	<0.01	<0.01	<0.01	<0.01	<0.01	<0.01	<0.01	<0.01
Ag_ppm	<2	<2	<2	<2	<2	<2	<2	<2	<2	<2	<2	<2	<2	<2
Ni_ppm	97.00	172.00	36.00	81.00	36.00	202.00	100.00	33.00	167.00	70.00	78.00	<10	375.00	181.00
Mo_ppm	0.20	0.21	0.25	0.16	0.15	0.39	0.23	0.29	0.26	0.19	0.30	0.34	0.08	0.24
Cu_ppm	7.76	10.56	5.02	6.06	2.22	11.07	9.85	6.70	11.45	5.11	8.77	2.31	299.24	44.30
Pb_ppm	0.27	0.23	0.21	0.30	0.22	0.20	0.23	0.17	0.16	0.14	0.22	0.18	0.32	0.28
Zn_ppm	14.40	27.70	7.70	23.40	13.50	29.00	13.60	6.80	33.50	20.80	26.40	2.60	25.60	14.40
Ag_ppb	10.00	12.00	4.00	60.00	53.00	10.00	8.00	8.00	51.00	59.00	14.00	6.00	339.00	34.00
Ni_ppm	73.20	154.30	32.00	73.30	30.80	182.00	49.90	25.10	147.30	64.70	65.00	7.70	284.40	137.90
Co_ppm	20.80	43.00	7.30	24.50	11.20	42.40	15.90	7.10	45.70	23.90	23.20	1.00	51.20	25.70
Mn_ppm	240.00	480.00	92.00	134.00	160.00	475.00	191.00	98.00	575.00	238.00	273.00	36.00	500.00	240.00
As_ppm	<0.1	<0.1	0.20	<0.1	<0.1	<0.1	1.30	0.10	0.20	<0.1	<0.1	<0.1	0.20	13.70
Au_ppb	<0.2	<0.2	<0.2	<0.2	0.60	<0.2	<0.2	<0.2	<0.2	<0.2	<0.2	<0.2	<0.2	0.50
Cd_ppm	<0.01	<0.01	<0.01	<0.01	<0.01	<0.01	<0.01	<0.01	<0.01	<0.01	<0.01	<0.01	0.03	0.05
Sb_ppm	<0.02	<0.02	<0.02	<0.02	<0.02	<0.02	<0.02	<0.02	<0.02	<0.02	<0.02	<0.02	<0.02	<0.02
Bi_ppm	<0.02	<0.02	<0.02	<0.02	<0.02	<0.02	<0.02	<0.02	<0.02	<0.02	<0.02	<0.02	<0.02	<0.02
Cr_ppm	10.00	7.30	31.80	7.30	24.00	11.30	91.60	5.00	34.60	6.20	123.70	38.00	99.30	383.50
Hg_ppb	<5	<5	<5	<5	<5	<5	<5	<5	<5	<5	<5	<5	<5	<5
Se_ppm	<0.1	<0.1	<0.1	<0.1	<0.1	<0.1	<0.1	<0.1	<0.1	<0.1	<0.1	<0.1	<0.1	<0.1
Te_ppm	<0.02	<0.02	<0.02	<0.02	<0.02	<0.02	<0.02	<0.02	<0.02	<0.02	<0.02	<0.02	<0.02	<0.02

Ge_ppm	<0.1	<0.1	<0.1	<0.1	<0.1	<0.1	<0.1	<0.1	<0.1	<0.1	<0.1	<0.1	<0.1	<0.1
In_ppm	<0.02	<0.02	<0.02	<0.02	<0.02	<0.02	<0.02	<0.02	<0.02	<0.02	<0.02	<0.02	<0.02	<0.02
Re_ppb	<1	<1	<1	<1	<1	<1	<1	<1	<1	<1	<1	<1	<1	<1
Be_ppm	<0.1	<0.1	<0.1	<0.1	<0.1	<0.1	<0.1	<0.1	<0.1	<0.1	<0.1	<0.1	<0.1	<0.1
Li_ppm	0.60	0.90	0.80	4.00	1.40	0.70	1.00	1.50	0.90	20.50	13.00	1.60	31.00	33.80
Pd_ppb	<10	<10	<10	<10	<10	<10	<10	<10	<10	<10	<10	<10	<10	<10
Pt_ppb	<2	<2	<2	<2	<2	<2	<2	<2	<2	<2	<2	<2	<2	<2
Au_ppb	3.00	3.00	3.00	3.00	2.00	2.00	3.00	2.00	4.00	2.00	2.00	3.00	3.00	3.00
Pt_ppb	0.20	0.30	0.30	0.20	0.20	0.20	0.10	0.20	0.20	0.10	0.20	0.20	0.30	0.30
Pd_ppb	0.70	0.80	0.60	0.70	0.50	<0.5	<0.5	0.50	0.50	<0.5	<0.5	0.60	0.80	0.70
B_ppm	3.00	3.00	<1	<1	<1	<1	<1	<1	13.00	2.00	2.00	5.00	2.00	9.00
Tl_ppm	<0.02	<0.02	<0.02	<0.02	<0.02	<0.02	<0.02	<0.02	<0.02	<0.02	<0.02	<0.02	<0.02	<0.02
LOI_pct	1.70	1.50	1.30	2.80	1.70	1.50	1.20	1.50	1.60	2.50	2.80	0.90	4.50	3.90
TOT/C_TC000_pct	0.06	0.07	0.03	0.03	0.07	0.05	0.04	0.12	0.04	0.04	0.21	0.03	0.27	0.09
TOT/S_pct	<0.02	<0.02	<0.02	<0.02	<0.02	<0.02	<0.02	<0.02	<0.02	<0.02	<0.02	<0.02	<0.02	<0.02
Ba_ppm	107.00	132.00	133.00	117.00	120.00	119.00	100.00	130.00	142.00	119.00	110.00	166.00	45.00	189.00
Sc_ppm	3.00	3.00	<1	2.00	3.00	2.00	22.00	<1	2.00	1.00	14.00	<1	46.00	20.00
Sum_pct	99.87	99.82	99.92	99.88	99.90	99.83	99.82	99.92	99.84	99.89	99.87	99.93	99.71	99.79
Cs_ppm	0.20	0.50	<0.1	0.80	<0.1	0.30	<0.1	<0.1	<0.1	<0.1	<0.1	<0.1	0.10	0.60
Ga_ppm	18.10	16.40	18.90	17.90	19.90	16.40	17.20	20.00	17.40	18.50	18.20	20.70	15.80	14.40
Hf_ppm	0.10	<0.1	<0.1	<0.1	<0.1	<0.1	0.40	<0.1	<0.1	<0.1	0.30	<0.1	0.20	0.20
Nb_ppm	0.40	0.10	<0.1	0.10	0.10	0.20	0.20	<0.1	<0.1	<0.1	0.10	<0.1	0.20	0.20
Rb_ppm	0.90	1.00	0.80	1.60	0.60	1.30	1.10	1.40	0.90	1.00	0.90	1.90	1.60	11.40
Sn_ppm	<1	<1	<1	<1	<1	<1	<1	<1	<1	<1	<1	<1	<1	<1
Sr_ppm	491.70	454.50	558.30	443.60	537.60	461.40	413.40	545.10	452.30	504.70	428.90	569.30	226.50	415.70

Ta_ppm	<0.1	<0.1	<0.1	<0.1	<0.1	<0.1	<0.1	<0.1	<0.1	<0.1	<0.1	<0.1	<0.1	<0.1
Th_ppm	<0.2	<0.2	<0.2	<0.2	<0.2	<0.2	<0.2	<0.2	<0.2	<0.2	<0.2	<0.2	<0.2	<0.2
U_ppm	<0.1	<0.1	<0.1	<0.1	<0.1	<0.1	<0.1	<0.1	<0.1	<0.1	<0.1	<0.1	<0.1	<0.1
V_ppm	26.00	20.00	15.00	15.00	26.00	15.00	159.00	<8	18.00	14.00	99.00	8.00	295.00	88.00
W_ppm	0.70	0.50	1.20	<0.5	0.90	1.20	1.10	0.90	1.30	0.60	0.70	1.80	<0.5	1.10
Zr_ppm	6.70	2.40	1.50	2.30	3.40	2.70	17.90	2.00	1.80	0.80	8.90	3.70	3.60	6.00
Y_ppm	1.50	1.00	0.50	0.50	1.20	0.70	6.90	0.60	0.60	0.60	4.00	0.50	3.20	4.20
La_ppm	1.60	1.00	1.30	1.00	1.60	1.50	1.60	1.40	1.20	1.20	1.50	1.50	0.40	1.00
Ce_ppm	3.00	2.00	2.60	1.90	3.30	2.80	4.00	2.40	2.20	2.10	2.80	2.80	0.80	2.00
Pr_ppm	0.35	0.24	0.24	0.20	0.31	0.30	0.57	0.23	0.18	0.22	0.40	0.25	0.14	0.26
Nd_ppm	1.60	0.90	1.10	0.90	1.60	1.40	2.90	1.20	1.00	1.00	2.30	1.20	0.90	1.70
Sm_ppm	0.28	0.17	0.17	0.18	0.29	0.20	0.88	0.18	0.12	0.10	0.56	0.18	0.32	0.50
Eu_ppm	0.58	0.57	0.65	0.61	0.71	0.55	0.71	0.68	0.57	0.71	0.70	0.70	0.15	0.42
Gd_ppm	0.35	0.18	0.18	0.16	0.35	0.20	1.14	0.20	0.11	0.16	0.71	0.17	0.52	0.69
Tb_ppm	0.05	0.02	0.01	0.02	0.04	0.02	0.20	0.02	0.01	0.01	0.12	0.02	0.09	0.12
Dy_ppm	0.727	0.10	0.10	0.08	0.22	0.11	1.24	0.08	0.06	0.07	0.72	0.13	0.61	0.78
Ho_ppm	0.06	0.03	<0.02	<0.02	0.05	0.02	0.26	<0.02	0.03	<0.02	0.16	<0.02	0.14	0.18
Er_ppm	0.17	0.08	0.06	0.05	0.13	0.07	0.77	0.04	0.08	0.06	0.43	0.04	0.39	0.54
Tm_ppm	0.02	<0.01	<0.01	<0.01	0.02	<0.01	0.11	<0.01	<0.01	<0.01	0.06	<0.01	0.05	0.07
Yb_ppm	0.14	0.08	<0.05	0.07	0.11	0.07	0.65	<0.05	0.07	<0.05	0.39	<0.05	0.36	0.39
Lu_ppm	0.02	<0.01	<0.01	<0.01	0.01	<0.01	0.10	<0.01	<0.01	<0.01	0.06	<0.01	0.05	0.06

Sample_ID	KAC418-1	KAC421-1	KAC421-2	KAC421-3	KAC423-1	KAC424-1	KAC425-1	KAC425-2	KAC426-1	KAC426-2	KAC428-1	KAC429-1	KAC429-2	KAC430-1	KAC432-3
Lat_S	-17.3771	-17.3777	-17.3777	-17.3777	-17.1351	-17.1363	-17.2709	-17.2709	-17.2732	-17.2732	-17.2724	-17.2723	-17.2723	-17.2721	-17.2757

Long_E	13.2647	13.2624	13.2624	13.2624	13.2369	13.2394	13.3141	13.3141	13.3153	13.3153	13.3172	13.3182	13.3182	13.3194	13.3174
Rocktype	metasomatized leuconorite	Leuconorite	Leuconorite	gneissic leuconorite	Leuconorite	Mgt-rich rock	Leuconorite	Mortar leuconorite	Leucotroctolite	Leucotrocolite	Leuconorite	Leuconorite	Leucotroctolite mortar	Leucotroctolite	Mortar leuconorite
Group	KC	KC	KC	KC	KC	KC	KC	KC	KC	KC	KC	KC	KC	KC	KC
SiO2_pct	49.18	47.41	38.66	45.86	45.48	37.31	50.51	51.70	46.49	48.22	52.09	51.63	51.98	46.40	52.12
TiO2_pct	0.31	0.23	3.37	0.29	0.06	0.04	0.43	0.17	0.10	0.12	0.10	0.15	0.12	0.11	0.16
Al2O3_pct	15.73	15.93	14.40	15.45	22.22	6.42	20.93	28.54	21.90	22.24	29.00	26.90	29.25	21.84	27.85
Fe2O3t_pct	6.77	6.05	16.04	5.89	7.34	17.35	5.09	0.95	8.15	7.81	0.88	1.30	0.63	7.49	1.15
MnO_pct	0.13	0.12	0.13	0.12	0.09	0.19	0.10	0.01	0.09	0.09	0.01	0.02	<0.01	0.08	0.02
MgO_pct	9.70	10.55	7.92	9.55	8.81	25.10	5.03	0.40	8.03	7.18	0.44	0.85	0.18	6.67	0.76
CaO_pct	12.91	9.51	5.87	7.23	8.43	2.83	13.35	11.62	7.35	9.57	11.31	12.27	11.50	9.50	10.31
Na2O_pct	1.89	2.63	0.03	0.02	2.89	0.50	3.11	4.56	3.33	3.09	4.77	4.17	4.84	2.83	4.87
K2O_pct	0.34	1.23	3.32	3.87	0.75	0.13	0.18	0.45	0.97	0.24	0.56	0.64	0.45	0.19	0.79
Cr2O3_pct	0.12	0.10	0.01	0.29	0.01	0.01	0.07	0.01	0.01	0.01	<0.002	0.02	0.00	0.01	0.01
P2O5_pct	<0.01	<0.01	0.61	0.02	<0.01	<0.01	<0.01	0.01	<0.01	<0.01	<0.01	<0.01	<0.01	<0.01	<0.01
Normalised *	97.07	93.78	90.42	88.70	96.10	89.95	98.84	98.41	96.50	98.61	99.13	97.92	98.93	95.13	98.11
SiO2_pct*	50.66	50.55	42.76	51.70	47.33	41.48	51.10	52.54	48.18	48.90	52.55	52.73	52.54	48.78	53.12
TiO2_pct*	0.32	0.24	3.45	0.30	0.06	0.04	0.44	0.17	0.10	0.12	0.10	0.15	0.12	0.11	0.16
Al2O3_pct*	50.66	50.55	42.76	51.70	47.33	41.48	51.10	52.54	48.18	48.90	52.55	52.73	52.54	48.78	53.12
Fe2O3t_pct *	6.97	6.45	17.74	6.64	7.64	19.29	5.15	0.97	8.45	7.92	0.89	1.33	0.64	7.87	1.17
FeO_pct*	5.93	5.48	15.08	5.64	6.49	16.40	4.38	0.82	7.18	6.73	0.75	1.13	0.54	6.69	1.00
Fe2O3_pct*	1.05	0.97	2.66	1.00	1.15	2.89	0.77	0.14	1.27	1.19	0.13	0.20	0.10	1.18	0.18
FeO*_pct	6.28	5.81	15.97	5.98	6.87	17.36	4.63	0.87	7.60	7.13	0.80	1.19	0.57	7.09	1.05
MnO_pct*	0.13	0.12	0.13	0.12	0.09	0.19	0.10	0.01	0.09	0.09	0.01	0.02	N/D	0.08	0.02

MgO_pct*	9.99	11.25	8.76	10.77	9.17	27.90	5.09	0.41	8.32	7.28	0.44	0.87	0.18	7.01	0.77
CaO_pct*	13.24	9.75	6.02	7.41	8.64	2.90	13.69	11.91	7.54	9.81	11.60	12.58	11.79	9.74	10.57
Na2O_pct*	1.94	2.70	0.03	0.02	2.96	0.51	3.19	4.68	3.41	3.17	4.89	4.28	4.96	2.90	4.99
K2O_pct*	0.35	1.26	3.40	3.97	0.77	0.13	0.18	0.46	0.99	0.25	0.57	0.66	0.46	0.19	0.81
Cr2O3_pct*	0.12	0.10	0.01	0.29	0.01	0.01	0.07	0.01	0.01	0.01	N/D	0.02	0.00	0.01	0.01
P2O5_pct*	N/D	N/D	0.63	0.02	N/D	N/D	N/D	0.01	N/D	N/D	N/D	N/D	N/D	N/D	N/D
Mg#	75.02	78.52	50.86	77.27	71.56	75.20	67.45	46.89	67.38	65.84	51.18	57.82	37.46	65.12	58.08
Mo_pct	<0.001	<0.001	<0.001	<0.001	<0.001	<0.001	<0.001	<0.001	<0.001	<0.001	<0.001	<0.001	<0.001	<0.001	<0.001
Cu_pct	0.01	0.00	0.01	<0.001	0.00	0.00	0.00	0.00	0.01	0.00	<0.001	0.00	0.00	0.00	<0.001
Pb_pct	<0.02	<0.02	<0.02	<0.02	<0.02	<0.02	<0.02	<0.02	<0.02	<0.02	<0.02	<0.02	<0.02	<0.02	<0.02
Zn_pct	<0.01	<0.01	<0.01	<0.01	<0.01	<0.01	<0.01	<0.01	<0.01	<0.01	<0.01	<0.01	<0.01	<0.01	<0.01
Ag_ppm	<2	<2	<2	<2	<2	<2	<2	2.00	<2	<2	2.00	<2	<2	<2	2.00
Ni_ppm	163.00	139.00	98.00	110.00	172.00	675.00	81.00	16.00	243.00	221.00	13.00	27.00	11.00	202.00	19.00
Mo_ppm	0.23	0.09	0.17	0.10	0.17	0.16	0.14	0.52	0.17	0.52	0.51	0.35	0.53	0.10	0.26
Cu_ppm	91.91	5.47	71.80	3.02	11.69	8.47	13.02	13.02	45.87	15.94	5.50	10.54	18.03	32.58	7.88
Pb_ppm	0.90	0.43	2.20	0.83	3.53	0.95	0.41	3.94	1.65	0.32	1.05	1.69	2.71	1.53	0.61
Zn_ppm	18.50	24.90	64.20	34.80	32.00	56.50	6.90	5.80	34.00	10.10	3.20	5.40	3.50	25.00	6.50
Ag_ppb	86.00	4.00	72.00	17.00	8.00	43.00	11.00	51.00	21.00	14.00	14.00	65.00	59.00	26.00	7.00
Ni_ppm	110.30	91.80	84.70	89.60	102.80	531.00	33.00	13.40	146.30	177.50	9.10	21.80	8.20	122.30	16.80
Co_ppm	26.30	30.60	55.00	30.60	33.40	143.20	8.80	3.60	36.30	42.80	2.60	4.70	1.50	35.90	4.20
Mn_ppm	380.00	479.00	957.00	838.00	416.00	1052.00	132.00	72.00	391.00	470.00	40.00	106.00	54.00	519.00	81.00
As_ppm	0.80	0.50	0.40	<0.1	0.30	0.10	0.30	0.30	0.10	<0.1	0.20	0.30	0.40	1.70	0.20
Au_ppb	0.40	0.70	<0.2	0.60	<0.2	0.40	0.20	<0.2	0.40	<0.2	<0.2	<0.2	0.70	<0.2	<0.2
Cd_ppm	0.02	0.01	0.05	0.04	0.01	0.01	0.01	0.02	0.01	<0.01	<0.01	0.02	0.01	0.01	<0.01
Sb_ppm	<0.02	<0.02	<0.02	<0.02	<0.02	<0.02	<0.02	<0.02	<0.02	<0.02	<0.02	<0.02	<0.02	<0.02	<0.02

Bi_ppm	<0.02	<0.02	<0.02	<0.02	<0.02	<0.02	<0.02	<0.02	0.03	<0.02	<0.02	<0.02	<0.02	<0.02	<0.02
Cr_ppm	229.00	259.50	11.50	734.30	22.70	15.00	144.30	9.30	26.30	16.30	7.50	83.70	11.60	24.70	44.20
Hg_ppb	<5	<5	<5	<5	<5	<5	<5	<5	<5	<5	<5	<5	<5	<5	<5
Se_ppm	<0.1	<0.1	<0.1	<0.1	<0.1	<0.1	<0.1	<0.1	<0.1	<0.1	<0.1	<0.1	<0.1	<0.1	<0.1
Te_ppm	<0.02	<0.02	<0.02	<0.02	<0.02	<0.02	<0.02	<0.02	<0.02	<0.02	<0.02	<0.02	<0.02	<0.02	<0.02
Ge_ppm	<0.1	<0.1	<0.1	<0.1	<0.1	0.20	<0.1	<0.1	<0.1	<0.1	<0.1	<0.1	<0.1	<0.1	<0.1
In_ppm	<0.02	<0.02	0.03	<0.02	<0.02	<0.02	<0.02	<0.02	<0.02	<0.02	<0.02	<0.02	<0.02	<0.02	<0.02
Re_ppb	<1	<1	<1	<1	<1	<1	<1	<1	<1	<1	<1	<1	<1	<1	<1
Be_ppm	<0.1	<0.1	0.70	<0.1	0.20	<0.1	<0.1	0.10	0.20	<0.1	<0.1	<0.1	0.10	<0.1	<0.1
Li_ppm	17.80	28.30	39.90	48.70	10.60	1.50	1.20	2.00	13.50	1.30	1.20	3.70	1.80	1.70	6.40
Pd_ppb	<10	<10	<10	<10	<10	<10	<10	<10	<10	<10	<10	<10	<10	<10	<10
Pt_ppb	<2	<2	<2	<2	<2	<2	<2	<2	<2	<2	<2	<2	<2	<2	<2
Au_ppb	3.00	3.00	3.00	4.00	3.00	4.00	2.00	2.00	3.00	3.00	3.00	3.00	6.00	4.00	3.00
Pt_ppb	0.30	0.30	0.60	0.50	0.20	0.30	0.20	0.10	0.20	0.60	0.30	0.30	0.30	0.40	0.20
Pd_ppb	1.00	0.90	0.90	1.60	0.80	1.30	1.60	<0.5	0.70	0.70	0.70	0.90	0.80	1.10	0.70
B_ppm	3.00	3.00	7.00	6.00	4.00	24.00	<1	2.00	4.00	<1	<1	5.00	4.00	<1	5.00
Tl_ppm	<0.02	<0.02	0.04	0.03	0.04	0.03	<0.02	<0.02	0.04	<0.02	0.02	<0.02	<0.02	<0.02	0.03
LOI_pct	2.70	6.00	9.30	11.10	3.70	9.60	1.00	1.50	3.30	1.20	0.80	2.00	1.00	4.70	1.80
TOT/C_TC000_pct	0.03	0.61	1.14	1.59	0.04	0.02	0.06	0.07	0.04	0.05	0.02	0.09	0.04	0.62	0.03
TOT/S_pct	<0.02	<0.02	<0.02	<0.02	<0.02	<0.02	<0.02	<0.02	<0.02	<0.02	<0.02	<0.02	<0.02	<0.02	<0.02
Ba_ppm	136.00	341.00	441.00	528.00	214.00	57.00	102.00	185.00	231.00	118.00	190.00	226.00	170.00	104.00	226.00
Sc_ppm	47.00	38.00	27.00	47.00	3.00	7.00	32.00	<1	3.00	3.00	<1	4.00	<1	4.00	3.00
Sum_pct	99.77	99.78	99.72	99.80	99.80	99.55	99.84	99.91	99.80	99.81	99.93	99.92	99.93	99.83	99.91
Cs_ppm	0.60	0.80	1.60	1.80	3.80	1.80	0.30	0.70	1.90	0.20	0.90	1.00	0.70	0.70	2.80
Ga_ppm	13.80	12.70	22.30	12.10	14.40	3.40	16.30	20.30	17.20	16.70	22.60	17.00	21.30	15.80	20.10

Hf_ppm	0.30	0.20	7.50	0.30	<0.1	<0.1	0.40	0.20	0.20	0.10	<0.1	0.10	0.10	<0.1	0.20
Nb_ppm	<0.1	<0.1	18.50	0.30	<0.1	<0.1	0.10	0.20	0.30	0.20	0.10	<0.1	0.40	0.30	0.40
Rb_ppm	7.00	16.90	49.10	57.00	27.10	4.60	0.90	7.70	33.40	1.80	14.00	12.80	7.30	2.00	18.50
Sn_ppm	<1	<1	2.00	<1	<1	<1	<1	<1	<1	<1	<1	<1	<1	<1	<1
Sr_ppm	193.60	174.20	77.80	62.80	370.30	103.60	383.80	564.80	460.80	417.20	538.50	456.60	552.50	388.00	613.00
Ta_ppm	<0.1	<0.1	1.20	<0.1	<0.1	<0.1	<0.1	<0.1	<0.1	<0.1	<0.1	<0.1	<0.1	<0.1	<0.1
Th_ppm	<0.2	<0.2	2.80	<0.2	<0.2	<0.2	<0.2	<0.2	0.40	0.30	<0.2	<0.2	0.30	<0.2	<0.2
U_ppm	<0.1	<0.1	1.80	0.60	<0.1	<0.1	<0.1	<0.1	0.30	<0.1	<0.1	<0.1	0.30	<0.1	<0.1
V_ppm	174.00	126.00	279.00	132.00	15.00	36.00	217.00	19.00	19.00	30.00	<8	39.00	9.00	28.00	25.00
W_ppm	0.70	<0.5	0.70	<0.5	0.60	<0.5	0.70	2.70	1.00	0.90	1.70	1.20	1.30	<0.5	1.10
Zr_ppm	6.10	4.50	316.90	10.40	1.70	2.40	12.60	6.20	6.70	4.50	2.10	3.80	3.40	4.40	6.50
Y_ppm	8.60	4.80	36.40	4.40	0.60	0.60	8.20	1.30	0.90	1.10	0.50	1.40	1.00	1.10	1.50
La_ppm	0.70	1.00	30.50	1.20	1.20	0.30	1.50	1.70	2.10	2.30	1.60	1.70	1.60	1.30	1.90
Ce_ppm	2.10	1.60	64.00	2.70	1.90	0.50	3.50	2.80	3.00	2.50	2.80	2.00	2.80	2.20	3.50
Pr_ppm	0.35	0.23	8.73	0.32	0.19	0.03	0.51	0.46	0.39	0.29	0.29	0.20	0.32	0.26	0.40
Nd_ppm	2.30	1.40	38.80	1.90	1.00	0.30	2.90	1.70	1.50	1.10	1.20	1.10	1.30	1.30	1.80
Sm_ppm	0.87	0.47	8.86	0.40	0.12	<0.05	0.99	0.25	0.24	0.23	0.12	0.17	0.18	0.14	0.28
Eu_ppm	0.48	0.30	2.62	0.28	0.33	0.05	0.73	0.73	0.60	0.62	0.75	0.62	0.65	0.52	0.71
Gd_ppm	1.27	0.66	8.92	0.79	0.18	0.11	1.42	0.31	0.20	0.27	0.15	0.38	0.22	0.23	0.29
Tb_ppm	0.22	0.12	1.32	0.13	0.02	0.01	0.23	0.05	0.02	0.04	0.02	0.04	0.03	0.03	0.04
Dy_ppm	1.54	0.85	7.46	0.85	0.09	0.10	1.51	0.25	0.15	0.26	0.12	0.28	0.18	0.14	0.24
Ho_ppm	0.33	0.18	1.43	0.20	<0.02	<0.02	0.32	0.05	0.03	0.06	0.02	0.05	0.03	0.04	0.06
Er_ppm	1.00	0.64	4.22	0.52	0.07	0.09	0.93	0.13	0.08	0.09	0.03	0.11	0.06	0.09	0.17
Tm_ppm	0.14	0.09	0.56	0.07	<0.01	0.01	0.14	0.01	0.01	0.03	<0.01	0.01	<0.01	0.01	0.02
Yb_ppm	0.81	0.56	3.64	0.45	0.06	0.10	0.77	0.06	0.08	0.13	<0.05	0.06	<0.05	0.08	0.12

Lu_ppm	0.12	0.07	0.52	0.06	<0.01	<0.01	0.11	0.02	0.02	0.02	<0.01	0.01	<0.01	0.02	0.01

Sample_ID	KAC435-1	KAC435-2	KAC437-1	KAC438-1	KAC439-1	KAC439-2	KAC439-4	KAC443-1	KAC445-1	KAC448-1	KAC448-2	KAC452-1	KAC453-1	KAC455-1
Lat_S	-17.2745	-17.2745	-17.2792	-17.2826	-17.2780	-17.2780	-17.2780	-17.3064	-17.3025	-17.2904	-17.2904	-17.2024	-17.2044	-17.2094
Long_E	13.3304	13.3304	13.3380	13.3319	13.3211	13.3211	13.3211	13.3266	13.3258	13.2866	13.2866	13.3754	13.3778	13.4014
Rocktype	Leucotroctolite	Leuconorite	Leucotroctolite	Leucotroctolite	Mottled leuconorite	Opx megacryst	Mortar anorthosite	Leucotroctolite	anorthosite rock	Foliated leuconorite	Noritic enclave	Leuconorite	Leucotroctolite	Leucotroctolite
Group	KC	KC	KC	KC	KC	KC	KC	KC	KC	KC	KC	KC	KC	KC
SiO2_pct	48.82	48.51	47.86	49.33	51.51	51.60	51.56	51.04	52.11	50.16	45.68	51.90	57.18	50.94
TiO2_pct	0.08	0.09	0.09	0.24	0.29	0.15	0.09	0.09	0.09	0.93	0.94	0.36	0.07	0.11
Al2O3_pct	23.95	24.29	22.93	23.62	25.65	27.78	29.22	28.27	28.90	18.85	16.53	22.21	17.70	25.57
Fe2O3t_pct	5.64	6.00	6.71	4.97	2.49	1.45	0.61	1.59	0.64	9.25	11.11	4.26	2.66	4.05
MnO_pct	0.06	0.06	0.07	0.07	0.03	0.02	<0.01	0.02	<0.01	0.18	0.21	0.08	0.06	0.04
MgO_pct	6.49	5.31	7.44	4.17	2.21	1.17	0.13	1.15	0.29	4.48	7.40	3.91	1.37	3.75
CaO_pct	10.30	10.30	9.87	10.92	11.63	11.85	12.23	12.24	11.93	8.52	10.49	10.76	12.44	10.54
Na2O_pct	2.94	3.42	3.08	3.71	4.04	4.41	4.48	4.10	4.39	4.17	2.14	3.35	4.30	3.79
K2O_pct	0.20	0.31	0.22	0.44	0.34	0.37	0.30	0.26	0.35	0.57	1.67	0.96	0.05	0.31
Cr2O3_pct	0.00	0.00	0.00	0.02	0.03	0.02	0.01	0.00	0.01	0.00	0.01	0.07	<0.002	0.00
P2O5_pct	<0.01	<0.01	<0.01	<0.01	<0.01	<0.01	<0.01	<0.01	<0.01	0.36	0.02	<0.01	<0.01	<0.01
Normalised *	98.54	98.35	98.32	97.55	98.29	98.81	98.64	98.82	98.73	97.54	96.33	97.86	95.83	99.17
SiO2_pct*	49.54	49.32	48.68	50.57	52.41	52.22	52.27	51.65	52.78	51.43	47.42	53.03	59.67	51.37
TiO2_pct*	0.08	0.09	0.09	0.25	0.30	0.15	0.09	0.09	0.09	0.95	0.96	0.37	0.07	0.11
Al2O3_pct*	49.54	49.32	48.68	50.57	52.41	52.22	52.27	51.65	52.78	51.43	47.42	53.03	59.67	51.37

Fe2O3t_pct*	5.72	6.10	6.82	5.09	2.53	1.47	0.62	1.61	0.65	9.48	11.53	4.35	2.78	4.08
FeO_pct*	4.87	5.19	5.80	4.33	2.15	1.25	0.53	1.37	0.55	8.06	9.80	3.70	2.36	3.47
Fe2O3_pct*	0.86	0.92	1.02	0.76	0.38	0.22	0.09	0.24	0.10	1.42	1.73	0.65	0.42	0.61
FeO*_pct	5.15	5.49	6.14	4.59	2.28	1.32	0.56	1.45	0.58	8.53	10.38	3.92	2.50	3.68
MnO_pct*	0.06	0.06	0.07	0.07	0.03	0.02	N/D	0.02	N/D	0.18	0.22	0.08	0.06	0.04
MgO_pct*	6.59	5.40	7.57	4.27	2.25	1.18	0.13	1.16	0.29	4.59	7.68	4.00	1.43	3.78
CaO_pct*	10.56	10.56	10.12	11.20	11.92	12.15	12.54	12.55	12.23	8.73	10.75	11.03	12.75	10.81
Na2O_pct*	3.01	3.51	3.16	3.80	4.14	4.52	4.59	4.20	4.50	4.28	2.19	3.43	4.41	3.89
K2O_pct*	0.21	0.32	0.23	0.45	0.35	0.38	0.31	0.27	0.36	0.58	1.71	0.98	0.05	0.32
Cr2O3_pct*	0.00	0.00	0.00	0.02	0.03	0.02	0.01	0.00	0.01	0.00	0.01	0.07	N/D	0.00
P2O5_pct*	N/D	N/D	N/D	N/D	N/D	N/D	N/D	N/D	N/D	0.37	0.02	N/D	N/D	N/D
Mg#	70.70	64.98	69.92	63.76	65.04	62.85	30.88	60.26	48.72	50.38	58.27	65.80	51.92	66.00
Mo_pct	<0.001	<0.001	<0.001	<0.001	<0.001	<0.001	<0.001	<0.001	<0.001	<0.001	<0.001	<0.001	<0.001	<0.001
Cu_pct	<0.001	0.00	<0.001	0.00	0.00	0.00	<0.001	<0.001	<0.001	0.01	0.00	0.00	0.00	0.00
Pb_pct	<0.02	<0.02	<0.02	<0.02	<0.02	<0.02	<0.02	<0.02	<0.02	<0.02	<0.02	<0.02	<0.02	<0.02
Zn_pct	<0.01	<0.01	<0.01	<0.01	<0.01	<0.01	<0.01	<0.01	<0.01	<0.01	<0.01	<0.01	<0.01	<0.01
Ag_ppm	<2	4.00	<2	2.00	<2	<2	<2	<2	3.00	<2	2.00	<2	<2	<2
Ni_ppm	218.00	178.00	259.00	117.00	45.00	20.00	<10	35.00	<10	12.00	76.00	62.00	50.00	114.00
Mo_ppm	0.34	0.23	0.23	0.16	0.60	0.21	0.40	0.57	0.29	0.19	0.08	0.23	0.72	0.15
Cu_ppm	6.66	12.46	7.73	29.55	22.20	11.71	2.92	11.20	1.98	71.78	7.53	15.93	9.67	11.80
Pb_ppm	1.27	0.59	0.29	4.44	2.57	0.88	0.73	0.37	0.24	0.82	0.97	7.06	9.39	0.24
Zn_ppm	9.20	13.10	14.50	14.80	5.30	5.00	2.90	5.50	3.00	62.70	60.50	8.20	11.20	3.80
Ag_ppb	147.00	138.00	57.00	25.00	39.00	15.00	3.00	10.00	8.00	31.00	82.00	29.00	12.00	7.00
Ni_ppm	177.10	157.90	224.70	75.10	18.10	13.40	8.50	35.30	8.70	11.10	52.50	17.20	45.60	79.20
Co_ppm	35.00	38.90	43.20	16.50	4.20	3.10	1.10	6.10	1.30	19.10	26.90	5.00	9.40	17.20

Mn_ppm	333.00	371.00	455.00	234.00	88.00	73.00	45.00	83.00	49.00	563.00	610.00	164.00	305.00	176.00
As_ppm	0.10	<0.1	<0.1	0.40	0.30	<0.1	0.40	0.50	<0.1	<0.1	<0.1	0.70	5.60	0.90
Au_ppb	<0.2	0.30	<0.2	<0.2	0.50	<0.2	0.20	0.40	0.40	0.60	<0.2	<0.2	0.30	<0.2
Cd_ppm	0.01	0.01	0.01	<0.01	<0.01	<0.01	<0.01	<0.01	<0.01	0.02	0.02	<0.01	0.01	<0.01
Sb_ppm	<0.02	<0.02	<0.02	<0.02	<0.02	<0.02	<0.02	0.02	<0.02	<0.02	<0.02	0.04	0.38	0.04
Bi_ppm	<0.02	<0.02	<0.02	<0.02	0.02	<0.02	<0.02	<0.02	<0.02	<0.02	<0.02	0.12	0.06	<0.02
Cr_ppm	9.80	28.40	12.00	41.70	58.80	46.20	42.70	11.20	32.80	24.30	58.40	127.70	15.60	18.20
Hg_ppb	<5	<5	<5	<5	5.00	<5	<5	<5	<5	<5	<5	<5	<5	<5
Se_ppm	<0.1	<0.1	<0.1	<0.1	<0.1	<0.1	<0.1	<0.1	0.20	0.30	0.30	<0.1	<0.1	<0.1
Te_ppm	<0.02	<0.02	<0.02	<0.02	<0.02	<0.02	<0.02	<0.02	<0.02	<0.02	<0.02	<0.02	<0.02	<0.02
Ge_ppm	<0.1	<0.1	<0.1	<0.1	<0.1	<0.1	<0.1	<0.1	<0.1	<0.1	<0.1	<0.1	0.20	<0.1
In_ppm	<0.02	<0.02	<0.02	<0.02	<0.02	<0.02	<0.02	<0.02	<0.02	<0.02	<0.02	<0.02	<0.02	<0.02
Re_ppb	<1	<1	<1	<1	<1	<1	<1	<1	<1	<1	<1	<1	<1	<1
Be_ppm	0.10	<0.1	<0.1	<0.1	0.20	<0.1	<0.1	<0.1	<0.1	0.20	0.20	0.30	1.40	<0.1
Li_ppm	3.40	3.20	2.50	3.30	3.50	2.70	1.60	1.80	0.90	7.60	8.80	2.00	5.80	0.90
Pd_ppb	<10	<10	<10	<10	<10	<10	<10	<10	<10	<10	<10	<10	<10	<10
Pt_ppb	<2	<2	<2	<2	<2	<2	<2	<2	<2	<2	5.00	<2	<2	<2
Au_ppb	3.00	2.00	3.00	3.00	3.00	4.00	2.00	2.00	2.00	4.00	3.00	4.00	4.00	3.00
Pt_ppb	0.30	0.20	0.20	0.40	0.60	0.50	0.20	0.20	0.20	1.60	9.20	0.50	0.30	0.20
Pd_ppb	0.80	0.60	0.70	1.00	1.50	1.40	0.50	<0.5	<0.5	2.20	1.30	1.30	0.90	0.80
B_ppm	5.00	8.00	8.00	3.00	<1	<1	2.00	<1	1.00	2.00	9.00	8.00	11.00	3.00
Tl_ppm	<0.02	<0.02	<0.02	<0.02	<0.02	<0.02	<0.02	<0.02	<0.02	<0.02	0.07	0.06	<0.02	<0.02
LOI_pct	1.30	1.50	1.50	2.30	1.60	1.10	1.30	1.10	1.20	2.20	3.40	2.00	4.10	0.70
TOT/C_TC000_pct	0.04	0.03	0.04	0.10	0.11	0.02	0.04	0.07	<0.02	<0.02	0.09	0.06	0.38	0.02
TOT/S_pct	<0.02	<0.02	<0.02	<0.02	<0.02	<0.02	<0.02	<0.02	<0.02	<0.02	<0.02	<0.02	<0.02	<0.02

Ba_ppm	95.00	126.00	107.00	153.00	157.00	131.00	115.00	128.00	137.00	462.00	920.00	223.00	36.00	147.00
Sc_ppm	2.00	2.00	2.00	10.00	13.00	5.00	<1	<1	<1	24.00	47.00	24.00	2.00	1.00
Sum_pct	99.84	99.85	99.82	99.85	99.89	99.91	99.94	99.92	99.93	99.74	99.73	99.86	99.93	99.87
Cs_ppm	0.80	0.70	0.70	1.00	0.80	0.90	0.90	<0.1	0.30	0.60	1.40	1.90	0.10	0.20
Ga_ppm	16.20	16.40	14.80	16.90	17.20	18.70	20.40	19.30	18.80	18.50	15.90	18.60	18.10	17.70
Hf_ppm	<0.1	<0.1	<0.1	0.30	0.30	0.10	<0.1	<0.1	<0.1	2.00	1.60	0.50	2.60	0.10
Nb_ppm	0.20	0.10	<0.1	0.30	0.30	<0.1	0.10	<0.1	<0.1	2.10	3.60	1.20	8.20	0.20
Rb_ppm	1.00	3.30	1.10	6.50	7.20	6.00	4.00	0.80	3.10	7.00	39.70	34.50	1.80	1.60
Sn_ppm	<1	<1	<1	<1	<1	<1	<1	<1	<1	<1	<1	<1	<1	<1
Sr_ppm	466.80	486.10	420.00	456.60	473.10	524.40	552.20	542.90	542.80	937.00	539.00	408.10	268.70	512.40
Ta_ppm	<0.1	<0.1	<0.1	<0.1	<0.1	<0.1	<0.1	<0.1	<0.1	<0.1	0.10	0.20	0.40	<0.1
Th_ppm	0.80	0.20	<0.2	<0.2	<0.2	<0.2	<0.2	<0.2	<0.2	<0.2	<0.2	0.70	54.90	<0.2
U_ppm	<0.1	<0.1	<0.1	<0.1	0.20	<0.1	<0.1	<0.1	<0.1	<0.1	<0.1	1.10	19.80	<0.1
V_ppm	12.00	13.00	17.00	75.00	91.00	42.00	8.00	11.00	9.00	223.00	356.00	174.00	19.00	23.00
W_ppm	0.90	2.50	0.60	1.40	1.70	0.90	2.80	1.20	1.60	1.30	<0.5	5.90	3.90	1.20
Zr_ppm	2.70	2.00	1.90	11.00	8.80	4.50	1.90	1.00	1.70	82.80	54.50	12.50	54.30	3.60
Y_ppm	0.40	0.60	0.60	4.20	4.30	1.90	0.40	0.40	0.40	16.60	23.10	7.70	2.50	0.60
La_ppm	2.30	1.60	1.10	1.80	1.60	1.60	1.40	1.50	1.30	16.90	12.50	2.30	2.60	1.60
Ce_ppm	3.50	2.70	2.30	4.00	3.20	2.70	2.30	2.50	2.50	35.60	33.80	4.80	6.20	2.80
Pr_ppm	0.38	0.29	0.25	0.53	0.44	0.33	0.24	0.25	0.25	4.76	4.95	0.66	0.63	0.30
Nd_ppm	1.40	1.30	1.00	2.60	2.00	1.40	1.20	1.00	1.10	20.60	22.10	3.60	2.60	1.30
Sm_ppm	0.16	0.13	0.17	0.60	0.59	0.33	0.09	0.12	0.16	4.17	4.80	1.05	0.68	0.15
Eu_ppm	0.47	0.53	0.48	0.70	0.65	0.63	0.61	0.57	0.56	1.62	1.33	0.78	1.09	0.54
Gd_ppm	0.17	0.12	0.13	0.81	0.75	0.37	0.12	0.12	0.13	3.71	4.57	1.35	0.59	0.20
Tb_ppm	0.01	0.02	0.02	0.12	0.12	0.05	0.01	0.01	0.01	0.50	0.66	0.22	0.07	0.02

Dy_ppm	0.06	0.10	0.08	0.77	0.70	0.32	0.09	0.08	0.08	2.92	4.01	1.41	0.42	0.09
Ho_ppm	<0.02	<0.02	<0.02	0.14	0.14	0.06	<0.02	<0.02	<0.02	0.56	0.82	0.29	0.07	0.02
Er_ppm	<0.03	0.04	0.05	0.44	0.44	0.14	<0.03	<0.03	0.04	1.63	2.42	0.79	0.23	0.05
Tm_ppm	<0.01	<0.01	<0.01	0.06	0.05	0.02	<0.01	<0.01	<0.01	0.22	0.32	0.11	0.02	<0.01
Yb_ppm	<0.05	<0.05	0.05	0.36	0.35	0.15	<0.05	<0.05	<0.05	1.40	2.10	0.67	0.19	<0.05
Lu_ppm	<0.01	<0.01	<0.01	0.05	0.05	0.02	<0.01	<0.01	<0.01	0.23	0.31	0.10	0.03	<0.01

Sample_ID	KAC455-2	KAC456-1	KAC457-1	KAC458-1	KAC461-1	KAC462-1	KAC462-3	KAC462-4	KSAT029/016	KSAT030/017	KSAT035/021	KSAT035/022	KSAT036/019	KSAT279/092
Lat_S	-17.2094	-17.2077	-17.2063	-17.2059	-17.2879	-17.2859	-17.2859	-17.2859	-15.8180	-15.8259	-15.7846	-15.7846	-15.7859	-15.7670
Long_E	13.4014	13.4035	13.4063	13.4117	13.2993	13.2985	13.2985	13.2985	13.7191	13.6868	13.5586	13.5586	13.5592	14.0577
Rocktype	Leucotroctolite	Leucotroctolite	Leucotroctolite	Mortar anorthosite	Leucotroctolite	Mortar leucotroctolite	Mortar leucotroctolite	Mortar leucotroctolite	Leuconorite / leucotroctolite	Anorthosite (metasomatised)	Leuconorite	Mottled anorthosite	Leuconorite	Foliated anorthosite
Group	KC	KC	KC	KC	KC	KC	KC	KC	KC	KC	KC	KC	KC	KC
SiO2_pct	50.46	53.33	50.96	52.67	49.99	51.85	52.12	50.87	48.04	47.57	49.68	48.98	47.97	52.73
TiO2_pct	0.11	0.12	0.11	0.11	0.17	0.18	0.12	0.15	0.48	0.31	0.78	0.51	0.47	0.11
Al2O3_pct	24.66	27.22	26.21	28.98	25.69	26.96	28.44	26.60	22.67	24.81	18.15	22.88	22.64	27.44
Fe2O3t_pct	4.28	1.28	3.57	0.57	3.93	1.91	1.02	3.62	6.95	4.89	8.46	5.03	5.36	1.84
MnO_pct	0.05	0.02	0.04	<0.01	0.05	0.03	0.02	0.05	0.09	0.06	0.11	0.07	0.08	0.02
MgO_pct	3.85	0.73	3.08	0.12	3.31	1.36	0.47	2.67	5.41	3.88	5.34	3.24	4.57	1.35
CaO_pct	10.37	10.30	10.79	11.88	11.32	12.52	12.25	11.39	10.88	11.00	9.51	9.43	10.41	10.82
Na2O_pct	3.95	4.78	3.99	4.50	3.74	3.99	4.29	3.49	2.90	3.49	2.80	3.30	2.69	4.41
K2O_pct	0.26	0.56	0.39	0.44	0.51	0.19	0.33	0.29	0.35	0.45	1.38	2.29	1.68	0.33
Cr2O3_pct	0.00	0.00	0.02	0.00	0.01	0.01	<0.002	0.00	0.04	0.03	0.01	0.00	0.01	0.00
P2O5_pct	0.01	<0.01	<0.01	<0.01	<0.01	<0.01	<0.01	<0.01	0.09	0.03	0.19	0.22	0.19	0.02

Normalised *	98.07	98.32	99.17	99.32	98.77	99.00	99.03	99.18	97.91	96.54	96.43	96.01	96.18	99.16
SiO2_pct*	51.45	54.24	51.39	53.03	50.61	52.37	52.63	51.29	49.07	49.27	51.52	51.02	49.88	53.18
TiO2_pct*	0.11	0.12	0.11	0.11	0.17	0.18	0.12	0.15	0.49	0.32	0.80	0.52	0.48	0.11
Al2O3_pct*	51.45	54.24	51.39	53.03	50.61	52.37	52.63	51.29	49.07	49.27	51.52	51.02	49.88	53.18
Fe2O3t_pct *	4.36	1.30	3.60	0.57	3.98	1.93	1.03	3.65	7.10	5.07	8.77	5.24	5.57	1.86
FeO_pct*	3.71	1.11	3.06	0.49	3.38	1.64	0.88	3.10	6.03	4.31	7.46	4.45	4.74	1.58
Fe2O3_pct*	0.65	0.20	0.54	0.09	0.60	0.29	0.15	0.55	1.06	0.76	1.32	0.79	0.84	0.28
FeO*_pct	3.93	1.17	3.24	0.52	3.58	1.74	0.93	3.28	6.39	4.56	7.90	4.72	5.02	1.67
MnO_pct*	0.05	0.02	0.04	N/D	0.05	0.03	0.02	0.05	0.09	0.06	0.11	0.07	0.08	0.02
MgO_pct*	3.93	0.74	3.11	0.12	3.35	1.37	0.47	2.69	5.53	4.02	5.54	3.37	4.75	1.36
CaO_pct*	10.63	10.56	11.06	12.18	11.61	12.84	12.56	11.68	11.15	11.28	9.75	9.67	10.67	11.09
Na2O_pct*	4.05	4.90	4.09	4.61	3.83	4.09	4.40	3.58	2.97	3.58	2.87	3.38	2.76	4.52
K2O_pct*	0.27	0.57	0.40	0.45	0.52	0.19	0.34	0.30	0.36	0.46	1.41	2.35	1.72	0.34
Cr2O3_pct*	0.00	0.00	0.02	0.00	0.01	0.01	N/D	0.00	0.04	0.03	0.01	0.00	0.01	0.00
P2O5_pct*	0.01	N/D	N/D	N/D	N/D	N/D	N/D	N/D	0.09	0.03	0.19	0.23	0.19	0.02
Mg#	65.35	54.46	64.40	30.62	63.84	59.88	49.14	60.73	62.00	62.45	56.96	57.45	64.13	60.60
Mo_pct	<0.001	<0.001	<0.001	<0.001	<0.001	<0.001	<0.001	<0.001	<0.001	<0.001	<0.001	<0.001	<0.001	<0.001
Cu_pct	<0.001	<0.001	0.00	<0.001	0.00	<0.001	<0.001	0.00	0.01	0.00	0.01	0.01	0.00	<0.001
Pb_pct	<0.02	<0.02	<0.02	<0.02	<0.02	<0.02	<0.02	<0.02	<0.02	<0.02	<0.02	<0.02	<0.02	<0.02
Zn_pct	<0.01	<0.01	<0.01	<0.01	<0.01	<0.01	<0.01	<0.01	<0.01	<0.01	<0.01	<0.01	<0.01	<0.01
Ag_ppm	<2	<2	<2	<2	<2	<2	<2	<2	<2	<2	<2	<2	<2	<2
Ni_ppm	107.00	21.00	94.00	<10	85.00	25.00	<10	36.00	100.00	73.00	99.00	71.00	110.00	16.00
Mo_ppm	0.51	0.16	0.33	0.13	0.30	0.15	0.25	0.12	0.16	0.10	0.57	0.86	0.54	0.14
Cu_ppm	6.86	6.65	9.98	3.21	11.76	4.42	5.18	11.38	70.19	17.12	105.07	65.69	6.82	4.46
Pb_ppm	2.88	10.71	0.19	0.21	0.82	0.23	0.27	0.27	1.42	0.69	5.59	5.61	4.49	0.30

Zn_ppm	16.30	10.50	4.20	1.80	6.70	6.40	3.60	7.20	25.40	15.10	44.20	39.10	33.20	3.50
Ag_ppb	215.00	87.00	7.00	5.00	13.00	9.00	12.00	21.00	36.00	18.00	52.00	91.00	9.00	4.00
Ni_ppm	66.20	20.10	71.80	4.10	60.60	12.40	4.50	12.80	56.10	49.70	66.30	60.50	79.00	8.90
Co_ppm	17.30	5.50	16.50	0.70	15.50	3.40	1.50	5.70	26.50	21.30	24.70	18.30	18.80	3.00
Mn_ppm	155.00	120.00	181.00	31.00	179.00	83.00	48.00	79.00	330.00	200.00	342.00	282.00	305.00	30.00
As_ppm	0.70	0.10	0.40	0.10	0.20	<0.1	<0.1	<0.1	0.20	0.40	0.70	7.30	0.80	<0.1
Au_ppb	<0.2	<0.2	<0.2	<0.2	<0.2	<0.2	<0.2	<0.2	<0.2	<0.2	1.00	<0.2	<0.2	<0.2
Cd_ppm	<0.01	<0.01	<0.01	<0.01	<0.01	<0.01	<0.01	<0.01	0.03	0.02	0.05	0.07	0.02	<0.01
Sb_ppm	0.04	<0.02	<0.02	<0.02	<0.02	<0.02	<0.02	<0.02	<0.02	<0.02	<0.02	<0.02	<0.02	<0.02
Bi_ppm	0.08	<0.02	<0.02	<0.02	<0.02	<0.02	<0.02	<0.02	<0.02	<0.02	<0.02	0.04	<0.02	<0.02
Cr_ppm	11.00	15.90	8.60	12.00	17.60	23.30	6.90	13.40	86.10	66.70	28.80	10.90	54.70	18.70
Hg_ppb	<5	<5	<5	<5	<5	<5	<5	<5	<5	<5	<5	<5	<5	<5
Se_ppm	<0.1	<0.1	<0.1	<0.1	<0.1	<0.1	<0.1	<0.1	<0.1	<0.1	<0.1	<0.1	<0.1	<0.1
Te_ppm	<0.02	<0.02	<0.02	<0.02	<0.02	<0.02	<0.02	<0.02	<0.02	<0.02	<0.02	<0.02	<0.02	<0.02
Ge_ppm	<0.1	<0.1	<0.1	<0.1	<0.1	<0.1	<0.1	<0.1	<0.1	<0.1	<0.1	<0.1	<0.1	<0.1
In_ppm	<0.02	<0.02	<0.02	<0.02	<0.02	<0.02	<0.02	<0.02	<0.02	<0.02	<0.02	<0.02	<0.02	<0.02
Re_ppb	<1	<1	<1	<1	<1	<1	<1	<1	<1	<1	<1	<1	<1	<1
Be_ppm	0.10	0.50	<0.1	<0.1	<0.1	<0.1	<0.1	<0.1	0.10	0.10	0.30	0.30	0.40	<0.1
Li_ppm	6.90	2.20	1.20	0.70	1.90	1.30	1.30	1.20	3.90	1.40	25.70	24.80	16.40	3.70
Pd_ppb	<10	<10	<10	<10	<10	<10	<10	<10	<10	<10	<10	<10	<10	<10
Pt_ppb	<2	<2	<2	<2	<2	<2	<2	<2	<2	<2	<2	<2	<2	<2
Au_ppb	3.00	3.00	3.00	3.00	4.00	4.00	4.00	4.00	3.00	2.00	3.00	3.00	3.00	3.00
Pt_ppb	0.20	0.20	0.20	0.20	0.50	0.60	0.40	0.20	4.30	0.20	0.30	0.30	0.50	0.30
Pd_ppb	0.90	0.80	0.60	0.60	1.00	0.90	0.80	0.80	2.00	0.80	0.50	0.80	0.90	0.80
B_ppm	2.00	4.00	1.00	<1	3.00	<1	<1	1.00	<1	<1	4.00	4.00	2.00	<1

Tl_ppm	<0.02	0.04	<0.02	<0.02	0.03	<0.02	<0.02	<0.02	<0.02	<0.02	0.03	0.08	0.03	<0.02
LOI_pct	1.80	1.60	0.70	0.60	1.10	0.90	0.90	0.70	1.90	3.30	3.30	3.80	3.60	0.70
TOT/C_TC000_pct	<0.02	0.03	0.03	<0.02	0.05	<0.02	<0.02	<0.02	<0.02	<0.02	0.13	0.16	0.17	<0.02
TOT/S_pct	<0.02	<0.02	<0.02	<0.02	<0.02	<0.02	<0.02	<0.02	<0.02	<0.02	<0.02	0.09	<0.02	<0.02
Ba_ppm	100.00	162.00	164.00	189.00	150.00	123.00	143.00	133.00	177.00	171.00	364.00	533.00	526.00	234.00
Sc_ppm	1.00	<1	<1	<1	5.00	9.00	2.00	5.00	7.00	4.00	22.00	9.00	8.00	1.00
Sum_pct	99.87	99.92	99.87	99.92	99.87	99.90	99.93	99.88	99.81	99.84	99.73	99.81	99.78	99.86
Cs_ppm	0.60	0.50	0.30	<0.1	1.00	0.20	0.40	0.30	<0.1	1.90	3.00	4.90	4.70	<0.1
Ga_ppm	17.80	21.00	18.60	20.00	19.30	17.10	17.80	17.40	15.20	15.50	17.70	19.10	17.50	19.00
Hf_ppm	0.20	0.60	<0.1	<0.1	0.10	0.30	0.10	0.20	1.50	0.40	2.80	1.60	1.70	<0.1
Nb_ppm	0.80	1.80	0.30	0.20	0.30	1.30	<0.1	0.50	3.20	0.70	4.40	4.80	3.90	<0.1
Rb_ppm	4.10	15.30	3.00	2.10	9.90	1.50	2.40	1.90	5.30	10.00	51.40	108.20	60.40	1.00
Sn_ppm	<1	<1	<1	<1	<1	<1	<1	<1	<1	<1	<1	1.00	2.00	<1
Sr_ppm	497.40	555.20	559.80	616.60	513.00	495.60	550.30	456.80	487.30	593.00	714.60	687.60	870.80	974.70
Ta_ppm	<0.1	<0.1	<0.1	<0.1	<0.1	<0.1	<0.1	<0.1	0.10	<0.1	0.30	0.30	0.20	<0.1
Th_ppm	0.70	1.90	<0.2	<0.2	<0.2	<0.2	<0.2	<0.2	0.90	0.20	4.30	3.90	2.60	<0.2
U_ppm	0.60	0.40	<0.1	<0.1	<0.1	<0.1	<0.1	<0.1	0.20	<0.1	0.90	0.80	0.50	<0.1
V_ppm	16.00	10.00	11.00	<8	47.00	70.00	27.00	43.00	70.00	45.00	246.00	90.00	62.00	13.00
W_ppm	1.80	0.80	1.10	0.80	1.00	1.20	0.90	0.90	0.60	<0.5	1.30	1.20	0.60	0.90
Zr_ppm	4.50	14.60	2.20	2.00	5.20	7.00	4.00	8.20	66.90	14.90	127.30	70.70	69.80	1.40
Y_ppm	1.40	0.70	0.70	0.50	2.30	3.00	1.20	1.30	8.10	2.90	12.00	9.50	9.00	0.50
La_ppm	1.90	2.20	1.80	1.70	1.60	1.90	1.80	1.50	9.80	3.00	28.30	27.00	24.30	2.80
Ce_ppm	3.10	3.80	2.90	3.00	3.10	3.10	3.40	2.50	20.10	6.80	52.60	56.20	45.70	4.40
Pr_ppm	0.36	0.41	0.33	0.35	0.40	0.40	0.38	0.31	2.26	0.75	5.92	5.85	5.10	0.47
Nd_ppm	1.50	1.60	1.30	1.40	1.60	2.00	1.50	1.40	9.30	3.00	23.10	21.50	20.60	1.80

Sm_ppm	0.33	0.32	0.23	0.23	0.29	0.37	0.24	0.17	1.89	0.60	3.98	3.47	3.28	0.18
Eu_ppm	0.60	0.69	0.59	0.64	0.71	0.76	0.77	0.63	0.73	0.59	1.12	1.13	1.21	0.67
Gd_ppm	0.27	0.25	0.20	0.20	0.45	0.55	0.30	0.25	1.75	0.65	3.05	2.54	2.55	0.24
Tb_ppm	0.04	0.02	0.03	0.02	0.06	0.06	0.05	<0.01	0.25	0.09	0.38	0.31	0.33	0.03
Dy_ppm	0.24	0.14	0.09	0.12	0.38	0.52	0.22	0.23	1.48	0.46	2.13	1.77	1.75	0.11
Ho_ppm	0.04	0.02	<0.02	<0.02	0.07	0.07	0.05	0.05	0.26	0.10	0.38	0.35	0.33	<0.02
Er_ppm	0.12	0.05	0.05	0.03	0.24	0.26	0.15	0.13	0.83	0.26	1.14	0.90	0.78	0.07
Tm_ppm	0.01	<0.01	0.01	0.01	0.03	0.03	0.02	<0.01	0.12	0.03	0.16	0.11	0.12	<0.01
Yb_ppm	0.10	<0.05	0.08	<0.05	0.16	0.29	0.12	0.18	0.71	0.28	0.99	0.75	0.71	<0.05
Lu_ppm	0.01	<0.01	<0.01	0.01	0.03	0.03	0.02	0.02	0.11	0.04	0.16	0.12	0.11	<0.01

Sample_ID	KSAT281/099	KSAT281/100	KSAT283/101	KSAT284/102	KSAT284/108	KSAT291/111	KSAT295/114	KSAT316-1	KSAT316-2	KSAT316-3	KSAT316-4	KSAT316-5	KSAT317-1	KSAT320-1
Lat_S	-17.2040	-17.2040	-17.2008	-17.1814	-17.1814	-17.0687	-17.1957	-17.4678	-17.4678	-17.4678	-17.4678	-17.4678	-17.4380	-17.4354
Long_E	13.2646	13.2646	13.2639	13.3197	13.3197	13.4757	13.3654	13.4342	13.4342	13.4342	13.4342	13.4342	13.4097	13.4288
Rocktype	Foliated anorthosite	Anorthosite	Foliated leuconorite	Leucotrocolite	White anorthosite	Leuconorite	Leuconorite	Diorite	Noritic schist	Micaceous leuconorite	Micaceous leuconorite	Micaceous leuconorite	Schistose leuconorite	Foliated leucotrocolite
Group	KC	KC	KC	KC	KC	KC	KC	KC	KC	KC	KC	KC	KC	KC
SiO2_pct	49.92	50.52	48.37	48.44	51.28	48.62	48.42	49.66	68.12	39.73	47.47	47.33	40.02	50.00
TiO2_pct	0.10	0.15	0.42	0.08	0.08	0.10	0.14	1.66	0.43	0.83	2.11	1.02	1.69	0.13
Al2O3_pct	26.74	27.68	17.54	24.46	29.52	26.40	23.43	16.58	15.81	16.54	17.55	18.32	17.87	25.99
Fe2O3t_pct	3.14	1.94	7.80	5.11	0.56	3.39	5.69	10.97	3.01	14.94	9.86	10.41	15.78	4.23
MnO_pct	0.04	0.02	0.13	0.06	<0.01	0.04	0.07	0.15	0.06	0.19	0.15	0.13	0.26	0.05
MgO_pct	2.78	1.41	9.07	5.94	0.27	2.61	5.92	6.10	1.03	8.85	6.43	8.82	7.82	3.68
CaO_pct	10.85	11.44	13.19	10.57	12.20	11.05	9.36	6.64	3.17	13.51	8.47	3.63	9.60	11.29

Na2O_pct	3.76	4.10	1.95	3.19	4.26	3.67	3.37	3.98	5.73	0.57	3.53	4.72	0.41	3.52
K2O_pct	0.50	0.53	0.21	0.21	0.25	1.22	0.88	0.80	1.14	0.14	0.62	0.32	0.09	0.32
Cr2O3_pct	0.00	0.00	0.18	0.00	<0.002	0.01	0.01	0.01	0.01	0.02	0.02	0.01	0.05	0.01
P2O5_pct	0.03	0.01	0.03	0.01	<0.01	<0.01	0.01	0.28	0.06	0.14	0.40	0.20	0.38	0.01
Normalised*	97.88	97.80	98.98	98.13	98.41	97.19	97.33	96.96	98.66	95.52	96.71	94.94	94.03	99.28
SiO2_pct*	51.00	51.66	48.87	49.36	52.11	50.03	49.75	51.22	69.05	41.59	49.08	49.85	42.56	50.36
TiO2_pct*	0.10	0.15	0.43	0.08	0.08	0.10	0.14	1.70	0.44	0.85	2.16	1.05	1.73	0.13
Al2O3_pct*	51.00	51.66	48.87	49.36	52.11	50.03	49.75	51.22	69.05	41.59	49.08	49.85	42.56	50.36
Fe2O3t_pct*	3.21	1.98	7.88	5.21	0.57	3.49	5.85	11.31	3.05	15.64	10.20	10.96	16.78	4.26
FeO_pct*	2.73	1.69	6.70	4.43	0.48	2.96	4.97	9.62	2.59	13.29	8.67	9.32	14.26	3.62
Fe2O3_pct*	0.48	0.30	1.18	0.78	0.09	0.52	0.88	1.70	0.46	2.35	1.53	1.64	2.52	0.64
FeO*_pct	2.89	1.79	7.09	4.69	0.51	3.14	5.26	10.18	2.75	14.08	9.18	9.87	15.10	3.83
MnO_pct*	0.04	0.02	0.13	0.06	N/D	0.04	0.07	0.15	0.06	0.19	0.15	0.13	0.27	0.05
MgO_pct*	2.84	1.44	9.16	6.05	0.27	2.69	6.08	6.29	1.04	9.27	6.65	9.29	8.32	3.71
CaO_pct*	11.12	11.73	13.52	10.84	12.51	11.33	9.60	6.81	3.25	13.85	8.68	3.72	9.84	11.57
Na2O_pct*	3.85	4.20	2.00	3.27	4.37	3.76	3.45	4.08	5.87	0.58	3.62	4.84	0.42	3.61
K2O_pct*	0.51	0.54	0.22	0.22	0.26	1.25	0.90	0.82	1.17	0.14	0.64	0.33	0.09	0.33
Cr2O3_pct*	0.00	0.00	0.18	0.00	N/D	0.01	0.01	0.01	0.01	0.02	0.02	0.01	0.05	0.01
P2O5_pct*	0.03	0.01	0.03	0.01	N/D	N/D	0.01	0.29	0.06	0.14	0.41	0.21	0.39	0.01
Mg#	64.99	60.38	70.91	70.90	50.27	61.75	68.57	53.83	41.77	55.39	57.76	63.98	50.95	64.59
Mo_pct	<0.001	<0.001	<0.001	<0.001	<0.001	<0.001	<0.001	<0.001	<0.001	<0.001	<0.001	<0.001	<0.001	<0.001
Cu_pct	<0.001	<0.001	0.01	<0.001	<0.001	<0.001	0.00	0.01	0.01	0.02	0.01	0.01	0.02	<0.001
Pb_pct	<0.02	<0.02	<0.02	<0.02	<0.02	<0.02	<0.02	<0.02	<0.02	<0.02	<0.02	<0.02	<0.02	<0.02
Zn_pct	<0.01	<0.01	<0.01	<0.01	<0.01	<0.01	<0.01	<0.01	<0.01	0.01	<0.01	<0.01	0.02	<0.01
Ag_ppm	<2	<2	<2	<2	<2	<2	<2	<2	<2	<2	<2	<2	<2	<2

Ni_ppm	71.00	46.00	135.00	156.00	<10	65.00	182.00	204.00	25.00	461.00	113.00	373.00	139.00	114.00
Mo_ppm	0.12	0.11	0.22	0.16	0.23	0.19	0.11	0.20	0.28	0.09	0.78	0.17	0.96	0.25
Cu_ppm	2.43	8.65	90.92	2.51	1.38	2.71	10.26	97.33	60.88	152.19	86.17	112.51	134.58	6.47
Pb_ppm	3.55	2.96	1.32	0.38	1.20	1.03	4.54	3.71	5.17	2.36	3.10	1.15	3.22	0.25
Zn_ppm	15.40	9.80	4.70	9.40	2.40	12.50	13.60	51.10	31.00	98.50	35.10	81.30	159.90	9.30
Ag_ppb	7.00	13.00	34.00	3.00	2.00	8.00	11.00	65.00	63.00	35.00	43.00	20.00	77.00	8.00
Ni_ppm	47.50	34.80	76.00	121.80	5.10	34.80	87.10	161.90	24.00	339.30	86.40	337.10	129.70	92.50
Co_ppm	13.20	9.20	16.50	33.20	1.70	10.20	20.70	38.70	5.40	43.80	41.80	49.90	51.70	21.40
Mn_ppm	142.00	107.00	162.00	328.00	33.00	124.00	155.00	386.00	295.00	586.00	306.00	687.00	1589.00	261.00
As_ppm	0.70	1.20	0.80	<0.1	0.60	2.00	8.30	0.20	<0.1	<0.1	<0.1	<0.1	0.90	<0.1
Au_ppb	<0.2	<0.2	0.30	<0.2	0.30	<0.2	<0.2	<0.2	<0.2	1.20	0.60	0.30	1.30	<0.2
Cd_ppm	0.02	0.02	0.01	<0.01	<0.01	0.01	0.01	0.05	0.02	0.02	0.07	0.03	0.02	<0.01
Sb_ppm	<0.02	<0.02	<0.02	<0.02	<0.02	0.07	0.11	<0.02	<0.02	<0.02	<0.02	<0.02	0.03	<0.02
Bi_ppm	0.05	0.03	<0.02	<0.02	<0.02	<0.02	0.02	0.06	<0.02	0.02	<0.02	<0.02	0.04	<0.02
Cr_ppm	4.70	19.80	191.20	6.40	3.90	20.60	23.80	28.00	36.90	66.20	52.10	35.00	251.60	29.70
Hg_ppb	<5	<5	<5	<5	<5	<5	<5	<5	<5	<5	<5	<5	<5	<5
Se_ppm	<0.1	<0.1	0.10	<0.1	<0.1	<0.1	<0.1	0.20	0.20	<0.1	0.20	0.20	0.30	<0.1
Te_ppm	<0.02	<0.02	<0.02	<0.02	<0.02	<0.02	<0.02	0.02	<0.02	0.04	<0.02	0.02	0.09	<0.02
Ge_ppm	<0.1	<0.1	<0.1	<0.1	<0.1	<0.1	<0.1	<0.1	<0.1	0.10	<0.1	<0.1	0.20	<0.1
In_ppm	<0.02	<0.02	<0.02	<0.02	<0.02	<0.02	<0.02	<0.02	<0.02	<0.02	<0.02	<0.02	0.02	<0.02
Re_ppb	<1	<1	<1	<1	<1	<1	<1	<1	<1	<1	<1	<1	2.00	<1
Be_ppm	0.30	<0.1	<0.1	<0.1	<0.1	<0.1	0.20	0.20	0.20	0.20	0.10	<0.1	1.40	<0.1
Li_ppm	17.20	9.80	1.90	1.90	1.20	11.10	6.70	7.40	2.20	8.90	9.50	19.00	11.80	1.80
Pd_ppb	<10	<10	<10	<10	<10	<10	<10	<10	<10	<10	<10	<10	<10	<10
Pt_ppb	<2	<2	<2	<2	<2	<2	<2	<2	<2	<2	<2	<2	<2	<2

Au_ppb	3.00	3.00	7.00	2.00	2.00	3.00	3.00	12.00	4.00	8.00	5.00	5.00	6.00	4.00
Pt_ppb	0.40	0.20	0.80	0.10	0.20	0.30	0.30	0.40	0.70	1.10	0.30	1.60	3.00	0.30
Pd_ppb	0.80	1.10	2.10	<0.5	<0.5	0.80	0.90	0.90	1.10	2.00	1.10	3.80	5.50	0.80
B_ppm	3.00	3.00	3.00	10.00	3.00	4.00	5.00	3.00	2.00	2.00	2.00	1.00	11.00	<1
Tl_ppm	0.03	0.03	0.06	<0.02	<0.02	0.02	0.06	0.14	0.02	0.05	0.02	0.03	0.03	<0.02
LOI_pct	2.00	2.10	0.80	1.70	1.50	2.70	2.50	2.80	1.20	4.20	3.00	4.80	5.60	0.60
TOT/C_TC000_pct	<0.02	0.03	0.03	0.02	<0.02	0.16	0.02	0.03	<0.02	0.08	0.04	0.03	0.06	0.07
TOT/S_pct	<0.02	<0.02	0.05	<0.02	<0.02	<0.02	<0.02	0.02	<0.02	<0.02	0.06	<0.02	0.11	<0.02
Ba_ppm	172.00	214.00	86.00	127.00	104.00	212.00	199.00	1293.00	555.00	300.00	630.00	215.00	110.00	133.00
Sc_ppm	<1	1.00	40.00	1.00	<1	1.00	4.00	14.00	11.00	10.00	22.00	10.00	53.00	1.00
Sum_pct	99.88	99.90	99.78	99.83	99.91	99.89	99.83	99.76	99.86	99.72	99.71	99.74	99.63	99.88
Cs_ppm	1.00	1.50	1.60	1.20	1.30	0.70	1.90	1.20	0.10	0.80	0.40	0.30	3.20	<0.1
Ga_ppm	16.00	16.20	13.90	12.30	17.90	15.90	15.20	15.40	16.00	20.80	17.40	12.80	22.60	16.60
Hf_ppm	0.10	0.10	0.60	<0.1	<0.1	0.10	0.30	2.50	7.20	1.40	4.90	2.00	3.70	0.10
Nb_ppm	0.80	<0.1	0.50	<0.1	0.20	0.20	1.00	5.70	8.30	3.30	12.40	4.80	8.40	0.10
Rb_ppm	16.50	16.80	8.00	1.30	8.20	37.90	38.70	32.50	27.10	8.10	14.10	9.90	3.00	1.30
Sn_ppm	<1	<1	<1	<1	<1	<1	<1	<1	2.00	<1	1.00	<1	2.00	<1
Sr_ppm	553.30	633.50	213.80	565.80	710.80	603.50	524.80	527.00	386.10	511.10	693.20	449.80	776.60	487.20
Ta_ppm	0.10	<0.1	<0.1	<0.1	<0.1	<0.1	0.20	0.40	0.60	0.20	0.60	0.30	0.30	<0.1
Th_ppm	<0.2	<0.2	0.30	<0.2	<0.2	<0.2	1.00	5.90	16.60	0.80	2.50	0.90	11.60	<0.2
U_ppm	0.50	<0.1	0.10	<0.1	<0.1	<0.1	0.50	0.60	1.60	0.20	0.50	0.10	0.60	<0.1
V_ppm	11.00	18.00	159.00	11.00	<8	12.00	29.00	158.00	52.00	96.00	195.00	100.00	365.00	17.00
W_ppm	<0.5	0.50	0.60	0.60	1.00	1.10	0.80	<0.5	1.40	<0.5	0.70	<0.5	1.20	0.80
Zr_ppm	2.10	5.10	25.30	1.60	3.80	5.50	5.60	102.40	284.20	62.70	211.10	82.90	133.20	4.80
Y_ppm	1.70	0.90	11.10	0.50	0.50	0.80	2.30	15.90	30.10	10.50	33.90	13.90	41.60	0.90

La_ppm	2.70	2.70	3.00	1.40	1.80	2.10	2.00	22.80	53.60	10.80	27.10	12.40	43.20	1.80
Ce_ppm	4.80	4.70	6.30	2.50	3.20	3.80	3.30	48.70	95.80	19.90	59.50	26.00	89.80	3.60
Pr_ppm	0.54	0.48	0.83	0.27	0.35	0.42	0.39	5.70	9.82	2.37	7.06	3.28	10.07	0.34
Nd_ppm	2.00	2.00	4.40	1.00	1.30	1.70	1.90	22.40	33.60	11.00	30.60	13.80	40.90	1.30
Sm_ppm	0.37	0.24	1.26	0.14	0.22	0.20	0.33	4.44	5.90	2.13	6.54	2.78	7.66	0.24
Eu_ppm	0.65	0.65	0.60	0.38	0.48	0.64	0.52	1.56	1.94	0.96	1.78	1.08	2.21	0.58
Gd_ppm	0.43	0.31	1.84	0.19	0.12	0.22	0.50	4.08	5.24	2.20	6.60	3.11	7.75	0.24
Tb_ppm	0.04	0.03	0.31	0.01	0.03	0.02	0.06	0.57	0.86	0.34	1.01	0.46	1.21	0.03
Dy_ppm	0.26	0.22	2.01	0.09	0.12	0.19	0.40	3.21	5.45	1.97	6.10	2.56	7.36	0.20
Ho_ppm	0.05	0.02	0.42	<0.02	0.03	0.02	0.07	0.59	1.04	0.40	1.21	0.55	1.55	0.04
Er_ppm	0.17	0.08	1.20	0.06	0.04	0.08	0.23	1.59	3.33	1.15	3.37	1.44	4.59	0.06
Tm_ppm	0.02	0.01	0.16	0.01	0.02	0.01	0.03	0.20	0.43	0.16	0.48	0.21	0.69	0.01
Yb_ppm	0.14	0.06	1.02	<0.05	<0.05	0.07	0.20	1.36	2.81	0.97	2.92	1.36	4.32	0.06
Lu_ppm	0.03	<0.01	0.15	<0.01	<0.01	0.01	0.03	0.18	0.40	0.15	0.42	0.18	0.70	0.01

Sample_ID	KSAT321-1	KAC040/041	KAC041/042a	KAC041/042b	KAC166/153	KAC084/135ab	KAC250/246	KSAT285/104	KSAT285/106	KSAT285/107	KAC007/009	KAC008/010	KAC009/011	KAC010/012
Lat_S	-17.2524	-16.5736	-16.5736	-16.5736	-15.4386		-16.8929	-17.1820	-17.1820	-17.1820	-17.1918	-17.2147	-17.1687	-17.1202
Long_E	13.3190	13.5523	13.5523	13.5523	13.7791		13.4636	13.3206	13.3206	13.3206	13.9800	13.9609	14.0137	14.0172
Rocktype	Leucotroctolite	Anorthosite	Leuconorite	Fine-g porphyritic material within 041/042a	Norite		leuconorite				Gabbro?	Granodiorite / diorite/ gabbro?	Granodiorite	Granodiorite
Group	KC	KC	KC	KC	KC	KC	KC	KC	KC	KC	KC	KC	KC	KC
SiO2_pct	50.92	50.61	51.33	46.60	45.07	50.93	49.73	34.83	48.98	35.73	48.03	43.90	46.35	57.90
TiO2_pct	0.17	0.26	0.84	1.17	0.08	0.60	0.88	0.19	0.08	0.13	0.63	0.67	0.60	0.85
Al2O3_pct	24.06	25.04	19.05	14.59	22.13	3.17	19.11	1.96	25.77	3.41	17.66	17.16	16.45	14.63

Fe2O3t_pct	4.45	4.51	9.49	16.74	8.91	19.24	6.31	25.11	4.11	24.85	8.39	10.88	8.91	7.54
MnO_pct	0.07	0.06	0.17	0.30	0.10	0.30	0.10	0.15	0.04	0.26	0.13	0.18	0.17	0.14
MgO_pct	3.41	3.68	5.13	8.33	10.29	23.69	4.04	27.70	4.82	26.72	9.75	11.89	8.58	4.86
CaO_pct	10.25	10.24	8.60	9.05	10.54	1.93	11.37	0.87	10.92	1.39	11.09	12.65	14.06	5.42
Na2O_pct	4.09	3.92	3.78	2.19	2.02	0.08	3.24	0.18	3.28	0.34	2.60	1.31	2.34	2.57
K2O_pct	0.68	0.38	0.36	0.17	0.13	0.01	0.25	<0.01	0.18	<0.01	0.27	0.07	0.67	3.18
Cr2O3_pct	0.01	0.03	0.02	0.06	0.01	0.13	0.02	0.01	0.00	0.00	0.03	0.08	0.02	0.04
P2O5_pct	<0.01	0.02	0.34	0.28	0.02	0.01	0.18	0.05	<0.01	0.05	0.02	0.02	0.09	0.26
Normalised*	98.17	98.74	99.22	99.54	99.36	100.15	95.23	91.10	98.24	93.00	98.63	98.90	98.28	97.47
SiO2_pct*	51.87	51.26	51.73	46.82	45.36	50.85	52.22	38.23	49.86	38.42	48.70	44.39	47.16	59.40
TiO2_pct*	0.17	0.27	0.86	1.20	0.08	0.62	0.90	0.19	0.08	0.13	0.65	0.69	0.62	0.87
Al2O3_pct*	51.87	51.26	51.73	46.82	45.36	50.85	52.22	38.23	49.86	38.42	48.70	44.39	47.16	59.40
Fe2O3t_pct*	4.53	4.57	9.56	16.82	8.97	19.21	6.63	27.56	4.18	26.72	8.51	11.00	9.07	7.74
FeO_pct*	3.85	3.88	8.13	14.29	7.62	16.33	5.63	23.43	3.56	22.71	7.23	9.35	7.71	6.58
Fe2O3_pct*	0.68	0.69	1.43	2.52	1.35	2.88	0.99	4.13	0.63	4.01	1.28	1.65	1.36	1.16
FeO*_pct	4.08	4.11	8.61	15.14	8.07	17.29	5.96	24.81	3.77	24.05	7.66	9.90	8.16	6.96
MnO_pct*	0.07	0.06	0.17	0.31	0.10	0.31	0.10	0.15	0.04	0.27	0.13	0.18	0.17	0.14
MgO_pct*	3.47	3.73	5.17	8.37	10.36	23.65	4.24	30.41	4.91	28.73	9.89	12.02	8.73	4.99
CaO_pct*	10.51	10.50	8.82	9.28	10.81	1.98	11.66	0.89	11.20	1.43	11.37	12.97	14.41	5.56
Na2O_pct*	4.19	4.02	3.88	2.25	2.07	0.08	3.32	0.18	3.36	0.35	2.67	1.34	2.40	2.63
K2O_pct*	0.70	0.39	0.37	0.17	0.13	0.01	0.26	N/D	0.18	N/D	0.28	0.07	0.69	3.26
Cr2O3_pct*	0.01	0.03	0.02	0.06	0.01	0.14	0.02	0.01	0.00	0.00	0.03	0.08	0.02	0.04
P2O5_pct*	N/D	0.02	0.35	0.29	0.02	0.01	0.18	0.05	N/D	0.05	0.02	0.02	0.09	0.27
Mg#	61.63	63.11	53.12	51.06	70.77	72.08	57.31	69.81	71.09	69.27	70.90	69.61	66.87	57.47
Mo_pct	<0.001	<0.001	<0.001	<0.001	<0.001	<0.001	<0.001	<0.001	<0.001	<0.001	<0.001	<0.001	<0.001	<0.001

Cu_pct	<0.001	0.00	0.00	0.12	<0.001	0.00	0.00	<0.001	<0.001	0.00	0.00	0.01	0.01	0.01
Pb_pct	<0.02	<0.02	<0.02	<0.02	<0.02	<0.02	<0.02	<0.02	<0.02	<0.02	<0.02	<0.02	<0.02	<0.02
Zn_pct	<0.01	<0.01	0.01	0.02	<0.01	0.01	<0.01	<0.01	<0.01	0.02	<0.01	<0.01	<0.01	<0.01
Ag_ppm	<2	<2	<2	<2	<2	<2	<2	<2	<2	<2	<2	<2	<2	<2
Ni_ppm	66.00	102.00	51.00	105.00	350.00	331.00	33.00	818.00	123.00	776.00	176.00	299.00	69.00	74.00
Mo_ppm	0.50	0.43	0.39	0.53	0.36	0.51	0.43	<0.01	0.10	0.05	0.58	0.78	0.53	1.03
Cu_ppm	5.14	10.62	19.99	1172.37	5.03	11.62	23.56	4.35	2.02	36.18	13.77	46.35	49.00	51.59
Pb_ppm	6.99	1.38	0.85	1.95	0.28	0.29	0.85	0.36	0.31	0.33	0.23	1.50	0.76	4.94
Zn_ppm	12.20	21.40	35.20	58.80	42.20	10.80	28.10	61.40	10.10	129.50	6.20	5.80	21.10	74.10
Ag_ppb	22.00	5.00	16.00	504.00	3.00	4.00	7.00	42.00	5.00	5.00	8.00	28.00	22.00	96.00
Ni_ppm	31.50	84.30	24.60	57.50	322.90	35.60	23.90	549.10	103.90	608.70	99.30	91.60	28.00	59.70
Co_ppm	12.00	24.80	10.20	18.00	66.80	9.70	19.80	150.90	28.70	166.50	27.20	13.40	15.40	21.10
Mn_ppm	188.00	381.00	114.00	171.00	736.00	137.00	496.00	856.00	278.00	1487.00	355.00	325.00	386.00	743.00
As_ppm	0.60	<0.1	<0.1	<0.1	<0.1	<0.1	<0.1	0.20	0.50	0.50	<0.1	<0.1	<0.1	0.10
Au_ppb	<0.2	0.40	1.60	10.50	<0.2	<0.2	<0.2	<0.2	0.30	<0.2	<0.2	0.80	0.80	1.20
Cd_ppm	0.01	<0.01	0.02	0.16	<0.01	<0.01	0.03	0.01	<0.01	0.02	<0.01	0.02	0.02	0.01
Sb_ppm	0.02	<0.02	<0.02	<0.02	<0.02	<0.02	<0.02	<0.02	<0.02	<0.02	<0.02	<0.02	<0.02	<0.02
Bi_ppm	0.05	<0.02	<0.02	0.39	<0.02	<0.02	<0.02	<0.02	<0.02	<0.02	<0.02	<0.02	<0.02	0.02
Cr_ppm	18.50	147.70	136.90	371.00	21.50	204.40	83.40	9.70	14.70	9.90	57.20	103.00	37.10	181.90
Hg_ppb	<5	<5	<5	<5	<5	<5	<5	<5	<5	<5	<5	<5	<5	<5
Se_ppm	<0.1	<0.1	<0.1	<0.1	<0.1	<0.1	0.10	<0.1	0.10	<0.1	<0.1	<0.1	<0.1	<0.1
Te_ppm	<0.02	<0.02	<0.02	0.03	0.04	<0.02	<0.02	<0.02	<0.02	<0.02	<0.02	0.03	0.03	<0.02
Ge_ppm	<0.1	<0.1	<0.1	0.10	<0.1	<0.1	<0.1	<0.1	<0.1	<0.1	<0.1	<0.1	<0.1	<0.1
In_ppm	<0.02	<0.02	<0.02	0.05	<0.02	<0.02	<0.02	<0.02	<0.02	<0.02	<0.02	<0.02	<0.02	<0.02
Re_ppb	<1	<1	<1	<1	<1	<1	<1	<1	<1	<1	<1	<1	<1	<1

Be_ppm	<0.1	<0.1	0.30	0.40	<0.1	<0.1	0.20	<0.1	<0.1	<0.1	<0.1	<0.1	0.30	0.40
Li_ppm	5.20	2.40	6.00	6.40	1.60	2.60	1.70	0.60	1.50	1.10	0.90	0.50	2.70	17.60
Pd_ppb	<10	<10	<10	19.00	<10	<10	<10	<10	<10	<10	<10	13.00	<10	<10
Pt_ppb	<2	<2	<2	7.00	<2	<2	<2	<2	<2	<2	<2	6.00	4.00	<2
Au_ppb	4.00	2.00	2.00	12.00	4.00	3.00	9.00	6.00	4.00	10.00	3.00	5.00	4.00	6.00
Pt_ppb	0.30	0.20	3.10	8.90	0.30	0.20	0.40	0.50	0.20	0.60	0.20	13.20	8.40	2.20
Pd_ppb	1.00	0.80	4.00	16.10	0.80	0.80	1.30	1.80	0.70	2.00	0.70	14.90	10.40	2.10
B_ppm	4.00	<1	<1	2.00	<1	<1	<1	23.00	7.00	5.00	<1	<1	<1	2.00
Tl_ppm	<0.02	<0.02	<0.02	<0.02	<0.02	<0.02	<0.02	<0.02	<0.02	<0.02	<0.02	<0.02	<0.02	0.23
LOI_pct	1.70	1.10	0.50	0.00	0.40	-0.60	4.60	8.40	1.60	6.50	1.10	0.80	1.40	2.30
TOT/C_TC000_pct	0.06	0.03	0.05	0.03	0.06	0.03	0.69	0.03	<0.02	0.04	0.12	0.10	0.03	0.17
TOT/S_pct	<0.02	<0.02	<0.02	0.15	<0.02	<0.02	<0.02	<0.02	<0.02	<0.02	<0.02	<0.02	<0.02	<0.02
Ba_ppm	241.00	249.00	562.00	578.00	90.00	10.00	156.00	30.00	116.00	46.00	159.00	83.00	260.00	986.00
Sc_ppm	8.00	<1	22.00	53.00	2.00	43.00	27.00	6.00	1.00	6.00	25.00	32.00	40.00	20.00
Sum_pct	99.87	99.84	99.72	99.54	99.76	99.55	99.83	99.50	99.84	99.50	99.73	99.70	99.68	99.77
Cs_ppm	1.00	0.40	<0.1	0.30	<0.1	<0.1	<0.1	2.40	1.80	1.50	0.10	<0.1	0.20	1.90
Ga_ppm	16.30	16.20	21.20	22.50	13.40	6.50	19.60	0.80	12.90	1.60	13.80	13.50	14.40	17.10
Hf_ppm	0.10	<0.1	1.80	5.20	<0.1	0.40	1.80	0.20	<0.1	0.20	0.40	0.60	1.60	5.60
Nb_ppm	<0.1	0.10	3.00	10.70	0.20	0.50	5.10	0.80	<0.1	0.60	0.30	0.40	2.40	8.10
Rb_ppm	11.60	2.00	1.80	3.80	0.90	0.50	3.20	0.90	0.60	0.60	1.30	1.00	12.30	98.90
Sn_ppm	<1	<1	<1	4.00	<1	<1	<1	<1	<1	<1	<1	<1	<1	2.00
Sr_ppm	486.90	755.60	1120.80	481.00	526.30	14.30	440.10	42.10	592.00	69.60	674.40	470.90	955.40	542.30
Ta_ppm	<0.1	<0.1	<0.1	0.40	<0.1	<0.1	0.30	<0.1	<0.1	<0.1	<0.1	<0.1	<0.1	0.40
Th_ppm	<0.2	<0.2	0.30	0.50	<0.2	<0.2	1.50	<0.2	<0.2	<0.2	<0.2	<0.2	0.20	6.70
U_ppm	0.10	<0.1	<0.1	0.10	<0.1	<0.1	0.80	<0.1	<0.1	<0.1	<0.1	<0.1	<0.1	1.30

V_ppm	69.00	35.00	198.00	303.00	<8	235.00	151.00	24.00	8.00	28.00	149.00	224.00	244.00	160.00
W_ppm	1.20	1.30	1.20	2.00	0.80	1.70	1.30	<0.5	<0.5	<0.5	1.90	2.00	1.20	1.50
Zr_ppm	3.90	3.10	68.20	201.50	2.90	11.40	72.80	9.40	1.40	8.10	9.80	13.60	72.10	218.20
Y_ppm	2.30	0.60	12.90	52.60	0.50	4.20	19.80	1.10	0.30	1.30	4.90	10.10	9.60	23.70
La_ppm	1.30	3.00	28.40	25.40	1.80	1.00	13.90	1.20	1.40	1.80	1.60	1.60	11.30	38.10
Ce_ppm	2.60	4.80	52.10	73.50	2.70	2.00	31.50	2.60	2.30	3.20	3.40	4.70	23.70	79.30
Pr_ppm	0.30	0.49	5.64	11.54	0.30	0.22	4.07	0.31	0.27	0.37	0.55	0.79	2.84	9.19
Nd_ppm	1.30	1.60	23.10	57.00	1.40	1.20	18.00	1.10	1.10	1.40	3.40	4.90	11.90	35.10
Sm_ppm	0.32	0.22	4.33	14.17	0.21	0.35	4.10	0.20	0.11	0.27	0.83	1.45	2.22	6.53
Eu_ppm	0.67	0.77	1.88	2.59	0.51	0.09	1.17	0.07	0.40	0.14	0.61	0.63	0.77	1.57
Gd_ppm	0.41	0.21	3.62	12.89	0.17	0.47	4.31	0.25	0.16	0.28	1.16	1.90	2.19	5.54
Tb_ppm	0.06	0.02	0.44	1.69	0.02	0.08	0.65	0.04	0.02	0.04	0.16	0.28	0.31	0.77
Dy_ppm	0.39	0.07	2.63	9.71	0.12	0.64	3.98	0.23	0.12	0.23	1.10	1.92	1.96	4.45
Ho_ppm	0.07	<0.02	0.42	1.88	0.02	0.16	0.74	0.04	0.02	0.05	0.19	0.40	0.36	0.83
Er_ppm	0.25	0.05	1.34	5.36	0.05	0.51	2.13	0.15	0.06	0.19	0.51	1.19	1.07	2.49
Tm_ppm	0.03	<0.01	0.16	0.71	<0.01	0.08	0.29	0.02	<0.01	0.03	0.07	0.14	0.15	0.33
Yb_ppm	0.20	<0.05	1.12	4.37	<0.05	0.57	1.75	0.15	<0.05	0.19	0.37	0.90	0.93	2.27
Lu_ppm	0.03	<0.01	0.15	0.66	<0.01	0.10	0.26	0.04	<0.01	0.04	0.06	0.13	0.15	0.34

Sample_ID	KAC012/016	KAC015/019	KAC020/025	KAC057/055	KAC058/056	KAC074/072	KAC154/147a	KAC154/147b	KAC154/147c	KAC155/148a	KAC155/148b	KAC158/149	KAC162/150	KAC168/154
Lat_S	-16.9913	-16.9923	-16.8569	-16.6117	-16.5996	-15.8375	-15.4874	-15.4874	-15.4874	-15.4875	-15.4875	-15.4863	-15.4875	-15.1911
Long_E	13.9144	13.7249	13.5096	13.8879	13.9075	13.9355	13.7453	13.7453	13.7453	13.7385	13.7385	13.7299	13.7229	13.9367
Rocktype	Porphyritic dolerite dyke	Norite	Norite	Norite	Melanorite/dolerite	Gabbroic rock	Garnet-bearing migmatitic granite	Garnet-bearing migmatitic granite	Garnet-bearing migmatitic granite	Dolerite/norite	Felsic rock (Anorth/LN/LT?)	Migmatitic granitoid?	Fine-g mafic rock in contact	Norite with granite

													with granite	
Group	KC	KC	KC	KC	KC	KC	KC	KC	KC	KC	KC	KC	KC	KC
SiO2_pct	48.08	54.05	47.77	48.90	42.86	56.15	40.05	36.28	39.66	44.51	53.38	54.93	50.34	47.30
TiO2_pct	1.95	0.95	0.58	3.09	2.19	1.27	0.41	0.17	0.19	2.81	0.63	0.28	1.22	1.73
Al2O3_pct	14.79	13.47	17.14	15.68	16.11	16.77	5.48	8.96	5.36	14.91	21.57	21.37	15.91	19.13
Fe2O3t_pct	13.87	10.77	9.03	13.30	15.08	9.82	4.32	6.41	4.03	18.22	6.72	5.76	9.49	11.63
MnO_pct	0.20	0.17	0.15	0.19	0.20	0.18	0.09	0.14	0.10	0.24	0.11	0.12	0.15	0.18
MgO_pct	5.72	5.93	8.70	5.62	9.86	2.87	19.93	26.03	20.35	6.52	3.06	3.44	6.53	4.02
CaO_pct	9.95	8.64	12.69	8.52	11.19	6.38	27.00	18.96	28.16	9.29	7.84	7.39	9.92	7.90
Na2O_pct	2.52	2.02	2.27	3.21	1.45	4.09	0.76	0.42	0.53	2.32	4.37	4.50	3.08	4.11
K2O_pct	0.45	1.32	0.22	0.51	0.28	1.26	0.10	0.05	0.09	0.43	1.09	0.98	1.81	1.87
Cr2O3_pct	0.02	0.02	0.17	0.00	0.03	0.01	0.00	0.00	0.00	0.02	0.01	0.01	0.05	0.00
P2O5_pct	0.22	0.10	<0.01	0.13	0.02	0.41	<0.01	<0.01	<0.01	0.38	0.37	0.29	0.30	0.88
Normalised*	97.76	97.49	98.78	99.25	99.30	99.35	98.14	97.44	98.44	99.71	99.39	99.09	98.93	98.88
SiO2_pct*	49.18	55.44	48.36	49.27	43.16	56.52	40.81	37.23	40.29	44.64	53.71	55.43	50.88	47.84
TiO2_pct*	2.00	0.97	0.59	3.17	2.25	1.30	0.42	0.17	0.19	2.88	0.65	0.29	1.25	1.77
Al2O3_pct*	49.18	55.44	48.36	49.27	43.16	56.52	40.81	37.23	40.29	44.64	53.71	55.43	50.88	47.84
Fe2O3t_pct*	14.19	11.05	9.14	13.40	15.19	9.88	4.40	6.58	4.09	18.27	6.76	5.81	9.59	11.76
FeO_pct*	12.06	9.39	7.77	11.39	12.91	8.40	3.74	5.59	3.48	15.53	5.75	4.94	8.15	10.00
Fe2O3_pct*	2.13	1.66	1.37	2.01	2.28	1.48	0.66	0.99	0.61	2.74	1.01	0.87	1.44	1.76
FeO*_pct	12.77	9.94	8.23	12.06	13.67	8.90	3.96	5.92	3.68	16.45	6.09	5.23	8.63	10.59
MnO_pct*	0.21	0.17	0.15	0.19	0.21	0.18	0.09	0.14	0.10	0.25	0.11	0.12	0.15	0.18
MgO_pct*	5.85	6.08	8.81	5.66	9.93	2.89	20.31	26.71	20.67	6.54	3.08	3.47	6.60	4.07

CaO_pct*	10.20	8.86	13.01	8.73	11.47	6.54	27.68	19.44	28.87	9.52	8.04	7.58	10.17	8.10
Na2O_pct*	2.58	2.07	2.33	3.29	1.49	4.19	0.78	0.43	0.54	2.38	4.48	4.61	3.16	4.21
K2O_pct*	0.46	1.35	0.23	0.52	0.29	1.29	0.10	0.05	0.09	0.44	1.12	1.00	1.86	1.92
Cr2O3_pct*	0.02	0.02	0.18	0.00	0.03	0.01	0.00	0.00	0.00	0.02	0.01	0.01	0.05	0.00
P2O5_pct*	0.23	0.10	N/D	0.13	0.02	0.42	N/D	N/D	N/D	0.39	0.38	0.30	0.31	0.90
Mg#	46.37	53.58	66.89	46.97	57.82	37.99	90.63	89.49	91.37	42.86	48.84	55.60	59.06	42.02
Mo_pct	<0.001	<0.001	<0.001	<0.001	<0.001	<0.001	<0.001	<0.001	<0.001	<0.001	<0.001	<0.001	<0.001	<0.001
Cu_pct	0.01	0.01	0.01	0.01	0.01	0.01	<0.001	0.00	<0.001	0.02	0.01	0.00	0.00	0.00
Pb_pct	<0.02	<0.02	<0.02	<0.02	<0.02	<0.02	<0.02	<0.02	<0.02	<0.02	<0.02	<0.02	<0.02	<0.02
Zn_pct	0.01	<0.01	<0.01	0.01	0.01	0.01	<0.01	<0.01	<0.01	0.02	<0.01	<0.01	<0.01	0.01
Ag_ppm	<2	<2	<2	<2	<2	<2	<2	<2	<2	<2	<2	<2	<2	<2
Ni_ppm	63.00	97.00	135.00	90.00	230.00	18.00	12.00	28.00	<10	93.00	50.00	30.00	88.00	<10
Mo_ppm	0.56	0.46	0.23	0.34	0.16	0.98	0.13	0.60	0.13	1.10	0.78	0.29	0.48	0.21
Cu_ppm	81.31	115.98	34.25	79.49	81.65	52.81	9.05	17.10	2.54	157.03	62.82	24.72	44.96	32.65
Pb_ppm	1.42	4.74	0.24	0.44	0.47	1.03	1.49	1.35	1.00	0.86	0.97	1.84	1.51	0.98
Zn_ppm	79.10	48.40	19.60	34.00	48.00	61.90	44.50	20.80	32.10	75.40	29.00	18.90	42.70	97.40
Ag_ppb	26.00	39.00	14.00	21.00	33.00	29.00	120.00	9.00	2.00	26.00	14.00	14.00	11.00	40.00
Ni_ppm	37.40	51.10	68.10	63.80	163.70	10.90	16.30	19.60	7.30	74.40	43.50	17.50	71.00	3.90
Co_ppm	33.10	23.30	24.30	23.10	48.60	10.30	13.00	12.80	7.90	39.20	13.30	6.50	25.30	19.60
Mn_ppm	516.00	431.00	458.00	123.00	657.00	135.00	755.00	948.00	600.00	162.00	165.00	124.00	261.00	530.00
As_ppm	<0.1	<0.1	<0.1	<0.1	<0.1	<0.1	0.50	0.40	0.40	<0.1	<0.1	0.20	0.20	<0.1
Au_ppb	<0.2	2.20	0.40	0.60	0.80	0.30	<0.2	<0.2	<0.2	<0.2	1.00	1.40	0.80	0.40
Cd_ppm	0.07	0.04	<0.01	0.02	0.03	0.01	0.05	0.06	0.03	<0.01	0.01	<0.01	0.01	0.03
Sb_ppm	<0.02	<0.02	<0.02	<0.02	<0.02	<0.02	<0.02	<0.02	<0.02	<0.02	<0.02	<0.02	<0.02	<0.02
Bi_ppm	0.03	0.06	<0.02	<0.02	<0.02	<0.02	<0.02	<0.02	<0.02	0.05	<0.02	<0.02	<0.02	<0.02

Cr_ppm	44.50	77.60	324.70	20.10	95.70	33.50	61.60	93.70	21.60	105.40	99.70	79.30	347.20	11.10
Hg_ppb	<5	<5	<5	<5	<5	<5	<5	<5	<5	6.00	8.00	<5	<5	<5
Se_ppm	<0.1	0.10	<0.1	<0.1	0.10	0.20	<0.1	<0.1	<0.1	<0.1	<0.1	<0.1	<0.1	0.20
Te_ppm	<0.02	<0.02	<0.02	<0.02	<0.02	<0.02	<0.02	<0.02	<0.02	<0.02	<0.02	<0.02	<0.02	<0.02
Ge_ppm	<0.1	<0.1	<0.1	<0.1	<0.1	<0.1	0.10	0.10	0.10	0.10	<0.1	<0.1	0.20	<0.1
In_ppm	0.04	<0.02	<0.02	<0.02	<0.02	<0.02	<0.02	<0.02	<0.02	0.04	<0.02	<0.02	<0.02	0.03
Re_ppb	1.00	1.00	<1	2.00	<1	<1	<1	<1	<1	2.00	1.00	<1	<1	<1
Be_ppm	0.40	0.20	<0.1	<0.1	0.10	0.20	0.60	0.40	0.70	0.30	0.20	0.30	0.20	0.30
Li_ppm	5.40	6.40	1.10	3.30	12.00	2.90	6.00	3.60	3.40	9.10	6.70	6.30	16.00	9.80
Pd_ppb	<10	<10	<10	<10	<10	<10	<10	<10	<10	<10	<10	<10	<10	<10
Pt_ppb	<2	5.00	<2	<2	<2	<2	<2	<2	<2	<2	<2	<2	<2	<2
Au_ppb	2.00	4.00	3.00	2.00	2.00	4.00	3.00	4.00	3.00	7.00	3.00	3.00	4.00	4.00
Pt_ppb	0.20	8.30	0.20	0.30	0.70	1.20	0.30	0.40	0.30	0.80	0.60	0.70	1.70	0.30
Pd_ppb	0.70	12.00	0.70	0.90	1.50	2.10	1.00	0.90	0.90	2.00	1.10	1.10	1.70	0.80
B_ppm	<1	1.00	<1	<1	<1	<1	6.00	6.00	8.00	<1	2.00	1.00	1.00	<1
Tl_ppm	0.02	0.04	<0.02	<0.02	<0.02	<0.02	<0.02	<0.02	<0.02	<0.02	<0.02	<0.02	0.23	0.14
LOI_pct	2.00	2.30	1.00	0.50	0.40	0.40	1.50	2.10	1.20	0.00	0.40	0.70	0.80	0.80
TOT/C_TC000_pct	0.25	0.05	0.02	0.04	0.03	0.04	0.16	0.25	0.12	0.03	0.05	0.04	0.05	<0.02
TOT/S_pct	0.13	0.03	0.04	0.15	0.04	0.08	<0.02	<0.02	<0.02	0.14	<0.02	<0.02	0.07	0.05
Ba_ppm	191.00	356.00	89.00	536.00	59.00	1221.00	70.00	58.00	84.00	399.00	1733.00	530.00	637.00	1306.00
Sc_ppm	36.00	31.00	37.00	27.00	29.00	23.00	2.00	3.00	2.00	35.00	9.00	9.00	28.00	21.00
Sum_pct	99.76	99.79	99.78	99.75	99.70	99.75	99.64	99.54	99.64	99.71	99.79	99.79	99.73	99.68
Cs_ppm	0.40	0.90	0.20	<0.1	0.10	<0.1	<0.1	<0.1	<0.1	<0.1	1.30	<0.1	1.00	0.10
Ga_ppm	18.30	14.70	13.80	17.50	17.80	20.90	6.80	12.10	6.30	21.40	23.40	23.20	15.30	22.00
Hf_ppm	3.30	3.30	0.40	2.50	0.90	10.20	0.70	0.10	0.20	4.30	0.50	1.30	3.30	5.00

Nb_ppm	6.80	5.10	0.30	7.80	3.20	9.30	2.70	0.30	0.70	10.30	1.20	1.50	15.70	13.20
Rb_ppm	9.80	45.40	1.60	2.00	5.30	11.10	0.50	0.50	0.50	3.30	13.30	8.80	67.70	43.80
Sn_ppm	1.00	2.00	<1	<1	<1	<1	<1	<1	<1	2.00	<1	<1	<1	1.00
Sr_ppm	284.80	144.20	325.50	528.50	452.40	653.10	152.10	94.80	108.20	353.70	906.60	949.30	587.50	1094.50
Ta_ppm	0.50	0.30	<0.1	0.40	0.20	0.30	0.20	<0.1	<0.1	0.60	<0.1	<0.1	0.70	0.40
Th_ppm	1.70	5.50	<0.2	<0.2	<0.2	0.20	1.40	<0.2	0.50	0.60	0.50	0.80	2.10	1.20
U_ppm	0.60	1.20	<0.1	<0.1	<0.1	0.10	0.30	<0.1	<0.1	<0.1	<0.1	0.20	0.50	0.40
V_ppm	333.00	298.00	235.00	341.00	338.00	142.00	18.00	29.00	14.00	346.00	141.00	73.00	237.00	214.00
W_ppm	0.90	1.20	0.70	1.10	1.00	2.20	1.40	1.50	1.70	1.80	1.60	2.30	1.30	1.00
Zr_ppm	121.90	128.50	12.00	99.50	18.60	439.80	19.90	5.50	7.90	174.80	20.30	51.10	135.20	229.80
Y_ppm	26.20	24.80	7.60	16.30	10.20	30.30	7.80	2.80	4.90	36.70	13.40	11.20	21.40	36.30
La_ppm	14.20	18.90	1.60	10.20	1.90	36.00	8.70	2.80	3.70	23.00	32.50	49.30	33.80	67.50
Ce_ppm	31.70	37.80	4.00	21.00	5.90	77.20	19.10	5.40	7.00	51.60	55.50	84.60	69.00	148.40
Pr_ppm	4.13	4.46	0.56	2.72	1.02	9.49	2.31	0.67	0.84	6.98	6.35	9.26	8.35	18.85
Nd_ppm	18.70	18.00	3.20	12.60	5.50	41.10	9.80	2.60	3.50	31.00	24.90	33.70	31.70	74.50
Sm_ppm	4.49	4.02	1.03	3.05	1.86	7.90	1.91	0.56	0.72	7.18	4.27	4.91	5.56	12.59
Eu_ppm	1.56	1.09	0.61	1.62	1.07	2.83	0.55	0.20	0.24	2.38	3.20	2.52	1.63	3.30
Gd_ppm	5.20	4.26	1.25	3.23	2.35	7.53	1.85	0.55	0.71	7.81	3.67	3.68	4.55	9.72
Tb_ppm	0.77	0.71	0.22	0.46	0.35	1.07	0.27	0.07	0.10	1.11	0.45	0.40	0.65	1.24
Dy_ppm	4.88	4.57	1.46	3.07	2.20	5.87	1.50	0.53	0.75	6.82	2.44	2.11	3.59	7.01
Ho_ppm	0.96	0.96	0.28	0.59	0.38	1.19	0.29	0.09	0.16	1.30	0.46	0.37	0.72	1.31
Er_ppm	2.86	2.71	0.81	1.84	1.02	3.05	0.89	0.27	0.49	3.72	1.27	1.01	2.05	3.57
Tm_ppm	0.38	0.40	0.11	0.22	0.13	0.45	0.11	0.04	0.07	0.50	0.15	0.14	0.29	0.46
Yb_ppm	2.38	2.49	0.72	1.49	0.76	2.54	0.70	0.33	0.49	3.21	0.95	0.90	1.89	3.01
Lu_ppm	0.36	0.38	0.10	0.25	0.11	0.37	0.09	0.06	0.09	0.47	0.14	0.14	0.28	0.45

Sample_ID	KAC168/155	KAC168/156	KAC168/157	KAC154/186A	KAC154/186B	KAC155/187B	KAC155/187C	KAC155/187D	KAC199/194	KAC202/196	KAC204/199	KAC227/226	KAC281-1	KAC281-2
Lat_S	-15.1911	-15.1911	-15.1911	-15.4874	-15.4874	-15.4875	-15.4875	-15.4875	-16.9093	-16.9101	-16.9096	-16.9159	-17.0771	-17.0771
Long_E	13.9367	13.9367	13.9367	13.7453	13.7453	13.7385	13.7385	13.7385	13.4621	13.4614	13.4631	13.4625	13.6299	13.6299
Rocktype	Porphyritic rock	Norite	Norite w irregular Pl phenocrysts	Calc-silicate/meta-ultramafic?	Calc-silicate/meta-ultramafic?	Fine-grained norite	Contact between fine-grained norite and medium-grained leuconorite	Fine-grained norite	Porphyritic dyke	Mafic dyke	Dolerite dyke in anorthosite	Dolerite dyke	Mafic intrusive? rock	
Group	KC	KC	KC	KC	KC	KC	KC	KC	KC	KC	KC	KC	KC	KC
SiO2_pct	47.09	45.50	46.00	39.66	42.08	47.39	46.58	46.48	50.24	46.21	46.43	45.94	51.48	50.27
TiO2_pct	0.93	0.95	1.49	0.87	0.27	2.44	2.57	2.45	2.79	1.64	1.38	1.78	2.17	1.10
Al2O3_pct	21.96	18.90	18.58	4.27	4.62	15.04	15.77	15.90	15.28	14.37	15.85	16.31	12.20	16.31
Fe2O3t_pct	8.57	10.71	11.64	4.15	2.23	16.53	16.06	16.45	10.75	12.96	12.23	13.58	14.95	10.16
MnO_pct	0.12	0.17	0.17	0.11	0.06	0.22	0.21	0.22	0.15	0.28	0.17	0.22	0.22	0.19
MgO_pct	5.01	6.84	6.73	22.76	14.59	6.06	6.06	5.85	3.84	8.47	7.23	6.76	4.21	4.93
CaO_pct	12.30	11.91	10.65	26.08	33.62	8.42	8.98	8.49	6.71	9.08	10.70	9.12	7.78	10.28
Na2O_pct	2.53	2.72	2.70	0.61	0.96	2.84	2.59	2.87	5.42	1.84	2.32	2.70	3.92	3.69
K2O_pct	0.34	0.48	0.26	0.07	0.23	0.42	0.47	0.64	0.41	1.94	0.53	0.93	0.84	0.51
Cr2O3_pct	0.01	0.01	0.02	0.01	0.00	0.02	0.01	0.02	0.04	0.08	0.13	0.03	0.01	0.03
P2O5_pct	0.11	0.30	0.19	<0.01	<0.01	0.32	0.36	0.32	1.16	0.44	0.12	0.44	0.30	0.12
Normalised *	99.01	98.58	98.46	98.59	98.72	99.75	99.73	99.74	96.77	97.40	97.17	97.90	98.08	97.69
SiO2_pct*	47.56	46.16	46.72	40.23	42.63	47.51	46.71	46.60	51.92	47.44	47.78	46.93	52.49	51.46

TiO2_pct*	0.95	0.97	1.53	0.89	0.28	2.50	2.63	2.51	2.86	1.68	1.41	1.82	2.22	1.13
Al2O3_pct*	47.56	46.16	46.72	40.23	42.63	47.51	46.71	46.60	51.92	47.44	47.78	46.93	52.49	51.46
Fe2O3t_pct*	8.66	10.86	11.82	4.21	2.26	16.57	16.10	16.49	11.11	13.31	12.59	13.87	15.24	10.40
FeO_pct*	7.36	9.23	10.05	3.58	1.92	14.09	13.69	14.02	9.44	11.31	10.70	11.79	12.96	8.84
Fe2O3_pct*	1.30	1.63	1.77	0.63	0.34	2.49	2.42	2.47	1.67	2.00	1.89	2.08	2.29	1.56
FeO*_pct	7.79	9.78	10.64	3.79	2.03	14.91	14.49	14.84	10.00	11.98	11.33	12.48	13.72	9.36
MnO_pct*	0.12	0.17	0.17	0.11	0.06	0.23	0.22	0.23	0.15	0.29	0.17	0.23	0.23	0.19
MgO_pct*	5.06	6.94	6.84	23.09	14.78	6.08	6.08	5.87	3.97	8.70	7.44	6.91	4.29	5.05
CaO_pct*	12.61	12.21	10.92	26.74	34.47	8.63	9.21	8.70	6.88	9.31	10.97	9.35	7.98	10.54
Na2O_pct*	2.59	2.79	2.77	0.63	0.98	2.91	2.66	2.94	5.56	1.89	2.38	2.77	4.02	3.78
K2O_pct*	0.35	0.49	0.27	0.07	0.24	0.43	0.48	0.66	0.42	1.99	0.54	0.95	0.86	0.52
Cr2O3_pct*	0.01	0.01	0.02	0.01	0.00	0.02	0.01	0.02	0.04	0.08	0.13	0.03	0.01	0.03
P2O5_pct*	0.11	0.31	0.19	#VALUE!	#VALUE!	0.33	0.37	0.33	1.19	0.45	0.12	0.45	0.31	0.12
Mg#	55.07	57.25	54.79	92.00	93.20	43.46	44.17	42.71	42.82	57.81	55.34	51.07	37.12	50.43
Mo_pct	<0.001	<0.001	<0.001	<0.001	<0.001	<0.001	<0.001	<0.001	<0.001	<0.001	<0.001	<0.001	<0.001	<0.001
Cu_pct	0.01	0.02	0.01	<0.001	<0.001	0.01	0.01	0.00	0.03	0.01	0.01	0.01	0.01	0.03
Pb_pct	<0.02	<0.02	<0.02	<0.02	<0.02	<0.02	<0.02	<0.02	<0.02	<0.02	<0.02	<0.02	<0.02	<0.02
Zn_pct	<0.01	<0.01	<0.01	<0.01	<0.01	0.01	0.01	0.01	0.01	0.02	0.01	0.01	0.01	<0.01
Ag_ppm	<2	<2	<2	<2	<2	<2	<2	<2	<2	<2	<2	<2	<2	<2
Ni_ppm	90.00	41.00	128.00	<10	<10	89.00	97.00	69.00	50.00	218.00	110.00	100.00	28.00	120.00
Mo_ppm	0.30	0.23	0.47	0.06	0.05	0.59	0.81	0.48	0.21	0.44	0.41	0.47	0.19	0.37
Cu_ppm	47.71	165.00	119.45	5.46	3.95	80.66	78.57	41.48	316.50	76.65	49.64	60.64	75.01	297.12
Pb_ppm	1.08	1.45	1.21	1.03	1.46	0.59	1.37	0.62	5.42	4.29	0.87	3.93	1.21	0.75
Zn_ppm	17.80	34.00	26.50	28.70	57.00	43.90	47.40	47.40	107.60	79.60	34.30	53.70	56.20	39.40
Ag_ppb	13.00	48.00	124.00	7.00	8.00	15.00	16.00	11.00	247.00	93.00	31.00	41.00	123.00	99.00

Ni_ppm	39.40	23.40	68.70	5.20	1.60	60.20	67.20	43.40	36.90	117.40	55.60	60.10	15.10	82.40
Co_ppm	13.60	19.00	23.40	7.50	5.40	28.30	30.80	28.40	24.90	28.80	23.30	30.90	20.70	25.50
Mn_ppm	169.00	392.00	288.00	700.00	407.00	106.00	83.00	106.00	839.00	677.00	382.00	302.00	531.00	578.00
As_ppm	<0.1	<0.1	<0.1	<0.1	2.80	<0.1	<0.1	<0.1	<0.1	0.20	<0.1	0.20	0.30	0.30
Au_ppb	<0.2	2.90	0.50	<0.2	<0.2	0.30	0.30	<0.2	1.30	1.90	0.60	<0.2	<0.2	0.20
Cd_ppm	0.01	0.03	0.02	0.03	0.03	0.02	0.01	0.01	0.09	0.06	0.06	0.03	0.06	0.05
Sb_ppm	<0.02	<0.02	<0.02	<0.02	<0.02	<0.02	<0.02	<0.02	0.03	<0.02	<0.02	<0.02	<0.02	<0.02
Bi_ppm	<0.02	<0.02	<0.02	<0.02	<0.02	<0.02	0.02	<0.02	0.02	0.05	<0.02	0.05	<0.02	<0.02
Cr_ppm	38.20	57.60	57.30	8.10	1.80	97.50	68.00	97.20	50.80	151.70	31.90	54.00	25.80	107.30
Hg_ppb	<5	<5	<5	<5	<5	<5	<5	<5	<5	<5	<5	<5	<5	<5
Se_ppm	0.20	0.30	0.20	0.20	0.20	0.10	0.20	<0.1	0.30	<0.1	<0.1	0.20	<0.1	<0.1
Te_ppm	0.03	0.04	0.03	<0.02	<0.02	<0.02	0.02	<0.02	0.03	<0.02	<0.02	0.03	<0.02	<0.02
Ge_ppm	<0.1	<0.1	<0.1	0.10	0.10	<0.1	<0.1	<0.1	0.20	<0.1	<0.1	<0.1	0.20	<0.1
In_ppm	<0.02	<0.02	<0.02	<0.02	<0.02	0.02	0.03	0.03	0.02	0.02	<0.02	<0.02	0.03	<0.02
Re_ppb	<1	<1	<1	<1	<1	<1	<1	<1	<1	<1	<1	<1	2.00	<1
Be_ppm	0.20	0.30	0.20	0.60	1.00	0.20	0.30	0.10	1.60	0.30	0.20	0.30	0.30	0.30
Li_ppm	3.70	5.50	5.30	3.10	8.00	5.40	6.10	5.70	12.50	25.60	10.70	10.00	4.60	12.10
Pd_ppb	<10	<10	<10	<10	<10	<10	<10	<10	<10	<10	<10	<10	<10	<10
Pt_ppb	<2	3.00	<2	<2	<2	<2	<2	<2	<2	<2	<2	<2	<2	<2
Au_ppb	3.00	6.00	4.00	3.00	4.00	7.00	4.00	4.00	4.00	4.00	3.00	6.00	6.00	4.00
Pt_ppb	0.40	6.70	0.40	0.30	0.30	1.00	0.70	0.40	0.40	1.10	0.20	0.60	0.40	0.20
Pd_ppb	0.90	9.80	1.10	0.80	1.10	2.40	1.30	1.10	0.80	2.50	0.80	1.80	1.30	0.80
B_ppm	<1	<1	<1	9.00	15.00	<1	<1	<1	4.00	2.00	3.00	2.00	1.00	<1
Tl_ppm	<0.02	<0.02	<0.02	<0.02	<0.02	<0.02	<0.02	<0.02	<0.02	0.06	<0.02	0.06	0.10	<0.02
LOI_pct	0.80	1.10	1.30	1.00	1.00	0.00	0.00	0.00	2.90	2.30	2.60	1.80	1.70	2.10

TOT/C_TC000_pct	<0.02	0.02	<0.02	0.15	0.09	0.03	<0.02	<0.02	0.05	0.03	0.11	0.09	<0.02	<0.02
TOT/S_pct	<0.02	0.19	0.05	<0.02	<0.02	<0.02	0.13	<0.02	<0.02	0.06	0.02	0.21	<0.02	<0.02
Ba_ppm	194.00	234.00	289.00	60.00	107.00	382.00	435.00	541.00	123.00	744.00	141.00	466.00	184.00	261.00
Sc_ppm	20.00	35.00	29.00	4.00	2.00	31.00	31.00	30.00	22.00	28.00	29.00	29.00	37.00	35.00
Sum_pct	99.81	99.68	99.76	99.59	99.72	99.75	99.73	99.74	99.67	99.70	99.77	99.70	99.78	99.79
Cs_ppm	0.10	<0.1	0.10	<0.1	<0.1	<0.1	0.30	0.10	0.30	1.30	0.50	1.20	0.70	<0.1
Ga_ppm	17.20	19.40	18.00	5.30	6.00	22.10	21.10	22.20	19.40	16.80	16.80	18.40	17.20	16.40
Hf_ppm	1.50	2.00	2.30	1.20	1.20	3.60	4.50	2.90	9.10	3.20	2.20	3.50	6.20	2.10
Nb_ppm	3.50	6.10	5.40	5.30	1.30	9.80	12.10	9.80	21.10	7.70	4.70	8.00	13.10	3.90
Rb_ppm	4.00	2.40	2.80	0.20	0.50	2.70	7.90	7.40	8.20	51.60	14.40	29.10	28.20	10.10
Sn_ppm	<1	<1	<1	<1	<1	1.00	2.00	1.00	2.00	1.00	<1	<1	2.00	<1
Sr_ppm	429.60	880.80	394.90	117.50	169.00	336.40	405.10	469.80	471.80	394.60	264.80	648.10	155.10	242.90
Ta_ppm	0.20	0.20	0.30	0.50	0.10	0.50	0.80	0.60	1.10	0.40	0.30	0.40	0.80	0.20
Th_ppm	0.40	0.20	<0.2	1.90	1.50	0.30	1.20	<0.2	4.00	0.80	1.00	1.10	4.50	1.20
U_ppm	<0.1	<0.1	<0.1	0.40	0.20	<0.1	0.40	<0.1	2.40	0.20	0.30	0.30	1.10	0.30
V_ppm	174.00	288.00	267.00	11.00	14.00	309.00	311.00	321.00	239.00	243.00	266.00	267.00	335.00	250.00
W_ppm	0.70	1.20	1.20	0.70	<0.5	1.30	1.40	1.30	1.50	1.10	0.50	0.90	0.70	1.10
Zr_ppm	54.40	64.90	80.60	42.10	44.50	145.80	190.00	116.10	431.60	125.80	82.70	138.20	228.50	73.50
Y_ppm	14.20	21.60	21.40	15.40	6.70	30.70	34.70	30.10	52.20	27.60	21.10	31.90	46.60	19.90
La_ppm	8.90	28.20	11.30	15.80	6.60	20.60	23.70	22.30	89.70	25.30	8.40	30.50	26.50	9.20
Ce_ppm	18.80	69.90	25.50	33.10	14.10	46.10	53.60	48.70	191.40	58.60	20.20	65.60	56.30	20.30
Pr_ppm	2.41	9.66	3.52	4.09	1.76	6.15	6.97	6.41	22.92	7.14	2.66	7.98	7.72	2.74
Nd_ppm	10.70	40.90	15.70	16.50	7.30	27.10	30.30	27.60	92.70	31.20	12.70	33.60	33.10	12.40
Sm_ppm	2.54	7.69	3.77	3.44	1.48	6.23	6.93	6.08	17.06	6.38	3.09	6.50	7.94	2.94
Eu_ppm	1.01	2.13	1.32	1.04	0.46	2.24	2.35	2.44	4.30	1.87	1.14	2.14	2.10	1.10

Gd_ppm	2.78	5.94	4.18	3.41	1.40	6.72	7.02	6.63	15.61	6.34	3.88	6.70	8.64	3.67
Tb_ppm	0.42	0.77	0.63	0.50	0.21	0.97	1.06	0.94	2.12	0.91	0.64	1.02	1.36	0.58
Dy_ppm	2.59	4.28	4.07	3.02	1.16	5.91	6.39	5.78	11.03	5.40	3.77	6.19	8.28	3.60
Ho_ppm	0.50	0.79	0.78	0.54	0.23	1.17	1.18	1.09	2.09	1.10	0.80	1.20	1.61	0.74
Er_ppm	1.43	2.13	2.26	1.61	0.66	3.32	3.57	3.16	5.62	3.12	2.50	3.63	4.93	2.11
Tm_ppm	0.20	0.30	0.29	0.21	0.09	0.45	0.47	0.40	0.74	0.48	0.35	0.49	0.66	0.27
Yb_ppm	1.24	1.89	1.90	1.38	0.48	2.69	2.97	2.57	4.61	2.88	2.13	3.16	4.33	1.72
Lu_ppm	0.20	0.27	0.28	0.20	0.08	0.43	0.47	0.41	0.69	0.42	0.33	0.48	0.67	0.27

Sample_ID	KAC300-1	KAC392-1	KAC392-2	KAC449-1	KSAT004/004	KSAT005/005	KSAT011/006	KSAT013/008	KSAT017/009	KSAT021/010	KSAT024/011	KSAT025/012	KSAT028/015	KSAT039/024A
Lat_S	-17.0713	-17.3781	-17.3781	-17.2904	-16.8777	-16.8767	-16.8740	-16.8668	-16.8440	-16.8479	-16.8504	-16.8506	-16.6997	-15.7595
Long_E	13.5391	13.3026	13.3026	13.2857	13.0442	13.0436	13.0284	13.0301	12.9679	12.9537	12.9492	12.9514	13.3532	13.5877
Rocktype	Mafic rock	Gabbro	Gabbro	Ultramafic	Dolerite	Dolerite	Dolerite	Mixed metavolcanic?	Dolerite	Dolerite	Dolerite	Dolerite	Pyroxenite	Pyroxenite (weakly layered)
Group	KC	KC	KC	KC	KC	KC	KC	KC	KC	KC	KC	KC	KC	KC
SiO2_pct	35.08	44.13	55.78	42.64	46.18	46.03	48.26	46.46	48.21	45.87	45.85	44.51	50.86	48.73
TiO2_pct	2.11	2.47	0.13	0.24	1.83	0.50	0.90	1.89	1.75	1.42	0.97	0.78	0.41	0.66
Al2O3_pct	21.61	15.60	23.80	10.90	16.37	17.68	12.56	15.90	13.54	16.46	16.90	17.02	4.63	15.69
Fe2O3t_pct	14.43	16.91	6.03	10.30	13.72	9.25	11.90	13.94	13.82	12.24	9.51	10.51	10.00	8.35
MnO_pct	0.14	0.21	0.06	0.18	0.19	0.13	0.21	0.17	0.22	0.17	0.14	0.14	0.22	0.14
MgO_pct	3.27	6.25	3.85	17.44	6.21	8.76	11.01	6.75	6.86	7.39	7.79	10.48	16.93	8.42
CaO_pct	18.99	9.15	3.26	13.09	8.58	10.84	10.77	6.66	9.00	10.63	11.14	9.93	14.05	12.19
Na2O_pct	<0.01	2.84	1.26	0.37	2.79	2.14	1.69	3.33	3.17	1.66	2.72	1.69	0.84	1.58
K2O_pct	<0.01	0.48	1.43	0.12	0.35	1.13	0.62	1.14	0.66	0.40	0.50	0.30	0.28	1.38

Cr2O3_pct	0.01	0.02	0.01	0.08	0.01	0.03	0.12	0.01	0.03	0.02	0.04	0.03	0.26	0.03
P2O5_pct	0.23	0.01	<0.01	<0.01	0.18	0.06	0.12	0.18	0.13	0.17	0.11	0.09	0.02	0.10
Normalised*	95.86	98.13	95.82	95.44	96.44	96.64	98.20	96.54	97.44	96.43	95.76	95.52	98.55	97.30
SiO2_pct*	36.60	44.97	58.21	44.68	47.88	47.63	49.14	48.13	49.48	47.57	47.88	46.60	51.61	50.08
TiO2_pct*	2.16	2.53	0.13	0.25	1.88	0.51	0.92	1.94	1.79	1.46	0.99	0.80	0.42	0.68
Al2O3_pct*	36.60	44.97	58.21	44.68	47.88	47.63	49.14	48.13	49.48	47.57	47.88	46.60	51.61	50.08
Fe2O3t_pct*	15.05	17.23	6.29	10.79	14.23	9.57	12.12	14.44	14.18	12.69	9.93	11.00	10.15	8.58
FeO_pct*	12.80	14.65	5.35	9.17	12.09	8.14	10.30	12.27	12.06	10.79	8.44	9.35	8.63	7.29
Fe2O3_pct*	2.26	2.58	0.94	1.62	2.13	1.44	1.82	2.17	2.13	1.90	1.49	1.65	1.52	1.29
FeO*_pct	13.55	15.51	5.66	9.71	12.80	8.61	10.91	13.00	12.76	11.42	8.94	9.90	9.13	7.72
MnO_pct*	0.14	0.22	0.06	0.18	0.19	0.13	0.22	0.17	0.23	0.17	0.14	0.14	0.23	0.14
MgO_pct*	3.41	6.37	4.02	18.27	6.44	9.06	11.21	6.99	7.04	7.66	8.13	10.97	17.18	8.65
CaO_pct*	19.47	9.38	3.34	13.42	8.80	11.11	11.04	6.83	9.23	10.90	11.42	10.18	14.40	12.50
Na2O_pct*	#VALUE!	2.91	1.29	0.38	2.86	2.19	1.73	3.41	3.25	1.70	2.79	1.73	0.86	1.62
K2O_pct*	#VALUE!	0.49	1.47	0.12	0.36	1.16	0.64	1.17	0.68	0.41	0.51	0.31	0.29	1.41
Cr2O3_pct*	0.01	0.02	0.01	0.08	0.01	0.03	0.12	0.01	0.03	0.02	0.04	0.03	0.26	0.03
P2O5_pct*	0.24	0.01	N/D	N/D	0.18	0.06	0.12	0.18	0.13	0.17	0.11	0.09	0.02	0.10
Mg#	32.21	43.66	57.24	78.02	48.69	66.50	65.98	50.38	51.00	55.86	63.20	67.64	78.02	67.89
Mo_pct	<0.001	<0.001	<0.001	<0.001	<0.001	<0.001	<0.001	<0.001	<0.001	<0.001	<0.001	<0.001	<0.001	<0.001
Cu_pct	<0.001	0.01	0.00	0.00	0.01	0.00	0.00	0.01	0.01	0.01	0.01	0.01	0.01	0.01
Pb_pct	<0.02	<0.02	<0.02	<0.02	<0.02	<0.02	<0.02	<0.02	<0.02	<0.02	<0.02	<0.02	<0.02	<0.02
Zn_pct	<0.01	0.01	0.02	<0.01	0.01	<0.01	0.01	0.01	<0.01	<0.01	<0.01	<0.01	0.01	<0.01
Ag_ppm	<2	<2	<2	<2	<2	<2	<2	<2	<2	<2	<2	<2	<2	<2
Ni_ppm	60.00	101.00	30.00	280.00	113.00	197.00	175.00	111.00	63.00	167.00	250.00	336.00	212.00	66.00
Mo_ppm	0.47	0.09	0.44	0.13	0.25	0.28	0.27	0.21	0.25	0.35	0.29	0.24	0.12	0.33

Cu_ppm	4.36	61.21	4.02	33.58	68.19	28.09	30.99	72.89	91.10	68.08	40.44	50.15	61.53	131.32
Pb_ppm	1.19	1.27	0.79	0.24	1.00	1.91	1.56	0.90	1.49	0.39	0.30	0.33	14.90	4.77
Zn_ppm	61.10	78.90	120.40	8.20	82.10	34.00	28.70	69.50	51.40	63.70	40.20	46.40	58.70	14.90
Ag_ppb	15.00	48.00	41.00	19.00	31.00	14.00	13.00	36.00	39.00	26.00	11.00	22.00	17.00	58.00
Ni_ppm	55.70	87.50	26.50	180.60	88.50	107.50	42.60	74.10	38.40	114.20	170.80	228.20	65.10	21.90
Co_ppm	31.80	53.10	20.50	45.80	44.80	35.70	17.30	40.10	30.90	41.40	31.00	44.50	13.20	14.40
Mn_ppm	611.00	298.00	425.00	489.00	655.00	418.00	410.00	633.00	652.00	564.00	438.00	550.00	310.00	190.00
As_ppm	0.30	0.20	<0.1	<0.1	0.30	5.70	11.00	1.70	0.10	<0.1	<0.1	0.10	<0.1	1.00
Au_ppb	<0.2	<0.2	<0.2	1.50	0.90	0.20	5.10	0.60	0.30	0.70	1.20	0.80	<0.2	0.70
Cd_ppm	<0.01	0.04	0.09	<0.01	0.11	0.02	0.01	0.09	0.10	0.07	0.01	0.03	0.05	0.05
Sb_ppm	0.02	<0.02	<0.02	<0.02	<0.02	0.03	0.73	<0.02	<0.02	<0.02	<0.02	<0.02	<0.02	<0.02
Bi_ppm	<0.02	<0.02	<0.02	<0.02	0.03	<0.02	0.13	<0.02	<0.02	<0.02	<0.02	<0.02	0.27	<0.02
Cr_ppm	38.80	71.70	26.00	119.20	46.00	44.60	374.40	50.20	157.10	46.00	26.70	35.50	240.50	58.60
Hg_ppb	<5	<5	6.00	<5	<5	<5	<5	<5	<5	<5	<5	<5	<5	<5
Se_ppm	<0.1	<0.1	<0.1	0.20	<0.1	<0.1	<0.1	<0.1	<0.1	<0.1	<0.1	<0.1	<0.1	<0.1
Te_ppm	0.03	<0.02	0.03	<0.02	<0.02	<0.02	0.07	<0.02	<0.02	<0.02	<0.02	<0.02	<0.02	<0.02
Ge_ppm	0.20	<0.1	<0.1	<0.1	<0.1	<0.1	0.10	0.10	0.10	<0.1	<0.1	<0.1	<0.1	<0.1
In_ppm	<0.02	<0.02	<0.02	<0.02	<0.02	<0.02	<0.02	<0.02	<0.02	<0.02	<0.02	<0.02	<0.02	<0.02
Re_ppb	<1	1.00	<1	<1	<1	<1	<1	<1	<1	<1	<1	<1	<1	<1
Be_ppm	0.20	<0.1	0.80	<0.1	<0.1	<0.1	0.30	<0.1	<0.1	0.20	<0.1	<0.1	<0.1	0.10
Li_ppm	17.80	2.90	20.30	6.30	14.90	16.20	3.80	34.60	24.70	8.60	3.50	5.30	1.80	12.10
Pd_ppb	<10	<10	<10	17.00	<10	<10	<10	<10	<10	<10	<10	<10	19.00	<10
Pt_ppb	<2	<2	<2	21.00	<2	<2	4.00	<2	<2	<2	<2	<2	45.00	5.00
Au_ppb	3.00	7.00	3.00	5.00	3.00	3.00	7.00	2.00	2.00	4.00	3.00	3.00	5.00	3.00
Pt_ppb	0.20	0.50	1.30	28.10	0.40	0.20	11.30	0.30	0.20	0.60	1.00	1.10	75.10	5.60

Pd_ppb	0.80	1.60	0.80	20.20	1.00	0.60	10.90	0.60	<0.5	2.20	3.10	3.20	21.10	5.40
B_ppm	2.00	2.00	5.00	42.00	3.00	5.00	6.00	4.00	3.00	2.00	<1	<1	<1	3.00
Tl_ppm	<0.02	0.03	0.05	0.03	0.02	0.03	0.09	0.02	<0.02	<0.02	<0.02	<0.02	<0.02	0.03
LOI_pct	3.70	1.60	4.00	4.20	3.30	3.10	1.50	3.20	2.30	3.30	4.00	4.20	1.10	2.40
TOT/C_TC000_pct	<0.02	<0.02	<0.02	0.14	0.08	0.02	0.02	<0.02	<0.02	0.03	0.39	0.07	0.03	0.05
TOT/S_pct	<0.02	0.34	<0.02	<0.02	0.03	<0.02	<0.02	0.03	0.07	0.04	<0.02	0.03	<0.02	<0.02
Ba_ppm	26.00	449.00	1564.00	35.00	278.00	378.00	150.00	792.00	255.00	149.00	191.00	114.00	57.00	285.00
Sc_ppm	30.00	31.00	11.00	42.00	33.00	24.00	37.00	32.00	50.00	26.00	28.00	18.00	52.00	43.00
Sum_pct	99.56	99.73	99.82	99.64	99.74	99.74	99.70	99.74	99.74	99.73	99.76	99.72	99.65	99.70
Cs_ppm	0.20	0.60	1.80	2.60	0.40	1.10	2.40	0.60	0.40	0.60	1.50	1.00	<0.1	1.50
Ga_ppm	41.30	20.10	38.70	6.60	19.60	16.40	12.90	18.80	16.40	16.80	15.80	14.60	5.10	14.20
Hf_ppm	2.50	0.50	0.70	0.30	3.10	1.00	1.40	3.00	3.00	2.30	1.40	1.20	0.70	1.50
Nb_ppm	7.80	0.20	0.10	<0.1	4.50	1.10	3.30	4.60	2.40	5.40	3.10	2.60	1.00	2.40
Rb_ppm	0.70	6.80	17.70	3.60	9.90	34.00	21.30	45.50	12.10	9.40	10.20	5.70	2.40	50.70
Sn_ppm	1.00	<1	<1	<1	1.00	<1	<1	<1	<1	<1	<1	<1	<1	<1
Sr_ppm	2416.90	608.60	450.60	326.70	517.50	615.10	352.80	398.20	327.20	558.00	426.40	500.40	86.10	691.10
Ta_ppm	0.40	<0.1	<0.1	<0.1	0.30	<0.1	0.20	0.20	0.10	0.40	0.20	0.10	<0.1	0.10
Th_ppm	0.60	<0.2	<0.2	<0.2	1.00	0.50	0.90	1.00	1.10	0.90	0.50	0.50	0.30	2.90
U_ppm	0.20	<0.1	<0.1	<0.1	0.30	<0.1	0.20	0.20	0.30	0.30	0.10	0.10	<0.1	0.60
V_ppm	417.00	462.00	165.00	134.00	292.00	143.00	256.00	288.00	376.00	231.00	201.00	139.00	191.00	219.00
W_ppm	1.20	<0.5	1.60	3.80	<0.5	0.90	0.50	1.00	<0.5	<0.5	0.50	0.60	0.50	0.80
Zr_ppm	82.20	6.10	22.30	6.10	103.50	33.60	52.90	104.50	105.90	84.10	51.60	42.40	21.50	58.00
Y_ppm	29.20	7.50	0.90	5.30	28.10	8.60	16.70	28.10	34.50	19.10	13.50	10.20	11.20	12.50
La_ppm	12.40	0.70	8.70	0.80	11.20	5.00	6.90	11.20	8.20	10.90	6.80	5.90	4.00	13.90
Ce_ppm	28.80	2.10	11.80	3.10	26.30	10.70	15.70	26.60	20.00	25.10	15.30	13.90	10.80	29.70

Pr_ppm	3.79	0.45	0.86	0.59	3.49	1.38	1.92	3.44	2.72	3.18	2.05	1.69	1.67	3.70
Nd_ppm	18.60	3.30	2.70	3.50	15.30	6.30	9.30	15.70	12.90	14.40	9.50	8.10	8.20	15.90
Sm_ppm	4.44	1.18	0.28	1.05	4.37	1.54	2.16	4.17	3.98	3.41	2.17	1.80	2.11	3.69
Eu_ppm	1.86	0.76	1.19	0.39	1.58	0.75	0.80	1.46	1.41	1.27	1.09	0.83	0.60	1.16
Gd_ppm	5.02	1.63	0.17	1.17	5.09	1.71	2.78	5.06	5.48	3.76	2.45	2.10	2.29	3.42
Tb_ppm	0.81	0.26	0.02	0.17	0.83	0.27	0.45	0.80	0.94	0.60	0.38	0.31	0.35	0.47
Dy_ppm	4.80	1.52	0.10	1.03	5.34	1.71	2.85	5.15	6.06	3.50	2.41	1.87	2.18	2.75
Ho_ppm	0.98	0.32	0.03	0.18	1.10	0.33	0.58	1.11	1.24	0.74	0.51	0.40	0.41	0.50
Er_ppm	2.69	0.89	0.13	0.60	3.22	0.95	1.69	3.03	3.76	2.14	1.36	1.19	1.20	1.34
Tm_ppm	0.37	0.11	0.02	0.07	0.43	0.12	0.25	0.44	0.51	0.27	0.19	0.15	0.17	0.19
Yb_ppm	2.42	0.60	0.15	0.42	2.80	0.82	1.52	2.67	3.30	1.85	1.21	1.00	1.11	1.24
Lu_ppm	0.34	0.09	0.04	0.07	0.42	0.12	0.22	0.41	0.48	0.30	0.20	0.16	0.16	0.17

Sample_ID	KSAT039/024B	KAC212/211	KSAT296/115	KSAT298/116	KSAT299/117	KSAT304/121	KAC030/033	KAC062/059	KAC074/071	KAC143/138	KAC164/151a	KAC164/151b	KAC198/193	KAC204/198
Lat_S	-15.7595	-16.9148	-17.2012	-17.1984	-17.1996	-17.4559	-16.9441	-16.4543	-15.8375	-15.3635	-15.4912	-15.4912	-17.0840	-16.9096
Long_E	13.5877	13.4499	13.3617	13.3615	13.3623	13.2033	13.4605	13.9333	13.9355	13.9465	13.7174	13.7174	13.5275	13.4631
Rocktype	Pyroxenite (distinctly layered)	Porphyritic trachyte?	Ultramafic dyke	Ultramafic dyke	Ultramafic dyke	Ultramafic dyke	Felsic metavolcanic	Granodiorite/tonalite (possible diatexite?)	Tonalite/ Granodiorite?	Host granitoid of 143/136	Migmatitic neosome	Leucosome resistite	Mica schist	Granodiorite paragneiss
Group	KC	KC	KC	KC	KC	KC	Basement	Basement	Baseement	Basement	Basement	Basement	Basement	Basement
SiO2_pct	49.28	47.80	41.81	44.72	42.35	52.37	64.76	73.10	63.18	58.29	63.62	48.35	47.68	67.84
TiO2_pct	0.80	1.42	4.28	3.74	4.28	1.72	0.59	0.16	0.56	0.64	0.74	0.76	1.95	0.55
Al2O3_pct	13.48	17.61	13.98	13.19	14.31	15.51	15.42	14.56	17.23	21.32	17.27	12.25	14.07	15.22
Fe2O3t_pct	8.98	11.17	16.91	16.94	17.40	12.83	4.28	1.92	5.21	3.38	5.52	10.19	14.32	4.69

MnO_pct	0.16	0.17	0.21	0.23	0.20	0.24	0.08	0.04	0.06	0.07	0.06	0.20	0.21	0.07
MgO_pct	9.04	5.19	5.34	4.11	5.37	1.70	1.18	0.47	2.48	0.40	2.21	13.02	6.04	1.50
CaO_pct	13.33	8.91	8.25	7.58	7.90	3.64	3.78	2.94	5.84	5.05	3.20	10.88	9.56	2.57
Na2O_pct	1.42	2.73	2.93	2.78	3.19	4.44	3.73	4.29	3.31	5.22	3.36	0.54	2.61	3.13
K2O_pct	0.64	1.91	1.29	1.65	0.72	4.49	3.49	1.57	0.87	4.08	2.91	1.56	0.76	2.00
Cr2O3_pct	0.07	0.10	0.01	<0.002	0.01	0.01	0.01	0.00	0.01	0.01	0.01	0.28	0.03	0.10
P2O5_pct	0.15	0.18	0.77	1.94	0.76	0.82	0.16	0.02	0.19	0.40	0.06	0.25	0.21	0.14
Normalised*	97.39	97.28	95.84	97.03	96.54	98.06	97.56	99.21	98.99	99.41	99.15	98.35	97.46	97.95
SiO2_pct*	50.60	49.14	43.62	46.09	43.87	53.41	66.38	73.68	63.82	58.64	64.17	49.16	48.92	69.26
TiO2_pct*	0.82	1.46	4.39	3.83	4.39	1.76	0.60	0.16	0.57	0.66	0.76	0.78	2.00	0.56
Al2O3_pct*	50.60	49.14	43.62	46.09	43.87	53.41	66.38	73.68	63.82	58.64	64.17	49.16	48.92	69.26
Fe2O3t_pct*	9.22	11.48	17.64	17.46	18.02	13.08	4.39	1.94	5.26	3.40	5.57	10.36	14.69	4.79
FeO_pct*	7.84	9.76	15.00	14.84	15.32	11.12	3.73	1.64	4.47	2.89	4.73	8.81	12.49	4.07
Fe2O3_pct*	1.38	1.72	2.65	2.62	2.70	1.96	0.66	0.29	0.79	0.51	0.84	1.55	2.20	0.72
FeO*_pct	8.30	10.33	15.88	15.71	16.22	11.78	3.95	1.74	4.74	3.06	5.01	9.32	13.22	4.31
MnO_pct*	0.16	0.17	0.22	0.24	0.21	0.25	0.08	0.04	0.06	0.07	0.06	0.21	0.22	0.07
MgO_pct*	9.28	5.34	5.57	4.24	5.56	1.73	1.21	0.47	2.51	0.40	2.23	13.24	6.20	1.53
CaO_pct*	13.67	9.13	8.46	7.77	8.10	3.73	3.88	3.01	5.99	5.18	3.28	11.15	9.80	2.63
Na2O_pct*	1.46	2.80	3.00	2.85	3.27	4.55	3.82	4.40	3.39	5.35	3.44	0.55	2.68	3.21
K2O_pct*	0.66	1.96	1.32	1.69	0.74	4.60	3.58	1.61	0.89	4.18	2.98	1.60	0.78	2.05
Cr2O3_pct*	0.07	0.10	0.01	N/D	0.01	0.01	0.01	0.00	0.01	0.01	0.01	0.29	0.03	0.10
P2O5_pct*	0.15	0.18	0.79	1.99	0.78	0.84	0.16	0.02	0.19	0.41	0.06	0.26	0.22	0.14
Mg#	67.85	49.34	39.83	33.72	39.28	21.74	36.63	33.91	49.95	19.88	45.63	72.82	46.93	40.14
Mo_pct	<0.001	<0.001	<0.001	<0.001	<0.001	<0.001	<0.001	<0.001	<0.001	<0.001	<0.001	<0.001	<0.001	<0.001
Cu_pct	0.01	0.01	0.01	0.00	0.01	0.00	0.00	<0.001	0.00	<0.001	<0.001	0.00	0.01	0.01

Pb_pct	<0.02	<0.02	<0.02	<0.02	<0.02	<0.02	<0.02	<0.02	<0.02	<0.02	<0.02	<0.02	<0.02	<0.02
Zn_pct	<0.01	0.01	0.01	0.02	0.01	0.02	<0.01	<0.01	<0.01	<0.01	<0.01	<0.01	0.01	<0.01
Ag_ppm	<2	<2	<2	<2	<2	<2	<2	<2	<2	<2	<2	<2	<2	<2
Ni_ppm	85.00	49.00	70.00	17.00	71.00	<10	13.00	<10	25.00	<10	32.00	274.00	59.00	16.00
Mo_ppm	0.22	0.71	0.99	1.12	0.93	0.89	1.29	1.31	0.51	0.62	0.36	0.78	0.31	2.22
Cu_ppm	92.31	78.77	43.29	29.17	45.45	9.69	28.92	4.94	22.19	8.26	5.65	19.98	87.02	70.10
Pb_ppm	2.80	2.87	1.64	5.47	10.34	8.85	19.07	2.99	1.82	0.62	2.94	2.40	12.77	8.75
Zn_ppm	29.00	46.80	47.90	57.30	39.00	118.20	66.40	25.30	26.60	20.90	33.70	11.20	56.80	66.60
Ag_ppb	33.00	45.00	17.00	27.00	20.00	28.00	89.00	115.00	181.00	274.00	6.00	110.00	10.00	63.00
Ni_ppm	27.10	26.70	53.30	13.30	51.90	8.70	12.30	3.00	19.70	10.00	32.60	105.00	36.60	16.50
Co_ppm	15.90	23.60	41.80	30.80	40.00	6.40	7.60	2.20	8.70	3.10	13.70	14.70	28.30	9.50
Mn_ppm	281.00	280.00	648.00	374.00	304.00	773.00	530.00	303.00	76.00	408.00	165.00	149.00	699.00	419.00
As_ppm	0.40	<0.1	<0.1	0.10	<0.1	<0.1	1.50	<0.1	<0.1	<0.1	<0.1	<0.1	<0.1	<0.1
Au_ppb	0.30	0.60	<0.2	<0.2	0.30	<0.2	2.00	<0.2	0.30	0.70	1.30	1.60	1.60	1.40
Cd_ppm	0.06	0.03	0.08	0.05	0.07	0.07	0.11	<0.01	<0.01	<0.01	<0.01	0.01	0.05	0.17
Sb_ppm	<0.02	<0.02	<0.02	<0.02	<0.02	<0.02	0.02	<0.02	<0.02	<0.02	<0.02	<0.02	0.03	<0.02
Bi_ppm	<0.02	0.03	<0.02	0.03	<0.02	0.06	0.22	<0.02	<0.02	<0.02	<0.02	0.06	<0.02	0.05
Cr_ppm	139.40	33.70	30.00	3.00	46.50	21.30	62.60	13.70	74.10	59.20	79.10	566.50	81.80	55.90
Hg_ppb	<5	<5	<5	<5	<5	<5	<5	<5	<5	<5	<5	<5	<5	<5
Se_ppm	<0.1	<0.1	0.20	0.50	0.30	0.60	<0.1	<0.1	<0.1	<0.1	<0.1	<0.1	<0.1	0.10
Te_ppm	<0.02	<0.02	<0.02	<0.02	<0.02	<0.02	0.05	<0.02	<0.02	<0.02	<0.02	0.07	<0.02	<0.02
Ge_ppm	<0.1	<0.1	<0.1	<0.1	<0.1	<0.1	0.20	<0.1	<0.1	<0.1	0.20	<0.1	<0.1	<0.1
In_ppm	<0.02	<0.02	0.04	0.04	0.05	0.10	<0.02	<0.02	<0.02	<0.02	0.03	<0.02	<0.02	0.03
Re_ppb	<1	<1	<1	<1	<1	<1	<1	<1	<1	<1	<1	<1	<1	<1
Be_ppm	0.10	0.20	0.50	0.60	0.50	1.20	1.20	0.30	0.30	<0.1	0.40	0.60	0.40	0.60

Li_ppm	9.30	11.10	4.40	5.20	2.00	4.10	17.60	6.70	4.60	2.20	11.20	3.60	13.80	9.90
Pd_ppb	<10	<10	<10	<10	<10	<10	<10	<10	<10	<10	<10	<10	<10	<10
Pt_ppb	3.00	<2	<2	<2	<2	<2	<2	<2	<2	<2	<2	2.00	<2	<2
Au_ppb	3.00	3.00	7.00	8.00	8.00	7.00	3.00	2.00	4.00	3.00	4.00	6.00	6.00	4.00
Pt_ppb	3.80	0.30	0.70	0.60	0.70	0.40	0.40	0.20	0.50	0.20	0.90	6.00	0.30	1.00
Pd_ppb	3.60	0.80	2.20	2.10	2.30	1.50	1.10	0.70	1.20	0.70	1.30	5.70	0.80	1.60
B_ppm	2.00	3.00	2.00	4.00	1.00	<1	2.00	<1	<1	<1	<1	2.00	<1	3.00
Tl_ppm	<0.02	0.05	0.29	0.25	0.20	0.19	0.03	0.05	<0.02	<0.02	0.10	0.26	0.04	0.09
LOI_pct	2.30	2.50	3.90	2.70	3.20	1.70	2.30	0.70	0.80	0.50	0.70	1.30	2.30	1.90
TOT/C_TC000_pct	0.02	0.19	0.67	0.16	0.40	0.18	0.04	0.02	0.04	0.03	0.03	0.15	0.02	0.07
TOT/S_pct	<0.02	0.08	0.10	0.05	0.09	<0.02	0.02	<0.02	0.03	<0.02	<0.02	0.03	<0.02	0.05
Ba_ppm	175.00	724.00	407.00	1485.00	371.00	2178.00	1169.00	1043.00	713.00	4607.00	1221.00	486.00	264.00	969.00
Sc_ppm	51.00	29.00	22.00	26.00	22.00	32.00	9.00	2.00	8.00	9.00	14.00	35.00	39.00	10.00
Sum_pct	99.69	99.78	99.74	99.73	99.74	99.76	99.86	99.91	99.79	99.91	99.85	99.65	99.76	99.85
Cs_ppm	0.30	0.70	3.60	1.50	1.90	0.70	0.70	0.30	<0.1	<0.1	0.20	4.10	0.30	1.30
Ga_ppm	13.00	17.40	18.60	20.10	19.90	25.90	18.30	15.80	17.30	22.60	18.90	12.30	18.60	16.30
Hf_ppm	1.80	2.70	4.90	8.30	4.60	14.60	5.60	4.00	8.60	0.40	6.90	2.20	3.20	5.50
Nb_ppm	3.00	5.60	16.80	24.50	16.90	37.90	11.30	8.80	3.00	0.40	7.70	4.20	6.50	9.90
Rb_ppm	22.70	57.80	28.50	26.70	14.10	73.50	77.20	35.90	5.60	20.60	55.60	87.60	40.00	42.20
Sn_ppm	<1	<1	1.00	2.00	2.00	3.00	2.00	<1	<1	<1	1.00	1.00	2.00	1.00
Sr_ppm	680.60	409.40	436.70	346.90	436.60	237.10	362.90	453.90	622.40	619.90	329.40	513.60	288.40	393.80
Ta_ppm	<0.1	0.20	1.00	1.30	1.10	1.90	0.70	0.50	<0.1	<0.1	0.20	0.20	0.40	0.60
Th_ppm	1.80	1.40	1.70	4.80	1.60	7.40	12.20	7.20	7.80	<0.2	14.60	2.00	2.10	12.10
U_ppm	0.60	0.40	0.50	1.30	0.40	2.00	2.40	1.30	0.30	<0.1	1.30	0.90	0.50	3.90
V_ppm	237.00	264.00	293.00	170.00	292.00	18.00	80.00	17.00	112.00	10.00	98.00	225.00	366.00	60.00

W_ppm	1.50	1.20	0.90	0.90	0.70	1.50	3.00	5.70	1.60	2.60	2.90	3.60	0.90	2.60
Zr_ppm	65.30	100.50	206.90	392.00	196.90	672.10	211.50	141.30	321.20	17.50	271.50	77.90	128.80	209.30
Y_ppm	18.30	20.10	29.00	58.40	27.90	67.10	17.20	37.10	4.50	4.10	22.60	18.80	29.60	24.20
La_ppm	15.20	12.50	25.30	64.40	25.80	90.00	66.20	28.20	61.80	6.90	55.00	25.30	16.40	46.70
Ce_ppm	36.50	28.80	57.70	143.20	56.60	188.60	122.60	57.10	108.40	11.60	100.70	56.80	36.40	94.90
Pr_ppm	4.62	3.57	7.21	17.81	7.20	22.35	12.71	6.24	10.84	1.52	11.59	7.48	4.82	10.21
Nd_ppm	21.30	16.10	32.70	78.00	32.40	91.20	44.70	24.20	37.50	7.50	41.80	32.00	21.50	39.40
Sm_ppm	4.83	3.70	7.15	15.76	7.17	17.58	6.91	5.30	4.38	1.45	6.95	6.28	5.15	6.57
Eu_ppm	1.36	1.40	2.58	4.84	2.59	5.68	1.70	1.05	1.43	8.15	1.79	2.02	1.67	1.47
Gd_ppm	4.44	4.17	7.17	14.89	7.28	16.28	4.92	5.92	2.74	1.50	5.34	5.13	5.61	5.32
Tb_ppm	0.65	0.68	1.04	2.08	1.04	2.42	0.64	0.89	0.26	0.16	0.71	0.64	0.86	0.76
Dy_ppm	3.56	4.07	5.90	11.86	6.13	13.52	3.21	5.95	1.13	0.84	4.07	3.53	5.64	4.40
Ho_ppm	0.70	0.81	1.16	2.29	1.13	2.73	0.61	1.28	0.18	0.16	0.79	0.59	1.10	0.97
Er_ppm	1.89	2.36	3.28	6.33	3.10	7.41	1.59	4.05	0.45	0.37	2.25	1.61	3.35	2.74
Tm_ppm	0.25	0.32	0.43	0.84	0.40	1.02	0.21	0.55	0.06	0.04	0.31	0.23	0.43	0.42
Yb_ppm	1.53	2.14	2.69	5.37	2.68	6.69	1.34	3.73	0.42	0.22	2.13	1.46	2.76	2.79
Lu_ppm	0.21	0.31	0.40	0.83	0.39	1.02	0.23	0.58	0.08	0.04	0.33	0.20	0.42	0.44

Sample_ID	KAC209/207	KAC210/208	KAC218/214	KAC219/215	KAC219/216	KAC220/217	KAC221/218	KAC227/227	KAC227/229	KAC251/247	KAC254/250	KAC256/248	KAC256/249	KAC287-2
Lat_S	-16.9111	-16.9109	-16.9877	-16.9856	-16.9856	-16.9838	-16.9324	-16.9159	-16.9159	-16.8877	-16.8740	-16.8714	-16.8714	-17.0935
Long_E	13.4587	13.4579	13.4551	13.4572	13.4572	13.4604	13.4631	13.4625	13.4625	13.4587	13.4524	13.4534	13.4534	13.5299
Rocktype	Brecciated pyroxenite	Migmatite	Granodiorite gneiss	Brecciated pyroxenite	Granite gneiss	Diorite	Granodiorite gneiss	Granodiorite	Migmatite	Granodiorite and fine grained granite	Granodiorite	migmatite	migmatite	
Group	Basement	Basement	Basement	Basement	Basement	Basement	Basement	Basement	Basement	Basement	Basement	Basement	Basement	Basement

SiO2_pct	59.51	66.55	58.21	50.13	68.41	55.15	56.57	65.53	70.09	66.65	61.44	64.92	68.58	51.79
TiO2_pct	0.30	0.77	0.83	0.89	0.37	0.85	0.72	0.70	0.41	0.56	0.63	0.62	0.49	1.97
Al2O3_pct	9.54	15.06	15.78	8.88	15.68	13.60	16.96	15.46	14.66	15.88	16.36	16.46	15.27	13.78
Fe2O3t_pct	6.98	4.97	7.34	10.68	2.71	9.48	7.51	5.45	3.24	3.48	6.03	4.67	4.31	14.24
MnO_pct	0.16	0.06	0.12	0.19	0.03	0.15	0.13	0.07	0.05	0.04	0.10	0.07	0.11	0.32
MgO_pct	9.76	1.88	3.51	13.15	1.04	5.68	4.05	2.02	1.22	0.99	2.76	1.38	1.30	2.11
CaO_pct	8.20	2.50	4.73	11.77	2.21	6.46	3.99	2.48	2.16	2.19	4.01	2.43	1.76	6.88
Na2O_pct	2.07	3.18	3.27	0.76	5.71	1.43	3.82	3.00	3.67	4.36	3.14	3.53	2.97	3.59
K2O_pct	1.54	3.38	3.24	0.96	1.75	4.27	2.59	3.26	2.27	3.97	2.66	3.36	3.11	2.40
Cr2O3_pct	0.09	0.14	0.19	0.18	0.02	0.09	0.01	0.04	0.07	0.00	0.01	0.01	0.01	0.00
P2O5_pct	0.05	0.06	0.24	0.25	0.07	0.23	0.27	0.06	0.09	0.16	0.28	0.09	0.07	0.65
Normalised*	98.25	98.71	97.55	97.86	98.06	97.55	96.76	98.22	98.07	98.44	97.60	97.74	98.07	97.96
SiO2_pct*	60.57	67.42	59.67	51.23	69.76	56.54	58.46	66.72	71.47	67.71	62.95	66.42	69.93	52.87
TiO2_pct*	0.31	0.79	0.85	0.91	0.38	0.87	0.74	0.72	0.42	0.57	0.65	0.64	0.50	2.02
Al2O3_pct*	60.57	67.42	59.67	51.23	69.76	56.54	58.46	66.72	71.47	67.71	62.95	66.42	69.93	52.87
Fe2O3t_pct*	7.10	5.03	7.52	10.91	2.76	9.72	7.76	5.55	3.30	3.54	6.18	4.78	4.39	14.54
FeO_pct*	6.04	4.28	6.40	9.28	2.35	8.26	6.60	4.72	2.81	3.00	5.25	4.06	3.74	12.36
Fe2O3_pct*	1.07	0.76	1.13	1.64	0.41	1.46	1.16	0.83	0.50	0.53	0.93	0.72	0.66	2.18
FeO*_pct	6.39	4.53	6.77	9.82	2.49	8.75	6.99	4.99	2.97	3.18	5.56	4.30	3.96	13.08
MnO_pct*	0.16	0.06	0.12	0.19	0.03	0.15	0.13	0.07	0.05	0.04	0.10	0.07	0.11	0.33
MgO_pct*	9.93	1.90	3.60	13.44	1.06	5.82	4.19	2.06	1.24	1.01	2.83	1.41	1.33	2.15
CaO_pct*	8.41	2.56	4.85	12.07	2.27	6.62	4.09	2.54	2.21	2.25	4.11	2.49	1.80	7.05
Na2O_pct*	2.12	3.26	3.35	0.78	5.85	1.47	3.92	3.08	3.76	4.47	3.22	3.62	3.04	3.68
K2O_pct*	1.58	3.47	3.32	0.98	1.79	4.38	2.66	3.34	2.33	4.07	2.73	3.44	3.19	2.46
Cr2O3_pct*	0.10	0.15	0.19	0.18	0.02	0.09	0.01	0.04	0.07	0.00	0.01	0.01	0.01	0.00

P2O5_pct*	0.05	0.06	0.25	0.26	0.07	0.24	0.28	0.06	0.09	0.16	0.29	0.09	0.07	0.67
Mg#	74.56	44.23	50.06	72.08	44.58	55.68	53.06	43.73	44.12	37.36	48.97	38.25	38.74	23.70
Mo_pct	<0.001	<0.001	<0.001	<0.001	<0.001	<0.001	<0.001	<0.001	<0.001	<0.001	<0.001	<0.001	<0.001	<0.001
Cu_pct	0.00	0.00	0.00	0.02	<0.001	0.01	0.00	0.01	0.01	0.00	0.00	<0.001	0.00	<0.001
Pb_pct	<0.02	<0.02	<0.02	<0.02	<0.02	<0.02	<0.02	<0.02	<0.02	<0.02	<0.02	<0.02	<0.02	<0.02
Zn_pct	<0.01	<0.01	<0.01	<0.01	<0.01	0.01	<0.01	<0.01	<0.01	<0.01	<0.01	<0.01	<0.01	0.02
Ag_ppm	<2	<2	<2	<2	<2	<2	<2	<2	<2	<2	<2	<2	<2	<2
Ni_ppm	95.00	41.00	26.00	149.00	<10	40.00	27.00	31.00	27.00	<10	22.00	14.00	18.00	<10
Mo_ppm	0.27	0.74	0.55	0.11	0.71	0.07	0.35	1.49	0.71	0.99	0.33	0.62	0.99	0.95
Cu_ppm	28.73	25.18	33.00	153.89	8.63	49.25	33.20	45.07	72.98	18.29	14.91	7.11	16.29	7.08
Pb_ppm	5.46	4.71	5.15	2.96	12.61	4.26	2.48	8.25	7.35	3.06	3.24	8.36	7.23	2.80
Zn_ppm	13.70	84.60	63.90	15.40	44.40	59.20	81.60	80.50	45.90	36.90	68.40	62.60	48.50	109.70
Ag_ppb	40.00	25.00	13.00	36.00	25.00	118.00	88.00	49.00	40.00	16.00	13.00	28.00	18.00	26.00
Ni_ppm	15.30	40.80	17.60	32.10	5.60	22.40	22.40	27.20	24.20	5.10	19.70	13.00	16.30	3.00
Co_ppm	4.80	14.70	15.60	13.00	5.10	19.90	19.40	11.80	8.60	6.50	16.30	8.60	8.30	10.20
Mn_ppm	141.00	408.00	528.00	239.00	199.00	553.00	682.00	454.00	289.00	236.00	599.00	377.00	408.00	1063.00
As_ppm	<0.1	<0.1	<0.1	0.20	<0.1	<0.1	0.20	<0.1	<0.1	<0.1	<0.1	<0.1	<0.1	<0.1
Au_ppb	0.30	1.10	1.00	0.60	0.40	0.20	0.70	0.80	0.60	0.90	<0.2	<0.2	<0.2	0.50
Cd_ppm	0.03	<0.01	0.02	0.03	0.03	0.03	0.02	0.04	0.03	0.01	0.03	0.03	0.01	0.13
Sb_ppm	<0.02	<0.02	<0.02	<0.02	<0.02	<0.02	<0.02	<0.02	<0.02	<0.02	<0.02	<0.02	<0.02	<0.02
Bi_ppm	0.03	0.03	<0.02	0.04	<0.02	<0.02	0.02	0.03	0.04	0.03	<0.02	0.07	0.06	<0.02
Cr_ppm	69.60	135.70	47.50	169.30	32.00	111.20	33.70	73.40	88.40	21.90	52.20	29.80	44.10	8.40
Hg_ppb	<5	<5	<5	<5	<5	<5	<5	<5	<5	<5	<5	<5	<5	<5
Se_ppm	<0.1	<0.1	<0.1	<0.1	<0.1	<0.1	<0.1	<0.1	0.10	<0.1	<0.1	0.10	<0.1	0.40
Te_ppm	<0.02	<0.02	<0.02	<0.02	<0.02	<0.02	<0.02	0.03	0.03	<0.02	<0.02	0.03	<0.02	<0.02

Ge_ppm	<0.1	<0.1	<0.1	<0.1	<0.1	<0.1	<0.1	<0.1	<0.1	<0.1	<0.1	<0.1	<0.1	0.20
In_ppm	<0.02	0.04	<0.02	<0.02	<0.02	<0.02	<0.02	0.04	0.02	<0.02	<0.02	0.03	<0.02	0.10
Re_ppb	<1	<1	<1	<1	<1	<1	<1	<1	<1	<1	<1	<1	<1	<1
Be_ppm	0.30	0.20	0.60	0.20	0.50	0.40	0.70	0.20	0.20	0.50	0.50	0.30	1.20	0.90
Li_ppm	1.00	20.50	15.30	1.70	4.80	6.00	35.20	17.40	13.00	6.10	16.80	17.30	21.90	8.40
Pd_ppb	<10	<10	<10	<10	<10	<10	<10	<10	<10	<10	<10	<10	<10	<10
Pt_ppb	5.00	<2	<2	<2	<2	3.00	<2	<2	<2	<2	<2	<2	<2	<2
Au_ppb	3.00	3.00	5.00	4.00	4.00	3.00	3.00	4.00	4.00	7.00	8.00	7.00	10.00	3.00
Pt_ppb	14.40	1.10	2.10	1.80	0.50	4.10	0.90	0.60	0.50	0.50	1.30	0.90	0.90	0.20
Pd_ppb	7.30	0.90	1.40	1.80	0.60	3.50	1.60	1.00	1.10	1.20	1.80	1.70	1.50	0.80
B_ppm	1.00	<1	5.00	2.00	5.00	2.00	3.00	1.00	1.00	1.00	<1	1.00	<1	2.00
Tl_ppm	0.02	0.29	0.03	<0.02	0.02	<0.02	0.02	0.28	0.05	0.02	0.02	0.04	0.11	<0.02
LOI_pct	1.50	1.10	2.20	1.80	1.80	2.20	3.00	1.60	1.80	1.40	2.20	2.10	1.80	1.70
TOT/C_TC000_pct	0.03	0.04	0.03	0.06	0.08	0.09	0.09	0.06	0.04	0.02	<0.02	0.06	0.05	0.16
TOT/S_pct	<0.02	<0.02	<0.02	<0.02	<0.02	<0.02	<0.02	0.02	<0.02	<0.02	<0.02	<0.02	<0.02	0.05
Ba_ppm	381.00	1446.00	1258.00	220.00	433.00	1545.00	1120.00	1377.00	870.00	1693.00	1705.00	1399.00	1235.00	1846.00
Sc_ppm	36.00	8.00	18.00	45.00	4.00	28.00	16.00	11.00	7.00	5.00	13.00	12.00	13.00	33.00
Sum_pct	99.75	99.81	99.75	99.66	99.86	99.75	99.76	99.82	99.87	99.84	99.80	99.84	99.87	99.66
Cs_ppm	0.30	1.70	0.60	0.20	0.40	0.70	1.40	2.10	0.90	0.50	0.40	1.10	1.60	0.20
Ga_ppm	11.40	16.20	17.40	12.30	17.60	16.60	18.10	16.00	14.00	16.70	16.60	16.70	15.10	19.70
Hf_ppm	0.70	7.90	6.10	2.10	5.00	3.60	3.50	7.10	3.10	6.00	2.90	6.20	5.70	23.00
Nb_ppm	5.00	11.90	10.00	5.00	3.10	8.00	6.90	10.90	7.60	8.60	6.60	12.60	7.30	79.20
Rb_ppm	45.40	83.10	83.10	24.20	47.90	107.30	79.80	81.90	58.30	61.30	49.70	68.50	74.70	26.40
Sn_ppm	3.00	<1	1.00	2.00	<1	1.00	<1	<1	<1	1.00	1.00	<1	<1	<1
Sr_ppm	298.30	469.00	713.20	109.90	561.60	512.50	807.60	478.10	502.80	595.50	858.00	485.90	386.40	376.60

Ta_ppm	0.40	0.60	0.60	0.30	0.30	0.20	0.40	0.80	0.50	0.60	0.50	0.50	0.50	3.40
Th_ppm	0.80	15.70	10.50	1.60	9.20	8.50	5.80	17.60	6.90	9.40	3.60	10.50	10.90	1.90
U_ppm	0.40	2.10	0.90	1.20	1.50	0.80	1.30	2.50	2.00	1.30	1.60	2.30	2.60	0.70
V_ppm	116.00	98.00	165.00	286.00	43.00	213.00	151.00	71.00	51.00	59.00	113.00	89.00	58.00	47.00
W_ppm	1.30	2.70	2.50	0.60	1.60	<0.5	1.10	2.70	2.50	2.30	1.50	2.50	1.70	2.10
Zr_ppm	20.00	304.50	241.20	69.70	209.00	140.80	137.10	255.60	129.50	255.70	114.80	222.80	210.90	1173.40
Y_ppm	38.30	11.70	24.50	19.60	5.50	24.10	17.90	19.30	19.60	17.60	15.40	26.60	34.50	78.30
La_ppm	9.50	57.80	53.30	15.80	33.70	42.30	39.90	59.20	28.60	64.80	24.60	40.10	39.10	81.20
Ce_ppm	27.20	115.20	108.10	45.20	56.40	86.40	80.10	119.80	57.80	125.10	53.20	81.80	78.40	180.60
Pr_ppm	4.59	12.21	11.76	6.13	5.18	9.84	8.75	13.00	6.07	13.13	6.49	9.25	8.86	22.91
Nd_ppm	21.60	46.40	45.60	25.80	17.50	38.80	33.80	48.60	21.60	46.00	25.60	34.30	33.40	104.10
Sm_ppm	5.58	7.74	7.56	5.13	2.45	7.28	5.52	8.23	3.85	6.83	4.60	5.94	5.66	20.61
Eu_ppm	0.93	1.66	1.87	1.50	0.85	1.66	1.59	1.63	1.38	1.46	1.40	1.66	1.61	5.04
Gd_ppm	5.78	5.80	6.38	4.56	1.77	6.08	4.67	5.84	3.14	4.85	3.88	4.86	5.00	19.55
Tb_ppm	1.09	0.71	0.86	0.65	0.20	0.84	0.64	0.76	0.50	0.57	0.52	0.72	0.77	2.87
Dy_ppm	6.97	2.88	4.74	3.86	1.03	4.44	3.44	3.76	3.34	3.13	2.89	4.48	5.61	16.47
Ho_ppm	1.38	0.45	0.94	0.72	0.18	0.93	0.63	0.74	0.69	0.57	0.53	0.92	1.23	3.35
Er_ppm	4.18	0.97	2.70	1.95	0.66	2.61	1.82	1.96	2.18	1.71	1.59	2.84	3.96	9.82
Tm_ppm	0.62	0.13	0.39	0.30	0.08	0.38	0.25	0.26	0.33	0.25	0.22	0.40	0.59	1.34
Yb_ppm	3.67	0.93	2.52	2.04	0.61	2.33	1.60	1.64	1.98	1.59	1.39	2.72	3.86	9.03
Lu_ppm	0.52	0.16	0.35	0.27	0.09	0.35	0.25	0.24	0.30	0.22	0.22	0.42	0.65	1.48

Sample_ID	KAC293	KAC301-2	KAC302-1	KAC302-2	KAC302-3	KAC303-2	KAC306	KAC307	KAC320-2	KAC334-1	KAC346	KAC347	KAC351-1	KAC356-2
Lat_S	-17.0842	-16.9629	-16.9327	-16.9327	-16.9327	-16.9343	-16.9470	-16.9502	-17.0289	-16.8581	-16.6720	-16.6774	-16.7461	-16.7415
Long_E	13.5234	13.3624	13.3369	13.3369	13.3369	13.3395	13.3556	13.3619	13.4970	13.4567	13.3941	13.3895	13.2116	13.2420

Rocktype										Migmatite	Granodiorite	Granodiorite	muscovite schist	Metasedimentary rock
Group	Basement	Basement	Basement	Basement	Basement	Basement	Basement	Basement	Basement	Basement	Basement	Basement	Basement	Basement
SiO2_pct	48.27	48.87	72.96	54.71	67.88	47.50	51.92	58.40	48.35	71.70	58.18	68.71	65.60	67.40
TiO2_pct	1.97	2.14	0.54	0.86	0.51	1.52	0.61	0.84	0.74	0.38	0.85	0.31	0.65	0.57
Al2O3_pct	13.64	13.11	14.01	16.13	16.82	16.07	7.95	15.72	13.51	14.87	15.77	15.24	17.93	17.49
Fe2O3t_pct	14.14	16.51	2.94	8.01	4.82	12.05	10.48	7.39	10.43	2.35	7.53	2.33	4.27	3.96
MnO_pct	0.21	0.23	0.11	0.14	0.06	0.17	0.22	0.12	0.18	0.03	0.12	0.03	0.06	0.04
MgO_pct	6.31	5.93	0.61	4.11	1.45	6.81	12.70	3.83	6.33	0.74	3.61	0.86	1.07	1.11
CaO_pct	9.73	7.00	1.78	7.63	0.52	8.78	12.17	5.14	14.72	2.86	5.97	2.38	0.97	0.96
Na2O_pct	2.45	2.59	5.23	3.38	1.03	2.62	0.94	3.30	1.17	3.93	3.24	3.32	2.31	1.76
K2O_pct	0.89	1.20	0.61	1.75	3.43	1.28	0.60	2.76	1.79	1.81	2.61	4.81	4.10	3.95
Cr2O3_pct	0.03	0.01	0.01	0.02	0.01	0.03	0.18	0.02	0.05	0.01	0.01	0.00	0.01	0.01
P2O5_pct	0.21	0.22	0.08	0.26	0.05	0.28	0.10	0.27	0.07	0.05	0.26	0.08	0.06	0.08
Normalised*	97.95	97.85	98.89	97.08	96.70	97.17	97.89	97.87	97.38	98.78	98.24	98.16	97.08	97.47
SiO2_pct*	49.28	49.94	73.78	56.36	70.20	48.88	53.04	59.67	49.65	72.59	59.22	70.00	67.57	69.15
TiO2_pct*	2.02	2.19	0.55	0.88	0.52	1.56	0.63	0.86	0.76	0.39	0.87	0.32	0.67	0.58
Al2O3_pct*	49.28	49.94	73.78	56.36	70.20	48.88	53.04	59.67	49.65	72.59	59.22	70.00	67.57	69.15
Fe2O3t_pct*	14.44	16.87	2.97	8.25	4.98	12.40	10.71	7.55	10.71	2.38	7.66	2.37	4.40	4.06
FeO_pct*	12.27	14.34	2.53	7.01	4.24	10.54	9.10	6.42	9.10	2.02	6.52	2.02	3.74	3.45
Fe2O3_pct*	2.17	2.53	0.45	1.24	0.75	1.86	1.61	1.13	1.61	0.36	1.15	0.36	0.66	0.61
FeO*_pct	12.99	15.19	2.68	7.43	4.49	11.16	9.64	6.80	9.64	2.14	6.90	2.14	3.96	3.66
MnO_pct*	0.22	0.24	0.11	0.14	0.06	0.17	0.23	0.12	0.18	0.03	0.12	0.03	0.06	0.04
MgO_pct*	6.44	6.06	0.62	4.23	1.50	7.01	12.97	3.91	6.50	0.75	3.67	0.88	1.10	1.14

CaO_pct*	9.98	7.18	1.82	7.82	0.53	9.00	12.48	5.27	15.09	2.93	6.12	2.44	0.99	0.98
Na2O_pct*	2.51	2.66	5.36	3.47	1.06	2.69	0.96	3.38	1.20	4.03	3.32	3.40	2.37	1.80
K2O_pct*	0.91	1.23	0.63	1.79	3.52	1.31	0.62	2.83	1.84	1.86	2.68	4.93	4.20	4.05
Cr2O3_pct*	0.03	0.01	0.01	0.02	0.01	0.03	0.19	0.02	0.05	0.01	0.01	0.00	0.01	0.01
P2O5_pct*	0.22	0.23	0.08	0.27	0.05	0.29	0.10	0.28	0.07	0.05	0.27	0.08	0.06	0.08
Mg#	48.34	42.95	30.31	51.82	38.68	54.23	71.76	52.07	55.99	39.76	50.13	43.62	34.44	37.01
Mo_pct	<0.001	<0.001	<0.001	<0.001	<0.001	<0.001	<0.001	<0.001	<0.001	<0.001	<0.001	<0.001	<0.001	<0.001
Cu_pct	0.01	0.01	0.00	0.00	<0.001	0.01	0.00	0.01	0.00	0.00	0.01	<0.001	<0.001	<0.001
Pb_pct	<0.02	<0.02	<0.02	<0.02	<0.02	<0.02	<0.02	<0.02	<0.02	<0.02	<0.02	<0.02	<0.02	<0.02
Zn_pct	0.01	0.01	<0.01	<0.01	<0.01	<0.01	<0.01	<0.01	<0.01	<0.01	<0.01	<0.01	<0.01	<0.01
Ag_ppm	<2	<2	<2	<2	<2	<2	<2	<2	<2	<2	<2	<2	<2	<2
Ni_ppm	73.00	47.00	<10	31.00	16.00	139.00	127.00	31.00	124.00	<10	26.00	<10	14.00	15.00
Mo_ppm	0.52	1.32	0.10	0.27	0.91	0.24	0.35	0.54	0.25	0.58	0.61	1.36	0.29	1.44
Cu_ppm	91.93	12.43	49.50	33.66	6.43	66.00	20.13	53.27	23.13	16.34	55.46	6.19	3.86	7.50
Pb_ppm	13.22	7.49	3.02	8.38	5.59	2.08	2.31	5.99	10.64	6.73	4.79	8.03	4.73	5.85
Zn_ppm	90.90	48.30	75.10	64.30	60.90	53.20	15.00	61.30	10.60	42.40	62.10	25.00	54.40	58.60
Ag_ppb	22.00	22.00	67.00	55.00	8.00	27.00	94.00	60.00	48.00	33.00	59.00	13.00	12.00	147.00
Ni_ppm	42.60	6.00	25.50	22.30	16.20	80.00	24.10	23.20	15.30	9.60	21.60	6.80	13.30	14.00
Co_ppm	22.80	4.40	26.50	16.40	7.70	26.50	8.70	16.50	6.00	5.20	17.80	5.30	7.90	6.80
Mn_ppm	549.00	380.00	842.00	564.00	332.00	477.00	255.00	545.00	218.00	133.00	393.00	165.00	360.00	170.00
As_ppm	0.20	0.30	<0.1	0.50	1.00	<0.1	<0.1	0.10	0.10	0.20	<0.1	<0.1	<0.1	<0.1
Au_ppb	<0.2	0.50	<0.2	1.40	0.50	0.30	<0.2	0.50	<0.2	0.40	1.60	0.30	0.40	0.30
Cd_ppm	0.05	0.03	0.03	0.07	0.01	0.04	0.02	0.07	0.03	0.03	0.02	0.01	0.03	<0.01
Sb_ppm	0.03	0.04	0.03	0.02	0.05	0.08	<0.02	<0.02	0.03	<0.02	<0.02	<0.02	<0.02	<0.02
Bi_ppm	<0.02	0.17	0.08	0.06	0.16	0.11	0.03	0.04	0.07	0.03	<0.02	<0.02	0.32	0.30

Cr_ppm	58.40	32.90	44.20	72.80	20.70	44.70	213.90	64.00	49.00	37.30	71.60	19.30	26.30	34.80
Hg_ppb	<5	<5	<5	<5	<5	<5	<5	<5	<5	<5	<5	<5	<5	<5
Se_ppm	0.20	<0.1	0.10	<0.1	<0.1	<0.1	<0.1	<0.1	<0.1	<0.1	<0.1	<0.1	<0.1	<0.1
Te_ppm	<0.02	<0.02	<0.02	<0.02	0.03	<0.02	<0.02	<0.02	0.03	0.03	<0.02	<0.02	0.04	0.03
Ge_ppm	0.10	<0.1	<0.1	<0.1	<0.1	<0.1	0.10	<0.1	0.10	<0.1	<0.1	<0.1	<0.1	<0.1
In_ppm	<0.02	<0.02	0.03	<0.02	<0.02	<0.02	<0.02	<0.02	<0.02	0.02	0.02	<0.02	<0.02	<0.02
Re_ppb	<1	<1	<1	<1	<1	<1	<1	<1	<1	<1	<1	<1	<1	<1
Be_ppm	0.40	0.20	0.80	0.80	0.80	0.20	0.40	0.50	0.20	0.10	0.30	0.60	0.60	0.30
Li_ppm	20.40	8.70	16.50	19.50	20.40	27.30	2.40	16.00	1.60	12.50	12.70	7.20	14.50	21.50
Pd_ppb	<10	<10	<10	<10	<10	<10	<10	<10	<10	<10	<10	<10	<10	<10
Pt_ppb	<2	<2	<2	<2	<2	<2	<2	<2	2.00	<2	<2	<2	<2	<2
Au_ppb	2.00	6.00	3.00	3.00	3.00	3.00	2.00	2.00	3.00	4.00	4.00	3.00	3.00	3.00
Pt_ppb	0.20	0.50	0.30	1.20	0.70	1.00	1.20	2.50	5.60	0.30	2.40	0.30	0.60	0.50
Pd_ppb	<0.5	1.80	0.70	1.60	1.10	2.20	0.90	2.80	3.60	1.00	2.30	0.60	0.60	0.60
B_ppm	1.00	1.00	2.00	7.00	2.00	3.00	2.00	5.00	2.00	1.00	1.00	1.00	2.00	2.00
Tl_ppm	0.02	0.09	<0.02	0.05	0.08	0.03	<0.02	0.08	<0.02	0.10	0.17	0.03	0.19	0.30
LOI_pct	1.80	1.90	1.00	2.70	3.20	2.60	1.80	1.90	2.40	1.10	1.50	1.70	2.80	2.40
TOT/C_TC000_pct	0.02	<0.02	0.03	0.12	0.02	0.02	0.04	<0.02	0.26	0.08	0.04	0.08	0.05	0.03
TOT/S_pct	<0.02	<0.02	<0.02	0.02	<0.02	<0.02	<0.02	<0.02	<0.02	<0.02	<0.02	<0.02	<0.02	<0.02
Ba_ppm	671.00	385.00	454.00	502.00	893.00	545.00	125.00	915.00	206.00	597.00	1150.00	1171.00	931.00	1091.00
Sc_ppm	39.00	45.00	9.00	21.00	12.00	29.00	68.00	19.00	36.00	5.00	19.00	4.00	14.00	12.00
Sum_pct	99.75	99.75	99.89	99.78	99.90	99.77	99.69	99.77	99.78	99.88	99.74	99.86	99.88	99.87
Cs_ppm	0.20	0.50	1.40	1.70	1.60	0.80	<0.1	1.50	0.20	0.70	1.40	0.40	3.50	5.20
Ga_ppm	18.30	19.00	13.20	19.10	17.90	15.10	13.50	18.30	13.70	15.00	17.00	15.20	18.40	17.40
Hf_ppm	3.80	3.80	4.90	3.80	5.20	3.30	1.30	5.10	1.10	4.00	5.50	4.50	4.90	6.00

Nb_ppm	7.20	9.20	7.40	8.00	12.20	6.10	4.00	9.40	1.50	6.70	8.00	8.70	11.50	12.10
Rb_ppm	51.80	45.70	20.60	55.70	127.40	62.70	10.20	75.10	47.90	48.70	64.10	89.60	109.90	120.00
Sn_ppm	<1	1.00	<1	1.00	1.00	<1	2.00	1.00	<1	<1	1.00	<1	2.00	2.00
Sr_ppm	207.20	156.30	380.70	552.90	94.40	340.80	178.70	624.10	471.60	558.10	746.30	526.40	185.20	199.80
Ta_ppm	0.50	0.60	0.60	0.50	1.00	0.30	0.20	0.50	<0.1	0.30	0.40	0.60	0.70	0.90
Th_ppm	2.20	1.50	6.60	4.80	19.80	1.10	0.70	7.40	<0.2	5.20	7.50	11.30	14.40	16.10
U_ppm	0.50	0.50	2.00	1.60	3.50	0.20	1.10	1.60	<0.1	0.90	0.70	1.30	3.40	4.10
V_ppm	376.00	434.00	34.00	182.00	65.00	211.00	286.00	160.00	261.00	34.00	159.00	35.00	75.00	50.00
W_ppm	0.90	1.30	2.60	0.70	3.00	0.90	0.60	1.60	0.90	2.00	0.70	1.40	2.10	3.30
Zr_ppm	130.70	145.20	196.50	135.50	178.60	136.30	34.90	199.70	39.30	149.80	223.80	182.00	179.70	217.10
Y_ppm	30.40	35.70	19.50	22.30	29.40	21.10	25.10	21.80	16.10	8.00	22.00	11.00	20.90	26.30
La_ppm	16.80	15.80	32.20	35.00	56.80	16.30	11.20	43.20	2.60	26.20	55.20	53.70	31.40	50.60
Ce_ppm	34.70	34.90	61.80	76.80	102.30	34.70	28.90	90.00	6.40	50.00	104.80	99.70	63.40	100.80
Pr_ppm	4.62	4.43	7.09	9.28	12.00	4.28	4.26	10.25	0.91	5.15	11.79	10.14	7.74	11.26
Nd_ppm	20.00	20.90	26.90	37.60	43.30	18.50	20.00	40.60	5.10	18.20	44.30	34.10	27.40	41.20
Sm_ppm	5.10	5.15	4.62	6.99	7.62	4.10	4.91	7.05	1.60	2.92	7.61	4.95	5.12	7.09
Eu_ppm	1.56	1.73	1.54	1.66	1.09	1.59	1.22	1.80	0.64	1.69	1.91	1.11	1.20	1.36
Gd_ppm	5.69	6.13	4.01	5.55	6.18	4.30	4.96	5.65	2.27	2.24	6.06	3.33	4.10	5.93
Tb_ppm	0.94	1.02	0.57	0.75	0.92	0.67	0.81	0.79	0.39	0.29	0.79	0.41	0.66	0.85
Dy_ppm	5.95	6.62	3.43	4.26	5.06	4.00	4.86	4.42	2.57	1.46	4.48	2.03	4.06	4.98
Ho_ppm	1.22	1.45	0.75	0.82	1.12	0.84	0.98	0.81	0.62	0.30	0.86	0.40	0.79	1.00
Er_ppm	3.52	4.21	2.05	2.46	3.19	2.39	2.91	2.42	1.83	0.91	2.32	1.09	2.60	2.96
Tm_ppm	0.48	0.58	0.32	0.34	0.48	0.33	0.41	0.34	0.25	0.12	0.34	0.16	0.41	0.46
Yb_ppm	3.30	3.56	2.10	2.13	3.28	2.17	2.54	2.24	1.71	0.92	2.20	1.00	2.75	3.33
Lu_ppm	0.46	0.55	0.33	0.31	0.49	0.30	0.37	0.34	0.25	0.15	0.31	0.17	0.43	0.50

Sample_ID	KAC357-1	KAC357-2	KAC358	KAC360	KAC363	KAC364	KAC369-2	KAC371-1	KAC371-2	KAC373	KAC384-1	KAC384-2	KAC384-3	KAC385-1
Lat_S	-16.7367	-16.7367	-16.7284	-16.7267	-16.7136	-16.7109	-16.7130	-16.8223	-16.8223	-16.8262	-17.4061	-17.4061	-17.4061	-17.4231
Long_E	13.2493	13.2493	13.2606	13.2610	13.2943	13.3077	13.4106	13.4801	13.4801	13.4743	13.2849	13.2849	13.2849	13.2822
Rocktype	Micaschist	Micaschist	Amphibolite	Granitoid	Granodiorite	Migmatites	Migmatite/gdt	GDT	GDT	Mafic phenocristic rock	Qtz-feldspathic gneiss	Metagabbro	Amphibolite and qtz-feld gneiss	Qtz-feldspathic gneiss
Group	Basement	Basement	Basement	Basement	Basement	Basement	Basement	Basement	Basement	Basement	Basement	Basement	Basement	Basement
SiO2_pct	55.36	57.53	45.94	57.15	60.68	69.69	55.99	59.27	57.17	53.40	77.03	45.12	72.67	78.08
TiO2_pct	0.79	0.90	1.20	0.80	0.72	0.39	0.99	0.78	0.92	0.88	0.11	1.72	0.64	0.12
Al2O3_pct	22.51	23.91	16.27	14.50	15.06	14.52	16.77	16.14	15.84	17.46	11.79	12.69	13.18	11.71
Fe2O3t_pct	7.16	7.29	12.97	7.59	5.56	3.09	9.14	6.64	7.38	9.00	1.20	15.74	2.50	0.96
MnO_pct	0.07	0.06	0.20	0.15	0.10	0.04	0.19	0.11	0.12	0.14	0.01	0.24	0.07	0.02
MgO_pct	1.86	1.68	5.97	3.96	2.96	1.69	4.69	3.29	3.61	4.97	0.20	8.33	0.91	0.31
CaO_pct	1.57	1.13	11.89	5.93	4.00	3.70	5.64	4.48	5.13	7.68	0.48	10.92	2.79	0.74
Na2O_pct	2.73	1.54	2.03	3.51	3.37	3.35	2.55	3.69	3.59	3.60	2.43	2.66	5.01	4.27
K2O_pct	4.99	2.53	1.40	4.52	3.25	1.24	1.97	2.84	3.52	1.25	5.81	0.67	0.79	2.77
Cr2O3_pct	0.01	0.02	0.02	0.02	0.01	0.01	0.01	0.01	0.01	0.02	0.01	0.02	0.01	0.00
P2O5_pct	0.05	0.27	0.19	0.17	0.24	0.03	0.33	0.26	0.34	0.32	<0.01	0.25	0.12	0.01
Normalised*	97.21	96.93	98.16	98.49	96.16	97.74	98.33	97.66	97.74	98.81	99.11	98.43	98.73	99.06
SiO2_pct*	56.95	59.35	46.80	58.03	63.10	71.30	56.94	60.69	58.49	54.04	77.72	45.84	73.60	78.82
TiO2_pct*	0.81	0.92	1.23	0.82	0.74	0.40	1.01	0.80	0.94	0.90	0.11	1.76	0.66	0.12
Al2O3_pct*	56.95	59.35	46.80	58.03	63.10	71.30	56.94	60.69	58.49	54.04	77.72	45.84	73.60	78.82
Fe2O3t_pct*	7.37	7.52	13.21	7.71	5.78	3.16	9.30	6.80	7.55	9.11	1.21	15.99	2.53	0.97

FeO_pct*	6.26	6.39	11.23	6.55	4.91	2.69	7.90	5.78	6.42	7.74	1.03	13.59	2.15	0.82
Fe2O3_pct*	1.10	1.13	1.98	1.16	0.87	0.47	1.39	1.02	1.13	1.37	0.18	2.40	0.38	0.15
FeO*_pct	6.63	6.77	11.89	6.94	5.20	2.85	8.37	6.12	6.80	8.20	1.09	14.39	2.28	0.87
MnO_pct*	0.07	0.06	0.21	0.15	0.10	0.04	0.19	0.11	0.12	0.14	0.01	0.25	0.07	0.02
MgO_pct*	1.91	1.73	6.08	4.02	3.08	1.73	4.77	3.37	3.69	5.03	0.20	8.46	0.92	0.31
CaO_pct*	1.61	1.16	12.19	6.08	4.10	3.79	5.78	4.59	5.26	7.87	0.49	11.20	2.86	0.76
Na2O_pct*	2.80	1.58	2.08	3.60	3.45	3.43	2.61	3.78	3.68	3.69	2.49	2.73	5.14	4.38
K2O_pct*	5.12	2.59	1.44	4.63	3.33	1.27	2.02	2.91	3.61	1.28	5.96	0.69	0.81	2.84
Cr2O3_pct*	0.01	0.02	0.02	0.02	0.01	0.01	0.01	0.01	0.01	0.02	0.01	0.02	0.01	0.00
P2O5_pct*	0.05	0.28	0.19	0.17	0.25	0.03	0.34	0.27	0.35	0.33	N/D	0.26	0.12	0.01
Mg#	35.26	32.58	49.11	52.24	52.74	53.41	51.82	50.95	50.63	53.65	25.89	52.60	43.28	40.37
Mo_pct	<0.001	<0.001	<0.001	<0.001	<0.001	<0.001	<0.001	<0.001	<0.001	<0.001	<0.001	<0.001	<0.001	<0.001
Cu_pct	0.00	0.00	0.01	0.00	0.05	0.00	0.01	0.00	0.01	0.00	<0.001	0.04	0.00	0.00
Pb_pct	<0.02	<0.02	<0.02	<0.02	<0.02	<0.02	<0.02	<0.02	<0.02	<0.02	<0.02	<0.02	<0.02	<0.02
Zn_pct	<0.01	<0.01	<0.01	<0.01	<0.01	<0.01	0.01	<0.01	<0.01	<0.01	<0.01	0.01	<0.01	<0.01
Ag_ppm	<2	<2	<2	<2	<2	<2	<2	<2	<2	<2	<2	<2	<2	<2
Ni_ppm	38.00	52.00	122.00	51.00	28.00	27.00	31.00	25.00	36.00	43.00	<10	115.00	11.00	<10
Mo_ppm	0.18	0.47	0.21	0.25	0.22	1.01	0.24	0.43	0.35	0.44	0.42	0.14	0.30	1.42
Cu_ppm	16.61	13.57	69.37	7.24	473.98	30.41	51.19	45.47	112.03	34.37	2.57	389.30	15.12	26.53
Pb_ppm	7.32	6.92	6.69	4.54	2.86	5.34	5.73	6.50	9.13	2.14	4.16	4.75	2.56	14.51
Zn_ppm	97.60	83.00	29.80	16.20	74.80	36.60	23.30	65.90	64.10	50.20	8.90	38.30	8.00	11.00
Ag_ppb	19.00	14.00	63.00	19.00	189.00	20.00	37.00	44.00	63.00	58.00	4.00	78.00	22.00	35.00
Ni_ppm	36.90	50.30	35.30	15.20	28.10	26.60	19.40	20.10	27.70	28.20	8.30	40.00	8.60	1.70
Co_ppm	13.50	15.80	18.10	7.20	18.60	10.20	10.20	15.80	17.50	16.40	1.40	31.00	2.70	1.00
Mn_ppm	327.00	358.00	398.00	338.00	688.00	229.00	155.00	544.00	527.00	161.00	71.00	593.00	215.00	105.00

As_ppm	<0.1	<0.1	<0.1	<0.1	<0.1	<0.1	<0.1	0.40	0.40	<0.1	<0.1	0.20	<0.1	<0.1
Au_ppb	<0.2	1.00	3.70	0.30	5.60	0.60	2.30	0.70	0.50	0.90	<0.2	2.70	<0.2	0.20
Cd_ppm	<0.01	0.02	0.04	0.05	<0.01	0.02	0.03	0.04	0.10	0.02	0.01	0.03	0.01	<0.01
Sb_ppm	<0.02	<0.02	<0.02	<0.02	<0.02	<0.02	<0.02	<0.02	0.02	<0.02	<0.02	<0.02	<0.02	<0.02
Bi_ppm	0.19	0.58	0.06	<0.02	<0.02	<0.02	<0.02	0.03	0.05	0.05	<0.02	<0.02	<0.02	<0.02
Cr_ppm	39.60	82.70	42.90	70.10	50.40	63.40	64.80	41.50	51.80	83.00	33.70	40.80	28.90	10.10
Hg_ppb	<5	<5	<5	<5	<5	<5	<5	<5	<5	<5	<5	<5	<5	<5
Se_ppm	<0.1	<0.1	<0.1	<0.1	0.50	<0.1	0.20	0.10	0.10	<0.1	0.40	0.40	0.20	0.20
Te_ppm	0.02	0.06	0.05	<0.02	<0.02	<0.02	<0.02	<0.02	<0.02	<0.02	<0.02	0.10	<0.02	<0.02
Ge_ppm	<0.1	<0.1	<0.1	<0.1	<0.1	<0.1	<0.1	<0.1	<0.1	<0.1	<0.1	0.10	<0.1	<0.1
In_ppm	0.02	<0.02	<0.02	<0.02	<0.02	<0.02	0.02	<0.02	<0.02	<0.02	<0.02	0.03	<0.02	<0.02
Re_ppb	<1	<1	<1	<1	<1	<1	<1	<1	<1	<1	<1	<1	<1	<1
Be_ppm	0.30	0.40	0.20	0.20	0.40	0.50	1.60	0.60	1.10	0.40	0.50	0.20	0.40	0.90
Li_ppm	49.00	72.40	4.60	1.50	15.60	8.60	5.30	18.10	14.80	6.20	1.10	2.40	1.20	1.20
Pd_ppb	<10	<10	16.00	<10	<10	<10	<10	<10	<10	<10	<10	<10	<10	<10
Pt_ppb	<2	<2	9.00	<2	<2	<2	2.00	<2	<2	<2	<2	<2	<2	<2
Au_ppb	3.00	3.00	7.00	2.00	7.00	3.00	4.00	3.00	2.00	3.00	2.00	5.00	3.00	2.00
Pt_ppb	0.90	0.90	17.80	2.20	0.50	0.90	3.20	1.20	1.00	1.40	0.20	1.10	0.30	0.10
Pd_ppb	0.90	0.80	17.40	1.80	0.60	1.30	3.70	1.90	1.10	1.10	<0.5	1.60	<0.5	<0.5
B_ppm	1.00	3.00	3.00	1.00	1.00	<1	1.00	2.00	2.00	<1	2.00	<1	3.00	3.00
Tl_ppm	0.40	0.19	0.03	<0.02	0.03	0.07	0.11	0.03	0.04	0.14	<0.02	<0.02	<0.02	0.02
LOI_pct	2.60	2.90	1.60	1.30	3.60	2.10	1.40	2.10	2.00	0.90	0.80	1.20	1.10	0.80
TOT/C_TC000_pct	<0.02	<0.02	<0.02	0.03	0.35	0.08	0.07	0.04	<0.02	0.06	<0.02	<0.02	0.03	0.04
TOT/S_pct	<0.02	<0.02	<0.02	<0.02	<0.02	<0.02	0.05	<0.02	<0.02	<0.02	<0.02	<0.02	<0.02	<0.02
Ba_ppm	1301.00	680.00	206.00	1987.00	1723.00	398.00	834.00	1202.00	863.00	655.00	206.00	230.00	388.00	758.00

Sc_ppm	18.00	18.00	43.00	20.00	16.00	8.00	29.00	16.00	15.00	22.00	3.00	37.00	12.00	3.00
Sum_pct	99.81	99.83	99.76	99.79	99.76	99.84	99.73	99.76	99.74	99.71	99.91	99.63	99.83	99.86
Cs_ppm	6.40	5.20	0.60	0.50	0.90	0.90	0.70	0.90	1.10	2.10	0.20	<0.1	0.20	0.10
Ga_ppm	25.70	21.70	18.10	14.10	14.80	13.10	20.00	17.50	17.30	21.00	13.10	16.10	13.90	9.60
Hf_ppm	7.30	6.80	2.10	1.90	3.50	6.70	2.60	3.80	4.30	3.10	6.50	1.60	12.60	7.90
Nb_ppm	15.10	14.70	3.20	4.70	7.10	6.40	11.00	8.10	9.20	5.10	14.30	3.30	18.20	9.00
Rb_ppm	175.70	120.00	31.30	53.50	60.90	46.60	66.70	75.90	119.20	40.60	129.50	5.30	20.10	43.10
Sn_ppm	3.00	1.00	<1	<1	1.00	<1	1.00	1.00	1.00	<1	<1	1.00	2.00	1.00
Sr_ppm	282.10	204.20	220.20	661.80	540.40	581.60	821.90	748.10	732.40	1071.30	90.60	393.70	384.90	279.80
Ta_ppm	1.00	1.20	0.20	0.20	0.30	0.40	0.80	0.50	0.40	0.40	1.10	0.20	1.00	0.70
Th_ppm	18.40	20.00	0.60	1.20	2.80	5.10	1.30	5.80	11.60	2.60	28.40	0.40	6.90	32.40
U_ppm	3.40	4.30	1.00	0.30	0.40	0.90	1.70	1.10	1.10	0.90	2.40	0.30	1.00	2.20
V_ppm	102.00	88.00	353.00	117.00	114.00	58.00	197.00	126.00	139.00	168.00	<8	492.00	33.00	<8
W_ppm	2.80	2.50	0.60	0.90	1.30	1.60	1.20	0.90	1.10	1.00	1.80	1.00	1.70	1.40
Zr_ppm	258.00	248.80	68.20	71.40	143.90	255.30	110.20	157.20	174.30	122.40	141.00	60.50	498.60	204.50
Y_ppm	35.10	39.00	22.10	21.00	20.30	3.70	14.70	18.20	17.50	12.90	72.10	25.30	45.20	51.50
La_ppm	50.50	64.10	5.70	33.40	31.70	22.80	18.30	39.70	48.60	26.40	59.20	11.60	69.30	118.50
Ce_ppm	107.80	127.00	13.40	76.30	58.70	36.20	40.20	79.40	92.60	49.50	119.80	25.50	130.40	241.40
Pr_ppm	12.29	14.21	1.92	9.28	7.63	3.67	5.23	9.15	10.48	5.83	14.17	3.49	14.57	25.65
Nd_ppm	46.60	51.20	9.80	36.80	31.60	12.20	22.60	35.90	39.10	23.30	53.70	16.30	53.50	86.50
Sm_ppm	8.47	9.33	2.80	6.54	5.84	1.69	5.20	6.47	6.40	4.84	11.27	4.00	8.82	14.52
Eu_ppm	1.73	1.85	1.02	1.57	1.54	1.29	1.37	1.69	1.56	1.65	0.32	1.48	2.00	0.84
Gd_ppm	7.39	8.04	3.64	5.48	5.22	1.14	4.55	4.92	4.79	4.10	11.77	4.64	8.06	11.45
Tb_ppm	1.07	1.20	0.63	0.77	0.72	0.13	0.65	0.68	0.65	0.54	1.98	0.74	1.29	1.79
Dy_ppm	6.39	7.38	3.94	4.04	4.07	0.76	3.63	3.57	3.25	2.66	12.69	4.54	7.96	10.24

Ho_ppm	1.30	1.48	0.90	0.84	0.77	0.12	0.63	0.67	0.65	0.53	2.75	0.97	1.73	2.11
Er_ppm	3.96	4.40	2.48	2.24	2.24	0.35	1.46	1.89	1.74	1.25	8.35	2.96	5.22	5.97
Tm_ppm	0.57	0.66	0.34	0.32	0.32	0.06	0.18	0.25	0.26	0.16	1.25	0.41	0.79	0.83
Yb_ppm	3.69	4.36	2.22	2.01	1.87	0.53	1.10	1.75	1.64	1.13	7.91	2.60	5.03	5.15
Lu_ppm	0.60	0.67	0.35	0.30	0.27	0.11	0.16	0.27	0.25	0.17	1.18	0.40	0.81	0.70

Sample_ID	KAC390-1	KAC413-1	KAC450-1	KSAT026/013	KSAT027/014	KSAT037/020	KSAT038/023	KSAT041/027A	KSAT043/029	KSAT045/030	KSAT053/035	KSAT054/036	KSAT054/037	KSAT055/038
Lat_S	-17.3839	-17.3939	-17.2904	-16.7417	-16.7148	-15.7867	-15.7379	-15.6579	-15.6050	-15.5190	-15.2789	-15.2700	-15.2700	-15.4080
Long_E	13.2917	13.2832	13.2848	13.2419	13.2881	13.5591	13.5533	13.5594	13.5828	13.6005	13.8280	13.8325	13.8325	13.6729
Rocktype	Metagabbro	Amphibolite and qtz-feld gneiss	folded amphibolite	Garnet-bearing migmatitic granite	Granodiorite	Granodiorite / monzodiorite	Granodiorite	Tonalite	Andalusite metapelite	Metasiltstone	Diorite	Diorite	Diorite	Diorite
Group	Basement	Basement	Basement	Basement	Basement	Basement	Basement	Basement	Basement	Basement	Basement	Basement	Basement	Basement
SiO2_pct	47.30	74.75	43.62	66.88	61.10	48.86	72.61	63.37	65.37	43.13	46.29	54.03	53.25	48.16
TiO2_pct	1.36	0.17	1.35	0.50	0.68	0.82	0.24	0.48	0.62	1.68	0.74	0.79	0.79	0.58
Al2O3_pct	14.25	13.18	16.86	17.79	16.24	15.21	13.58	15.08	18.71	8.16	14.47	12.87	11.69	16.81
Fe2O3t_pct	11.74	1.36	13.32	3.74	6.28	8.29	2.04	4.72	5.86	14.60	10.13	8.29	8.72	7.98
MnO_pct	0.18	0.02	0.22	0.04	0.10	0.14	0.03	0.07	0.04	0.18	0.13	0.15	0.16	0.12
MgO_pct	8.51	0.41	7.93	0.81	2.75	8.84	0.54	3.21	1.46	17.74	9.83	7.62	8.32	8.84
CaO_pct	10.29	1.63	8.34	1.76	4.43	10.58	1.63	4.62	0.50	11.39	13.36	10.30	11.11	11.83
Na2O_pct	1.89	3.06	2.98	3.33	2.98	2.11	2.75	2.79	0.61	0.17	1.52	3.19	2.63	1.84
K2O_pct	0.09	4.12	0.98	2.75	2.27	1.39	5.56	3.53	5.17	0.08	0.60	0.94	1.28	0.69
Cr2O3_pct	0.03	0.01	0.05	0.01	0.01	0.04	0.01	0.02	0.02	0.35	0.02	0.04	0.06	0.01
P2O5_pct	0.08	0.03	0.98	0.09	0.19	0.18	0.04	0.16	0.09	0.16	0.11	0.25	0.22	0.11

Normalised *	95.71	98.93	96.68	97.77	97.11	96.52	99.11	98.22	98.57	97.76	97.27	98.49	98.31	96.99
SiO2_pct*	49.42	75.56	45.12	68.41	62.92	50.62	73.26	64.52	66.32	44.12	47.59	54.86	54.17	49.65
TiO2_pct*	1.39	0.17	1.38	0.51	0.70	0.84	0.25	0.49	0.64	1.72	0.76	0.81	0.81	0.59
Al2O3_pct*	49.42	75.56	45.12	68.41	62.92	50.62	73.26	64.52	66.32	44.12	47.59	54.86	54.17	49.65
Fe2O3t_pct *	12.27	1.37	13.78	3.83	6.47	8.59	2.06	4.81	5.95	14.93	10.41	8.42	8.87	8.23
FeO_pct*	10.43	1.17	11.71	3.25	5.50	7.30	1.75	4.08	5.05	12.69	8.85	7.15	7.54	6.99
Fe2O3_pct *	1.84	0.21	2.07	0.57	0.97	1.29	0.31	0.72	0.89	2.24	1.56	1.26	1.33	1.23
FeO*_pct	11.04	1.24	12.40	3.44	5.82	7.73	1.85	4.32	5.35	13.44	9.37	7.58	7.98	7.40
MnO_pct*	0.18	0.02	0.23	0.04	0.10	0.14	0.03	0.07	0.04	0.18	0.13	0.15	0.16	0.12
MgO_pct*	8.89	0.41	8.20	0.83	2.83	9.16	0.54	3.27	1.48	18.15	10.11	7.74	8.46	9.11
CaO_pct*	10.55	1.67	8.55	1.80	4.54	10.85	1.67	4.74	0.51	11.68	13.70	10.56	11.39	12.13
Na2O_pct*	1.94	3.14	3.06	3.41	3.06	2.16	2.82	2.86	0.63	0.17	1.56	3.27	2.70	1.89
K2O_pct*	0.09	4.22	1.00	2.82	2.33	1.43	5.70	3.62	5.30	0.08	0.62	0.96	1.31	0.71
Cr2O3_pct *	0.03	0.01	0.05	0.01	0.01	0.04	0.01	0.02	0.02	0.35	0.02	0.04	0.06	0.01
P2O5_pct*	0.08	0.03	1.00	0.09	0.19	0.18	0.04	0.16	0.09	0.16	0.11	0.26	0.23	0.11
Mg#	60.31	38.73	55.52	31.23	47.86	69.09	35.69	58.78	34.31	71.81	67.04	65.84	66.67	69.90
Mo_pct	<0.001	<0.001	<0.001	<0.001	<0.001	<0.001	<0.001	<0.001	<0.001	<0.001	<0.001	<0.001	<0.001	<0.001
Cu_pct	0.01	<0.001	0.01	<0.001	0.01	0.01	0.00	0.00	0.01	0.01	0.02	0.01	0.01	0.03
Pb_pct	<0.02	<0.02	<0.02	<0.02	<0.02	<0.02	<0.02	<0.02	<0.02	<0.02	<0.02	<0.02	<0.02	<0.02
Zn_pct	<0.01	<0.01	0.01	<0.01	<0.01	<0.01	<0.01	<0.01	<0.01	<0.01	<0.01	<0.01	<0.01	<0.01
Ag_ppm	<2	<2	<2	<2	<2	<2	<2	<2	<2	<2	<2	<2	<2	<2
Ni_ppm	100.00	<10	48.00	12.00	29.00	136.00	<10	50.00	41.00	925.00	88.00	58.00	64.00	107.00
Mo_ppm	0.18	0.88	0.09	1.06	0.36	0.19	1.21	1.08	0.61	0.91	0.15	0.32	0.22	0.27
Cu_ppm	59.20	7.83	47.85	9.81	40.46	124.73	10.76	25.76	86.21	53.92	146.22	51.88	46.26	231.65
Pb_ppm	0.94	4.25	2.78	8.78	4.59	21.07	12.85	6.67	4.00	0.28	1.34	1.57	1.61	2.21

Zn_ppm	79.90	9.10	83.50	41.10	71.10	30.70	21.40	33.50	61.00	9.20	17.40	15.50	20.20	20.20
Ag_ppb	47.00	17.00	100.00	30.00	48.00	86.00	17.00	32.00	80.00	11.00	73.00	21.00	18.00	118.00
Ni_ppm	83.20	7.30	29.30	10.90	27.50	72.70	5.40	35.50	38.20	473.00	42.90	20.40	22.30	42.60
Co_ppm	43.50	2.60	22.60	7.50	18.10	21.20	3.40	13.50	14.00	49.30	18.20	8.20	10.50	19.70
Mn_ppm	828.00	98.00	785.00	94.00	614.00	315.00	157.00	317.00	277.00	589.00	255.00	227.00	283.00	233.00
As_ppm	0.30	0.40	2.60	0.20	0.30	0.70	0.10	0.50	0.50	1.30	<0.1	0.10	<0.1	<0.1
Au_ppb	<0.2	<0.2	0.30	<0.2	0.80	0.30	<0.2	<0.2	2.00	0.60	7.00	<0.2	1.00	11.60
Cd_ppm	0.10	<0.01	0.02	0.02	0.02	0.07	<0.01	0.01	0.03	0.04	0.05	0.03	0.02	0.04
Sb_ppm	<0.02	<0.02	0.07	<0.02	<0.02	<0.02	<0.02	<0.02	<0.02	0.06	<0.02	<0.02	<0.02	<0.02
Bi_ppm	<0.02	<0.02	0.17	0.18	<0.02	0.08	<0.02	<0.02	0.50	0.03	<0.02	<0.02	0.03	0.03
Cr_ppm	145.10	16.80	185.50	27.60	63.80	66.40	25.30	101.40	99.50	246.20	49.00	48.20	76.90	26.00
Hg_ppb	<5	<5	<5	<5	<5	<5	<5	<5	<5	<5	6.00	<5	<5	<5
Se_ppm	0.10	<0.1	<0.1	<0.1	<0.1	<0.1	<0.1	<0.1	<0.1	<0.1	<0.1	<0.1	<0.1	<0.1
Te_ppm	<0.02	<0.02	<0.02	0.02	<0.02	0.03	<0.02	<0.02	0.04	<0.02	0.03	<0.02	0.02	0.03
Ge_ppm	<0.1	<0.1	<0.1	<0.1	0.10	<0.1	0.10	0.10	0.10	0.20	<0.1	0.10	<0.1	<0.1
In_ppm	<0.02	<0.02	0.02	<0.02	<0.02	<0.02	<0.02	<0.02	0.05	<0.02	<0.02	<0.02	<0.02	<0.02
Re_ppb	<1	<1	<1	<1	<1	<1	<1	<1	<1	<1	<1	<1	<1	<1
Be_ppm	<0.1	0.10	0.30	0.20	0.60	0.20	0.40	<0.1	1.70	0.20	<0.1	0.40	0.30	0.10
Li_ppm	1.90	1.50	11.90	16.40	11.50	16.90	9.50	30.00	27.70	3.90	5.70	4.10	7.70	12.00
Pd_ppb	<10	<10	<10	<10	<10	<10	<10	<10	<10	<10	23.00	<10	<10	<10
Pt_ppb	<2	<2	3.00	<2	<2	2.00	<2	<2	<2	<2	12.00	7.00	3.00	6.00
Au_ppb	2.00	3.00	4.00	3.00	4.00	3.00	3.00	2.00	4.00	8.00	8.00	3.00	3.00	13.00
Pt_ppb	0.10	0.20	3.50	0.40	1.20	2.40	0.20	0.70	0.80	5.30	23.50	12.70	7.20	11.30
Pd_ppb	<0.5	<0.5	3.80	0.90	1.50	1.40	0.60	0.70	1.30	6.40	37.60	10.20	8.70	1.80
B_ppm	<1	1.00	6.00	1.00	2.00	2.00	<1	<1	<1	5.00	2.00	<1	1.00	1.00

Tl_ppm	<0.02	<0.02	0.04	0.12	0.13	0.02	0.08	0.32	0.61	<0.02	<0.02	<0.02	<0.02	<0.02
LOI_pct	4.00	1.00	3.00	2.10	2.70	3.20	0.80	1.60	1.30	1.80	2.40	1.20	1.40	2.70
TOT/C_TC000_pct	0.19	<0.02	<0.02	<0.02	0.05	0.18	<0.02	0.07	<0.02	0.06	0.07	0.03	0.10	0.12
TOT/S_pct	0.17	<0.02	<0.02	<0.02	<0.02	<0.02	<0.02	<0.02	0.03	<0.02	0.02	<0.02	<0.02	0.04
Ba_ppm	96.00	1883.00	355.00	671.00	720.00	524.00	770.00	1165.00	857.00	58.00	215.00	275.00	517.00	272.00
Sc_ppm	43.00	1.00	31.00	10.00	14.00	35.00	3.00	12.00	14.00	31.00	47.00	41.00	45.00	32.00
Sum_pct	99.71	99.93	99.68	99.87	99.81	99.72	99.91	99.82	99.87	99.56	99.67	99.69	99.71	99.69
Cs_ppm	<0.1	0.30	1.60	2.90	1.30	2.20	1.60	4.40	11.10	0.70	0.70	0.50	0.40	1.00
Ga_ppm	15.30	10.60	18.60	14.90	15.90	12.30	12.20	13.60	20.80	13.40	14.90	15.00	12.10	14.60
Hf_ppm	1.40	3.30	1.60	5.80	4.00	2.30	4.80	3.20	4.50	2.90	1.40	5.50	2.60	1.50
Nb_ppm	2.30	1.10	3.80	10.10	7.90	9.50	5.40	5.20	11.70	8.00	2.40	5.10	4.70	2.10
Rb_ppm	0.90	44.70	22.80	87.30	76.10	45.90	141.20	117.60	198.80	2.70	10.80	17.70	22.50	11.40
Sn_ppm	<1	<1	<1	1.00	1.00	<1	<1	1.00	2.00	<1	<1	<1	<1	<1
Sr_ppm	452.80	361.80	703.10	344.70	620.40	470.70	213.70	529.70	75.40	417.60	656.30	734.30	619.60	667.60
Ta_ppm	0.10	<0.1	0.10	0.70	0.30	0.50	0.40	0.40	0.90	0.50	<0.1	0.30	0.10	0.10
Th_ppm	0.40	7.60	<0.2	11.80	5.40	3.50	40.40	11.30	17.80	0.70	1.00	3.20	2.00	1.90
U_ppm	<0.1	0.30	0.40	2.50	0.90	0.60	5.10	1.00	3.70	0.20	0.20	0.70	0.50	0.40
V_ppm	353.00	16.00	328.00	50.00	127.00	187.00	24.00	89.00	80.00	271.00	301.00	203.00	216.00	155.00
W_ppm	<0.5	1.80	2.20	2.80	1.10	0.90	1.80	3.20	3.90	1.50	0.90	0.70	0.90	<0.5
Zr_ppm	46.00	120.40	47.70	219.20	172.20	84.50	165.40	140.10	162.20	108.80	40.40	262.40	97.40	51.80
Y_ppm	21.90	2.50	23.10	23.90	17.10	14.50	8.20	11.20	27.30	14.50	13.70	20.00	19.20	11.10
La_ppm	7.50	35.50	36.50	45.10	36.50	22.00	40.80	37.30	57.50	11.30	11.60	26.50	22.50	12.80
Ce_ppm	17.20	52.80	79.50	91.70	73.10	48.10	75.60	68.80	109.50	27.50	27.40	57.60	50.50	28.70
Pr_ppm	2.34	5.07	10.90	9.65	8.11	5.23	6.91	6.92	11.60	3.56	3.85	6.73	6.20	3.51
Nd_ppm	11.40	16.60	45.30	36.10	30.70	20.60	22.50	24.50	42.00	15.80	17.50	27.50	26.30	15.60

Sm_ppm	3.057	1.91	8.39	6.48	5.25	3.83	2.90	3.94	7.14	3.63	3.88	5.12	4.99	3.20
Eu_ppm	1.24	0.94	2.15	1.75	1.35	1.08	0.74	1.11	1.47	1.28	1.10	1.51	1.38	0.95
Gd_ppm	3.81	1.24	6.65	5.10	4.11	3.33	2.22	2.79	6.11	4.00	3.73	4.95	4.81	2.77
Tb_ppm	0.64	0.12	0.83	0.74	0.56	0.47	0.28	0.39	0.88	0.59	0.49	0.67	0.66	0.38
Dy_ppm	4.07	0.59	4.46	4.34	3.21	2.70	1.57	2.10	5.15	3.32	2.73	3.73	3.77	2.27
Ho_ppm	0.85	0.07	0.83	0.89	0.65	0.53	0.29	0.38	1.02	0.56	0.50	0.75	0.73	0.41
Er_ppm	2.52	0.24	2.27	2.82	1.82	1.43	0.79	1.13	2.87	1.64	1.45	2.19	2.18	1.10
Tm_ppm	0.35	0.04	0.29	0.39	0.26	0.20	0.13	0.17	0.40	0.18	0.19	0.30	0.28	0.13
Yb_ppm	2.18	0.25	1.91	2.73	1.75	1.27	0.82	1.02	2.82	1.18	1.15	2.00	1.80	0.96
Lu_ppm	0.34	0.05	0.26	0.40	0.26	0.19	0.14	0.17	0.42	0.16	0.17	0.31	0.25	0.14

Sample_ID	KSAT059/039	KSAT062/040	KSAT062/041	KSAT063/042	KSAT068/044	KSAT073/045	KSAT075/046	KSAT080/047	KSAT082/048	KSAT086/049	KSAT088/050	KSAT099/053	KSAT103/054	KSAT110/055
Lat_S	-15.4092	-15.4112	-15.4112	-15.4113	-15.4109	-15.4056	-15.4024	-15.4020	-15.4055	-15.3938	-15.3950	-15.3951	-15.3960	-15.3982
Long_E	13.6201	13.6227	13.6227	13.6221	13.6245	13.6306	13.6320	13.6268	13.6227	13.6257	13.6258	13.6302	13.6327	13.6337
Rocktype	Lherzolite	Amphibole gabbro	Porphyritic amphibole gabbro	Diorite	Amphibolite	Leucogabbro/anorthosite	Lherzolite/harzburgite	Diorite	Leucogabbro	Foliated diorite	Diorite	Tonalite	Diorite	Ol leucogabbro ('hybrid' rock)
Group	Basement	Basement	Basement	Basement	Basement	Basement	Basement	Basement	Basement	Basement	Basement	Basement	Basement	Basement
SiO2_pct	38.05	49.22	48.68	49.80	50.15	44.87	39.17	49.80	49.22	51.46	50.76	58.41	49.93	46.09
TiO2_pct	0.18	0.91	0.82	1.02	0.92	0.44	0.31	0.66	1.11	0.93	0.73	0.68	0.75	0.61
Al2O3_pct	3.71	18.09	19.21	17.63	14.22	22.34	3.99	9.33	20.93	15.55	11.75	19.49	11.93	14.92
Fe2O3t_pct	14.72	10.11	10.30	10.44	10.47	5.38	14.69	8.77	4.88	10.53	9.19	5.55	9.19	8.60
MnO_pct	0.17	0.14	0.11	0.16	0.20	0.07	0.18	0.17	0.07	0.20	0.16	0.04	0.15	0.11
MgO_pct	33.43	3.99	3.72	4.60	8.68	8.63	33.10	11.15	4.13	5.63	9.75	1.93	11.18	12.25

CaO_pct	1.79	9.01	7.96	8.16	8.58	10.57	2.15	15.50	11.14	9.28	12.10	5.08	11.23	11.07
Na2O_pct	0.25	3.36	3.74	3.68	3.09	2.42	0.43	1.52	3.63	2.91	1.98	4.42	2.06	1.91
K2O_pct	0.04	1.32	1.54	1.33	1.14	0.29	0.06	0.74	1.09	0.95	0.90	1.75	0.93	0.23
Cr2O3_pct	0.35	0.00	<0.002	0.00	0.04	0.01	0.31	0.03	0.01	0.01	0.13	0.00	0.12	0.06
P2O5_pct	0.03	0.75	0.87	0.34	0.16	0.06	0.03	0.18	0.10	0.21	0.19	0.08	0.16	0.04
Normalised *	93.00	96.99	97.00	97.20	97.78	95.16	94.60	97.89	96.35	97.73	97.71	97.49	97.69	95.98
SiO2_pct*	40.91	50.75	50.19	51.23	51.29	47.15	41.41	50.87	51.08	52.66	51.95	59.91	51.11	48.02
TiO2_pct*	0.18	0.93	0.84	1.05	0.94	0.45	0.32	0.68	1.14	0.95	0.75	0.70	0.77	0.63
Al2O3_pct *	40.91	50.75	50.19	51.23	51.29	47.15	41.41	50.87	51.08	52.66	51.95	59.91	51.11	48.02
Fe2O3t_pct *	15.83	10.42	10.62	10.74	10.71	5.65	15.53	8.96	5.06	10.77	9.41	5.69	9.41	8.96
FeO_pct*	13.45	8.86	9.03	9.13	9.10	4.81	13.20	7.62	4.31	9.16	7.99	4.84	8.00	7.62
Fe2O3_pct *	2.37	1.56	1.59	1.61	1.61	0.85	2.33	1.34	0.76	1.62	1.41	0.85	1.41	1.34
FeO*_pct	14.25	9.38	9.56	9.67	9.64	5.09	13.98	8.06	4.56	9.70	8.46	5.12	8.47	8.06
MnO_pct*	0.17	0.14	0.11	0.16	0.21	0.07	0.18	0.17	0.07	0.21	0.16	0.04	0.15	0.11
MgO_pct*	35.95	4.11	3.84	4.73	8.88	9.07	34.99	11.39	4.29	5.76	9.98	1.98	11.44	12.76
CaO_pct*	1.84	9.24	8.16	8.37	8.80	10.84	2.20	15.89	11.42	9.51	12.41	5.21	11.51	11.35
Na2O_pct*	0.26	3.44	3.83	3.77	3.17	2.48	0.44	1.56	3.72	2.98	2.03	4.53	2.11	1.96
K2O_pct*	0.04	1.35	1.58	1.36	1.17	0.30	0.06	0.76	1.12	0.97	0.92	1.79	0.95	0.24
Cr2O3_pct *	0.36	0.00	N/D	0.00	0.04	0.01	0.32	0.03	0.01	0.01	0.13	0.00	0.13	0.06
P2O5_pct*	0.03	0.77	0.89	0.35	0.16	0.06	0.03	0.18	0.10	0.22	0.19	0.08	0.16	0.04
Mg#	82.64	45.28	43.09	48.02	63.48	77.08	82.53	72.72	63.95	52.85	68.98	42.16	71.83	74.91
Mo_pct	<0.001	<0.001	<0.001	<0.001	<0.001	<0.001	<0.001	<0.001	<0.001	<0.001	<0.001	<0.001	<0.001	<0.001
Cu_pct	0.01	0.02	0.01	0.01	0.01	0.00	0.00	0.00	0.00	0.01	0.01	0.00	0.00	0.01
Pb_pct	<0.02	<0.02	<0.02	<0.02	<0.02	<0.02	<0.02	<0.02	<0.02	<0.02	<0.02	<0.02	<0.02	<0.02
Zn_pct	<0.01	<0.01	<0.01	<0.01	<0.01	<0.01	<0.01	<0.01	<0.01	<0.01	<0.01	<0.01	<0.01	<0.01

Ag_ppm	<2	<2	<2	<2	<2	<2	<2	<2	<2	<2	<2	<2	<2	<2
Ni_ppm	1788.00	11.00	21.00	17.00	85.00	399.00	1723.00	55.00	42.00	33.00	80.00	<10	158.00	238.00
Mo_ppm	0.14	5.08	0.26	0.20	0.19	0.15	0.42	0.18	0.30	0.25	0.19	0.96	0.21	0.23
Cu_ppm	53.63	200.21	132.83	113.27	61.45	26.20	36.63	25.50	29.33	53.86	53.41	40.42	10.13	115.11
Pb_ppm	0.29	4.19	3.27	1.95	3.17	2.18	0.30	3.54	5.70	2.64	3.41	8.10	2.14	0.97
Zn_ppm	66.10	42.10	37.10	40.80	24.40	27.90	75.80	18.30	29.90	33.30	14.80	66.40	15.20	21.50
Ag_ppb	19.00	92.00	51.00	33.00	23.00	11.00	15.00	25.00	27.00	21.00	18.00	42.00	6.00	68.00
Ni_ppm	1826.20	8.10	19.80	12.20	46.60	310.10	1749.40	19.10	31.30	16.10	24.80	8.90	47.30	186.70
Co_ppm	150.00	27.20	18.90	21.10	13.90	34.10	149.80	10.70	14.10	19.00	9.20	15.60	11.00	49.40
Mn_ppm	1228.00	439.00	390.00	404.00	412.00	292.00	1269.00	218.00	198.00	494.00	257.00	243.00	246.00	266.00
As_ppm	<0.1	<0.1	<0.1	<0.1	0.10	<0.1	<0.1	0.80	<0.1	<0.1	0.20	<0.1	<0.1	<0.1
Au_ppb	1.10	6.90	4.20	3.20	1.00	1.40	0.80	1.10	<0.2	1.20	0.50	0.50	<0.2	2.10
Cd_ppm	0.03	0.02	0.02	0.01	0.02	0.02	0.03	0.02	0.05	0.03	<0.01	0.01	0.02	0.02
Sb_ppm	<0.02	<0.02	<0.02	<0.02	<0.02	0.02	<0.02	<0.02	<0.02	<0.02	<0.02	<0.02	<0.02	<0.02
Bi_ppm	<0.02	0.07	0.03	0.03	<0.02	<0.02	<0.02	<0.02	<0.02	0.03	<0.02	<0.02	<0.02	<0.02
Cr_ppm	119.20	10.30	3.20	14.30	198.80	41.80	156.00	47.00	36.90	52.60	179.70	14.30	108.50	100.90
Hg_ppb	<5	<5	<5	<5	<5	<5	<5	<5	<5	<5	<5	<5	<5	<5
Se_ppm	<0.1	0.50	<0.1	0.20	<0.1	0.10	<0.1	<0.1	<0.1	<0.1	<0.1	<0.1	<0.1	0.60
Te_ppm	0.02	0.08	0.04	<0.02	0.04	0.05	<0.02	0.03	<0.02	<0.02	<0.02	<0.02	<0.02	0.07
Ge_ppm	<0.1	<0.1	<0.1	<0.1	<0.1	<0.1	<0.1	<0.1	<0.1	<0.1	<0.1	<0.1	<0.1	<0.1
In_ppm	<0.02	<0.02	<0.02	<0.02	<0.02	<0.02	<0.02	<0.02	<0.02	<0.02	<0.02	<0.02	<0.02	<0.02
Re_ppb	<1	11.00	<1	<1	<1	<1	<1	<1	<1	<1	<1	<1	<1	1.00
Be_ppm	<0.1	0.40	0.50	0.30	0.30	0.20	0.10	0.10	0.20	0.40	0.20	0.30	0.30	<0.1
Li_ppm	3.00	11.10	10.60	9.90	8.10	5.80	2.10	10.50	19.80	8.50	7.00	17.50	7.70	1.70
Pd_ppb	16.00	<10	<10	<10	<10	65.00	10.00	12.00	<10	<10	<10	<10	<10	29.00

Pt_ppb	<2	<2	<2	3.00	3.00	12.00	<2	8.00	<2	4.00	5.00	<2	2.00	4.00
Au_ppb	6.00	9.00	6.00	5.00	3.00	5.00	4.00	4.00	3.00	4.00	3.00	3.00	3.00	4.00
Pt_ppb	3.00	0.30	0.20	4.70	9.60	17.50	1.90	12.60	2.40	5.90	8.10	0.30	6.40	10.40
Pd_ppb	20.00	0.70	0.80	6.40	7.90	72.90	11.50	15.70	11.60	4.60	9.80	0.60	6.20	28.40
B_ppm	<1	2.00	2.00	2.00	3.00	1.00	<1	2.00	4.00	2.00	1.00	1.00	<1	2.00
Tl_ppm	<0.02	<0.02	0.02	<0.02	0.03	0.05	<0.02	<0.02	<0.02	0.02	<0.02	0.06	0.02	<0.02
LOI_pct	6.40	2.70	2.70	2.50	1.90	4.60	4.80	1.80	3.40	2.00	2.00	2.30	2.00	3.70
TOT/C_TC000_pct	0.07	0.07	0.04	0.08	0.02	0.29	0.11	0.07	0.09	0.08	0.02	0.03	0.03	0.22
TOT/S_pct	0.05	0.21	0.03	0.17	<0.02	<0.02	0.04	<0.02	<0.02	0.03	<0.02	0.12	<0.02	0.42
Ba_ppm	27.00	657.00	675.00	602.00	750.00	100.00	40.00	365.00	443.00	915.00	262.00	668.00	345.00	112.00
Sc_ppm	6.00	17.00	14.00	23.00	41.00	5.00	9.00	62.00	22.00	27.00	59.00	5.00	28.00	47.00
Sum_pct	99.40	99.69	99.70	99.70	99.68	99.76	99.40	99.69	99.75	99.73	99.71	99.79	99.69	99.68
Cs_ppm	<0.1	1.10	1.00	0.80	0.60	0.40	<0.1	0.40	2.50	0.70	0.40	1.20	0.20	0.10
Ga_ppm	4.00	19.10	19.40	18.70	15.70	14.10	4.20	11.00	17.00	16.90	11.30	26.00	12.20	11.80
Hf_ppm	0.30	2.10	1.60	3.00	2.80	0.70	0.70	1.40	1.30	2.10	1.10	3.80	2.40	0.90
Nb_ppm	0.70	4.50	3.70	4.60	4.10	2.50	1.70	1.70	5.40	5.40	1.80	4.90	4.10	2.30
Rb_ppm	1.20	25.00	32.70	26.70	26.50	4.50	1.60	13.20	30.90	28.30	20.80	57.40	25.10	3.10
Sn_ppm	<1	<1	<1	<1	<1	<1	<1	<1	<1	1.00	<1	<1	<1	<1
Sr_ppm	91.00	1212.50	1247.70	1011.50	734.70	648.10	94.10	560.90	1145.90	717.20	483.90	622.50	509.50	557.90
Ta_ppm	<0.1	0.10	0.20	0.10	0.20	0.20	0.10	0.10	0.40	0.30	<0.1	0.20	0.20	0.20
Th_ppm	<0.2	2.10	1.80	1.70	2.60	0.30	<0.2	1.20	0.50	2.80	1.10	29.20	2.70	0.30
U_ppm	<0.1	0.60	0.50	0.40	0.60	<0.1	<0.1	0.30	0.10	0.90	0.30	0.50	0.70	<0.1
V_ppm	43.00	242.00	230.00	265.00	270.00	50.00	59.00	233.00	172.00	291.00	258.00	97.00	185.00	159.00
W_ppm	2.20	2.50	1.90	0.70	2.10	<0.5	16.60	0.60	<0.5	7.50	1.00	0.80	1.70	<0.5
Zr_ppm	10.70	75.60	57.50	121.60	96.60	28.00	30.10	34.00	49.00	75.20	39.90	161.00	86.50	29.50

Y_ppm	1.40	16.70	16.30	20.50	21.20	3.90	2.40	13.10	9.30	18.40	14.10	7.20	18.80	7.30
La_ppm	1.20	34.60	35.70	28.40	21.40	3.90	1.50	13.90	7.20	24.60	14.90	90.20	20.30	4.10
Ce_ppm	2.50	73.30	70.50	61.40	46.40	7.80	3.80	30.80	15.00	46.60	29.20	186.40	38.50	9.00
Pr_ppm	0.34	9.08	9.16	7.75	5.88	1.01	0.44	4.37	1.94	5.84	3.91	22.00	4.94	1.26
Nd_ppm	1.30	37.00	38.10	32.40	25.80	4.40	1.80	19.80	8.90	24.00	18.40	83.00	19.70	5.70
Sm_ppm	0.23	6.57	6.63	5.90	5.38	1.00	0.38	4.52	1.94	4.63	3.70	13.10	4.02	1.51
Eu_ppm	0.14	2.04	2.04	1.75	1.48	0.56	0.23	1.42	0.91	1.34	1.17	1.77	1.18	0.66
Gd_ppm	0.32	5.06	5.45	5.18	5.10	0.93	0.50	4.05	2.11	4.31	3.44	7.48	3.81	1.55
Tb_ppm	0.05	0.65	0.66	0.72	0.73	0.14	0.08	0.54	0.32	0.60	0.49	0.66	0.58	0.24
Dy_ppm	0.29	3.34	3.40	3.95	4.28	0.88	0.50	2.81	1.83	3.55	2.84	2.30	3.41	1.45
Ho_ppm	0.06	0.61	0.68	0.79	0.88	0.16	0.09	0.51	0.37	0.73	0.54	0.27	0.70	0.28
Er_ppm	0.18	1.62	1.76	2.25	2.42	0.45	0.26	1.38	1.08	1.84	1.58	0.42	1.97	0.80
Tm_ppm	0.02	0.22	0.22	0.30	0.33	0.06	0.04	0.19	0.13	0.28	0.20	0.05	0.29	0.10
Yb_ppm	0.16	1.37	1.39	1.89	2.18	0.43	0.25	1.02	0.97	1.71	1.35	0.43	1.81	0.59
Lu_ppm	0.03	0.20	0.21	0.31	0.33	0.06	0.04	0.15	0.12	0.26	0.21	0.06	0.27	0.08

Sample_ID	KSAT112/056	KSAT119/057	KSAT127/058A	KSAT127/058B	KSAT139/059	KSAT152/060	KSAT167/061	KSAT189/062	KSAT202/063	KSAT203/064	KSAT207/068	KSAT209/070	KSAT214/072	KSAT217/073
Lat_S	-15.3993	-15.3999	-15.4174	-15.4174	-15.3941	-15.3906	-15.4023	-15.4121	-15.4063	-15.6130	-15.6176	-15.5983	-15.7854	-15.7858
Long_E	13.6343	13.6304	13.6171	13.6171	13.6388	13.6451	13.6400	13.6166	13.6171	13.6378	13.6405	13.6262	13.5590	13.5591
Rocktype	Ultramafic	Granite	Diorite + granite	Diorite + granite	Ol gabbro ('hybrid' rock)	Ol leucogabbro ('hybrid' rock)	Foliated diorite	Ultramafic	Ultramafic	Amphibolite	Paragneiss	Paragneiss	Diorite	Diorite + leucodiorite
Group	Basement	Basement	Basement	Basement	Basement	Basement	Basement	Basement	Basement	Basement	Basement	Basement	Basement	Basement
SiO2_pct	38.92	75.45	49.43	44.85	39.47	47.57	41.77	39.05	39.34	46.67	52.03	64.21	46.87	48.11
TiO2_pct	0.31	0.08	1.15	1.36	0.68	0.70	1.77	0.51	0.39	1.74	1.47	0.71	0.67	0.36

Al2O3_pct	5.29	13.15	16.28	18.05	5.43	22.39	12.56	4.90	4.96	13.38	24.49	18.95	15.38	24.67
Fe2O3t_pct	14.37	0.76	11.46	13.12	14.66	5.92	18.43	14.39	13.72	14.61	10.60	5.89	11.41	4.01
MnO_pct	0.17	0.01	0.11	0.12	0.18	0.09	0.18	0.18	0.17	0.21	0.07	0.06	0.15	0.06
MgO_pct	30.96	0.45	4.83	5.87	28.17	6.07	9.61	30.85	30.92	7.00	3.67	1.62	12.41	3.20
CaO_pct	2.69	0.95	8.08	8.78	3.49	10.45	10.14	2.90	2.84	12.70	0.77	0.99	7.49	10.03
Na2O_pct	0.53	3.53	2.74	2.36	0.69	2.98	2.14	0.44	0.51	2.29	0.99	1.84	1.41	3.19
K2O_pct	0.06	4.51	1.87	2.13	0.18	0.78	0.89	0.14	0.08	0.22	3.85	4.12	1.17	2.07
Cr2O3_pct	0.29	0.01	<0.002	<0.002	0.26	0.03	0.01	0.32	0.31	0.02	0.03	0.02	0.01	0.01
P2O5_pct	0.05	<0.01	0.47	0.14	0.09	0.07	0.19	0.08	0.05	0.13	0.04	0.06	0.19	0.10
Normalised*	93.83	98.95	96.56	96.91	93.46	97.06	97.79	93.93	93.53	99.05	98.25	98.57	97.26	95.90
SiO2_pct*	41.48	76.25	51.19	46.28	42.23	49.01	42.71	41.57	42.06	47.12	52.96	65.14	48.19	50.17
TiO2_pct*	0.32	0.08	1.18	1.39	0.70	0.72	1.81	0.52	0.40	1.78	1.51	0.73	0.69	0.37
Al2O3_pct*	41.48	76.25	51.19	46.28	42.23	49.01	42.71	41.57	42.06	47.12	52.96	65.14	48.19	50.17
Fe2O3t_pct*	15.31	0.77	11.87	13.54	15.69	6.10	18.85	15.32	14.67	14.75	10.79	5.98	11.73	4.18
FeO_pct*	13.02	0.65	10.09	11.51	13.33	5.18	16.02	13.02	12.47	12.54	9.17	5.08	9.97	3.55
Fe2O3_pct*	2.30	0.12	1.78	2.03	2.35	0.91	2.83	2.30	2.20	2.21	1.62	0.90	1.76	0.63
FeO*_pct	13.78	0.69	10.68	12.18	14.12	5.49	16.96	13.79	13.20	13.28	9.71	5.38	10.56	3.76
MnO_pct*	0.17	0.01	0.11	0.12	0.18	0.09	0.18	0.18	0.17	0.22	0.07	0.06	0.15	0.06
MgO_pct*	33.00	0.45	5.00	6.06	30.14	6.25	9.83	32.84	33.06	7.07	3.74	1.64	12.76	3.34
CaO_pct*	2.76	0.97	8.28	9.00	3.58	10.71	10.40	2.97	2.91	13.02	0.79	1.01	7.68	10.28
Na2O_pct*	0.54	3.62	2.81	2.42	0.71	3.06	2.19	0.45	0.52	2.35	1.01	1.89	1.45	3.27
K2O_pct*	0.06	4.62	1.92	2.18	0.18	0.80	0.91	0.14	0.08	0.23	3.95	4.22	1.20	2.12
Cr2O3_pct*	0.30	0.01	N/D	N/D	0.26	0.03	0.01	0.32	0.31	0.02	0.03	0.02	0.01	0.01
P2O5_pct*	0.05	N/D	0.48	0.14	0.09	0.07	0.19	0.08	0.05	0.13	0.04	0.06	0.19	0.10
Mg#	81.87	55.38	46.91	48.40	80.11	68.25	52.23	81.80	82.53	50.11	42.06	36.57	69.51	62.59

Mo_pct	<0.001	<0.001	<0.001	<0.001	<0.001	<0.001	<0.001	<0.001	<0.001	<0.001	<0.001	<0.001	<0.001	<0.001
Cu_pct	0.00	<0.001	0.05	0.06	0.01	0.01	0.04	0.01	0.00	0.01	<0.001	0.00	0.00	<0.001
Pb_pct	<0.02	<0.02	<0.02	<0.02	<0.02	<0.02	<0.02	<0.02	<0.02	<0.02	<0.02	<0.02	<0.02	<0.02
Zn_pct	<0.01	<0.01	<0.01	<0.01	<0.01	<0.01	0.01	0.01	<0.01	<0.01	0.01	<0.01	<0.01	<0.01
Ag_ppm	<2	<2	<2	<2	<2	<2	<2	<2	<2	<2	<2	<2	<2	<2
Ni_ppm	1640.00	20.00	15.00	19.00	1465.00	166.00	52.00	1692.00	1695.00	114.00	85.00	38.00	381.00	90.00
Mo_ppm	0.18	2.95	0.16	0.25	0.17	0.30	0.10	0.15	0.10	0.18	0.68	0.58	0.23	0.14
Cu_ppm	40.39	3.72	438.41	580.04	59.58	86.67	383.26	49.91	27.38	102.66	4.34	14.84	43.79	4.05
Pb_ppm	0.36	12.98	3.21	3.54	0.45	11.86	1.82	9.06	0.33	0.49	3.35	4.82	2.10	5.25
Zn_ppm	68.00	6.00	35.30	39.00	73.50	56.80	42.20	74.40	69.90	26.90	44.10	61.90	35.30	33.70
Ag_ppb	14.00	6.00	192.00	185.00	24.00	87.00	213.00	43.00	11.00	26.00	6.00	12.00	21.00	7.00
Ni_ppm	1584.70	18.70	11.60	11.80	1395.20	140.70	22.40	1500.70	1605.50	55.90	58.10	37.20	214.70	75.70
Co_ppm	136.40	2.70	22.10	24.20	125.40	36.40	26.70	127.70	129.90	20.80	14.50	13.40	36.60	16.70
Mn_ppm	1205.00	86.00	327.00	324.00	1169.00	290.00	439.00	1054.00	1133.00	358.00	166.00	371.00	281.00	317.00
As_ppm	<0.1	<0.1	0.70	0.30	<0.1	<0.1	<0.1	<0.1	<0.1	0.10	<0.1	<0.1	0.20	0.60
Au_ppb	0.60	<0.2	19.60	11.90	0.80	<0.2	10.90	0.60	<0.2	<0.2	1.10	0.80	0.70	0.40
Cd_ppm	0.02	<0.01	0.03	0.04	0.03	0.14	0.03	0.07	0.02	0.03	0.01	<0.01	0.01	0.03
Sb_ppm	<0.02	<0.02	<0.02	0.02	<0.02	<0.02	<0.02	<0.02	<0.02	<0.02	<0.02	<0.02	<0.02	0.04
Bi_ppm	<0.02	<0.02	0.03	0.03	<0.02	<0.02	0.03	<0.02	<0.02	<0.02	0.02	0.24	<0.02	0.03
Cr_ppm	167.70	24.90	8.70	3.20	204.90	33.80	47.80	204.20	147.70	40.20	96.50	93.30	15.90	44.20
Hg_ppb	<5	<5	8.00	<5	<5	<5	<5	<5	<5	<5	<5	<5	<5	<5
Se_ppm	<0.1	<0.1	0.10	0.30	<0.1	<0.1	0.20	<0.1	<0.1	<0.1	<0.1	0.10	<0.1	<0.1
Te_ppm	<0.02	<0.02	0.03	0.03	0.02	0.02	0.03	<0.02	<0.02	0.02	<0.02	0.03	0.02	<0.02
Ge_ppm	<0.1	<0.1	<0.1	<0.1	<0.1	<0.1	<0.1	<0.1	<0.1	<0.1	<0.1	<0.1	<0.1	<0.1
In_ppm	<0.02	<0.02	<0.02	<0.02	<0.02	<0.02	0.02	<0.02	<0.02	0.02	0.04	0.06	<0.02	<0.02

Re_ppb	<1	<1	<1	<1	<1	<1	<1	<1	<1	<1	<1	<1	<1	<1
Be_ppm	<0.1	0.30	0.20	0.20	0.10	0.10	0.20	<0.1	<0.1	0.20	1.40	2.30	0.20	0.40
Li_ppm	2.20	2.20	14.00	16.00	3.10	9.90	6.00	6.70	2.10	4.20	13.70	31.30	12.10	13.80
Pd_ppb	<10	<10	<10	<10	11.00	<10	29.00	16.00	<10	<10	<10	<10	<10	<10
Pt_ppb	<2	<2	<2	2.00	<2	<2	6.00	<2	<2	<2	<2	<2	<2	<2
Au_ppb	3.00	2.00	20.00	18.00	6.00	3.00	16.00	6.00	6.00	6.00	3.00	3.00	8.00	3.00
Pt_ppb	1.50	0.20	1.70	2.90	2.30	0.30	20.70	3.00	0.80	1.50	1.90	0.70	0.80	0.30
Pd_ppb	10.70	0.80	4.90	7.60	13.30	0.70	38.60	19.80	5.20	2.40	1.10	1.20	2.20	0.80
B_ppm	<1	<1	2.00	2.00	<1	4.00	<1	2.00	<1	1.00	<1	1.00	1.00	4.00
Tl_ppm	<0.02	<0.02	0.03	0.04	<0.02	0.03	<0.02	<0.02	<0.02	<0.02	0.12	0.50	0.09	0.05
LOI_pct	5.60	1.00	3.10	2.70	6.00	2.70	1.80	5.50	5.90	0.70	1.50	1.30	2.40	3.90
TOT/C_TC000_pct	0.13	0.03	0.12	0.08	0.09	0.08	0.03	0.07	0.04	0.03	0.04	<0.02	0.15	0.14
TOT/S_pct	0.05	<0.02	0.05	0.05	0.07	0.23	0.03	<0.02	0.03	<0.02	<0.02	<0.02	<0.02	<0.02
Ba_ppm	43.00	655.00	883.00	867.00	79.00	261.00	498.00	51.00	45.00	105.00	1820.00	715.00	477.00	574.00
Sc_ppm	8.00	2.00	29.00	38.00	13.00	8.00	56.00	10.00	10.00	41.00	15.00	15.00	14.00	4.00
Sum_pct	99.43	99.95	99.66	99.61	99.46	99.76	99.59	99.43	99.43	99.75	99.75	99.87	99.66	99.80
Cs_ppm	<0.1	0.80	1.00	1.20	0.30	1.40	0.20	0.20	<0.1	0.30	2.10	6.10	3.20	5.30
Ga_ppm	4.60	12.00	18.00	18.40	6.40	16.10	17.60	4.60	4.60	16.00	27.60	20.30	13.70	18.60
Hf_ppm	0.60	2.00	2.10	1.30	1.10	0.90	1.80	0.90	0.50	2.50	12.10	5.80	1.80	1.40
Nb_ppm	1.60	6.40	4.20	3.50	3.90	4.10	3.50	3.00	1.90	5.90	20.30	12.40	5.30	3.00
Rb_ppm	1.70	87.30	45.30	57.70	4.40	17.20	11.10	3.40	2.10	5.10	94.90	167.40	35.80	72.40
Sn_ppm	<1	<1	<1	<1	<1	<1	1.00	<1	<1	<1	<1	1.00	<1	<1
Sr_ppm	132.30	218.90	980.80	1019.50	153.00	748.60	641.50	108.30	113.50	257.10	171.10	86.70	653.50	965.30
Ta_ppm	<0.1	0.70	0.20	0.10	0.10	0.20	0.10	0.20	0.10	0.40	1.10	0.70	0.20	0.10
Th_ppm	<0.2	7.80	3.30	1.60	0.40	0.30	1.00	0.30	0.20	0.50	25.80	17.90	3.40	2.80

U_ppm	<0.1	2.60	0.70	0.60	0.10	<0.1	0.30	<0.1	<0.1	0.10	3.10	3.20	0.60	0.50
V_ppm	58.00	13.00	376.00	486.00	103.00	83.00	588.00	79.00	72.00	372.00	182.00	90.00	108.00	44.00
W_ppm	12.50	3.80	0.80	0.70	<0.5	<0.5	<0.5	<0.5	<0.5	0.70	1.30	1.90	0.60	0.70
Zr_ppm	24.20	48.20	72.90	36.70	38.60	36.70	61.70	28.00	20.10	94.40	443.80	215.90	61.80	63.80
Y_ppm	2.60	6.00	15.60	14.00	6.20	6.50	19.20	4.90	3.70	22.00	33.80	28.90	10.60	4.90
La_ppm	2.30	14.70	26.70	16.50	4.60	5.80	18.60	3.30	2.40	7.50	87.60	56.50	19.10	20.90
Ce_ppm	4.80	26.20	55.70	32.70	10.40	11.90	42.50	7.90	5.10	19.80	168.70	110.70	40.20	35.20
Pr_ppm	0.58	2.92	7.20	4.51	1.33	1.49	6.13	1.02	0.64	2.77	18.72	12.23	4.89	3.67
Nd_ppm	2.70	10.80	31.00	21.10	6.20	5.90	28.10	4.60	3.00	13.40	68.30	43.60	21.10	12.90
Sm_ppm	0.54	1.91	6.03	4.44	1.29	1.28	6.60	0.98	0.74	3.84	11.49	7.59	3.70	1.94
Eu_ppm	0.22	0.43	1.65	1.46	0.50	0.70	1.93	0.36	0.28	1.32	3.50	1.63	1.04	1.04
Gd_ppm	0.54	1.51	4.91	4.03	1.43	1.51	5.73	1.06	0.79	4.46	9.18	6.00	3.19	1.34
Tb_ppm	0.09	0.20	0.62	0.51	0.21	0.22	0.75	0.16	0.11	0.69	1.31	0.90	0.40	0.17
Dy_ppm	0.55	1.11	3.47	2.60	1.23	1.19	3.84	1.00	0.65	4.27	6.93	5.50	2.23	0.98
Ho_ppm	0.11	0.18	0.62	0.51	0.25	0.27	0.70	0.18	0.14	0.86	1.34	1.09	0.41	0.17
Er_ppm	0.31	0.58	1.63	1.35	0.72	0.62	1.97	0.57	0.39	2.34	3.82	3.25	1.09	0.44
Tm_ppm	0.04	0.09	0.22	0.17	0.09	0.09	0.26	0.07	0.05	0.33	0.52	0.49	0.15	0.07
Yb_ppm	0.28	0.72	1.41	1.07	0.64	0.57	1.51	0.47	0.34	2.02	3.63	3.11	0.94	0.51
Lu_ppm	0.05	0.11	0.19	0.16	0.09	0.09	0.23	0.06	0.05	0.32	0.61	0.46	0.14	0.07

Sample_ID	KSAT223/074	KSAT228/076	KSAT231/077	KSAT234/082	KSAT238/078	KSAT245/079	KSAT251/080	KSAT255/081	KSAT259/083	KSAT260/084	KSAT261/086	KSAT264/087	KSAT267/088	KSAT269/089
Lat_S	-15.7871	-15.7880	-15.7852	-15.7840	-15.7844	-15.7863	-15.7893	-15.7902	-15.7839	-15.7840	-15.7758	-15.7650	-15.7649	-15.7644
Long_E	13.5590	13.5602	13.5627	13.5570	13.5580	13.5579	13.5577	13.5564	13.5579	13.5579	13.5539	13.5817	13.5809	13.5811

Rocktype	Diorite	Sheared leucodiorite	Diorite + leucodiorite	Granite	Mottled leucodiorite	Diorite	Diorite	Diorite	Leucodiorite	Leucodiorite	Diorite	Diorite	Diorite	Diorite
Group	Basement	Basement	Basement	Basement	Basement	Basement	Basement	Basement	Basement	Basement	Basement	Basement	Basement	Basement
SiO2_pct	48.29	46.57	42.08	71.60	47.79	50.64	51.69	51.13	50.70	49.84	55.55	49.16	53.58	54.33
TiO2_pct	0.63	0.55	1.67	0.29	0.70	1.42	0.68	0.84	0.64	0.55	0.76	0.72	0.53	0.78
Al2O3_pct	16.33	22.81	17.00	14.14	22.68	16.57	17.81	17.19	18.41	21.68	9.22	8.80	9.45	11.60
Fe2O3t_pct	6.78	5.89	16.39	2.12	6.29	11.15	7.17	8.87	7.35	5.52	6.49	9.46	9.29	9.51
MnO_pct	0.11	0.08	0.13	0.03	0.09	0.14	0.12	0.12	0.12	0.08	0.13	0.19	0.19	0.16
MgO_pct	8.78	4.46	6.18	0.73	4.08	3.65	6.17	5.83	5.52	3.42	8.55	12.56	10.58	8.03
CaO_pct	12.10	12.02	11.00	0.76	8.85	7.63	8.77	8.47	9.67	10.06	12.51	15.09	10.89	10.07
Na2O_pct	2.09	2.88	1.55	3.78	2.88	3.30	2.54	2.80	2.44	2.90	2.59	1.45	1.56	2.11
K2O_pct	1.03	0.80	0.72	5.21	2.41	1.84	1.39	1.48	1.67	1.94	2.66	0.58	1.52	1.17
Cr2O3_pct	0.05	0.02	0.00	0.01	0.01	0.00	0.03	0.02	0.00	0.01	0.02	0.09	0.08	0.03
P2O5_pct	0.13	0.13	0.10	0.11	0.20	0.91	0.30	0.33	0.25	0.21	0.27	0.12	0.34	0.03
Normalised*	96.34	96.28	96.83	98.92	96.09	97.29	96.70	97.19	96.84	96.28	98.87	98.27	98.10	97.86
SiO2_pct*	50.12	48.37	43.46	72.38	49.73	52.05	53.45	52.61	52.35	51.77	56.18	50.03	54.62	55.52
TiO2_pct*	0.65	0.56	1.71	0.30	0.72	1.46	0.70	0.86	0.66	0.56	0.78	0.74	0.54	0.80
Al2O3_pct*	50.12	48.37	43.46	72.38	49.73	52.05	53.45	52.61	52.35	51.77	56.18	50.03	54.62	55.52
Fe2O3t_pct*	7.04	6.12	16.93	2.14	6.55	11.46	7.41	9.13	7.59	5.73	6.56	9.63	9.47	9.72
FeO_pct*	5.98	5.20	14.39	1.82	5.56	9.74	6.30	7.76	6.45	4.87	5.58	8.18	8.05	8.26
Fe2O3_pct*	1.06	0.92	2.54	0.32	0.98	1.72	1.11	1.37	1.14	0.86	0.98	1.44	1.42	1.46
FeO*_pct	6.33	5.51	15.23	1.93	5.89	10.31	6.67	8.21	6.83	5.16	5.91	8.66	8.52	8.75
MnO_pct*	0.11	0.08	0.13	0.03	0.09	0.14	0.12	0.12	0.12	0.08	0.13	0.19	0.19	0.16
MgO_pct*	9.11	4.63	6.38	0.74	4.25	3.75	6.38	6.00	5.70	3.55	8.65	12.78	10.78	8.21

CaO_pct*	12.41	12.32	11.28	0.78	9.07	7.82	8.99	8.68	9.91	10.31	12.83	15.47	11.16	10.32
Na2O_pct*	2.14	2.95	1.59	3.88	2.95	3.38	2.60	2.87	2.50	2.97	2.66	1.49	1.60	2.16
K2O_pct*	1.06	0.82	0.74	5.34	2.47	1.89	1.43	1.52	1.71	1.99	2.73	0.59	1.56	1.20
Cr2O3_pct*	0.05	0.02	0.00	0.01	0.01	0.00	0.03	0.02	0.00	0.01	0.02	0.10	0.08	0.03
P2O5_pct*	0.13	0.13	0.10	0.11	0.21	0.93	0.31	0.34	0.26	0.22	0.28	0.12	0.35	0.03
Mg#	73.08	61.35	44.15	41.92	57.62	40.70	64.34	57.95	61.16	56.50	73.42	73.57	70.48	63.90
Mo_pct	<0.001	<0.001	<0.001	<0.001	<0.001	<0.001	<0.001	<0.001	<0.001	<0.001	<0.001	<0.001	<0.001	<0.001
Cu_pct	0.01	0.01	0.03	<0.001	0.01	0.00	0.02	0.02	0.01	0.01	0.06	0.02	0.01	0.05
Pb_pct	<0.02	<0.02	<0.02	<0.02	<0.02	<0.02	<0.02	<0.02	<0.02	<0.02	<0.02	<0.02	<0.02	<0.02
Zn_pct	<0.01	<0.01	<0.01	<0.01	<0.01	0.01	<0.01	<0.01	<0.01	<0.01	<0.01	<0.01	<0.01	<0.01
Ag_ppm	<2	<2	<2	<2	<2	<2	<2	<2	<2	<2	<2	<2	<2	<2
Ni_ppm	169.00	90.00	67.00	<10	95.00	<10	102.00	103.00	64.00	43.00	285.00	109.00	124.00	67.00
Mo_ppm	0.27	0.39	0.61	1.66	0.33	0.47	0.26	0.33	0.22	0.25	0.30	0.10	0.09	0.28
Cu_ppm	108.52	47.80	232.40	7.81	77.16	31.78	138.75	175.14	80.34	59.53	589.44	212.79	57.29	491.58
Pb_ppm	4.44	3.33	2.90	5.31	4.65	5.66	5.14	4.75	4.17	5.33	7.72	1.48	5.65	8.53
Zn_ppm	23.00	43.20	52.30	27.50	39.60	84.60	37.00	40.50	33.70	30.60	14.20	17.20	22.60	16.40
Ag_ppb	60.00	36.00	68.00	11.00	104.00	38.00	84.00	52.00	37.00	43.00	364.00	52.00	20.00	197.00
Ni_ppm	82.20	78.70	43.70	9.40	69.50	3.40	59.10	63.70	38.60	26.40	126.10	27.00	36.60	14.10
Co_ppm	18.30	24.60	54.00	4.30	19.60	21.80	17.50	21.80	17.30	13.50	13.00	14.30	12.20	12.00
Mn_ppm	276.00	326.00	329.00	249.00	324.00	451.00	283.00	314.00	290.00	263.00	188.00	255.00	356.00	223.00
As_ppm	0.70	10.90	1.40	0.20	8.00	<0.1	0.20	0.20	0.30	1.60	<0.1	0.30	0.40	0.40
Au_ppb	2.60	0.40	7.80	0.50	0.40	0.30	2.70	1.90	0.40	0.80	4.10	4.40	0.60	4.20
Cd_ppm	0.02	0.07	0.03	<0.01	0.07	0.04	0.03	0.03	0.02	0.02	0.06	0.05	0.03	0.17
Sb_ppm	<0.02	<0.02	0.05	0.04	0.04	0.02	<0.02	<0.02	<0.02	0.03	0.03	<0.02	0.02	0.06
Bi_ppm	0.03	<0.02	0.05	0.04	0.08	0.04	0.04	0.02	<0.02	0.02	0.22	0.04	0.05	0.05

Cr_ppm	99.60	112.10	19.10	31.70	16.00	6.60	81.90	50.40	20.90	12.20	23.90	140.80	109.70	37.40
Hg_ppb	<5	<5	<5	<5	<5	<5	<5	<5	<5	<5	<5	<5	<5	<5
Se_ppm	0.10	0.10	0.10	<0.1	0.20	0.10	0.20	<0.1	0.10	<0.1	0.50	0.20	<0.1	0.10
Te_ppm	0.03	<0.02	0.02	<0.02	<0.02	<0.02	<0.02	<0.02	<0.02	<0.02	0.06	0.03	<0.02	0.03
Ge_ppm	<0.1	<0.1	<0.1	<0.1	<0.1	<0.1	<0.1	<0.1	<0.1	<0.1	<0.1	<0.1	<0.1	<0.1
In_ppm	<0.02	<0.02	<0.02	<0.02	<0.02	<0.02	<0.02	<0.02	<0.02	<0.02	<0.02	<0.02	<0.02	<0.02
Re_ppb	<1	<1	<1	<1	<1	<1	<1	<1	<1	<1	<1	<1	<1	<1
Be_ppm	0.20	0.20	0.20	1.10	0.40	0.60	0.40	0.40	0.40	0.50	0.30	0.20	0.40	0.40
Li_ppm	25.40	41.20	10.80	12.40	39.00	23.10	20.00	18.10	27.40	27.20	3.80	7.90	3.40	4.00
Pd_ppb	<10	<10	<10	<10	<10	<10	<10	<10	<10	<10	<10	18.00	<10	<10
Pt_ppb	5.00	<2	<2	<2	<2	<2	<2	<2	<2	<2	11.00	11.00	6.00	5.00
Au_ppb	6.00	3.00	14.00	2.00	2.00	3.00	5.00	7.00	7.00	8.00	7.00	12.00	9.00	10.00
Pt_ppb	7.40	0.40	0.50	0.20	0.30	0.20	1.40	0.80	0.60	0.50	14.70	13.90	10.10	7.40
Pd_ppb	3.30	0.70	1.90	<0.5	<0.5	0.50	0.90	1.00	2.00	1.80	8.60	18.80	10.60	9.80
B_ppm	3.00	3.00	2.00	2.00	3.00	2.00	2.00	1.00	2.00	3.00	2.00	3.00	2.00	2.00
Tl_ppm	0.02	0.02	0.03	0.04	0.07	0.05	0.03	0.03	0.04	0.06	0.02	<0.02	0.02	0.03
LOI_pct	3.40	3.50	2.80	1.00	3.70	2.40	3.00	2.50	2.90	3.50	0.80	1.40	1.60	1.80
TOT/C_TC000_pct	0.06	0.09	0.06	0.03	0.08	0.06	0.05	0.03	0.12	0.14	<0.02	0.02	0.03	0.06
TOT/S_pct	<0.02	<0.02	0.03	<0.02	0.20	0.08	<0.02	<0.02	0.04	0.03	<0.02	<0.02	<0.02	<0.02
Ba_ppm	283.00	348.00	246.00	754.00	680.00	886.00	542.00	556.00	505.00	529.00	631.00	121.00	460.00	304.00
Sc_ppm	28.00	8.00	30.00	5.00	13.00	21.00	21.00	22.00	22.00	15.00	36.00	74.00	47.00	42.00
Sum_pct	99.74	99.78	99.63	99.92	99.79	99.69	99.70	99.69	99.74	99.78	99.67	99.67	99.70	99.66
Cs_ppm	1.80	4.00	2.50	3.90	5.20	2.30	2.00	1.80	2.20	3.40	1.80	0.50	0.70	1.60
Ga_ppm	11.00	16.40	21.30	16.30	20.60	23.00	17.40	19.40	18.40	19.50	11.40	10.20	11.00	13.30
Hf_ppm	1.80	1.20	1.70	4.30	2.60	4.60	3.20	3.10	2.70	2.50	3.10	1.50	3.10	3.00

Nb_ppm	7.90	3.50	2.50	10.20	6.20	10.30	6.30	7.10	5.80	5.60	9.40	2.40	4.80	6.90
Rb_ppm	39.70	32.80	24.20	178.40	118.40	55.20	40.90	50.40	71.10	93.40	81.30	18.00	48.30	55.70
Sn_ppm	<1	<1	1.00	3.00	2.00	2.00	<1	<1	<1	2.00	1.00	<1	<1	1.00
Sr_ppm	419.70	890.30	845.80	233.50	650.70	994.30	906.20	869.30	827.40	817.90	375.90	253.10	326.50	423.70
Ta_ppm	0.30	0.20	0.10	0.80	0.30	0.50	0.30	0.30	0.20	0.30	0.60	0.20	0.20	0.60
Th_ppm	2.20	2.60	2.00	23.70	4.50	5.70	4.40	3.60	5.00	4.60	8.10	1.30	4.50	7.20
U_ppm	0.40	0.70	0.50	6.00	0.90	1.40	1.00	0.70	0.80	0.90	2.50	0.30	1.10	3.10
V_ppm	146.00	106.00	655.00	27.00	123.00	238.00	136.00	221.00	139.00	135.00	156.00	275.00	203.00	366.00
W_ppm	0.80	1.20	3.40	2.70	1.90	1.40	1.10	1.00	<0.5	0.90	0.70	0.60	<0.5	0.80
Zr_ppm	69.90	46.80	72.60	130.80	99.10	205.20	147.40	139.50	111.60	104.30	122.90	42.30	127.10	114.40
Y_ppm	10.90	7.40	9.10	13.40	12.30	23.40	15.20	15.10	13.10	12.30	16.60	17.50	20.70	16.60
La_ppm	16.90	16.30	15.50	42.50	31.10	74.10	40.80	45.80	34.80	34.70	36.90	11.80	43.50	23.00
Ce_ppm	35.60	30.50	31.40	83.00	63.50	149.80	78.20	92.30	70.30	65.30	76.80	27.30	79.10	47.80
Pr_ppm	4.19	3.45	3.85	8.11	6.96	16.73	8.50	9.98	7.49	7.24	8.76	3.55	9.01	5.36
Nd_ppm	16.20	13.30	16.20	28.70	28.50	67.40	32.90	36.30	28.40	27.20	35.00	16.20	33.40	20.60
Sm_ppm	2.91	2.31	3.03	4.63	4.59	10.38	5.20	6.04	4.97	4.65	6.16	3.90	5.95	4.13
Eu_ppm	0.93	0.84	0.96	0.89	1.24	2.63	1.44	1.64	1.39	1.32	1.72	1.12	1.37	0.85
Gd_ppm	2.60	1.80	2.55	3.36	3.74	8.15	4.24	4.67	4.01	3.37	5.12	3.83	5.18	3.65
Tb_ppm	0.38	0.24	0.33	0.48	0.48	1.02	0.54	0.60	0.52	0.45	0.63	0.58	0.72	0.52
Dy_ppm	1.92	1.33	1.80	2.47	2.53	5.24	3.04	3.11	2.94	2.37	3.57	3.34	3.89	3.36
Ho_ppm	0.43	0.25	0.32	0.49	0.51	0.97	0.54	0.53	0.52	0.43	0.68	0.66	0.75	0.59
Er_ppm	1.08	0.71	0.94	1.40	1.25	2.47	1.60	1.53	1.31	1.26	1.79	1.85	2.10	1.69
Tm_ppm	0.16	0.09	0.12	0.20	0.18	0.33	0.18	0.20	0.20	0.18	0.24	0.25	0.31	0.26
Yb_ppm	0.97	0.63	0.79	1.15	1.09	1.96	1.35	1.27	1.21	1.07	1.52	1.56	1.76	1.54
Lu_ppm	0.16	0.09	0.11	0.19	0.17	0.29	0.19	0.20	0.19	0.16	0.24	0.24	0.28	0.24

Sample_ID	KSAT275/090	KSAT277/091	KAC449-1	KSAT004/004	KSAT005/005	KSAT011/006	KSAT013/008	KSAT017/009	KSAT021/010	KSAT024/011	KSAT025/012	KSAT028/015	KSAT039/024A	KSAT039/024B
Lat_S	-15.7605	-15.7608	-17.2904	-16.8777	-16.8767	-16.8740	-16.8668	-16.8440	-16.8479	-16.8504	-16.8506	-16.6997	-15.7595	-15.7595
Long_E	13.5859	13.5871	13.2857	13.0442	13.0436	13.0284	13.0301	12.9679	12.9537	12.9492	12.9514	13.3532	13.5877	13.5877
Rocktype	Diorite	Diorite	Ultramafic	Dolerite	Dolerite	Dolerite	Mixed metavolcanic?	Dolerite	Dolerite	Dolerite	Dolerite	Pyroxenite	Pyroxenite (weakly layered)	Pyroxenite (distinctly layered)
Group	Basement	Basement	Basement	Basement	Basement	Basement	Basement	Basement	Basement	Basement	Basement	Basement	Basement	Basement
SiO2_pct	47.57	48.00	42.64	46.18	46.03	48.26	46.46	48.21	45.87	45.85	44.51	50.86	48.73	49.28
TiO2_pct	0.46	1.13	0.24	1.83	0.50	0.90	1.89	1.75	1.42	0.97	0.78	0.41	0.66	0.80
Al2O3_pct	14.61	16.67	10.90	16.37	17.68	12.56	15.90	13.54	16.46	16.90	17.02	4.63	15.69	13.48
Fe2O3t_pct	8.23	11.51	10.30	13.72	9.25	11.90	13.94	13.82	12.24	9.51	10.51	10.00	8.35	8.98
MnO_pct	0.14	0.16	0.18	0.19	0.13	0.21	0.17	0.22	0.17	0.14	0.14	0.22	0.14	0.16
MgO_pct	10.48	6.55	17.44	6.21	8.76	11.01	6.75	6.86	7.39	7.79	10.48	16.93	8.42	9.04
CaO_pct	13.93	10.62	13.09	8.58	10.84	10.77	6.66	9.00	10.63	11.14	9.93	14.05	12.19	13.33
Na2O_pct	1.24	1.79	0.37	2.79	2.14	1.69	3.33	3.17	1.66	2.72	1.69	0.84	1.58	1.42
K2O_pct	0.79	0.93	0.12	0.35	1.13	0.62	1.14	0.66	0.40	0.50	0.30	0.28	1.38	0.64
Cr2O3_pct	0.03	0.01	0.08	0.01	0.03	0.12	0.01	0.03	0.02	0.04	0.03	0.26	0.03	0.07
P2O5_pct	0.09	0.07	<0.01	0.18	0.06	0.12	0.18	0.13	0.17	0.11	0.09	0.02	0.10	0.15
Normalised*	97.57	97.51	95.44	96.44	96.64	98.20	96.54	97.44	96.43	95.76	95.52	98.55	97.30	97.39
SiO2_pct*	48.75	49.23	44.68	47.88	47.63	49.14	48.13	49.48	47.57	47.88	46.60	51.61	50.08	50.60
TiO2_pct*	0.47	1.16	0.25	1.88	0.51	0.92	1.94	1.79	1.46	0.99	0.80	0.42	0.68	0.82
Al2O3_pct*	48.75	49.23	44.68	47.88	47.63	49.14	48.13	49.48	47.57	47.88	46.60	51.61	50.08	50.60
Fe2O3t_pct*	8.43	11.80	10.79	14.23	9.57	12.12	14.44	14.18	12.69	9.93	11.00	10.15	8.58	9.22

FeO_pct*	7.17	10.03	9.17	12.09	8.14	10.30	12.27	12.06	10.79	8.44	9.35	8.63	7.29	7.84
Fe2O3_pct*	1.27	1.77	1.62	2.13	1.44	1.82	2.17	2.13	1.90	1.49	1.65	1.52	1.29	1.38
FeO*_pct	7.59	10.62	9.71	12.80	8.61	10.91	13.00	12.76	11.42	8.94	9.90	9.13	7.72	8.30
MnO_pct*	0.14	0.16	0.18	0.19	0.13	0.22	0.17	0.23	0.17	0.14	0.14	0.23	0.14	0.16
MgO_pct*	10.74	6.72	18.27	6.44	9.06	11.21	6.99	7.04	7.66	8.13	10.97	17.18	8.65	9.28
CaO_pct*	14.28	10.89	13.42	8.80	11.11	11.04	6.83	9.23	10.90	11.42	10.18	14.40	12.50	13.67
Na2O_pct*	1.27	1.84	0.38	2.86	2.19	1.73	3.41	3.25	1.70	2.79	1.73	0.86	1.62	1.46
K2O_pct*	0.81	0.95	0.12	0.36	1.16	0.64	1.17	0.68	0.41	0.51	0.31	0.29	1.41	0.66
Cr2O3_pct*	0.03	0.01	0.08	0.01	0.03	0.12	0.01	0.03	0.02	0.04	0.03	0.26	0.03	0.07
P2O5_pct*	0.09	0.07	N/D	0.18	0.06	0.12	0.18	0.13	0.17	0.11	0.09	0.02	0.10	0.15
Mg#	72.75	54.40	78.02	48.69	66.50	65.98	50.38	51.00	55.86	63.20	67.64	78.02	67.89	67.85
Mo_pct	<0.001	<0.001	<0.001	<0.001	<0.001	<0.001	<0.001	<0.001	<0.001	<0.001	<0.001	<0.001	<0.001	<0.001
Cu_pct	0.03	0.01	0.00	0.01	0.00	0.00	0.01	0.01	0.01	0.01	0.01	0.01	0.01	0.01
Pb_pct	<0.02	<0.02	<0.02	<0.02	<0.02	<0.02	<0.02	<0.02	<0.02	<0.02	<0.02	<0.02	<0.02	<0.02
Zn_pct	<0.01	<0.01	<0.01	0.01	<0.01	0.01	0.01	<0.01	<0.01	<0.01	<0.01	0.01	<0.01	<0.01
Ag_ppm	<2	<2	<2	<2	<2	<2	<2	<2	<2	<2	<2	<2	<2	<2
Ni_ppm	106.00	31.00	280.00	113.00	197.00	175.00	111.00	63.00	167.00	250.00	336.00	212.00	66.00	85.00
Mo_ppm	0.10	0.29	0.13	0.25	0.28	0.27	0.21	0.25	0.35	0.29	0.24	0.12	0.33	0.22
Cu_ppm	277.16	86.68	33.58	68.19	28.09	30.99	72.89	91.10	68.08	40.44	50.15	61.53	131.32	92.31
Pb_ppm	1.72	2.62	0.24	1.00	1.91	1.56	0.90	1.49	0.39	0.30	0.33	14.90	4.77	2.80
Zn_ppm	12.60	37.70	8.20	82.10	34.00	28.70	69.50	51.40	63.70	40.20	46.40	58.70	14.90	29.00
Ag_ppb	184.00	29.00	19.00	31.00	14.00	13.00	36.00	39.00	26.00	11.00	22.00	17.00	58.00	33.00
Ni_ppm	34.40	16.30	180.60	88.50	107.50	42.60	74.10	38.40	114.20	170.80	228.20	65.10	21.90	27.10
Co_ppm	14.60	23.00	45.80	44.80	35.70	17.30	40.10	30.90	41.40	31.00	44.50	13.20	14.40	15.90
Mn_ppm	186.00	322.00	489.00	655.00	418.00	410.00	633.00	652.00	564.00	438.00	550.00	310.00	190.00	281.00

As_ppm	<0.1	<0.1	<0.1	0.30	5.70	11.00	1.70	0.10	<0.1	<0.1	0.10	<0.1	1.00	0.40
Au_ppb	3.50	0.50	1.50	0.90	0.20	5.10	0.60	0.30	0.70	1.20	0.80	<0.2	0.70	0.30
Cd_ppm	0.02	0.03	<0.01	0.11	0.02	0.01	0.09	0.10	0.07	0.01	0.03	0.05	0.05	0.06
Sb_ppm	<0.02	<0.02	<0.02	<0.02	0.03	0.73	<0.02	<0.02	<0.02	<0.02	<0.02	<0.02	<0.02	<0.02
Bi_ppm	0.02	<0.02	<0.02	0.03	<0.02	0.13	<0.02	<0.02	<0.02	<0.02	<0.02	0.27	<0.02	<0.02
Cr_ppm	36.00	19.20	119.20	46.00	44.60	374.40	50.20	157.10	46.00	26.70	35.50	240.50	58.60	139.40
Hg_ppb	<5	<5	<5	<5	<5	<5	<5	<5	<5	<5	<5	<5	<5	<5
Se_ppm	0.30	0.20	0.20	<0.1	<0.1	<0.1	<0.1	<0.1	<0.1	<0.1	<0.1	<0.1	<0.1	<0.1
Te_ppm	0.05	0.02	<0.02	<0.02	<0.02	0.07	<0.02	<0.02	<0.02	<0.02	<0.02	<0.02	<0.02	<0.02
Ge_ppm	<0.1	<0.1	<0.1	<0.1	<0.1	0.10	0.10	0.10	<0.1	<0.1	<0.1	<0.1	<0.1	<0.1
In_ppm	<0.02	<0.02	<0.02	<0.02	<0.02	<0.02	<0.02	<0.02	<0.02	<0.02	<0.02	<0.02	<0.02	<0.02
Re_ppb	<1	<1	<1	<1	<1	<1	<1	<1	<1	<1	<1	<1	<1	<1
Be_ppm	0.20	0.30	<0.1	<0.1	<0.1	0.30	<0.1	<0.1	0.20	<0.1	<0.1	<0.1	0.10	0.10
Li_ppm	7.00	10.20	6.30	14.90	16.20	3.80	34.60	24.70	8.60	3.50	5.30	1.80	12.10	9.30
Pd_ppb	10.00	<10	17.00	<10	<10	<10	<10	<10	<10	<10	<10	19.00	<10	<10
Pt_ppb	4.00	<2	21.00	<2	<2	4.00	<2	<2	<2	<2	<2	45.00	5.00	3.00
Au_ppb	10.00	8.00	5.00	3.00	3.00	7.00	2.00	2.00	4.00	3.00	3.00	5.00	3.00	3.00
Pt_ppb	7.70	0.80	28.10	0.40	0.20	11.30	0.30	0.20	0.60	1.00	1.10	75.10	5.60	3.80
Pd_ppb	12.60	2.10	20.20	1.00	0.60	10.90	0.60	<0.5	2.20	3.10	3.20	21.10	5.40	3.60
B_ppm	1.00	1.00	42.00	3.00	5.00	6.00	4.00	3.00	2.00	<1	<1	<1	3.00	2.00
Tl_ppm	0.03	<0.02	0.03	0.02	0.03	0.09	0.02	<0.02	<0.02	<0.02	<0.02	<0.02	0.03	<0.02
LOI_pct	2.10	2.20	4.20	3.30	3.10	1.50	3.20	2.30	3.30	4.00	4.20	1.10	2.40	2.30
TOT/C_TC000_pct	0.04	0.03	0.14	0.08	0.02	0.02	<0.02	<0.02	0.03	0.39	0.07	0.03	0.05	0.02
TOT/S_pct	0.08	0.20	<0.02	0.03	<0.02	<0.02	0.03	0.07	0.04	<0.02	0.03	<0.02	<0.02	<0.02
Ba_ppm	137.00	302.00	35.00	278.00	378.00	150.00	792.00	255.00	149.00	191.00	114.00	57.00	285.00	175.00

Sc_ppm	42.00	33.00	42.00	33.00	24.00	37.00	32.00	50.00	26.00	28.00	18.00	52.00	43.00	51.00
Sum_pct	99.67	99.71	99.64	99.74	99.74	99.70	99.74	99.74	99.73	99.76	99.72	99.65	99.70	99.69
Cs_ppm	3.90	1.90	2.60	0.40	1.10	2.40	0.60	0.40	0.60	1.50	1.00	<0.1	1.50	0.30
Ga_ppm	11.70	18.80	6.60	19.60	16.40	12.90	18.80	16.40	16.80	15.80	14.60	5.10	14.20	13.00
Hf_ppm	1.10	1.90	0.30	3.10	1.00	1.40	3.00	3.00	2.30	1.40	1.20	0.70	1.50	1.80
Nb_ppm	2.40	4.60	<0.1	4.50	1.10	3.30	4.60	2.40	5.40	3.10	2.60	1.00	2.40	3.00
Rb_ppm	27.50	27.40	3.60	9.90	34.00	21.30	45.50	12.10	9.40	10.20	5.70	2.40	50.70	22.70
Sn_ppm	<1	1.00	<1	1.00	<1	<1	<1	<1	<1	<1	<1	<1	<1	<1
Sr_ppm	666.90	701.90	326.70	517.50	615.10	352.80	398.20	327.20	558.00	426.40	500.40	86.10	691.10	680.60
Ta_ppm	<0.1	0.30	<0.1	0.30	<0.1	0.20	0.20	0.10	0.40	0.20	0.10	<0.1	0.10	<0.1
Th_ppm	0.80	3.50	<0.2	1.00	0.50	0.90	1.00	1.10	0.90	0.50	0.50	0.30	2.90	1.80
U_ppm	0.20	0.90	<0.1	0.30	<0.1	0.20	0.20	0.30	0.30	0.10	0.10	<0.1	0.60	0.60
V_ppm	174.00	353.00	134.00	292.00	143.00	256.00	288.00	376.00	231.00	201.00	139.00	191.00	219.00	237.00
W_ppm	<0.5	0.80	3.80	<0.5	0.90	0.50	1.00	<0.5	<0.5	0.50	0.60	0.50	0.80	1.50
Zr_ppm	34.90	69.40	6.10	103.50	33.60	52.90	104.50	105.90	84.10	51.60	42.40	21.50	58.00	65.30
Y_ppm	10.70	17.60	5.30	28.10	8.60	16.70	28.10	34.50	19.10	13.50	10.20	11.20	12.50	18.30
La_ppm	10.10	19.40	0.80	11.20	5.00	6.90	11.20	8.20	10.90	6.80	5.90	4.00	13.90	15.20
Ce_ppm	24.00	44.40	3.10	26.30	10.70	15.70	26.60	20.00	25.10	15.30	13.90	10.80	29.70	36.50
Pr_ppm	2.99	5.55	0.59	3.49	1.38	1.92	3.44	2.72	3.18	2.05	1.69	1.67	3.70	4.62
Nd_ppm	12.90	23.50	3.50	15.30	6.30	9.30	15.70	12.90	14.40	9.50	8.10	8.20	15.90	21.30
Sm_ppm	2.93	4.69	1.05	4.37	1.54	2.16	4.17	3.98	3.41	2.17	1.80	2.11	3.69	4.83
Eu_ppm	0.96	1.49	0.39	1.58	0.75	0.80	1.46	1.41	1.27	1.09	0.83	0.60	1.16	1.36
Gd_ppm	2.76	4.33	1.17	5.09	1.71	2.78	5.06	5.48	3.76	2.45	2.10	2.29	3.42	4.44
Tb_ppm	0.39	0.64	0.17	0.83	0.27	0.45	0.80	0.94	0.60	0.38	0.31	0.35	0.47	0.65
Dy_ppm	2.20	3.73	1.03	5.34	1.71	2.85	5.15	6.06	3.50	2.41	1.87	2.18	2.75	3.56

Ho_ppm	0.41	0.65	0.18	1.10	0.33	0.58	1.11	1.24	0.74	0.51	0.40	0.41	0.50	0.70
Er_ppm	1.09	2.06	0.60	3.22	0.95	1.69	3.03	3.76	2.14	1.36	1.19	1.20	1.34	1.89
Tm_ppm	0.15	0.29	0.07	0.43	0.12	0.25	0.44	0.51	0.27	0.19	0.15	0.17	0.19	0.25
Yb_ppm	1.00	1.67	0.42	2.80	0.82	1.52	2.67	3.30	1.85	1.21	1.00	1.11	1.24	1.53
Lu_ppm	0.14	0.25	0.07	0.42	0.12	0.22	0.41	0.48	0.30	0.20	0.16	0.16	0.17	0.21

Sample_ID	KSAT049/032	KSAT051/033	KSAT052/034	KAC091/088	KAC097/091a	KAC097/091b	KAC098/092	KAC118/108	KAC119/109	KAC121/110	KAC165/152	KAC168/158	KAC199/195	KSAT012/007
Lat_S	-15.4384	-15.4100	-15.4095	-15.3087	-14.9517	-14.9517	-14.9451	-14.8335	-14.8001	-15.0577	-15.4931	-15.1911	-16.9093	-16.8731
Long_E	13.6132	13.6146	13.6169	13.8504	14.0281	14.0281	14.0373	14.4340	14.4253	14.0045	13.7279	13.9367	13.4621	13.0276
Rocktype	Gabbro?	Ultramafic	Ultramafic	Granite/ tonalite/granodiorite	Granite	Porphyritic rhyolite	Granite?	Granite	Porphyritic granite/ tonalite?	Microgranite	Granite	Granite	Granitoid gneiss	Granite
Group	Basement	Basement	Basement	Basement	Basement	Basement	Basement	Basement	Basement	Basement	Basement	Basement	Basement	Basement
SiO2_pct	54.57	38.04	39.42	64.56	62.63	77.57	65.01	72.39	74.69	72.22	65.58	74.34	62.30	72.02
TiO2_pct	0.82	0.10	0.08	0.66	0.93	0.15	0.81	0.20	0.26	0.41	0.66	0.25	0.71	0.54
Al2O3_pct	14.01	4.36	8.55	16.37	17.03	11.95	15.96	14.68	13.07	13.96	15.91	13.34	16.94	13.17
Fe2O3t_pct	9.05	13.31	11.11	4.76	4.85	0.85	4.68	1.90	1.39	2.21	3.80	1.48	5.62	3.69
MnO_pct	0.14	0.18	0.13	0.07	0.14	0.02	0.10	0.04	0.02	0.06	0.05	0.02	0.22	0.07
MgO_pct	6.33	34.30	28.74	1.48	1.04	0.05	1.08	0.54	0.32	0.42	1.15	0.30	1.60	0.95
CaO_pct	8.23	2.79	4.30	4.06	2.68	0.33	3.03	2.08	1.56	1.24	2.83	1.33	3.23	1.00
Na2O_pct	2.73	0.20	0.69	4.60	4.65	3.24	3.92	3.22	2.82	3.56	3.24	3.08	4.08	3.49
K2O_pct	2.00	0.07	0.10	2.02	4.71	5.01	4.18	3.39	4.87	5.15	5.32	5.11	2.52	3.10
Cr2O3_pct	0.04	0.26	0.12	0.01	<0.002	0.01	0.00	0.01	0.01	0.01	0.01	0.01	0.23	0.01
P2O5_pct	0.26	0.02	0.02	0.20	0.24	<0.01	0.24	0.07	0.05	0.06	0.16	0.04	0.20	0.13
Normalised*	98.24	93.88	93.48	98.83	99.10	99.17	99.24	98.62	99.05	99.49	98.85	99.43	97.82	98.33

SiO2_pct*	55.55	40.52	42.17	65.32	63.20	78.22	65.51	73.40	75.41	72.59	66.34	74.77	63.69	73.24
TiO2_pct*	0.84	0.10	0.08	0.68	0.95	0.15	0.83	0.21	0.27	0.42	0.68	0.26	0.73	0.55
Al2O3_pct*	55.55	40.52	42.17	65.32	63.20	78.22	65.51	73.40	75.41	72.59	66.34	74.77	63.69	73.24
Fe2O3t_pct*	9.21	14.18	11.88	4.82	4.89	0.86	4.72	1.93	1.40	2.22	3.84	1.49	5.75	3.75
FeO_pct*	7.83	12.05	10.10	4.09	4.16	0.73	4.01	1.64	1.19	1.89	3.27	1.27	4.88	3.19
Fe2O3_pct*	1.38	2.13	1.78	0.72	0.73	0.13	0.71	0.29	0.21	0.33	0.58	0.22	0.86	0.56
FeO*_pct	8.29	12.76	10.70	4.33	4.82	0.84	4.64	1.90	1.38	2.19	3.79	1.47	5.66	3.70
MnO_pct*	0.14	0.18	0.13	0.07	0.14	0.02	0.10	0.04	0.02	0.06	0.05	0.02	0.23	0.07
MgO_pct*	6.44	36.54	30.74	1.50	1.05	0.05	1.09	0.55	0.32	0.42	1.16	0.30	1.64	0.97
CaO_pct*	8.44	2.86	4.41	4.16	2.75	0.34	3.11	2.13	1.60	1.27	2.90	1.36	3.31	1.03
Na2O_pct*	2.80	0.21	0.71	4.72	4.77	3.32	4.02	3.30	2.89	3.65	3.32	3.16	4.18	3.58
K2O_pct*	2.05	0.07	0.10	2.07	4.83	5.14	4.29	3.48	4.99	5.28	5.45	5.24	2.58	3.18
Cr2O3_pct*	0.04	0.27	0.12	0.01	#VALUE!	0.01	0.00	0.01	0.01	0.01	0.01	0.01	0.24	0.01
P2O5_pct*	0.27	0.02	0.02	0.21	0.25	#VALUE!	0.25	0.07	0.05	0.06	0.16	0.04	0.21	0.13
Mg#	59.45	84.38	84.43	39.46	31.01	10.98	32.61	37.34	32.55	28.49	38.82	29.82	37.38	35.05
Mo_pct	<0.001	<0.001	<0.001	<0.001	<0.001	<0.001	<0.001	<0.001	<0.001	<0.001	<0.001	<0.001	<0.001	<0.001
Cu_pct	0.01	<0.001	<0.001	0.00	<0.001	<0.001	<0.001	<0.001	<0.001	<0.001	0.00	<0.001	0.00	<0.001
Pb_pct	<0.02	<0.02	<0.02	<0.02	<0.02	<0.02	<0.02	<0.02	<0.02	<0.02	<0.02	<0.02	<0.02	<0.02
Zn_pct	<0.01	<0.01	<0.01	<0.01	0.01	<0.01	<0.01	<0.01	<0.01	<0.01	<0.01	<0.01	<0.01	<0.01
Ag_ppm	<2	<2	<2	<2	<2	<2	<2	<2	<2	<2	<2	<2	<2	<2
Ni_ppm	45.00	1931.00	1616.00	<10	<10	<10	<10	<10	<10	<10	14.00	<10	17.00	<10
Mo_ppm	0.13	0.22	0.48	0.41	1.60	1.03	1.46	0.37	2.47	0.82	0.64	0.46	1.00	1.90
Cu_ppm	51.35	8.38	4.39	23.87	5.99	6.13	7.94	2.06	3.58	3.02	22.45	9.34	19.90	9.13
Pb_ppm	4.44	0.28	0.26	1.24	5.04	6.72	2.27	4.57	9.18	2.99	2.30	3.36	7.45	18.58
Zn_ppm	30.10	57.80	50.80	16.60	62.60	39.50	63.70	20.30	29.90	38.60	27.20	11.00	80.80	49.10

Ag_ppb	68.00	10.00	11.00	33.00	9.00	149.00	17.00	9.00	12.00	36.00	21.00	16.00	68.00	18.00
Ni_ppm	21.30	1689.50	1478.80	8.70	3.40	6.00	3.60	6.70	3.70	8.50	13.90	7.70	16.90	5.40
Co_ppm	15.00	144.10	127.00	7.40	5.80	0.50	5.40	2.50	2.90	1.70	5.70	2.10	10.50	5.30
Mn_ppm	317.00	1255.00	992.00	248.00	382.00	130.00	229.00	279.00	205.00	307.00	135.00	115.00	477.00	376.00
As_ppm	0.20	<0.1	0.20	<0.1	<0.1	<0.1	<0.1	0.10	<0.1	<0.1	<0.1	<0.1	<0.1	0.30
Au_ppb	<0.2	<0.2	<0.2	0.20	<0.2	<0.2	<0.2	<0.2	<0.2	<0.2	<0.2	<0.2	0.60	<0.2
Cd_ppm	0.06	0.02	<0.01	0.02	0.05	0.02	0.02	<0.01	0.02	0.02	<0.01	<0.01	0.07	0.08
Sb_ppm	<0.02	<0.02	<0.02	<0.02	<0.02	<0.02	<0.02	<0.02	0.03	<0.02	<0.02	<0.02	<0.02	0.04
Bi_ppm	<0.02	<0.02	<0.02	<0.02	<0.02	<0.02	<0.02	0.02	0.20	<0.02	<0.02	<0.02	0.03	0.02
Cr_ppm	75.10	92.80	88.90	35.80	9.50	39.70	13.80	35.60	31.20	47.70	61.10	41.80	57.60	31.60
Hg_ppb	<5	<5	<5	<5	<5	<5	<5	<5	<5	<5	<5	<5	<5	<5
Se_ppm	<0.1	<0.1	<0.1	<0.1	<0.1	<0.1	<0.1	<0.1	0.10	0.30	0.20	<0.1	0.20	<0.1
Te_ppm	<0.02	<0.02	<0.02	<0.02	<0.02	<0.02	<0.02	<0.02	<0.02	<0.02	<0.02	<0.02	0.02	<0.02
Ge_ppm	<0.1	0.20	0.20	0.10	0.20	<0.1	0.10	<0.1	0.10	<0.1	<0.1	<0.1	<0.1	0.10
In_ppm	<0.02	<0.02	<0.02	<0.02	0.07	0.05	0.03	<0.02	<0.02	0.03	<0.02	<0.02	0.03	0.02
Re_ppb	<1	<1	<1	<1	<1	<1	<1	<1	<1	<1	<1	<1	<1	<1
Be_ppm	0.40	<0.1	<0.1	0.20	0.60	<0.1	<0.1	0.70	0.50	0.20	0.10	0.10	0.40	1.00
Li_ppm	13.00	8.00	1.50	4.90	8.80	1.80	3.70	14.80	25.60	12.70	7.30	4.40	19.40	10.80
Pd_ppb	<10	<10	<10	<10	<10	<10	<10	<10	<10	<10	<10	<10	<10	<10
Pt_ppb	<2	<2	<2	<2	<2	<2	<2	<2	<2	<2	<2	<2	<2	2.00
Au_ppb	3.00	6.00	2.00	3.00	3.00	3.00	3.00	4.00	3.00	2.00	3.00	3.00	4.00	2.00
Pt_ppb	1.30	0.40	0.20	0.50	0.20	0.20	0.20	0.40	0.30	0.20	0.30	0.20	1.30	0.20
Pd_ppb	1.80	1.90	0.60	1.20	0.90	0.70	0.80	0.90	0.80	0.60	0.80	0.60	1.80	<0.5
B_ppm	<1	5.00	1.00	<1	<1	<1	<1	<1	<1	<1	<1	<1	2.00	4.00
Tl_ppm	0.03	<0.02	<0.02	<0.02	0.10	0.11	0.04	0.11	0.19	0.08	0.04	0.03	0.06	0.04

LOI_pct	1.50	5.50	6.00	1.00	0.70	0.80	0.60	1.30	0.90	0.40	1.00	0.50	2.00	1.50
TOT/C_TC000_pct	0.04	0.06	0.12	0.14	0.04	<0.02	0.05	0.02	<0.02	<0.02	0.06	<0.02	0.06	0.03
TOT/S_pct	<0.02	0.03	<0.02	0.06	<0.02	<0.02	0.02	<0.02	<0.02	<0.02	<0.02	<0.02	<0.02	<0.02
Ba_ppm	600.00	38.00	17.00	591.00	1377.00	77.00	1698.00	1016.00	259.00	1414.00	1271.00	912.00	1205.00	1003.00
Sc_ppm	24.00	5.00	4.00	11.00	19.00	2.00	8.00	4.00	2.00	4.00	8.00	4.00	13.00	11.00
Sum_pct	99.74	99.38	99.48	99.83	99.80	99.97	99.84	99.92	99.95	99.89	99.85	99.93	99.82	99.83
Cs_ppm	0.70	0.20	<0.1	<0.1	0.30	0.10	0.10	1.90	3.70	0.10	0.10	0.30	1.20	0.70
Ga_ppm	14.70	2.60	3.40	17.90	19.90	16.40	19.30	15.20	13.10	14.10	16.50	13.20	18.50	16.60
Hf_ppm	3.60	0.20	<0.1	5.80	12.00	4.50	9.20	3.20	3.60	7.00	9.40	4.50	5.80	13.00
Nb_ppm	7.60	0.30	<0.1	7.10	35.00	12.30	18.20	7.70	8.20	12.40	11.00	4.20	10.70	21.70
Rb_ppm	49.70	1.30	0.30	18.20	127.90	161.10	64.60	117.60	164.00	110.50	119.50	73.20	61.10	85.40
Sn_ppm	<1	<1	<1	<1	3.00	2.00	1.00	1.00	1.00	2.00	<1	<1	<1	2.00
Sr_ppm	611.50	164.20	199.60	566.10	283.40	13.70	375.90	333.40	114.60	251.80	354.50	248.10	582.70	181.00
Ta_ppm	0.40	<0.1	<0.1	0.40	3.10	0.50	0.90	0.80	0.90	1.00	0.40	0.20	0.50	1.50
Th_ppm	4.60	<0.2	<0.2	4.60	12.10	17.50	5.80	13.10	25.00	7.70	7.70	8.70	10.90	27.40
U_ppm	1.20	<0.1	<0.1	0.30	1.60	0.90	0.60	2.60	3.10	0.70	0.90	0.50	2.10	4.80
V_ppm	192.00	32.00	22.00	89.00	48.00	<8	46.00	23.00	14.00	14.00	59.00	12.00	90.00	30.00
W_ppm	0.70	<0.5	1.00	1.10	2.10	2.00	2.90	3.10	2.60	2.40	2.50	2.30	1.40	3.80
Zr_ppm	127.30	4.70	1.80	246.00	476.20	115.90	358.90	108.60	111.20	255.60	367.10	159.30	220.50	510.30
Y_ppm	23.70	0.70	0.50	18.80	68.60	28.70	31.40	12.70	17.40	37.70	12.20	3.60	29.30	58.20
La_ppm	26.10	0.80	0.40	63.70	79.70	22.00	61.60	35.00	33.90	68.50	62.50	50.60	45.60	81.50
Ce_ppm	55.20	1.90	0.90	117.50	188.50	38.40	122.00	66.70	70.30	140.70	112.10	83.70	90.00	165.70
Pr_ppm	6.49	0.17	0.08	12.72	22.70	4.24	13.88	7.23	6.73	16.31	12.33	8.14	9.83	18.25
Nd_ppm	25.00	0.80	0.40	45.20	81.90	14.70	53.60	25.80	24.20	60.90	43.00	26.30	37.60	68.10
Sm_ppm	5.23	0.17	0.06	6.81	14.01	2.95	9.90	4.14	4.75	10.69	5.88	2.93	6.91	12.80

Eu_ppm	1.30	0.08	0.11	2.24	2.55	0.66	3.10	0.88	0.68	1.93	1.69	0.97	1.79	2.10
Gd_ppm	4.83	0.17	0.11	5.57	12.02	2.86	8.22	3.20	3.83	8.76	4.26	1.91	5.86	11.75
Tb_ppm	0.75	0.02	<0.01	0.72	1.84	0.56	1.12	0.45	0.58	1.24	0.48	0.17	0.87	1.84
Dy_ppm	4.38	0.13	0.08	3.70	11.03	3.69	6.26	2.56	3.39	7.13	2.46	0.83	5.15	10.63
Ho_ppm	0.87	0.03	<0.02	0.73	2.34	0.80	1.21	0.44	0.64	1.39	0.43	0.12	1.11	2.20
Er_ppm	2.62	0.10	0.04	1.90	7.49	2.49	3.24	1.33	1.94	3.97	1.19	0.31	3.31	6.16
Tm_ppm	0.36	0.01	<0.01	0.25	1.16	0.34	0.42	0.19	0.28	0.59	0.16	0.05	0.52	0.85
Yb_ppm	2.59	0.10	0.06	1.54	7.79	2.24	2.64	1.27	2.00	3.71	1.04	0.40	3.53	5.56
Lu_ppm	0.35	0.01	<0.01	0.24	1.20	0.32	0.38	0.19	0.30	0.53	0.17	0.08	0.52	0.86

Sample_ID	KAC031/035	KAC034/037b	KAC079/074	KAC035-1	KAC035-2	KAC035-3	KAC035-4	KAC032/236	KAC186/188	KAC190/192	KAC208/205	KAC208/206	KAC226/225	KAC233/234
Lat_S	-16.9415	-16.6818	-15.7844	-16.5931	-16.5931	-16.5931	-16.5931	-16.7670	-15.4142	-15.7615	-16.9105	-16.9105	-16.9373	-16.7586
Long_E	13.4700	13.4410	13.8355	13.4497	13.4497	13.4497	13.4497	13.4884	14.0818	14.0865	13.4590	13.4590	13.4763	13.4688
Rocktype	Red granite	Porphyritic granite (37a) + xenolith	Porphyritic syenite	Fine-grained dark rock - tonalite	Mix tonalite - Red Granite gneiss	Mix tonalite - Red Granite gneiss	Red granite gneiss	Gneiss	Granite	Aplite	Felsic dyke	Felsic dyke	Granite	Pyroxene-bearing granitoid
Group	KC	KC	KC	KC	KC	KC	KC	KC	KC	KC	KC	KC	KC	KC
SiO2_pct	65.75	67.44	53.42	68.19	62.69	61.53	66.47	64.20	65.89	52.87	71.62	72.16	59.68	50.75
TiO2_pct	0.63	0.63	0.81	0.63	0.82	0.91	0.77	0.98	0.18	0.16	0.29	0.29	1.63	1.09
Al2O3_pct	15.00	14.38	14.23	14.15	15.93	16.48	14.23	14.24	15.70	28.52	14.76	14.29	14.88	17.12
Fe2O3t_pct	4.36	4.19	13.72	4.28	5.32	5.80	4.94	6.16	3.88	1.01	1.74	1.96	9.48	10.91
MnO_pct	0.07	0.09	0.35	0.06	0.08	0.09	0.08	0.12	0.06	<0.01	0.03	0.03	0.15	0.19
MgO_pct	0.89	0.62	0.19	0.78	1.02	1.04	1.01	1.34	0.12	0.12	0.57	0.52	0.29	5.71

CaO_pct	1.57	1.69	6.34	2.22	2.67	2.72	2.38	2.88	4.79	11.36	1.33	1.14	2.80	8.48
Na2O_pct	3.48	3.09	4.88	3.37	3.44	3.46	2.97	3.37	3.54	4.55	3.75	3.54	3.79	3.19
K2O_pct	6.33	6.12	4.20	4.79	6.10	6.16	5.31	4.58	4.11	0.51	4.36	4.52	4.68	1.10
Cr2O3_pct	0.00	0.00	0.00	0.00	0.01	0.00	0.01	0.01	0.01	0.01	0.00	0.01	0.12	0.05
P2O5_pct	0.14	0.16	0.22	0.18	0.19	0.21	0.25	0.31	0.03	<0.01	0.05	0.07	0.12	0.37
Normalised *	98.39	98.61	98.50	98.82	98.40	98.58	98.59	98.34	98.39	99.20	98.58	98.69	98.59	99.08
SiO2_pct*	66.83	68.39	54.23	69.00	63.71	62.42	67.42	65.28	66.97	53.30	72.65	73.12	60.53	51.22
TiO2_pct*	0.65	0.65	0.83	0.65	0.84	0.93	0.79	1.00	0.18	0.16	0.30	0.30	1.67	1.12
Al2O3_pct*	66.83	68.39	54.23	69.00	63.71	62.42	67.42	65.28	66.97	53.30	72.65	73.12	60.53	51.22
Fe2O3t_pct *	4.43	4.25	13.93	4.33	5.41	5.88	5.01	6.26	3.94	1.02	1.77	1.99	9.62	11.01
FeO_pct*	3.77	3.61	11.84	3.68	4.60	5.00	4.26	5.32	3.35	0.87	1.50	1.69	8.17	9.36
Fe2O3_pct*	0.66	0.64	2.09	0.65	0.81	0.88	0.75	0.94	0.59	0.15	0.26	0.30	1.44	1.65
FeO*_pct	3.99	3.82	12.54	3.90	4.87	5.30	4.51	5.64	3.55	0.92	1.59	1.79	8.65	9.91
MnO_pct*	0.07	0.09	0.36	0.06	0.08	0.09	0.08	0.12	0.06	N/D	0.03	0.03	0.15	0.19
MgO_pct*	0.90	0.63	0.19	0.79	1.04	1.05	1.02	1.36	0.12	0.12	0.58	0.53	0.29	5.76
CaO_pct*	1.61	1.73	6.50	2.28	2.74	2.79	2.44	2.95	4.91	11.65	1.36	1.17	2.87	8.69
Na2O_pct*	3.57	3.17	5.00	3.45	3.53	3.55	3.04	3.45	3.63	4.66	3.84	3.63	3.89	3.27
K2O_pct*	6.49	6.27	4.31	4.91	6.25	6.32	5.44	4.70	4.21	0.52	4.47	4.63	4.80	1.13
Cr2O3_pct*	0.00	0.00	0.00	0.00	0.01	0.00	0.01	0.01	0.01	0.01	0.00	0.01	0.12	0.05
P2O5_pct*	0.14	0.16	0.23	0.18	0.19	0.22	0.26	0.32	0.03	N/D	0.05	0.07	0.12	0.38
Mg#	29.97	23.68	2.82	27.64	28.67	27.32	30.00	31.32	6.09	19.94	40.72	35.74	6.03	52.32
Mo_pct	<0.001	<0.001	<0.001	<0.001	<0.001	<0.001	<0.001	<0.001	<0.001	<0.001	<0.001	<0.001	<0.001	<0.001
Cu_pct	0.00	0.00	0.00	<0.001	0.00	0.00	0.00	<0.001	<0.001	<0.001	<0.001	0.00	0.00	0.01
Pb_pct	<0.02	<0.02	<0.02	<0.02	<0.02	<0.02	<0.02	<0.02	<0.02	<0.02	<0.02	<0.02	<0.02	<0.02
Zn_pct	<0.01	0.01	0.03	<0.01	<0.01	<0.01	<0.01	0.01	<0.01	<0.01	<0.01	<0.01	0.02	0.01

Ag_ppm	<2	<2	<2	<2	<2	<2	<2	<2	<2	<2	<2	<2	<2	<2
Ni_ppm	<10	<10	<10	<10	<10	<10	<10	<10	<10	<10	<10	<10	<10	51.00
Mo_ppm	1.68	1.93	2.83	1.42	1.32	2.26	0.49	0.38	1.17	0.84	0.89	0.31	2.01	0.36
Cu_ppm	32.68	35.82	18.31	9.75	19.11	17.15	13.56	5.27	5.58	3.47	9.36	11.44	8.76	98.91
Pb_ppm	11.94	9.52	6.88	7.18	7.24	7.00	7.82	7.88	5.22	1.25	5.51	10.42	7.53	1.46
Zn_ppm	56.90	53.10	188.30	63.00	72.50	70.10	66.00	96.00	6.60	4.70	28.50	31.90	81.80	39.40
Ag_ppb	47.00	66.00	85.00	19.00	33.00	33.00	26.00	21.00	2.00	7.00	4.00	16.00	50.00	48.00
Ni_ppm	6.20	3.30	3.70	3.30	7.10	4.30	6.60	4.70	6.00	2.60	5.10	7.50	1.30	31.80
Co_ppm	6.80	4.00	1.10	5.50	8.20	8.00	6.20	7.10	2.70	1.20	3.70	3.40	1.80	15.70
Mn_ppm	385.00	374.00	1028.00	352.00	408.00	334.00	368.00	711.00	284.00	38.00	202.00	222.00	368.00	150.00
As_ppm	<0.1	<0.1	<0.1	<0.1	<0.1	<0.1	<0.1	<0.1	<0.1	<0.1	<0.1	<0.1	<0.1	<0.1
Au_ppb	0.60	0.60	1.70	<0.2	0.60	0.20	<0.2	<0.2	0.40	0.30	<0.2	0.50	0.40	2.60
Cd_ppm	0.05	0.06	0.53	0.04	0.05	0.05	0.04	0.06	0.03	<0.01	<0.01	<0.01	0.09	0.03
Sb_ppm	<0.02	<0.02	<0.02	<0.02	<0.02	<0.02	<0.02	<0.02	<0.02	<0.02	<0.02	<0.02	<0.02	<0.02
Bi_ppm	<0.02	<0.02	<0.02	<0.02	<0.02	<0.02	<0.02	0.02	<0.02	<0.02	<0.02	<0.02	<0.02	<0.02
Cr_ppm	17.20	19.40	23.50	12.30	18.70	8.80	25.80	19.50	15.90	14.40	18.60	34.00	7.40	126.20
Hg_ppb	<5	<5	<5	<5	<5	<5	<5	<5	<5	<5	<5	<5	<5	<5
Se_ppm	<0.1	<0.1	0.60	0.20	0.20	0.30	0.30	0.40	<0.1	<0.1	<0.1	<0.1	0.20	0.30
Te_ppm	<0.02	<0.02	<0.02	<0.02	<0.02	<0.02	<0.02	<0.02	<0.02	<0.02	<0.02	<0.02	<0.02	0.02
Ge_ppm	0.20	0.20	0.60	<0.1	<0.1	<0.1	<0.1	<0.1	<0.1	<0.1	<0.1	<0.1	0.10	<0.1
In_ppm	0.04	0.08	0.13	0.04	0.06	0.05	0.05	0.07	0.07	<0.02	<0.02	<0.02	0.12	<0.02
Re_ppb	<1	<1	<1	<1	<1	<1	<1	<1	<1	<1	<1	<1	<1	<1
Be_ppm	1.10	0.90	0.20	0.80	0.60	0.80	1.00	1.40	0.60	0.30	0.50	0.70	0.90	0.30
Li_ppm	14.60	14.20	0.60	17.10	23.10	19.30	18.40	24.30	0.70	1.50	4.00	4.90	2.50	5.00
Pd_ppb	<10	<10	<10	<10	<10	<10	<10	<10	<10	<10	<10	<10	<10	<10

Pt_ppb	<2	<2	<2	<2	<2	<2	<2	<2	<2	<2	<2	<2	<2	2.00
Au_ppb	2.00	2.00	5.00	3.00	4.00	4.00	3.00	3.00	3.00	3.00	3.00	3.00	4.00	5.00
Pt_ppb	0.10	0.20	0.40	0.20	0.30	0.20	0.20	0.20	0.20	0.20	0.30	0.30	0.10	3.70
Pd_ppb	0.60	0.60	1.10	0.60	0.70	0.70	<0.5	<0.5	0.80	0.80	0.60	0.80	0.60	4.60
B_ppm	5.00	3.00	10.00	2.00	1.00	3.00	2.00	3.00	2.00	<1	<1	2.00	2.00	<1
Tl_ppm	0.05	0.03	<0.02	0.06	0.20	0.05	0.07	0.09	0.03	<0.02	0.03	0.06	0.03	<0.02
LOI_pct	1.40	1.10	1.00	1.00	1.40	1.20	1.20	1.40	1.30	0.70	1.30	1.20	1.10	0.60
TOT/C_TC000_pct	0.05	0.03	0.03	<0.02	0.08	0.09	<0.02	0.04	0.07	<0.02	<0.02	0.18	0.02	0.08
TOT/S_pct	<0.02	<0.02	<0.02	<0.02	<0.02	0.03	<0.02	<0.02	<0.02	<0.02	<0.02	<0.02	<0.02	0.09
Ba_ppm	1431.00	1814.00	1433.00	1039.00	1250.00	1537.00	1418.00	1540.00	516.00	239.00	997.00	1005.00	9055.00	745.00
Sc_ppm	8.00	12.00	9.00	8.00	8.00	9.00	10.00	13.00	4.00	<1	4.00	4.00	19.00	26.00
Sum_pct	99.79	99.71	99.50	99.82	99.80	99.78	99.79	99.74	99.69	99.90	99.88	99.89	99.69	99.68
Cs_ppm	0.60	0.30	<0.1	0.80	0.80	0.50	0.80	1.30	0.10	<0.1	0.60	0.40	1.10	<0.1
Ga_ppm	16.50	18.40	23.30	16.80	17.40	18.20	17.80	20.70	26.20	18.80	18.20	18.10	26.40	19.20
Hf_ppm	11.80	18.30	53.60	9.90	12.30	13.90	12.20	15.80	10.10	0.10	3.90	4.20	27.80	3.20
Nb_ppm	22.20	48.30	46.30	22.30	26.00	29.60	28.30	37.50	40.00	1.10	4.00	7.10	32.60	8.10
Rb_ppm	129.60	122.20	42.20	109.00	137.00	131.00	124.00	104.00	59.50	9.50	94.10	98.30	83.60	13.00
Sn_ppm	2.00	1.00	<1	2.00	1.00	1.00	2.00	3.00	4.00	<1	<1	<1	3.00	<1
Sr_ppm	292.00	314.10	131.00	284.20	318.80	362.70	322.00	329.90	832.60	859.10	477.50	458.30	488.40	1006.10
Ta_ppm	0.90	1.70	1.50	1.10	1.10	1.50	1.20	1.70	1.90	<0.1	0.10	0.40	1.80	0.20
Th_ppm	15.20	11.90	0.90	12.60	10.50	10.00	10.20	10.20	19.30	0.30	11.90	8.50	9.40	<0.2
U_ppm	1.40	0.70	0.50	1.30	0.90	1.10	0.90	1.50	2.80	<0.1	1.10	1.40	2.60	<0.1
V_ppm	41.00	24.00	<8	41.00	45.00	47.00	47.00	41.00	21.00	27.00	33.00	35.00	14.00	254.00
W_ppm	23.00	3.80	6.50	1.60	1.00	1.10	1.40	1.40	2.70	1.80	1.80	1.50	2.00	1.30
Zr_ppm	492.60	801.20	2774.50	412.00	515.80	578.10	530.70	677.20	296.90	4.30	153.40	149.50	1327.90	123.20

Y_ppm	52.30	89.60	75.10	40.90	38.80	44.10	54.90	70.40	87.00	4.00	3.40	8.50	60.70	20.00
La_ppm	160.30	193.10	50.70	109.50	105.40	118.90	96.90	145.40	326.70	3.80	37.50	38.50	39.90	31.30
Ce_ppm	272.90	394.90	134.90	217.00	205.20	243.90	209.50	290.40	610.50	6.40	65.40	68.00	93.40	67.40
Pr_ppm	32.16	42.78	20.18	24.70	24.66	28.48	26.22	35.45	65.83	0.70	6.10	7.30	11.72	8.01
Nd_ppm	113.60	157.90	97.80	87.20	90.50	105.70	99.60	130.70	229.70	3.00	18.50	24.40	50.80	33.80
Sm_ppm	17.60	27.93	20.84	13.62	14.35	16.89	18.17	22.37	34.48	0.45	2.23	3.97	11.59	5.87
Eu_ppm	2.70	4.08	8.03	2.27	2.32	2.65	2.65	4.05	2.17	0.64	0.58	0.87	9.77	1.99
Gd_ppm	13.52	22.07	19.53	10.10	10.65	12.16	13.72	17.02	26.45	0.50	1.25	2.56	12.40	5.12
Tb_ppm	1.67	3.11	2.70	1.31	1.40	1.61	1.82	2.29	3.34	0.07	0.12	0.33	1.93	0.66
Dy_ppm	9.42	17.81	15.26	7.29	7.77	8.90	10.56	13.53	17.50	0.50	0.60	1.65	11.48	3.97
Ho_ppm	1.73	3.14	3.24	1.41	1.42	1.63	1.89	2.46	2.93	0.11	0.10	0.33	2.37	0.71
Er_ppm	4.74	8.70	9.13	3.93	3.90	4.49	5.22	7.15	7.91	0.42	0.31	0.85	7.28	2.05
Tm_ppm	0.69	1.12	1.44	0.55	0.52	0.61	0.73	0.99	1.14	0.05	0.03	0.12	1.09	0.29
Yb_ppm	4.18	6.77	10.75	3.48	3.28	3.87	4.58	6.23	7.87	0.34	0.37	0.94	7.54	2.00
Lu_ppm	0.67	0.94	2.07	0.55	0.49	0.58	0.69	0.96	1.26	0.05	0.04	0.14	1.26	0.30

Sample_ID	KAC269/268	KAC269/270	KAC283	KAC291	KAC301-1	KAC310-1	KAC310-2	KAC335	KAC337	KAC338	KAC341	KAC422-1	KAC423-2	KAC423-3
Lat_S	-15.5956	-15.5956	-17.0783	-17.0845	-16.9629	-16.9778	-16.9778	-16.5975	-16.5964	-16.5936	-16.6675	-17.4682	-17.1351	-17.1351
Long_E	13.8898	13.8898	13.6306	13.5271	13.3624	13.3619	13.3619	13.4511	13.4594	13.4636	13.4273	13.4327	13.2369	13.2369
Rocktype	Red Granite gneiss	Red Granite gneiss						Red Granite gneiss	Red Granite gneiss	leucogranite	Red Granite gneiss	Granitoid gneiss	Granite dyke	Granitoid gneiss
Group	KC	KC	KC	KC	KC	KC	KC	KC	KC	KC	KC	KC	KC	KC
SiO2_pct	76.48	74.83	72.63	73.01	74.55	65.35	54.04	64.47	71.46	75.81	66.78	65.88	71.94	73.55

TiO2_pct	0.07	0.10	0.39	0.33	0.28	0.89	2.00	0.96	0.39	0.02	0.73	0.80	0.09	0.06
Al2O3_pct	13.54	13.07	12.32	12.54	11.83	14.62	14.40	14.03	12.93	13.48	14.67	14.34	16.26	15.43
Fe2O3t_pct	0.70	1.68	3.49	3.06	3.32	5.10	11.32	6.07	3.62	0.92	4.46	5.48	0.69	0.68
MnO_pct	0.01	0.04	0.05	0.05	0.03	0.08	0.17	0.11	0.07	0.12	0.08	0.10	0.01	0.01
MgO_pct	0.09	0.05	0.29	0.25	0.32	0.84	3.73	1.13	0.29	0.10	0.71	1.62	0.24	0.20
CaO_pct	1.54	0.58	1.71	1.26	0.57	2.77	4.88	3.26	1.42	1.88	2.41	3.17	1.41	0.98
Na2O_pct	6.33	3.39	2.59	3.54	2.89	3.08	3.70	3.05	2.71	6.52	3.68	2.98	7.79	7.85
K2O_pct	0.10	5.26	5.05	4.80	5.28	5.67	2.80	4.78	5.83	0.07	4.65	3.17	0.25	0.24
Cr2O3_pct	0.00	0.00	0.01	0.01	0.01	0.00	0.01	0.01	0.01	0.00	0.00	0.01	0.01	0.01
P2O5_pct	<0.01	<0.01	0.04	0.05	0.02	0.13	0.42	0.33	0.10	0.02	0.25	0.18	<0.01	<0.01
Normalised*	98.82	99.02	98.65	98.95	99.24	98.57	97.51	98.36	98.89	98.92	98.60	97.84	98.72	99.03
SiO2_pct*	77.39	75.57	73.62	73.78	75.12	66.30	55.42	65.54	72.26	76.64	67.73	67.33	72.87	74.27
TiO2_pct*	0.07	0.10	0.40	0.34	0.29	0.91	2.05	0.98	0.40	0.02	0.75	0.82	0.09	0.06
Al2O3_pct*	77.39	75.57	73.62	73.78	75.12	66.30	55.42	65.54	72.26	76.64	67.73	67.33	72.87	74.27
Fe2O3t_pct*	0.71	1.70	3.54	3.09	3.35	5.17	11.61	6.17	3.66	0.93	4.52	5.60	0.70	0.69
FeO_pct*	0.60	1.44	3.01	2.63	2.84	4.40	9.87	5.25	3.11	0.79	3.84	4.76	0.59	0.58
Fe2O3_pct*	0.11	0.25	0.53	0.46	0.50	0.78	1.74	0.93	0.55	0.14	0.68	0.84	0.10	0.10
FeO*_pct	0.64	1.53	3.18	2.78	3.01	4.66	10.45	5.55	3.29	0.84	4.07	5.04	0.63	0.62
MnO_pct*	0.01	0.04	0.05	0.05	0.03	0.08	0.17	0.11	0.07	0.12	0.08	0.10	0.01	0.01
MgO_pct*	0.09	0.05	0.29	0.25	0.32	0.85	3.83	1.15	0.29	0.10	0.72	1.66	0.24	0.20
CaO_pct*	1.58	0.59	1.75	1.29	0.58	2.84	5.00	3.34	1.46	1.93	2.47	3.25	1.45	1.00
Na2O_pct*	6.49	3.48	2.66	3.63	2.96	3.16	3.79	3.13	2.78	6.68	3.77	3.06	7.99	8.05
K2O_pct*	0.10	5.39	5.18	4.92	5.41	5.81	2.87	4.90	5.98	0.07	4.77	3.25	0.26	0.25
Cr2O3_pct*	0.00	0.00	0.01	0.01	0.01	0.00	0.01	0.01	0.01	0.00	0.00	0.01	0.01	0.01
P2O5_pct*	N/D	N/D	0.04	0.05	0.02	0.13	0.43	0.34	0.10	0.02	0.26	0.18	N/D	N/D

Mg#	21.23	5.87	14.84	14.62	16.81	25.67	40.86	28.07	14.38	18.56	25.02	38.26	42.17	38.14
Mo_pct	<0.001	<0.001	<0.001	<0.001	<0.001	<0.001	<0.001	<0.001	<0.001	<0.001	<0.001	<0.001	<0.001	<0.001
Cu_pct	0.01	<0.001	0.00	<0.001	<0.001	<0.001	<0.001	0.00	0.00	<0.001	<0.001	0.01	0.00	0.00
Pb_pct	<0.02	<0.02	<0.02	<0.02	<0.02	<0.02	<0.02	<0.02	<0.02	<0.02	<0.02	<0.02	<0.02	<0.02
Zn_pct	<0.01	<0.01	<0.01	<0.01	<0.01	<0.01	0.02	0.01	<0.01	<0.01	<0.01	<0.01	<0.01	<0.01
Ag_ppm	<2	<2	<2	<2	<2	<2	<2	<2	<2	<2	<2	<2	<2	<2
Ni_ppm	<10	<10	<10	<10	<10	<10	47.00	<10	<10	<10	<10	16.00	<10	<10
Mo_ppm	0.82	1.04	0.94	0.55	1.30	0.53	0.25	1.22	0.85	0.84	0.88	0.38	0.33	0.38
Cu_ppm	47.79	2.72	15.46	6.55	2.98	2.32	3.12	21.28	10.27	5.52	8.24	71.70	9.27	16.82
Pb_ppm	3.51	8.20	22.25	23.02	7.79	5.23	7.07	11.20	16.31	3.03	12.93	5.99	89.87	55.78
Zn_ppm	7.40	47.80	65.90	81.30	44.60	54.40	145.00	90.30	81.70	12.10	74.90	52.60	6.60	5.00
Ag_ppb	<2	<2	<2	72.00	14.00	4.00	10.00	55.00	161.00	8.00	39.00	15.00	11.00	33.00
Ni_ppm	5.20	4.90	5.00	4.50	3.30	5.60	33.20	4.70	7.50	3.10	1.50	15.10	7.40	9.60
Co_ppm	1.70	1.90	3.00	2.10	1.60	6.00	18.50	7.90	3.70	1.20	4.80	11.80	2.10	2.10
Mn_ppm	91.00	304.00	313.00	296.00	232.00	311.00	724.00	494.00	384.00	326.00	390.00	440.00	75.00	67.00
As_ppm	0.60	0.60	0.10	<0.1	<0.1	<0.1	<0.1	<0.1	<0.1	1.40	<0.1	0.40	0.70	1.90
Au_ppb	<0.2	<0.2	<0.2	<0.2	<0.2	<0.2	<0.2	0.30	<0.2	<0.2	<0.2	<0.2	<0.2	0.30
Cd_ppm	0.01	<0.01	0.11	0.07	0.02	0.05	0.08	0.08	0.11	<0.01	0.21	0.04	0.05	0.01
Sb_ppm	<0.02	0.05	<0.02	0.03	0.03	0.02	<0.02	<0.02	<0.02	0.04	<0.02	<0.02	0.02	0.06
Bi_ppm	<0.02	0.03	0.04	0.04	0.07	<0.02	<0.02	0.04	<0.02	0.58	0.05	0.02	0.02	0.25
Cr_ppm	13.10	21.00	19.50	23.30	21.80	12.70	46.60	16.20	26.30	12.70	9.10	54.00	35.50	33.20
Hg_ppb	<5	<5	6.00	<5	<5	<5	<5	<5	<5	<5	<5	<5	<5	<5
Se_ppm	<0.1	<0.1	<0.1	0.20	0.20	0.50	0.60	<0.1	0.30	0.20	0.20	<0.1	<0.1	<0.1
Te_ppm	<0.02	<0.02	0.02	<0.02	<0.02	<0.02	<0.02	<0.02	<0.02	<0.02	<0.02	<0.02	<0.02	<0.02
Ge_ppm	0.10	0.10	0.20	0.20	<0.1	<0.1	<0.1	0.10	<0.1	0.20	<0.1	<0.1	<0.1	<0.1

In_ppm	0.03	0.07	0.06	0.07	0.10	0.06	0.08	0.06	0.05	<0.02	0.04	0.03	<0.02	<0.02
Re_ppb	<1	<1	<1	<1	<1	<1	<1	<1	<1	<1	2.00	<1	<1	<1
Be_ppm	1.30	0.70	1.00	1.70	1.30	0.90	1.20	1.70	0.90	2.10	1.60	0.60	1.10	1.10
Li_ppm	1.30	1.70	3.40	7.00	2.90	4.10	16.40	19.10	3.50	0.60	17.80	8.80	0.90	0.60
Pd_ppb	<10	<10	<10	<10	<10	<10	<10	<10	<10	<10	<10	<10	<10	<10
Pt_ppb	<2	<2	<2	<2	<2	<2	<2	<2	<2	<2	<2	<2	<2	<2
Au_ppb	7.00	10.00	4.00	2.00	3.00	2.00	2.00	3.00	3.00	2.00	3.00	2.00	2.00	5.00
Pt_ppb	0.40	0.80	0.20	0.10	0.20	0.10	0.20	0.20	0.20	0.50	0.10	0.60	0.10	0.30
Pd_ppb	1.00	2.00	0.60	<0.5	0.70	0.50	0.70	0.80	0.70	<0.5	<0.5	0.80	0.50	0.80
B_ppm	2.00	2.00	<1	1.00	2.00	2.00	5.00	2.00	1.00	<1	2.00	9.00	3.00	3.00
Tl_ppm	<0.02	0.14	0.02	0.10	0.03	0.02	0.03	0.07	0.04	<0.02	0.07	0.12	0.02	0.02
LOI_pct	1.10	0.90	1.20	0.90	0.60	1.10	2.10	1.40	0.90	1.00	1.20	2.00	1.20	0.90
TOT/C_TC000_pct	<0.02	0.02	<0.02	0.05	0.04	<0.02	0.09	0.03	<0.02	0.05	<0.02	0.02	<0.02	<0.02
TOT/S_pct	<0.02	<0.02	<0.02	<0.02	<0.02	<0.02	<0.02	<0.02	<0.02	<0.02	<0.02	<0.02	<0.02	<0.02
Ba_ppm	54.00	269.00	928.00	561.00	958.00	447.00	660.00	1554.00	774.00	34.00	1522.00	665.00	145.00	116.00
Sc_ppm	<1	<1	6.00	4.00	4.00	8.00	16.00	14.00	6.00	3.00	10.00	17.00	<1	<1
Sum_pct	99.92	99.92	99.85	99.85	99.84	99.67	99.61	99.76	99.79	99.92	99.80	99.84	99.92	99.93
Cs_ppm	0.40	3.30	0.30	1.30	0.80	0.20	0.80	0.90	0.30	<0.1	0.70	1.00	0.30	0.30
Ga_ppm	18.90	21.40	16.10	21.10	17.20	26.80	26.40	19.50	17.90	18.60	17.70	15.60	17.40	17.20
Hf_ppm	8.60	9.20	13.40	12.40	15.10	30.90	23.20	16.80	12.80	5.20	12.60	8.30	4.40	3.20
Nb_ppm	59.60	48.60	29.30	31.20	35.00	84.80	74.60	37.00	45.00	30.20	23.50	10.80	3.80	6.60
Rb_ppm	5.50	232.20	98.00	164.20	139.80	81.80	58.70	116.30	164.90	1.50	97.50	143.50	7.40	7.70
Sn_ppm	4.00	6.00	8.00	8.00	6.00	2.00	2.00	3.00	2.00	6.00	2.00	2.00	<1	<1
Sr_ppm	121.70	31.80	125.90	95.80	63.30	161.70	195.00	334.00	250.20	198.00	314.90	273.00	337.70	316.10
Ta_ppm	3.00	3.40	2.00	2.10	2.10	2.70	3.20	1.60	1.30	3.50	1.90	0.40	0.20	0.80

Th_ppm	28.40	28.70	23.40	27.60	21.10	16.40	10.60	5.50	19.80	13.10	6.50	20.90	43.90	40.50
U_ppm	2.50	4.10	5.60	6.00	5.50	3.00	2.10	2.00	0.90	12.10	3.40	2.20	5.80	5.60
V_ppm	<8	<8	11.00	10.00	32.00	43.00	139.00	57.00	12.00	<8	28.00	91.00	<8	<8
W_ppm	2.50	3.20	2.10	1.70	3.30	1.40	1.40	1.70	1.40	2.00	5.80	1.60	2.20	1.90
Zr_ppm	179.70	270.20	537.10	434.40	559.60	1251.70	965.40	743.50	485.60	53.30	517.20	327.40	106.80	84.70
Y_ppm	71.30	54.00	67.10	76.60	61.80	159.40	144.50	59.40	83.60	191.40	47.40	39.40	2.40	5.60
La_ppm	15.60	18.10	67.80	91.30	92.00	139.20	173.20	70.00	154.10	17.60	78.90	59.30	19.90	21.50
Ce_ppm	45.90	91.40	138.10	185.40	181.50	297.80	352.30	174.50	319.80	61.90	168.00	119.40	34.00	43.40
Pr_ppm	5.51	5.59	16.48	19.86	21.06	36.66	41.22	23.36	35.46	7.67	19.89	13.13	3.21	4.48
Nd_ppm	22.80	22.20	59.30	74.80	80.10	147.20	163.90	97.80	127.20	31.80	78.60	50.20	10.60	15.10
Sm_ppm	6.56	5.34	11.65	14.06	14.04	31.55	32.24	18.71	22.89	12.30	13.51	9.25	1.53	2.09
Eu_ppm	0.32	0.71	1.44	1.12	1.65	1.51	3.67	3.18	1.79	0.06	2.95	1.68	0.91	0.80
Gd_ppm	8.02	5.62	10.97	13.25	12.44	31.79	31.75	14.74	18.44	14.09	11.17	8.06	0.90	1.30
Tb_ppm	1.69	1.12	1.78	2.16	1.97	5.31	4.76	2.12	2.92	3.03	1.48	1.20	0.10	0.17
Dy_ppm	11.97	8.16	11.11	13.72	12.12	31.96	28.49	11.84	16.32	23.45	8.41	7.12	0.45	0.90
Ho_ppm	2.70	1.86	2.32	2.92	2.57	6.46	5.75	2.29	3.31	5.96	1.76	1.44	0.08	0.16
Er_ppm	8.18	6.51	7.31	8.87	7.56	18.11	16.64	6.53	9.28	21.52	4.74	4.48	0.25	0.56
Tm_ppm	1.22	1.08	1.05	1.28	1.11	2.44	2.20	0.94	1.25	4.00	0.72	0.62	0.03	0.07
Yb_ppm	7.65	7.55	7.09	8.42	7.51	14.54	13.99	6.20	7.50	31.48	4.99	4.06	0.22	0.58
Lu_ppm	1.14	1.16	1.05	1.21	1.11	2.21	2.03	0.93	1.05	5.19	0.79	0.59	0.04	0.09

Sample_ID	KAC425-3	KAC433-1	KAC433-2	KAC439-3	KSAT290/110	KAC043/043	KAC043/044	KAC043/045	KAC045/046	KAC061/058	KAC221/219	KAC228/231A	KAC285	KAC289
Lat_S	-17.2709	-17.2731	-17.2731	-17.2780	-17.0318	-16.5505	-16.5505	-16.5505	-16.5480	-16.4996	-16.9324		-17.0801	-17.0908
Long_E	13.3141	13.3246	13.3246	13.3211	13.4763	13.6780	13.6780	13.6780	13.7478	13.9233	13.4631		13.6318	13.5254

Rocktype	Granite dyke	granite sheet	granite sheet	gneissic anorthositic rock	Granite	Augen gneiss	Fine-g porphyritic dyke within 043/043	Foliated porphyritic granite	Graphic granite	Granite (Chela?)	Felsic vein			Granodiorite
Group	KC	KC	KC	KC	KC	KC	KC	KC	KC	KC	KC	KC	KC	KC
SiO2_pct	58.69	69.65	71.10	52.56	67.12	64.64	61.77	75.52	77.49	72.76	74.12	62.99	53.03	45.21
TiO2_pct	0.30	0.36	0.28	0.09	0.37	0.56	0.85	0.05	0.08	0.27	0.15	0.96	1.80	2.77
Al2O3_pct	19.80	15.44	15.04	25.30	15.26	15.98	16.90	13.31	12.66	12.71	13.39	15.67	12.41	19.80
Fe2O3t_pct	4.41	2.47	2.10	2.51	4.87	4.89	5.32	0.63	0.83	3.18	1.17	5.68	13.96	12.02
MnO_pct	0.05	0.02	0.02	0.03	0.02	0.08	0.08	0.01	0.02	0.04	0.02	0.08	0.21	0.15
MgO_pct	0.05	0.92	0.78	1.99	0.14	0.62	1.15	0.05	0.13	0.16	0.29	1.42	5.33	3.84
CaO_pct	8.03	1.41	2.13	7.39	0.65	2.05	2.64	0.85	1.52	1.05	1.31	3.75	6.11	7.72
Na2O_pct	7.09	7.35	6.94	5.85	5.00	3.62	3.65	3.45	5.32	2.91	4.02	3.35	3.01	2.78
K2O_pct	<0.01	0.14	0.07	1.00	5.38	5.30	5.09	5.15	0.63	5.74	4.16	4.08	0.84	2.46
Cr2O3_pct	0.01	<0.002	0.00	<0.002	0.00	0.01	<0.002	0.01	0.01	0.02	0.11	0.22	0.00	0.00
P2O5_pct	0.03	0.06	0.05	<0.01	0.05	0.18	0.21	<0.01	<0.01	0.05	0.02	0.18	0.16	0.33
Normalised*	98.42	97.87	98.56	96.81	98.95	98.21	97.84	99.08	98.72	99.02	98.83	98.44	96.88	97.16
SiO2_pct*	59.63	71.17	72.14	54.29	67.83	65.82	63.13	76.22	78.49	73.48	75.00	63.99	54.74	46.53
TiO2_pct*	0.31	0.37	0.29	0.09	0.38	0.57	0.87	0.05	0.08	0.28	0.15	0.98	1.85	2.84
Al2O3_pct*	59.63	71.17	72.14	54.29	67.83	65.82	63.13	76.22	78.49	73.48	75.00	63.99	54.74	46.53
Fe2O3t_pct*	4.48	2.52	2.13	2.59	4.92	4.98	5.44	0.64	0.84	3.21	1.18	5.77	14.41	12.37
FeO_pct*	3.81	2.15	1.81	2.20	4.18	4.23	4.62	0.54	0.71	2.73	1.01	4.90	12.25	10.52
Fe2O3_pct*	0.67	0.38	0.32	0.39	0.74	0.75	0.82	0.10	0.13	0.48	0.18	0.87	2.16	1.86
FeO*_pct	4.03	2.27	1.92	2.33	4.43	4.48	4.89	0.57	0.76	2.89	1.07	5.19	12.97	11.13
MnO_pct*	0.05	0.02	0.02	0.03	0.02	0.08	0.08	0.01	0.02	0.04	0.02	0.08	0.22	0.15
MgO_pct*	0.05	0.94	0.79	2.06	0.14	0.63	1.18	0.05	0.13	0.16	0.29	1.44	5.50	3.95

CaO_pct*	8.23	1.45	2.18	7.58	0.67	2.10	2.71	0.87	1.56	1.08	1.34	3.84	6.26	7.91
Na2O_pct*	7.27	7.54	7.12	6.00	5.13	3.71	3.74	3.54	5.45	2.98	4.12	3.43	3.09	2.85
K2O_pct*	N/D	0.14	0.07	1.03	5.52	5.43	5.22	5.28	0.65	5.88	4.26	4.18	0.86	2.52
Cr2O3_pct*	0.01	N/D	0.00	N/D	0.00	0.01	N/D	0.01	0.01	0.02	0.11	0.22	0.00	0.00
P2O5_pct*	0.03	0.06	0.05	N/D	0.05	0.18	0.22	N/D	N/D	0.05	0.02	0.18	0.16	0.34
Mg#	2.32	43.85	43.78	62.44	5.68	21.00	31.19	14.27	24.72	9.54	34.19	34.39	44.46	40.11
Mo_pct	<0.001	<0.001	<0.001	<0.001	<0.001	<0.001	<0.001	<0.001	<0.001	<0.001	<0.001	<0.001	<0.001	<0.001
Cu_pct	0.02	0.00	0.00	<0.001	0.02	0.00	0.00	0.01	0.01	<0.001	0.01	0.01	0.01	0.02
Pb_pct	<0.02	<0.02	<0.02	<0.02	<0.02	<0.02	<0.02	<0.02	<0.02	<0.02	<0.02	<0.02	<0.02	<0.02
Zn_pct	<0.01	<0.01	<0.01	<0.01	<0.01	<0.01	<0.01	<0.01	<0.01	<0.01	<0.01	<0.01	0.01	0.01
Ag_ppm	<2	<2	<2	<2	<2	<2	<2	<2	<2	<2	<2	<2	<2	<2
Ni_ppm	<10	<10	<10	59.00	<10	<10	<10	12.00	<10	11.00	<10	12.00	30.00	34.00
Mo_ppm	1.25	0.98	0.42	0.21	0.60	0.98	0.78	0.79	3.28	1.96	0.19	1.31	0.13	0.55
Cu_ppm	204.16	28.46	22.66	4.36	149.87	21.91	19.30	106.40	73.06	6.92	41.83	53.51	52.90	168.46
Pb_ppm	13.56	160.75	136.34	7.40	22.35	8.79	12.19	5.82	2.92	3.97	2.50	11.24	1.36	6.71
Zn_ppm	2.30	30.20	25.80	16.80	8.20	51.90	80.60	6.80	8.90	47.60	7.40	44.70	91.80	86.90
Ag_ppb	67.00	182.00	29.00	5.00	248.00	11.00	27.00	31.00	<2	19.00	41.00	36.00	169.00	89.00
Ni_ppm	4.40	4.80	6.90	58.00	4.00	6.40	8.90	11.40	4.00	11.80	4.30	7.60	19.50	25.80
Co_ppm	1.80	4.60	4.30	14.70	1.10	5.60	10.00	2.20	1.60	2.10	1.80	9.70	30.00	35.30
Mn_ppm	135.00	140.00	154.00	227.00	98.00	293.00	426.00	94.00	98.00	233.00	91.00	283.00	953.00	368.00
As_ppm	0.60	0.20	0.30	1.20	<0.1	0.20	0.30	<0.1	0.20	<0.1	0.10	<0.1	<0.1	0.60
Au_ppb	3.10	<0.2	<0.2	0.40	0.20	1.20	<0.2	1.70	1.20	0.30	0.60	<0.2	0.50	0.30
Cd_ppm	0.02	0.17	0.04	<0.01	0.05	0.09	0.04	<0.01	0.01	0.03	<0.01	0.05	0.02	0.08
Sb_ppm	0.09	0.04	0.02	0.03	0.02	<0.02	<0.02	<0.02	<0.02	<0.02	<0.02	<0.02	<0.02	0.02
Bi_ppm	0.10	0.03	0.03	0.06	<0.02	<0.02	<0.02	<0.02	<0.02	<0.02	<0.02	0.04	<0.02	<0.02

Cr_ppm	19.20	14.90	25.10	5.70	11.40	38.40	10.40	72.80	31.50	79.80	20.90	17.30	16.70	6.00
Hg_ppb	<5	5.00	<5	<5	<5	<5	<5	<5	<5	<5	<5	<5	<5	<5
Se_ppm	<0.1	<0.1	<0.1	<0.1	0.80	<0.1	<0.1	<0.1	<0.1	0.20	<0.1	0.10	<0.1	0.10
Te_ppm	0.06	0.04	0.05	<0.02	<0.02	0.02	<0.02	<0.02	<0.02	<0.02	<0.02	<0.02	<0.02	<0.02
Ge_ppm	0.40	0.20	0.20	<0.1	<0.1	0.20	0.20	<0.1	<0.1	<0.1	<0.1	<0.1	<0.1	<0.1
In_ppm	<0.02	<0.02	<0.02	<0.02	0.14	0.04	0.05	<0.02	<0.02	0.05	<0.02	0.02	0.03	<0.02
Re_ppb	<1	<1	<1	<1	<1	<1	<1	<1	<1	<1	<1	<1	<1	<1
Be_ppm	0.30	0.70	1.20	0.80	1.20	0.70	0.40	<0.1	2.80	0.40	0.30	1.10	0.70	0.40
Li_ppm	0.10	2.40	2.20	14.00	<0.1	2.70	11.40	0.60	0.70	3.40	1.50	15.90	12.40	29.40
Pd_ppb	<10	<10	<10	<10	<10	<10	<10	<10	<10	<10	<10	<10	<10	<10
Pt_ppb	<2	<2	<2	<2	<2	<2	<2	<2	<2	<2	<2	<2	<2	<2
Au_ppb	4.00	2.00	3.00	4.00	3.00	3.00	3.00	2.00	2.00	2.00	3.00	3.00	3.00	2.00
Pt_ppb	0.20	0.10	0.20	0.20	0.20	0.30	0.20	0.20	0.20	0.20	0.20	0.10	0.10	0.10
Pd_ppb	0.90	0.50	0.60	0.60	0.80	0.80	0.90	0.70	0.70	0.80	0.60	0.50	0.90	0.50
B_ppm	1.00	<1	3.00	6.00	2.00	3.00	3.00	<1	<1	<1	2.00	4.00	2.00	3.00
Tl_ppm	<0.02	<0.02	<0.02	0.06	<0.02	0.04	0.03	0.03	<0.02	0.04	0.04	0.04	<0.02	0.06
LOI_pct	1.20	1.90	1.30	3.10	0.80	1.50	1.90	0.90	1.20	0.80	1.10	1.40	2.90	2.60
TOT/C_TC000_pct	0.04	0.04	<0.02	0.15	<0.02	0.05	0.05	0.03	<0.02	0.04	0.08	0.03	0.04	0.05
TOT/S_pct	<0.02	<0.02	<0.02	<0.02	<0.02	<0.02	<0.02	<0.02	<0.02	<0.02	<0.02	<0.02	<0.02	<0.02
Ba_ppm	19.00	157.00	93.00	265.00	557.00	3036.00	2021.00	168.00	54.00	1237.00	614.00	893.00	198.00	880.00
Sc_ppm	1.00	1.00	1.00	<1	3.00	8.00	9.00	<1	1.00	4.00	2.00	11.00	38.00	11.00
Sum_pct	99.62	99.77	99.86	99.91	99.75	99.71	99.74	99.98	99.92	99.82	99.93	99.84	99.78	99.76
Cs_ppm	<0.1	0.20	0.10	2.70	<0.1	0.20	0.20	<0.1	0.40	0.30	1.10	0.80	0.30	1.50
Ga_ppm	23.00	18.20	16.10	17.00	23.10	18.20	18.90	15.20	15.60	18.60	12.10	19.40	15.40	19.50
Hf_ppm	9.90	10.90	8.40	0.20	20.90	13.20	14.70	2.70	0.80	9.80	3.40	4.20	5.40	2.00

Nb_ppm	6.60	10.80	4.10	1.70	49.10	13.00	25.00	1.00	79.40	22.10	6.80	9.80	11.40	5.70
Rb_ppm	0.10	3.40	2.30	31.80	110.80	95.50	86.80	79.80	21.50	107.50	89.60	107.40	19.20	103.40
Sn_ppm	<1	1.00	<1	<1	<1	<1	1.00	<1	<1	1.00	<1	4.00	2.00	1.00
Sr_ppm	1415.40	414.40	216.60	438.30	82.40	453.20	349.60	42.20	346.00	118.80	340.50	370.30	104.60	552.20
Ta_ppm	0.30	0.60	<0.1	0.10	2.00	0.50	0.80	<0.1	2.20	0.90	0.60	0.90	0.70	0.30
Th_ppm	133.00	134.30	93.00	2.70	27.40	23.20	17.80	0.90	21.40	26.30	10.90	7.80	4.20	1.60
U_ppm	10.10	5.50	4.50	2.00	3.80	0.70	1.00	0.40	3.10	1.20	2.10	1.50	1.20	0.30
V_ppm	51.00	18.00	17.00	<8	74.00	29.00	45.00	<8	<8	8.00	14.00	112.00	353.00	349.00
W_ppm	2.40	3.40	1.40	0.60	2.00	1.30	2.30	2.70	6.30	3.20	1.10	3.20	<0.5	1.10
Zr_ppm	338.10	371.60	274.10	4.50	885.90	579.00	678.50	63.60	19.00	377.00	116.10	172.00	189.50	84.60
Y_ppm	9.10	10.90	3.60	1.50	102.90	26.50	41.00	1.50	47.60	54.10	8.00	20.90	36.30	12.90
La_ppm	261.10	223.90	118.50	2.30	94.40	320.10	174.20	16.60	12.60	227.00	27.30	72.40	24.00	14.20
Ce_ppm	450.50	391.60	214.10	4.60	243.80	547.20	329.30	17.30	34.90	420.50	49.30	137.20	49.50	29.80
Pr_ppm	42.12	36.06	19.98	0.52	27.72	51.93	33.00	1.76	4.78	41.41	4.95	13.70	6.23	3.59
Nd_ppm	118.60	103.60	59.70	1.90	105.60	170.00	114.00	4.90	22.10	139.90	16.50	45.50	27.30	15.60
Sm_ppm	12.35	11.31	7.10	0.41	23.29	18.53	16.90	0.57	7.65	20.15	2.66	6.33	5.92	3.10
Eu_ppm	2.37	2.41	1.51	0.52	2.32	4.59	2.43	0.72	0.33	2.14	0.62	1.83	1.52	1.44
Gd_ppm	5.78	5.34	2.83	0.35	21.80	10.57	12.15	0.45	9.76	15.01	1.92	4.89	6.63	2.98
Tb_ppm	0.57	0.56	0.26	0.05	3.44	1.10	1.51	0.06	1.74	2.02	0.25	0.68	1.11	0.43
Dy_ppm	2.06	2.33	0.93	0.25	21.65	5.50	7.89	0.33	11.37	11.48	1.39	3.89	6.91	2.55
Ho_ppm	0.26	0.30	0.09	0.04	4.15	0.91	1.49	0.07	2.34	2.03	0.31	0.80	1.50	0.52
Er_ppm	0.55	0.81	0.30	0.10	12.64	2.58	3.75	0.20	6.64	5.58	0.81	2.19	4.38	1.44
Tm_ppm	0.10	0.11	0.04	0.02	1.76	0.36	0.52	0.03	0.88	0.75	0.14	0.37	0.60	0.20
Yb_ppm	0.60	0.68	0.32	0.11	11.24	2.20	3.17	0.23	5.10	4.45	0.98	2.26	3.77	1.32
Lu_ppm	0.10	0.10	0.05	0.01	1.76	0.40	0.48	0.04	0.73	0.66	0.17	0.39	0.62	0.19

Sample_ID	KAC304	KAC316-1	KAC311	KAC316-2	KAC320-1	KAC330
Lat_S	-16.9369	-16.9771	-16.9780	-16.9771	-17.0289	-16.8681
Long_E	13.3444	13.4522	13.4527	13.4522	13.4970	13.4629
Rocktype						Foliated reddish rock
Group	KC	KC	KC	KC	KC	KC
SiO2_pct	73.95	72.86	74.82	74.92	46.79	72.33
TiO2_pct	0.10	0.03	0.05	0.11	0.73	0.44
Al2O3_pct	14.10	15.11	13.98	13.74	14.30	12.83
Fe2O3t_pct	1.08	0.41	0.47	0.87	11.27	2.69
MnO_pct	0.03	<0.01	0.01	0.01	0.18	0.04
MgO_pct	0.20	0.15	0.10	0.17	6.62	0.44
CaO_pct	1.17	0.66	0.64	0.57	15.25	1.42
Na2O_pct	4.05	3.12	3.60	4.33	1.33	2.25
K2O_pct	4.18	5.97	5.40	4.21	0.68	5.87
Cr2O3_pct	0.01	0.00	0.00	0.01	0.05	0.01
P2O5_pct	0.05	0.09	0.01	0.04	0.06	0.11
Normalised*	98.95	98.80	99.17	99.04	97.26	98.55
SiO2_pct*	74.73	73.74	75.45	75.65	48.11	73.39
TiO2_pct*	0.10	0.03	0.05	0.11	0.75	0.45
Al2O3_pct*	74.73	73.74	75.45	75.65	48.11	73.39
Fe2O3t_pct*	1.09	0.41	0.47	0.88	11.59	2.73
FeO_pct*	0.93	0.35	0.40	0.75	9.85	2.32

Fe2O3_pct*	0.16	0.06	0.07	0.13	1.74	0.41
FeO*_pct	0.98	0.37	0.43	0.79	10.43	2.46
MnO_pct*	0.03	N/D	0.01	0.01	0.18	0.04
MgO_pct*	0.20	0.15	0.10	0.17	6.81	0.45
CaO_pct*	1.20	0.68	0.66	0.58	15.63	1.46
Na2O_pct*	4.15	3.20	3.69	4.44	1.36	2.31
K2O_pct*	4.29	6.12	5.54	4.32	0.70	6.02
Cr2O3_pct*	0.01	0.00	0.00	0.01	0.05	0.01
P2O5_pct*	0.05	0.09	0.01	0.04	0.06	0.11
Mg#	27.97	43.41	30.85	29.06	55.19	25.54
Mo_pct	<0.001	<0.001	<0.001	<0.001	<0.001	<0.001
Cu_pct	<0.001	<0.001	<0.001	0.00	0.01	<0.001
Pb_pct	<0.02	<0.02	<0.02	<0.02	<0.02	<0.02
Zn_pct	<0.01	<0.01	<0.01	<0.01	<0.01	<0.01
Ag_ppm	<2	3.00	<2	<2	<2	<2
Ni_ppm	<10	<10	<10	<10	125.00	<10
Mo_ppm	1.06	0.74	0.49	0.30	0.48	2.49
Cu_ppm	5.51	3.22	2.61	13.76	69.91	5.33
Pb_ppm	2.35	7.58	5.28	8.22	19.33	7.71
Zn_ppm	7.40	4.40	7.90	11.50	11.70	36.50
Ag_ppb	11.00	177.00	305.00	32.00	174.00	14.00
Ni_ppm	2.80	1.20	1.30	6.50	18.00	6.30
Co_ppm	1.10	0.60	1.00	1.40	7.50	3.80
Mn_ppm	106.00	32.00	73.00	84.00	226.00	223.00
As_ppm	<0.1	0.10	<0.1	0.20	0.20	<0.1

Au_ppb	0.20	<0.2	<0.2	0.20	<0.2	0.40
Cd_ppm	0.02	<0.01	<0.01	<0.01	0.05	0.05
Sb_ppm	<0.02	<0.02	<0.02	<0.02	0.03	<0.02
Bi_ppm	0.04	<0.02	0.08	0.07	0.09	<0.02
Cr_ppm	18.30	12.70	8.80	30.10	42.90	15.40
Hg_ppb	<5	<5	<5	<5	<5	<5
Se_ppm	<0.1	<0.1	<0.1	<0.1	<0.1	<0.1
Te_ppm	<0.02	<0.02	<0.02	0.02	0.04	<0.02
Ge_ppm	<0.1	<0.1	<0.1	<0.1	0.10	<0.1
In_ppm	<0.02	<0.02	<0.02	<0.02	<0.02	0.02
Re_ppb	<1	<1	<1	<1	<1	<1
Be_ppm	0.30	0.20	0.20	0.20	0.20	0.50
Li_ppm	1.90	0.70	1.20	1.50	2.30	2.50
Pd_ppb	<10	<10	<10	<10	<10	<10
Pt_ppb	<2	<2	<2	<2	2.00	<2
Au_ppb	2.00	2.00	2.00	1.00	3.00	3.00
Pt_ppb	0.20	0.10	0.10	0.10	5.00	0.30
Pd_ppb	0.50	<0.5	0.50	<0.5	4.20	0.90
B_ppm	2.00	2.00	<1	<1	2.00	<1
Tl_ppm	0.04	0.02	0.03	0.02	<0.02	0.06
LOI_pct	1.00	1.10	0.80	0.90	2.50	1.30
TOT/C_TC000_pct	<0.02	0.03	<0.02	0.02	0.21	<0.02
TOT/S_pct	<0.02	<0.02	<0.02	<0.02	<0.02	<0.02
Ba_ppm	403.00	3378.00	413.00	532.00	124.00	1113.00
Sc_ppm	2.00	<1	1.00	2.00	36.00	4.00

Sum_pct	99.95	99.90	99.97	99.94	99.76	99.85
Cs_ppm	1.30	0.80	1.30	1.30	<0.1	0.40
Ga_ppm	16.10	7.90	13.00	15.20	14.70	15.90
Hf_ppm	1.90	1.10	2.70	3.00	1.00	8.50
Nb_ppm	10.10	0.50	3.70	5.20	1.30	18.70
Rb_ppm	98.50	105.30	131.30	98.80	17.30	93.60
Sn_ppm	1.00	<1	<1	<1	<1	<1
Sr_ppm	210.40	687.00	177.50	312.20	523.80	215.80
Ta_ppm	1.00	<0.1	0.50	0.40	<0.1	0.40
Th_ppm	9.20	3.10	5.90	8.70	<0.2	19.80
U_ppm	1.80	0.90	3.20	2.20	<0.1	0.80
V_ppm	17.00	<8	<8	10.00	273.00	24.00
W_ppm	1.90	1.70	1.20	1.40	0.90	1.80
Zr_ppm	56.40	43.40	78.90	82.60	36.70	334.20
Y_ppm	9.60	22.80	4.10	5.40	15.80	22.80
La_ppm	29.00	16.80	4.40	16.30	2.40	153.80
Ce_ppm	46.30	28.90	7.70	31.50	6.20	304.60
Pr_ppm	5.12	3.20	0.93	2.83	0.89	25.74
Nd_ppm	19.30	11.30	3.30	9.70	4.60	78.70
Sm_ppm	3.50	2.07	0.73	1.36	1.56	9.94
Eu_ppm	0.74	1.68	0.39	0.35	0.62	1.80
Gd_ppm	2.71	2.26	0.75	1.04	2.29	6.57
Tb_ppm	0.33	0.43	0.09	0.16	0.39	0.87
Dy_ppm	1.73	3.19	0.71	0.85	2.62	4.55
Ho_ppm	0.30	0.82	0.13	0.18	0.63	0.80

Er_ppm	0.81	2.70	0.41	0.58	1.81	2.27
Tm_ppm	0.13	0.39	0.06	0.09	0.26	0.33
Yb_ppm	1.01	2.43	0.52	0.58	1.68	2.10
Lu_ppm	0.15	0.36	0.09	0.08	0.28	0.31